ISSN 0031 - 9465

PHYTOPATHOLOGIA MEDITERRANEA

Plant health and food safety

Volume 65 • No. 1 • April 2026

The international journal of the
Mediterranean Phytopathological Union

FIRENZE UNIVERSITY PRESS

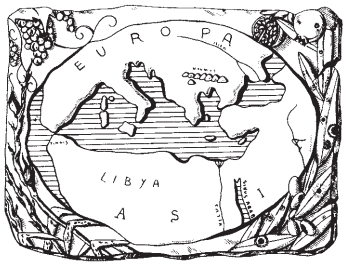

PHYTOPATHOLOGIA MEDITERRANEA

Plant health and food safety

The international journal edited by the Mediterranean Phytopathological Union
founded by A. Ciccarone and G. Goidànich

Phytopathologia Mediterranea is an international journal edited by the Mediterranean Phytopathological Union. The journal's mission is the promotion of plant health for Mediterranean climate and regions, safe food production, and the transfer of knowledge on diseases and their sustainable management.
The journal deals with all areas of plant pathology, including epidemiology, disease control, biochemical and physiological aspects, and utilization of molecular technologies. All types of plant pathogens are covered, including fungi, nematodes, protozoa, bacteria, phytoplasmas, viruses, and viroids. Papers on mycotoxins, biological and integrated management of plant diseases, and the use of natural substances in disease and weed control are also strongly encouraged. The journal focuses on phytopathology and closely related fields in the Mediterranean agro-ecological regions. The journal includes three issues each year, publishing Reviews, Original research papers, Research notes, New or unusual disease reports, News and opinion, Current topics, Commentaries, and Letters to the Editor.

EDITORS-IN-CHIEF

Laura Mugnai – University of Florence, DAGRI, Plant pathology and Entomology section, P.le delle Cascine 28, 50144 Firenze, Italy
Phone: +39 055 2755861
E-mail: laura.mugnai@unifi.it

Richard Falloon – New Zealand Institute for Plant & Food Research (retired)
Phone: +64 3 337 1193 or +64 27 278 0951
Email: richardefalloon@gmail.com

CONSULTING EDITOR

G. Surico, DAGRI, University of Florence, Italy

EDITORIAL BOARD

J. Armengol, Universidad Politécnica de Valencia, Spain
S. Banniza, University of Saskatchewan, Canada
A. Bertaccini, Alma Mater Studiorum, University of Bologna, Italy
A.G. Blouin, Plant & Food Research, Auckland, New Zealand
R. Buonaurio, University of Perugia, Italy
N. Buzkan, Imam University, Turkey
T. Caffi, Università Cattolica del Sacro Cuore, Piacenza, Italy
I.L.P.M. da Conceição, University of Coimbra, Portugal
U. Damm, Senckenberg Museum of Natural History Görlitz, Germany
A.M. D'Onghia, CIHEAM/Mediterranean Agronomic Institute of Bari, Italy
A. Eskalen, University of California, Davis, CA, United States
T.A. Evans, University of Delaware, Newark, DE, USA
A. Evidente, University of Naples Federico II, Italy
M. Garbelotto, University of California, Berkeley, CA, USA
S. Gargouri, INRAT-Tunisi, Tunisia
L. Ghelardini, University of Florence, Italy
V. Guarnaccia, University of Turin, Italy
P. Kinay Teksür, Ege University, Bornova Izmir, Turkey
S. Kumari, ICARDA, Terbol Station, Lebanon
A. Lanubile, Università Cattolica del Sacro Cuore, Piacenza, Italy
M. Masiello, National Research Council, (CNR), Bari, Italy
L. Mostert, Faculty of AgriSciences, Stellenbosh, South Africa
J. Murillo, Universidad Publica de Navarra, Spain
J.A. Navas-Cortes, CSIC, Cordoba, Spain
L. Palou, Centre de Tecnologia Postcollita, Valencia, Spain
E. Paplomatas, Agricultural University of Athens, Greece
I. Pertot, University of Trento, Italy
A. Picot, Univerisité de Bretagne Occidental, LUBEM, Plouzané, France
D. Rubiales, Institute for Sustainable Agriculture, CSIC, Cordoba, Spain
J-M. Savoie, INRA, Villenave d'Ornon, France
A. Siah, Yncréa HdF, Lille, France
A. Tekauz, Cereal Research Centre, Winnipeg, MB, Canada
D. Tsitsigiannis, Agricultural University of Athens, Greece
J.R. Úrbez-Torres, Agriculture and Agri-Food Canada, Canada
J.N. Vanneste, Plant & Food Research, Sandringham, New Zealand
M. Vurro, National Research Council (CNR), Bari, Italy
A.S Walker, BIOGER, INRAE, Thiverval-Grignon, France
M.J. Wingfield, University of Pretoria, South Africa

DIRETTORE RESPONSABILE

Giuseppe Surico, DAGRI, University of Florence, Italy
E-mail: giuseppe.surico@unifi.it

EDITORIAL OFFICE STAFF

DAGRI, Plant pathology and Entomology section, University of Florence, Italy
E-mail: phymed@unifi.it, Phone: ++39 055 2755861/862
Editorial Assistant - **Sonia Fantoni**
Editorial office staff - **Angela Gaglier**

PHYTOPATHOLOGIA MEDITERRANEA

The international journal of the Mediterranean Phytopathological Union

Volume 65, April, 2026

Firenze University Press

Phytopathologia Mediterranea. The international journal of the Mediterranean Phytopathological Union
https://www.fupress.com/pm
ISSN 0031-9465 (print) | ISSN 1593-2095 (online)
Published three times a year

Editor-in-Chief:
Laura Mugnai, University of Florence, Italy
Richard Falloon, New Zealand Institute for Plant & Food Research, New Zealand

Direttore Responsabile: Giuseppe Surico, University of Florence, Italy
Iscritto al Tribunale di Firenze con il n° 4923 del 5-1-2000

© 2026 Author(s)

Content license: except where otherwise noted, the present work is released under Creative Commons Attribution 4.0 International license (CC BY 4.0: https://creativecommons.org/licenses/by/4.0/legalcode). This license allows you to share any part of the work by any means and format, modify it for any purpose, including commercial, as long as appropriate credit is given to the author, any changes made to the work are indicated and a URL link is provided to the license.

Metadata license: all the metadata are released under the Public Domain Dedication license (CC0 1.0 Universal: https://creativecommons.org/publicdomain/zero/1.0/legalcode).

Published by Firenze University Press

Firenze University Press
Università degli Studi di Firenze
via Cittadella, 7, 50144 Firenze, Italy
www.fupress.com

Phytopathologia Mediterranea
The international journal of the
Mediterranean Phytopathological Union

Firenze University Press
www.fupress.com/pm

Research Papers

Evaluation of *Trichoderma asperellum* ICC012 and *T. gamsii* ICC080 to protect almond pruning wounds from infections caused by fungal trunk pathogens

Hamza Bin SAJID, Maya HACHICHA, Yan-Jiun HUANG, Mónica BERBEGAL, Josep ARMENGOL*

Instituto Agroforestal Mediterráneo, Universitat Politècnica de València, Camino de Vera S/N, 46022-Valencia
*Corresponding author. E-mail: jarmengo@eaf.upv.es

OPEN ACCESS

Citation: Sajid, H. B., Hachicha, M., Huang, Y.-J., Berbegal, M., & Armengol, J. (2026). Evaluation of *Trichoderma asperellum* ICC012 and *T. gamsii* ICC080 to protect almond pruning wounds from infections caused by fungal trunk pathogens. *Phytopathologia Mediterranea* 65(1): 3-13. doi: 10.36253/phyto-16809

Accepted: January 18, 2026

Published: March 16, 2026

©2026 Author(s). This is an open access, peer-reviewed article published by Firenze University Press (https://www.fupress.com) and distributed, except where otherwise noted, under the terms of the CC BY 4.0 License for content and CC0 1.0 Universal for metadata.

Data Availability Statement: All relevant data are within the paper and its Supporting Information files.

Competing Interests: The Author(s) declare(s) no conflict of interest.

Editor: Akif Eskalen, University of California, Davis, CA, United States.

ORCID:
HBS: 0000-0002-9439-9918
MH: 0009-0000-3429-0358
YJH: 0009-0002-4180-7946
MB: 0000-0002-5773-3104
JA: 0000-0003-3815-8578

Summary. This study evaluated the potential of *Trichoderma asperellum* ICC012 and *T. gamsii* ICC080 to protect almond pruning wounds from infections caused by three major almond trunk pathogens: *Diplodia seriata*, *Eutypa lata*, and *Neofusicoccum parvum*. Dual-culture antagonism assays and two *in planta* wound protection trials were conducted to assess their efficacy. In the first trial, treatments with *T. asperellum* ICC012 + *T. gamsii* ICC080 were applied one or seven days before or after pathogen inoculation to test the impact of application timing, while the second trial focused on preventive strategies, comparing single versus double applications prior to inoculation. Both *Trichoderma* strains alone and mixed were able to inhibit pathogen growth *in vitro*. Experiments *in planta* showed that only pre-infection applications significantly protected pruning wounds, though their efficacy differed by pathogen and treatment strategy. Protection was highest against *E. lata* and *D. seriata*, in which a single treatment prevented infection, whereas *N. parvum* proved more challenging; only a double pre-inoculation application markedly improved its control. Our results demonstrate that preventive wound protection by *T. asperellum* ICC012 + *T. gamsii* ICC080 is essential for effective control. Incorporating these biocontrol agents into almond orchard management can substantially reduce trunk disease infections and limit reliance on synthetic fungicides in Mediterranean production systems.

Keywords. *Diplodia seriata*, *Eutypa lata*, *Neofusicoccum parvum*, nut crops, *Prunus dulcis*.

INTRODUCTION

Almond (*Prunus dulcis* [Mill.] D.A.Webb) is a widely grown nut crop in many Mediterranean countries, as well as in California (USA), South Africa, and some countries in South America and Australasia. Almond trees are well adapted to Spanish semiarid Mediterranean conditions mainly found in the southeastern regions and parts of the Ebro Valley (Gradziel, 2017). Accord-

ing to Food and Agriculture Organization (FAO, 2024), Spain is one of the top producers of almonds after California (USA).

Fungal trunk diseases on fruit and nut crops affecting different cultivars and caused by many diverse pathogens are currently becoming one of the main concerns worldwide, due to important production losses and their negative economic impact (Guarnaccia *et al*., 2022; Martino *et al*., 2025; Luque-Cruz et al., 2026). Fungal trunk diseases of almond trees have been associated with pathogenic species belonging to several distinct taxonomic groups, including members of the families *Botryosphaeriaceae*, *Calosphaeriaceae*, *Cytosporaceae*, *Diaporthaceae*, *Diatrypaceae*, *Togniniaceae*, *Hymenochaetaceae*, *Pleosporaceae*, and *Tympanidaceae* (Slippers *et al*., 2007; Inderbitzin *et al*., 2010; Gramaje *et al*., 2012; Olmo *et al*., 2016; Markakis *et al*., 2017; Lawrence *et al*., 2018; Nouri *et al*., 2018; León *et al*., 2020; Holland *et al*., 2021b; Goura *et al*., 2023).

The role of wounds in the epidemiology and management of fungal trunk diseases in fruit and nut crops is crucial (Guarnaccia *et al*., 2022). In almond cultivation, pruning wounds serve as important infection courts for various fungal pathogens that cause trunk diseases, leading to sunken cankers, vascular tissue girdling, branch dieback, and, in severe cases, tree death (Inderbitzin *et al*., 2010; Gramaje *et al*., 2012; Holland *et al*., 2021b).

Researchers both in California and Spain have explored a variety of management strategies to protect pruning wounds in almonds through chemical and biological control. In Spain, Olmo *et al*. (2017) demonstrated the effectiveness of the fungicide thiophanate-methyl for pruning wound protection against infections caused by Botryosphaeriaceae species. Subsequently, Holland *et al*. (2021a) confirmed the efficacy of the same product in California against five almond trunk pathogens *Botryosphaeria dothidea* (Moug.) Ces. & De Not., *Neofusicoccum parvum* (Pennycook & Samuels) Crous, Slippers & A.J.L. Phillips, *Cytospora sorbicola* Norph., Bulgakov, T.C. Wen & K.D. Hyde, *Ceratocystis destructans* L.A. Holland, D.P. Lawr. & Trouillas and *Eutypa lata* (Pers.) Tul. & C. Tul.

However, biological control has gained a strong interest in managing pruning wound diseases due to the progressive banning of chemical fungicides together with the high restrictions that they currently face worldwide due to their harmful effects on human health and the environment (Lahlali *et al*., 2022). Biological control agents (BCAs) such as *Trichoderma atroviride* P. Karst. SC1, *T. paratroviride* Jaklitsch & Voglmayr RTFT014, and *Clonostachys rosea* (Link) Schroers, Samuels, Seifert & W. Gams J1446 had proven their efficacy to protect almond wounds against fungal trunk pathogens in California (Holland *et al*., 2021a; Travadon *et al*., 2023a, b). While in Spain, the BCA *Pseudomonas aeruginosa* (Schroeter 1872) Migula 1900 AC17 has recently been suggested as the best candidate for the biological control of Botryosphaeriaceae fungi infecting almond pruning wounds (Romero-Cuadrado *et al*., 2024).

Apart from the application of BCAs based on bacterial strains in Spain, all other biological control studies have been performed in California investigating BCAs products authorised or developed there. Nevertheless, in Mediterranean European almond producing countries, there is a lack of information about management strategies that may be useful for wound protection against trunk pathogens using fungal based BCAs. Thus, the objective of our work was to determine the potential biocontrol activity and wound protection of *Trichoderma asperellum* Samuels, Lieckf. & Nirenberg (isolate ICC012) and *T. gamsii* Samuels & Druzhin. (isolate ICC080) against three frequently found almond trunk disease pathogens in Mediterranean conditions: *Diplodia seriata* De Not., *E. lata*, and *N. parvum*.

MATERIALS AND METHODS

Fungal isolates

In this study, we used three isolates of the following species of almond trunk pathogens: *D. seriata* (BAL-45, Binissalem, Balearic Islands), *E. lata* (GIHF-311, Caravaca de la Cruz, Murcia), and *N. parvum* (BAL-42, Sant Llorenç des Cardassar, Balearic Islands). These isolates were obtained from almond trees showing symptoms of cankers and internal wood necrosis. They were hyphal tipped prior to storage in 15% glycerol solution at -80°C into 1.5 mL cryovials at the fungal collection of the Instituto Agroforestal Mediterráneo, Universitat Politècnica de València, Spain. Moreover, *Trichoderma asperellum* (isolate ICC012) and *T. gamsii* (isolate ICC080) cultures, which are the components of the commercial product Blindar®, were provided by Gowan Crop Protection Limited, and they were also stored as described before.

Dual culture antagonism assay

Antagonistic effect of the *Trichoderma* isolates against the selected almond trunk pathogens was determined using dual culture assays on Potato Dextrose Agar (PDA, Biokar-Diagnostics, Zac de Ther, France) plates.

Pathogens inoculum was obtained from the margins of seven-day-old colonies actively growing on PDA. From these edges, mycelial plugs (6 mm in diam-

eter) were extracted for use in the confrontation assays. *Trichoderma* isolates were cultured on PDA and incubated for ten days at 25°C in darkness. To harvest conidia, the agar surface was flooded with 10 mL of sterile distilled water (SDW) and gently scraped with a sterile spatula. The suspension was filtered through a double layer of cheesecloth and adjusted using a hemocytometer to a final concentration of 10^6 conidia mL^{-1}. Moreover, these conidial suspensions were used to prepare an additional *Trichoderma* suspension containing a mixture of both isolates (*T. asperellum* + *T. gamsii,* 50% each), which was also adjusted to 10^6 conidia mL^{-1}. Drops (20 µL) of the three different *Trichoderma* conidial suspensions were used for the dual confrontation experiments.

The assay was performed in 90 mm Petri dishes containing PDA. A six mm pathogen plug was placed on one side of the dish, while a 20 µL drop of the corresponding *Trichoderma* suspension was placed at the opposite edge. All plates were incubated at 25°C in darkness for seven days. Control treatments consisted of PDA plates inoculated solely with the pathogen plug under the same incubation conditions to provide a baseline for radial growth comparison.

The experiment was conducted twice with four replicate plates per pathogen/*Trichoderma* suspension combination, and the area occupied by each microorganism was measured using ImageJ software (Rueden *et al*., 2017), based on a reference distance common to all images. The percent of mycelium growth inhibition was calculated using the formula: Percent Growth Inhibition (PGI) = [(B – A) / B] × 100, where A is the area of pathogen mycelium growth coinoculated with *Trichoderma* and B is the area of the pathogen mycelium growth alone in the control plate (Úrbez-Torres *et al*., 2020).

Pruning wound protection trials

Two different pruning wound protection trials against selected trunk pathogens were established using 1-y-old almond plants 'Avijor' grafted onto GF-677 rootstock.

Pathogens inoculum preparation

Inoculum of *D. seriata* and *N. parvum* were prepared as conidial suspensions according to Elena and Luque (2016). A mycelial plug of each pathogen, previously grown on PDA for seven days at 25°C, was put on a center of a water agar plate (WA) (Bacto Agar; BD Biosciences, NJ). Several sterile fragments (approximately n = 20) of pine needles (three cm long) were put on the media surface at about 1.5 cm surrounding the mycelial plug. Plates were incubated for four weeks at 25°C under combined near-UV and white fluorescent light (Philips TL-D 18W BLB and Sylvania Standard F18W/33-640-TS cool white, respectively) at a photoperiod of 12 and 12 h, until pycnidia formation. One day before inoculation, pine needles (approximately n = 30) with pycnidia were placed in a 250 mL Erlenmeyer flask containing 50 mL of sterile distilled water. The solution was kept overnight (approximately 16 h) at 4°C to prevent conidia germination, and in constant agitation with the help of a magnetic stirrer to induce conidia release from the pycnidia. On the next day, the suspension was vacuum-filtered through a 60-µm Steriflip filter (Millipore Corporation, Billerica, MA) to get a cleaner suspension. The conidial suspension was adjusted to 2×10^4 conidia mL^{-1} using a hemocytometer. Inoculum of *E. lata* consisted of a suspension of mycelial fragments from liquid cultures, which was prepared as described by Travadon *et al*., (2013). To produce the starter culture, ten 2 × 2-mm plugs from a seven-day culture on PDA were inoculated into a 250 mL Erlenmeyer flask containing 100 mL of potato dextrose broth (PDB; Condalab, Spain) and incubated five days at 25°C and 150 rpm. A blender cup (Oster 4655ESP) was used to homogenize 40 mL of the PDB culture (one min, speed three), and two mL of this homogenized starter culture was then inoculated to a 125 mL Erlenmeyer flask containing 40 mL of PDB. After incubation five days at 25°C and 150 rpm, the entire 40 mL liquid culture was homogenized and the concentration of mycelial fragments, which were primarily <0.5 mm in length, was adjusted with SDW to 2×10^4 fragments mL^{-1} using a hemocytometer.

Trichoderma treatments preparation

A water suspension of formulated *T. asperellum* ICC012 + *T. gamsii* ICC080 (Blindar®; 3×10^7 CFU per gram of formulated product) at ten g L^{-1} was used. The viability of the conidia in the commercial product was checked to be at a minimum of 90% before each trial. For this purpose, a serial dilution of the conidia suspension was plated on PDA and the colony forming units were counted after 24–48 h incubation at room temperature.

First pruning wound protection trial

Main stems (0.5 cm diameter) of one-year-old potted almond plants 'Avijor' grafted onto GF-677 rootstock were pruned to 30 cm above the grafting point to simulate a fresh pruning wound. For each pathogen four dif-

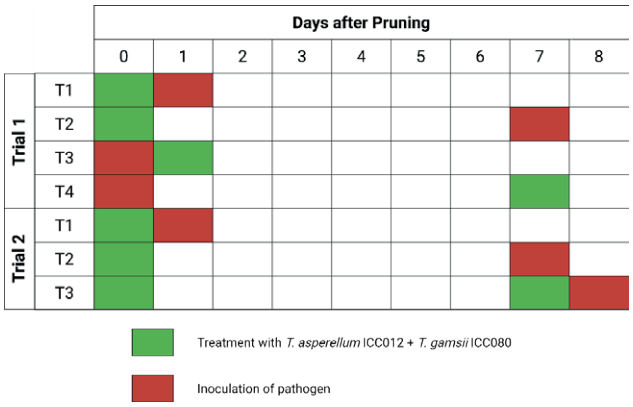

Figure 1. Schematic diagram illustrating the experimental design and treatment timing across the first and second pruning trials. In the first trial, for each pathogen (*Diplodia seriata*, *Eutypa lata* or *Neofusicoccum parvum*) four different treatments with *Trichoderma asperellum* ICC012 + *T. gamsii* ICC080 were evaluated: two pre-infection strategies (T1 and T2) and two post-infection strategies (T3 and T4). In the second trial, three pre-infection strategies with one (T1 and T2) or two (T3) *T. asperellum* ICC012 + *T. gamsii* ICC080 applications were evaluated.

ferent treatments with *T. asperellum* ICC012 + *T. gamsii* ICC080 were evaluated: two pre-infection strategies (T1-Plants treated immediately after pruning and inoculated 24 h after the treatment; and T2-Plants treated immediately after pruning and inoculated 7 d after the treatment) and two post-infection strategies (T3-Plants inoculated immediately after pruning and treated 24 h after infection; and T4-Plants inoculated immediately after pruning and treated seven days after infection) (Figure 1). Positive controls included non-treated but inoculated wounds with each pathogen at 24 h or seven days after pruning. Negative controls included pruned non-treated and non-inoculated plants to determine if natural infections occurred. *Trichoderma* treatments and the inoculation with each of the pathogens were performed by pipetting a drop of 20 µL onto the pruning wound, respectively. For each combination of treatment and pathogen, nine replicates (plants) were used. Plants were maintained in a temperature-controlled greenhouse and arranged in a completely randomized design. The experiment was repeated.

The plants were maintained in the greenhouse for two months. After this time, a three cm fragment of the main stem of each plant was cut below the wound and collected. In the laboratory, these three cm fragments were flame sterilized with 70% ethanol. Then, the bark around the fragments was removed. In each fragment, a tissue piece (≈ one mm) from the surface of the pruning wound was discarded, and five small pieces of necrotic tissue were plated onto one plate of two% malt extract agar (MEA) (Oxoid Ltd., Basingstoke, Hants, England) supplemented with 0.5 g L^{-1} of streptomycin sulphate (Sigma-Aldrich, St. Louis, MO, USA) (MEAS), in an attempt to recover the inoculated fungi and evaluate fungal colonization. Plates were incubated for up to 10 d at 25°C in the dark. If a piece of necrotic tissue yielded either *D. seriata*, *E. lata* or *N. parvum*, it was rated as colonized by the respective pathogen. From the data of these isolations, the mean percent recovery (MPR) (number of pieces colonized by each pathogen relative to the total number of pieces plated) was determined from all positive controls and treatments. Treatment effectiveness was calculated as the mean percent disease control (MPDC) using the formula: MPDC = 100 × [1 - (MPR treated plants / MPR non-treated control plants)] (Úrbez-Torres *et al*., 2020).

Second pruning wound protection trial

In this trial, inoculum preparation of the pathogens and *Trichoderma*, pathogens inoculation, and *Trichoderma* treatments were conducted as described previously.

Three pre-infection strategies with one or two *T. asperellum* ICC012 + *T. gamsii* ICC080 applications were studied: T1-Plants treated immediately after pruning and inoculated 24 h after treatment; T2-Plants treated immediately after pruning and inoculated seven days after treatment; and T3-Plants treated immediately after pruning and seven days later, and inoculated 24 h after the second treatment (Figure 1). Positive controls included non-treated but inoculated wounds with each pathogen at 24 h or seven days after pruning. Negative controls included non-treated and non-inoculated plants to determine if natural infections occurred. For each combination of treatment and pathogen, eight replicates (plants) were used. Plants were maintained in a temperature-controlled greenhouse for two months and arranged in a completely randomized design. The experiment was repeated. Fungal isolation, MPR and MPDC calculation were performed as described before.

Statistical analyses

For the dual culture antagonism assay the antagonistic activity of *Trichoderma* spp. against the fungal trunk pathogens was evaluated as the mean percent inhibition (MPI) of mycelial growth measured after seven days, calculated from the corresponding replicates (four per experiment and repetition). Regarding the pruning wounds protection experiments, the MPR by each pathogen was determined from all positive con-

trols and treatments calculated from the corresponding replicates (nine and eight plants per experiment in the first and second trials, respectively). Statistical analyses were conducted using R version 4.2.0 (R Core Team, 2024). For the experiment and treatment effect, values were analyzed using the Kruskal–Wallis multiple comparison test ($P < 0.05$). When differences were significant, Dunn's post hoc test was applied using the packages "agricolae" and "dunn.test" (De Mendiburu, 2023; Dinno, 2024).

RESULTS

Dual culture antagonism assay

The antagonistic activity of *T. asperellum* ICC012, *T. gamsii* ICC080, and a 50% mixture of both isolates was evaluated against three fungal trunk pathogens*: E. lata*, *D. seriata*, and *N. parvum*, as shown in Figure 2. The mean percent inhibition (MPI) of mycelial growth after seven days of incubation is presented in Figure 3.

The percentage of inhibition of mycelial growth of *D. seriata*, *E. lata* and *N. parvum* by *Trichoderma* strains used in this experiment ranged from 59.35% (*T. gamsii* ICC080 with *D. seriata*) to 80.89% (*T. asperellum* ICC012 + *T. gamsii* ICC080 with *N. parvum*).

For *E. lata*, the *T. asperellum* ICC012 strain resulted in an MPI of 80.57%, the *T. gamsii* ICC080 treatment in 61.06%, and the *T. asperellum* ICC012 + *T. gamsii* ICC080 mixture in 80%. The *T. asperellum* ICC012 alone and the *T. asperellum* ICC012 + *T. gamsii* ICC080 mixture significantly inhibited the growth of *E. lata* compared to *T. gamsii* ICC080 alone. In the case of *D. seriata*, the *T. asperellum* confrontation had an MPI of 73.85%, *T. gamsii* resulted in 59.35%, and the *T. asperellum* ICC012 + *T. gamsii* ICC080 mixture showed 65.48% inhibition. Again, *T. asperellum* ICC012 alone resulted in the highest inhibition, followed by the *T. asperellum* ICC012 + *T. gamsii* ICC080 mixture and *T. gamsii*

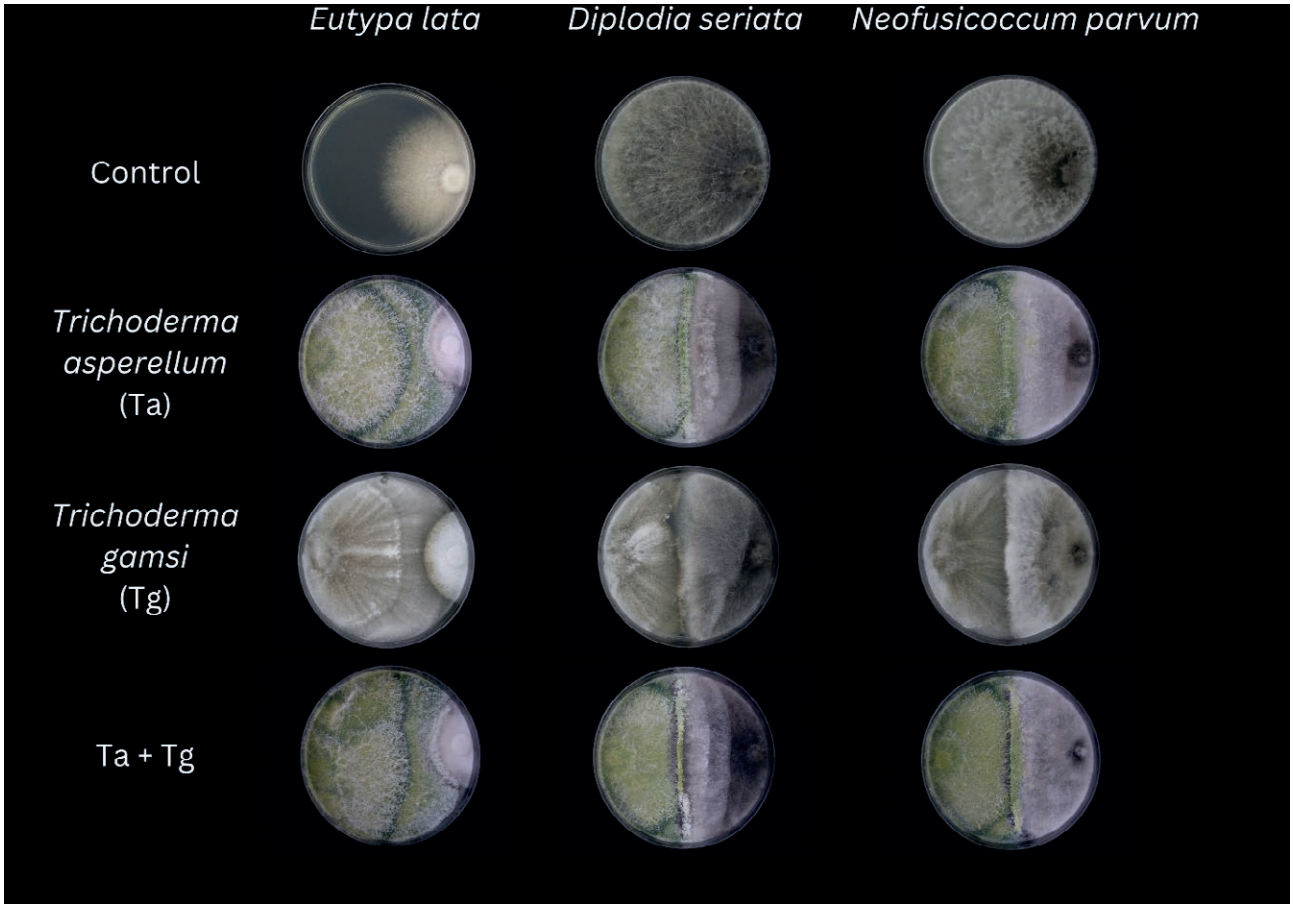

Figure 2. Dual culture antagonism experiment. Petri plates show antagonistic activity of each *Trichoderma* strain used in this study and the mixture of both strains (left side of the plate) against the fungal trunk pathogens: *Eutypa lata*, *Diplodia seriata*, and *Neofusicoccum parvum* (right side of Petri plate) seven days after incubation on PDA at 25°C.

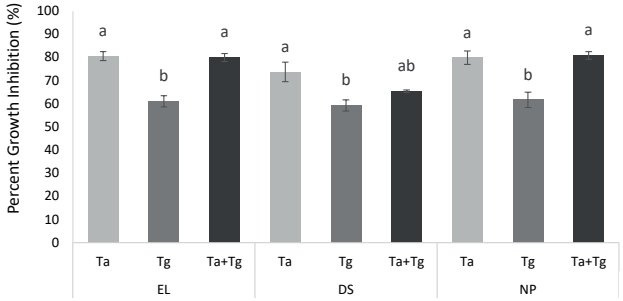

Figure 3. Antagonistic activity of *Trichoderma asperellum* isolate ICC012 (Ta), *T. gamsii* isolate ICC080 (Tg) and *T. asperellum* + *T. gamsii* 50% each isolate (Ta+Tg) against fungal trunk pathogens *Eutypa lata* (EL), *Diplodia seriata* (DS), and *Neofusicoccum parvum* (NP). Values represent the mean percent inhibition of mycelial growth measured after seven days calculated from eight replicates and bars represent standard errors of the means. For each pathogen, columns with the same letter were not statistically different according to Dunn's post hoc test ($P < 0.05$).

ICC080. For *N. parvum*, *T. asperellum* ICC012 showed an MPI of 79.96%, *T. gamsii* ICC080 had 61.77%, and the *T. asperellum* ICC012 + *T. gamsii* ICC080 mixture resulted in 80.89%. As occurred with *E. lata*, *T. asperellum* ICC012 and the *T. asperellum* ICC012 + *T. gamsii* ICC080 mixture exhibited significant inhibition compared to *T. gamsii* ICC080 alone.

Results analysis showed that the inhibition effects of *T. asperellum* ICC012 and *T. asperellum* ICC012 + *T. gamsii* ICC080 were not significantly different for any of the pathogens. For *E. lata* and *N. parvum* both *T. asperellum* ICC012 and *T. asperellum* ICC012 + *T. gamsii* ICC080 were significantly more effective for mycelial growth inhibition than *T. gamsii* ICC080 alone. But, for *D. seriata* there were statistically significant differences only between *T. asperellum* ICC012 and *T. gamsii* ICC080.

Pruning wound protection trials

First pruning wound protection trial

The efficacy of *T. asperellum* ICC012 + *T. gamsii* ICC080 was evaluated using four different treatment strategies: two pre-infection treatments and two post-infection treatments. Statistical analysis showed no significant differences between the two experimental replicates (*E. lata* $P = 0.727$; *D. seriata* $P = 0.262$; *N. parvum* $P = 0.056$), so data were pooled. The MPR and MPDC values are presented in Table 1. Fungal pathogens were not isolated from the non-inoculated negative controls.

For *E. lata*, the pre-infection treatment T1 presented a MPR of 16.6% and a MPDC of 79.9%. Pre-infection treatment T2 led to a MPR of 7.7% and a MPDC of 90.6%, while the post-infection treatments T3 and T4 exhibited MPR values of 38.8% and 54.4%, respectively, with corresponding MPDC values of 53.1% and 34.4%. For *D. seriata,* the treatment T1 had a MPR value of 37.7% and a MPDC of 57.5%, and treatment T2 had a MPR of 35.5% and a MPDC of 60.1%. Post-infection treatments T3 and T4 had MPR values of 75.5% and 66.6%, with MPDC values of 15.1% and 25.1%, respectively. For *N. parvum*, the pre-infection treatments T1 and T2 resulted in MPRs of 64.4% and 84.4%, with

Table 1. First trial. Mean percent recovery (MPR) and mean percent disease control (MPDC) of *Eutypa lata*, *Diplodia seriata* and *Neofusicoccum parvum* from pruning wounds treated with *Trichoderma asperellum* ICC012 + *T. gamsii* ICC080 in preventive (T1-Plants treated immediately after pruning and inoculated 24 h after the treatment; and T2-Plants treated immediately after pruning and inoculated seven days after the treatment) or curative strategies (T3-Plants inoculated immediately after pruning and treated 24 h after; and T4-Plants inoculated immediately after pruning and treated seven days after).

Treatment	Inoculation day	Value	*Eutypa lata*		*Diplodia seriata*		*Neofusicoccum parvum*	
Control			83.3±5.6	A	88.8±6.1	A	93.3±5.6	A
T1	1 after treatment	MPR	16.6±7.2	B	37.7±9.2	CD	64.4±9.9	B
		MPDC	79.9		57.5		30.7	
T2	7 after treatment	MPR	7.7±4.8	B	35.5±10.1	D	84.4±6.3	A
		MPDC	90.6		60.1		9.2	
T3	1 before treatment	MPR	38.8±10.9	A	75.5±9.9	B	91.1±5.9	A
		MPDC	53.1		15.1		2.03	
T4	7 before treatment	MPR	54.4±9.4	A	66.6±9.2	BC	90±6.9	A
		MPDC	34.4		25.1		3.2	

MPR, mean percent recovery.
MPDC, mean percent disease control was calculated as 100 x [1-(MPR treatment/MPR control)].
Values followed by the same letter(s) in each column were not statistically different using the Kruskal-Wallis multiple comparison test. When differences were significant, Dunn's post hoc test was applied.

Table 2. Second trial. Mean percent recovery (MPR) and mean percent disease control (MPDC) of *Eutypa lata*, *Diplodia seriata* and *Neofusicoccum parvum* from pruning wounds treated with *Trichoderma asperellum* ICC012 + *T. gamsii* ICC080 in three preventative strategies (T1-Plants treated immediately after pruning and inoculated 24 h after treatment; T2-Plants treated immediately after pruning and inoculated seven days after treatment; and T3-Plants treated immediately after pruning and seven days later, and inoculated 24 h after the second treatment).

Treatment	Inoculation day/ number of applications	Value	*Eutypa lata*		*Diplodia seriata*		*Neofusicoccum parvum*	
Control 1			73.3±12.3	A	53.3±18.4	A	66.6±16.05	A
T1	1 day/1	MPR	12.5±5.1	B	7.5±3.5	B	57.5±10.6	A
		MPDC	82.95		85.9		13.7	
Control 2			20±13.6	A	0	-	40±20	A
T2	7 days/1	MPR	0	B	1.2±1.2	-	13.7±5.9	AB
		MPDC	100		nc		65.6	
T3	7 days/2	MPR	1.2±1.2	B	0	-	5±5	B
		MPDC	93.7		nc		87.5	

MPR, mean percent recovery.
MPDC, mean percent disease control was calculated as 100 x [1-(MPR treatment/MPR control)].
Values followed by the same letter(s) in each column were not statistically different regarding its respective control using the Kruskal–Wallis multiple comparison test. When differences were significant, Dunn's post hoc test was applied.

MPDC values of 30.7% and 9.2%, respectively. The post-infection treatments T3 and T4 yielded MPR values of 91.1% and 90.0%, with MPDC values of 2.03% and 3.2%, respectively.

These results indicated that the application of *T. asperellum* ICC012 + *T. gamsii* ICC080 was most effective when applied in preventive strategies than curative strategies. This was very clear in the case of inoculation with *E. lata*, in which only preventive treatments T1 and T2 showed statistically significant differences with the untreated control ($P = 0.0002$). For *D. seriata* all treatments were significantly different from the untreated control ($P = 1.7\ 10^{-7}$), and for *N. parvum* only the preventive treatment T1 was significantly different from the untreated control ($P = 0.008$).

Second pruning wound protection trial

The pruning wound protection efficacy of *T. asperellum* ICC012 + *T. gamsii* ICC080 was further evaluated using only three pre-infection strategies with one or two applications of the product. Statistical analysis showed no significant differences between the two experimental replicates (*E. lata* $P = 0.896$; *D. seriata* $P = 0.223$; *N. parvum* $P = 0.226$), so data were pooled. The MPR and MPDC values are presented in Table 2. Fungal pathogens were not isolated from the non-inoculated negative controls.

For *E. lata*, the treatment T1 resulted in a MPR of 12.5% and an MPDC of 82.9%, treatment T2 had a MPR of 0% and a MPDC of 100%, while treatment T3 showed a MPR of 1.2% and a MPDC of 93.7%. For *D. seriata*, the treatment T1 resulted in a MPR of 7.5% and a MPDC of 85.9%, but this fungus could not be reisolated from the control plants infected seven days after pruning, thus invalidating the evaluation of the efficacy of the treatments T2 and T3, although their MPR values were very low (1.2% and 0%, respectively). For *N. parvum,* the treatment T1 resulted in a MPR of 57.5% and a MPDC of 13.7%, while treatments T2 and T3 had a MPR of 13.7% and a MPDC of 65.6%, and a MPR of 5% and a MPDC of 87.5%, respectively.

For *E. lata*, all preventive treatments with *T. asperellum* ICC012 + *T. gamsii* ICC080 were significantly different from their respective untreated controls ($P = 0.0007$ for T1 and $P = 0.031$ for T2 and T3). In *D. seriata* the treatment T1 was also significantly different from the untreated control ($P = 0.008$). But, for *N. parvum* only the treatment T3, with two applications of *T. asperellum* ICC012 + *T. gamsii* ICC080, was significantly different from its control ($P = 0.047$).

DISCUSSION

The dual culture and pruning wound assays collectively demonstrate that *T. asperellum* ICC012 + *T. gamsii* ICC080 can protect pruning wounds from infections caused by some of the major almond trunk pathogens in both *in vitro* and *in planta* experiments.

Our *in vitro* data showed *T. asperellum* is a potent antagonist against *D. seriata*, *E. lata*, and *N. parvum*. The combination of the strains *T. asperellum* ICC012

+ *T. gamsii* ICC080 showed inhibition levels statistically comparable to *T. asperellum* alone for all three pathogens, whereas *T. gamsii* alone was less effective. This is similar to the findings by Holland *et al*. (2021a), who observed that a mixed *T. harzianum* Rifai + *T. virens* (J.H. Mill., Giddens & A.A. Foster) Arx product (RootShield Plus®) was considerably less effective (only ~63% protection) than a single-strain *T. atroviride* treatment (93% protection) in almond trials. According to our results, the composition and compatibility of strains in a bioproduct are thus crucial for ensuring its effectiveness. In our case, combining *T. asperellum* ICC012 and *T. gamisii* ICC080 did not compromised antagonism performance relative to the one showing the best results alone, suggesting these two are complementary. Indeed, the species *T. asperellum* and *T. gamsii* have distinct but synergistic traits: *T. asperellum* produces a rich arsenal of antibiotics, competes aggressively for nutrients/space, and mycoparasitizes pathogens (Verma *et al*., 2007; Wu *et al*., 2017), while *T. gamsii* is noted for prolific volatile antifungal metabolites and an ability to tolerate cooler temperatures (Rinu *et al.,* 2014). By combining biological control agents, the product can exploit multiple modes of action and remain active under a wider range of environmental conditions. In fact, Di Marco *et al*. (2022) already showed that the *T. asperellum* ICC012 + *T. gamsii* ICC080 mixture was effective against diverse fungal grapevine trunk pathogens such as *Fomitiporia mediterranea* M. Fisch., *N. parvum* and *Phaeomoniella chlamydospora* (W. Gams, Crous, M.J. Wingf. & Mugnai) Crous & W. Gams.

In planta, preventive treatments of pruning wounds with the mixture of *T. asperellum* ICC012 + *T. gamsii* ICC080 provided substantial protection, whereas post-infection (curative) applications were far less effective. These results underscore that the *Trichoderma* biocontrol is most effective as a protectant applied to fresh wounds, and notably less so as a curative applied after pathogen infection has occurred (Guzmán-Guzmán *et al*., 2023).

Neofusicoccum parvum proved to be the most challenging pathogen as it is an aggressive, fast-colonizing fungus known to cause extensive almond dieback (Holland *et al.,* 2021b). Our curative treatments were not effective for *N. parvum* (recovery of the fungus from inoculated wounds remained high), and even a single pre-infection application sometimes showed suboptimal control. Recovery of *N. parvum* from inoculated wounds was significantly reduced only when two consecutive pre-infection applications were used, probably allowing *Trichoderma* strains to firmly establish in the wounded area. Travadon *et al*. (2023a) reported that wound protection against *N. parvum* significantly improved when the pathogen was inoculated seven days after *Trichoderma* application, instead of 24 hours. They attributed this result to *N. parvum* high virulence and rapid wood colonization, whereas *E. lata* (a less virulent and more slowly invading pathogen) infections could be reduced by *Trichoderma* even with a shorter establishment period. Consistently, in our study *E. lata* was effectively controlled by a single pre-infection treatment, highlighting that preventive wound colonization by *Trichoderma* can almost completely supress infections by this pathogen. However, when *E. lata* was allowed to infect wounds before treatment, *Trichoderma* was much less effective. On the other hand, *D. seriata* exhibited intermediate aggressiveness between *N. parvum* and *E. lata*. Its generally less aggressive behaviour when compared with *N. parvum* can made wounds easier to protect. Our results showed that even one preventive treatment of *T. asperellum* ICC012 + *T. gamsii* ICC080 provided effective control of *D. seriata*.

These patterns reinforce that the timing of BCAs application is critical, and that pathogen aggressiveness based on how fast it is able to colonize the wound niche influence how effective the BCA wound protectant effect will be. Holland *et al*. (2021a) reported that a single application of *T. atroviride* SC1 (a commercial strain in product Vintec®) achieved 81–100% protection of almond pruning wounds against various pathogens, like the results obtained with the best fungicide (thiophanate-methyl). Similarly, Travadon *et al*. (2023a) conducted almond field trials in California and demonstrated that *T. atroviride* SC1 and an experimental *T. paratroviride* strain could prevent *E. lata* and *N. parvum* infections as effectively as thiophanate-methyl, when applied after pruning. *Trichoderma* treatments provided optimal protection when wounds were treated immediately post-pruning, before rainfall, as it can contribute to spore dispersal (Úrbez-Torres *et al*., 2010; Fujiyoshi *et al*., 2021; Jiménez Luna *et al*., 2022; Travadon *et al.,* 2023a).

Finally, it is interesting to note that our results using *T. asperellum* ICC012 + *T. gamsii* ICC080 extend the successful use of *Trichoderma*-based biocontrol in Mediterranean conditions, because these strains (originally formulated as "Remedier®"/"Blindar®") had already been used in Europe for grapevine fungal trunk diseases management and are known to colonize woody tissues effectively (Di Marco *et al*., 2022).

In Spain, Olmo *et al*. (2017) demonstrated that pruning wound protection in almonds orchards could be achieved with chemical fungicides; thiophanate-methyl was shown to be the most effective fungicide reducing *Botryosphaeriaceae* infections and lesion lengths, and it

was recommended for inclusion in integrated pest management (IPM) strategies. The BCAs used in our experimental treatments provide an alternative to such chemicals. As regulatory trends in the Europe, EU is limiting fungicide use. Thus, many chemical pesticides (including thiophanate-methyl) have been phased out due to environmental and health concerns. Consequently, interest in BCAs for fungal trunk disease management has increased. In California, a range of BCAs has already been explored in addition to *Trichoderma*-based products. A *C. rosea* strain J1446 showed excellent wound protection on almond and cherry, even matching fungicide control for *E. lata* and *N. parvum* in those hosts (Travadon *et al.,* 2023b). Until recently, comparable biocontrol research in Mediterranean almonds was scarce. Romero-Cuadrado *et al*. (2024) reported one of the first such Spanish studies, focusing on bacterial antagonist *P. aeruginosa* strain (AC17), which suppressed *N. parvum*, *B. dothidea*, and *D. seriata* cankers on almond, with efficacy equivalent to *T. atroviride* and conventional fungicide treatments. Their work confirms that multiple biocontrol agents (fungal and bacterial) can deliver high levels of protection. Together, these findings show that biological wound protectants can effectively complement or replace chemical fungicides in almond trunk diseases management. An IPM approach to trunk diseases should combine cultural measures (sanitation, optimal pruning timing) with wound protection using fungicides or BCAs across the nursery and orchard stages (Guarnaccia *et al*., 2022). Our findings strongly support this approach, offering a practical biological tool for the wound protection component.

In conclusion, *T. asperellum* ICC012 + *T. gamsii* ICC080, especially when applied as a preventive biocontrol treatment (e.g. at pruning), showed high efficacy in protecting almond pruning wounds from infection by *D. seriata*, *E. lata*, and *N. parvum*. This efficacy is comparable to that reported for other successful BCAs and fungicides in California and Spain. The success of *T. asperellum* ICC012 + *T. gamsii* ICC080 in our study contributes to the progressive adoption of BCAs for the management of fruit and nut crops diseases.

ACKNOWLEDGEMENTS

Funded by the European Union. Views and opinions expressed are however those of the author(s) only and do not necessarily reflect those of the European Union or the European Education and Culture Executive Agency (EACEA). Neither the European Union nor EACEA can be held responsible for them.

LITERATURE CITED

De Mendiburu F., 2023. *Agricolae: Statistical Procedures for Agricultural Research*, R package version 1.3-7. R Core Team, Vienna, Austria. https://doi.org/10.32614/CRAN.package.agricolae

Di Marco S., Metruccio E.G., Moretti S., Nocentini M., Carella G., ..., Mugnai L., 2022. Activity of *Trichoderma asperellum* strain ICC 012 and *Trichoderma gamsii* strain ICC 080 toward diseases of Esca complex and associated pathogens. *Frontiers in Microbiology* 12: 813410. https://doi.org/10.3389/fmicb.2021.813410

Dinno A., 2024. *dunn.test: Dunn's Test of Multiple Comparisons Using Rank Sums*, R package version 1.3.6. https://doi.org/10.32614/CRAN.package.dunn.test

Elena G., Luque J., 2016. Seasonal susceptibility of grapevine pruning wounds and cane colonization in Catalonia, Spain following artificial infection with *Diplodia seriata* and *Phaeomoniella chlamydospora*. *Plant Disease* 100(8): 1651–1659. https://doi.org/10.1094/PDIS-10-15-1186-RE

FAO, 2024. Food and Agriculture Organization of the United Nations, Statistical Databases. Available at: http://www.fao.org. Accessed March 19, 2024.

Fujiyoshi P.T., Lawrence D.P., Travadon R., Cooper M., Verdegaal P., Schwebs S., Baumgartner K., 2021. Detection of spores of causal fungi of dieback-type trunk diseases in young, asymptomatic vineyards and mature, symptomatic vineyards. *Crop Protection* 150: 105798. https://doi.org/10.1016/j.cropro.2021.105798

Goura K., Lahlali R., Bouchane O., Baala M., Radouane N., ...Tahiri A., 2023. Identification and characterization of fungal pathogens causing trunk and branch cankers of almond trees in Morocco. *Agronomy* 13(1): 130. https://doi.org/10.3390/agronomy13010130

Gradziel T.M., 2017. History of cultivation. In: *Almonds: Botany, Production and Uses*, CABI, Wallingford, United Kingdom, 43–69. https://doi.org/10.1079/9781780643540.0043

Gramaje D., Agustí-Brisach C., Pérez-Sierra A., Moralejo E., Olmo D., ... Armengol J., 2012. Fungal trunk pathogens associated with wood decay of almond trees on Mallorca (Spain). *Persoonia: Molecular Phylogeny and Evolution of Fungi* 28: 1–13. https://doi.org/10.3767/003158512X626155

Guarnaccia V., Kraus C., Markakis E., Alves A., Armengol J., … Gramaje D., 2022. Fungal trunk diseases of fruit trees in Europe: pathogens, spread and future directions. *Phytopathologia Mediterranea* 61(3): 563–599. https://doi.org/10.36253/phyto-14167

Guzmán-Guzmán P., Kumar A., de Los Santos-Villalobos S., Parra-Cota F.I., Orozco-Mosqueda M.D.C., … Santoyo, G., 2023. *Trichoderma* species: Our best fungal allies in the biocontrol of plant diseases—A review. *Plants* 12(3), 432. https://doi.org/10.3390/plants12030432

Holland L.A., Travadon R., Lawrence D.P., Nouri M.T., Trouillas F., 2021a. Evaluation of pruning wound protection products for the management of almond canker diseases in California. *Plant Disease* 105(11): 3368–3375. https://doi.org/10.1094/PDIS-11-20-2371-RE

Holland L.A., Trouillas F.P., Nouri M.T., Lawrence D.P., Crespo M., … Fichtner E.J., 2021b. Fungal pathogens associated with canker diseases of almond in California. *Plant Disease* 105(2): 346–360. https://doi.org/10.1094/PDIS-10-19-2128-RE

Inderbitzin P., Bostock R.M., Trouillas F.P., Michailides T.J., 2010. A six locus phylogeny reveals high species diversity in Botryosphaeriaceae from California almond. *Mycologia* 102(6): 1350–1368. https://doi.org/10.3852/10-006

Jiménez Luna I., Doll D., Ashworth V.E.T.M., Trouillas F.P., Rolshausen P.E., 2022. Comparative profiling of wood canker pathogens from spore traps and symptomatic plant samples within California almond and walnut orchards. *Plant Disease* 106(8): 2182–2190. https://doi.org/10.1094/PDIS-05-21-1057-RE

Lahlali R., Ezrari S., Radouane N., Kenfaoui J., Esmaeel Q., … Barka, E. A., 2022. Biological control of plant pathogens: A global perspective. *Microorganisms* 10(3): 596. https://doi.org/10.3390/microorganisms10030596

Lawrence D.P., Holland L.A., Nouri M.T., Travadon R., Abramians A., Michailides T.J., Trouillas F.P., 2018. Molecular phylogeny of *Cytospora* species associated with canker diseases of fruit and nut crops in California, with the descriptions of ten new species and one new combination. *IMA Fungus* 9(2): 333–369. https://doi.org/10.5598/imafungus.2018.09.02.07

León M., Berbegal M., Rodríguez-Reina J.M., Elena G., Abad-Campos P., …Armengol J., 2020. Identification and characterization of *Diaporthe* spp. associated with twig cankers and shoot blight of almonds in Spain. *Agronomy* 10(8): 1062. https://doi.org/10.3390/agronomy10081062

Luque-Cruz C., Capote N., Marco-Noales E., Palomares-Rius J. E., Romero-Cuadrado L., Morán, F., … Agustí-Brisach, C., 2026. Insights Into the Aetiology of Almond Canker Diseases and Decline Syndromes: An Emerging and Complex Phytopathological Challenge. *Plant Pathology* 75: e70126. https://doi.org/10.1111/ppa.70126

Markakis E.A., Kavroulakis N., Ntougias S., Koubouris G.C., Sergentani C.K., Ligoxigakis E.K., 2017. Characterization of fungi associated with wood decay of tree species and grapevine in Greece. *Plant Disease* 101(11): 1929–1940. https://doi.org/10.1094/PDIS-12-16-1761-RE

Martino I., Spadaro D., Guarnaccia V., 2025. Fungal trunk pathogens of fruit and nut tree crops: identification, characterization, detection, and perspectives for a critical global issue. *Plant Disease* 109(6): 1192–1210. https://doi.org/10.1094/PDIS-10-24-2069-FE

Nouri M.T., Lawrence D.P., Yaghmour M.A., Michailides T.J., Trouillas F.P., 2018. *Neoscytalidium dimidiatum* causing canker, shoot blight and fruit rot of almond in California. *Plant Disease* 102(8): 1638–1647. https://doi.org/10.1094/PDIS-12-17-1967-RE

Olmo D., Armengol J., León M., Gramaje D., 2016. Characterization and pathogenicity of Botryosphaeriaceae species isolated from almond trees on the island of Mallorca (Spain). *Plant Disease* 100(12): 2483–2491. https://doi.org/10.1094/PDIS-05-16-0676-RE

Olmo D., Gramaje D., Armengol J., 2017. Evaluation of fungicides to protect pruning wounds from Botryosphaeriaceae species infections on almond trees. *Phytopathologia Mediterranea* 56: 118–129. https://doi.org/10.14601/Phytopathol_Mediterr-19428

R Core Team, 2024. R: *A Language and Environment for Statistical Computing*. R Foundation for Statistical Computing, Vienna, Austria. https://www.R-project.org/

Rinu K., Sati P., Pandey A., 2014. *Trichoderma gamsii* (NFCCI 2177): a newly isolated endophytic, psychrotolerant, plant growth promoting, and antagonistic fungal strain. *Journal of Basic Microbiology* 54(5): 408–417. https://doi.org/10.1002/jobm.201200579

Romero-Cuadrado L., Picos M.C., Camacho M., Ollero F.J., Capote N., 2024. Biocontrol of almond canker diseases caused by Botryosphaeriaceae fungi. *Pest Management Science* 80(4): 1839–1848. https://doi.org/10.1002/ps.7919

Rueden C.T., Schindelin J., Hiner M.C., DeZonia B.E., Walter A.E., Arena E.T., Eliceiri K.W., 2017. ImageJ2: ImageJ for the next generation of scientific image data. *BMC Bioinformatics* 18(1): 529. https://doi.org/10.1186/s12859-017-1934-z

Slippers B., Smit W.A., Crous P.W., Coutinho T.A., Wingfield B.D., Wingfield M.J., 2007. Taxonomy, phylogeny and identification of Botryosphaeriaceae associated with pome and stone fruit trees in South Africa and other regions of the world. *Plant Pathology* 56(1): 128–139. https://doi.org/10.1111/j.1365-3059.2006.01486.x

Travadon R., Lawrence D.P., Li S., Trouillas F.P., 2023a. Evaluation of biological control agents for the protection of almond pruning wounds against infection by fungal canker pathogens. *Phytopathology* 113(8): 1417–1427. https://doi.org/10.1094/PHYTO-02-23-0075-R

Travadon R., Lawrence D.P., Li S., Trouillas F.P., 2023b. Field evaluation of biological wound treatments for the management of almond, cherry, and grapevine fungal canker diseases. *Biological Control* 185: 105292. https://doi.org/10.1016/j.biocontrol.2023.105292

Travadon R., Rolshausen P.E., Gubler W.D., Cadle-Davidson L., Baumgartner K., 2013. Susceptibility of cultivated and wild *Vitis* spp. to wood infection by fungal trunk pathogens. *Plant Disease* 97(12): 1529–1536. https://doi.org/10.1094/PDIS-05-13-0525-RE

Úrbez-Torres J.R., Battany M., Bettiga L.J., Gispert C., McGourty G., Roncoroni J., Smith R.J., Verdegaal P., Gubler W.D., 2010. Botryosphaeriaceae species spore-trapping studies in California vineyards. *Plant Disease* 94(6): 717–724. https://doi.org/10.1094/PDIS-94-6-0717

Úrbez-Torres J.R., Tomaselli E., Pollard-Flamand J., Boule J., Gerin D., Pollastro S., 2020. Characterization of *Trichoderma* isolates from southern Italy, and their potential biocontrol activity against grapevine trunk disease fungi. *Phytopathologia Mediterranea* 59(3): 425–440. https://doi.org/10.14601/Phyto-11273

Verma M., Brar S.K., Tyagi R.D., Surampalli R.Y., Valéro J.R., 2007. Antagonistic fungi, *Trichoderma* spp.: Panoply of biological control. *Biochemical Engineering Journal* 37(1): 1–20. https://doi.org/10.1016/j.bej.2007.05.012

Wu Q., Sun R., Ni M., Yu J., Li Y., Yu C., Dou K., Ren J., Chen J., 2017. Identification of a novel fungus, *Trichoderma asperellum* GDFS1009, and comprehensive evaluation of its biocontrol efficacy. *PLOS ONE* 12: 1–20. https://doi.org/10.1371/journal.pone.0179957

Phytopathologia Mediterranea
The international journal of the
Mediterranean Phytopathological Union

Firenze University Press
www.fupress.com/pm

Research Papers

Phylogenetic diversity and pathogenicity of *Colletotrichum* species associated with avocado anthracnose in Chile

Marcelo I. BUSTAMANTE[1,2,*], Ysadora FERNÁNDEZ[1], Claudio OSORIO-NAVARRO[1,3], Cristóbal CÁRDENAS[1], Tyler B. BOURRET[4], Akif ESKALEN[2], José Luis HENRÍQUEZ-SÁEZ[1]

[1] *Departamento de Sanidad Vegetal, Facultad de Ciencias Agronómicas, Universidad de Chile, La Pintana, 8820808, Santiago, Chile*
[2] *Department of Plant Pathology, University of California, Davis, CA 95616, USA*
[3] *Plant Molecular Biology Centre, Department of Biology, Faculty of Sciences, University of Chile, Ñuñoa, 7800003, Santiago, Chile*
[4] *Mycology and Nematology Genetic Diversity and Biology Laboratory, Agricultural Research Service, United States Department of Agriculture, Beltsville, MD 20705, USA*
* Corresponding author. E-mail: mibustamante@ucdavis.edu

Summary. Anthracnose, caused by *Colletotrichum* species, is a major disease of avocado (*Persea americana*) that significantly reduces fruit quality and export potential in Chile. *Colletotrichum* species associated with this disease were identified and their pathogenicity to avocado was assessed. In the summer of 2018, healthy fruits (n = 1,335) were sampled from three commercial groves located in the Metropolitan, O'Higgins and Valparaíso regions of Chile, and from a non-commercial grove and local markets. Fruits were stored until symptoms developed, indicating anthracnose incidence in commercial groves ranging from 10 to 50%. A total of 146 fungal isolates were obtained from symptomatic fruit and were initially identified as *Colletotrichum* spp. Fifty representative isolates were further identified through multilocus phylogenetic analyses. Ten species belonging to four species complexes were identified. *Colletotrichum* cf. *cigarro* was the most frequent taxon (n = 17), followed by *C. pyricola* (n = 9), *C. gloeosporioides* (n = 6), *C. jiangxiense* (n = 5), *C. karsti* (n = 4), *C. anthrisci* (n = 3), *C. brassicicola* (n = 3), *C. laurosilvaticum* (n = 1), *C. fructicola* (n = 1), and *C. perseae* (n = 1). Pathogenicity tests reproduced anthracnose symptoms in inoculated fruits, whereas control fruits remained symptomless, and revealed differences in virulence among isolates and species. This study provides the first report of *C. brassicicola, C. laurosilvaticum* and *C. pyricola* as causal agents of avocado anthracnose, highlights the diversity of *Colletotrichum* species in Chilean avocado groves, and provides insights for improved management strategies for avocado anthracnose.

Keywords. Etiology, *Persea americana*, postharvest disease.

OPEN ACCESS

Citation: Bustamante, M. I., Fernández, Y., Osorio-Navarro, C., Cárdenas, C., Bourret, T. B., Eskalen, A., & Henríquez-Sáez, J. L. (2026). Phylogenetic diversity and pathogenicity of *Colletotrichum* species associated with avocado anthracnose in Chile. *Phytopathologia Mediterranea* 65(1): 15-31. doi: 10.36253/phyto-16790

Accepted: November 23, 2025

Published: March 16, 2026

©2026 Author(s). This is an open access, peer-reviewed article published by Firenze University Press (https://www.fupress.com) and distributed, except where otherwise noted, under the terms of the CC BY 4.0 License for content and CC0 1.0 Universal for metadata.

Data Availability Statement: All relevant data are within the paper and its Supporting Information files.

Competing Interests: The Author(s) declare(s) no conflict of interest.

Editor: Vladimiro Guarnaccia, DiSAFA - University of Torino, Italy.

ORCID:
MIB: 0000-0001-7887-7230
YF: 0009-0002-5683-4955
CON: 0000-0002-0589-3392
TBB: 0000-0003-2223-0440
AE: 0000-0002-8829-7413
JLHS: 0000-0003-4979-6962

INTRODUCTION

Avocado (*Persea americana* Mill.) is an economically important fruit crop in Chile, with approx. 33,000 ha cultivated mainly between the Coquimbo and O'Higgins regions (latitudes 29°30' to 35°45' S) (ODEPA-CIREN, 2024). The cultivar Hass dominates production and fruit of which are the only ones exported. During the 2024-2025 season, Chile produced approximately 240,000 tons of avocados, exporting 139,091 tons primarily to Europe (76.9%), Latin America (17.1%), Asia (3.5%), and North America (2.4%) (Comité de Paltas de Chile, 2025; FAOSTAT 2025). Avocado fruit is susceptible to anthracnose, a major postharvest disease caused by species of *Colletotrichum* (Dann *et al.,* 2013). Infections occur in the field, where these pathogens penetrate young fruit and remain latent until ripening after harvest (Prusky and Plumbley, 1992). Because of long distances to export markets, fruit is stored at low temperatures (4–5°C) for 17 to 45 d (Ferreyra and Defilippi, 2012). This period allows for fruit ripening and activation of latent pathogen infections, often resulting in anthracnose development and significant postharvest losses (Ramírez-Gil *et al.,* 2020).

During the last two decades, incidence of anthracnose in avocados has increased in Chile, particularly in high-density groves located in humid areas. The disease is most severe in coastal areas, where high relative humidity and prolonged dew periods favour infections. Symptoms first appear as small circular lesions on fruit skins that enlarge rapidly, becoming dark and sunken. Soon after, the pathogens produce acervuli that rupture fruit epidermis and sporulate, forming orange to pink, waxy masses of conidia (Nelson, 2008). As the disease progresses, the fruit pulp beneath the lesions begins to rot and separates easily from the skin, leaving characteristic cavities when skin is removed. In the field, damaged infected fruit may ripen prematurely, leading to pre-harvest fruit drop. Infected avocado leaves and twigs often remain attached to the trees, serving as inoculum sources for subsequent infection cycles (Fitzell, 1987).

Avocado anthracnose is caused by fungi of the genus *Colletotrichum*, with approx. 26 species reported. Most species associated with this disease belong to the *Colletotrichum gloeosporioides* species complex (CGSC), followed by the *C. acutatum* species complex (CASC), and the *C. boninense* species complex (CBSC). Comprehensive studies investigating species associated with avocado anthracnose have been conducted in several major avocado producing countries, including Mexico (Fuentes-Aragón *et al*., 2020), Colombia (Gañán *et al*., 2015), Kenya (Kimaru *et al*., 2018), Brazil (Soares *et al*., 2020), Chile (Bustamante *et al*., 2022), Israel (Sharma *et al*., 2017), and Vietnam (Thanh *et al*., 2025). In other important avocado-producing countries such as Indonesia, the Dominican Republic, and Peru, only *C. gloeosporioides sensu lato* has been documented (Zakaria, 2021). Additional reports of this disease from regions with low avocado production volumes include China (Li *et al*., 2022), the United States of America (Nelson, 2008, Faber *et al*., 2016), Australia (Shivas and Tan, 2009; Giblin *et al*., 2018), South Africa (Weir *et al*., 2012), New Zealand (Weir *et al*., 2012; Hofer *et al*., 2021), Türkiye (Akgül *et al*., 2016), Greece (Malandrakis *et al*., 2023), Sri Lanka (Dissanayake *et al*., 2021), and Ghana (Honger *et al*., 2016). Studies from countries with emerging avocado industries include Taiwan (Wu *et al*., 2023), Thailand (Armand and Jayawardena, 2024), and Italy (Guarnaccia *et al*., 2016). Species belonging to the *C. gigasporum* species complex have been reported in Sri Lanka, *C. magnum* species complex in Mexico, and *C. dematium* species complex (CDSC) in Chile. These represent infrequent detections compared with dominant species complexes associated with avocado anthracnose (Hunupolagama *et al*., 2015; Fuentes-Aragón *et al*., 2020; Bustamante *et al*., 2022).

In Chile, only *C. gloeosporioides sensu lato* and *C. anthrisci* have been formally documented as causal agents of avocado anthracnose (Morales *et al*., 1979; Bustamante *et al*., 2022). Research in other avocado-growing regions has shown that diversity and prevalence of *Colletotrichum* species vary considerably, depending on geographical location and environmental conditions. Accurate identification of *Colletotrichum* species is a critical prerequisite for the development of effective disease management strategies (Downling *et al*., 2020; Camiletti *et al*., 2022). Therefore, a clear understanding of the species composition and pathogenic potential of *Colletotrichum* associated with avocado anthracnose in Chile is required to support the implementation of integrated disease management programs. To address this gap, the present study aimed to isolate, identify, and assess the pathogenicity of *Colletotrichum* species associated with anthracnose symptoms on avocado fruits in Chile.

MATERIALS AND METHODS

Fruit sampling and incubation

During the 2018 growing season, a total of 1,335 apparently healthy avocado fruits (cv. Hass) were collected from three commercial groves, a non-commercial grove, and from local markets. The commercial groves were located in the Metropolitan (33°43'60"S), O'Higgins

(34°23'46"S), and Valparaíso (33°38'00"S) regions of Chile. The non-commercial grove was located approx. 10 km southeast of the commercial grove, near Naltahua in the Metropolitan region. Fruits were randomly collected from harvest bins, trees, and grove floors. Locally grown fruit from domestic markets within the Metropolitan region were also randomly sampled. In the laboratory, collected fruits were incubated in cardboard packaging at room temperature (20–25°C) under a 12 h photoperiod with fluorescent light and maintained at 40 to 50% humidity for 14 d until anthracnose symptoms developed.

Fungal isolations

Symptomatic fruits were inspected for anthracnose by observing acervuli formation and fruit rot underneath sunken lesions. Fruits were surface-disinfected by spraying with 70% ethanol, and isolations were carried out individually from one sporulating lesion per fruit, following methods of Hu *et al*. (2015). Symptomatic tissue pieces (each approx. 2 × 2 mm) beneath lesions were excised and plated onto potato dextrose agar (PDA) amended with streptomycin (100 mg L^{-1}). Pure cultures were established using single-conidium and hyphal tip isolation methods (Senanayake *et al*., 2020), and each isolate was obtained from a different symptomatic fruit. Preliminary identifications of isolated fungi were based on observation of acervuli, setae, and conidia using a microscope (Axiostar Plus, Carl Zeiss) at 100× and 400× magnifications. For isolates that did not sporulate on PDA, casitone-yeast extract agar (CYA: 1.7 g L^{-1} of casitone, 0.35 g L^{-1} of yeast extract, 2.0 g L^{-1} of glucose, 5.0 g L^{-1} of agar) was used to induce acervulus formation. Subsequently, isolates were cultured on PDA for colony observations, and representative isolates from each location were selected for phylogenetic analyses.

DNA extraction, amplification, and sequencing of representative isolates

Selected isolates (n = 50) were each cultured on PDA for 7 d, and DNA was extracted using the Fungi/Yeast Genomic DNA isolation kit (Norgen Biotek Corp.). The rDNA internal transcribed spacer (ITS), along with fragments of the glyceraldehyde-3-phosphate dehydrogenase (*gapdh*) and beta-tubulin (*tub2*) genes, were amplified by PCR for all the selected isolates using the primer pairs ITS1/ITS4 for ITS (White *et al*., 1990), GDF1/GDR1 for *gapdh* (Guerber *et al*., 2003), and T1/Bt2b for *tub2* (Glass and Donaldson, 1995; O'Donnell and Cigelnik, 1997). Additionally, for isolates within the *C. gloeosporioides* species complex (CGSC), the glutamine synthetase (*gs*) gene was amplified using GSF1/GSR1 (Guerber *et al*., 2003), and the intergenic region between the DNA lyase (*Apn2*) and the mating type *MAT1-2* genes (referred to as ApMat) was amplified using AMF1/AMR1 (Silva *et al*., 2012b). For isolates within the *C. dematium* species complex (CDSC), the actin (*act*) gene was amplified using ACT-512F/ACT-783R, and the chitin synthase (*chs1*) gene was amplified using CHS-79F/CHS-354R (Carbone and Kohn, 1999). PCRs were each carried out in a final volume of 25 µL, containing 1× GoTaq® Green Master Mix (Promega), 200 nM of each primer, 50 to 100 ng of genomic DNA, and Nanopure water to complete the volume. The thermocycling conditions were: an initial denaturation at 94°C for 5 min, followed by 30 cycles each of 30 s at 94°C, 45 s at 48°C for ITS, or 52°C for *gapdh, tub2*, *gs* and ApMat, or 61°C for *act*, or 58°C for *chs1*, and 40 s at 72°C, then with final extension of 7 min at 72°C. PCR products were sequenced by Psomagen USA (Rockville, MD, USA), and consensus sequences were obtained by assembling forward and reverse sequences using CAP3 (Huang and Madan, 1999).

Phylogenetic analyses

Four data sets, consisting of sequences of different DNA markers (ITS, *gapdh*, *tub2*, *gs*, ApMat, *act*, and *chs1*) of *Colletotrichum* species, were constructed by combining reference sequences from the NCBI database with the sequences obtained from the Chilean isolates (Supplementary Tables S1 to S4). Sequences were aligned by locus using MAFFT 7 selecting the L-INS-i refinement method (Katoh *et al*., 2019), and were trimmed manually on BioEdit 7 (Hall, 1999). Each locus of the concatenated data sets was partitioned by coding and non-coding regions (but not by codon position), resulting in 20 partitioned subsets. Maximum likelihood (ML) reconstructions were carried out in IQ-TREE 2 (Minh *et al*., 2020), with the following options: linked branch lengths for partitioned analysis, 'greedy' algorithm for merging partitions, 'merge-model all' and 'merge-rate all', to employ the widest range of evolutionary models, corrected Akaike information criterion for model testing, 'allnni' for a more thorough tree search, and the ultrafast approximation of 1,000 bootstrap replicates for support values. Each species complex was analyzed separately using concatenated data sets of ITS-*gapdh*-*tub2*. When resolution was insufficient, the markers ApMat, *gs*, *act* and *chs1* were incorporated individually or in combination, to improve phylogenetic informativeness of the dataset. Bayesian inference (BI) was assessed using MrBayes 3.2.7 (Ronquist *et al*., 2012), following the methodology of Bourret

et al., (2018). Resulting ML and BI trees were examined, and support values were combined in TreeGraph2 (Stöver and Müller, 2010). Visual edits were carried out using Inkscape 0.92 (http://inkscape.org). Final sequences were submitted to GenBank following analyses.

Conidium characterization

Representative isolates of each *Colletotrichum* species were cultured on CYA plates at 22°C for 7 to 14 d until acervuli formed. For each isolate, 30 conidia were measured for length and width using a light microscope (Axiostar Plus, Carl Zeiss) at 400× magnification. Conidium dimensions were recorded as minimum, mean ± standard deviation, and maximum for lengths and widths, and length-to-width ratios were calculated from mean values. Conidium dimensions were compared to published data of reference strains of each species (Damm *et al*., 2009; 2012a; 2012b; Liu *et al*., 2015; Prihastuti *et al*., 2009; Ramos *et al*., 2016; Sharma *et al*., 2017).

Pathogenicity tests

One or two isolates per species were selected (n = 17) to conduct assessments of Koch's postulates on healthy 'Hass' avocado fruits. Three fruits per isolate were inoculated, and each fruit received two inoculations. The isolates were cultured on CYA plates for 14 d at 22°C to induce acervulus formation. Conidia were washed from sporulating acervuli using sterile distilled water, and conidium suspensions were diluted up to 10^6 conidia mL^{-1} by counting with hemocytometer. Fruits were each disinfected with 0.5% sodium hypochlorite for 3 min and then rinsed with sterile distilled water. The fruits were each then wounded at two points using a sterile needle (0.5 mm diameter) to 1 mm of depth. Inoculations each consisted of pipetting 20 µL of the conidium suspension onto each wound, while inoculation control fruits received sterile water. Fruits were then incubated at 22°C for 7 d in humid chambers (>80% RH), which were polystyrene containers containing moistened paper towels. Evaluations were carried out by removing the skin from each fruit and measuring diameters of necrotic lesions, with each lesion measured in two perpendicularly opposite directions using a caliper. Re-isolations were carried out by culturing pulp pieces (each approx. 16 mm^2) from lesions margins on PDA for 7 d at 22°C. Resulting fungal colonies were identified morphologically. Data of lesion diameters were subjected to analysis of variance (ANOVA) using generalized linear models with the corresponding R packages in InfoStat v2008 (Grupo InfoStat, FCA), and means were separated using Fisher's least significant difference (LSD) test (α = 0.05). The pathogenicity assessment was carried out twice, and data were combined for treatments that were not significantly different ($P > 0.05$) for the two experiments.

RESULTS

Symptoms on sampled fruit

Black, circular lesions developed on the fruit skins after ripening, with one to several lesions per fruit. Lesions appeared within 7 to 14 d after harvest, as fruits ripened under incubation at room temperature (20 to 25°C, 40–50% relative humidity). Over time, lesions expanded progressively, and waxy conidium masses developed in the lesion centres. Conidium masses varied in colour, from orange to pink (Figure 1 A), and less frequently, from white to grey (Figure 1 B). As the disease progressed, adjacent lesions coalesced and became sunken (Figure 1 C). Internally, the pulp beneath each lesions was dark brown, forming a rounded pattern toward the fruit centre. When symptomatic fruits were bisected, the necrotic pulp detached easily from the surrounding healthy tissues, leaving characteristic cavities (Figure 1 D).

Fungal isolations

Isolations from individual fruits yielded 146 fungal isolates: 48 were from a commercial grove in the Metropolitan region, 40 were from Valparaíso, 18 were from O'Higgins, 27 were from a non-commercial grove in the Metropolitan region, and 13 were from locally grown fruit purchased in markets. All isolates were morphologically consistent with *Colletotrichum* spp., showing diagnostic structures including acervuli, setae, and conidia on PDA and CYA cultures (Barnett and Hunter 1998). Colony morphology on PDA at 22°C had overlap among isolates, so was not used for species identifications. Representative isolates from each location were selected for multilocus phylogenetic analyses for species identification.

Phylogenetic analyses

The consensus sequence lengths ranged from 535 to 577 bp for ITS, 254 to 278 bp for *gapdh*, 724 to 751 bp for *tub2*, 922 to 997 bp for *gs*, 906 to 961 bp for ApMat, 252 to 254 bp for *act*, and 288 to 301 bp for *chs1*. BLAST searches confirmed that the 50 analyzed isolates belonged to *Colletotrichum*. Phylogenetic reconstruc-

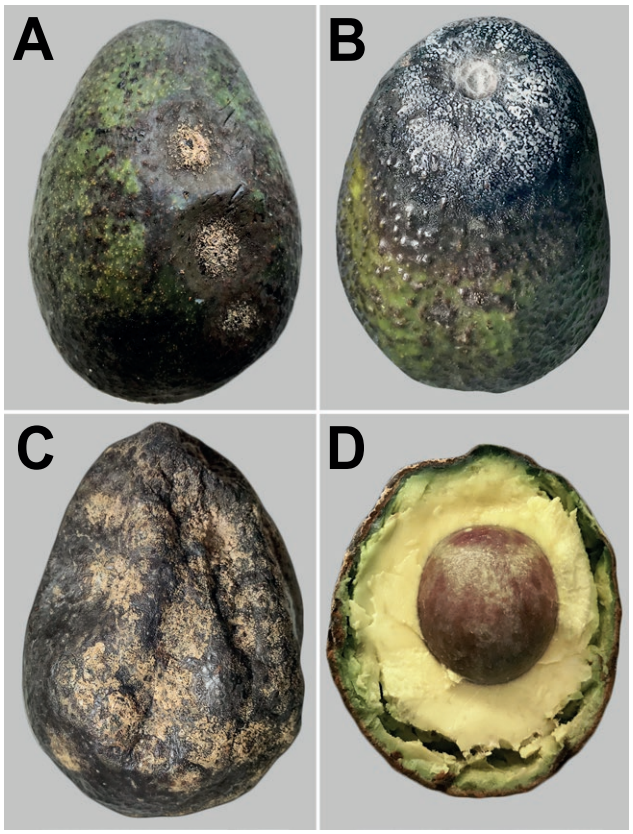

Figure 1. Symptoms of anthracnose on 'Hass' avocado fruits during postharvest. A, Lesions on fruit skin with orange to pink sporulation. B, Lesion on the stem end skin of a fruit showing the least frequent white to grey sporulation. C, Advanced symptoms showing coalescing, sunken lesions. D, Characteristic cavity formed between healthy and colonized pulp after cutting open an anthracnose symptomatic fruit.

tions using maximum likelihood (ML) and Bayesian posterior probability (PP) methods showed that the isolates clustered with reference strains of ten species across four species complexes (Figures 2 to 5). A predominance of members of the *C. gloeosporioides* species complex (CGSC; *n* = 30 isolates) was detected, followed by the species complexes *C. acutatum* (CASC; *n* = 9), *C. boninense* (CBSC; *n* = 8), and *C. dematium* (CDSC; *n* = 3).

For the CGSC, the combined dataset ITS-*gapdh*-*tub2*-ApMat-*gs* provided high resolution (Figure 2). Isolates formed strongly supported clades with reference strains of *C. fructicola*, *C. gloeosporioides, C. jiangxiense*, and *C. perseae*, all with ML/PP support values of 100%/1.0. The remaining isolates formed a well-supported cluster (100%/1.0) with the strains ICMP 12952, ICMP 12953, and PR432, previously reported as *C. cigarro*. However, the ex-type strain of *C. cigarro* (ICMP 18539) formed a separate clade as a sister taxon of *C. helleniense*. Consequently, these isolates were designated as *C.* cf. *cigarro*. For CASC and CBSC, the concatenated dataset ITS-*gapdh-tub2* was phylogenetically informative (Figures 3 and 4). Chilean isolates formed well-supported clades with reference strains of *C. pyricola* (100%/1.0), *C. karsti* (99%/1.0), *C. laurosilvaticum* (99%/1.0), and *C. brassicicola* (100%/1.0). The CDSC was resolved with the combined dataset ITS-*gapdh-tub2-act-chs1*, which revealed a well-supported clade between Chilean isolates and strains of *C. anthrisci* (100%/1.0) (Figure 5). Species identifications and their respective frequencies are summarized in Table 1. GenBank accession numbers of analyzed isolates are listed in Tables 2, 3 and 4.

Conidium characterization

Selected isolates of each *Colletotrichum* species produced acervuli on CYA plates after 7 to 14 days at 22°C. Isolates from the CGSC and CBSC formed cylindrical to oval, aseptate conidia with straight or slightly rounded ends. Isolates of *C. pyricola* (CASC) formed cylindrical to fusiform, aseptate conidia, each with one end slightly pointed and the other end rounded. In contrast, *C. anthrisci* (CDSC) produced curved fusiform conidia, which were almost straight in the central regions but bending abruptly toward both ends. Conidium dimensions of all analyzed isolates, together with reference strains, are presented in Table 5. Due to the high morphological variability within this group, 12 isolates of *C.* cf. *cigarro* were examined. Conidium lengths ranged from 12.0 to 21.0 µm and widths from 4.0 to 7.0 µm, exhibiting overlaps across isolates and significant differences in length, width, and length-to-width ratios (Figure S1).

Pathogenicity assessments

All assessed isolates induced anthracnose symptoms on inoculated avocado fruits within 7 days at 22 °C, whereas non-inoculated control fruits remained symptomless. Mean lesions diameters ranged from 20.9 to 34.1 mm, with significant differences detected among isolates ($P < 0.0001$) (Table 6). The most virulent isolates were *C. fructicola* (MER-06; mean lesion diameter = 34.1 mm) and *C.* cf. *cigarro* (MER-11; mean = 33.0 mm). Intermediate virulence was observed for *C.* cf. *cigarro* (SDO-03), *C. anthrisci* (NAL-54) and *C. pyricola* (FAM-20 and FAM-23), with mean lesion diameters between 28.3 and 30.9 mm. The remaining isolates of *C. gloeosporioides* (MER-07 and FAM-01), *C. jiangxiense* (SDO-38 and NAL-03), *C. perseae* (NAL-19), *C. karsti*

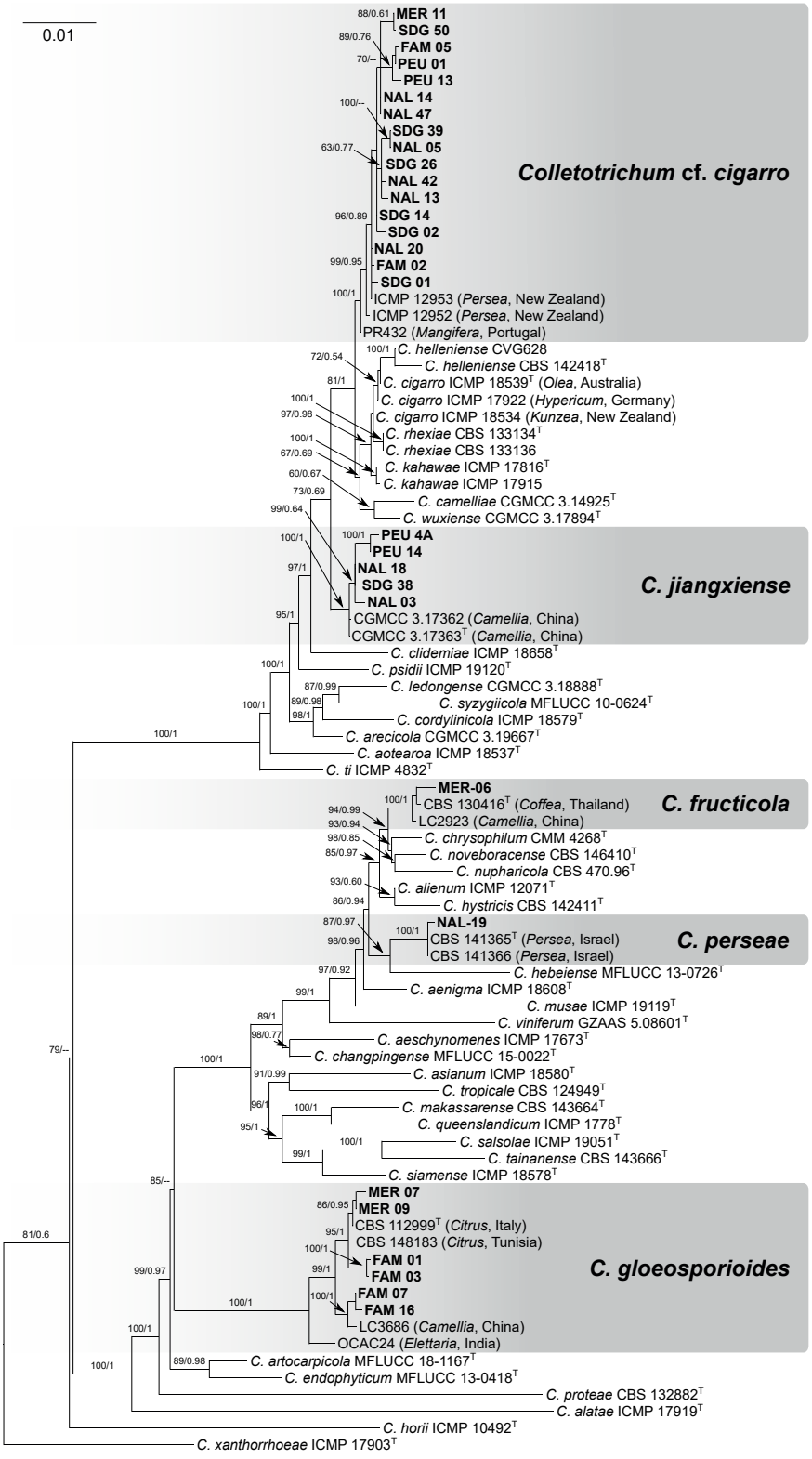

Figure 2. Maximum likelihood phylogenetic analysis of the *Colletotrichum gloeosporioides* species complex (CGSC). Chilean isolates are shown in bold font, and ex-type strains are each accompanied with a superscript T. Maximum likelihood bootstrap values and Bayesian posterior probabilities are indicated above the tree branches. The tree was inferred from a data set consisting of sequences of five DNA markers (ITS, *gapdh*, *tub2*, ApMat, and *gs*), and was rooted with *C. xanthorrhoeae*. Scale bar = substitutions per site.

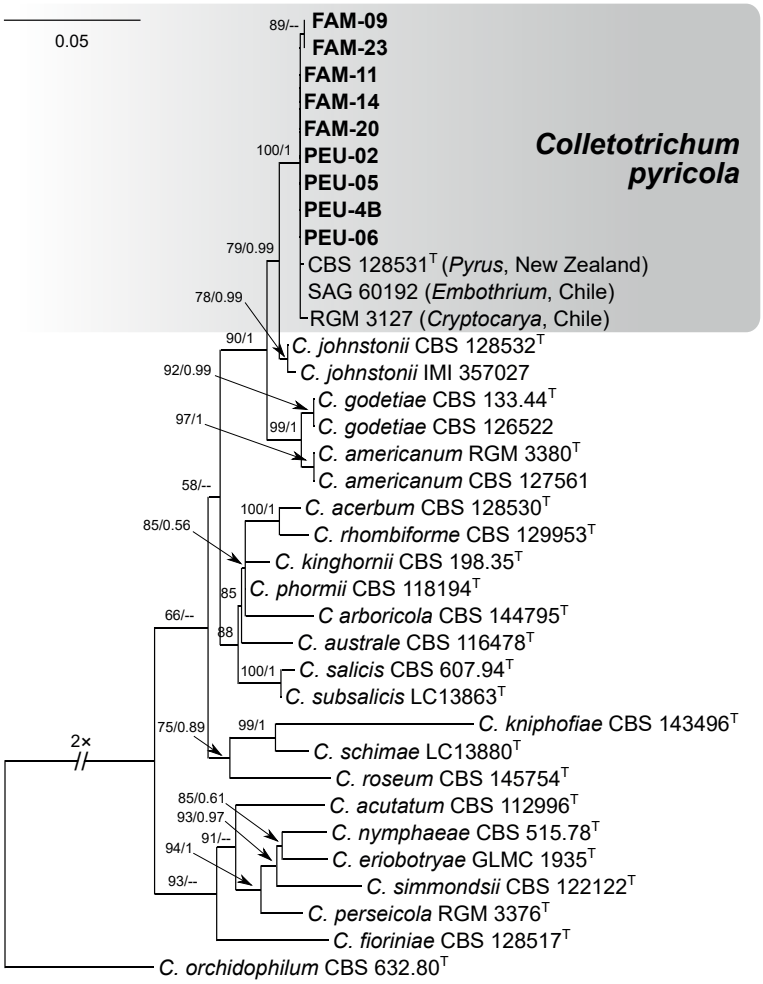

Figure 3. Maximum likelihood phylogenetic analysis of the *Colletotrichum acutatum* species complex (CASC). Chilean isolates are shown in bold font, and ex-type strains are each accompanied with a superscript T. Maximum likelihood bootstrap values and Bayesian posterior probabilities are indicated above the tree branches. The tree was inferred from a data set consisting of sequences of three DNA markers (ITS, *gapdh*, and *tub2*) and was rooted with *C. orchidophilum*. Scale bar = substitutions per site.

(NAL-33 and NAL-35), *C. anthrisci* (NAL-53), *C. brassicicola* (NAL-32 and FAM-06), and *C. laurosilvaticum* (NAL-17), were less virulent, with mean lesion diameters from 20.9 to 27.4 mm. Figure 6 illustrates representative species showing contrasting levels of virulence. The same isolates as those inoculated were consistently re-isolated on PDA plates from the necrotic pulp of symptomatic fruit, with identities confirmed by morphology, and no *Colletotrichum* colonies were recovered from the non-inoculated control fruits.

DISCUSSION

This study provides a comprehensive assessment of the etiology of avocado anthracnose in Chile. Ten *Colletotrichum* species were identified through combined morphological and multilocus phylogenetic analyses, representing four species complexes: CGSC (30 isolates), CASC (eight isolates), CBSC (eight isolates), and CDSC (three isolates). From other countries, approx. 26 *Colletotrichum* species have been previously identified causing avocado anthracnose, with members of the CGSC most frequently observed (Shivas and Tan, 2009; Cannon *et al*., 2012; Hunupolagama *et al*., 2015; Sharma *et al*., 2017; Giblin *et al*., 2018; Fuentes-Aragón *et al*., 2020; Soares *et al*., 2020; Hofer *et al*., 2021; Wu *et al*., 2023). The present study detected greater diversity of species in Chile than previously documented, including three species reported on avocado for the first time.

The most frequent species found in the present study was *C.* cf. *cigarro* (CGSC), detected across all sam-

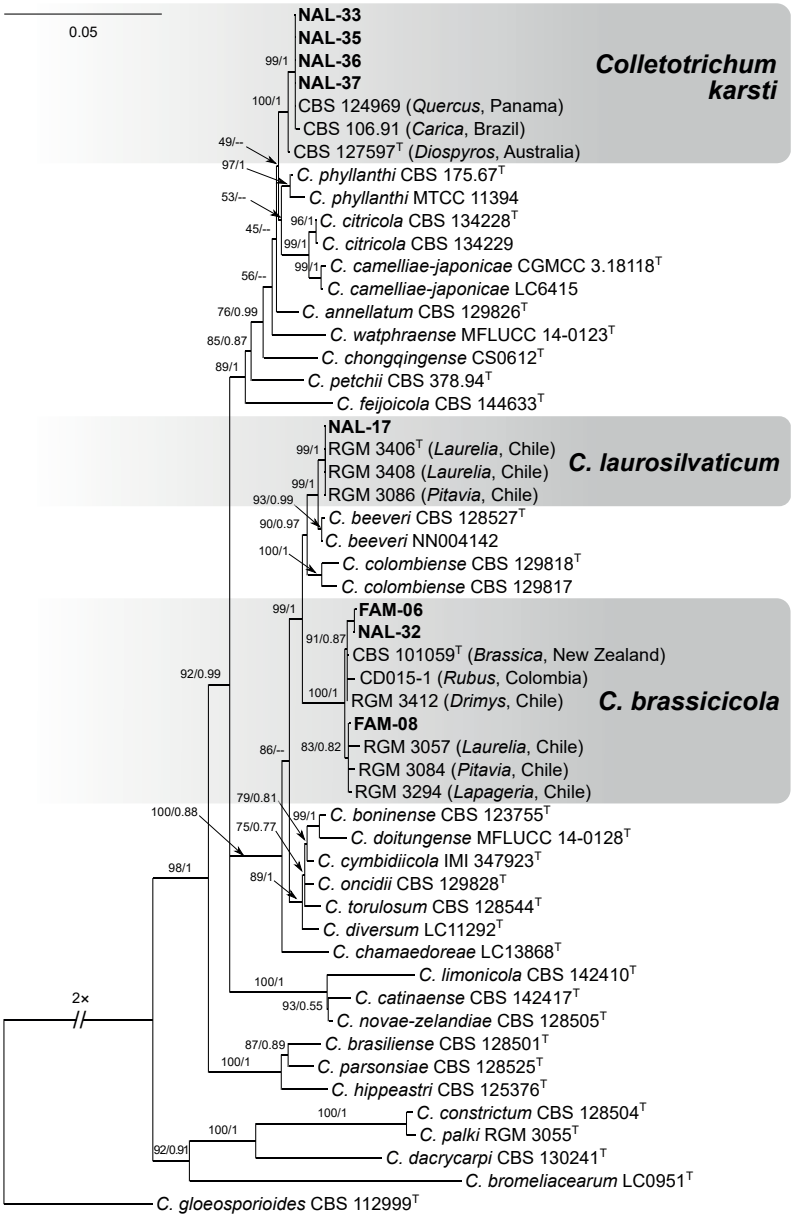

Figure 4. Maximum likelihood phylogenetic analysis of the *Colletotrichum boninense* species complex (CBSC). Chilean isolates are shown in bold font, and ex-type strains are each accompanied with a superscript T. Maximum likelihood bootstrap values and Bayesian posterior probabilities are indicated above the tree branches. The tree was inferred from a data set consisting of sequences of three DNA markers (ITS, *gapdh*, and *tub2*) and was rooted with *C. gloeosporioides*. Scale bar = substitutions per site.

pled sites. These isolates were morphologically diverse and indistinguishable from *C. jiangxiense* or *C. fructicola*, but clustered phylogenetically with strains reported as *C. cigarro* from avocado and mango. Their genetic divergence from the type strain of *C. cigarro* suggests they may represent a distinct, undescribed species, a hypothesis that requires further taxonomic investigation. The second most common species was *C. pyricola* (CASC), previously reported on various hosts in Australia, New Zealand, and Chile (Damm *et al*., 2012a; Zapata and Opazo, 2017). Its detection on avocado represents a new host record, and indicates a wider distribution in Chile than previously recognized, supporting the hypothesis by Zapata *et al*., (2024) of its endemic origin in southern South America.

Other notable species included *C. gloeosporioides* and *C. jiangxiense*, both members of the CGSC. The present study provides the first molecular confirmation of *C. gloe-*

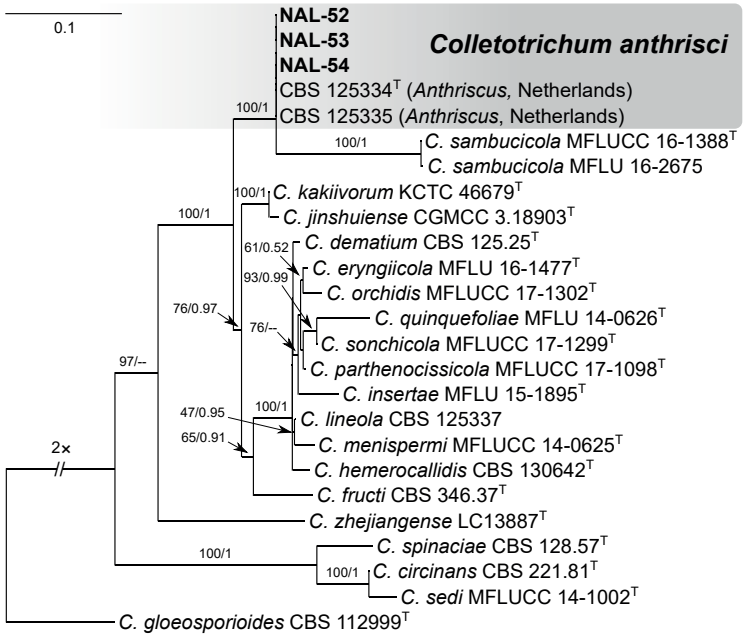

Figure 5. Maximum likelihood phylogenetic analysis of the *Colletotrichum dematium* species complex (CDSC). Chilean isolates are shown in bold font, and ex-type strains are each accompanied with a superscript T. Maximum likelihood bootstrap values and Bayesian posterior probabilities are indicated above the tree branches. The tree was inferred from a data set consisting of sequences of five DNA markers (ITS, *gapdh*, *tub2*, *act*, and *chs1*) and was rooted with *C. gloeosporioides*. Scale bar = substitutions per site.

Table 1. Isolate frequencies and geographical origins for *Colletotrichum* species associated with avocado anthracnose in Chile.

Species complex and species	Frequency of isolates (*n*)				
	Metropolitan Region	Valparaiso Region	O'Higgins Region	Total	Relative frequency (%)
C. gloeosporioides species complex (CGSC)					
C. cf. *cigarro*	9	6	2	17	34.0
C. gloeosporioides	6	0	0	6	12.0
C. jiangxiense	2	1	2	5	10.0
C. fructicola	1	0	0	1	2.0
C. perseae	1	0	0	1	2.0
C. acutatum species complex (CASC)					
C. pyricola	5	0	4	9	18.0
C. boninense species complex (CBSC)					
C. karsti	4	0	0	4	8.0
C. brassicicola	3	0	0	3	6.0
C. laurosilvaticum	1	0	0	1	2.0
C. dematium species complex (CDSC)					
C. anthrisci	3	0	0	3	6.0
Total	35	7	8	50	100.0

osporioides on avocado in Chile, clarifying previous morphology-based reports (Morales *et al*., 1979; Montealegre *et al*., 2002). Conversely, *C. jiangxiense*, previously reported only in Mexico on avocado (Ayvar-Serna *et al*., 2021), is here documented for the first time in Chile, extending the known geographical range of this pathogen.

Within the CBSC, *C. karsti*, *C. brassicicola*, and *C. laurosilvaticum* were identified at low frequencies.

Table 2. GenBank accession numbers and sampling sites of *Colletotrichum gloeosporioides* species complex (CGSC) isolates obtained from avocado anthracnose in Chile and included in phylogenetic analyses.

Species	Isolate	Sampling site	Location, region	GenBank accession number				
				ITS	*gapdh*	*tub2*	ApMat	*gs*
C. cf. *cigarro*	FAM-02	Non-commercial grove	Isla de Maipo, Metropolitan	PQ167786	PQ178841	PQ195572	PQ217744	PQ217774
C. cf. *cigarro*	FAM-05	Non-commercial grove	Isla de Maipo, Metropolitan	PQ167787	PQ178842	PQ195573	PQ217745	PQ217775
C. cf. *cigarro*	MER-11	Local market	Santiago, Metropolitan	PQ167788	PQ178843	PQ195574	PQ217746	PQ217776
C. cf. *cigarro*	NAL-05	Commercial grove	Isla de Maipo, Metropolitan	PQ167789	PQ178844	PQ195575	PQ217747	PQ217777
C. cf. *cigarro*	NAL-13	Commercial grove	Isla de Maipo, Metropolitan	PQ167790	PQ178845	PQ195576	PQ217748	PQ217778
C. cf. *cigarro*	NAL-14	Commercial grove	Isla de Maipo, Metropolitan	PQ167791	PQ178846	PQ195577	PQ217749	PQ217779
C. cf. *cigarro*	NAL-20	Commercial grove	Isla de Maipo, Metropolitan	PQ167792	PQ178847	PQ195578	PQ217750	PQ217780
C. cf. *cigarro*	NAL-42	Commercial grove	Isla de Maipo, Metropolitan	PQ167793	PQ178848	PQ195579	PQ217751	PQ217781
C. cf. *cigarro*	NAL-47	Commercial grove	Isla de Maipo, Metropolitan	PQ167794	PQ178849	PQ195580	PQ217752	PQ217782
C. cf. *cigarro*	PEU-01	Commercial grove	Peumo, O'Higgins	PQ167795	PQ178850	PQ195581	PQ217753	PQ217783
C. cf. *cigarro*	PEU-13	Commercial grove	Peumo, O'Higgins	PQ167796	PQ178851	PQ195582	PQ217754	PQ217784
C. cf. *cigarro*	SDO-01	Commercial grove	Santo Domingo, Valparaíso	PQ167797	PQ178852	PQ195583	PQ217755	PQ217785
C. cf. *cigarro*	SDO-02	Commercial grove	Santo Domingo, Valparaíso	PQ167798	PQ178853	PQ195584	PQ217756	PQ217786
C. cf. *cigarro*	SDO-14	Commercial grove	Santo Domingo, Valparaíso	PQ167799	PQ178854	PQ195585	PQ217757	PQ217787
C. cf. *cigarro*	SDO-26	Commercial grove	Santo Domingo, Valparaíso	PQ167800	PQ178855	PQ195586	PQ217758	PQ217788
C. cf. *cigarro*	SDO-39	Commercial grove	Santo Domingo, Valparaíso	PQ167801	PQ178856	PQ195587	PQ217759	PQ217789
C. cf. *cigarro*	SDO-50	Commercial grove	Santo Domingo, Valparaíso	PQ167802	PQ178857	PQ195588	PQ217760	PQ217790
C. fructicola	MER-06	Local market	Santiago, Metropolitan	PQ167773	PQ178828	PQ195559	PQ217731	PQ217761
C. gloeosporioides	FAM-01	Non-commercial grove	Isla de Maipo, Metropolitan	PQ167774	PQ178829	PQ195560	PQ217732	PQ217762
C. gloeosporioides	FAM-03	Non-commercial grove	Isla de Maipo, Metropolitan	PQ167775	PQ178830	PQ195561	PQ217733	PQ217763
C. gloeosporioides	FAM-07	Non-commercial grove	Isla de Maipo, Metropolitan	PQ167776	PQ178831	PQ195562	PQ217734	PQ217764
C. gloeosporioides	FAM-16	Non-commercial grove	Isla de Maipo, Metropolitan	PQ167777	PQ178832	PQ195563	PQ217735	PQ217765
C. gloeosporioides	MER-07	Local market	Santiago, Metropolitan	PQ167778	PQ178833	PQ195564	PQ217736	PQ217766
C. gloeosporioides	MER-09	Local market	Santiago, Metropolitan	PQ167779	PQ178834	PQ195565	PQ217737	PQ217767
C. jiangxiense	NAL-03	Commercial grove	Naltahua, Metropolitan	PQ167780	PQ178835	PQ195566	PQ217738	PQ217768
C. jiangxiense	NAL-18	Commercial grove	Naltahua, Metropolitan	PQ167781	PQ178836	PQ195567	PQ217739	PQ217769
C. jiangxiense	PEU-4A	Commercial grove	Peumo, O'Higgins	PQ167782	PQ178837	PQ195568	PQ217740	PQ217770
C. jiangxiense	PEU-14	Commercial grove	Peumo, O'Higgins	PQ167783	PQ178838	PQ195569	PQ217741	PQ217771
C. jiangxiense	SDO-38	Commercial grove	Santo Domingo, Valparaíso	PQ167784	PQ178839	PQ195570	PQ217742	PQ217772
C. perseae	NAL-19	Commercial grove	Isla de Maipo, Metropolitan	PQ167785	PQ178840	PQ195571	PQ217743	PQ217773

Table 3. GenBank accession numbers and sampling sites of isolates of the *Colletotrichum acutatum* (CASC) and *C. boninense* (CBSC) species complexes obtained from avocado anthracnose in Chile and included in phylogenetic analyses.

Species	Species complex	Isolate	Sampling site	Location, region	GenBank accession number		
					ITS	*gapdh*	*tub2*
C. brassicicola	CBSC	FAM-06	Non-commercial grove	Isla de Maipo, Metropolitan	PQ167805	PQ195525	PQ195542
C. brassicicola	CBSC	FAM-08	Non-commercial grove	Isla de Maipo, Metropolitan	PQ167806	PQ195526	PQ195543
C. brassicicola	CBSC	NAL-32	Commercial grove	Isla de Maipo, Metropolitan	PQ167807	PQ195527	PQ195544
C. karsti	CBSC	NAL-33	Commercial grove	Isla de Maipo, Metropolitan	PQ167808	PQ195528	PQ195545
C. karsti	CBSC	NAL-35	Commercial grove	Isla de Maipo, Metropolitan	PQ167809	PQ195529	PQ195546
C. karsti	CBSC	NAL-36	Commercial grove	Isla de Maipo, Metropolitan	PQ167810	PQ195530	PQ195547
C. karsti	CBSC	NAL-37	Commercial grove	Isla de Maipo, Metropolitan	PQ167811	PQ195531	PQ195548
C. laurosilvaticum	CBSC	NAL-17	Commercial grove	Isla de Maipo, Metropolitan	PQ167812	PQ195532	PQ195549
C. pyricola	CASC	FAM-09	Non-commercial grove	Isla de Maipo, Metropolitan	PQ167813	PQ195533	PQ195550
C. pyricola	CASC	FAM-11	Non-commercial grove	Isla de Maipo, Metropolitan	PQ167814	PQ195534	PQ195551
C. pyricola	CASC	FAM-14	Non-commercial grove	Isla de Maipo, Metropolitan	PQ167815	PQ195535	PQ195552
C. pyricola	CASC	FAM-20	Non-commercial grove	Isla de Maipo, Metropolitan	PQ167816	PQ195536	PQ195553
C. pyricola	CASC	FAM-23	Non-commercial grove	Isla de Maipo, Metropolitan	PQ167817	PQ195537	PQ195554
C. pyricola	CASC	PEU-02	Commercial grove	Peumo, O'Higgins	PQ167818	PQ195538	PQ195555
C. pyricola	CASC	PEU-4B	Commercial grove	Peumo, O'Higgins	PQ167819	PQ195539	PQ195556
C. pyricola	CASC	PEU-05	Commercial grove	Peumo, O'Higgins	PQ167820	PQ195540	PQ195557
C. pyricola	CASC	PEU-06	Commercial grove	Peumo, O'Higgins	PQ167821	PQ195541	PQ195558

Table 4. GenBank accession numbers and sampling sites of *Colletotrichum anthrisci* isolates obtained from avocado anthracnose in Chile included in phylogenetic analyses.

Species	Isolate	Sampling site	Location, region	GenBank accession number				
				ITS	*gapdh*	*tub2*	*act*	*chs1*
C. anthrisci	NAL-52	Commercial grove	Isla de Maipo, Metropolitan	MN203633	MN207466	MN207160	OM055666	OM037442
C. anthrisci	NAL-53	Commercial grove	Isla de Maipo, Metropolitan	MN203634	MN207467	MN207161	OM055667	OM037443
C. anthrisci	NAL-54	Commercial grove	Isla de Maipo, Metropolitan	MN203635	MN207468	MN207162	OM055668	OM037444

Table 5. Conidial dimensions of isolates of *Colletotrichum* spp. associated with avocado anthracnose in Chile compared to reference strains.

Species	Isolate/strain[a]	Conidial size (µm) (L × W)[b]	Mean (µm) (L × W)	Mean L/W ratio	Reference
C. anthrisci	CBS 125334^T	(22.0–)23.9–26.9(–28.5) × (3.0–)3.3–3.7(–4.0)	26.3 × 3.4	7.8	Damm *et al.* (2009)
C. anthrisci	NAL-53	(20.0–)22.0–25.3(–27.5) × (2.5–)2.3–3.1(–3.8)	23.6 × 2.7	8.7	This study
C. brassicicola	CBS 101059^T	(9.0–)11.4–13.4(–14.5) × (5.0–)5.3–5.9(–6.0)	12.2 × 5.6	2.2	Damm *et al.* (2012b)
C. brassicicola	FAM-06	(11.0–)11.8–12.3(–12.2) × (4.5–)4.9–5.2(–5.4)	12.0 × 5.0	2.4	This study
C. cigarro	ICMP 18534	(11.0–)12.4–14.5(–16.0) × (3.0–)3.5–4.5(–6.0)*	13.4 × 4.2	3.3	Cabral *et al.* (2020)
C. cigarro	ICMP 18539^T	(12.0–)16.0–19.5(–29.0) × (4.5–)5.0(–8.0)*	17.8 × 5.1	3.5	Weir *et al.* (2012)
C. cf. *cigarro*	ICMP 12953	(10.5–)13.0–14.4(–15.5) × (5.0–)5.5–6.6(–6.0)*	13.4 × 5.6	2.4	Cabral *et al.* (2020)
C. cf. *cigarro*	FAM-05	(14.0–)16.1–18.4(–20.0) × (4.0–)4.4–6.3(–7.0)	16.8 × 5.3	3.2	This study
C. cf. *cigarro*	MER-11	(12.0–)13.4–17.0(–20.0) × (5.0–)5.1–6.1(–6.0)	15.2 × 5.6	2.7	This study
C. cf. *cigarro*	NAL-05	(13.0–)14.3–16.7(–18.0) × (5.0–)4.8–6.0(–7.0)	15.4 × 5.2	3.0	This study
C. cf. *cigarro*	NAL-13	(15.0–)15.8–18.3(–20.0) × (5.0–)5.7–7.1(–7.0)	16.9 × 6.4	2.6	This study
C. cf. *cigarro*	NAL-42	(13.0–)14.2–16.6(–18.0) × (4.0–)4.9–6.0(–6.0)	15.4 × 5.4	2.9	This study
C. cf. *cigarro*	PEU-13	(14.0–)15.0–17.5(–19.0) × (5.0–)4.8–5.6(–6.0)	16.2 × 5.2	3.1	This study
C. cf. *cigarro*	PR432	(11.0–)12.5–14.0(–15.5) × (4.5–)5.5–6.3(–7.0)*	13.3 × 5.9	2.3	Cabral *et al.* (2020)
C. cf. *cigarro*	SDO-01	(15.0–)17.2–20.1(–21.0) × (5.0–)5.0–6.4(–7.0)	18.3 × 5.7	3.2	This study
C. cf. *cigarro*	SDO-02	(13.0–)14.2–16.4(–18.0) × (4.0–)4.9–6.0(–6.0)	15.3 × 5.5	2.8	This study
C. cf. *cigarro*	SDO-14	(14.0–)14.7–16.4(–18.0) × (4.0–)5.0–6.7(–7.0)	15.5 × 5.8	2.7	This study
C. cf. *cigarro*	SDO-26	(14.0–)14.8–17.0(–18.0) × (5.0–)4.8–5.7(–6.0)	15.9 × 5.2	3.1	This study
C. cf. *cigarro*	SDO-39	(14.0–)15.0–17.4(–19.0) × (5.0–)5.1–6.2(–7.0)	16.2 × 5.6	2.9	This study
C. cf. *cigarro*	SDO-50	(13.0–)15.0–19.3(–21.0) × (5.0–)5.0–6.5(–7.0)	17.2 × 5.7	3.0	This study
C. fructicola	ICMP 18581^T	(9.7–)10.5–12.6(–14.0) × (3.0–)3.2–3.9(–4.3)	11.4 × 3.5	3.3	Prihastuti *et al.* (2009)
C. fructicola	MER-06	(14.0–)14.1–14.8(–15.0) × (4.5–)4.6–5.0(–5.0)	14.4 × 4.8	3.0	This study
C. gloeosporioides	LC3312	(11.0–)12.3–14.7(–15.5) × (4.5–)5.2–5.8(–6.0)	13.5 × 5.5	2.5	Liu *et al.* (2015)
C. gloeosporioides	MER-07	(19.0–)19.4–20.5(–22.0) × (4.8–)4.9–5.0(–5.0)	19.9 × 5.0	4.0	This study
C. gloeosporioides	PR411	(17.8–)19.5(–21.6) × (4.8–)6.1(–6.9)	19.5 × 6.1	3.2	Ramos *et al.* (2016)
C. jiangxiense	CGMCC 3.17363^T	(13.0–)14.2–16.2(–19.0) × (4.0–)4.8–5.6(–6.0)	15.2 × 5.2	2.9	Liu *et al.* (2015)
C. jiangxiense	NAL-03	(12.0–)13.7–16.7(–18.0) × (6.0–)5.9–7.5(–8.0)	15.2 × 6.7	2.3	This study
C. karsti	CBS 127597^T	(12.0–)12.9–15.1(–16.5) × (5.5–)5.4–6.0(–6.5)	13.1 × 5.8	2.2	Damm *et al.* (2012b)
C. karsti	NAL-33	(14.5–)14.8–15.0(–15.0) × (5.0–)5.4–7.0(–7.0)	14.9 × 6.2	2.4	This study
C. laurosilvaticum	NAL-17	(12.3–)12.7–13.9(–14.0) × (6.0–)6.5–7.1(–7.0)	13.3 × 6.8	2.0	This study
C. laurosilvaticum	RGM 3406^T	(13.5–)12.9–14.3(–16.5) × (5.0–)6.1–6.7(–6.5)	13.6 × 6.4	2.1	Zapata *et al.* (2024)
C. perseae	CBS 141365^T	(13.0–)15.7(–19.0) × (4.0–)5.2(–6.5)	15.7 × 5.2	3.0	Sharma *et al.* (2017)
C. perseae	NAL-19	(15.0–)17.2–20.1(–21.0) × (5.0–)5.0–6.4(–7.0)	18.6 × 5.7	3.3	This study
C. pyricola	CBS 128531^T	(9.5–)13.8–17.0(–18.5) × (4.0–)4.4–5.2(–5.5)	15.4 × 4.8	3.2	Damm *et al.* (2012a)
C. pyricola	PEU-02	(14.2–)14.5–15.5(–16.2) × (4.5–)4.7–5.1(–5.2)	15.0 × 4.9	3.1	This study

[a] Type strains are highlighted in bold and a superscript T.
[b] L × W = length by width, data represents (minimum–) average–standard deviation [SD] – average+SD (–maximum).
Data marked with an asterisk (*) represents (minimum–) first quartile – third quartile (–maximum).

While *C. karsti* has been previously reported on avocado (Damm *et al*., 2012b), this study provides the first records of *C. brassicicola* and *C. laurosilvaticum* on avocado, thereby expanding their known host ranges and distribution to central Chile (Zapata *et al*., 2024). The species *C. anthrisci* (CDSC) was also recovered at low frequency, supporting its limited epidemiological relevance, in agreement with previous observations (Rose and Damm, 2024). Likewise, *C. fructicola* and *C. perseae* (CGSC) were detected only sporadically, extending their known geographical distributions to Chile yet suggesting that both species constitute minor and likely incidental components of the local pathogen composition.

The *Colletotrichum* identification results obtained in this study are consistent with previous reports of these pathogens on avocado and other hosts (Diao *et al*., 2017; Sharma *et al*., 2017; Armand and Jayawardena, 2024). Multilocus phylogenetic analyses were essential for accu-

Table 6. Mean lesion diameters (mm) caused by *Colletotrichum* species inoculated into healthy avocado fruits (cv. Hass) after 7 d at 20°C. Means accompanied by the same letter are not significantly different ($P > 0.05$) according to Fisher's LSD test.

Species	Isolate	Mean lesion diameter (mm)	Standard error	LSD test
C. fructicola	MER-06	34.05	0.55	a
C. cf. *cigarro*	MER-11	33.03	1.56	a b
C. cf. *cigarro*	SDO-03	30.93	1.17	b
C. anthrisci	NAL-54	30.30	1.59	b c
C. pyricola	FAM-23	30.08	1.36	b c
C. pyricola	FAM-20	28.32	1.81	b c d
C. gloeosporioides	MER-07	27.38	0.80	c d
C. jiangxiense	SDO-38	25.83	0.31	d
C. perseae	NAL-19	25.27	0.38	d e
C. jiangxiense	NAL-03	25.05	0.18	d e
C. gloeosporioides	FAM-01	25.05	1.03	d e
C. karsti	NAL-33	24.92	1.23	d e
C. anthrisci	NAL-53	24.35	1.03	d e
C. karsti	NAL-35	24.08	0.62	e
C. brassicicola	NAL-32	22.77	1.09	e f
C. brassicicola	FAM-06	22.70	1.41	e f
C. laurosilvaticum	NAL-17	20.91	0.25	f
Control	n/a	0.09	0.10	g

rate species delimitation. Concatenated ITS, *gapdh,* and *tub2* sequences resolved species within CASC and CBSC, as reported previously (Velho *et al*., 2015; Khodadadi *et al*., 2020). By contrast, in the CDSC, incorporation of *act* and *chs1* was required to resolve *C. anthrisci*, consistent with previous studies (Lee and Jung, 2018; Fu *et al*., 2019). Similarly, in the CGSC, inclusion of ApMat and *gs* was necessary to separate closely related taxa (Liu *et al*., 2015). Chilean isolates identified as *C.* cf. *cigarro* clustered with strains reported as *C. cigarro* from avocado in New Zealand and mango in Portugal, whereas the type strain grouped separately with isolates from other hosts in Germany and New Zealand. These results support previous observations that isolates identified as *C. cigarro* do not form a monophyletic clade, and may represent multiple species (Silva *et al*., 2012a; Doyle *et al*., 2013; Vieira *et al*., 2018; Cabral *et al*., 2020; Kreth *et al*., 2025). Additionally, Conidia of Chilean isolates of *C.* cf. *cigarro* were generally longer than those measured by Cabral *et al*., (2020), and although they overlapped with the type strain, statistically significant differences in conidium size were detected among isolates (Figure S1). Collectively, these results suggest that the Chilean isolates, along with strains ICMP 12952, ICMP 12953 and PR432, may constitute a new species that requires formal taxonomic evaluation. From a morphological perspective, conidium features of representative isolates from all identified species were consistent with type strain descriptions, although size variation was expected given the known overlap across species (Damm *et al*., 2009; 2012a; 2012b; Weir *et al*., 2012).

Pathogenicity tests confirmed all ten species as causal agents of avocado anthracnose. Isolates from the CGSC and CASC exhibited greater virulence than those from CBSC and CDSC, consistent with previous studies on avocado and other hosts (Munir *et al*., 2016; Sharma *et al*., 2017; Oo *et al*., 2018; Fuentes-Aragón *et al*., 2020; Wu *et al*., 2023). Variation in virulence among species complexes, species, and isolates highlights the importance of species-level identification for disease management (Guarnaccia *et al*., 2017; Chung *et al*., 2020; Riolo *et al*., 2021; Camiletti *et al*., 2022).

In conclusion, the present study documents an unprecedented diversity of *Colletotrichum* species associ-

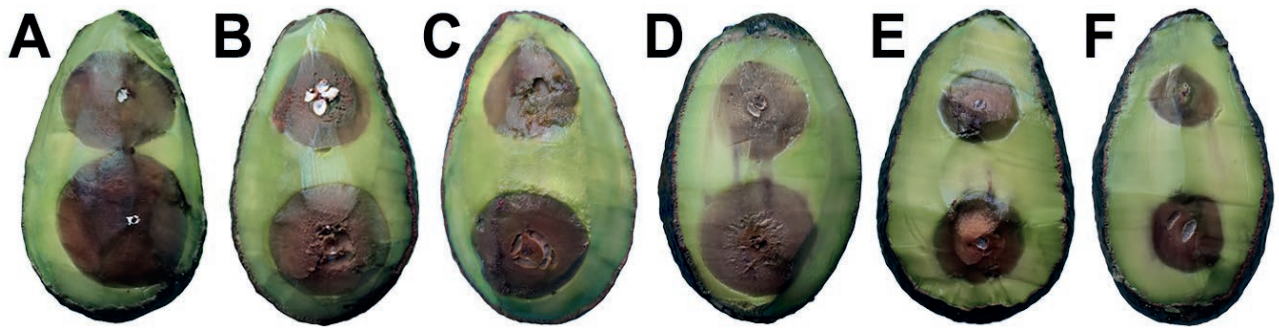

Figure 6. Pathogenicity tests showing internal lesions caused by the most frequently isolated *Colletotrichum* species with differential virulences on cv. 'Hass' avocado fruits at 7 d after inoculations. A and B, the most virulent species. C and D, moderately virulent species. E and F, least virulent species. A, *Colletotrichum* cf. *cigarro* isolate SDO-03. B, *C. pyricola* isolate FAM-23. C, *C. anthrisci* isolate NAL-54. D, *C. gloeosporioides* isolate MER-07. E, *C. karsti* isolate NAL-35. F, *C. brassicicola* isolate FAM-06.

ated with avocado anthracnose in Chile, including three species reported for the first time on avocado. These results provide information on the most frequent species, extend the known geographic distributions of several pathogens, reveal differences in virulence, and emphasize the need for further taxonomic clarification of *C.* cf. *cigarro*. Further research should address the epidemiology of the most prevalent *Colletotrichum* species to support the development of effective disease management strategies for Chilean avocado production.

LITERATURE CITED

Akgül D.S., Awan Q.N., Güler P.G., Önelge N., 2016. First report of anthracnose and stem end rot diseases caused by *Colletotrichum gloeosporioides* and *Neofusicoccum australe* on avocado fruits in Turkey. *Plant Disease* 100: 1792. https://doi.org/10.1094/PDIS-03-16-0305-PDN

Armand A., Jayawardena R.S., 2024. Morphomolecular identification and pathogenicity of *Colletotrichum* species associated with avocado anthracnose in northern Thailand. *Plant Pathology* 73: 186–197. https://doi.org/10.1111/ppa.13792

Ayvar-Serna S., Díaz-Nájera J.F., Vargas-Hernández M., Camacho-Tapia M., Valencia-Rojas G.A., … Tovar-Pedraza J.M., 2021. First report of *Colletotrichum jiangxiense* causing avocado anthracnose in Mexico. *Plant Disease* 105: 502. https://doi.org/10.1094/PDIS-03-20-0459-PDN

Barnett H.L., Hunter B.B., 1998. *Illustrated Genera of Imperfect Fungi*, 4th ed. APS Press, St. Paul, MN, USA.

Bourret T.B., Choudhury R.A., Mehl H.K., Blomquist C.L., McRoberts N., Rizzo D.M., 2018. Multiple origins of downy mildews and mitonuclear discordance within the paraphyletic genus *Phytophthora*. *PLoS ONE* 13: e0192502. https://doi.org/10.1371/journal.pone.0192502

Bustamante M.I., Osorio-Navarro C., Fernández Y., Bourret T.B., Zamorano A., Henríquez-Saez J.L., 2022. First record of *Colletotrichum anthrisci* causing anthracnose on avocado fruits in Chile. *Pathogens* 11: 1204. https://doi.org/10.3390/pathogens11101204

Cabral A., Azinheira H.G., Talhinhas P., Batista D., Ramos A.P., … Várzea V., 2020. Pathological, morphological, cytogenomic, biochemical and molecular data support the distinction between *Colletotrichum cigarro* comb. et stat. nov. and *Colletotrichum kahawae*. *Plants* 9: 502. https://doi.org/10.3390/plants9040502

Camiletti B.X., Lichtemberg P.S.F., Paredes J.A., Carraro T.A., Velascos J., Michailides T.J., 2022. Characterization of *Colletotrichum* isolates causing *Colletotrichum* dieback of citrus in California. *Phytopathology* 112: 1454–1466. https://doi.org/10.1094/PHYTO-10-21-0434-R

Cannon P.F., Damm U., Johnston P.R., Weir B.S., 2012. *Colletotrichum* – current status and future directions. *Studies in Mycology* 73: 181–213. https://doi.org/10.3114/sim0014

Carbone I., Kohn L.M., 1999. A method for designing primer sets for speciation studies in filamentous ascomycetes. *Mycologia* 91: 553–556. https://doi.org/10.1080/00275514.1999.12061051

Chung P.C., Wu H.Y., Wang Y.W., Ariyawansa H.A., Hu H.P., … Chung C.L., 2020. Diversity and pathogenicity of *Colletotrichum* species causing strawberry anthracnose in Taiwan and description of a new species, *Colletotrichum miaoliense* sp. nov. *Scientific Reports* 10: 14664. https://doi.org/10.1038/s41598-020-70878-2

Comité de Paltas de Chile. 2025. Estadísticas. Presencia en principals mercados globales. Available online: https://paltahass.cl/estadisticas/

Dann E.K., Ploetz R.C., Coates L.M., Pegg K.G., 2013. Foliar, fruit and soilborne diseases. In: *The Avocado: Botany*, Production and Uses, 2nd ed, pp. 380–422. (Schaffer B., Wolstenholme B.N., Whiley A.W., ed.). CAB International, Wallingford, United Kingdom.

Damm U., Cannon P.F., Woudenberg J.H.C., Crous P.W., 2012a. The *Colletotrichum acutatum* species complex. *Studies in Mycology* 73: 37–113. https://doi.org/10.3114/sim0010

Damm U., Cannon P.F., Woudenberg J.H.C., Johnston P.R., Weir B.S., Tan Y.P., Shivas R.G., Crous P.W., 2012b. The *Colletotrichum boninense* species complex. *Studies in Mycology* 73: 1–36. https://doi.org/10.3114/sim0002

Damm U., Woudenberg J.H.C., Cannon P.F., Crous P.W., 2009. *Colletotrichum* species with curved conidia from herbaceous hosts. *Fungal Diversity* 39: 45–87.

Diao Y.-Z., Zhang C., Liu F., Wang W.-Z., Liu L., Cai L., Liu X.-L., 2017. *Colletotrichum* species causing anthracnose disease of chili in China. *Persoonia* 38: 20–37. https://doi.org/10.3767/003158517X692788

Dissanayake D.M.S., Adikaram N.K.B., Yakandawala D.M.D., Jayasinghe L., 2021. Molecular phylogeny-based identification of *Colletotrichum endophytica and C. siamense* as causal agents of avocado anthracnose in Sri Lanka. *Ceylon Journal of Science* 50: 449–458. https://doi.org/10.4038/cjs.v50i4.7943

Dowling M., Peres N., Villani S., Schnabel G. 2020. Managing *Colletotrichum* on fruit crops: a "complex" challenge. *Plant Disease* 104: 2301–2316. https://doi.org/10.1094/PDIS-11-19-2378-FE

Doyle V.P., Oudemans P.V., Rehner S.A., Litt A., 2013. Habitat and host indicate lineage identity in *Colletotrichum gloeosporioides* s.l. from wild and agricultural landscapes in North America. *PLoS ONE* 8(5): e62394. https://doi.org/10.1371/journal.pone.0062394

Faber B.A., Wilen C.A., Eskalen A., Morse J.G., Hanson B.R., Hoddle M.S., 2016. UC IPM Pest Management Guidelines: Avocado (UC ANR Publication 3436). University of California Agriculture and Natural Resources. https://ipm.ucanr.edu/PMG/selectnewpest.avocado.html

FAOSTAT, 2025. Crops and livestock products database. Food and Agriculture Organization of the United Nations. Available at: https://www.fao.org/faostat/en/#data/QCL

Ferreyra R., Defilippi B., 2012. Factores de precosecha que afectan la postcosecha de palta Hass: clima, suelo y manejo. Quillota, Chile: Boletín INIA 248.

Fitzell R.D., 1987. Epidemiology of anthracnose disease of avocados. *South African Avocado Growers' Association Yearbook* 10: 113–116.

Fu M., Crous P.W., Bai Q., Zhang P.F., Xiang J., … Wang G.P., 2019. *Colletotrichum* species associated with anthracnose of *Pyrus* spp. in China. *Persoonia* 42: 1–35. https://doi.org/10.3767/persoonia.2019.42.01

Fuentes-Aragón D., Silva-Rojas H.V., Guarnaccia V., Mora-Aguilera J.A., Aranda-Ocampo S., … Téliz-Ortíz D., 2020. *Colletotrichum* species causing anthracnose on avocado fruit in Mexico: current status. *Plant Pathology* 69: 1513–1528. https://doi.org/10.1111/ppa.13234

Gañán L., Álvarez E., Castaño-Zapata J., 2015. Identificación genética de aislamientos de *Colletotrichum* spp. causantes de antracnosis en frutos de aguacate, banano, mango y tomate de árbol. *Revista de la Academia Colombiana de Ciencias Exactas, Físicas y Naturales* 39: 339–347. https://doi.org/10.18257/raccefyn.192

Giblin F.R., Tan Y.P., Mitchell R., Coates L.M., Irwin J.A.G., Shivas R.G., 2018. *Colletotrichum* species associated with pre- and postharvest diseases of avocado and mango in eastern Australia. *Australasian Plant Pathology* 47: 269–276.

Glass N.L., Donaldson G.C., 1995. Development of primer sets designed for use with the PCR to amplify conserved genes from filamentous ascomycetes. *Applied and Environmental Microbiology* 61: 1323–1330. https://doi.org/10.1128/aem.61.4.1323-1330.1995

Guarnaccia V., Groenewald J.Z., Polizzi G., Crous P.W., 2017. High species diversity in *Colletotrichum* associated with citrus diseases in Europe. *Persoonia* 39: 32–50. https://doi.org/10.3767/persoonia.2017.39.02

Guarnaccia V., Vitale A., Cirvilleri G., Aiello D., Susca A., Epifani F., Perrone G., Polizzi G., 2016. Characterisation and pathogenicity of fungal species associated with branch cankers and stem-end rot of avocado in Italy. *European Journal of Plant Pathology* 146: 963–976. https://doi.org/10.1007/s10658-016-0973-z

Guerber J.C., Liu B., Correll J.C., Johnston P.R., 2003. Characterization of diversity in *Colletotrichum acutatum* sensu lato by sequence analysis of two gene introns, mtDNA and intron RFLPs, and mating compatibility. *Mycologia* 95: 872–895. https://doi.org/10.2307/3762016

Hall T.A., 1999. BioEdit: a user-friendly biological sequence alignment editor and analysis program for Windows 95/98/NT. *Nucleic Acids Symposium Series* 41:95-98.

Hofer K.M., Braithwaite M., Braithwaite L.J., Sorensen S., Siebert B., … Toome-Heller M., 2021. First report of *Colletotrichum fructicola*, *C. perseae*, and *C. siamense* causing anthracnose disease of avocado (*Persea americana*) in New Zealand. *Plant Disease* 105: 1564. https://doi.org/10.1094/PDIS-06-20-1313-PDN

Honger J.O., Offei S.K., Oduro K.A., Odamtten G.T., Nyaku S.T., 2016. Identification and molecular characterisation of *Colletotrichum* species from avocado, citrus and pawpaw in Ghana. *South African Journal of Plant and Soil* 33: (online). https://doi.org/10.1080/02571862.2015.1125958

Hu M.-J., Grabke A., Schnabel G., 2015. Investigation of the *Colletotrichum gloeosporioides* species complex causing peach anthracnose in South Carolina. *Plant Disease* 99: 797–805. https://doi.org/10.1094/PDIS-10-14-1076-RE

Huang X., Madan A., 1999. CAP3: A DNA sequence assembly program. *Genome Research* 9: 868–877. https://doi.org/10.1101/gr.9.9.868

Hunupolagama D.M., Wijesundera R.L.C., Chandrasekharan N.V., Wijesundera W.S.S., Kathriarachchi H.S., Fernando T.H.P.S., 2015. Characterization of *Colletotrichum* isolates causing avocado anthracnose and first report of *C. gigasporum* infecting avocado in Sri Lanka. *Plant Pathology Quarantine* 5: 132–143. https://doi.org/10.5943/ppq/5/2/10

Katoh K., Rozewicki J., Yamada K.D., 2019. MAFFT online service: Multiple sequence alignment, interactive sequence choice, and visualization. *Briefings in Bioinformatics* 20: 1160–1166. https://doi.org/10.1093/bib/bbx108

Khodadadi F., González J.B., Martin P.L., Giroux E., Bilodeau G.J., Peter K.A., Doyle V.P., Aćimović S.G., 2020. Identification and characterization of *Colletotrichum* species causing apple bitter rot in New

York and description of *C. noveboracense* sp. nov. *Scientific Reports* 10: 11043. https://doi.org/10.1038/s41598-020-66761-9

Kimaru S.K., Monda E., Cheruiyot R.C., Mbaka J., Alakonya A., 2018. Morphological and molecular identification of the causal agent of anthracnose disease of avocado in Kenya. *International Journal of Microbiology* 2018: 4568520. https://doi.org/10.1155/2018/4568520

Kreth L.-S., Damm U., Götz M., 2025. A new name for an old problem—*Colletotrichum cigarro* is the cause of St John's wilt of *Hypericum perforatum*. *Frontiers in Fungal Biology* 5: 1534080. https://doi.org/10.3389/ffunb.2024.1534080

Lee S.Y., Jung H.Y., 2018. *Colletotrichum kakivorum* sp. nov., a new leaf spot pathogen of persimmon in Korea. *Mycological Progress* 17: 1113–1121. https://doi.org/10.1007/s11557-018-1424-3

Li M., Feng W., Yang J., Gao Z., Zhang Z., … Hu M., 2022. First report of anthracnose caused by *Colletotrichum siamense* on avocado fruits in China. *Crop Protection* 155: 105922. https://doi.org/10.1016/j.cropro.2021.105922

Liu F., Weir B.S., Damm U., Crous P.W., Wang Y., … Cai L., 2015. Unravelling *Colletotrichum* species associated with *Camellia*: employing ApMat and GS loci to resolve species in the *C. gloeosporioides* complex. *Persoonia* 35: 63–86. https://doi.org/10.3767/003158515X687597

Malandrakis A.A., Kissandraki M., Mikalef L., Ntougias S., Kavroulakis N., 2023. First record of *Neofusicoccum luteum* and *Colletotrichum gloeosporioides* causing anthracnose and stem end rot on avocado fruits in Greece. Plant Disease 107: 3308. https://doi.org/10.1094/PDIS-12-22-2826-RE

Minh B.Q., Schmidt H.A., Chernomor O., Schrempf D., Woodhams M.D., von Haeseler A., Lanfear R., 2020. IQ-TREE 2: New models and efficient methods for phylogenetic inference in the genomic era. *Molecular Biology and Evolution* 37: 1530–1534. https://doi.org/10.1093/molbev/msaa015

Montealegre J., Herrera F., Mondaca C., Herrera R., 2002. *Colletotrichum gloeosporioides* as causal agent of postharvest avocado rots. XI National Conference of Phytopathology, Santa Cruz, Chile. *Fitopatología* 37: 67–108.

Morales A., Berger H., Luza J., 1979. Identificación de hongos causantes de pudriciones en almacenaje refrigerado de paltas (*Persea americana* Mill.) Fuerte y Negra La Cruz. *Investigación Agrícola* 5: 1–4.

Munir M., Amsden B., Dixon E., Vaillancourt L., Ward Gauthier N.A., 2016. Characterization of *Colletotrichum* species causing bitter rot of apple in Kentucky orchards. *Plant Disease* 100: 2194–2203. https://doi.org/10.1094/PDIS-10-15-1144-RE

Nelson S.C., 2008. Anthracnose of avocado. *Plant Disease* 58: 1–6. https://www.ctahr.hawaii.edu/oc/freepubs/pdf/PD-58.pdf

ODEPA-CIREN, 2024. Catastro frutícola: principals resultados. Región de O'Higgins. Oficina de Estudios y Políticas Agrarias (ODEPA) – Centro de Información de Recursos Naturales (CIREN), Santiago, Chile. Available online: https://bibliotecadigital.odepa.gob.cl/bitstream/handle/20.500.12650/71984/Catastro_Fruticola_REGION_MAULE.pdf

O'Donnell K., Cigelnik E., 1997. Two divergent intragenomic rDNA ITS2 types within a monophyletic lineage of the fungus *Fusarium* are nonorthologous. *Molecular Phylogenetics and Evolution* 7: 103–116. https://doi.org/10.1006/mpev.1996.0376

Oo M.M., Yoon H.Y., Jang H.A., Oh S.K., 2018. Identification and characterization of *Colletotrichum* species associated with bitter rot disease of apple in South Korea. *Plant Pathology Journal* 34: 480–489. http://doi.org/10.5423/PPJ.FT.10.2018.0201

Prihastuti H., Cai L., Chen H., McKenzie E.H.C., Hyde K.D., 2009. Characterization of *Colletotrichum* species associated with coffee berries in northern Thailand. *Fungal Diversity* 39: 89–109. https://doi.org/10.3114/sim0011

Prusky D., Plumbley R.A., 1992. Quiescent infections of *Colletotrichum* in tropical and subtropical fruits. In: *Colletotrichum: Biology, Pathology and Control*, 1st ed.; (Bailey J.A., Jeger M.J., eds). CABI, Wallingford, UK, pp. 289–307.

Ramírez-Gil J.G., López J.H., Henao-Rojas J.C., 2020. Causes of Hass avocado fruit rejection in preharvest, harvest, and packinghouse: economic losses and associated variables. *Agronomy* 10: 8. https://doi.org/10.3390/agronomy10010008

Ramos A.P., Talhinhas P., Sreenivasaprasad S., Oliveira H., 2016. Characterization of *Colletotrichum gloeosporioides* as the main causal agent of citrus anthracnose, and *C. karstii* as species preferentially associated with lemon twig dieback in Portugal. *Phytoparasitica* 44: 549–561. https://doi.org/10.1007/s12600-016-0537-y

Riolo M., Aloi F., Pane A., Cara M., Cacciola S.O., 2021. Twig and shoot dieback of citrus, a new disease caused by *Colletotrichum* species. *Cells* 10: 449. https://doi.org/10.3390/cells10020449

Ronquist F., Teslenko M., van der Mark P., Ayres D.L., Darling A., … Huelsenbeck J., 2012. MrBayes 3.2: Efficient Bayesian phylogenetic inference and model choice across a large model space. *Systematic Biology* 61: 539–542. https://doi.org/10.1093/sysbio/sys029

Rose C., Damm, U., 2024. Diversity of *Colletotrichum* species on strawberry (*Fragaria* × *ananassa*) in Germany. *Phytopathologia Mediterranea* 63: 155–178. https://doi.org/10.36253/phyto-15094

Senanayake I.C., Rathnayaka A.R., Marasinghe D.S., Calabon M.S., Gentekaki E., … Xiang M.M., 2020. Morphological approaches in studying fungi: collection, examination, isolation, sporulation and preservation. *Mycosphere* 11(1): 2678–2754. https://doi.org/10.5943/mycosphere/11/1/20

Sharma G., Maymon M., Freeman S., 2017. Epidemiology, pathology and identification of *Colletotrichum* including a novel species associated with avocado (*Persea americana*) anthracnose in Israel. *Scientific Reports* 7: 15839. https://doi.org/10.1038/s41598-017-15946-w

Shivas R.G., Tan Y.P., 2009. A taxonomic re-assessment of *Colletotrichum acutatum*, introducing *C. fioriniae* comb. et stat. nov. and *C. simmondsii* sp. nov. *Fungal Diversity* 39: 111–122.

Silva D.N., Talhinhas P., Cai L., Manuel L., Gichuru E.K., Loureiro A., Várzea V., Paulo O.S., Batista D., 2012a. Host-jump drives rapid and recent ecological speciation of the emergent fungal pathogen *Colletotrichum kahawae*. *Molecular Ecology* 21: 2655–2670. https://doi.org/10.1111/j.1365-294X.2012.05557.x

Silva D.N., Talhinhas P., Várzea V., Paulo O.S., Batista D., 2012b. Application of the Apn2/MAT locus to improve the systematics of the *Colletotrichum gloeosporioides* complex: An example from coffee (*Coffea* spp.) hosts. *Mycologia* 104(2): 396–409. https://doi.org/10.3852/11-145

Soares M.G.O., Alves E., Silveira A.L., Pereira F.D., Guimarães S.S.C., 2020. *Colletotrichum siamense* is the main aetiological agent of anthracnose of avocado in south-eastern Brazil. *Plant Pathology* 70: 154–166. https://doi.org/10.1111/ppa.13262

Stöver B.C., Müller K.F., 2010. TreeGraph 2: Combining and visualizing evidence from different phylogenetic analyses. *BMC Bioinformatics* 11: 7. https://doi.org/10.1186/1471-2105-11-7

Thanh L.T.H., Tien N.T.T., Trang N.T.T., Nguyen T.T.T., Le K.Q., Bui T.Q. et al.,, 2025. First report of *Colletotrichum siamense* and *Colletotrichum endophyticum* associated with anthracnose on avocado (*Persea americana*) in Vietnam. *Journal of Plant Pathology* 107: 633–647. https://doi.org/10.1007/s42161-024-01813-x

Velho A.C., Alaniz S., Casanova L., Mondino P., Stadnik M.J., 2015. New insights into the characterization of *Colletotrichum* species associated with apple diseases in southern Brazil and Uruguay. *Fungal Biology* 119(4): 229–244. https://doi.org/10.1016/j.funbio.2014.12.009

Vieira A., Silva D.N., Várzea V., Salgueiro Paulo O., Batista D., 2018. Novel insights on colonization routes and evolutionary potential of *Colletotrichum kahawae*, a severe pathogen of *Coffea arabica*. *Molecular Plant Pathology* 19: 2488–2501. https://doi.org/10.1111/mpp.12726

Weir B.S., Johnston P.R., Damm U., 2012. The *Colletotrichum gloeosporioides* species complex. *Studies in Mycology* 73: 115–180. https://doi.org/10.3114/sim0011

White T.J., Bruns T., Lee S., Taylor J., 1990. Amplification and direct sequencing of fungal ribosomal RNA genes for phylogenetics. In: *PCR Protocols: A Guide to Methods and Applications*. (Innis M.A., Gelfand D.H., Shinsky J.J., White T.J., ed.). Academic Press, San Diego, CA, USA, pp. 315–322.

Wu C.-J., Lin M.-C., Ni H.-F., 2023. *Colletotrichum* species causing anthracnose disease on avocado fruit in Taiwan. *European Journal of Plant Pathology* 165: 629–647. https://doi.org/10.1007/s10658-022-02635-2

Zakaria L., 2021. Diversity of *Colletotrichum* species associated with anthracnose disease in tropical fruit crops: a review. *Agriculture* 11: 297. https://doi.org/10.3390/agriculture11040297

Zapata M., Rodríguez-Serrano E., Castro J.F., Santelices C., Carrasco-Fernández J., Damm U., Palfner G., 2024. Novel species and records of *Colletotrichum* associated with native woody plants in south-central Chile. *Mycological Progress* 23: 18. https://doi.org/10.1007/s11557-024-01956-2

Zapata M., Opazo A., 2017. Detection of *Colletotrichum pyricola* on urban trees of *Embothrium coccineum* in Chile. *Bosque (Valdivia)* 38: 195–201. https://doi.org/10.4067/S0717-92002017000100019

Phytopathologia Mediterranea
The international journal of the
Mediterranean Phytopathological Union

Firenze University Press
www.fupress.com/pm

Research Papers

Beyond the primary host: survival of *Heterodera schachtii* (*Nematoda, Heteroderidae*) through alternative hosts

Diogo AZEVEDO[1], Eugénia de ANDRADE[2,3], Maria L. INÁCIO[2,3,*], Ana Paula RAMOS[4,5,*], Maria João CAMACHO[2,3]

[1] *Instituto Superior de Agronomia (ISA), Universidade de Lisboa, Tapada da Ajuda, 1349-017 Lisboa, Portugal*
[2] *Instituto Nacional de Investigação Agrária e Veterinária (INIAV, I.P.), Quinta do Marquês, 2780-159 Oeiras, Portugal*
[3] *Green-it Bioresources for Sustainability, ITQB NOVA, 2780-159 Oeiras, Portugal*
[4] *Linking Landscape, Environment, Agriculture and Food Research Centre (LEAF), Associate Laboratory TERRA, Instituto Superior de Agronomia, Universidade de Lisboa, Tapada da Ajuda, 1349-017, Lisbon, Portugal*
[5] *Laboratório de Patologia Vegetal Veríssimo de Almeida (LPVVA), Instituto Superior de Agronomia, Universidade de Lisboa, Tapada da Ajuda, 1349-017, Lisbon, Portugal*
*Corresponding authors. E-mail: lurdes.inacio@iniav.pt, pramos@isa.ulisboa.pt

Summary. Plant-parasitic nematodes are an underestimated cause of crop yield losses. Cyst nematodes, particularly *Heterodera* spp., are important pests of sugar beet, cereals, and soybean. Presence of these nematodes was investigated in a plot near Lisbon (Golegã), where problems with cyst nematode infestations had been detected. *Heterodera* cysts were extracted and isolated from soil samples, and were identified morphologically and using PCR and DNA sequencing. Morphological identifications were difficult, but molecular analyses confirmed the presence of *H. schachtii*, linking this with the plot's history. This nematode had remained viable in the soil for more than 15 years, despite absence of sugar beet, the primary host.

Keywords. Cyst nematodes resilience, population dynamics, host range, morphological identification, molecular identification.

OPEN ACCESS

Citation: Azevedo, D., de Andrade, E., Inácio, M. L., Ramos, A. P., & Camacho, M. J. (2026). Beyond the primary host: survival of *Heterodera schachtii* (*Nematoda*, *Heteroderidae*) through alternative hosts. *Phytopathologia Mediterranea* 65(1): 33-42. doi: 10.36253/phyto-16650

Accepted: November 4, 2025

Published: March 16, 2026

© 2026 Author(s). This is an open access, peer-reviewed article published by Firenze University Press (https://www.fupress.com) and distributed, except where otherwise noted, under the terms of the CC BY 4.0 License for content and CC0 1.0 Universal for metadata.

Data Availability Statement: All relevant data are within the paper and its Supporting Information files.

Competing Interests: The Author(s) declare(s) no conflict of interest.

Editor: Isabel Luci Pisa Mata da Conceição, University of Coimbra, Portugal.

ORCID:
EDA: 0000-0002-6781-5234
MLI: 0000-0002-6883-5288
APR: 0000-0001-5974-7481
MJC: 0000-0002-2432-1234

INTRODUCTION

Nematodes in soil are commonly classified into functional groups based on their feeding strategies which reflect their roles in soil ecosystems (Yeates *et al*., 1993; Decraemer and Hunt, 2013). The plant-parasitic nematodes predominantly occupy upper soil layers, where organic matter and plant roots are abundant. Their stylets inject enzymes into plant cells to extract cell contents for feeding (Camacho *et al*., 2020).

Cyst nematodes are economically important (Camacho *et al*., 2017), contributing to yield losses in agricultural crops (Sikora *et al*., 2023). Their

damage is intensified by the interactions with biotic and abiotic factors including soil pathogens, low soil fertility, reduced soil biodiversity, and climate variability (Sikora *et al*., 2023). The most important cyst nematode species belong to the genera *Heterodera* and *Globodera,* which are endoparasites of plant roots (Lilley *et al*., 2005; Smiley and Nicol, 2009). Moreover, eggs and juvenile forms can survive in the soil within cysts for long periods, potentially lasting several years, until a susceptible host is present in the area (Lilley *et al*., 2005; Hunt, 2008; Smiley and Nicol, 2009). Although it is difficult to predict how long sugar beet cyst nematodes may survive in soil without hosts, a small percentage of eggs within each cyst can survive for 12 years under fallow conditions (Khan *et al*., 2021). This longevity is particularly important because it limits the effectiveness of control methods and reduces the growth of specific crops.

Heterodera life cycles begin with eggs and progress through four juvenile stages, each separated by moults, before reaching adult stages (male or female) (Lilley *et al*., 2005; Hunt, 2008). Each female can contain 100 to 600 eggs enclosed in a lemon-shaped cyst (Hunt, 2008; Smiley and Nicol, 2009). Nematodes of this genus complete their life cycles in 21 to 25 days (Inagaki and Tsutsumi, 1971), and can have more than one generation per year (Turner and Subbotin, 2013), due to the short life cycle, adaptability to warm climates, and reduced dormancy requirements, and thus cause damage in crop fields. The most important *Heterodera* species are *Heterodera glycines* Ichinohe (soybean cyst nematode), *Heterodera avenae* Wollenweber (cereal cyst nematode), *Heterodera schachtii* Schmidt (sugar beet cyst nematode) and *Heterodera zeae* Koshy, Swarup & Sethi (corn cyst nematode) (Lilley *et al*., 2005; Moens *et al*., 2018).

Traditionally, *Heterodera* species are identified using cyst and juvenile morphology and morphometrics (Golden, 1986; Rivoal *et al.,* 2003). This is time-consuming and requires knowledge and experience (Yan and Smiley, 2009). However, morphological identification is not always reliable, making it important to confirm results through molecular identification methods (Seesao *et al*., 2016; Camacho *et al*., 2017), and several DNA-based methods are used to study nematodes biodiversity. These include amplification of barcoding sequences by conventional PCR followed by DNA sequencing. The most used barcoding sequences are the LSU (28S rDNA), SSU (18S rDNA), the full ITS-rDNA region and mt*COI* gene (Nisa *et al*., 2022; Camacho *et al*., 2025). Given these challenges, the primary goal of the present study was to investigate the presence and survival of Heterodera schachtii cyst nematodes in agricultural fields in the Golegã region of Portugal, due to their historical occurrence in soils where sugar beet had been cultivated for approximately 15 years.

MATERIALS AND METHODS

Location and establishment of study plots

This study was carried out in agricultural fields in the Golegã region, central Portugal (39°23′07″N; 8°29′26″W). These fields had been cultivated over the previous 15 years with crops of wheat, corn, potatoes, and peas, as well as cover crops including brassicas, grasses, and legumes, either as single species or as mixtures, namely: (A) *Avena strigosa* and *Raphanus sativus* var. *oleiferus*; (B) *Avena strigosa*, *Brassica carinata*, *Brassica napus*, *Lathyrus sativus*, *Lolium multiflorum*, *Pisum sativum*, *Raphanus sativus* var. *longipinnatus*, *Raphanus sativus* var. *oleiferus*, *Sinapis alba*, *Trifolium* spp., and *Vicia sativa*; and (C) *Avena sativa*, *Lolium multiflorum*, *Trifolium* spp., and *Vicia sativa*. Although sugar beet was no longer cultivated in these fields, this crop had been grown until 2008.

Sampling and processing of soil samples

Sampling was carried out in agricultural fields according to Annex II of DL 87/2010 (Portuguese Ministry of Agriculture, 2010). Twenty soil samples, each of approx. 1 L, were randomly collected from bare soil, across a zigzag pattern, and at depth of 20 to 25 cm, which corresponded to the depth of the rhizosphere. The top layer of soil was removed to avoid plant debris and possible contaminants. The samples were then stored in labelled plastic bags.

The samples were transported to the Nematology Laboratory of the Instituto Nacional de Investigação Agrária e Veterinária, I.P. - INIAV in Oeiras, Portugal, where they were kept at room temperature for 3 days to dry. The Fenwick can then was used to extract cyst nematodes from samples of maximum weight 400 g, according to EPPO protocols PM7/119(1) (EPPO, 2013a) and PM7/40(3) (EPPO, 2013b). The samples were then assessed using a light microscope (Olympus Bx51) equipped with a Leica MC190 HD optical camera, and software version LAS V4.12 (Leica Microsystems). When lemon-shaped cysts characteristic of *Heterodera* were observed, they were isolated and stored at room temperature to be used in later analyses (Fenwick, 1940; EPPO, 2013b).

Morphological identification of Heterodera *spp.*

Vulval cones were cut from isolated cysts with an ophthalmic scalpel, and released eggs and second-stage juveniles (J2) were mounted in sterile tap water. Morphological and morphometric characteristics of ten second-stage juveniles from each selected cyst were then assessed, and were compared with available descriptions (Subbotin *et al*., 2010).

Molecular identification of Heterodera *spp.*

DNA extraction and amplification: Viable juveniles from cysts analysed morphologically were used for DNA extractions using the QIAamp® DNA Mini Kit (Qiagen), following the manufacturer's instructions. The mt*COI* gene, and the 18S rDNA and 28S rDNA regions were amplified as described in Table 1. PCR reactions were carried out using a Biometra TOne Gradient thermocycler (Biometra). Possible contaminations were evaluated by including non-template controls (NTC) without DNA.

Amplified products were loaded onto a 1.5% agarose gel in TAE, and then subjected to electrophoresis at 5 V cm^{-1} in a Mupid One System (Nippon Genetics Europe). This system allows visualization and detection of DNA fragments during each run, using direct staining of DNA with Midori Green (Nippon Genetics Europe) together with safe Blues LEDs that do not degrade or mutate DNA.

Sequencing and sequence quality control: PCR products were enzymatically purified using ExoSAP-IT PCR Product Cleanup (Thermo Fisher), following the manufacturer's instructions (incubation for 15 min at 37°C, followed by 15 min at 85°C). Cycle sequencing was carried out with the ABI BigDye Cycle sequencing kit (Applied Biosystems) on an ABI Prism 3130XL capillary sequencer (Applied Biosystems), in both directions using the same PCR primers. Sanger sequencing was outsourced at the molecular biology laboratory of INIAV (Oeiras, Portugal).

Chromatograms were visualized and nucleotide sequences were edited and analysed using BioEdit v7.2.0 (Ibis Biosciences) and MEGA X version 10.2.6 (Pennsylvania State University). Unidirectional sequences were each considered successful when the sequence of the complementary primer was present at the 3'end, no double peaks were observed, and high fluorescence was measured along the entire sequence. The mt*COI* sequence was translated using the translation table 5 for invertebrate mtDNA genetic code and aligned. Non-stop codons were not visualized.

When all the quality criteria were fulfilled, the primer sequences were trimmed, and a consensus sequence was generated. The resulting mt*COI*, 18S rDNA and 28S rDNA consensus sequences were used to investigate, by a blast search the "core nucleotide database (core-nt)" in NCBI GenBank, to identify the most similar sequences within *Heterodera* species.

Phylogenetic analyses

The nucleotide alignments were also used to construct distance trees. All sequences were aligned by CLUSTAW with default parameters. The pairwise aligned sequences were phylogenetically analysed by the Neighbor-Joining Tree-Built method and the Tamura-Nei Genetic Distance model employing MEGA X version 10.2.6 software (Pennsylvania State University). A bootstrap analysis with 1000 replications was also conducted to infer robustness of the phylogenetic trees. Sequences from *Globodera rostochiensis* were selected as the outgroup.

RESULTS

Morphological identification of Heterodera *spp.*

Cysts were light to dark brown. By cutting the vulval cone of *Heterodera* cysts, it was possible to identify eggs (Figure 1 A), second-stage juveniles (Figure 1 B), and the vulval cone characteristics (Figure 2).

Second-stage juveniles were vermiform, with annulated bodies that tapered at both ends (Figure 1 B). Mean body length was 429 (± 18) µm, the heads were offset, and the cuticles were regularly annulated, each with four lateral fields extending from near the head to the tail (Figure 1 C). Stylets were well developed of mean length 23 (± 1) µm, with anterior concave knobs. The tails gradually tapered towards finely rounded termini, and were mean length 49 (± 2) µm, with hyaline parts of mean length 25 (± 1) µm. The vulvas were ambifenestrate and each divided into two semifenestrae by a vulval bridge (Figure 2 A), and within the cone, remains of a vagina was attached to side walls by a well-developed underbridge and a number of irregularly arranged, dark brown bullae situated a short distance beneath vulval bridge (Figure 2 B). By comparing the data reported by Subbotin *et al*. (2010), these nematodes were identified as *Heterodera schachtii.*

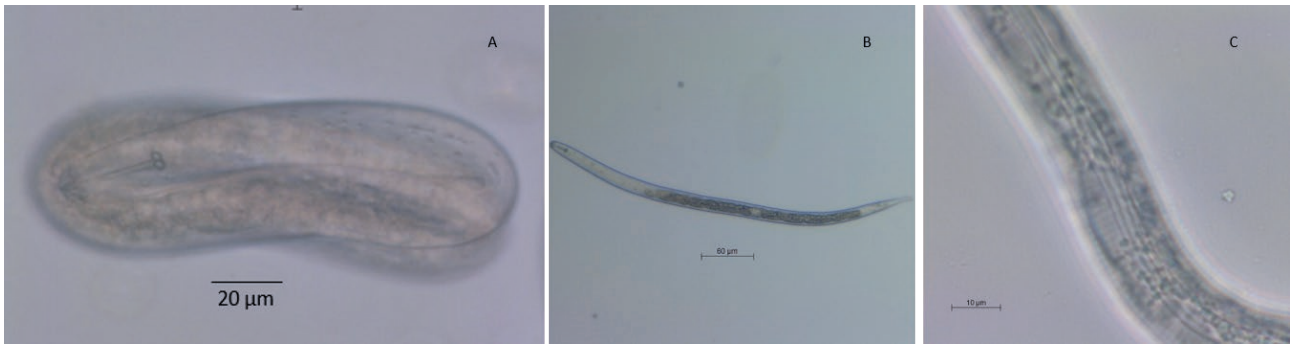

Figure 1. A: Egg of *Heterodera* nematode containing a fully developed second-stage juvenile, ready to emerge. B: Fully developed second-stage juvenile. C: Juvenile cuticle regularly annulated with four lateral fields (C).

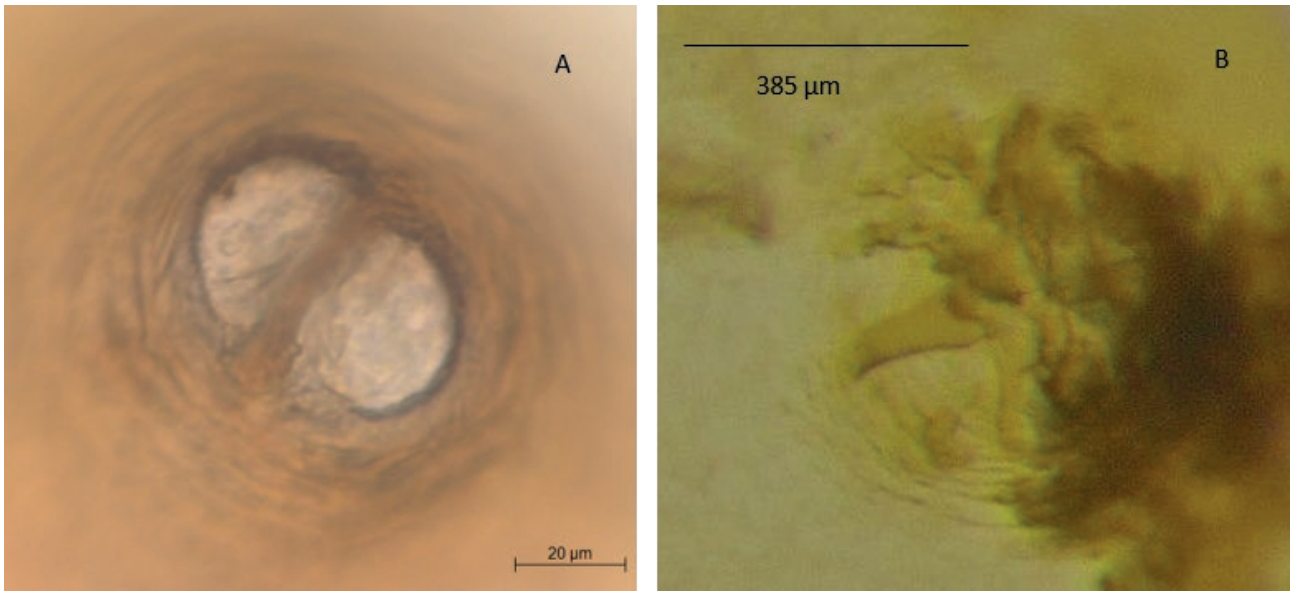

Figura 2. A: *Heterodera* vulval cone, vulva ambifenestrate divided into two semifenestrae by the vulval bridge. B: The cone has bullae and a well-developed underbridge.

Molecular identification of Heterodera schachtii

Using the procedure previously described, all primer pairs allowed amplification in the tested samples. Assembled sequences were compared with the GenBank database to confirm nematode identity. For the mt*COI* sequence, all hits had coverage of 99%, that allowed identification of the *H. schachtii*. The nucleotide sequences had 100% similarity with other *H. schachtii* sequences from the Iberian region (Sevilla, Spain -MW345380-MW345391; Faro and Leiria, Portugal -PQ462045-PQ462046). For the 18S rDNA sequence, all hits had coverage of 99%, that allowed identification of *H. schachtii*. The nucleotide sequences had 100% similarity with *H. schachtii* sequences from Gent University, Belgium (EU306355). For the 28S rDNA sequence, all hits had coverage of 96%, that allowed identification of *H. schachtii*. The nucleotide sequences had 99.72% similarity with *H. schachtii* sequences from Jeongseon, South Korea (MN720062).

The sequences were deposited at NCBI database under accession numbers PQ462055 (for mt*COI*), PV351709 (for 18S rDNA), and PV351741 (for 28S rDNA), and were also used to obtain the phylogenetic tree at NCBI platform through the Neighbour Joining method as a confirmation step of identification (data not shown).

Table 1. PCR conditions, master mix used: Supreme NZYTaq II 2× Green Master Mix (NZYTech).

Primers (Reference)	Primers sequences	Amplicon size	Thermal cycling conditions	Reaction mix
18S rDNA gene region				
988F/1912R and 1813F/2646R (Hu *et al*., 2002)	988F: 5'-CTC AAA GAT TAA GCC ATG C-3' 1912R: 5'-TTT ACG GTC AGA ACT AGG G-3' 1813F: 5'-CTG CGT GAG AGG TGA AAT-3' 2646R: 5'-GCT ACC TTG TTA CGA CTT TT-3'	98 0bp and 880 bp, resulting a 1730 bp	Initial denaturation of 94°C for 5 min 53 cycles (94°C for 30 s, 45°C for 30 s and 72°C for 70 s) 35 cycles (94°C for 30 s, 54°C for 30 s and 72°C for 70 s) Final extension of 72°C for 10 min	– 5 µL of template DNA – 12.5 µL of Master Mix (NZYTech) – 1.5 µL of each primer – 4.5 µL of water
28S rDNA region				
D2A/D3B (Holterman *et al*., 2006)	D2A: 5´-ACA AGT ACC GTG AGG GAA AGT TG-3´ D3B:5´-TCG GAA GGA ACC AGC TAC TA-3´	780 bp	Initial denaturation of 95°C for 10 min 40 cycles (95°C for 30 s, 60°C for 45 s and 72°C for 45 s) Final extension of 72°C for 10 min	– 2 µL of template DNA – 12.5 µL of Master Mix – 0.75 µL of each primer – 9 µL of water
Mitochondrial cytochrome oxidase subunit one (mt*COI*) gene region				
JB3/ JB5 (Ley *et al*., 1999)	JB3: 5´- TTT TTT GGG CAT CCT GAG GTT TAT -3´ JB5: 5'- AGC ACC TAA ACT TAA AAC ATA ATG AAA ATG -3´	447 bp	Initial denaturation of 98°C for 1 min 40 cycles (8°C for 10 s, 41°C for 20 s and 72°C for 30 seg) Final extension of 72°C for 10 min	– 5 µL of template DNA – 12.5 µL of Master Mix – 1.5 µL of each primer – 4.5 µL of water

The phylogenetic relationship of the present study specimen with other *Heterodera* species based on the mt*COI* gene region (Figure 3) was within the *H. schachtii* clade, and was highly supported by a 99% Bootstrap value. Similar situations were observed for the 18S rDNA and 28S rDNA trees (Figures 4 and 5).

The high sequence similarity and consistent phylogenetic results provide robust molecular confirmation of the species identity. These results are consistent with the conclusions of Huston *et al*. (2022) and Camacho *et al*., 2025), who demonstrated the reliability and utility of standard gene sequence barcodes, including mt*COI*, 18S rDNA, and 28S rDNA regions, for accurate identification and differentiation of cyst nematodes within *Heterodera*.

DISCUSSION

Morphological data showed that the cysts obtained in this study were of *Heterodera schachtii*. However, because morphological identification of nematodes is not always reliable, confirmation using molecular methods is recommended (Seesao *et al*., 2016 and Camacho *et al*., 2017)). In the present case, the morphological and molecular analyses confirmed the identification of *H. schachtii*, with JB3-JB5 being the best primer pair for *H. schachtii* identification. This is in agreement with previous research that highlights the reliability of standard gene sequence barcodes for identification of *Heterodera* species (Huston *et al*., 2022, Camacho *et al*., 2025).

Heterodera schachtii is a parasite of several plant families, including *Brassicaceae*, *Chenopodiaceae* and *Cruciferae* (Raski, 1950), with sugar beet being its primary host (Mwamula *et al*., 2019). Given the history of the plot assessed in the present study and known hosts of *H. schachtii*, presence of these nematodes was likely. The present results show that cysts of *H. schachtii* remained viable after more than 15 years without cultivation of sugar beet, the main host crop this nematode. However, during this period, the plot was intermittently covered by many different plants, including associations with brassicas, particularly forage radish (*Raphanus sativus* var. *longipinnatus* and *Raphanus sativus* var. *oleiferus*), as well as plants used for green manuring, and weeds (*Avena sativa, Avena strigosa, Brassica carinata, Brassica napus, Lathyrus sativus*, *Lolium multiflorum, Pisum sativum, Sinapis alba, Trifolium* spp. and *Vicia sativa*). Among the plant species that have been cultivated in the studied plot, several have been described as hosts of *H. schachtii* (Goodey *et al*., 1965). Although the *R. sativus* cultivars used are resistant to *H. schachtii* (Eberlein *et al*., 2020), and were grown as a trap crop to reduce nem-

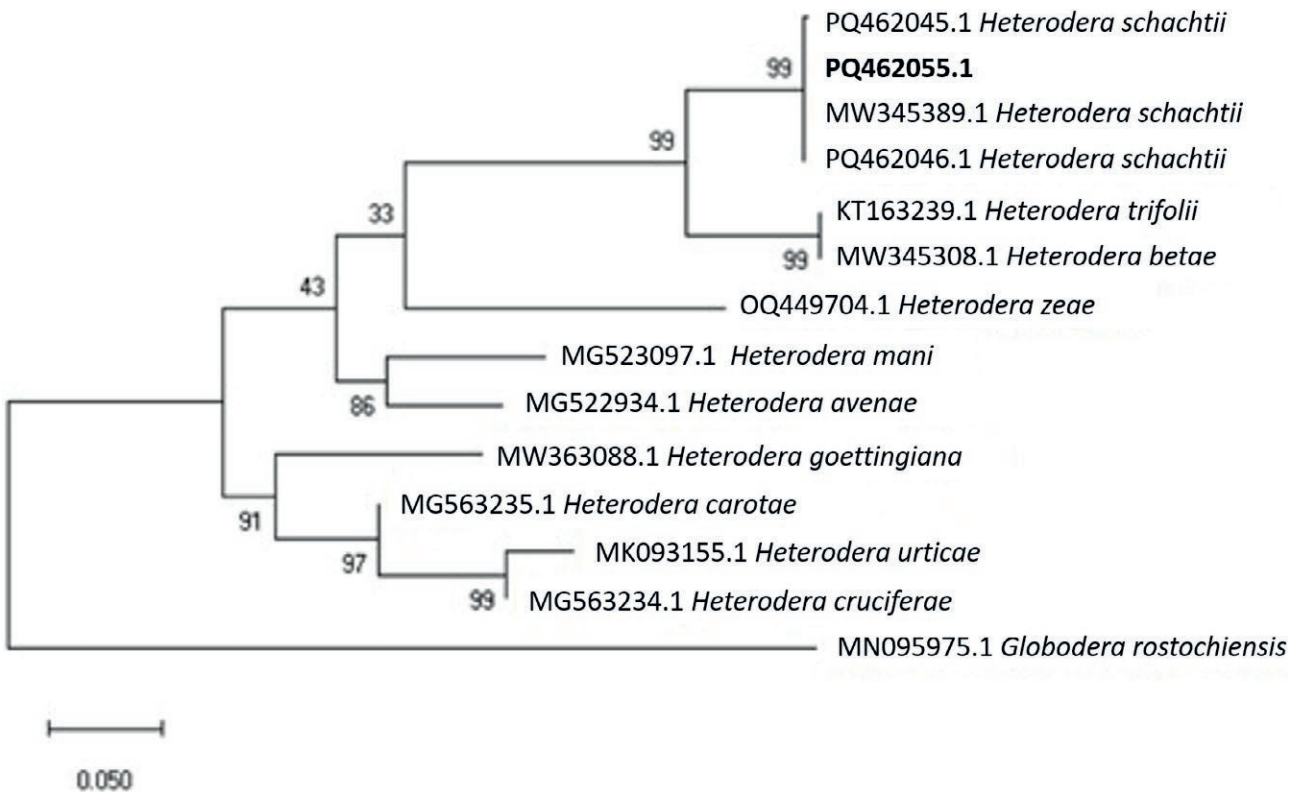

Figure 3. Phylogenetic tree for *Heterodera* spp. based on sequence alignment of the mitochondrial cytochrome oxidase subunit one (mt*COI*) gene. The analysis involved 14 nucleotide sequences, including the PQ462055.1 sequence, identified as *Heterodera schachtii. Globodera rostochiensis* was used as the outgroup taxon. The condensed phylogenetic tree was generated using the Neighbor-Joining method with 1,000 bootstrap replications. Bootstrap values are indicated at the nodes.

atode densities, other brassicas may have contributed to persistence of the population. However, it is not possible to retrospectively determine whether any weed species harboured *H. schachtii* populations, or whether the brassicas used as cover crops, despite being considered nematode-resistant, may have sustained them. Previous studies allowing for greater control of variables, have been time restricted. This highlights the relevance of the present work, as it provides new insights into the prevalence of these nematodes in agricultural fields that have been without primary hosts for more than 15 years. Besides, no brassicas were included in the crop rotations over the past 3 years, yet *Heterodera* populations remained viable in the soil.

In the study of Westphal and Becker (2001), neither resistant nor susceptible radish cultivars allowed *H. schachtii* development. Therefore, it is concluded that for management of these nematodes in infested fields, brassicas can be used as cover crops unless resistant varieties to *H. schachtii* are selected.

Heterodera eggs within cysts can remain viable in soil, but dormant for several years (Lilley *et* al., 2005**;** Smiley *et al.,* 2009; Hunt, 2008). However, previous studies have not provided specific observations on duration of cyst viability in the absence of primary hosts. The present study documents the prolonged survival of lemon-shaped cysts of *H. schachtii,* in the absence of the nematode's primary host. This underscores the challenges for control of these nematodes, as their extended longevity in soil diminishes the effectiveness of inoculum reduction methods such as fallowing and crop rotations. Therefore, alternative strategies such as using trap crops or resistant cultivars are likely to be the most promising approaches for managing problems caused by *H. schachtii*.

AUTHOR CONTRIBUTIONS

Conceptualization, ML.I. and MJ.C.; methodology, E.A., ML.I., AP.R. and MJ.C.; software, E.A. and MJ.C.; validation, D.A.; E.A. ML.I., AP.R., and MJ.C.; formal analysis, D.A.; E.A., and MJ.C.; resources, E.A. and ML.I.; data curation, E.A. and ML.I; writing-orig-

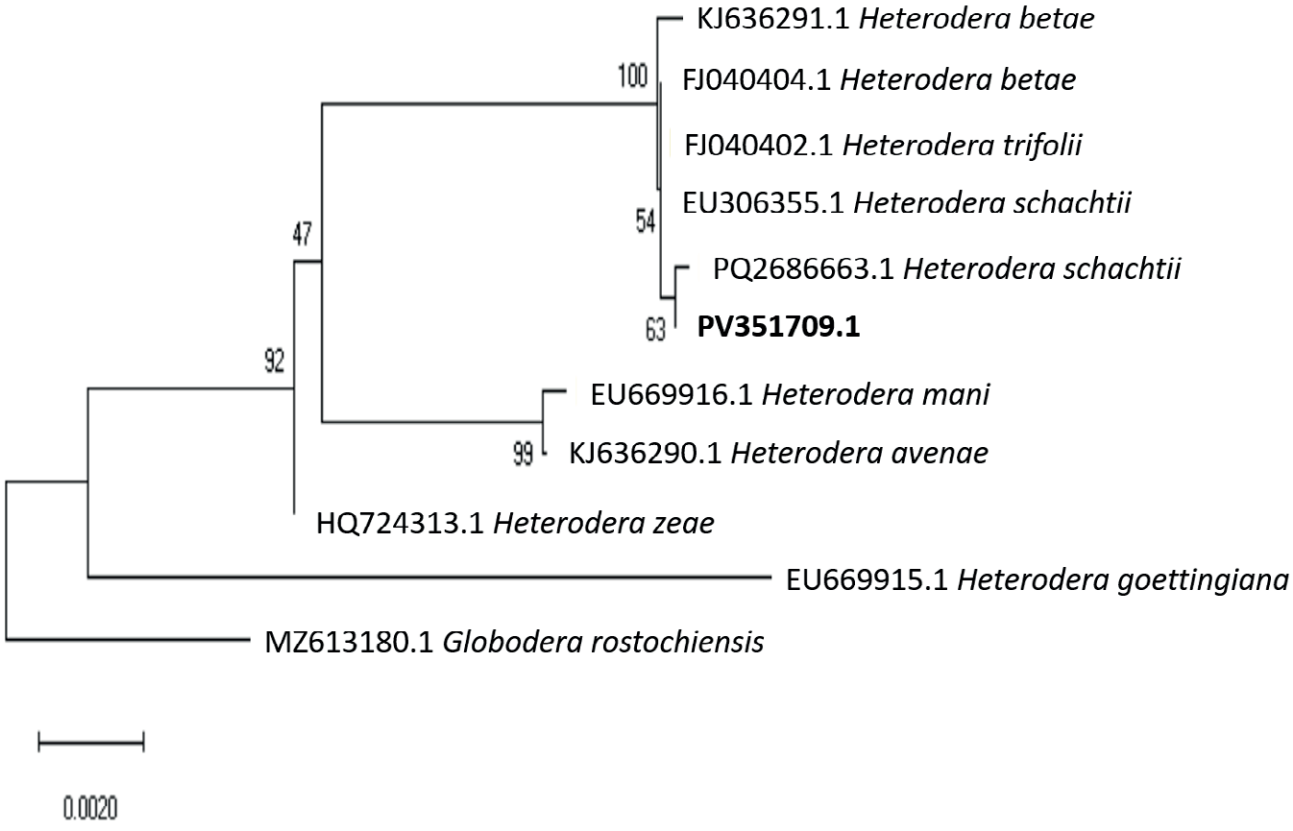

Figure 4. Phylogenetic tree for *Heterodera* spp. based on the sequence alignment of 18S rDNA gene region. The analysis involved 11 nucleotide sequences, including the PV351709.1 sequence, identified as *Heterodera schachtii*. *Globodera rostochiensis* was used as the outgroup taxon. The condensed phylogenetic tree was generated using the Neighbor-Joining method with 1,000 bootstrap replications. Bootstrap values are indicated at the nodes.

inal draft preparation, D.A.; ML.I. and M.J.C.; writing—review and editing, D.A.; ML.I., E.A., ML.I., AP.R. and MJ.C.; visualization, D.A.; ML.I., E.A., ML.I., AP.R. and MJ.C; supervision, ML.I., AP.R. and MJ.C.; project administration, ML.I.; funding acquisition, ML.I. and E.A. All authors have read and agreed to the published version of the manuscript.

FUNDING

LPVVA— Laboratório de Patologia Vegetal Veríssimo de Almeida, Instituto Superior de Agronomia, under Protocol LPVVA - Câmara Municipal de Lisboa,

ACKNOWLEDGMENTS

This research was supported in part by GREEN-IT "BioResources 4 Sustainability" https://doi.org/10.54499/UIDB/04551/2020 and by LPVVA— Laboratório de Patologia Vegetal Veríssimo de Almeida, Instituto Superior de Agronomia, under Protocol LPVVA - Câmara Municipal de Lisboa, and FCT – Fundação para a Ciência e Tecnologia, I.P. through project UID/04129/2025 (https://doi.org/10.54499/UID/04129/2025) of LEAF-Linking Landscape, Environment, Agriculture and Food. The authors extend sincere gratitude to Margarida Fontes and Nídia Laureano for their technical assistance and valuable contributions to parts of the practical work, as well as for the shared enthusiasm and passion for nematode research.

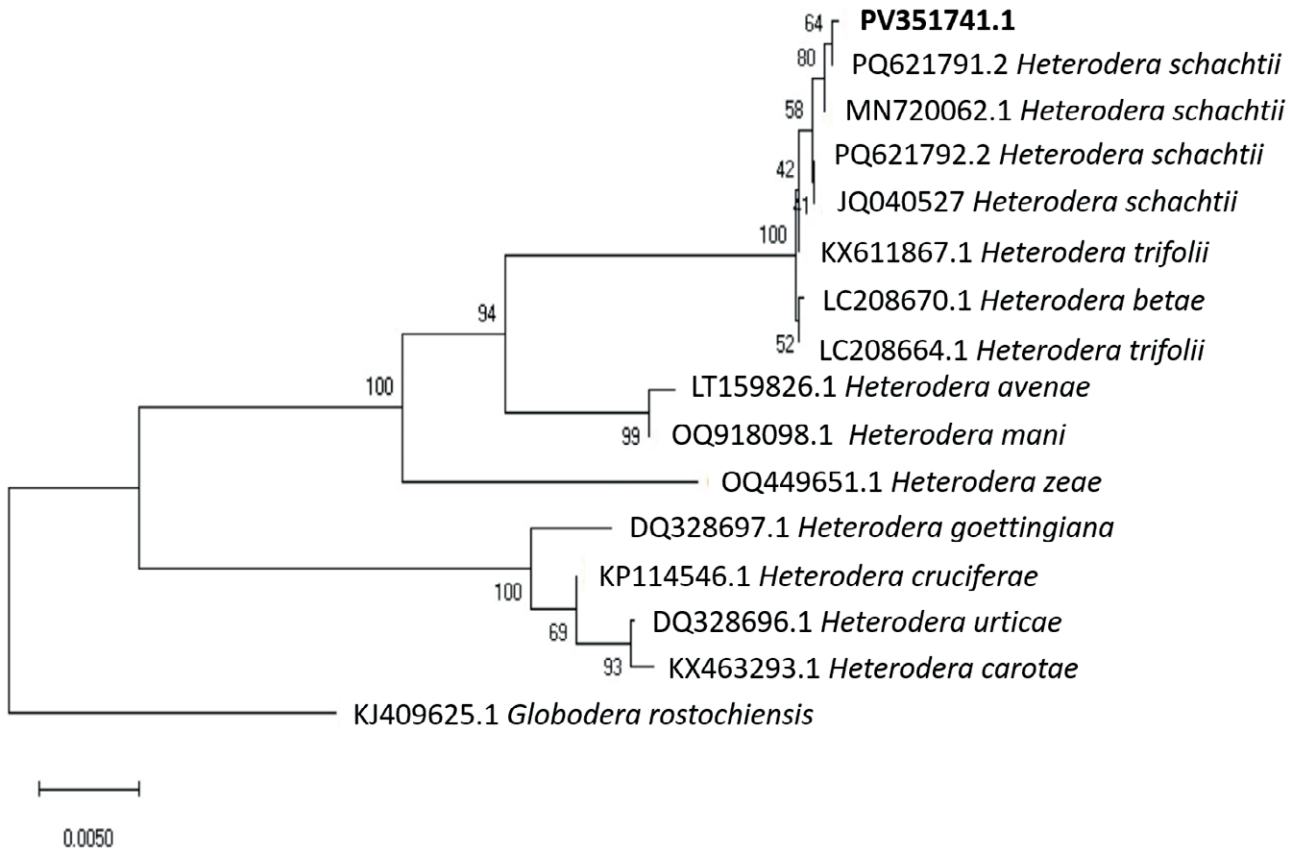

Figure 5. Phylogenetic tree for *Heterodera* spp. based on the sequence alignment of 28S rDNA gene region. The analysis involved 16 nucleotide sequences, including the PV351741.1 sequence, identified as *Heterodera schachtii*. *Globodera rostochiensis* was used as the outgroup taxon. The condensed phylogenetic tree was generated using the Neighbor-Joining method with 1,000 bootstrap replications. Bootstrap values are indicated at the nodes.

LITERATURE CITED

Camacho M.J., Nóbrega F., Lima A., Mota M., Inácio M.L., 2017. Morphological and molecular identification of potato nematodes (*Globodera rostochiensis* and *G. pallida*) in Portuguese potato fields. *Nematology* 19: 883–889. https://doi.org/10.1163/15685411-23000003094

Camacho M.J., Andrade E., Mota M., Nóbrega F., Vicente C., ... Inácio M.L., 2020. Potato cyst nematodes: geographical distribution, phylogenetic relationships and integrated pest management outcomes in Portugal. *Frontiers in Plant Science* 11. https://doi.org/10.3389/fpls.2020.606178

Camacho M. J., Inácio M. L., Andrade E. d., 2025. Multi-Marker Approach for the Identification of Different Heterodera Species (Nematoda: Heteroderidae). *Pathogens* 14: 1052. https://doi.org/10.3390/pathogens14101052

Decraemer W., Hunt D.J., 2013. Structure and classification. In: *Plant Nematology*, 2nd ed. (Perry R.N., Moens M. ed.). CAB International, Wallingford, UK. pp. 3–39.

Eberlein C., Heuer H., Westphal A., 2020. Biological suppression of populations of *Heterodera schachtii* adapted to different host genotypes of sugar beet. *Frontiers in Plant Science* 11: 812. https://doi.org/10.3389/fpls.2020.00812

European and Mediterranean Plant Protection Organization. 2013a. Nematode extraction PM 7/119 (1). *EPPO Bulletin* 43: 471–495. https://doi.org/10.1111/epp.12077

European and Mediterranean Plant Protection Organization. 2013b. *Globodera rostochiensis* and *Globodera pallida* PM 7/40 (3). *EPPO Bulletin* 39: 354–368. https://doi.org/10.1111/epp.12025

Fenwick D., 1940. Methods for the recovery and counting of cysts of *Heterodera schachtii* from soil. *Journal Helminthology* 18: 155–172. http://dx.doi.org/10.1017/S0022149X00031485

Golden A.M., 1986. Morphology and identification of cyst nematodes. In *Cyst Nematodes*. (Lamberti F., Taylor C.E. ed.). Springer, Boston, MA., USA, Volume 121. pp. 23–45. https://doi.org/10.1007/978-1-4613-2251-1_2

Goodey J.B., Franklin M.T., Hooper D.J., 1965. *The Nematode Parasites of Plants Catalogued under their Hosts*. 3rd ed. Commonwealth Agricultural Bureaux, Farnham Royal, UK. 214 pp.

Holterman M., van der Wurff A., Van den Elsen S., Van Megen H., Bongers T., … Helder J., 2006. Phylum-wide analysis of SSU rDNA reveals deep phylogenetic relationships among nematodes and accelerated evolution toward crown clades. *Molecular Biology and Evolution* 23: 1792–1800. https://doi.org/10.1093/molbev/msl044

Hu M., Höglund J., Chilton N.B., Zhu X.Q., Gasser R.B., 2002. Mutation scanning analysis of mitochondria cytochrome c oxidase subunit 1 reveals limited gene flow among bovine lungworm subpopulations in Sweden. *Electrophoresis* 23: 3357–3363. https://doi.org/10.1002/1522-2683(200210)23:19<3357::AID-ELPS3357>3.0.CO;2-B

Hunt D., 2008. *Heterodera glycines* (soybean cyst nematode). *CABI Compendium*. https://doi.org/10.1079/cabicompendium.27027

Huston D.C., Khudhir M., Hodda M., 2022. Reliability and utility of standard gene sequence barcodes for the identification and differentiation of cyst nematodes of the genus *Heterodera*. *Journal of Nematology* 54: e2022-0024. https://doi.org/10.2478/jofnem-2022-0024

Inagaki H., Tsutsumi M., 1971. Survival of the soybean cyst nematode, *Heterodera glycines* Ichinohe (Tylenchida: Heteroderidae) under certain storing conditions. *Applied Entomology and Zoology* 6: 156–162. https://doi.org/10.1303/aez.6.156

Khan M.F.R., Arabiat S., Chanda A.K., Yan G., 2021. Sugarbeet Cyst Nematode. In: *Plant Disease Management (NDSU Extension)*, PP1788.

Ley P.D., Felix M., Frisse L., Nadler S., Sternberg P., Thomas W.K., 1999. Molecular and morphological characterisation of two reproductively isolated species with mirror-image anatomy (Nematoda: Cephalobiidae). *Nematology* 1(6): 591–612. https://doi.org/10.1163/156854199508559

Lilley C.J., Atkinson H.J., Urwin P.E., 2005. Molecular aspects of cyst nematodes. *Molecular Plant Pathology* 6: 577–588. https://doi.org/10.1111/j.1364-3703.2005.00306.x

Moens M., Perry R.N., Jones J.T., 2018. Cyst nematodes – life cycle and economic importance. In *Cyst Nematodes*, 1st ed. (Perry R.N., Moens M., Jones J.T. ed.). CAB International, Wallingford, UK. pp. 1–26. https://doi.org/10.1079/9781786390837.0001

Mwamula A.O., Ko H.R., Kim Y., Kim Y.H., Lee J.K., Lee D.W., 2019. Morphological and molecular characterization of *Heterodera schachtii* and the newly recorded cyst nematode, *H. trifolii*, associated with Chinese cabbage in Korea. *Plant Pathology Journal* 35: 90. https://doi.org/10.5423/PPJ.ER.12.2017.0262

Nisa R.U., Tantray A.Y., Shah A.A., 2022. Shift from morphological to recent advanced molecular approaches for the identification of nematodes. *Genomics* 114: 1–12. https://doi.org/10.1016/j.ygeno.2022.110295.

Portuguese Ministry of Agriculture, 2010. Decreto-lei n.º 87/2010 de 16 de julho – Controlo dos nemátodes de quisto da batateira. *Diário da República* I série, nº 137. Available online: www.dre.pt (accessed September 3, 2024).

Raski D.J., 1950. The life history and morphology of the sugar beet nematode, *Heterodera schachtii* Schmidt. *Phytopathology* 40: 135–151.

Rivoal R., Valette S., Bekal S., Gauthier J.P., Yahyaoui A., 2003. Genetic and phenotypic diversity in the graminaceous cyst nematode complex, inferred from PCR-RFLP of ribosomal DNA and morphometric analysis. *European Journal of Plant Pathology* 109: 227–241. https://doi.org/10.1023/A:1022838806268

Seesao Y., Gaya M., Merlinc S., Viscogliosi E., Aliouat-Denis C., Audebet C., 2016. A review of methods for nematode identification. *Journal of Microbiological Methods* 138: 37–49. https://doi.org/10.1016/j.mimet.2016.05.030

Sikora R.A., Helder J., Molendijk L.P.G., Desaeger J., Eves-van den Akker S., Mahlein A.K., 2023. Integrated nematode management in a world in transition: constraints, policy, processes, and technologies for the future. *Annual Review of Phytopathology* 61: 209–230. https://doi.org/10.1146/annurev-phyto-021622-113058

Smiley R.W., Nicol J.M., 2009. Nematodes which challenge global wheat production. In: *Wheat: Science and Trade*, 1st ed.; (Carver B.F., ed). Wiley, Iowa, USA. pp. 171–187.

Subbotin S.A., Mundo-Ocampo M., Baldwin J.G., 2010. Systematics of cyst nematodes (Nematoda: Heteroderinae). In: *Nematology Monographs and Perspectives* 8A; Hunt D.J., Perry R.N. (eds). Brill, Leiden. 351 pp.

Turner S.J., Subbotin S.A., 2013. Cyst nematodes. In: *Plant Nematology*. (Perry R.N., Moens M. ed.). CABI, UK. pp. 110–143.

Westphal A., Becker J.O., 2001. Soil suppressiveness to *Heterodera schachtii* under different cropping sequences. *Nematology* 3: 551–558. https://doi.org/10.1163/156854101753389167

Yan G.P., Smiley R.W., 2009. Distinguishing *Heterodera filipjevi* and *H. avenae* using polymerase chain reaction–restriction fragment length polymorphism and cyst morphology. *Phytopathology* 100: 216–224. https://doi.org/10.1094/PHYTO-100-3-0216

Yeates G., Bongers T., de Goede R., Freckman D., Georgieva S., 1993. Feeding habits in soil nematode families and genera – an outline for soil ecologists. *Journal of Nematology* 25: 315–331.

Phytopathologia Mediterranea
The international journal of the
Mediterranean Phytopathological Union

Firenze University Press
www.fupress.com/pm

Research Papers

Cross-infection and asymptomatic colonization by *Botryosphaeriaceae* fungi on lignified stems of apple and olive, and dormant cuttings of grapevine

Laura HERNÁNDEZ[1], Pedro MONDINO[1], María Julia CARBONE[1], Victoria MOREIRA[1], Oscar BENTANCUR[2], Sandra ALANIZ[1,*]

[1] *Departamento de Protección Vegetal, Facultad de Agronomía, Universidad de la República, Montevideo, Uruguay*
[2] *Departamento de Biometría, Estadística y Computación, Facultad de Agronomía, Universidad de la República, Montevideo, Uruguay*
*Corresponding author. E-mail: salaniz@fagro.edu.uy

Summary. *Botryosphaeriaceae* pathogens have broad host ranges and can move between hosts, particularly those with overlapping geographic distributions. Cross-infection potential and virulence were assessed for 40 isolates of *Botryosphaeria*, *Diplodia*, and *Neofusicoccum* (11 species), originally isolated from apple, olive, or grapevine crops. Progression of asymptomatic colonization beyond visible necrotic lesions was also assessed, to determine minimum pruning distances required for effective pathogen removal. The assays were conducted using detached lignified stems of apple and olive, and dormant cuttings of grapevine. All the isolates cross-infected and colonized stems or cuttings of the three potential hosts, confirming host-independence of these pathogens. Most of the *Neofusicoccum* isolates consistently caused the largest lesions across the three inoculated hosts. Asymptomatic colonization was not detected at distances of 20 or 30 cm beyond visible lesions. However, at 10 cm, one isolate of *N. parvum* colonized the three hosts, and one isolate of *D. seriata* colonized olive host. These results highlight the challenges for managing these pathogens in fruit crops growing in close proximity, and emphasize the urgency of revising the minimum pruning distances required for successful pathogen removal.

Keywords. *Botryosphaeria*, *Diplodia*, *Neofusicoccum,* host jumping, sanitation practices.

OPEN ACCESS

Citation: Hernández, L., Mondino, P., Carbone, M. J., Moreira, V., Bentancur, O., & Alaniz, S. (2026). Cross-infection and asymptomatic colonization by *Botryosphaeriaceae* fungi on lignified stems of apple and olive, and dormant cuttings of grapevine. *Phytopathologia Mediterranea* 65(1): 43-53. doi: 10.36253/phyto-16717

Accepted: December 12, 2025

Published: March 16, 2026

©2026 Author(s). This is an open access, peer-reviewed article published by Firenze University Press (https://www.fupress.com) and distributed, except where otherwise noted, under the terms of the CC BY 4.0 License for content and CC0 1.0 Universal for metadata.

Data Availability Statement: All relevant data are within the paper and its Supporting Information files.

Competing Interests: The Author(s) declare(s) no conflict of interest.

Editor: Vladimiro Guarnaccia, DiSAFA - University of Torino, Italy.

ORCID:
LH: 0000-0003-0473-2682
PM: 0000-0002-4494-5271
MJC: 0000-0003-1845-9277
VM: 0000-0001-5784-5918
OB: 0000-0003-0509-5793
SA: 0000-0002-6530-7279

INTRODUCTION

Botryosphaeriaceae includes fungi widely recognized for abilities to infect a broad range of woody hosts, both native and introduced (Slippers and Wingfield 2007; Phillips *et al.,* 2013; Batista *et al.,* 2021; Guarnaccia *et al.,* 2022). These fungi pathogens frequently act as latent pathogens, becoming virulent when their hosts are in stress conditions (Slippers and Wing-

field 2007; Slippers *et al.,* 2013; Hrycan *et al*., 2020; Batista *et al.,* 2021). The most common symptoms caused by *Botryosphaeriaceae* include fruit rot, leaf spot, dieback, and canker (Slippers and Wingfield 2007; Phillips *et al.,* 2013; Yang *et al.,* 2017), with cankers being the most destructive, as they can lead to the death of stems, branches or whole trees (Slippers and Wingfield 2007; Delgado *et al*., 2016; Úrbez-Torres *et al*., 2016; Hernández *et al*., 2022; Valdez-Tenezaca *et al*., 2025).

Botryosphaeriaceae are known for their broad host ranges and ability for host jumping, particularly among hosts with overlapping geographic distributions (Amponsah *et al*., 2011; Cloete *et al*., 2011; Úrbez-Torres *et al*., 2013; Sessa *et al*., 2016; Zlatković *et al*., 2018; Silva-Valderrama *et al*., 2024). Recent studies have confirmed the capacity of various host species to be inoculum sources for other susceptible hosts (Mojeremane *et al*., 2020; Díaz *et al*., 2022; Hernández *et al*., 2025).

In Uruguay, *Botryosphaeriaceae* have been isolated from healthy and symptomatic tissues of commercial and native *Myrtaceae* species (Pérez *et al*., 2009; 2010), and from cankers and fruit rots of several fruit crops, including grapevine (Abreo *et al*., 2013), apple (Delgado *et al*., 2016; Sessa *et al*., 2016), pear, peach (Sessa *et al*., 2016), blueberry (Sessa *et al*., 2018), and olive (Hernández *et al*., 2022). Most of these crops are cultivated in close proximity, highlighting the risks of cross-infection occurrence (Silva-Valderrama *et al*., 2024). Furthermore, the majority of identified *Botryosphaeriaceae* in *Botryosphaeria*, *Diplodia*, and *Neofusicoccum*, and have been found infecting most of these hosts (Abreo *et al*., 2013; Delgado *et al*., 2016; Pérez *et al*., 2009; 2010; Sessa *et al*., 2016; 2018; Hernández *et al*., 2022).

Multiple studies of pathogen virulence have shown that species of *Neofusicoccum* are the most virulent, regardless of their origins. For example, most isolates of *N. luteum* and *N. parvum* originating from grapevine (Úrbez-Torres *et al*., 2011; Belleé *et al*., 2017), apple (Delgado *et al*., 2016), almond (Olmo *et al*., 2016), or walnut (Antony *et al*., 2024), caused longer necrotic wood lesions compared to other related species when inoculated into the respective hosts. A similar pattern was observed in cross-inoculation studies, where most *Neofusicoccum* species exhibited the greatest levels of virulence (Sessa *et al*., 2016; Diaz *et al*., 2022; Hernández *et al*., 2025).

Once wood is infected and cankers become visible, removing diseased stems, branches or trunks is the most appropriate recommendation to extend the productive life of the trees (Úrbez-Torres, 2011; Alaniz *et al*., 2012; Delgado *et al*., 2016). Pruning should extend several centimeters beyond the visible margins of necrotic lesions, as it has been documented that *Botryosphaeriaceae* hyphae can colonize asymptomatic tissues, mainly xylem, beyond visible lesions (Brown and Hendrix, 1981; Muniz *et al*., 2011; Obrador-Sánchez and Hernández-Martínez, 2020; Antony *et al*., 2024). For example, in nut crops, Moral *et al*., (2019) recommended pruning approx. 5 to 6 cm below external canker margins, whereas Úrbez-Torres (2011) suggested removing all infected grapevine wood at least 10 cm below visible vascular symptoms. However, no studies have established the precise amount of tissue that must be removed to ensure complete pathogen elimination. Incomplete removal will lead to canker recurrence, as residual pathogens can continue to colonize host tissues.

The aims of the present study were: i) to investigate the occurrence of cross-infections by *Botryosphaeria*, *Diplodia* and *Neofusicoccum* species originating from apple, olive or grapevine, and to evaluate their virulence in these hosts; ii) to estimate the asymptomatic colonization distances of *Botryosphaeria*, *Diplodia*, and *Neofusicoccum* species from visible lesion margins in apple, olive, and grapevine fruit crops. Experiments were conducted using detached lignified stems of apple and olive, and dormant cuttings of grapevine, which were inoculated with local isolates of *Botryosphaeriaceae*.

MATERIAL AND METHODS

Fungal isolates

Forty *Botryosphaeriaceae* isolates, representing eleven species of *Botryosphaeria*, *Diplodia* or *Neofusicoccum* (maximum of three isolates per species, according to availability) were used for direct and cross inoculation assessments. Twelve isolates of the seven most relevant species from these genera, with a maximum of three isolates per species, were used for asymptomatic colonization progression assessments (Table 1). The isolates were obtained from apple stem cankers, dieback, or fruit rot (Delgado *et al*., 2016), olive stem canker (Hernández *et al*., 2022), or from grapevine wood canker samples collected from commercial orchards and vineyards in the south of Uruguay (Supplementary material 1). *Botryosphaeriaceae* isolates from grapevine were initially identified by their fast-growing mycelium, which was white and cottony in early growth in culture, on the first days and turning to grey or grey-green a few days later. Isolates were subcultured on water agar with sterilized pine needles on the agar surface, and incubated at 25°C under near UV-light with a 12-h photoperiod. When mature pycnidia were formed, conidium shapes and colour were assessed. For species

Table 1. Designations, hosts, localities, and relevant references for Uruguayan isolates of *Botryosphaeria*, *Diplodia* and *Neofusicoccum* used in this study.

Species	Isolate	Host	Locality	Reference
B. dothidea	B14 a	Apple	Melilla/Montevideo	Delgado *et al.,* 2016
	B49	Apple	Villa Nueva, Canelones	Delgado *et al.,* 2016
	B108	Apple	Canelón Chico, Canelones	Delgado *et al.,* 2016
	O28	Olive	19 de Abril, Rocha	Hernández *et al.,* 2022
	V2	Grapevine	n/d	Present study
	V13	Grapevine	Las Brujas, Canelones	Present study
	V22 a	Grapevine	Progreso, Canelones	Present study
B. wangensis	O7 a	Olive	Garzón, Maldonado	Hernández *et al.,* 2022
	O22	Olive	Melilla, Montevideo	Hernández *et al.,* 2022
D. intermedia	B5	Apple	Melilla, Montevideo	Delgado *et al.,* 2016
	B118	Apple	Melilla, Montevideo	Delgado *et al.,* 2016
	B144	Apple	Progreso, Canelones	Delgado *et al.,* 2016
D. mutila	O36	Olive	Melilla, Montevideo	Hernández *et al.,* 2022
D. pseudoseriata	V 14	Grapevine	Las Brujas, Canelones	Present study
D. seriata	B27	Apple	El Colorado, Canelones	Delgado *et al.,* 2016
	B69	Apple	Kiyu, San José	Delgado *et al.,* 2016
	B157 a	Apple	Juanicó, Canelones	Delgado *et al.,* 2016
	O14 a	Olive	San Jacinto, Canelones	Hernández *et al.,* 2022
	O19	Olive	Montevideo, Melilla	Hernández *et al.,* 2022
	V1 a	Grapevine	n/d	Present study
	V5	Grapevine	n/d	Present study
	V23	Grapevine	Progreso, Canelones	Present study
N. australe	B112	Apple	Melilla, Montevideo	Delgado *et al.,* 2016
N. cryptoaustrale	O6	Olive	Garzón, Maldonado	Hernández *et al.,* 2022
	O21 a	Olive	Melilla, Montevideo	Hernández *et al.,* 2022
	O24	Olive	Villa Nueva, Canelones	Hernández *et al.,* 2022
N. luteum	B55	Apple	Melilla, Montevideo	Delgado *et al.,* 2016
	B107	Apple	Canelón Chico, Canelones	Delgado *et al.,* 2016
	B129 a	Apple	Juanicó, Canelones	Delgado *et al.,* 2016
	O10 a	Olive	Garzón, Maldonado	Hernández *et al.,* 2022
	O20	Olive	Melilla, Montevideo	Hernández *et al.,* 2022
	O27	Olive	Villa Nueva, Canelones	Hernández *et al.,* 2022
N. occulatum	O12 a	Olive	Garzón, Maldonado	Hernández *et al.,* 2022
	O29	Olive	19 de Abril, Rocha	Hernández *et al.,* 2022
N. parvum	B60	Apple	Melilla, Montevideo	Delgado *et al.,* 2016
	B146	Apple	Progreso, Canelones	Delgado *et al.,* 2016
	B168 a	Apple	Melilla, Montevideo	Delgado *et al.,* 2016
	V4	Grapevine	C. de Sierra, Canelones	Present study
	V28	Grapevine	Las Brujas, Canelones	Present study
	V35 a	Grapevine	Las Brujas, Canelones	Present study

[a] Isolates used to study progression of infections in asymptomatic host tissues.
n/d no data.

identification, the isolate genomic regions translation elongation factor 1-α (TEF), beta-tubulin (TUB2), and internal transcribed spacer regions (ITS) were analyzed (Supplementary material 2).

Plant material and inoculation method

Apparently healthy 1-year-old detached lignified stems or dormant cuttings of lengths approx. 50 or 80 cm and 1 cm diam. of apple 'Red Delicious', olive 'Arbe-

quina', or grapevine 'Marseland', were used for pathogenicity assessments. These cultivars are among the most planted of the respective fruit crops in Uruguay. The stems and cuttings were collected during winter, from mature commercial orchards with no known previous *Botryosphaeriaceae* infections, that were located in Canelones and Montevideo Department, of southern Uruguay. The climate of the region where these orchards are established is characterized by persistent high humidity, frequent rainfall (approx. 1,100 mm per year) and moderate temperatures. The collected stems or cuttings were immediately placed in 200 mL capacity glass jars each containing 50 mL of sterile moist sand.

For direct and cross-inoculation assays, a central internode of each stem or cutting was surface-disinfected with cotton soaked in 70% ethanol. For asymptomatic colonization progression assays, the upper internode of each stem or cutting was disinfected under the same conditions. A wound (5 mm diam.) was immediately made by removing the bark with a sterile scalpel to expose the cambium. Mycelium plugs (5 mm diam.) were cut from the margins of *Botryosphaeriaceae* colonies on PDA growing at 25°C in darkeners for 1 week, and were each placed onto a wound with the mycelium surface facing the stem cambium. Cotton soaked in sterile water was attached to the inoculated wound and wrapped with parafilm, to prevent desiccation.

Direct and cross inoculations on detached host stems and cuttings

For each fruit crop host, eight detached 50-cm-long stems or cuttings were inoculated with each *Botryosphaeriaceae* isolate, while eight stems or cuttings were inoculated with sterile agar plugs as inoculation controls. Glass jars (see above) containing the inoculated stems or cuttings were randomly arranged in a temperature-controlled room (24 ± 2°C), and the sand in each jar was periodically moistened. After five weeks, the plant stem or cutting bark was removed, and lengths of necrotic lesions as discolored wood extending from the inoculation sites, were measured using a digital caliper (Kamasa, EEUU). The experiment was repeated once.

Lesion length data were analyzed using generalized linear models, assuming a gamma distribution for the variable, with natural Log as link function. The GLIMMIX procedure in SAS program (Statistical Analysis System, version 9.4, SAS Institute Inc.) was used. The model included the following factors: host origins of the isolates, *Botryosphaeriaceae* species within host origin, and isolates within *Botryosphaeriaceae* species and host origin. Means were compared using the Tukey-Kramer test and a significance level of $P \leq 0.05$.

Asymptomatic colonization progression on detached host stems and cuttings

For each fruit host, five detached 80-cm-long stems or cuttings were inoculated with each *Botryosphaeriaceae* isolate, while five stems or cuttings inoculated with sterile agar plugs were used as inoculation controls. Glass jars (see above) containing the inoculated stems or cuttings were randomly arranged in a temperature-controlled room (24 ± 2°C), and the sand in each jar was periodically moistened. After 4 weeks, the bark of each stem or cutting was removed, and isolations were made by removing tissue pieces from the lower edges of visible necrotic lesions, as well as from 10, 20 and 30 cm towards the lower parts of stems or cuttings (Figure 1).

For re-isolations, five 1–2 mm cross-sectional discs were cut at each distance, and were placed on potato dextrose agar (PDA) and incubated at 25°C in darkness. After 3 to 6 d, the presence of *Botryosphaeriaceae* colonies was recorded, and the re-isolated cultures were compared with the original isolates based on colony morphology and conidium characteristics. The proportion of stems or cuttings with positive re-isolations was estimated for each fruit crop and isolate combination at

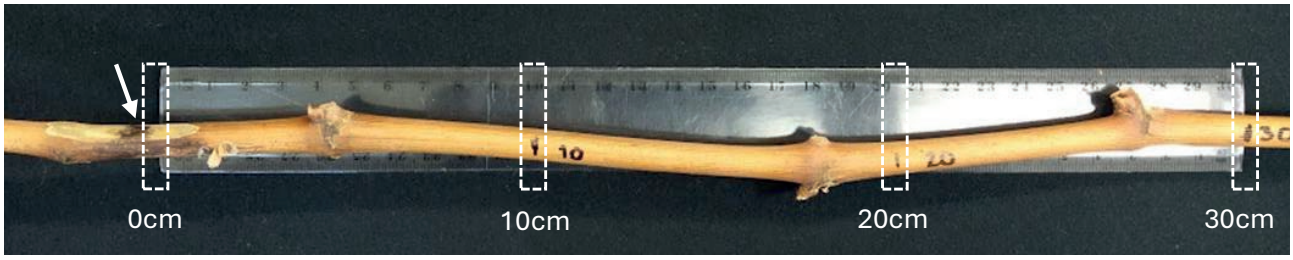

Figure 1. Illustration showing the four distances on detached lignified stems of apple and olive or detached dormant cuttings of grapevine, used for re-isolations of *Botryosphaeriaceae* isolates inoculated onto host tissues. The distances were from the necrotic lesion margin (indicated by the white arrow).

the four specified re-isolation distances (0, 10, 20 and 30 cm) from inoculation points. At least one of the five stem discs plated in PDA yielding a *Botryosphaeriaceae* colony was considered as a positive infection. The experiment was repeated once.

RESULTS

Direct and cross inoculations on detached host stems and cuttings

The forty inoculated *Botryosphaeriaceae* isolates caused necrotic lesions on detached stems of apple and olive, and detached cuttings of grapevine, extending upwards and downwards from the points of inoculation. Cicatrized wounds developed on detached stems and cuttings used as inoculation controls. Necrotic lesions consisted of dark discolouration and internal wood streaking (Figure 2). For all the inoculated isolates, the mean necrotic lesions lengths ranged from 1.3 to 29.4 cm on apple stems, from 2.1 to 19.6 cm on olive stems, and from 2.4 to 20.3 cm in grapevine cuttings.

For each fruit crop, statistical analyses indicated statistically significant effects of host origin of isolates ($P < 0.0001$), *Botryosphaeriaceae* species within host origin ($P < 0.0001$), and isolates within species and host origin ($P < 0.0001$). However, regardless of isolate host origin or inoculated host, most *Neofusicoccum* spp. isolates caused the longest lesions on all three hosts, with statistically significant differences in most cases compared with the mean lesion lengths caused by isolates of *Diplodia* spp. or *Botryosphaeria* spp. The mean necrotic lesion lengths caused by *Neofusicoccum* spp. ranged from 3.3 to 28.3 cm on apple stems, from 8.3 to 15.9 cm on olive stems, and from 7.5 to 13.8 cm on grapevine cuttings. *Diplodia* spp. isolates produced necrotic lesions averaging from 1.3 to 12.8 cm on apple stems, from 1.9 to 4.7 cm on olive stems, and from 4.5 to 9.9 cm on grapevine cuttings. *Botryosphaeria* spp. isolates caused necrotic lesions averaging from 3.9 to 6.8 cm on apple stems, 3.4 to 8.1 cm on olive stems, and 3.8 to 8.1 cm on grapevine cuttings (Figure 3).

Asymptomatic colonization progression on detached hosts stems or cuttings

All the detached apple and olive stems and detached grapevine cuttings inoculated with the 12 *Botryosphaeriaceae* isolates developed necrotic lesions on the host wood. Inoculated fungi were consistently re-isolated from the advancing margins of lesions on all the host stems or cuttings, exhibiting the morphological characteristics of the inoculated isolates.

Asymptomatic colonization was detected in re-isolations from 10 cm beyond the visible lesion margins. The isolate V35 of *N. parvum* was re-isolated from 60% of inoculated olive stems and from 20% of inoculated apple stems and grapevine cuttings. Isolate M157 of *D. seriata* was re-isolated from 20% of inoculated olive stems. No isolates were recovered at 20 or 30 cm from the lesion margins, in any of the three plant hosts. Additionally, no *Botryosphaeriaceae* growth was observed from inoculation control stems or cuttings, either at the callused wound margins (0 cm) or at any of the three distances (10, 20 and 30 cm) from inoculations (Table 2).

DISCUSSION

In this study, *Botryosphaeriaceae* fungi capacities to cross-infect wood plant tissues beyond their original host species were assessed. Several isolates of *B. dothidea*, *B. wangensis*, *D. intermedia*, *D. mutila*, *D. pseudoseriata*, *D. seriata*, *N. australe*, *N. cryptoaustrale*, *N. luteum*, *N. occulatum*, and *N. parvum*, were evaluated for ability to infect and colonize lignified detached stems of apple and olive, and detached cuttings of grapevine, that were both the original and alternative fruit crop hosts for each isolate. The forty inoculated isolates caused necrotic lesions on detached stems or cuttings of the three hosts, providing evidence that host origin does not affect the ability of these pathogens to infect multiple hosts, and showing their capacities for cross-infection.

This knowledge poses significant challenges for fruit crop production in Uruguay, as *Botryosphaeriaceae* hosts are typically cultivated in close proximity, frequently on the same farm, facilitating the spread of these pathogens. While this study was focused on apple, olive, and grapevine, which are among the most economically important fruit crops in Uruguay (MGAP 2023), other co-cultivated fruit crops such as pear, peach, or blueberry are also known hosts of *Botryosphaeriaceae* (Sessa *et al*., 2016; Sessa *et al*., 2018), further highlighting the relevance of these results.

As in the present study, ability of *Botryosphaeriaceae* to infect multiple fruit hosts was previously demonstrated by Cloete *et al*., (2011) in South Africa and Amponsah *et al*., (2011) in New Zealand, who found that isolates of *Botryosphaericeae* from pear, apple, olive, broom, and pine trees could infect grapevine. Similarly, in Uruguay Sessa *et al*., (2016) provided evidence that isolates of *Diplodia*, *Lasiodiplodia* and *Neofusicoccum* isolated from apple, peach, or pear cross-infected these hosts.

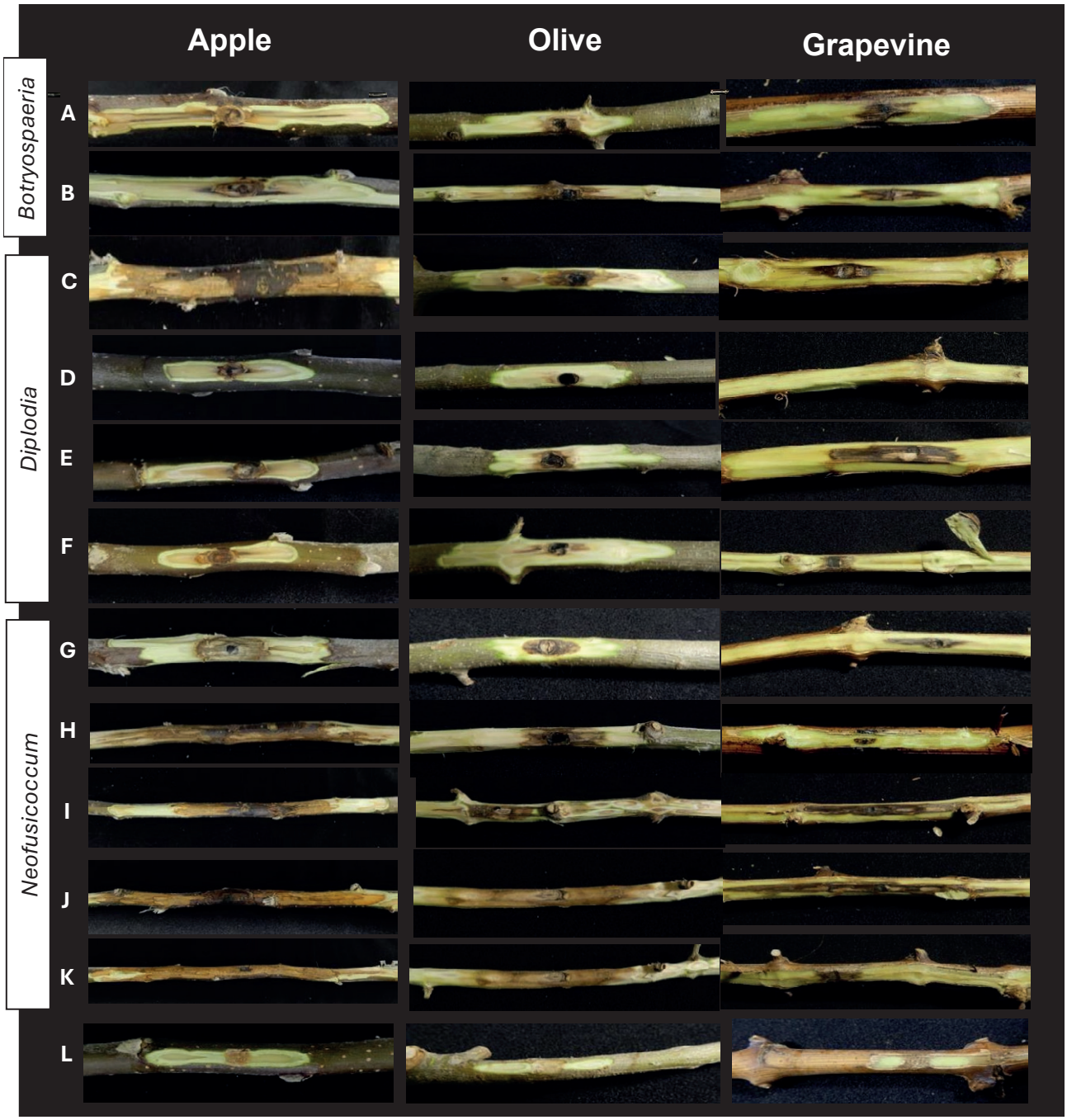

Figure 2. Necrotic lesions developed on detached lignified stems of apple and olive, or detached cuttings of grapevine, 5 weeks after inoculations with *Botryosphaeriaceae* isolates obtained from these three fruit crops. A) *Botryosphaeria dothidea* (B14); B) *B. wangensis* (O22); C) *Diplodia intermedia* (B5); D) *D. mutila* (O36); E*) D. pseudoseriata* (V14); F) *D. seriata* (O19); G) *Neofusicoccum australe* (B112); H) *N. cryptoaustrale* (O6); I) *N. luteum* (B107); J) *N. parvum* (V18); and K) *N. occulatum* (O12). L) Inoculation controls.

Mojeremane *et al*., (2020) in South Africa showed that isolates of *N. australe* and *N. stellenboschiana* obtained from grapevine, plum, apple, olive, Peruvian pepper, and fig were pathogenic on these hosts. In Chile, Díaz *et al*., (2022) and Hernández *et al*., (2025) confirmed cross-infection potential of isolates belonging to *Diplodia*, *Dothiorella*, *Lasiodiplodia*, and *Neofusicoccum*, after induction of necrotic lesions in pear, walnut, and grape-

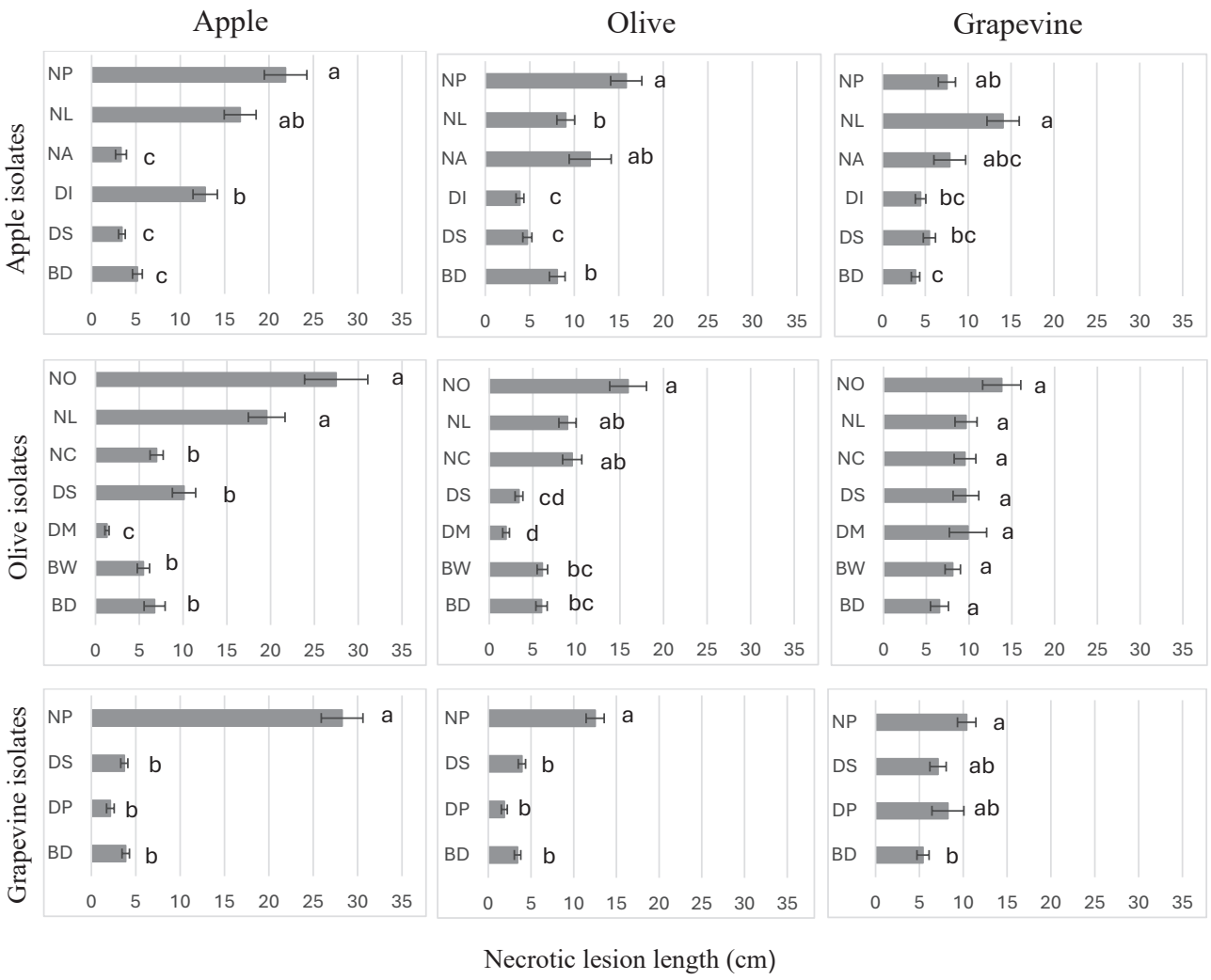

Figure 3. Mean necrotic lesion lengths measured in detached lignified stems of apple and olive, or detached dormant cuttings of grapevine, 5 weeks after direct and cross inoculations with 40 isolates of 11 species of *Botryosphaeriaceae* isolated from apple, olive, or grapevine crops. NP: *Neofusicoccum parvum*, NL: *N. luteum*, NA: *N. australe*, NO: *N. occulatum*, NC: *N. cryptoaustrale*, DS: *Diplodia seriata*, DI: *D. intermedia*, DM: *D. mutila*, DP: *D. pseudoseriata*, BD: *Botryosphaeria dothidea*, and BW: *B. wangensis*. Vertical bars indicate standard errors of the means. Values followed by different letters differ significantly ($P \geq 0.05$), according to the Tukey test.

vine using grapevine-derived isolates, and caused cankers in grapevine using isolates obtained from, respectively, apple, blueberry, or walnut. Some of these studies also examined hosts beyond fruit crops, including forestry, horticultural, and ornamental species, demonstrating that the host ranges and potential for cross-infection extend across a wide and diverse variety of woody plants. Collectively, these findings underscore the epidemiological complexity of this group of *Botryosphaeriaceae* pathogens (Silva-Valderrama *et al*., 2024).

In the present study, virulence of *Botryosphaeriaceae* species varied both among and within species. However, most *Neofusicoccum* isolates consistently caused the longest lesions in the three inoculated fruit hosts, confirming that their high virulence is independent of *Neofusicoccum* origin. These results are consistent with previous studies that have identified *Neofusicoccum* species as among the most virulent *Botryosphaeriaceae*, whether inoculated on their original hosts (Pérez *et al*., 2010; Úrbez-Torres *et al*., 2011; Delgado *et al*., 2016; Olmo *et al*., 2016, Antony *et al*., 2024) or on alternative hosts (Cloete *et al*, 2011; Amponsah *et al*., 2011; Sessa *et al*., 2016; Díaz *et al*., 2022; Hernández *et al*., 2025).

The virulence of *Neofusicoccum* species may be attributed to the expansion of gene families linked to virulence, specifically those encoding carbohydrate-

Table 2. Percentages of positive re-isolations from four distances from necrotic lesion margins for seven species of *Botryosphaeria*, *Diplodia* or *Neofusicoccum* inoculated into detached lignified stems of apple and olive, or detached dormant cuttings of grapevine. Each datum is the percentage for five host stems or cuttings.

Specie	Isolate	Percentage of re-isolation from different distances from lesion margins											
		Apple				Olive				Grapevine			
		0 cm	10cm	20cm	30cm	0cm	10cm	20cm	30cm	0cm	10cm	20cm	30cm
B. dothidea	M14	100	0	0	0	100	0	0	0	100	0	0	0
	V22	100	0	0	0	100	0	0	0	100	0	0	0
B. wangensis	O7	100	0	0	0	100	0	0	0	100	0	0	0
D. seriata	M157	100	0	0	0	100	20	0	0	100	0	0	0
	O14	100	0	0	0	100	0	0	0	100	0	0	0
	V1	100	0	0	0	100	0	0	0	100	0	0	0
N. cryptoaustale	O21	100	0	0	0	100	0	0	0	100	0	0	0
N. luteum	M129	100	0	0	0	100	0	0	0	100	0	0	0
	O10	100	0	0	0	100	0	0	0	100	0	0	0
N. occulatum	O12	100	0	0	0	100	0	0	0	100	0	0	0
N. parvum	M168	100	0	0	0	100	0	0	0	100	0	0	0
	V35	100	20	0	0	100	60	0	0	100	20	0	0
Control (non-inoculated)		0	0	0	0	0	0	0	0	0	0	0	0

active enzymes (CAZymes), peptidases, and components of secondary metabolism. These genetic features give fungi enhanced capacities to degrade lignified tissues and circumvent plant defense mechanisms (Morales-Cruz *et al*., 2015, Belleé *et al*., 2017). Supporting this, Belair *et al*. (2023) conducted a comparative genomic analysis across six *Botryosphaeriaceae* genera, and found that *Neofusicoccum,* particularly a specific isolate of *N. parvum,* exhibited enrichment in genes encoding CAZymes and peptidases, highlighting its superior pathogenic potential.

The present study also assessed the ability of *Botryosphaeriaceae* isolates to colonize asymptomatic woody tissues beyond the margins of visible lesions. One month after inoculation, inoculated isolates were absent at distances of 20 and 30 cm beyond visible necroses in all inoculated stems and cuttings of the three fruit hosts assessed. However, although only occasionally, the inoculated pathogens were re-isolated from up to 10 cm beyond the visible lesion edges in stems of apple and olive, and cuttings of grapevine. In apple, this latent colonization may explain, at least in part, the reactivation of disease that can be observed in commercial apple crops after pruning sanitization (Alaniz *et al*., 2012). This finding highlights the need to revise current pruning recommendations of removing up to 10 cm below visible lesion edges (Alaniz *et al*., 2012) to establish the minimum pruning lengths necessary for effective pathogen eradication. Additionally, the susceptibility of pruning wounds at different ages, and the effect of pruning timing on infection, should be included in studies to establish successful sanitation pruning recommendations (Valdez-Tenezaca *et al*., 2025).

One isolate of *N. parvum* was the only pathogen recovered from asymptomatic tissues across all three host species. This supports that particular isolates of *N. parvum* may have ability to colonize woody tissues beyond the visible lesions more rapidly than other members of this family. This may be through vascular pathways such as xylem vessels (Muniz *et al*., 2011; Han *et al*., 2016; Obrador-Sánchez and Hernández-Martínez 2020; Antony *et al*., 2024).

In summary, the present study has highlighted the challenges of managing diseases caused by *Botryosphaeriaceae* where multiple susceptible hosts are grown in close proximities, as is common in fruit production systems in Uruguay. In these situations, effective disease management should account for the potential for cross-infection among co-cultivated species, recognizing that each host can serve as an inoculum source for others. For example, the status of *Botryosphaeriaceae* cankers in neighbouring fruit orchards should be evaluated before establishing new plantings. Additionally, pruning distance required to ensure the complete elimination of these pathogens needs to be revised. Susceptibility of pruning wounds, effects of pruning time, and protection of pruning wounds should be evaluated under local conditions to prevent infections or re-infections by these

pathogens. Environmentally friendly treatment alternatives, such as fungicides approved for use in integrated management programs, biological control agents, or natural fungicidal compounds, should be considered in these investigations.

AUTHOR CONTRIBUTIONS

Laura Hernández was responsible for experimental assays, data analyses, and preparation of the draft manuscript. María Julia Carbone and Victoria Moreira assisted in experimental assays and contributed to the data analyses and manuscript review. Oscar Bentancur was responsible for experimental designs and statistical analyses of data. Pedro Mondino provided project conceptualization, and draft manuscript review. Sandra Alaniz provided project conceptualization, data analyses, preparation of the draft manuscript, and its review and editing. All authors approved the final version of the manuscript.

LITERATURE CITED

Abreo E., Martínez S., Bettucci L., Lupo S., 2013. Characterization of Botryosphaeriaceae species associated with grapevines in Uruguay. *Australasian Plant Pathology* 42: 241–249. https://doi.org/10.1007/s13313-013-0200-8

Antony S., Billones-Baaijens R., Steel C.C., Stodart B.J., Savocchia S., 2024. Pathogenicity and progression of Botryosphaeriaceae associated with dieback in walnut orchards in Australia. *European Journal of Plant Pathology* 168(4): 723–742. https://doi.org/10.1007/s10658-023-02794-w

Amponsah N.T., Jones E.E., Ridgway H.J., Jaspers M.V., 2011. Identification, potential inoculum sources and pathogenicity of Botryosphaeriaceous species associated with grapevine dieback disease in New Zealand. *European Journal of Plant Pathology* 131: 467–482. https://doi.org/10.1007/s10658-011-9823-1

Alaniz S., Delgado L., Leoni C., Mondino P., 2012. Situación actual de los cancros del manzano: distribución, descripción de síntomas, agentes causales, pautas de manejo. Seminario de actualización técnica en frutales de hoja caduca. In: *Seminario de Actualización Técnica Frutales de Pepita* (pp. 29–34). *Serie de Actividades de Difusión* N° 687, INIA, Montevideo.

Batista A., Lopes A., Alves A., 2021. What do we know about Botryosphaeriaceae? an overview of a worldwide cured dataset. *Forest* 12(3):.313-330. https://doi.org/10.3390/f12030313

Belair M., Restrepo-Leal J.D., Praz C., Fontaine F., Rémond C., Fernandez O., Besaury L., 2023. Botryosphaeriaceae gene machinery: Correlation between diversity and virulence. *Fungal Biology* 127(5): 1010–1031. https://doi.org/10.1016/j.funbio.2023.03.004

Belleé A., Comont G., Nivault A., Abou-Mansour E., … Dufour M.C., Corio-Costet M.F.., 2017. Life traits of four Botryosphaeriaceae species and molecular responses of different grapevine cultivars or hybrids. *Plant Pathology* 66(5): 763–776. https://doi.org/10.1111/ppa.12623

Brown E.A., Hendrix F.F., 1981. Pathogenicity and histopathology of *Botryosphaeria dothidea* on apple stems. *Phytopathology* 71: 375–379

Cloete M., Fourie P.H., Damm U., Crous P.W., Mostert L., 2011. Fungi associated with die-back symptoms of apple and pear trees, a possible inoculum source of grapevine trunk disease pathogens. *Phytopathologia Mediterranea* 50: S176-S190. https://doi.org/10.1094/Phyto-71-375.

Delgado L., Mondino P., Alaniz S., 2016. Botryosphaeriaceae species associated with stem canker, dieback and fruit rot on apple in Uruguay. *European Journal of Plant Pathology* 146: 637–655. https://doi.org/10.1007/s10658-016-0949-z

Díaz G.A., Valdez A., Halleen F., Ferrada E., Lolas M., Latorre B.A., 2022. Characterization and pathogenicity of *Diplodia*, *Lasiodiplodia*, and *Neofusicoccum* species causing Botryosphaeria canker and dieback of apple trees in central Chile. *Plant Disease* 106(3): 925–937. https://doi.org/10.1094/PDIS-06-21-1291-RE

Guarnaccia V., Kraus C., Markakis E., Alves A., Armengol J., … Gramaje D., 2022. Fungal trunk diseases of fruit trees in Europe: Pathogens, spread and future directions. *Phytopathologia Mediterranea* 61: 563–599. https://doi.org/10.36253/phyto-14167

Han Q., Gao X., Wang J., Wang H., Huang L., 2016. Cytological and histological studies of the interaction between *Botryosphaeria dothidea* and apple twigs. *Scientia Horticulturae* 202: 142–149. https://doi.org/10.1016/j.scienta.2016.03.002

Hernández-Rodríguez L., Mondino-Hintz P., Alaniz-Ferro S., 2022. Diversity of Botryosphaeriaceae species causing stem canker and fruit rot in olive trees in Uruguay. *Journal of Phytopathology* 170(4): 264–277. https://doi.org/10.1111/jph.13078

Hernández Y., Lolas M., Elfar K., Eskalen A., Gainza-Cortés F., Díaz G.A., 2025. Host Jumps and Pathogenicity of Botryosphaeriaceae Species on Grapevines (*Vitis vinifera*) in Chile. *Microorganisms*

13(2): 331. https://doi.org/10.3390/microorganisms13020331

Hrycan J., Miranda H.A.R.T., Bowen P., Forge T., Urbez-Torres J.R. 2020. Grapevine trunk disease fungi: Their roles as latent pathogens and stress factors that favour disease development and symptom expression. *Phytopathologia Mediterranea* 59(3): 395–424. 10.14601/Phyto-11275

MGAP (Ministerio de Ganadería, Agricultura y Pesca). 2023. Anuario estadístico agropecuario 2023. Dirección de Estadísticas Agropecuarias (DIEA). https://descargas.mgap.gub.uy/DIEA/Anuarios/Anuario2023/ANUARIO2023WEB.pdf

Mojeremane K., Lebenya P., Du Plessis I.L., van Der Rijst M., Mostert L., ... Halleen F., 2020. Cross pathogenicity of *Neofusicoccum australe* and *Neofusicoccum stellenboschiana* on grapevine and selected fruit and ornamental trees. *Phytopathologia Mediterranea* 59(3): 581–594. https://doi:10.14601/Phyto-11609

Moral J., Morgan D., Michailides T.J., 2019. Management of *Botryosphaeria* canker and blight diseases of temperate zone nut crops. *Crop Protection* 126: 104927. https://doi.org/10.1016/j.cropro.2019.104927

Morales-Cruz A., Amrine K.C., Blanco-Ulate B., Lawrence D.P., Travadon R.,.... Cantu D., 2015. Distinctive expansion of gene families associated with plant cell wall degradation, secondary metabolism, and nutrient uptake in the genomes of grapevine trunk pathogens. *BMC Genomics* 16: 469. https://doi.org/10.1186/s12864-015-1624-z

Muniz C.R., Freirea F.C.O., Vianaa F.M.P., Cardosoa J.E., Cookeb P., ... Guedesd M.I.F., 2011. Colonization of cashew plants by *Lasiodiplodia theobromae*: Microscopical. *Micron* 42: 419–428. https://doi.org/10.1016/j.micron.2010.12.003

Obrador-Sánchez J.A., Hernandez-Martinez R., 2020. Microscope observations of Botryosphaeriaceae spp. in the presence of grapevine wood. *Phytopathologia Mediterranea* 59(1): 119–129. https://doi.org/10.36253/phyto-11040

Olmo D., Armengol J., León M., Gramaje D., 2016. Characterization and pathogenicity of Botryosphaeriaceae species isolated from Almond trees on the Island of Mallorca (Spain). *Plant Disease* 100: 2483–2491. https://doi.org/10.1094/PDIS-05-16-0676-RE

Pérez C.A., Wingfield M.J., Slippers B., Altier N.A., Blanchette R.A., 2009. *Neofusicoccum eucaliptorum*, a Eucaliptus pathogen, on native *Myrtaceae* in Uruguay. *Plant Pathology* 58: 964–970. https://doi.org/10.1111/j.1365-3059.2009.02116.x

Pérez C.A., Wingfield M.J., Slippers B., Altier N.A., Blanchette R.A. 2010. Endophytic and canker-associated Botryosphaeriaceae occurring on non-native *Eucalyptus* and native *Myrtaceae* trees in Uruguay. *Fungal Diversity* 41: 53–69. https://doi.org/10.1007/s13225-009-0014-8

Phillips A.J.L., Alves A., Abdollahzadeh J., Slippers B., Wingfield M.J., ... Crous P.W., 2013. The Botryosphaeriaceae: genera and species known from culture. *Studies in Mycology* 76: 51–167. https://doi.org/10.3114/sim0021.

Sessa L., Abreo E., Bettucci L., Lupo S., 2016. Botryosphaeriaceae species associated with wood diseases of stone and pome fruits trees: symptoms and virulence across different hosts in Uruguay. *European Journal of Plant Pathology* 146: 519–530. https://doi.org/10.1007/s10658-016-0936-4

Sessa L., Abreo E., Lupo S., 2018. Diversity of fungal latent pathogens and true endophytes associated with fruit trees in Uruguay. *Journal of Phytopathology* 166: 633–647. https://doi.org/10.1111/jph.12726

Silva-Valderrama I., Úrbez-Torres J.R., Davies T.J., 2024. From host to host: The taxonomic and geographic expansion of Botryosphaeriaceae. *Fungal Biology Reviews* 48: 100352. https://doi.org/10.1016/j.fbr.2023.100352

Slippers B., Wingfield M.J. 2007. Botryosphaeriaceae as endophytes and latent pathogens of woody plants: diversity, ecology and impact. *Fungal Biology Reviews* 21: 90–106. https://doi.org/10.1016/j.fbr.2007.06.002

Slippers B., Boissin E., Phillips A.J.L., Groenewald J.Z., Lombard L., ... Crous P.W., 2013. Phylogenetic lineages in the Botryosphaeriales: a systematic and evolutionary framework. *Studies in Mycology* 76: 31–49. https://doi.org/10.3114/sim0020

Úrbez-Torres J.R. 2011. The status of Botryosphaeriaceae species infecting grapevines. *Phytopathologia Mediterranea* 50: S5–S45. https://doi.org/10.14601/Fitopatología_Mediterr- 9316

Úrbez-Torres J.R., Gubler W., 2011. Susceptibility of grapevine pruning wounds to infection by *Lasiodiplodia theobromae* and *Neofusicoccum parvum*. *Plant Pathology* 60: 261–270. https://doi.org/10.1111/j.1365-3059.2010.02381.x

Úrbez-Torres J.R., Peduto F., Vossen P.M., Krueger W.H., Gubler W.D., 2013. Olive twig and branch dieback: etiology, incidence, and distribution in California. *Plant Disease* 97: 231–244. https://doi.org/10.1094/PDIS-04-12-0390-RE

Úrbez-Torres J.R., Castro-Medina F., Mohali S.R., Gubler W.D., 2016. Botryosphaeriaceae species associated with cankers and dieback symptoms of *Acacia mangium* and *Pinus caribaea* var. *hondurensis* in Ven-

ezuela. *Plant Disease* 100(12): 2455–2464. https://doi.org/10.1094/PDIS-05-16-0612-RE

Valdez-Tenezaca A., Latorre B.A., Díaz G.A., 2025. Susceptibility of pruning wounds of apple trees to *Diplodia mutila*, *D. seriata*, *Lasiodiplodia theobromae*, and *Neofusicoccum arbuti* Infections and conidial release of Botryosphaeriaceae spp. in the Maule Region, Chile. *Plant Disease* 109(5): 1121–1129. https://doi.org/10.1094/PDIS-07-24-1498-RE

Yang T., Groenewald J.Z., Cheewangkoon R., Jami F., Abdollahzadeh J., ... Crous P.W., 2017. Families, genera, and species of Botryosphaeriales. *Fungal Biology* 121(4): 322–346. https://doi.org/10.1016/j.funbio.2016.11.001

Zlatković M., Wingfield M.J., Jami F., Slippers B., 2018. Host specificity of co-infecting Botryosphaeriaceae on ornamental and forest trees in the Western Balkans. *Forest Pathology* 48(2): e12410. https://doi.org/10.1111/efp.12410

Phytopathologia Mediterranea
The international journal of the
Mediterranean Phytopathological Union

Firenze University Press
www.fupress.com/pm

Research Papers

Occurrence and genetic diversity of grapevine leafroll-associated virus 4 in Algeria

Anfel DJENAOUI[1]*, Osamah ALISAWI[2], Manel EL AIR[3], Nour Elhouda LAIDOUDI[4], Imene MAHDID[1], Rima Hind BOUDCHICHA[5], Naima MAHFOUDHI[3], Arezki LEHAD[1]*

[1] *Laboratoire de Phytopathologie et Biologie Moléculaire, Département de Botanique, Ecole Nationale Supérieure Agronomique (ENSA-ES 1603), Avenue Hassan Badi, El-Harrach, Algiers, 16200, Algeria*
[2] *Department of Plant Protection, Faculty of Agriculture, University of Kufa, Najaf, Iraq*
[3] *Laboratoire de Protection des Végétaux, Institut National de la Recherche Agronomique de Tunisie, Rue Hedi Karray, 1004 El Menzah, Tunis, Tunisia*
[4] *Laboratoire de Microbiologie Appliquée, Faculté des Sciences de la Nature et de la Vie, Université Ferhat Abbas Sétif 1, Setif, Algeria*
[5] *Biotechnology Research Center, Constantine (CRBT), Constantine, Algeria*
Corresponding authors. E-mail: anfel.dje@gmail.com; lehad.arezki@gmail.com

Summary. Grapevine leafroll-associated virus 4 (GLRaV-4, *Ampelovirus tetravitis*) has considerable genetic diversity. A survey was conducted in central, western, and southern Algeria to investigate the distribution and the genetic diversity of GLRaV-4 in commercial and autochthonous grape cultivars. DAS-ELISA detected an overall grapevine infection rate of 18.2%, and infections in a subset of samples were confirmed by RT-PCR. Analysis of the P23 protein gene sequence revealed six known phylogenetic groups, with Algerian isolates clustering in strains -4, -5, -6, -9, and -Pr of GLRaV-4. In addition to this virus, three viruses and two viroids were identified using high throughput sequencing: grapevine Pinot gris virus (GPGV, *Trichovirus pinovitis*), grapevine leafroll-associated virus 2 (GLRaV-2, *Closterovirus vitis*), grapevine fanleaf virus (GFLV, *Nepovirus foliumflabelli*), hop stunt viroid (HSVd, *Hostuviroid impedihumuli*) and grapevine yellow speckle viroid 1 (GYSVd-1, *Apscaviroid alphaflavivitis*). This study was the first research on genetic diversity of GLRaV-4 in Algeria.

Keywords. GLRaV-4, RT-PCR, genetic diversity, P23, high throughput sequencing.

OPEN ACCESS

Citation: Djenaoui, A., Alisawi, O., El Air, M., Laidoudi, N. E., Mahdid, I., Boudchicha, R. H., Mahfoudhi, N., & Lehad, A. (2026). Occurrence and genetic diversity of grapevine leafroll-associated virus 4 in Algeria. *Phytopathologia Mediterranea* 65(1): 55-65. doi: 10.36253/phyto-16539

Accepted: December 19, 2025

Published: March 16, 2026

© 2026 Author(s). This is an open access, peer-reviewed article published by Firenze University Press (https://www.fupress.com) and distributed, except where otherwise noted, under the terms of the CC BY 4.0 License for content and CC0 1.0 Universal for metadata.

Data Availability Statement: All relevant data are within the paper and its Supporting Information files.

Competing Interests: The Author(s) declare(s) no conflict of interest.

Editor: Arnaud G Blouin, Institut des sciences en production végétale IPV, DEFR, Agroscope, Nyon, Switzerland.

ORCID:
AD: 0009-0004-1790-1320
OA: 0000-0002-8344-1113
MEA: 0009-0000-3546-8090
NEL: 0009-0006-6594-9411
IM: 0009-0006-9417-757X
RHB: 0000-0001-9336-0280
NM: 0000-0001-5157-5099
AL: 0000-0001-6653-4425

INTRODUCTION

Grapevine leafroll disease (GLD), one of the most economically important virus disease affecting grapevines, results from infection by one or more grapevine leafroll-associated viruses (GLRaVs), a group of genetically distinct species in the family *Closteroviridae* (Naidu *et al.*, 2015; Atallah *et al.*, 2012). Among these viruses, grapevine leafroll-associated virus 4 (GLRaV-4, *Ampelovirus tetravitis*) is a recognized species within *Ampelovirus*, which includes several genetically diverse variants known as GLRaV-4 Strains -4, -5,

-6, -9, -Car, -Pr, and -Ob (Martelli *et al*., 2012; Aboughanem-Sabanadzovic *et al*., 2017). GLRaV-4 and its strains are identified by positive RNA molecules of genome size between 13.6 and 13.8 kb, along with six open reading frames (ORFs), flanked by short 5′ or 3′ untranslated regions (UTRs). The virus sequence encodes six proteins (in the 5′ to 3′ direction): the replication-associated polyprotein (expressed via +1 ribosomal frameshift of two partially overlapping ORFs), a small hydrophobic protein (p5), heat shock protein 70 homologue (HSP70h), heat shock protein 90 homologue (HSP90h or p60), virus coat protein (CP), and a protein of unknown function with a molecular mass of 23K (p23). GLRaVs are known to spread through infected host planting material, and through grafting practices (Abou Ghanem-Sabanadzovic *et al*., 2012; Aboughanem-Sabanadzovic *et al*., 2017; Adiputra *et al*., 2019).

Members of *Ampelovirus* responsible for grapevine leafroll are primarily transmitted by specific hemipteran insect vectors, mainly mealybugs and soft scales (Herrbach *et al*., 2017). Additionally, several species of mealybugs and soft-scale insects have been identified as vectors of GLRaV-4, semi-persistently transmitting the virus within and between neighbouring vineyards (Naidu *et al*., 2015; Aboughanem-Sabanadzovic *et al*., 2017). In contrast to the severe symptoms typically associated with GLRaV-1, GLRaV-2, and GLRaV-3, infections by GLRaV-4 strains generally induce milder symptoms (Maree *et al*., 2013; Reynard *et al*., 2015; Abou Ghanem-Sabanadzovic *et al*., 2017).

High-throughput sequencing (HTS) technologies and bioinformatics have revolutionized identification of viral pathogens without knowledge of their primary structures (Maliogka *et al*., 2018). HTS has been instrumental for identifying and characterizing new grapevine virus species, the study of unknown diseases, identification of candidate disease-associated agents, and improvements to existing diagnostic assays for some viruses (Saldarelli *et al*., 2017). HTS has been recently applied to identify and characterize grapevine viruses in Algeria (Bachir *et al*., 2024; Laidoudi *et al*., 2025; Mahdid *et al*., 2025).

Few studies have focused on occurrence of grapevine leafroll disease in Algeria. While GLRaV-1, -2, and -3 have been investigated (Lehad *et al*., 2015a; 2015b; 2019), the present study focused on GLRaV-4 in this country. The main objective of this research was to determine occurrence and genetic diversity of the grapevine virus GLRaV-4 associated with grapevine leafroll disease in Algeria.

MATERIALS AND METHODS

Plant material

During the winter of 2021/2022, 444 grapevine samples were collected from the major grapevine growing regions of central, western, and southern Algeria (Figure 1). Cuttings from different grapevine cultivars were randomly collected from commercial cultivars (421 samples), and from 23 cultivars (23 samples) from the autochthonous grapevine collection at the Institut Technique de l'Arboriculture Fruitière et de la Vigne (ITAFV) (Supplementary Table 1). Additionally, an analysis of 122 grapevine samples (bark scrapings from mature canes) was included, that were randomly collected in 2012 and were provided by the plant protection laboratory of INRAT from vineyards in the wine-growing regions of Algeria (Supplementary Table 2).

DAS-ELISA

Preliminary detection of GLRaV-4 presence in the 444 collected grapevine samples was carried out using DAS-ELISA (Clark and Adams, 1977), employing a commercial kit (GLRaV-4 strains Complete kit 480, Bioreba AG). An extraction was carried out from phloem tissue of each field sample (bark scrapings from mature canes) following the kit manufacturer's instructions, using the provided PBS grinding buffer. The absorbance was measured at wavelength 405 nm using a microplate spectrophotometer (SunriseTM absorbance microplate reader, Tecan Trading AG). Two positive controls and two negative controls supplied by Bioreba AG were used on each plate. In addition, one control well containing only the buffer without antibodies was included per plate. To reduce the risk of false-positive results, a sample was considered positive only if its absorbance value was equal to or exceeded three times the mean absorbance of the negative controls.

Extraction of TNA from the phloem tissue

Total nucleic acids (TNA) were extracted from 0.2 g of phloem tissue from each mature grapevine cane sample, using the CTAB-based protocol of Gambino *et al*. (2008), with minor modifications. This involved grinding the material with liquid nitrogen, extraction with CTAB buffer at 65°C, followed by extraction with a chloroform/isoamyl alcohol mixture, precipitation with isopropanol, an ethanol wash, and then resuspending the TNA in sterile ultrapure water before storing at -20°C. The quality of the TNA was assessed through

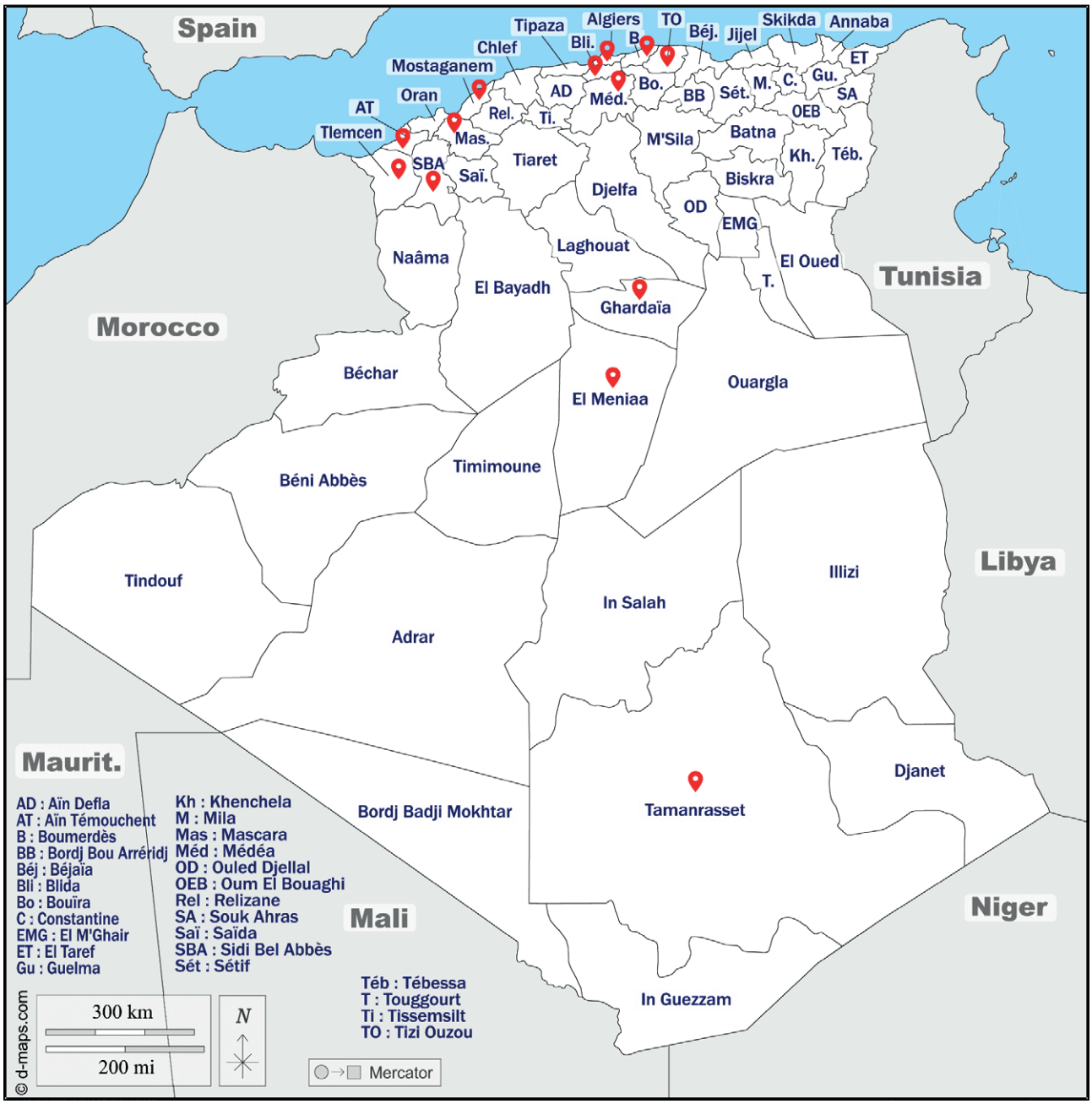

Figure 1. Map of the primary sampling regions in Algeria for this study. The symbols indicate the locations where samples were collected.

agarose gel electrophoresis, while their concentrations were determined using a spectrophotometer (NanoDrop® ND-100 spectrophotometer, Thermo Scientific).

Reverse transcription-polymerase chain reaction (RT-PCR)

A two-step RT-PCR protocol was followed for synthesis of cDNA. In the first step of reverse transcription, the random primer (1 µg µL^{-1}; Invitrogen™) was added with 1.5 µL of sterile water to 10 µL of TNA, and the reaction was incubated at 95°C for 5 min. Then, the components necessary for reverse transcription, including 0.5 µL dNTPs (10mM), 4µL RT 5× Buffer, DTT (0.1M), and M-MLV Reverse Transcriptase (200 U µL^{-1}) (Invitrogen™), were introduced for the second step. The reaction was incubated at 39°C for 1 h to allow cDNA

synthesis, followed by enzyme inactivation at 70°C for 10 min. The total reaction volume was 20 µL.

The PCRs was carried out using the primers LRAmp-F and LRAmp-R, designed by N. Abou Ghanem-Sabanadzovic *et al.* (2012), to amplify 485 bp fragments for the p23 protein (ORF6) gene region. The reactions were each carried out with 2.5 µL of denatured cDNA, 0.5 µL of each primer (20 µM), and DreamTaq DNA Polymerase (5U μL^{-1}) (Thermo Scientific™) in a total volume of 25 µL. They included initial denaturation at 94°C for 5 min, followed by 40 cycles, each of denaturation at 94°C for 30 sec, annealing at 50°C for 35 sec, then extension at 72°C for 45 sec, and a final extension at 72°C for 7 min. The PCR products were analyzed by electrophoresis on 1.2% TBE agarose gel, and visualized using ethidium bromide staining. RT-PCR was carried out specifically for the ELISA-positive samples. Additionally, 122 samples were used that were from plant material collected during another sampling in 2012 from grapevine growing regions in Algeria. Phloem tissues were used for RNA extractions, and the samples were stored as cDNA at –80°C at the plant protection laboratory of INRAT. Quality control of the cDNA was carried out using a positive control plant sample infected by GLRaV-4, which showed a positive reaction and confirmed good conservation of the cDNA.

Some virus isolates were selected for sequencing of the p23 protein gene regions using the Sanger method, and the obtained sequences were submitted in the NCBI database. A total of 14 positive samples were selected for sequencing based on their geographic and grapevine cultivar origins, to assess the genetic diversity of their partial p23 gene. The PCR products were processed for Sanger sequencing by Carthagenomics (Tunisia).

High throughput sequencing

Total RNA extraction and Illumina-HTS

To complement the DAS-ELISA and RT-PCR tests, a single grapevine sample from the autochthonous cultivar 'Cherchalli', collected in Medea and confirmed positive for GLRaV-4, was selected for HTS to detect the potential infections by other viruses and viroids. A 0.5 × 0.5 cm piece of leaf tissue from this GLRaV-4–infected plant was placed in an Eppendorf tube and immersed in RNALater solution, and then sent to JS-Link Company (South Korea). The RNA was extracted from plant sample using the RNeasy® Plant Mini Kit (QIAGEN). To obtain the cDNA, reverse transcription was carried out using M-MLV Reverse Transcriptase, following the manufacturer's instructions (JS-Link Company). To prepare the Illumina-HTS library, the Company used the TruSeq total DNA library prep kit. The sequences of total DNA were obtained using NovaSeq6000, 2×101PE (Platform: NovaSeq6000; Application: WTS/mRNA), after DNA quality was determined using an Agilent 2100 Expert Bioanalyzer (Agilent). Trimmomatic-0.39 and BBduk v 37.22 were used to trim raw reads in Geneious Prime® 2024.0.5 (Minimum quality = 6) Both ends were trimmed and minimum read length was 10 (Adapter/Quality Trimming Version 38.84; Brian Bushnell) (Kearse *et al.* 2012; www.geneious.com).

Map to reference

Geneious Prime® 2024.0.5 was used to map the DNA-Seq data to the reference sequences. The mapping was carried out with parameters set to "Medium-Low Sensitivity", using the Geneious DNA mapper. The DNA clean reads were mapped to a package of all the 5040 plant virus sequences available in GenBank (downloaded 24 August, 2024). These sequences were concatenated into a single representative sequence (76,145,671 nt), to ensure comprehensive detection of all virus and viroid elements present in the sample data. The results were displayed in a report that included the total number of reads used and the number of assembled reads (Khaffajah *et al.*, 2022).

Phylogenetic analyses

Blastn search was used for sequence comparisons, and multiple nucleotide sequence alignments were carried out using the ClustalW algorithm implemented in the Molecular Evolutionary Genetics Analysis software (MEGA 11.0.10) (Tamura *et al.* 2021). These alignments included sequences obtained in the present study and additional sequences retrieved from the GenBank database (www.cbi.nlm.nih.gov), some of which correspond to reference sequences from previously characterized strains of GLRaV-4 (Table 1). The p-distance method was used to calculate percent similarity values. A phylogenetic tree was then constructed based on nucleotide identity distances, using the neighbor-joining (NJ) method (Kimura 2-parameter model) with 1000 bootstrap replicates and the best-fit alignment (318 nt).

RESULTS

The DAS-ELISA test showed that GLRaV-4 was detected in 81 (18.2%) of the 444 samples assessed.

Table 1. Strain reference sequences of GLRaV-4 selected for phylogenetic analysis of the P23 gene.

Accession number	Isolates	Strain	Origin	Reference
FJ467503.1	LR106	Strain 4	USA	Abou Ghanem-Sabanadzovic *et al.* 2012
MF669482.1	WALA-9	Strain 9	USA	Adiputra *et al.* 2019
MF669481.1	WASB-5	Strain 5	USA	Adiputra *et al.* 2019
FJ467504.1	Estellat	Strain 6	USA	Abou Ghanem-Sabanadzovic *et al.* 2012
AM182328.4	Pr	Strain Pr	Greece	Maliogka *et al.* 2008
KP313764.1	Ob	Strain Ob	Switzerland	Reynard *et al.* 2015

GLRaV-4 was detected in different grapevine varieties. Among the varieties assessed, Ahmar Bouamar had an infection rate of 26.8%. Ladhari and Valensi each had rates of 40%, while Alicante had 30% infection, and Muscat had 20% GLRaV-4 infection. The 23 autochthonous grapevine accessions collected from ITAF had a combined infection rate of 39.1% (Table 2). The greatest highest infection rate (36.8% grapevines infected) was detected in the southern region of Algeria, particularly in Ghardaïa (36.4% infected). The central region followed, with an overall infection rate of 18.1%, particularly in Boumerdès and Médéa (approx. 23% positive samples. Lowest GLRaV-4 prevalence (16.7%) was detected in the western region (Table 3). These results highlighted variations in GLRaV-4 incidence among different grapevine varieties and viticultural regions.

Table 2. Infection rates of GLRaV-4 in surveyed grapevine cultivars, detected using DAS-ELISA.

Cultivar	Number of samples	Number of infected samples	Infection rate (%)
Ahmar Bouamar	41	11	26.8
Dattier	46	2	4.3
Michele Palieri	10	0	0.0
Muscat Italia	28	2	7.1
Cinsault	70	8	11.4
Gros noir	29	4	13.8
Red globe	20	3	15.0
Sabel	22	4	18.2
Cardinal	35	4	11.4
Ladhari	20	8	40.0
Carignan	20	4	20.0
Alicante	10	3	30.0
Merseguerra	10	0	0.0
Muscat	20	4	20.0
Valensi	20	8	40.0
Autochthonous	23	9	39.1
Unknown	20	7	35.0
Total	444	81	18.2

Some DAS-ELISA positive samples were further analyzed by RT-PCR using primers targeting the P23 protein (ORF6) gene, to assess genetic variability of GLRaV-4. Among the 81 positive samples (obtained in 2021/2022) assessed using DAS-ELISA for the presence of the virus, 59 were selected for further analyses by RT-PCR. Of these 29 were confirmed as positive for GLRaV-4. The PCR analyses of the 122 samples from the 2012 sampling showed that 16 samples were positive. Combining these results with those from the 2021/2022 samples collected, a total of 45 GLRaV-4 positive samples were detected. Among the positive samples, 14 were Sanger-sequenced, and two using HTS, selected from different grapevine cultivars and viticultural regions in the central, eastern, western, and southern parts of Algeria (Table 4).

Phylogenetic analysis revealed that Pairwise P23 nucleotide identities ranged from 71 to 100% for the

Table 3. Distribution of GLRaV-4 infections across major grapevine sampling regions and wilayas in Algeria.

Region	Wilaya	Number of samples	Number of infected samples	Infection rate (%)
Central	Medea	99	23	23.2
	Boumerdes	43	10	23.3
	Blida	40	1	2.5
	Tizi Ouzou	31	5	16.1
	Algiers	2	0	0.0
	Total	215	39	18.1
Western	Mostaganem	60	8	13.3
	Aïn Temouchent	70	11	15.7
	Tlemcen	20	3	15.0
	Sidi Bel Abbès	10	0	0.0
	Mascara	50	13	26.0
	Total	210	35	16.7
Southern	El Menia	4	1	25.0
	Ghardaia	11	4	36.4
	Tamanrasset	4	2	50.0
	Total	19	7	36.8

Table 4. GenBank accession numbers of Algerian GLRaV-4 isolates sequenced for the P23 protein gene.

Isolate	Cultivar	Origin	Sequencing method	Accession number
ALG85	Cinsault	Aïn Temouchent	Sanger	PQ406674
ALG107	Cherchali	Medea	HTS	PP983228
ALG108	Cherchali	Medea	HTS	PP983229
ALG122	Muscat	Aïn Temouchent	Sanger	PQ633193
ALG130	Muscat	Aïn Temouchent	Sanger	PQ619712
ALG157	Valensi	Mascara	Sanger	PQ633194
ALG212	Unknown	Ghardaia	Sanger	PQ633195
ALG253	Gros noir	Boumerdes	Sanger	PQ518714
ALG265	Sabel	Boumerdes	Sanger	PQ633197
ALG378	Unknown	Tamenrasset	Sanger	PQ619713
ALG383	Ahmar de Machetras	Medea	Sanger	PQ633196
ALG388	Ghanez	Medea	Sanger	PQ800099
ALG424	Ahmar Bouamar	Medea	Sanger	PQ807038
ALG20-12	Gros noir	Mascara	Sanger	PQ816343
ALG26-12	Gros noir	Mascara	Sanger	PQ816344
ALG373-12	Cargnan	Mascara	Sanger	PQ821896

Algerian isolates, that indicate a close relationship between Algerian isolates, except for the isolate ALG253 which showed less than 76% identity to the other Algerian sequences, indicating a highly divergent variant (Supplementary Table 3).

The Blast analysis revealed that the Algerian isolates share high sequence identity with NCBI isolates reported from several countries worldwide. As a result, we observed strong similarity with isolates from India, the USA, France, and other geographically distant regions (Table 5).

The phylogenetic tree, based on the P23 protein sequences of Algerian GLRaV-4 isolates and related international sequences available in GenBank, revealed six distinct phylogenetic groups (Figure 2). Among these, the Algerian sequences obtained in the present study clustered into five groups, each corresponding to a specific strain of GLRaV-4, as indicated by reference sequences from previous studies (Table 1). Distribution of the Algerian isolates across these strains was: Strain 4, isolates ALG383, ALG20-12, and ALG378; Strain 5, isolates ALG373-12, ALG157, and ALG85; Strain 6, isolates ALG107, ALG108, ALG265, ALG424, and ALG26-12; Strain 9, isolates ALG122, ALG130, ALG212, and ALG388; and Strain Pr, isolate ALG253. This clustering highlights the genetic diversity of GLRaV-4 within the Algerian isolates and provides valuable insights into their relationships with reference strains.

More than 95% nucleotide similarity was shown within the GLRaV-4 strain groups 4, 5, 6, and 9, except for Strain Ob, which had 90% similarity (Supplementary Table 4). In contrast, the between-group similarity percentages ranged from 62% to 90%, highlighting significant genetic diversity among isolates from different strains, especially Strain Pr and Strain Ob, with similarities of less than 75%.

Table 5. Pairwise nucleotide similarities between Algerian isolates of GLRaV-4 and reference sequences available in NCBI.

Algerian isolate	Strain	Reference isolate	Origin	Similarity (%)
ALG20-12 ALG378 ALG383	Strain 4	GDR-I (KT933072)	India	90–99.7
		LR106 (FJ467503)	USA	
ALG85 ALG157 ALG373-12	Strain 5	WASB-5 (MF669481)	USA	96–98
ALG26-12 ALG107 ALG108 ALG265 ALG424	Strain 6	WIL24N5 (OP752662)	Australia	94–97
		Estellat (FJ467504)	USA	
ALG122 ALG130 ALG212 ALG388	Strain 9	WALA-9 (MF669482)	USA	95–98
		LC12_N5 (OP752665)	Australia	
ALG253	Strain Pr	Pr (AM182328)	Greece	97.6

The between-group identity analyses showed that Strain 9 and Strain 5 had close phylogenetic relationship (90%). Strain 6 had 89% similarity with Strain 9 and 88% with Strain 5, indicating strong genetic connections between these strains. Strain 4 had moderate similar-

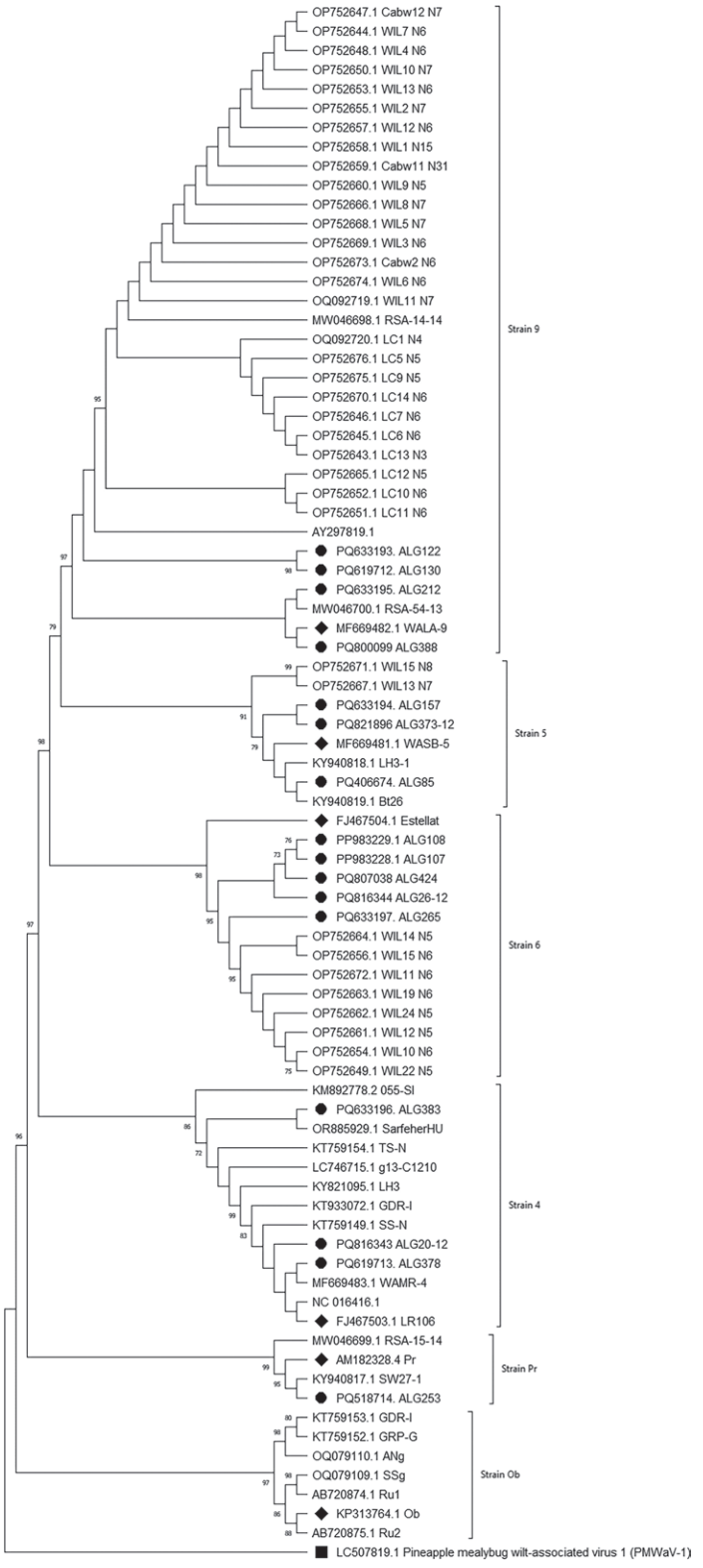

Figure 2. Phylogenetic tree of grapevine leafroll associated virus 4 (GLRaV-4, *Ampelovirus tetravitis*) isolates obtained in the present study and retrieved from GenBank. The tree was constructed with sequences of the 318 nt fragment of the P23 gene, with percentage of bootstrap support (≥70%) with 1,000 bootstrap replicates. Pineapple mealybug wilt-associated virus (LC507819: PMWaV-1, *Ampelovirus unananas*) was used as the outgroup. ● indicates Algerian sequences, and ♦ indicates the reference sequence for the group.

ity (83%) with Strain 6 and Strain 5 (83%), and Strain 9 (84%), suggesting a closer genetic relationship within these strains compared to others. Strain Pr had low similarity (maximum of 74%) across all comparisons, indicating divergent genetic composition in this strain. Strain Ob had the lowest similarity (62% to 64%), indicating increased degree of genetic divergence compared to the other strains (Supplementary Table 5).

Total RNAseq data generated by the Illumina platform included 47,039,345 raw reads that were trimmed to obtain 47,034,642 short clean reads of 101 bases. In Geneious software, all RNA reads were paired and mapped against suspected virus and viroid genomes. The P23 protein genes of the GLRaV-4 were reconstructed (isolates ALG107, PP983228 and ALG108, PP983229). Additionally, the complete genomes of hop stunt viroid (HSVd, *Hostuviroid impedihumuli*) isolate ALG305 (PQ059409) and grapevine yellow speckle viroid 1 (GYSVd-1, *Apscaviroid alphaflavivitis*) isolate ALG302 (PQ059408) were obtained. Furthermore, fragmented sequences corresponding to three viruses were also identified: grapevine Pinot gris virus (GPGV, *Trichovirus pinovitis*) isolate ALG400, grapevine leafroll-associated virus 2 (GLRaV-2, *Closterovirus vitis*) isolate ALG301, and grapevine fanleaf virus (GFLV, *Nepovirus foliumflabelli*) isolate ALG226, registered, respectively, under accession numbers PQ059410.1, PQ059407.1, and PQ059404.1.

DISCUSSION

GLRaV-4 has been reported as one of the viruses responsible for grapevine leafroll in many regions, and is often found in mixed infections with other GLRaVs (Aboughanem-Sabanadzovic *et al*., 2017).

The present study is the first to report occurrence and genetic diversity of GLRaV-4 in Algeria, covering the different viticultural regions across the country. Previous surveys in Algerian vineyards reported GLRaV-3 as the most prevalent grapevine leafroll-associated virus, with incidences ranging from 44% to 55.3%, while GLRaV-2 and GLRaV-1 were detected at incidences of, respectively, 15.8% and 5.4% (Lekikot *et al*., 2012; Lehad *et al*., 2015a; 2015b; 2019). Based on the 18.2% incidence of GLRaV-4 detected in the present study, this virus probably ranks between GLRaV-2 and GLRaV-3 in prevalence among grapevine leafroll-associated viruses reported so far in Algeria.

The discrepancy observed in the present study between ELISA and RT-PCR results likely resulted from the high genetic variability of the virus, which limits the ability of the primers designed by Abou Ghanem-Sabanadzovic *et al.* (2012) to detect all variants. In contrast, ELISA uses polyclonal antibodies that recognize a broad range of variants, making it more reliable than RT-PCR for large-scale virus detections.

Nucleotide comparisons showed that the Algerian GLRaV-4 sequences exhibited genetic relationships for the P23 gene, with sequence similarity ranging from 71% to 100%. This high level of genetic diversity reflects the presence of distinct GLRaV-4 strains, as confirmed by Martelli *et al.* (2012). They described GLRaV-4 as a virus with multiple genetically diverse variants, including Strains 4, 5, 6, 9, Pr, and others, which are serologically related and share similar genome structures, sizes, and biological and epidemiological characteristics. The similarities observed between strains, ranging from 62% to 90%, further confirms the significant genetic diversity among GLRaV-4 strains.

The analyses showed strong relationships between some virus isolates obtained from different regions and grapevine varieties. Isolates ALG122, ALG130, ALG212, and ALG388 had high nucleotide similarity (97% to 100%). Isolates ALG26-12, ALG107, ALG108, ALG265, and ALG424 were also similar, with nucleotide similarities between 96% and 100%. Additionally, isolates ALG85, ALG157, and ALG373-12 shared nucleotide similarities from 96% to 98%. In contrast, isolate ALG253 had low similarity compared to other Algerian sequences, suggesting the isolate was more genetically distinct. The results showed no correlations between percentage of nucleotide similarity and either the geographical origin or the grapevine cultivar from which the isolates were obtained. Comparable results were obtained by Orfanidou *et al.* (2021).

Most of the Algerian sequences obtained in the present study, from different grapevine cultivars and regions, clustered with the reference sequences of GLRaV-4 Strain 4, Strain 5, Strain 6, and Strain 9, while only one sequence grouped with GLRaV-4 Strain Pr. No Algerian sequence clustered with GLRaV-4 Strain Ob. Based on the comparison with the reference sequences, isolates ALG20-12, ALG378, and ALG383 were closely related to the reference isolate LR106 (FJ467503), with 92 to 99% similarity, identifying them as GLRaV-4 Strain 4. Isolates ALG85, ALG157, and ALG373-12 were closely related (96 to 98% similar) to the reference isolate WASAB-5 (MF669481), identifying them as GLRaV-4 Strain 5. Isolates ALG26-12, ALG107, ALG108, ALG265, and ALG424 were 94% similar to the reference isolate Estellat (FJ467504), identifying them as GLRaV-4 Strain 6. Isolates ALG122, ALG130, ALG212, and ALG388 had nucleotide similarities of 97% to 98% to the refer-

ence isolate WALA-9 (MF669482), classifying them as GLRaV-4 Strain 9. Isolate ALG253 had 99% similarity to the reference isolate Pr (AM182328), identifying it as GLRaV-4 Strain Pr.

These results are consistent with those reported by other authors. The phylogenetic analysis of Wu *et al.* (2023) showed that Australian isolates were of five major groups, of Strains 4, 5, 6, 9 and Pr, for the complete genome sequence and sequences of the RdRp, HPS70h and CP genes. Argentinian isolates (Talquenca *et al*., 2023) grouped within GLRaV-4 Strain 5, Strain 6, and Strain 9, based on their coat protein (CP) gene sequences, while no sequence was found to cluster with GLRaV-4 Strain 4, Strain Pr, or Strain Ob. Du *et al.* (2025) built on earlier work that had separated GLRaV-4 into the strain groups 4, 5, 6, 9, Car, Pr and Ob, using CP sequences. Using combined CP and HSP70 phylogenies, they redefined this diversity into seven groups: the distinct strain groups 5, 6, 9, Pr and Car, plus two additional clusters designated as GLRaV-4 Group 1 and Group 2. In this updated framework, Group 1 corresponds to the original GLRaV-4 lineage containing the reference isolate LR106 (NC_016416), while Group 2 corresponds to the former Ob strain lineage. With this updated grouping scheme, the Algerian isolates were found, in the present study, to belong to GLRaV-4 Group 1 and to the previously defined strain groups 5, 6, 9 and Pr.

The P23 gene protein homology analysis in the present study indicated that Strains 5, 6, and 9 are phylogenetically more similar to each other than to Strains 4, Pr, and Ob. The sequences corresponding to GLRaV-4 Strain Ob and GLRaV-4 Strain Pr exhibited the greatest genetic diversity compared to sequences from other groups. This was already observed by Wu *et al.* (2023) in their study of the coat protein (CP) gene of Australian isolates. The Slovenian isolate 055-SI was 87% similar to the reference sequence LR106, and only 61% similar to Strain Ob (Ru1, AB720874.1), for the P23 protein gene (Štrukelj *et al*., 2016). Indian GLRaV-4 isolates GRP-G and GDR-I also had genetic divergence in their P23 gene compared with other GLRaV-4 isolates (Rai *et al*., 2017). The phylogenetic tree based on the P23 gene in the present study (Figure 2) is consistent with the taxonomic revision proposed by Martelli *et al.* (2012), which was based on amino acid sequence divergence from RNA-dependent RNA polymerase (RdRp), heat shock protein 70 homologue (HSP70h), and coat protein (CP).

HTS confirmed GLRaV-4 infections and supported mixed infections of this virus with HSVd, GYSVd 1, GPGV, GLRaV-2, and GFLV. These results reflect the previously reported common occurrence of mixed virus infections observed in grapevines (Fajardo *et al*., 2017).

Limited studies have been conducted specifically on the P23 protein gene within GLRaV-4. Du *et al.* (2025) showed that P23 interacts with HSP70 and CP, playing a key role in virus particle assembly, replication, and grapevine leafroll pathogenesis. Further research is required to provide increased understanding of genetic diversity of the P23 gene across different virus strains. Additionally, observed symptoms caused by GLRaV-4 are closely related to mixed virus infections, and cannot be attributed to any specific virus, viroid or to synergies between these pathogens.

There have been few studies examining GLRaV vectors and transmission in Algeria. However, the mealybug *Planococcus ficus* has been reported to be a vector of GLRaV-4 in other viticultural regions (Tsai *et al*., 2010), and has been recorded in the Mitidja region of Algeria (Bissaad *et al*., 2017). Presence of this insect suggests a potential role in the local transmission of GLRaV-4. Information on the distribution of mealybugs and soft scale insects, specifically *P. ficus* and *Phenacoccus aceris*, is important for controlling GLRaV-4 dissemination in viticultural systems. Practical disease management strategies should include the use of certified virus-free planting material (obtained through sanitation and *in vitro* culture protocols), monitoring and control of insect vectors such as mealybugs and soft scale, and removal of infected grapevines to reduce virus spread and protect vineyard productivity.

ACKNOWLEDGEMENTS

This work was funded by the Algerian Ministry of Higher Education and Scientific Research (MESRS), through the Directorate-General of Scientific Research and Technological Development (DGRSDT) and the Algero-Tunisian project “INNOVITIS”.

LITERATURE CITED

Abou Ghanem-Sabanadzovic N., Sabanadzovic S., Gugerli P., Rowhani A., 2012. Genome organization, serology, and phylogeny of *Grapevine leafroll-associated viruses* 4 and 6: Taxonomic implications. *Virus Research* 163(1): 120–128. https://doi.org/10.1016/j.virusres.2011.09.001

Aboughanem-Sabanadzovic N., Maliogka V., Sabanadzovic S., 2017. Grapevine leafroll-associated virus 4. In: *Grapevine Viruses: Molecular Biology, Diagnostics and Management* (Meng B., Martelli G.P., Golino D.A., Fuchs M., ed.). Springer International Publish-

ing, pp. 197–202. https://doi.org/10.1007/978-3-319-57706-7_9

Adiputra J., Jarugula S., Naidu R.A., 2019. Intra-species recombination among strains of the ampelovirus Grapevine leafroll-associated virus 4. *Virology Journal* 16(1): 1–13. https://doi.org/10.1186/s12985-019-1243-4

Atallah S.S., Gómez M.I., Fuchs M.F., Martinson T.E., 2012. Economic impact of *Grapevine Leafroll Disease* on *Vitis vinifera* cv. Cabernet franc in Finger Lakes vineyards of New York. *American Journal of Enology and Viticulture* 63(1): 73–79. https://doi.org/10.5344/ajev.2011.11055

Bachir A., El Air M., Alisawi O., Djenaoui A., Laidoudi N., … Lehad, A., 2024. Genetic diversity of GRSPaV-associated virus in Algeria. *Phytopathologia Mediterranea* 63(3): 443–451. https://doi.org/10.36253/phyto-15554

Bissaad F. Z., Bounaceur F., Doumandji, M. B., 2017. Dynamique spatio-temporelle de *Planococcus ficus* (Signoret, 1875) dans les vignobles de la mitidja (Algeria). *Lebanese Science Journal* 1: 24–46.

Clark M.F., Adams A.N., 1977. Characteristics of the microplate method of enzyme-linked immunosorbent assay for the detection of plant viruses. *Journal of General Virology* 34(3): 475–483. https://doi.org/10.1099/0022-1317-34-3-475

Du T., Hao Y., Gao J., Qiao S., Hu G., Ren F., Fan X., Dong, Y., 2025. Complete Sequence Analysis of Grapevine Leafroll-Associated Virus 4 and Interactions Between the Encoded Proteins. *Viruses* 17(7): 952. https://doi.org/10.3390/v17070952

Fajardo T. V., Silva F. N., Eiras M., Nickel O., 2017. High-throughput sequencing applied for the identification of viruses infecting grapevines in Brazil and genetic variability analysis. *Tropical Plant Pathology* 42: 250–260. https://doi.org/10.1007/s40858-017-0142-8

Gambino G., Perrone I., Gribaudo I., 2008. A rapid and effective method for RNA extraction from different tissues of grapevine and other woody plants. *Phytochemical Analysis* 19(6): 520–525. https://doi.org/10.1002/pca.1078

Herrbach E., Alliaume A., Prator C.A., Daane K.M., Cooper M.L., Almeida R.P.P., 2017. Vector transmission of *Grapevine leafroll-associated viruses*. In: *Grapevine Viruses: Molecular Biology, Diagnostics and Management* (Meng B., Martelli G.P., Golino D.A., Fuchs M., ed.). Springer, pp. 483–503. https://doi.org/10.1007/978-3-319-57706-7_24

Kearse M., Moir R., Wilson A., Stones-Havas S., Cheung M., … Drummond A., 2012. Geneious Basic: an integrated and extendable desktop software platform for the organization and analysis of sequence data. *Bioinformatics* 28(12): 1647–1649. https://doi.org/10.1093/bioinformatics/bts199

Khaffajah B., Alisawi O., Al Fadhl F., 2022. Genome sequencing of eggplant reveals Eggplant mild leaf mottle virus existence with associated two endogenous viruses in diseased eggplant in Iraq. *Archives of Phytopathology and Plant Protection* 55(16): 1930–1943. https://doi.org/10.1080/03235408.2022.2123601

Laidoudi N. E., Alisawi O., Yahiaoui B., Djenaoui A., Mahdid I., … Lehad A., 2025. Occurrence of *Grapevine fanleaf virus* in Algerian vineyards, and complete genome sequencing. *Phytopathologia Mediterranea* 64(2): 219–228. https://doi.org/10.36253/phyto-15993

Lehad A., Selmi I., Louanchi M., Aitouada M., Mahfoudhi N., 2015a. Survey and genetic diversity of *Grapevine leafroll-associated virus 2* in Algeria. *International Journal of Phytopathology* 4(1): 35–42. https://doi.org/10.33687/phytopath.004.01.1074

Lehad A., Selmi I., Louanchi M., Aitouada M., Mahfoudhi N., 2015b. Genetic diversity of *Grapevine leafroll-associated virus 3* in Algeria. *Journal of Plant Pathology* 97(1): 203–207. http://www.jstor.org/stable/24579152

Lehad A., Selmi I., Louanchi M., Aitouada M., Mahfoudhi N., 2019. Occurrence and diversity of *Grapevine leafroll-associated virus 1* in Algeria. *Phytopathologia Mediterranea* 58(2): 277–281. https://doi.org/10.14601/Phytopathol_Mediter-10615

Lekikot K., Elbeaino T., Ghezli C., Digiaro M., 2012. Preliminary Survey of Grapevine Viruses in Algeria. *Proceedings of 17th Congress of ICVG*, Davis, California, USA. 194–197.

Mahdid I., Alisawi O., Djenaoui A., Laidoudi N., Mahfoudhi N., Lehad A., 2025. Assessment of Grapevine Fleck Virus (GFkV) infection in Algerian vineyards. *Acta Phytopathologica et Entomologica Hungarica* 60: 59–70. https://doi.org/10.1556/038.2025.00238

Maliogka V.I., Dovas C.I., Katis N.I., 2008. Evolutionary relationships of virus species belonging to a distinct lineage within the *Ampelovirus* genus. *Virus Research* 135(1): 125–135. https://doi.org/10.1016/j.virusres.2008.02.015

Maliogka V.I., Minafra A., Saldarelli P., Ruiz-García A.B., Glasa M., Katis N., Olmos A., 2018. Recent advances on detection and characterization of fruit tree viruses using high-throughput sequencing technologies. *Viruses* 10(8): 1–23. https://doi.org/10.3390/v10080436

Maree H.J., Almeida R.P.P., Bester R., Chooi K.M., Cohen D., … P., Burger J.T., 2013. Grapevine leafroll-*associated virus 3. Frontiers in Microbiology* 4: 1–21. https://doi.org/10.3389/fmicb.2013.00082

Martelli G.P., Abou Ghanem-Sabanadzovic N., Agranovsky A.A., Al Rwahnih M., Dolja V.V., … Saldarelli P., 2012. Taxonomic revision of the family *Closteroviridae* with special reference to the *Grapevine Leafroll-Associated* members of the genus *Ampelovirus* and the putative species unassigned to the family. *Journal of Plant Pathology* 94(1): 7–19. https://www.jstor.org/stable/45156004

Naidu R.A., Maree H.J., Burger J.T., 2015. Grapevine leafroll disease and associated viruses: A unique pathosystem. *Annual Review of Phytopathology* 53: 613–634. https://doi.org/10.1146/annurev-phyto-102313-045946

Orfanidou C.G., Moraki K., Panailidou P., Lotos L., Katsiani A., … Maliogka V.I. 2021. Prevalence and genetic diversity of viruses associated with rugose wood complex in Greek vineyards. *Plant Disease* 105(11), 3677–3685. https://doi.org/10.1094/PDIS-02-21-0266-RE

Rai R., Khurana S.P., Kumar S., Sharma S.K., Watpade S., Baranwal V.K., 2017. Characterization of Grapevine leafroll-associated virus 4 from Indian vineyards. *Journal of Plant Pathology* 99: 255–259. https://www.jstor.org/stable/44280598

Reynard J.S., Schneeberger P.H., Frey J.E., Schaerer S., 2015. Biological, serological, and molecular characterization of a highly divergent strain of *Grapevine leafroll-associated virus 4* causing grapevine leafroll disease. *Phytopathology* 105(9): 1262–1269. https://doi.org/10.1094/PHYTO-12-14-0386-R

Saldarelli P., Giampetruzzi A., Maree H.J., Al Rwahnih M., 2017. High-throughput sequencing: advantages beyond virus identification. In: *Grapevine Viruses: Molecular Biology, Diagnostics and Management* (Meng B., Martelli G., Golino D., Fuchs M., ed.). Springer, Cham, pp.625–642.

Štrukelj M., Pleško I., Urek G., 2016. Molecular characterization of a *Grapevine leafroll-associated virus 4* from Slovenian vineyards. *Acta Virologica* 60(2): 174–180. https://doi.org/10.4149/AV_2016_02_174

Talquenca S. G., Volpe M. L., Setien N., Gracia O., Grau O., 2023. Serological relationships among strains of grapevine leafroll-associated virus 4 reflect the evolutive behavior of its coat protein gene. *Revista de la Facultad de Ciencias Agrarias UNCuyo*, 55(1): 104–114. https://doi.org/10.48162/rev.39.100

Tamura K., Stecher G., Kumar S., 2021. MEGA11: Molecular Evolutionary Genetics Analysis version 11. *Molecular Biology and Evolution* 38(7): 3022–3027. https://doi.org/10.1093/molbev/msab120

Tsai C. W., Rowhani A., Golino D. A., Daane K. M., Almeida, R. P. 2010. Mealybug transmission of grapevine leafroll viruses: an analysis of virus–vector specificity. *Phytopathology* 100(8): 830–834. https://doi.org/10.1094/PHYTO-100-8-0830

Wu Q., Habili N., Kinoti W.M., Tyerman S.D., Rinaldo A., Zheng L., Constable F.E., 2023. A metagenomic investigation of the viruses associated with Shiraz disease in Australia. *Viruses* 15(3): 774. https://doi.org/10.3390/v15030774

Phytopathologia Mediterranea
The international journal of the
Mediterranean Phytopathological Union

Firenze University Press
www.fupress.com/pm

Research Notes

Virome analysis reveals apple mosaic virus in the monumental tree *Castagno dei cento cavalli* in Sicily

Matilde TESSITORI[1,*], Marina CIUFFO[2], Cristina MARZACHÌ[2], Marco FORGIA[2]

[1] *Department of Agriculture, Food and Environment (Di3A), University of Catania, 95123 Catania, Italy*
[2] *Institute of Sustainable Plant Protection on National Research Council (IPSP-CNR), 10135 Torino, Italy*
*Corresponding author. E-mail: mtessitori@unict.it

Summary. The *Castagno dei cento cavalli* (One hundred horse chestnut) is a monumental *Castanea sativa* (sweet chestnut) located on the eastern slope of Mount Etna in Sicily (Italy), and is the oldest (>2000 years) known sweet chestnut in the world. In the spring of 2022, symptoms indicating virus infection were observed on this tree. Attempts to visualize virus particles from extracts using transmission electron microscopy were unsuccessful, so high-throughput RNA sequencing was carried out. This identified a tripartite genome (RNA1, RNA2, and RNA3) corresponding to apple mosaic virus (species *Ilarvirus ApMV*). Serological analyses using polyclonal antiserum confirmed infection in symptomatic but not in asymptomatic leaf samples. This is the first report of ApMV infecting *C. sativa*, and this virus possibly threatens monumental trees elsewhere internationally. Although efficient ApMV vectors are lacking, limiting the risk of spread, this knowledge highlights the need for monitoring monumental trees as potential reservoirs of novel host-virus associations, and the importance of careful management of this Sicilian botanical monument.

Keywords. HTS-based virus detection, *Castanea sativa*, chlorotic mottling, ApMV host range.

OPEN ACCESS

Citation: Tessitori, M., Ciuffo, M., Marzachì, C., & Forgia, M. (2026). Virome analysis reveals apple mosaic virus in the monumental tree *Castagno dei cento cavalli* in Sicily. *Phytopathologia Mediterranea* 65(1): 67-73. doi: 10.36253/phyto-16807

Accepted: January 8, 2026

Published: March 16, 2026

© 2026 Author(s). This is an open access, peer-reviewed article published by Firenze University Press (https://www.fupress.com) and distributed, except where otherwise noted, under the terms of the CC BY 4.0 License for content and CC0 1.0 Universal for metadata.

Data Availability Statement: All relevant data are within the paper and its Supporting Information files.

Competing Interests: The Author(s) declare(s) no conflict of interest.

Editor: Arnaud G Blouin, Institut des sciences en production végétale IPV, DEFR, Agroscope, Nyon, Switzerland.

ORCID:
MT: 0000-0003-4285-8569
MC: 0000-0003-0422-408X
CM: 0000-0002-1084-6048
MF: 0000-0003-0101-1046

INTRODUCTION

The One Hundred Horse Chestnut (*Castagno dei Cento Cavalli*) is a monumental *Castanea sativa* Mill. located in Sant'Alfio (Catania Province, Sicily, Italy; 37°45'00.66" N, 15°07'49.34" E), at 710 m a.s.l., about 10 km from the Etna crater (Figure 1). Estimated to be 2,000 to 3,000 years old, this tree is regarded as the world's oldest *C. sativa* specimen, and has survived multiple Etna eruptions and extreme climatic events (Schicchi and Raimondo, 2007). Recognized by UNESCO as a "World Heritage messenger of peace," the tree holds European records for size and longevity. Molecular analyses have shown that the tree, once believed to be three individuals, is a single

plant, with three trunks sharing a common root system probably resulting from radial fragmentation of an ancient trunk (Pereira-Lorenzo et al., 2019; Mattioni et al., 2020; Nunziata et al., 2022). Radial growth estimates indicate that the tree is at least 2,276 years old (Pereira-Lorenzo et al., 2019).

The apple mosaic virus (ApMV, species *Ilarvirus ApMV*) belongs to *Ilarvirus* (*Bromoviridae*). Early classification of this virus relied on serology, but was later refined through genomic data into four molecular subgroups (Pallas *et al*., 2013). The term "ilar-" derives from "**i**sometric **la**bile **r**ingspot." These thermolabile viruses often mask symptoms at high temperatures (Aramburu and Rovira, 1998; Dal Zotto et al., 1999). ApMV particles are quasi-spherical and contain a tripartite, positive-sense RNA genome and RNA3, and produce a subgenomic RNA that carries the open reading frame (ORF) encoding the coat protein (Roossinck *et al*., 2005). All three RNA components are required for host plant infection (Grimová et al., 2016). The virus occurs widely in woody and herbaceous hosts, mainly *Malus domestica* and *Rubus idaeus* (Manzoor *et al*., 2023), but has been detected in more than 65 plant species (Grimová *et al*., 2016; EPPO, 2024).

This paper reports the results of virome analysis carried out on the monumental sweet chestnut tree using high-throughput sequencing, and documents the first detection of ApMV in *C. sativa*.

MATERIAL AND METHODS

Following a report from the Regional Plant Protection Service, a first survey of *Castagno dei Cento Cavalli* was conducted in June 2022, the symptoms of which indicated viral infection. Foliar symptoms of chlorotic ring mottling, spotting, and oak-leaf patterns were observed on suckers and apical branches of one of the three main trunks of the tree (Figure 2), while the other two trunks had no symptoms. Leaf samples were collected from all three trunks. Additional surveys in spring and autumn 2023 and 2024 confirmed persistence and localization of symptoms on the tree. Field observations were also extended to the surrounding area to record comparable symptoms in other plant species, including hazelnut (*Corylus avellana*), an abandoned apple orchard, and another monumental chestnut (*Castagno della Nave*) located about 600 m away from *Castagno dei Cento Cavalli*.

Attempts to visualize virus particles using transmission electron microscopy (TEM) were unsuccessful, probably due to virion instability. For virome analy-

Figure 1. The *Castagno dei Cento Cavalli* (One hundred horse chestnut) *Castanea sativa* tree in Sant'Alfio (Catania), Sicily, Italy.

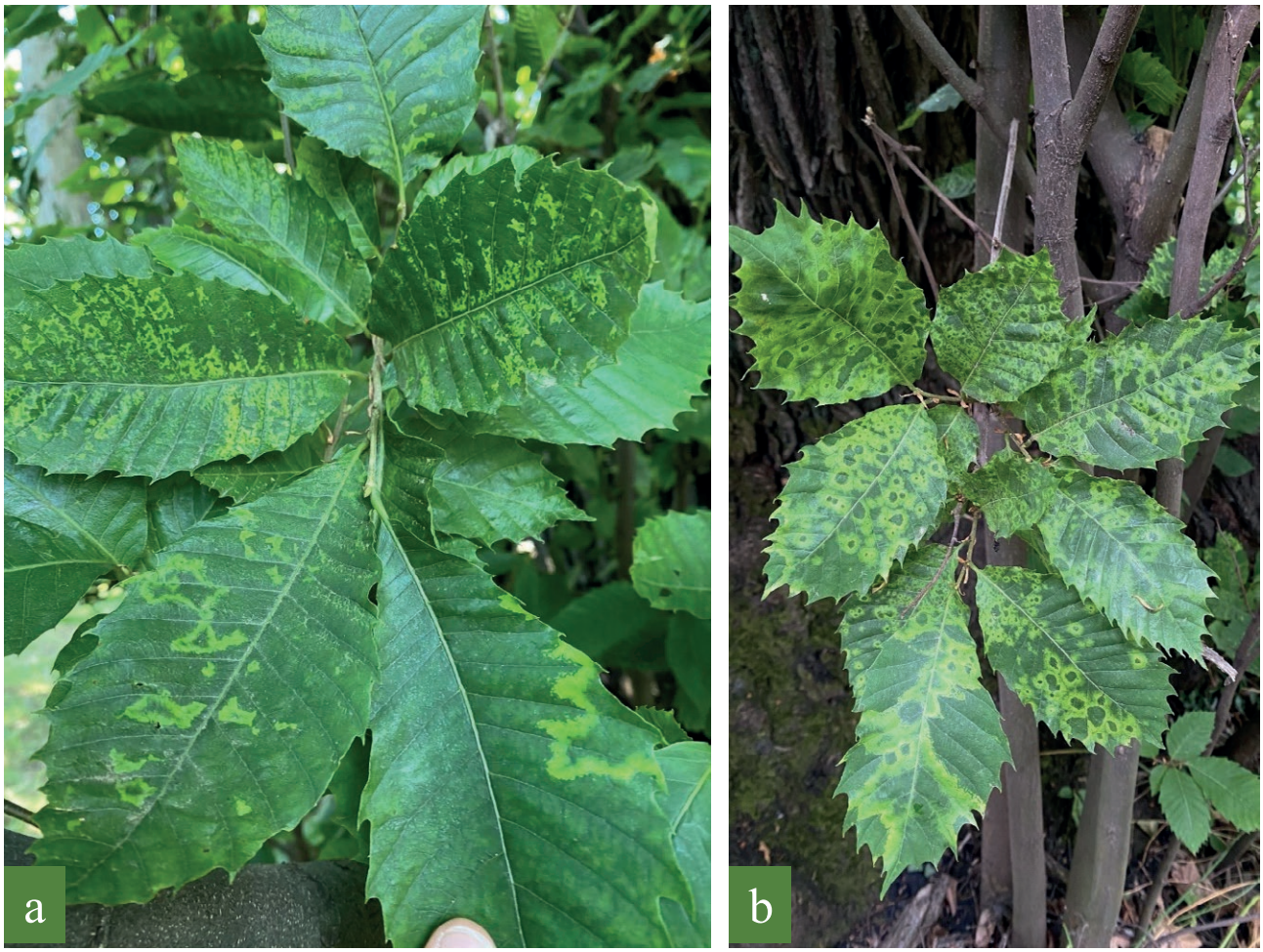

Figure 2. Symptoms of leaf chlorotic ring mottling, oak-like leaf, and chlorotic spotting on suckers, in initial (a) and advanced (b) stages of symptom development on the monumental chestnut tree *Castagno dei Cento Cavalli*.

sis, leaf samples were freeze-dried and stored at –20°C. Total RNA was extracted using the Spectrum™ Plant Total RNA Kit (Merck). RNA integrity was checked by 1% agarose gel electrophoresis, and RNA was quantified using a NanoDrop spectrophotometer (Thermo Fisher Scientific). Total RNA was processed by Macrogen Inc. (Seoul, Republic of Korea), for rRNA depletion (TruSeq Stranded Total RNA with Ribo-Zero Plant, Illumina), library preparation, and high-throughput sequencing on an Illumina NovaSeq 6000 platform. Resulting 150 bp paired-end reads were quality-filtered using the Joint Genome Institute (JGI) pipeline (https://doi.org/10.17504/protocols.io.gydbxs6), and were assembled *de novo* with Trinity v2.3.0. Viral contigs were identified through BLAST search against the NCBI nr database (e-value $1e^{-10}$), as described by Forgia *et al.* (2022). Filtering with the *dplyr* package (R software) and manual check yielded three contigs blasting against the protein coded by RNA1, RNA2 and RNA3 of ApMV. Read mapping was performed with Bowtie2 (Langmead and Salzberg, 2012), and alignments visualized with Tablet. ApMV detection was validated by RT-qPCR on cDNA synthesized from the same RNA used for HTS, using primers specifically designed on RNA1 by using Primer3 (Untergasser *et al.*, 2012) (amplicon 70–120 bp, 60°C annealing) (Table 1). cDNA synthesis employed the High-Capacity cDNA Reverse Transcription Kit (Thermo Fisher Scientific), and RT-qPCR was run in 10 µL reactions with three technical replicates using iTaq Universal SYBR Green Supermix (Bio-Rad) on a CFX Connect System (Bio-Rad) (Picarelli *et al.*, 2019). Open reading frames (ORFs) prediction and identification of domains in the putative proteins were carried out using the NCBI ORF Finder tool. The RNA-dependent RNA polymerase (RdRp) of the ApMV isolate MT3 was aligned with RdRp sequences of recognized *Ilarvirus*

species (ICTV database). Multiple sequence alignment was performed using MAFFT (Katoh and Standley, 2013), and a maximum-likelihood tree was constructed with IQ-TREE (Trifinopoulos *et al*., 2016) under automatic model selection and 1,000 ultrafast bootstraps. The resulting tree was edited using MEGA version X.

To confirm presence of the ApMV, and its association with observed symptoms, four asymptomatic and four symptomatic leaf samples were collected during each spring and autumn of 2023 and 2024 (total of 16 asymptomatic and 16 symptomatic samples). The samples were assessed using DAS-ELISA. Serological analyses were carried out using a polyclonal antiserum raised against the ApMV-hop isolate (LOEWE), following the manufacturer's instructions, using 1 g of leaf tissue homogenized in extraction buffer. To validate the three RNA sequences obtained by HTS and to verify possible insertions, deletions, or SNPs in comparison with genomes available in GenBank, specific primers were designed and used for RT-PCR on total RNA from four symptomatic samples collected in spring 2024 (Supplementary Table S1). Two asymptomatic samples served as negative controls. Amplicons were sequenced in both directions by Sanger sequencing.

RESULTS AND DISCUSSION

Illumina sequencing produced 102,025,671 raw reads, of which 91,999,781 high-quality reads were retained, and these were assembled *de novo* with Trinity, yielding 409,219 contigs. All raw sequencing data generated in this study have been deposited in the NCBI Sequence Read Archive (SRA) under accession number SRR36266065. The HTS library was established through the collection of diverse plant specimens suspected of containing virus infections. Each of the identified viruses (prunus necrotic ringspot virus, prune dwarf virus, eggplant mottled dwarf nucleorhabdovirus) were checked in the chestnut samples through qRT-PCR (protocol described above).

Virus screening exclusively identified three viral contigs corresponding to the complete coding sequences of a novel ApMV isolate, designated MT3. These sequences were deposited in GenBank, under accession numbers PQ137752 (RNA2), PQ137753 (RNA1), and PQ137751 (RNA3). Read mapping using Bowtie2 confirmed coverage of all genomic segments (40,882 reads for RNA1, 21,078 for RNA2, and 76,316 for RNA3). RT-qPCR assays with primers targeting RNA1 (Supplementary Table S1) confirmed ApMV presence in RNA extracted from symptomatic chestnut leaves collected in spring 2023. BLAST analyses of each RNA sequence (July 2025 NCBI release) revealed that RNA1 and RNA2 of ApMV MT3 were most similar to the Iranian apple isolate Alborz-A2 (92.7% similarity for RNA1, 89.5% for RNA2). In contrast, RNA3 of ApMV MT3 exhibited greater divergence, with 87.9% similarity with its closest match, a German ApMV isolate from *Rubus* sp. (DSMZ PV-0742). The predicted proteins shared 88.8 to 94.8% similarity with ApMV homologs (Table 1). Phylogenetic analysis of the RdRp amino acid sequence positioned ApMV MT3 within the established ApMV clade (Figure. 3). Mutations in regions containing indels or

Table 1. BLAST analysis results of the nucleotide and protein sequences of ApMV MT3.

Genomic segment	Isolate	Blastn best hit						
		Query cover	E value	Percent similarity	Acc. Len	Accession	Host	Origin
RNA1	Alborz-A2	98%	0.0	92.67%	3440	OR537857.1	*Malus domestica*	Iran
RNA2	Alborz-A2	98%	0.0	89.45%	2979	OR537858.1	*Malus domestica*	Iran
RNA3	DSMZ PV-0742	100%	0.0	87.88%	2104	OR477282.1	*Rubus* sp.	Germany

Genomic Segment	Protein	Isolate	Blastp best hit						
			Query cover	E value	Percent similarity	Acc. Len	Accession	Host	Origin
RNA1	Replicase	Alborz-A2	100%	0.0	94.84%	1047	XCO66467.1	*Malus domestica*	Iran
RNA2	RNA-dependent RNA polymerase	DSMZ PV-0742	100%	0.0	91.45%	877	WNS50456.1	*Rubus* sp.	Germany
RNA3	Movement protein	ApMV_RNA3_hop_pool_2021	100%	0.0	88.77%	285	XQU58012.1	*Humulus lupulus*	Germany
RNA3	Coat protein	India3	100%	0.0	89.24%	223	ACJ44917.1	*Malus domestica*	India

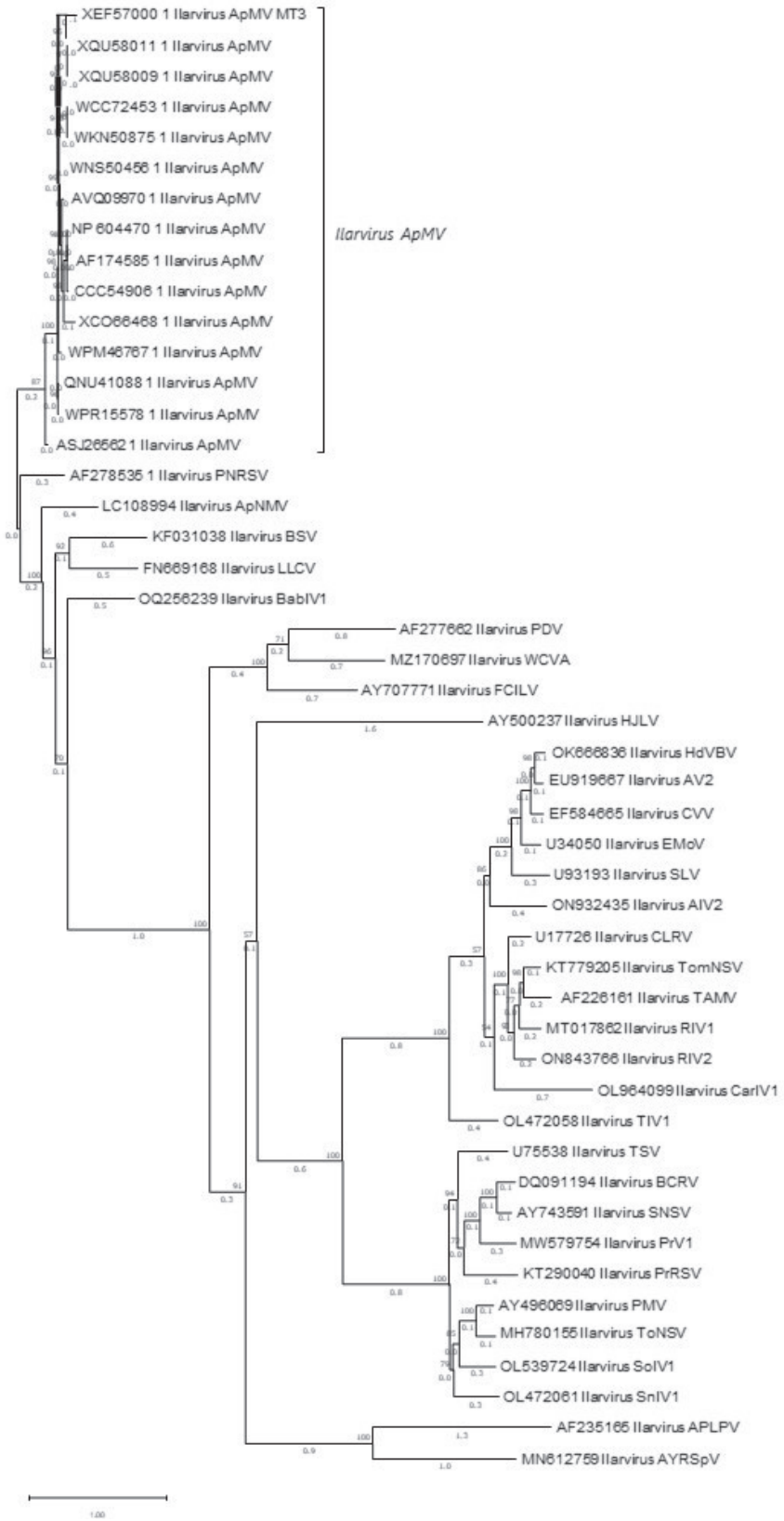

Figure 3. Maximum likelihood phylogenetic tree of RdRp sequences from all viruses accepted in *Ilarvirus*.

SNPs, initially identified in the original sample, were confirmed by RT-PCR with specific primers and Sanger sequencing, using RNA extracts from samples collected in autumn 2024.

DAS-ELISA consistently detected ApMV only in the symptomatic trunk of the monumental chestnut tree, while the other two trunks remained virus-free. Visual surveys conducted during 2023 to 2024 did not reveal virus- or ApMV-like symptoms in nearby hazelnut or apple trees, nor in the *Castagno della Nave* tree (600 m away from *Castagno dei Cento Cavalli*). While latent or asymptomatic infections cannot be ruled out without molecular analyses, no symptomatic hosts were detected in the surrounding vegetation. The restriction of ApMV detection to a single trunk may reflect limited systemic movement of the virus within the monumental chestnut, potentially constrained by the age and structural complexity of the host.

This study highlights the sensitivity and specificity of HTS-based virus detection. *Castagno dei Cento Cavalli* lacked symptom-based indicators associated with specific viruses in *C. sativa*, and this combined with inconclusive electron microscopy results, made conventional diagnostic approaches ineffective. High throughput sequencing was the only method that enabled the detection of ApMV in this newly reported host. The present paper is the first to report virome characterization of a monumental tree, and the first detection of ApMV in *C. sativa* and within *Fagaceae*. Although sequence divergence exists, nucleotide and protein identities, along with phylogenetic placement and serological reactivity, confirm the classification of ApMV MT3 as a member of apple mosaic virus. These results expand the known host range of ApMV, confirming that sweet chestnut can be naturally infected. For the monumental *Castagno dei Cento Cavalli*, this detection can inform future pruning or management interventions for the tree, helping to prevent potential virus spread within this historically important tree.

ACKNOWLEDGEMENTS

The authors acknowledge Giuseppe Campo, Regional Phytosanitary Service, for original reports of the disease in the monumental chestnut tree, and Emanuele Distefano, Concita Blancato and Massimiliano Cultrona (formerly in Di3A, University of Catania) for field surveys and preliminary virus detection analysis. Prof. Franco Raimondo provided information on the history of the magnificent tree. This research was funded by PIACERI, of the University of Catania 2024/2026, 'Diagnosis of poorly known or emerging diseases and development of innovative and environmentally sustainable defence strategies (DIME-SIECO)'.

LITERATURE CITED

Aramburu J.M., Rovira M., 1998. The effects of Apple mosaic ilarvirus (ApMV) on hazelnut (*Corylus avellana* L.). *Journal of Horticultural Sciences & Biotechnology* 73(1): 97-101. https://doi.org/10.1080/14620316.1998.11510950

Dal Zotto A., Nome S.F., Di Rienzo J.A., Docampo D.M., 1999. Fluctuations of Prunus necrotic ringspot virus (PNRSV) at various phenological stages in peach cultivars. *Plant Disease* 83(11): 1055–1057. https://doi.org/10.1094/PDIS.1999.83.11.1055

EPPO, 2024. EPPO Global Database. https://gd.eppo.int

Forgia M., Chiapello M., Daghino S., Pacifico D., Crucitti D., … Turina M., 2022. Three new clades of putative viral RNA-dependent RNA polymerases with rare or unique catalytic triads discovered in libraries of ORFans from powdery mildews and the yeast of oenological interest *Starmerella bacillaris*. *Virus Evolution* 8 (1), veac038. https://doi.org/10.1093/ve/veac038

Grimová L., Winkowska L., Konrady M., Ryšánek P., 2016. Apple mosaic virus. *Phytopathologia Mediterranea* 55(1), 1–19. https://doi.org/10.14601/Phytopathol_Mediterr-16295

International Committee on Taxonomy of Viruses (ICTV). https://ictv.global/taxonomy/

Katoh K., Standley D.M., 2013. MAFFT multiple sequence alignment software version 7: improvements in performance and usability. *Molecular Biology and Evolution* 30(4): 772–780. https://doi.org/10.1093/molbev/mst010

Langmead B., Salzberg S., 2012. Fast gapped-read alignment with Bowtie 2. *Nature Methods* 9: 357–359. https://doi.org/10.1038/nmeth.1923

Manzoor S., Nabi S.U., Baranwal V. K., Verma M.K., Parveen S., … Shafi M., 2023. Overview on century progress in research on mosaic disease of apple (*Malus domestica* Borkh) incited by apple mosaic virus / apple necrotic mosaic virus. *Virology* 587: 109846. https://doi.org/10.1016/j.virol.2023.109846

Mattioni C., Ranzino L., Cherubini M., Leonardi L., La Mantia T., … Simeone M.C., 2020. Monuments unveiled: Genetic characterization of large old chestnut (*Castanea sativa* Mill.) trees using comparative nuclear and chloroplast DNA analysis. *Forests* 11(10), 1118. https://doi.org/10.3390/f11101118

Nunziata A., Ferlito F., Magri A., Ferrara E., Petriccione M., 2022. The Hundred Horses Chestnut: a model system for studying mutation rate during clonal propagation in superior plants. *Forestry* 95(5): 678-685. https://doi.org/10.1093/forestry/cpac020

Pallas V., Aparicio F., Herranz M. C., Sánchez-Navarro J.A., Scott S. W., 2013. The molecular biology of ilarviruses. *Advances in Virus Research* 87: 139–181. https://doi.org/10.1016/b978-0-12-407698-3.00005-3

Pereira-Lorenzo S., Ramos-Cabrer A.M., Barreneche T., Mattioni C., Villani F., ... Martín A., 2019. Instant domestication process of European chestnut cultivars. *Annals of Applied Biology* 174: 74-85. https://doi.org/10.1111/aab.12474

Picarelli M.A.S., Forgia M., Rivas E. B., Nerva L., Chiapello M., Turina M., Colariccio A., 2019. Extreme diversity of mycoviruses present in isolates of Rhizoctonia solani AG2-2 LP from Zoysia japonica from Brazil. *Frontiers in Cellular and Infection Microbiology* 9: 244. https://doi.org/10.3389/fcimb.2019.00244

Roossinck M. J., Bujarski J., Ding S. W., Hajimarad R., Hanada K., Scott S., Tousignant M., 2005. Bromoviridae (pp. 1049–105). In: *Virus Taxonomy. Eighth Report of the International Committee on Taxonomy of Viruses*. (Fauquet C.M., Mayo M.A., Maniloff J., Desselberger, U., Ball L.A., ed.). Elsevier/Academic Press, London.

Schicchi R., Raimondo F.M., 2007. I grandi alberi di Sicilia. Palermo: Azienda Foreste demaniali della Sicilia.

Trifinopoulos J., Nguyen L.T., von Haeseler A., Minh B.Q., 2016. W-IQ-TREE: a fast online phylogenetic tool for maximum likelihood analysis. *Nucleic Acids Research* 44(W1), W232–W235. https://doi.org/10.1093/nar/gkw256

Untergasser A., Cutcutache I., Koressaar T., Ye J., Faircloth B.C., Remm M., Rozen S.G., 2012. Primer3—new capabilities and interfaces. *Nucleic Acids Research* 40(15): e115. https://doi.org/10.1093/nar/gks596

Phytopathologia Mediterranea
The international journal of the
Mediterranean Phytopathological Union

Firenze University Press
www.fupress.com/pm

Research Papers

Assessment of damage potential of *Gnomoniopsis castaneae* to fruit and trees of European Chestnut (*Castanea sativa*)

Francesca CARLONI[1], Carlo BREGANT[2], Benedetto T. LINALDEDDU[2], Giorgio MARESI[3], Sergio MUROLO[1,*]

[1] *Department of Agricultural, Food and Environmental Sciences, Marche Polytechnic University, Via Brecce Bianche 10, 60131, Ancona, Italy*
[2] *Department of Land and Agro-Forestry Systems, University of Padua, Viale dell'Università, 16, 35020 Legnaro, Italy*
[3] *Fondazione Edmund Mach, Technology Transfer Center, Via E. Mach 1, 38010 San Michele all'Adige, Trento, Italy*
*Corresponding author. E-mail: s.murolo@staff.univpm.it

Summary. *Gnomoniopsis castaneae* has become an important pathogen of European chestnut (*Castanea sativa*), affecting fruits and colonizing shoots and branches, as well as galls caused by the oriental chestnut gall wasp (*Dryocosmus kuriphilus*). On apparently asymptomatic fruits, *G. castaneae* can colonize the endosperms, causing quality issues, especially in post-harvest. Given the alarming spread of *G. castaneae* infections in Italy and the current knowledge gaps regarding aspects of *G. castaneae* biogeography and virulence, research was addressed to: 1) evaluate occurrence of *G. castaneae* in chestnut nuts and branches in different Italian regions; 2) study occurrence and distribution of the two known *G. castaneae* haplotypes throughout Italy; and 3) evaluate their virulence on chestnut under different water regimes. Fungal isolation from representative chestnut branch and nut samples consistently yielded colonies that were morphologically consistent with *G. castaneae*, the identity of which was confirmed by analysis of ITS sequences. Analysis of *β-tubulin* sequences confirmed the presence of two distinct genetic lineages (*Gc*-haplotypes A and B). To assess pathogenicity, *G. castaneae* isolates were inoculated onto chestnuts, chestnut cuttings and 3-year-old young plants grown under two water regimes. All assessed isolates were pathogenic on chestnut, and water-stressed plants exhibited more extensive necrosis than well-watered plants when inoculated with the *Gc*-haplotype A, highlighting the influence of environmental conditions on disease expression. This study expands current knowledge on the distribution, genetic diversity, and effects of water stress on the pathogenic potential of *G. castaneae* on chestnut.

Keywords. Endophytic and pathogenic behaviours, molecular typing, pathogenicity test, water stress.

OPEN ACCESS

Citation: Carloni, F., Bregant, C., Linaldeddu, B. T., Maresi, G., & Murolo, S. (2026). Assessment of damage potential of *Gnomoniopsis castaneae* to fruit and trees of *Castanea sativa* (chestnut). *Phytopathologia Mediterranea* 65(1): 75-92. doi: 10.36253/phyto-16789

Accepted: December 27, 2025

Published: March 16, 2026

© 2026 Author(s). This is an open access, peer-reviewed article published by Firenze University Press (https://www.fupress.com) and distributed, except where otherwise noted, under the terms of the CC BY 4.0 License for content and CC0 1.0 Universal for metadata.

Data Availability Statement: All relevant data are within the paper and its Supporting Information files.

Competing Interests: The Author(s) declare(s) no conflict of interest.

Editor: Luisa Ghelardini, University of Florence, Italy.

ORCID:
FC: 0009-0007-1245-5423
CB: 0000-0003-1353-7993
BTL: 0000-0003-2428-9905
GM: 0000-0001-6806-6135
SM: 0000-0001-7269-1734

INTRODUCTION

European chestnut (*Castanea sativa* Mill.) is a versatile forest tree species, that is strongly related to human activities in Mediterranean mountain

areas (Conedera *et al*., 2004). Over centuries, chestnut cultivation has directly contributed to food security (Gabrielli, 1994), as these trees are important food resources of rural areas. Chestnut trees enabled development of local economies based on the production and commercialization of high-quality nuts, valuable timber, and a wide range of traditional processed products (Pezzi *et al*., 2022). Beyond its socio-economic importance, chestnut orchards provide key ecosystem services, including soil protection, slope stability, and erosion mitigation in mountainous environments (Bassanelli *et al*., 2013). *Castanea sativa* is also relevant for biodiversity conservation, hosting a wide range of plant and animal species, and is an efficient carbon sink (Mattioli *et al*., 2016; Prada *et al*., 2016).

In Europe, *C. sativa* is primarily cultivated in southern countries, with Spain and Portugal leading production, followed by Italy and France (Pérez-Girón *et al*., 2020). Chestnut fruits are commercialized to many countries, because they are appreciated for their low-fat content, richness in essential nutrients such as starch, sugars and proteins, and because they are gluten-free (Suna *et al*., 2021; Rodrigues *et al*., 2022; Santos *et al*., 2022).

Chestnut fruit production has declined (Maresi *et al*., 2013; Freitas *et al*., 2021), due to neglect of chestnut groves, sometimes accompanied by replacement of chestnut with more remunerative agricultural crops, and abandonment in mountainous regions as rural populations migrated (Freitas *et al*., 2021). Additional threats to chestnut ecosystems include climate change (rising temperatures), which may alter chestnut tree phenological stages, affecting fruit quality (Freitas *et al*., 2021). Spread of well-known pests and diseases, such as Asian wasp gall, chestnut blight, ink disease, and (more recently) mosaic disease, have impacted chestnut vitality and production (Battisti *et al*., 2014; Rigling and Prospero, 2018; Marais *et al*., 2021; Pezzi *et al*., 2022; Prospero *et al*., 2023). Further detrimental impacts on post-harvest production have been associated with nut rots caused by *Phomopsis endogena*, *Ciboria batschiana*, *Colletotrichum acutatum*, *Neofusicoccum parvum* and species of *Aspergillus*, *Fusarium*, *Alternaria* and *Botrytis* (Washington *et al*., 1997; Donis-González *et al*., 2009; Visentin *et al*., 2012; Gaffuri *et al*., 2017; Nicoletti *et al*., 2021; Seddaiu *et al*., 2021).

Gnomoniopsis castaneae has become an increasing threat to chestnut fruit production, causing brown rot. This fungus was independently described in 2012 by two research teams, in Italy (Visentin *et al*., 2012) and Australia (Shuttleworth, 2012), and a comprehensive review was later published by Lione *et al*. (2019). High nut infection rates have been observed in North and South America, Asia, Australia, and in Europe, particularly Switzerland (50 to 91% infection) and Italy (20 to 94%) (Lema *et al*., 2023). Origin of the fugus remains unknown, and its biology is still not fully understood (Dobry and Campbell, 2023). The life cycle of *G. castaneae* includes sexual and asexual phases. During winter, the fungus survives as mycelium and propagules in leaf litter, and galls caused by *Dryocosmus kuriphilus* in the previous chestnut growing season. In spring, ascospores released from perithecia are dispersed by wind and insects, infecting host plant female flowers, leaves and branches (Lema *et al*., 2023). During flowering, and fruit development and maturation, the fungus invades chestnut kernels, causing endosperm and embryo necrosis resulting in internal nut decay, while outer shells remain visually unaffected (Lema et al., 2023). Asexual reproduction of the pathogen, involving conidial differentiation, may occur inside infected nuts, on *D. kuriphilus* galls, or in infected flower buds, leaves or branches (Maresi *et al*., 2013; Dobry and Campbell, 2023; Topalidou *et al*., 2024).

Gnomoniopsis castaneae can be a latent pathogen able to persist endophytically within the hosts, so it is frequently isolated from apparently healthy chestnut plant woody tissues and fruits (Ugolini *et al*., 2014; Lema *et al*., 2023). Generally, its pathogenicity is associated with high levels of fruit colonization, causing brown rot, but the fungus can also induce cankers in host stem and shoots (Dar and Ray, 2015; Dobry and Campbell, 2023). Nevertheless, the biological mechanisms regulating the transition from endophytic colonization to pathogenic behaviour have not been fully elucidated (Maresi *et al*., 2013; Lione *et al*., 2016; Pasche *et al*., 2016; Shuttleworth and Guest, 2017).

The host range of *G. castaneae* is not restricted to chestnut species. The fungus has been recorded on oak (*Quercus cerris* L., *Quercus ilex* L.), pine (*Pinus pinaster* Aiton), hazelnut (*Corylus avellana* L.), and ash (*Fraxinus ornus* L.) (Visentin *et al*., 2012; Linaldeddu *et al*., 2016; EPPO, 2017; Lione *et al*., 2019; Dobry and Campbell, 2023), where it is related to cankers, fruit rot and leaf necrosis of these hosts.

Given the severe damage caused by *G. castaneae* in many countries, and the current knowledge gaps regarding some aspects of its biogeography and virulence, the present study was conducted to: 1) evaluate the occurrence of *G. castaneae* in chestnut nuts and branches across different Italian regions; 2) ascertain distributions of the two *G. castaneae* haplotypes in Italy; and 3) assess their ability to induce canker lesions on artificially inoculated chestnut stems under water-stress conditions.

MATERIAL AND METHODS

Field surveys, sampling and isolation from cankered branches

In summer 2017, the health status of chestnut trees was monitored in two orchards located in Sardinia (Aritzo: 39.950563, 9.196157) and a coppice in Veneto (Torreglia: 45.319230, 11.711188). The chestnut trees (approx. 40–50 years old) were inspected for the presence of necrosis on Asian wasp galls and for cankers on branches. A total of 20 shoots per site showing cankers, different on the colour and appearance from the ones caused by *C. parasitica*, were randomly chosen for diagnostic analysis and fungal isolations. Disease incidence (D) was calculated as the percentage of affected chestnut trees out of the total number of chestnut trees along two linear (50 m long) transects per site. Branch samples were initially disinfected with 70% ethanol for 30 s, and then used for isolation by aseptically taking ten small tissue fragments (each 5 × 5 mm) from margins of the necrotic lesions of inner bark, after removal of outer bark with a sterile scalpel. All tissue fragments were placed onto 90 mm diam. Petri dishes containing Potato Dextrose Agar (PDA, 39 g L^{-1}, DIFCO) and incubated at 25°C for 7 d in the dark. Hyphal tips from emerging colonies were then sub-cultured onto PDA in 60 mm diam. Petri dishes and then incubated at 25°C in the dark.

Nut sources and brown rot assessments

As part of the Chestnut Fruit Exhibition (Ascoli Piceno, Italy) on November 11th, 2023, the Department of Agricultural, Food and Environmental Sciences (D3A) at UNIVPM received 117 chestnut fruit samples from more than 100 chestnut varieties. Some of the trees were cultivated and preserved at the Chestnut Biodiversity Repository Fields located in Piedmont, Tuscany, Emilia-Romagna and Campania, and others were from commercial orchards in Lombardy, Trentino-Alto Adige, Marche and Sardinia (Table S1). The fruit samples (each 300 to 400 g) were collected in mid-October 2023 from the different locations. They were immediately sent to UNIVPM (Ancona, Italy), where they were stored in a cold room at 2 to 4°C under high humidity conditions until the Chestnut Fruit Exhibition, and then kept at room temperature (23°C) for 20 d prior to analyses.

Depending on nut availability for each of the 117 samples, ten to 20 chestnuts were analyzed to record morphological characteristics of the episperms (colour and texture) and, after longitudinal dissection, any signs of endosperm alterations. Green mold, and black, pink or brown rots, were recorded, along with insect larvae feeding within the nut endosperms. A more detailed assessment was conducted for chestnut brown rot, focusing on disease incidence, severity and McKinney Index.

Disease incidence (D) was calculated as the percentage of affected chestnuts (out of 20 assessed per sample).

Severity (S) was assessed by classifying each 20 chestnut sample using an empirical scale (Figure 1) (Gonzalez *et al.*, 2016 with modifications), and was calculated using the following formula:

$$S = (c \times f) / n$$

where: S = severity; c = severity class (0 to 5); f = frequency; and n = number of symptomatic chestnuts.

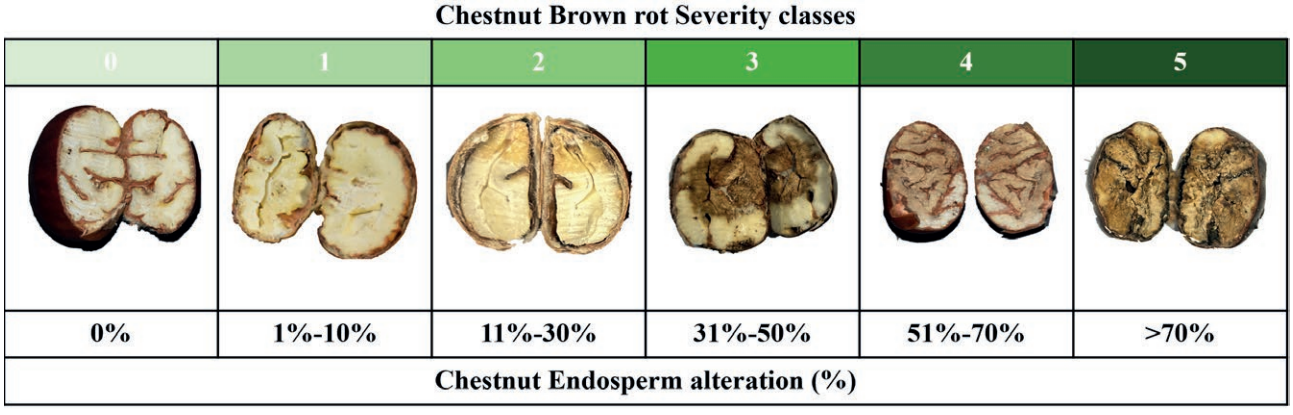

Figure 1. Chestnut brown rot severity scores, according to the percentage of endosperm alterations, as used in the present study. Six severity classes were: 0 = no disease; 1 = up to 10% diseased tissue; 2 = 11 to 30%; 3 = 31 to 50%; 4 = 51 to 70%; 5 = more than 70% endosperm diseased.

Considering both Incidence (D) and Severity (S), the McKinney Index (MI) was then calculated using the formula (McKinney, 1923; Possamai *et al*., 2023):

$$MI\ (\%) = (\Sigma(n_i \times v_i) / N \times V) \times 100$$

where: MI = McKinney Index; n_i = number of symptomatic fruits in severity class; v_i = severity class (0 to 5); N = total number of chestnuts observed; and V = maximum value of severity class.

Isolations from nut samples and morphological identification of isolated fungi

After visual assessments, microorganisms associated with tissue rot were isolated from five to ten chestnuts per sample. Fruits were surface sterilized with 90% ethanol (2 min), 2% sodium hypochlorite (2 min), then rinsed in sterile water (2 min), and then dried on sterile absorbent paper under a laminar flow hood. The fruits were then cut longitudinally with sterile blades, and asymptomatic or visibly deteriorated endosperm tissues were selected. From each fruit, five tissue pieces were placed in a Petri dish (90 mm diam.) containing 15 mL of PDA supplemented with antibiotic solution (150 mg L^{-1} ampicillin + 150 mg L^{-1} streptomycin). To assess microorganism diversity across the visual disease categories, the same procedure was repeated for 60 representative chestnuts spanning the severity classes 0 to 5. Petri plates were incubated at room temperature (23 ± 1°C) for 7 d. Resulting fungal colonies were then subcultured to obtain pure isolates. Isolate mycelium colour and structure of fruiting bodies were observed for identifications using a light microscope (Leica DM 500) at ×40 magnification, and appropriate images were captured with an ICC50W microscopic Digital USB Camera (Leica Microsystems).

DNA extraction, PCR amplification and sequencing

Among *Gnomoniopsis* isolates, 23 were randomly selected for molecular analyses, including 17 from northern Italy, two from central Italy, one from southern Italy, and three from Italian islands. Fungal DNA was extracted from each isolate using the CTAB protocol (Doyle and Doyle, 1990, with minor modifications), and was used for further molecular analyses.

Amplification reactions (total volume 25 µL) each contained 9.1 µL of MilliQ H_2O, 12.5 µL EmeraldAmp MAX PCR Master Mix 2× (Takara), 1.2 µL of each primer (10 µM), and 1 µL of DNA (50 ng). The primers used were ITS1/ITS4 (White *et al*., 1990) targeting the ITS region, and Bt2a/Bt2b (Glass and Donaldson, 1995) targeting the *β-tubulin* gene. Amplifications was carried out in a DNA iCycler (Bio-Rad), with an initial denaturation step at 95°C for 3 min, then 35 cycles, each of denaturation at 95°C for 30 s, annealing at 55°C for 30 s, and extension at 72°C for 60 s, and a final elongation step of 5 min at 72 °C for both primer sets. Products were visualized on 1.5% agarose gel in 1× TAE buffer (45 mM Tris-borate, 1 mM EDTA, pH 8), which was stained with GelRed (Biotium), and acquired using a Gel Doc system (Bio-Rad, USA). A 100 bp DNA ladder (Sigma-Adrich) was included as the size marker. Specific ITS and *β-tubulin* amplicons of the 23 representative isolates were purified and sequenced in both directions (Genewiz), then nucleotide sequences were compared with those in the NCBI database (on 16th August 2025) by nucleotide Blast Analysis (https://blast.ncbi.nlm.nih.gov/Blast.cgi). *β-tubulin* amplicon sequences were aligned with reference strains by BioEdit v. 7.2.1 (https://bioedit.software.informer.com/7.2/) to distinguish between *Gc*-haplotypes A and B, according to SNPs in the conserve region. The nucleotide sequences of ITS and *β-tubulin* regions were validated by NCBI, and were deposited in GenBank (on 3rd September 2025).

Pathogenicity tests on chestnut cuttings

Two-year-old chestnut stems (1 to 1.5 cm diam.) were harvested from ten ungrafted *C. sativa* trees without visible damage or disease symptoms. The stems, protected in plastic bags to prevent dehydration, were then stored at 4°C in a cold room for 16 h, and then cut into ~10 cm sections, which were surface-disinfected with 90% ethanol solution, and wounded (3 mm diam.) to expose the cambium. Based on previous results and molecular typing, 16 *G. castaneae* isolates were selected, including five of *Gc*-haplotype A and 11 of *Gc*-haplotype B (*sensu* Seddaiu *et al*., 2023), and two reference isolates (PD-ST30, PD-ST55) provided by the fungal collection of TESAF Department (UNIPD, Padova, Italy). Mycelium plugs from 5-d-old *G. castaneae* PDA cultures were inserted into inoculated stem wounds using sterile tools, and were then sealed with parafilm (Table 1). Negative inoculation controls received only PDA disks. The upper end of each chestnut cutting was then sealed with grafting wax, and the lower 1.2 cm portion was immersed in 3 mL of sterile water in a 50 mL tube without a cap. Cuttings were then maintained at 23±1°C for 30 d in the incubator. Length extension of necrosis on each cutting was then measured using by digital caliper (Metrica). Organism re-isolation was carried out

Table 1. Representative *Gnomoniopsis castaneae* (GC) isolates obtained from different chestnut varieties, and the respective ITS and bt nucleotide sequence registration numbers, originating from different Italian regions and molecularly characterized as Haplotype A or B based on *β-tubulin* gene typing (Seddaiu *et al*., 2021).

Gnomoniopsis isolates ID	Geographical region	Haplotype A or B	Nucleotide sequence	
			ITS	bt
GC_SanPietro	Campania	A		PX259707
GC_Barrile	Sardinia	A	PX242886	PX259715
GC_Castel del Rio-MO	Emilia Romagna	A	PX242877	PX259708
GC_Castagna di Val di Castro-SITE 1	Marche	A	PX242891	PX259719
GC_Castagna bionda di Lunano	Marche	A	PX242885	PX259714
GC_Santu Giuanni-ARI3	Sardinia	B	PX242880	PX259710
GC_Bouche de Betizac	Piedmont	B	PX242898	PX259725
GC_Marrone di Viterbo	Piedmont	B	PX242887	PX259716
GC_Precoce Migoule	Piedmont	B	PX242882	PX259712
GC_Chiusa Pesio	Piedmont	B	PX242883	PX259713
GC_Marrone scuro-2710	Lombardy	B	PX242888	PX259717
GC_Patriarca-3595	Lombardy	B	PX242889	PX259718
GC_Marrone di Perledo-3419	Lombardy	B	PX242896	PX259723
GC_Rossera-2412	Lombardy	B	PX242881	PX259711
GC_Tosca/Garfagnana-MO	Emilia Romagna	B	PX242892	PX259720
GC_Pilistella	Emilia Romagna	B	PX242899	PX259726

by removing the external layer of bark of each cutting, excising four pieces of inner bark tissues and placing the pieces onto PDA.

Pathogenicity tests on chestnut fruits

For the pathogenicity test on fruits, the local chestnut variety 'Marrone Classico di Acquasanta Terme' (from Ascoli Piceno, Marche, Italy) was selected. This variety was recorded to be poorly affected during the preliminary assessment of the present investigation. The nuts were disinfected with a superficial treatment in 90% ethanol solution for 1 min, followed by 2% sodium hypochlorite solution for 1 min), and the rinsing in sterile water, and were then left to dry on 3 mm blotting paper (Whatman) at room temperature under a laminar flow cabinet.

The 16 selected *G. castaneae* isolates (as above) were each inoculated onto four chestnut fruits, by inserting a mycelium plug (3 mm diam.), between the pericarp and perisperm of each fruit, and sealing the inoculation site with parafilm. For inoculation controls, PDA disks without mycelium were similarly added to chestnut fruits. All fruits were then incubated at 23°C (± 1°C) for 30 d, and necrotic areas were then measured as ellipses. Organism re-isolation were then carried out cutting each nut into two parts, picking out four pieces of symptomatic inner tissue and placing these onto PDA.

Pathogenicity test on chestnut seedlings under different water regimes

A greenhouse pot experiment was carried out with 3-year-old chestnut seedlings (*C. sativa*) grown in 3 L pots, that were filled with soil collected from a chestnut orchard in Montemonaco (Ascoli Piceno, Italy). All the pots were water-saturated, then two water regimes were applied: 150 mL water per week (designated WR_A) or 150 mL water per month (WR_B). The 16 *G. castaneae* isolates (as above) were then inoculated onto the seedlings. Each isolate was applied to wounds (3 mm diam.) made on the seedlings at 3, 12 and 21 cm above the soil line. After 30 d at 26°C, in greenhouse, lengths of cortex necroses were measured using a digital caliper (Metrica). Fungus re-isolations were made by removing the external layer of bark of each seedling, then excising four pieces of symptomatic inner bark tissue and placing these onto PDA in Petri plates.

Statistical analysis

For each pathogenicity test, data were tested for homogeneity of variances using Levene's test, and for normality of residuals using the Shapiro–Wilk test, prior to analyses of variance (ANOVA). When assumptions of normality and homogeneity were met, one-way ANOVAs were carried out to assess effects (at $P < 0.05$) of the different iso-

lates on sizes of necrotic tissues. If the statistical analysis showed the data were not normally distributed, the dataset was transformed using the function "Boxcox". All statistical analyses were conducted using R version 4.4.3.

RESULTS

Field symptoms and disease incidence

On monitored trees at the Sardinia and Veneto sites, chestnut blight, ink disease and Asian wasp galls were widespread. In addition, 42% of the assessed trees showed branch cankers characterized by dark necrotic bark lesions, sometimes accompanied by a reddish discolouration, mainly along the canker margins (Figure 2). The branch cankers often started from Asian wasp galls, and then progressively necrotized and advanced from the shoots towards the branches causing wilting of the distal portions. During the summer survey, affected branches were recognizable as the leaves lost their turgidity, turned from pale green to brown, and withered. Colonies of *G. castaneae* were isolated from all 60 assessed branches showing these symptoms.

Three further fungi, identified as *Dothiorella iberica* (seven isolates), *Cryphonectria parasitica* (four), and *Neofusicoccum luteum* (three) were sporadically isolated from the assessed canker samples.

Figure 2. a) Chestnut necrotic shoots; b) branch cankers starting from Asian wasp galls; c) a wilted distal portion of a tree branch; d) a canker induced by *Gnomoniopsis castaneae*.

Assessments of chestnut fruit rot

During visual inspections, the fruits generally did not show significant anomalies of pericarp colour, which are mostly due to host intraspecific variability. However, investigation of inner fruits tissues was different. After dissection, 1251 (69.04%) of 1812 chestnut samples showed endosperm diseases. More than 90% of these chestnut fruits showed no external alteration of episperm colour. From observations of the dissected fruits, the most frequent disease symptom (disease incidence; D) was brown rot (59.05%), followed by green mold (15.95%), black rot (7.06%) and pink rot (4.02%).

Chestnut brown rot was individually predominant, even when recorded with green rot (9.05%) as well as black rot (4.97%), pink rot (2.04%) and insect damage (13.74%). The different fruit rot symptoms are illustrated in Figure 3.

Focusing on the brown rot-related alteration, the average disease severity (S), was expressed as a score from 0 to 5. Most of the samples were evaluated in class 3 (31–50% of nuts), with an average severity around 3.2 (Table 2).

Combining disease incidence and severity, McKinney Index (MI) was calculated with an overall average value of approx. 42% for fruit samples of different varieties and origins (Table 2). Chestnut brown rot differently affected the varieties cultivated in the Regional Chestnut Repositories of Piedmont, Emilia-Romagna, Toscana and Campania (Table 2). Varieties most affected included 'Castagna della Madonna' (Piedmont), 'San Pietro' and 'Lucente' (Campania), 'Marrone di Loiano' (Tuscany), as well as 'Castel del Rio' and 'Bovalghe' (Emilia-Romagna), all showing high MI values (ranging from 42% to 93%). In contrast, the varieties 'Sborgà' (Emilia-Romagna), 'Salvana' (Emilia-Romagna, Tuscany), 'Marrone buono' (Tuscany), 'Ishyzuki precoce' (Piedmont), and 'Verdole' (Campania) displayed low susceptibility, with MI values ranging from 0 to 22% (Table 2).

For samples coming from chestnut orchards in Lombardy, Marche and Sardinia, some varieties had different MI values. 'Marrone scuro' (Lombardy), 'Pallante' (Marche) and 'Craeddu – CRAV' (Sardinia) were the most affected, with MI values from 33 to 100%. Conversely, several varieties had no brown rot symptoms (MI = 0%), including 'Marrone Classico di Acquasanta Terme' and 'Castagna di Val di Castro' from site 1 (MI

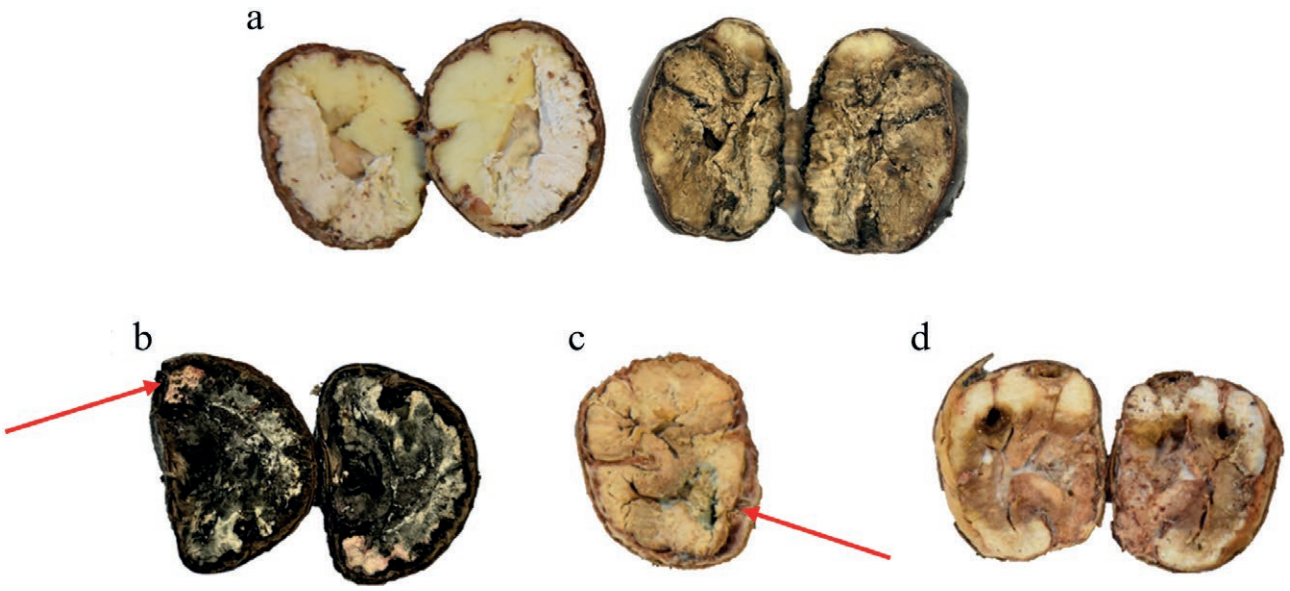

Figure 3. Symptoms recorded during visual inspections after fruit dissection. a) Chestnut brown rot; b) (arrow) black rot and pink rot; c) (arrow), green mold; and d) insect damage and brown rot.

= 0%) (Marche). Similarly, in Sardinia, the varieties 'Luccheddu – LOCG2' and 'Ildubba – ILDP' (MI = 0%) were also unaffected.

Pathogens associated with nut diseases

Most of the *in vitro* isolations from brown rot affected chestnuts from each of the 117 varieties were identified as *G. castaneae* [481 (68.52%) of 702 isolates]. In addition, *Penicillium* (4.85%), *Aspergillus* (7.41%), *Fusarium* (9.12%), *Alternaria* (6.13%) and *Trichoderma* (4.13%) were isolated at minor frequencies.

In vitro isolations from 60 chestnuts representative of the different disease severity classes (1 to 5) and asymptomatic samples (class 0), gave different proportions of *G. castaneae* isolates (Table 3). Samples of class 3 (98.3% *G. castaneae*) and 2 (95%) gave greatest proportions, followed by class 4 samples (70%), 1 (50%), and 5 (37% of samples). *Gnomoniopsis castaneae* was also isolated from 5% of asymptomatic episperms. The frequencies of *Penicillium, Trichoderma, Aspergillus, Fusarium* and *Alternaria* spp. isolations were generally greater from fruit with chestnut brown rot severity classes of 4 or 5.

Molecular identification and characterization of Gnomoniopsis castaneae

The 23 selected *G. castaneae* isolates subjected to total DNA extractions yielded from 75 and 172 ng μL^{-1} of DNA, of quality enough for further analyses (ratio 260 nm/280 nm > 1.8). All the isolates, including those with values below the quality threshold, were analyzed using the primers ITS1/ITS4 and Bt2a/Bt2b. Twenty-two of the 23 samples positively amplified for the ITS region, each showing a specific band of approx. 600 bp. For amplifications with *β-tubulin* primers, 20 of the 23 isolates gave specific bands of approx. 300 bp. Blast analysis gave 100% sequence identity when the present study *G. castaneae* isolate ITS regions were compared with that of the ex-type culture (HM142946). Blast analyses based on *β-tubulin* sequences discriminated two different *Gc*-haplotypes (A and B), according to single nucleotide polymorphisms (SNPs) in conserved position, as previously described by Seddaiu *et al.* (2023). *Gc*-haplotype A was recorded in isolates from Campania, Sardinia, Marche and Emilia Romagna, while *Gc*-haplotype B was recorded from Piedmont, Sardinia, Lombardy and Emilia-Romagna (Table 1).

Pathogenicity test on chestnut cuttings

The 16 isolates of *G. castaneae,* (five of *Gc*-haplotype A and 11 of *Gc*-haplotype B, as shown by *β-tubulin* molecular typing) induced necrotic lesions on chestnut cuttings (Figure 4A; Supplementary Table 2). From the statistical analyses, *G. castaneae* isolates of *Gc*-haplotype A were not pathogenically different ($P > 0.05$) from the *Gc*-haplotype B isolates. However, differences were found among the *G.*

Table 2. Brown rot incidence, severity and McKinney indices in chestnuts from different regions in Italy.

Chestnut variety	Region	Chestnut brown rot		
		Incidence D (%)	Severity S	McKinney Index MI (%)
Marrone di Comunanza	Marche	27.78	4.20	23.33
Insita site 1	Marche	54.55	3.33	36.36
Marrone rugoso di Acquasanta Terme	Marche	0.00	0.00	0.00
Marrone gentile di Acquasanta Terme site 1	Marche	11.11	2.00	4.44
Marrone delle Piagge	Marche	5.26	3.00	3.16
Marroncino dell'ascensione site 1	Marche	20.00	3.75	15.00
Marrone classico di Acquasanta Terme	Marche	0.00	0.00	0.00
Castagna di Val di Castro site 1	Marche	0.00	0.00	0.00
Marroncino dell'Ascensione site2	Marche	75.00	2.07	31.00
Marrone gentile di Acquasanta Terme site 2	Marche	27.78	2.40	13.33
Insita site 2	Marche	82.35	2.29	37.65
Pallante	Marche	85.00	3.24	55.00
Marrone della Sibilla di Montemonaco	Marche	25.00	3.00	15.00
Castagna di Val di Castro site 2	Marche	65.00	1.92	25.00
Castagna bionda di Lunano	Marche	10.00	2.00	4.00
Average		32.59	2.21	17.55
Marrone di Limonta – 1001	Lombardy	70.00	5.00	70.00
Marrone di Limonta – 1007	Lombardy	100.00	4.21	84.21
Agostana - 2211	Lombardy	90.00	5.00	90.00
Agostana - 2230	Lombardy	78.95	2.93	46.32
Agostana - 2233	Lombardy	95.00	4.00	76.00
Marronessa - 2338	Lombardy	94.44	4.06	76.67
Marronessa - 2339	Lombardy	100.00	4.67	93.33
Marronessa - 2340	Lombardy	93.33	4.07	76.00
Unknown - 2412	Lombardy	100.00	4.47	89.47
Rossera - 2414	Lombardy	100.00	4.15	83.00
Rossera - 2415	Lombardy	100.00	4.20	84.00
Piata - 2417	Lombardy	100.00	4.82	96.47
Enset de Piaz - 2450	Lombardy	82.35	3.79	62.35
Settembrana - 2452	Lombardy	100.00	4.53	90.59
Verdala - 2695	Lombardy	94.74	4.33	82.11
Unknown - 2896	Lombardy	100.00	4.11	82.22
Unknown - 2697	Lombardy	85.00	4.00	68.00
Marrone scuro - 2710	Lombardy	100.00	5.00	100.00
Topia - 2747	Lombardy	80.00	3.50	56.00
Barucana - 2750	Lombardy	81.25	4.00	65.00
Donegai - 3029	Lombardy	100.00	3.53	70.53
Bonela - 3039	Lombardy	95.00	2.95	56.00
Catot - 3365	Lombardy	66.67	3.40	45.33
Catot - 3366	Lombardy	100.00	3.53	70.59
Marrone - 3367	Lombardy	88.89	3.19	56.67
Catot - 3368	Lombardy	72.22	2.85	41.11
Longone - 3369	Lombardy	94.44	3.35	63.33
Marrone di Perledo - 3407	Lombardy	100.00	3.82	76.47
Marrone di Perledo - 3412	Lombardy	100.00	4.53	90.53
Marrone di Perledo - 3414	Lombardy	100.00	3.67	73.33
Marrone di Perledo - 3419	Lombardy	80.00	3.58	57.33

(Continued)

Table 2. (Continued).

Chestnut variety	Region	Chestnut brown rot		
		Incidence D (%)	Severity S	McKinney Index MI (%)
Marrone di Perledo - 3422	Lombardy	88.24	4.20	74.12
Patriarca - 3595	Lombardy	75.00	3.07	46.00
Bunela - 4712	Lombardy	100.00	4.65	93.00
Galdana - 2442	Lombardy	100.00	4.39	87.78
Average		91.59	3.99	73.54
Centa S. Nicolo'	Trentino Alto Adige	9.09	2.00	3.64
Castione	Trentino Alto Adige	55.56	3.60	40.00
Roncegno	Trentino Alto Adige	20.00	2.50	10.00
Drena	Trentino Alto Adige	22.22	3.00	13.33
Average		26.72	2.78	16.74
Loccheddu – LOCG2	Sardinia	0.00	0.00	0.00
Migheli Urru - MURG	Sardinia	66.67	2.33	31.11
Ildubba - ILDP	Sardinia	0.00	0.00	0.00
Barrile - BARV	Sardinia	55.56	2.80	31.11
Craeddu - CRAV	Sardinia	50.00	3.33	33.33
Santu Giuanni – ARI3	Sardinia	25.00	5.00	25.00
Average		32.87	2.24	20.09
Salvana	Tuscany	14.29	2.50	7.14
Marrone di Loiano	Tuscany	80.00	3.50	56.00
Marron buono di Marradi	Tuscany	26.32	1.80	9.47
Average		40.20	2.60	24.21
Verdole	Campania	35.00	3.14	22.02
Marrone di Scala	Campania	77.78	3.50	54.4
Santimango	Campania	84.21	1.44	24.21
San Pietro	Campania	100.00	4.29	85.71
Olefarella	Campania	57.89	2.91	33.68
Lucente	Campania	100.00	4.10	82.00
Tempestiva	Campania	100.00	4.05	81.00
Napoletana	Campania	100.00	3.65	73.00
Average		81.86	3.38	57.01
Marrone di Zocca - UNIBO	Emilia-Romagna	50.00	2.00	20.00
Svizzera - UNIBO	Emilia-Romagna	45.45	2.60	23.64
Pastinese - UNIBO	Emilia-Romagna	27.27	4.33	23.64
Ceppa - UNIBO	Emilia-Romagna	13.33	3.50	9.33
Sborga' site 1 - UNIBO	Emilia-Romagna	40.00	1.00	8.00
Marrone di Castel del Rio - UNIBO	Emilia-Romagna	22.22	4.50	20.00
Pelosa - UNIBO	Emilia-Romagna	50.00	3.86	38.57
Bovalghe - UNIBO	Emilia-Romagna	72.73	2.88	41.82
Pastanese - UNIBO	Emilia-Romagna	53.85	3.57	38.46
Sborga' site 2- UNIBO	Emilia-Romagna	0.00	0.00	0.00
Pastinese - MO	Emilia-Romagna	28.57	1.00	5.71
Ceppa - MO	Emilia-Romagna	30.00	4.00	24.00
Marrone di Zocca - MO	Emilia-Romagna	30.00	2.67	16.00
Carrarese - MO	Emilia-Romagna	56.25	3.89	43.75
Tosca/Garfagnana - MO	Emilia-Romagna	15.79	2.33	7.37
Madonna - MO	Emilia-Romagna	50.00	2.67	26.67
Loglia - MO	Emilia-Romagna	25.00	2.00	10.00

(Continued)

Table 2. (Continued).

Chestnut variety	Region	Chestnut brown rot		
		Incidence D (%)	Severity S	McKinney Index MI (%)
Biancherina - MO	Emilia-Romagna	46.15	2.83	26.15
Svizzero - MO	Emilia-Romagna	30.00	2.67	16.00
Pilistella - MO	Emilia-Romagna	42.86	2.67	22.86
Loiola - MO	Emilia-Romagna	44.44	2.00	17.78
Lisanese - MO	Emilia-Romagna	20.00	2.00	8.00
Salvane - MO	Emilia-Romagna	13.33	3.00	8.00
Bovalghe - MO	Emilia-Romagna	43.75	3.43	30.00
Pelosa - MO	Emilia-Romagna	77.78	3.43	53.33
Molana - MO	Emilia-Romagna	31.25	2.40	15.00
Montemarano - MO	Emilia-Romagna	66.67	3.07	40.95
Castel del Rio - MO	Emilia-Romagna	90.00	3.00	54.00
Garron Rosso - MO	Emilia-Romagna	73.68	2.21	32.63
Marron Buono - MO	Emilia-Romagna	20.00	3.25	13.00
Castagna - MO	Emilia-Romagna	5.00	1.00	1.00
Average		39.29	2.69	22.44
Castagna della Madonna	Piedmont	100.00	4.65	93.,00
Colossal	Piedmont	33.33	3.20	21.33
Marsol	Piedmont	64.71	3.82	49.41
Marlhac	Piedmont	57.14	3.25	37.14
Maridonne	Piedmont	71.43	3.40	48.57
Ishyzuki precoce	Piedmont	26.32	3.00	15.79
Ishyzuki tardiva	Piedmont	52.38	3.91	40.95
Tsukuba	Piedmont	53.85	3.57	38.46
Precoce Migoule	Piedmont	65.00	3.08	40.00
Bouche de Betizac	Piedmont	90.91	4.70	85.45
Laguepie	Piedmont	55.00	3.45	38.00
Marrubia	Piedmont	85.71	3.61	61.90
Marrone di Susa	Piedmont	75.00	3.40	51.00
Marrone di Chiusa Pesio	Piedmont	47.62	3.40	32.38
Marrone di Viterbo	Piedmont	36.84	4.57	33.68
Average		61.02	3.67	45.81

Table 3. Fungal genera isolated from a total of 360 chestnuts which were classified after visual inspection into chestnut brown rot (CBR) severity classes (0 to 5) based on the proportions of internal nut tissue deterioration (see text). Numbers in parentheses indicate the percentages.

CBR Severity class	Number of samples	Fungal genera detected (%)					
		Gnomoniopsis	*Penicillium*	*Trichoderma*	*Aspergillus*	*Alternaria*	*Fusarium*
0	60	3 (5)	0	0	0	0	0
1	60	30 (50)	2 (3)	1 (1.6)	1 (1.6)	2 (3)	2 (3)
2	60	57 (95)	3 (5)	2 (3)	1 (1.6)	2 (3)	0
3	60	59 (98.3)	2 (3)	0	0	0	4 (6.6)
4	60	42 (70)	2 (3)	1 (1.6)	3 (5)	1 (1.6)	1 (1.6)
5	60	22 (36.6)	2(3)	4 (6.6)	2 (3)	5 (8.3)	2 (3)
Total	360	213 (59.2)	11 (3)	8 (2)	7 (1.9)	10 (2.7)	9 (2.5)

Figure 4. A) (a-s). Necrotic lesions formed on chestnut cuttings (*Castanea sativa*) 20 d after inoculation with *Gnomoniopsis castaneae* isolates of haplotype A [a) 'GC_Castagna di Val di Castro-SITE 1'; b) 'GC_Barrile-BARV'; c) 'GC_Castagna bionda di Lunano'; d) 'GC_SanPietro'; e) 'GC_Castel del Rio-MO'; f) isolate 'PD-ST30'; and g) inoculation control.] Inoculations with *G. castaneae* isolates of haplotype B [h) 'GC_Marrone scuro-2710'; i) 'GC_Marrone di Chiusa Pesio'; j) 'GC_Rossera-2414'; k) 'GC_Tosca/Garfagnana'; l) 'GC_Patriarca-3595'; m) 'GC_Bouche de Betizac'; n) 'GC_Santu Giuanni-ARI3'; o) 'GC_Pilistella'; p) 'GC_Precoce Migoule'; q) 'GC_Marrone di Viterbo'; r) 'GC_Marrone di Perledo-3419'; or s) isolate 'PD-ST55'. B)] Necrosis lenghts (cm) in stems of cuttings of different chestnut varieties previously inoculated with different *Gnomoniopsis castaneae* isolates. Means accompanied by the same lowercase letter are not different ($P \geq 0.05$).

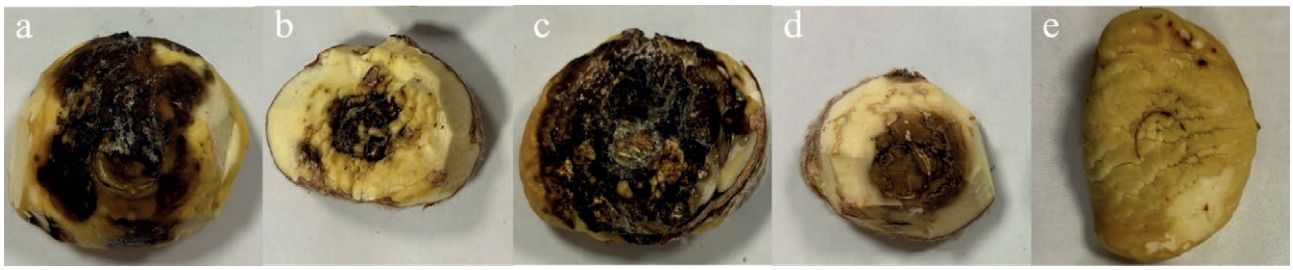

Figure 5. Necrotic lesions formed in the endosperm tissues of chestnut (*Castanea sativa*) fruits 16 d after inoculations with *Gnomoniopsis castaneae* isolates molecularly characterized as Gc-haplotype A and B based on *β-tubulin* gene sequences typing: a) 'GC_Castagna bionda di Lunano'; b) 'GC_Marrone scuro-2710'; c) 'GC_Rossera-2414'; d) 'GC_Marrone di Chiusa Pesio'; and e) the inoculation control.

castaneae isolates within each *Gc*-haplotype group (Confidence level used: 0.95, $P > 0.5$) (Figure 4B). Among the *Gc*-haplotype A isolates, the isolates 'GC_Castagna bionda di Lunano' and 'GC_Castagna di Val di Castro' site 1 (Marche) were the most aggressive, producing a longer necrosis compared to the other isolates. Within *Gc*-haplotype B, the most aggressive isolate was 'GC_Tosca Garfagnana from Emilia Romagna' (Figure 4B).

Pathogenicity test on chestnut fruits

The 16 isolates of *G. castaneae,* five of *Gc*-haplotype A and 11 of *Gc*-haplotype B, all induced necrotic lesions on fruits 16 d post inoculation (Supplementary Table 3). Mean areas of necrosis ranged from 0.84 (± 0.63) cm^2, induced by isolate 'GC_Precoce Migoule', up to 11.21 (± 5.97) cm^2 induced by isolate 'GC_Santu Giuanni_ARI3' (Figure 5). Statistical analyses showed that these data were not normally distributed, so the dataset was transformed using the function "Boxcox" and a lambda value of 0.26. With the transformed data, the ANOVA test showed no statistically significant difference ($P = 0.4787$) between necrosis caused by the two *Gc*-haplotype groups.

Pathogenicity test on chestnut seedlings under different water regimes

An additional pathogenicity test was performed inoculating the 16 *G. castaneae* isolates (*Gc*-haplotypes A and B) on 3-year-old chestnut seedlings, cultivated in two different water regimes (WR) in controlled conditions for 30 days. All 16 *G. castaneae* isolates induced cortical necrosis on seedlings (Supplementary Table 4). ANOVA tests showed no statistically significant ($P > 0.05$) differences within each water regime in necrosis produced by the different *G. castaneae* isolates (Figure 6A). Generally, necrosis induced by each isolate were longer for WR_B (150 mL $month^{-1}$) than for WR_A (150 mL $week^{-1}$). Exceptions were for 'GC_Marrone di Perledo' and 'GC_Marrone di Chiusa Pesio', where mean necrosis length for WR_A (150 mL $week^{-1}$) was 3.86 cm (± 1.91), while for the WR_B (150 mL $month^{-1}$) plants mean lesion length was 3.33 cm (± 1.83) (Supplementary Table 4).

Differences were detected in severity of necroses caused by *Gc*-haplotypes A and B. The *Gc*-haplotype A isolates produced longer necroses in plants under WR_B than for WR_A. In contrast, *Gc*-haplotype B showed no difference ($P > 0.05$) in necrosis between the two water regimes (Figure 6B).

DISCUSSION

Results from this study have demonstrated the importance of *G. castaneae* as an emerging pathogen causing diseases in European chestnut in Italy. Approximately 69% of the 1812 assessed nuts from 100 of the varieties growing in the Italian Biodiversity Repository Fields, located in Piedmont, Tuscany, Emilia-Romagna, and Campania, and in commercial orchards in Lombardy, Trentino Alto-Adige, Marche and Sardinia, were affected by fruit rots. Occasionally, pink and black rots as well as internal green mold were recorded in fruit samples. The most frequently detected postharvest alteration was brown rot of nut endosperms, although the nuts had been harvested and selected for the Fruit Exhibition showing no external symptoms, no loss of consistency, or other significant visible defects. These results indicate that visual inspection of nuts is often insufficient for an accurate assessment of brown rot and detection of *G. castaneae*, which was also reported by Vettraino *et al.* (2021). Consequently, nuts that appear externally healthy may be internally compromised and unmarketable (Shuttleworth and Guest, 2017). Reliable detection of chestnut rots currently relies on destructive methods or advanced techniques such as X-ray comput-

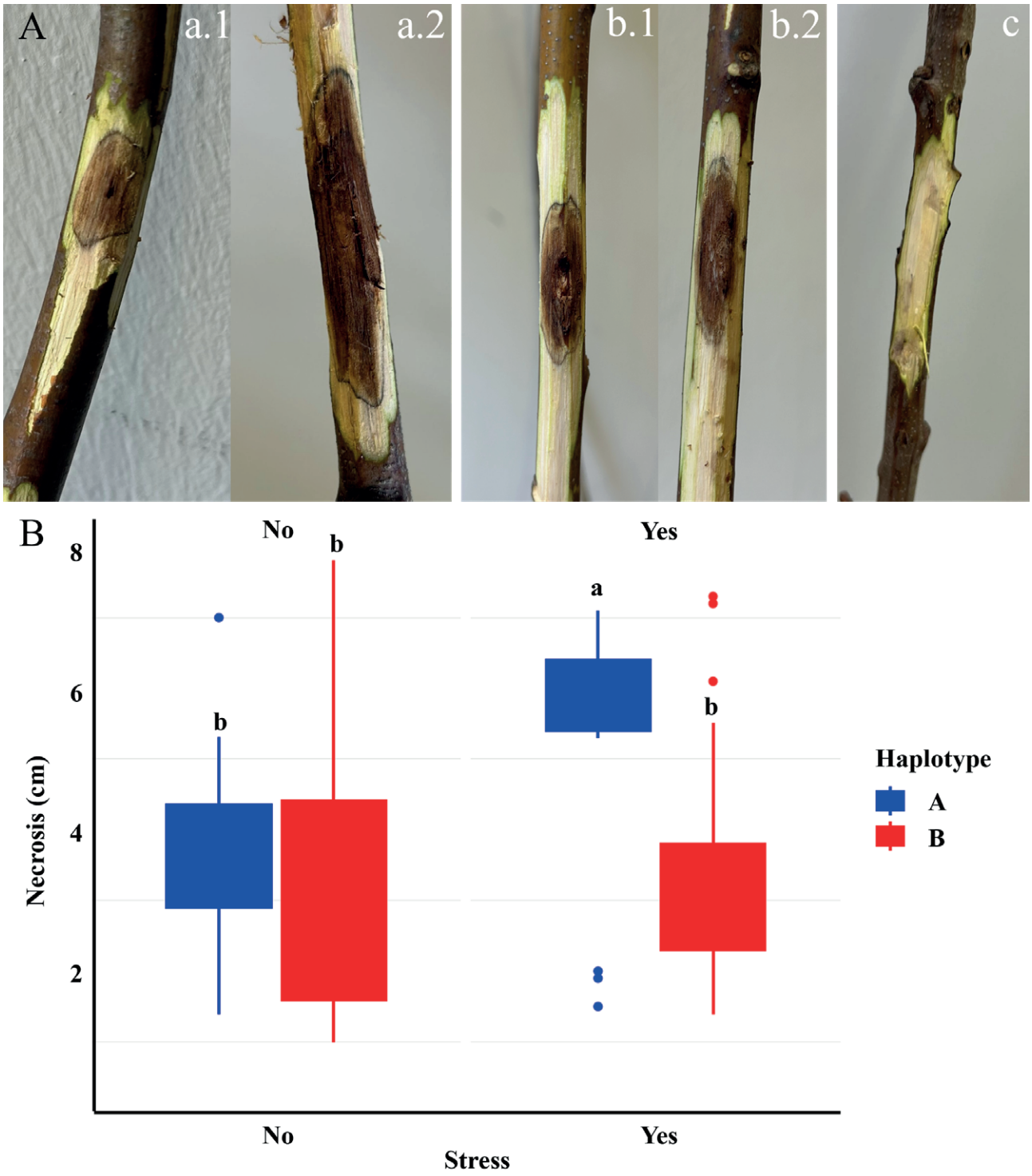

Figure 6. A) (a–c). Necrotic lesions formed on chestnut (*Castanea sativa*) seedlings 30 d after inoculations with *Gnomoniopsis castaneae* isolates. The seedlings received two different water regimes to simulate no stress or stress conditions. a.1) Haplotype A: 'GC_Castagna di Val di Castro – SITE 1', in the 150 mL week^{-1} irrigation treatment, and a-2) in the 150 mL month^{-1} treatment; b.1) 'GC_Castagna Bionda di Lunano' in the 150 mL week^{-1} irrigation treatment, and b.2) in the 150 mL month^{-1} treatment; c) experimental control. B) Lengths (cm) of necroses in stems of cuttings of different chestnut varieties that were previously inoculated with different *Gnomoniopsis castaneae* isolates. Means accompanied by the same lowercase letter are not different ($P \geq 0.05$). Statistical analysis showing the significantly different behaviour of the Haplotype A isolates when comparing necrosis under different water stress conditions.

ed tomography (CT), which provides deep penetration capability (Bernard *et al*., 2020; Matsui *et al*., 2022).

After nut bi-dissection, brown rot was detected in more than half of the nuts analyzed, with different levels of disease severity in nut endosperms. The McKinney Index gave good assessments of the impact of brown rot on chestnut fruit. This Index synthesizes incidence (D) and severity (S) of this disease. The present study results showed that average Mckinney index was 42.19%, with different Italian regional situations, ranging from 16% (Trentino Alto Adige) to 72% (Lombardy). Most of the assessed chestnut varieties had fruit brown rots. Epidemiological data from Australia, Italy and Portugal have showed that most chestnut germplasm can be affected, though severity and extent of endosperm alteration can be variable (Lione, 2016; Shuttleworth and Guest, 2017; Possamai *et al*., 2023). The present study showed that from chestnuts showing brown rot, *G. castaneae* was isolated from fruits, the endosperms of which involved from 11 to 50% of tissues (disease severity classes 2 and 3). Brown rot was not observed in a few varieties, including: 'Marrone Rugoso di Acquasanta Terme', 'Castagna di Val di Castro' site 1 and 'Marrone Classico di Acquasanta Terme' (Marche); 'Sborgà' (Emilia-Romagna); and 'Loccheddu- LOCG2' and 'Ildubba-ILDP' (Sardinia).

Gnomoniopsis castaneae was occasionally also isolated from nuts classified as McKinney Index MI = 0 (no visible episperm alterations), confirming the pathogen's latent stage, as has been previously reported by Maresi *et al*. (2013) and Dennert *et al*. (2015). This can also explain how apparently healthy nuts were found infected after 2 weeks of storage at room temperature, without any source of inoculum. This ability to latently persist, and its widespread distribution, underlies the success of this pathogen. The ubiquity and ability to infect different chestnut tree components was demonstrated by Topalidou *et al*. (2024), who detected *G. castaneae* using Bar-HRM analysis, at varying success rates from different chestnut tissues (buds, flowers, or nuts), and across multiple seasonal stages. Ability to cause damage on fruit is likely to be related to nut storage conditions, temperature shown to be important in the present study.

Factors such as pre-harvest litter management, climate conditions (Shuttleworth *et al*., 2013; Lione *et al*., 2015, 2021), and especially storage time and temperature are all likely to influence the transition from latent to active nut infections, accelerating post-harvest disease progression (Morales-Rodriguez *et al*., 2022). These factors could explain the ambiguous results obtained from the particular varieties (i.e. 'Ceppa', 'Pelosa', 'Bovalghe', 'Pastanese', 'Svizzera') cultivated in two different Germoplasm Repositories of Emilia Romagna.

Gnomoniopsis castaneae was identified in the present study using morphological characteristics and molecular assays, and ITS sequence analyses were effective for species-level resolutions. Further genotyping based on the *β-tubulin* sequences confirmed the two *G. castaneae* haplotypes (A and B) recently described by Seddaiu *et al*. (2023). The results of the present study have expanded knowledge on the geographical distribution of the two haplotypes, by obtaining information on their presence/absence in Emilia-Romagna (*Gc*-haplotypes A and B), Marche (A) and Campania (A). According to previous findings, 64% of Italian isolates belonged to *Gc*-haplotype A (mainly found in central Italy), while 36% belonged to *Gc*-haplotype B (more common in the north Italian regions) (Seddaiu *et al*., 2023). Although the two haplotypes are morphologically indistinguishable, they differ in virulence, particularly in ability to rapidly induce necroses in inoculated fruits. This was indicated by Seddaiu *et al*. (2023), after conducting pathogenic tests on chestnut fruits with seven representative Sardinian isolates of *G. castaneae* (*Gc*-haplotypes A and B). In the present study assessments conducted on Marche fruits and chestnut cuttings, inoculating 16 *G. castaneae* isolates (five of *Gc*-haplotype A and 11 of *Gc*-haplotypes B), no statistically significant differences were detected between the two *Gc*-haplotypes in their necrotic effects on fruits or chestnut cuttings. Both haplotypes induced cankers when inoculated onto cuttings, consistent results of similar damage in other *Fagaceae* hosts (Droby *et al*., 2023). Ability of *G. castaneae* to cause branch cankers and necroses was also recorded in chestnut trees in Veneto and Sardinia. From branch cankers, which turned shoot tissues from pale green to brown and withered, *G. castaneae* was commonly isolated, while *Do. iberica, C. parasitica*, *N. luteum* were only sporadically isolated. Symptoms in chestnut canopies were generally associated to *C. parasitica* (Rigling and Prospero, 2018). Cankers caused by *G. castaneae* are distinguishable from those caused by *C. parasitica*, due to their dark brown bark, while for *C. parasitica* outer bark cankers are typically red-orange with swollen and fissured host cortical tissues.

Plants, cultivated at the same temperature, but subjected to prolonged water stress and inoculated with *Gc*-haplotype A, developed more severe symptoms than those receiving regular irrigation, indicating that water stress promoted aggressiveness of *Gc*-haplotypes. From the present study data, when the pathogenicity tests were carried out on seedlings, water stress conditions did not affect the pathogenicity of *Gc*-haplotype B, but only that of *Gc*-haplotype A. On the other hand, *G. castaneae* has been frequently isolated from different tissues of healthy

plants (Ugolini *et al*., 2014; Pasche *et al*., 2016; Kolp *et al*., 2020). As suggested by Topalidou *et al*. (2024), buds and flowers can be reservoirs of the fungal inoculum, and *G. castaneae* can then shift from endophytic to pathogenic behaviour due to favourable environmental conditions for the pathogen combined with host stress induced by abiotic and/or biotic conditions. Several studies have shown that under conditions of stress, inoculation of endophytes into plant tissues can result in disease symptoms (necrosis or chlorosis) and/or growth inhibition of host plants (Schulz *et al*., 1998).

CONCLUSIONS

Gnomoniopsis castaneae has increasing impacts on chestnut hosts, as the pathogen can take advantage of conducive conditions after fruit harvest, and of abiotic stress conditions for affecting plants. The data presented here of Gc-haplotype virulence, and the recent availability of *Castanea sativa* chromosome-level genome and mitogenome (Bianco *et al.,* 2024; Villa *et al*., 2025), may provide a useful background for further studies of short and medium term adaptive disease management strategies. Detailed investigations into the mechanisms involving fungal behaviour and tree physiology in climate change context would be worthwhile.

ACKNOWLEDGMENTS

The Authors express gratitude to Francesco Carosi, Riccardo Falappa, Pietro Turchi and Simone Piancatelli for technical assistance in laboratory activities and data elaboration. The Piedmont Chestnut R&D Center at Chiusa Pesio (Cuneo), the Foundation E. Mach (San Michele all'Adige, Trento), the National Chestnut Biodiversity Center (Granaglione, Bologna), the University Alma Mater Bologna, Study and Documentation Center for the Chestnut in Marradi (Firenze), CREA OFA Caserta (Caserta), the Agro-Silvo Chestnut Consortium of the Modena Apennines (Modena), and AGRIS Sardinia supported the research reported in this paper. Lombardy Chestnut accessions were previously studied by the Experimental Agricultural Center at IBE CNR Follonica (Grosseto).

AUTHOR CONTRIBUTIONS

F.C. methodology, investigation, formal analysis, writing - original draft; C.B. investigation, formal analysis, writing - original draft; B.T.L. conceptualization, formal analysis investigation, formal analysis, Writing – Review & Editing funding acquisition, supervision; G.M. Writing – Review & Editing, supervision; S.M. conceptualization formal analysis, Writing – Review & Editing; funding acquisition, supervision.

LITERATURE CITED

Bassanelli C., Bischetti G.B., Chiaradia E.A., Rossi L., Vergani, C., 2013. The contribution of chestnut coppice forests on slope stability in abandoned territory: a case study. *Journal of Agricultural Engineering* 44: (s2). https://doi.org/10.4081/jae.2013.254

Battisti A., Bevegnu I., Colombari F., Haack R.A., 2014. Invasion by the chestnut gall wasp in Italy causes significant yield loss in *Castanea sativa* nut production. *Agricultural and Forest Entomology* 16: 75–79. https://doi.org/10.1111/afe.12036

Bianco L., Fontana P., Marchesini A., Torre S., Moser M., … Palmieri L., 2024. The *de novo*, chromosome-level genome assembly of the sweet chestnut (*Castanea sativa* Mill.) Cv. Marrone Di Chiusa Pesio. *BMC Genomic Data* 25(1): 64. https://doi.org/10.1186/s12863-024-01245-7

Bernard A., Hamdy S., Le Corre L., Dirlewanger E., Lheureux, F., 2020. 3D characterization of walnut morphological traits using X-ray computed tomography. *Plant Methods* 16(1): 115. https://doi.org/10.1186/s13007-020-00657-7

Conedera M., Krebs P., Tinner W., Pradella M., … Torriani D., 2004. The cultivation of *Castanea sativa* (Mill.) in Europe, from its origin to its diffusion on a continental scale. *Vegetation History and Archaeobotany* 13(3): 161–179. https://doi.org/10.1007/s00334-004-0038-7

Dar M.A., Rai M., 2015. *Gnomoniopsis smithogilvyi*, a canker causing pathogen on *Castanea sativa*: First report. *Mycosphere* 6(3): 327–336. https://doi.org/10.5943/mycosphere/6/3/8

Dennert F.G., Broggini G.A.L., Gessler C., Storari M., 2015. *Gnomoniopsis castaneae* is the main agent of chestnut nut rot in Switzerland. *Phytopathologia Mediterranea* 54: 199–211. https://doi.org/10.14601/Phytopathol_Mediterr-14712

Dobry E., Campbell M., 2023. *Gnomoniopsis castaneae*: an emerging plant pathogen and global threat to chestnut systems. *Plant Pathology* 72: 218–231. https://doi.org/10.1111/ppa.13670

Doyle J.J., Doyle J.L., 1990. Isolation of plant DNA from fresh tissue. *Focus* 12: 13–15.

Donis González I.R., Fulbright D.W., Ryser E.T., Guyer D., 2009. Shell mold and kernel decay of fresh chestnuts in Michigan. In *I European Congress on Chestnut-Castanea 2009* 866: 353–362. https://doi.org/10.17660/ActaHortic.2010.866.45

European and Mediterranean Plant Protection Organization, 2017. EPPO Reporting Service No. 02–2017 Num. Article: 2017/047. Available online: http://archives.eppo.int/EPPOReporting/2017/Rse-1702.pdf (accessed 22 March 2021).

Freitas T.R., Santos J.A., Silva A.P., Fraga H., 2021. Influence of climate change on chestnut trees: a review. *Plants* 10: 1463. https://doi.org/10.3390/plants10071463

Gabrielli A., 1994. La civiltà del castagno. *Monti e boschi* 65: 3.

Gaffuri F., Longa C.M.O., Turchetti T., Danti R., Maresi G., 2017. 'Pink rot': infection of *Castanea sativa* fruits by *Colletotrichum acutatum*. *Forest Pathology* 47: e12307. https://doi.org/10.1111/efp.12307

Glass N.L., Donaldson G.C., 1995. Development of primer sets designed for use with the PCR to amplify conserved genes from filamentous ascomycetes. *Applied and Environmental Microbiology* 61: 1323–1330. https://doi.org/10.1128/AEM.61.4.1323-1330.1995

González I.R., Guyer D.E., Fulbright D.W., 2016. Quantification and identification of microorganisms found on shell and kernel of fresh edible chestnuts in Michigan. *Journal of the Science of Food and Agriculture* 96: 4514–4522. https://doi.org/10.1002/jsfa.7667

Kolp M., Double M. L., Fulbright D. W., MacDonald W. L., Jarosz A. M., 2020. Spatial and temporal dynamics of the fungal community of chestnut blight cankers on American chestnut (*Castanea dentata*) in Michigan and Wisconsin. *Fungal Ecology* 45:100925. https://doi.org/10.1016/j.funeco.2020.100925

Lema F., Baptista P., Oliveira C., Ramalhosa E., 2023. Brown rot caused by *Gnomoniopsis smithogilvyi* (syn. *Gnomoniopsis castaneae*) at the level of the chestnut tree (*Castanea sativa* Mill.). *Applied Sciences* 13: 3969. https://doi.org/10.3390/app13063969

Linaldeddu B.T., Deidda A., Scanu B., Franceschini A., Alves A., … Phillips A.J.L., 2016. Phylogeny, morphology and pathogenicity of *Botryosphaeriaceae, Diatrypaceae* and *Gnomoniaceae* associated with branch diseases of hazelnut in Sardinia (Italy). *European Journal of Plant Pathology* 146(2): 259–279. https://doi.org/10.1007/s10658-016-0912-z

Lione G., Giordano L., Sillo, F., Gonthier P., 2015. Testing and modelling the effects of climate on the incidence of the emergent nut rot agent of chestnut *Gnomoniopsis castanea*. *Plant Pathology* 64: 852–863. https://doi.org/10.1111/ppa.12319

Lione G.G., 2016. Ecology and epidemiology of the emerging plant pathogen *Gnomoniopsis castaneae*. *Journal of Plant Pathology* 98(4): S5-S5.

Lione G., Danti R., Fernandez-Conradi P., Ferreira-Cardoso J.V., Lefort F., … Gonthier P., 2019. The emerging pathogen of chestnut *Gnomoniopsis castaneae*: the challenge posed by a versatile fungus. *European Journal of Plant Pathology* 153: 671–685. https://doi.org/10.1007/s10658-018-1597-2

Lione G., Giordano L., Sillo F., Brescia F., Gonthier P., 2021. Temporal and spatial propagule deposition patterns of the emerging fungal pathogen of chestnut *Gnomoniopsis castaneae* in orchards of north-western Italy. *Plant Pathology* 70(9): 2016–2033. https://doi.org/10.1111/ppa.13451

Marais A., Murolo S., Faure C., Brans Y., Larue C., … Candresse, T., 2021. Sixty years from the first disease description, a novel badnavirus associated with chestnut mosaic disease. *Phytopathology* 111(6): 1051–1058. https://doi.org/10.1094/PHYTO-09-20-0420-R

Maresi G., Oliveira Longa C.M., Turchetti T., 2013. Brown rot on nuts of *Castanea sativa* Mill: an emerging disease and its causal agent. *iForest* 6: 294–301. https://doi.org/10.3832/ifor0952-006

Mattioli W., Mancini L. D., Portoghesi L., Corona P., 2016. Biodiversity conservation and forest management: The case of the sweet chestnut coppice stands in Central Italy. *Plant Biosystems-An International Journal Dealing with all Aspects of Plant Biology* 150(3): 592–600. https://doi.org/10.1080/11263504.2015.1054448

Matsui H., 2022. Biological Sensing Using Infrared. *Biosignal Processing* 209.

McKinney H.H., 1923. Influence of soil temperature and moisture on infection of wheat seedlings by *Helminthosporium sativum*. *Journal of Agricultural Research* 26: 195–218.

Morales-Rodriguez C., Bastianelli G., Caccia R., Bedini G., Massantini R., … Vannini A., 2022. Impact of 'brown rot' caused by *Gnomoniopsis castaneae* on chestnut fruits during the post-harvest process: critical phases and proposed solutions. *Journal of the Science of Food and Agriculture* 102: 680–687. https://doi.org/10.1002/jsfa.11397

Nicoletti R., Beccaro G.L., Sekara A., Cirillo C., Di Vaio C., 2021. Endophytic fungi and ecological fitness of chestnuts. *Plants* 10: 542. https://doi.org/10.3390/plants10030542

Pasche S., Calmin G., Auderset G., Crovadore J., Pelleteret P., … Lefort F., 2016. *Gnomoniopsis smithogilvyi*

causes chestnut canker symptoms in *Castanea sativa* shoots in Switzerland. *Fungal Genetics and Biology* 87: 9–21. https://doi.org/10.1016/j.fgb.2016.01.002

Pérez-Girón J.C., Álvarez-Álvarez P., Díaz-Varela E.R., Mendes Lopes D.M., 2020. Influence of climate variations on primary production indicators and on the resilience of forest ecosystems in a future scenario of climate change: application to sweet chestnut agroforestry systems in the Iberian Peninsula. *Ecological Indicators* 113: 106199. https://doi.org/10.1016/j.ecolind.2020.106199

Pezzi G., Ferretti F., Maltoni A., Krebs P., Conedera M., Maresi G., 2022. The chestnut orchards in the Bolognese Apennines: A vanishing socio-ecological habitat. In *Historical Ecology: Learning from the Past to Understand the Present and Forecast the Future of Ecosystems* pp. 195–205.

Possamai G., Dallemole-Giaretta R., Gomes-Laranjo J., Sampaio A., Rodrigues P., 2023. Chestnut brown rot and *Gnomoniopsis smithogilvyi*: Characterization of the causal agent in Portugal. *Journal of Fungi* 9(4): 401. https://doi.org/10.3390/jof9040401

Prada M., Bravo F., Berdasco L., Canga E., Martínez-Alonso C., 2016. Carbon sequestration for different management alternatives in sweet chestnut coppice in northern Spain. *Journal of Cleaner Production* 135: 1161–1169. https://doi.org/10.1016/j.jclepro.2016.07.041

Prospero S., Heinz M., Augustiny E., Chen Y. Y., Engelbrecht J., … Fonti P., 2023. Distribution, causal agents, and infection dynamic of emerging ink disease of sweet chestnut in Southern Switzerland. *Environmental Microbiology* 25(11): 2250–2265. https://doi.org/10.1111/1462-2920.16455

Rigling D., Prospero S., 2018. *Cryphonectria parasitica*, the causal agent of chestnut blight: invasion history, population biology and disease control. *Molecular Plant Pathology* 19(1): 7–20. https://doi.org/10.1111/mpp.12542

Rodrigues P., Driss O.J., Gomes-Laranjo J., Sampaio A., 2022. Impact of cultivar, processing and storage on the mycobiota of European chestnut fruits. *Agriculture* 12: 1930. https://doi.org/10.3390/agriculture12111930

Santos M.J., Pinto T., Vilela A., 2022. Sweet chestnut (*Castanea sativa* Mill.) nutritional and phenolic composition interactions with chestnut flavor physiology. *Foods* 11: 4052. https://doi.org/10.3390/foods11244052

Schulz B., Guske S., Dammann U., Boyle C., 1998. Endophyte host interactions II. Defining symbiosis of the endophyte-host interaction. *Symbiosis* 25: 213–227.

Seddaiu S., Mello A., Sechi C., Cerboneschi A., Linaldeddu B.T., 2021. First Report of *Neofusicoccum parvum* associated with chestnut nut rot in Italy. *Plant Disease* 105: 3743. https://doi.org/10.1094/PDIS-01-21-0072-PDN

Seddaiu S., Mello A., Sarais L., Mulas A., Sechi C., Ruiu P.A., … Linaldeddu B.T., 2023. Haplotypes distribution and virulence of *Gnomoniopsis castaneae* in Italy. *Journal of Plant Pathology* 105: 1135–1140. https://doi.org/10.1007/s42161-023-01459-1

Shuttleworth L.A., 2012 . Fungal planet description sheet 108: *Gnomoniopsis smithogilvyi* LA Shuttleworth, ECY Liew & DI Guest, sp. nov. *Persoonia* 28: 142–143. https://doi.org/10.3767/003158512X652633

Shuttleworth L.A., Liew E.C.Y., Guest D.I., 2013. Survey of the incidence of chestnut rot in south-eastern Australia. *Australasian Plant Pathology* 42: 63–72. https://doi.org/10.1007/s13313-012-0170-2

Shuttleworth L.A., Guest D.I., 2017. The infection process of chestnut rot, an important disease caused by *Gnomoniopsis smithogilvyi* (*Gnomoniaceae, Diaporthales*) in Oceania and Europe. *Australasian Plant Pathology* 46(5): 397–405. https://doi.org/10.1007/s13313-017-0502-3

Suna S., Avşar B., Koçer S., Çopur Ö.U., 2021. Effects of different pretreatments on the physicochemical characteristics and quality criteria of chestnut (*Castanea sativa* Mill.) pickle: a new value-added product. *Journal of Food Processing and Preservation* 45:e15669. https://doi.org/10.1111/jfpp.15669

Topalidou E., Lagiotis G., Bosmali I., Stefanidou E., Tsirogiannis D., Vettraino A.M., Madesis P., 2024. Water stress enhances the pathogenicity of *Gnomoniopsis castaneae* in chestnut trees. *Journal of Plant Pathology* 106: 345–352. https://doi.org/10.1016/j.funbio.2024.06.003

Ugolini F., Massetti L., Pedrazzoli F., Tognetti R., Vecchione A., … Maresi G., 2014. Ecophysiological responses and vulnerability to other pathologies in European chestnut coppices, heavily infested by the Asian chestnut gall wasp. *Forest Ecology and Management* 314: 38–49. https://doi.org/10.1016/j.foreco.2013.11.031

Vettraino A. M., Luchi N., Rizzo D., Pepori A. L., Pecori F., Santini A., 2021. Rapid diagnostics for *Gnomoniopsis smithogilvyi* (syn. *Gnomoniopsis castaneae*) in chestnut nuts: new challenges by using LAMP and real-time PCR methods. *AMB Express* 11(1): 105. https://doi.org/10.1186/s13568-021-01266-w

Villa S., Marchesini A., Torre S., Bianco L., Fontana P., De Quattro C., … Sebastiani F., 2025. First complete mitogenome assembly of *Castanea sativa*: structure,

comparative genomics, and phylogeny. *Tree Genetics & Genomes* 21(4): 22. https://doi.org/10.1007/s11295-025-01707-8

Visentin I., Gentile S., Valentino D., Gonthier P., Tamietti G., Cardinale F., 2012. *Gnomoniopsis castaneae* sp. nov. (*Gnomoniaceae*, *Diaporthales*) as the causal agent of nut rot in sweet chestnut. *Journal of Plant Pathology* 94: 411–419. http://www.jstor.org/stable/45156050.

Washington W.S., Allen A.D., Dooley L.B., 1997. Preliminary studies on *Phomopsis castanea* and other organisms associated with healthy and rotted chestnut fruit in storage. *Australasian Plant Pathology* 26: 37–43. https://doi.org/10.1071/AP97006

White T.J., Bruns T., Lee S., Taylor J.W., 1990. Amplification and direct sequencing of fungal ribosomal RNA genes for phylogenetics. In: *PCR protocols: a guide to methods and applications*. (Innis M.A., Gelfand D.H., Sninsky J.J., White T.J. ed.). San Diego, C, USA, Academic Press, 315–322.

Phytopathologia Mediterranea
The international journal of the
Mediterranean Phytopathological Union

Firenze University Press
www.fupress.com/pm

Research Papers

Preserving autochthonous Albanian plum germplasm: Plum pox virus-free status and *in vitro* sanitation perspectives for the 'Tropojane' cultivar

Magdalena CARA[1,2], Serafina Serena AMOIA[3,*], Valbona SOTA[4,7], Jordan MERKURI[2], Orges CARA[5,2], Klevis HOXHALLARI[1,2], Elektra PAPAKOSTA[6], Efigjeni KONGJIKA[7], Angelantonio MINAFRA[3]

[1] *Agricultural University of Tirana, Faculty of Agriculture and Environment, Rruga Paisi Vodica 1025, Tirana, Albania*
[2] *NanoBalkan, Academy of Sciences of Albania, Murat Toptani Avenue, 1000 Tirana, Albania*
[3] *Institute for Sustainable Plant Protection (IPSP)—National Research Council, Via Amendola 122/D, Bari 70126, Italy*
[4] *Department of Biotechnology, Faculty of Natural Sciences, University of Tirana, Albania, Bul. Zog. 1, 1001, Tirana, Albania*
[5] *International Centre for Advanced Mediterranean Agronomic Studies (CIHEAM of Bari), Valenzano, Italy*
[6] *Agricultural Technology Transfer Center, Shamogjin, Vlora, Albania*
[7] *Research Center of Biotechnology and Genetics, Academy of Sciences of Albania, Murat Toptani Avenue, 1000, Tirana, Albania*
*Corresponding author. E-mail: serafinaserena.amoia@cnr.it

Summary. The stone fruit industry, particularly plum (*Prunus domestica*) production, is important to the Albanian economy. The *Prunus domestica* 'Tropojane' predominates due to its high and stable productivity, adaptability, and superior organoleptic qualities. Assessing phytosanitary status of this fruit plant is important, to ensure sustainable production and preserve genetic resources. During the spring seasons of 2022, 2023 and 2024, 129 samples of 'Tropojane' plum were collected across the regions of Tropoja, Kukës, Has, Puka, Durrës, Paskuqan, and Kamëz of Albania. All samples were tested by ELISA, PCR, and qPCR to detect plum pox virus (PPV), the most destructive virus infecting plum, and to screen for additional stone fruit viruses including *Prunus* necrotic ringspot virus (PNRSV), prune dwarf virus (PDV), apple mosaic virus (ApMV), and apple chlorotic leafspot virus (ACLSV). ELISA tests demonstrated that PPV was present in 35.5% of the samples, whereas RT-PCR and RT-qPCR assays detected PPV in 45.6% of the samples, confirming greater sensitivity of the PCR assays for virus detection. No infections with other assessed stone fruit viruses were detected. PPV identity was confirmed by sequencing, and phylogenetic analyses showed that the Albanian isolates clustered within the Rec strain group, also indicating their possible regional origin. Meristem culture was employed as a sanitation strategy for PPV-infected explants. Differences in regeneration capacity among plum populations were observed, yet stable *in vitro* cultures were established in all cases, and molecular diagnostics confirmed that regenerated plantlets were PPV-free. *In vitro* shoots were successfully subcultured, rooted, and acclimatized. These results highlight the need to

OPEN ACCESS

Citation: Cara, M., Amoia, S. S., Sota, V., Merkuri, J., Cara, O., Hoxhallari, K., Papakosta, E., Kongjika, E., & Minafra, A. (2026). Preserving autochthonous Albanian plum germplasm: Plum pox virus-free status and *in vitro* sanitation perspectives for the 'Tropojane' cultivar. *Phytopathologia Mediterranea* 65(1): 93-105. doi: 10.36253/phyto-17066

Accepted: March 4, 2026

Published: May 14, 2026

©2026 Author(s). This is an open access, peer-reviewed article published by Firenze University Press (https://www.fupress.com) and distributed, except where otherwise noted, under the terms of the CC BY 4.0 License for content and CC0 1.0 Universal for metadata.

Data Availability Statement: All relevant data are within the paper and its Supporting Information files.

Competing Interests: The Author(s) declare(s) no conflict of interest.

Editor: Assunta Bertaccini, Alma Mater Studiorum, University of Bologna, Italy.

ORCID:
MC: 0000-0002-1715-8635
SSA: 0000-0002-1661-8417
VS: 0000-0002-5840-0387
JM: 0009-0004-5610-763X
OC: 0009-0000-0682-0796
KH: 0009-0002-7618-7660
EP: 0009-0005-4601-4920
EK: 0000-0002-5328-3919
AM: 0000-0002-0547-7129

conserve native plum germplasm, and enforce the use of certified planting material, to ensure the long-term preservation of autochthonous cultivars, while preventing further spread of PPV.

Keywords. Plum pox virus, Sharka disease, virus detection, *in vitro* sanitation, meristem tip culture.

INTRODUCTION

Albania has a long tradition in the cultivation of stone fruits (*Prunus* spp.), which have considerable socio-economic importance. The European plum (*Prunus domestica* L.) is the most widely grown *Prunus* species in Albania. Both native and foreign plum varieties are cultivated across all regions, with total production of 40,196 tons over 2,559 ha in 2024 (ISTAT, 2024). Albanian germplasm includes more than 20 autochthonous plum varieties, among which the *Prunus domestica* 'Tropojane' predominates, accounting for more than 50% of all plum trees in the country (Çakalli *et al*., 2007). 'Tropojane', also known as "Kumbulla e Hasit", derives its name from the area where it originated, and is cultivated throughout Albania due to its high adaptability and desirable agronomic and pomological traits. This cultivar is late flowering, and produces large, dark-skinned, elliptic fruits (each approx. 60 g) that ripen in September each year. The fruit flesh is yellow-reddish, juicy, aromatic, and moderately firm (Kokaj, 2025). 'Tropojane' plum is used extensively for fresh consumption and processing (*e.g*., dried prunes, jams, and traditional alcoholic drinks), underscoring its importance as a valuable genetic resource within Albanian *Prunus* germplasm.

Nevertheless, plums are susceptible to numerous pests and diseases, among which virus infections pose significant threats, leading to yield losses and deterioration of fruit quality (Rubio *et al*., 2017). In particular, *Potyvirus plumpoxi* (plum pox virus, PPV), the etiological agent of Sharka, is considered one of the most harmful virus pathogens that internationally affect plums and other stone fruits, with cumulative losses estimated to value € 2.4 billion over the last 28 years (Cambra *et al*., 2024). For these reasons, PPV is ranked as either a quarantine pest or a regulated non-quarantine pest (RNQP), due to its widespread endemic presence [EPPO PM 7/32 (2)].

PPV (*Potyvirus*, *Potyviridae*) has flexuous filamentous particles. It possesses a positive-sense single-stranded RNA (ssRNA) genome of approx. 9.7 kb (García *et al*., 2014), which encodes a single large open reading frame (ORF). To date, ten independent strains have been identified, varying in established sequences, geographical distributions, and host ranges: D, M, EA, Rec, T, C, CR, CV, W, and An (García *et al*.,2025). The M (Marcus), D (Dideron), and Rec (Recombinant) strains are considered the most epidemiologically important, with the D and Rec strains exhibiting preference for plum hosts (Sihelská *et al*. 2017). The symptoms caused by this virus variants are strongly influenced by the host cultivar, environmental conditions (*e.g*., temperature), and age and physiological stage of the infected plants (Clemente-Moreno *et al*., 2015). PPV induces yellowish to olive-green bands, rings, spots and mottling on host leaves, which may be associated with leaf malformation. On plum fruits, PPV infections cause shallow depressions that deepen as fruits ripen, leading to deformations and irregular line patterns on the fruit surfaces. Infected fruits are tasteless and fibrous, making them unmarketable, and, in some cases, all fruits may prematurely drop (Llácer and Cambra, 2006; Pedrelli *et al*., 2024).

PPV was first reported in 1918 in Bulgaria infecting plums (Atanasoff, 1932), and has since spread to other European countries, the Near and Middle East, Asia, North Africa, and America (EPPO, 2025). In Albania, several studies of PPV on stone fruits have been conducted, confirming its presence in plum, apricot, and peach and showing high infection rates in tested plants from orchards, nurseries, and mother plots (Myrta *et al*., 1995; Musa *et al*., 2010). Myrta *et al*. (1998) and Stamo *et al*. (2003) reported that PPV-M and PPV-D were the predominant strains. In contrast, Palmisano *et al*. (2015) confirmed the presence of PPV-Rec and PPV-T, with the latter representing one of the few occurrences of the virus recorded outside Türkiye. PPV transmission pathways explain this widespread distribution. Long-distance dissemination of the virus is primarily facilitated by the movement of infected propagation material, often introduced through insufficiently regulated commercial or illegal exchanges. Approximately 30 aphid species mediate natural non-persistent plant-to-plant transmission of PPV (Rimbaud *et al*., 2015). Among these aphids, *Myzus persicae*, *Aphis spiraecola*, and *Hyalopterus pruni* are the most efficient vectors in the Mediterranean region (Cambra and Vidal, 2016). Effective surveillance and implementation of preventive containment strategies remain essential to mitigate spread and impacts of PPV.

Virus-free host propagation through *in vitro* meristem culture is widely recognized as an effective strat-

egy for eliminating PPV and other graft-transmissible pathogens from infected plant material (Bhat and Rao, 2020; Szabó *et al*., 2024). Shoot apex (0.4 to 0.7 mm) meristems often do not have systemic infections, because viruses typically fail to invade the actively dividing cells within the apical domes and youngest leaf primordia (Mori and Hosokawa, 1977; Mochizuki and Ohki, 2015; Vivek and Modgil, 2018; Singh, 2025). Use of the meristem culture, alone or combined with thermotherapy, is efficient for producing PPV-free plants in many stone fruit species, including plum (Kabylbekova *et al*., 2025), sweet cherry (Naddaf *et al*., 2021), nectarine (Manganaris *et al*., 2003), peach (Dessoky *et al*., 2018), and apricot (Pérez-Caselles *et al*., 2025). Although the regenerative potential after meristem excision can decrease due to the reduced explant size, optimizing the physicochemical culture factors can regenerate high numbers of healthy plantlets during subculturing stages, and these can be used as mother plants for certified propagation programs. The effectiveness of meristem culture can be reliably confirmed through the integration of molecular diagnostics, particularly PCR-based assays, which enable rapid and highly sensitive detection of virus infections in regenerated plantlets (Gong *et al*., 2019; Kang *et al*., 2025).

Given the significant socio-economic value of the autochthonous European plum (*Prunus domestica* 'Tropojane') in Albania, and the potential threats posed by Sharka, the present study aimed to assess prevalence and distribution of PPV in native plum germplasm across this country's major plum-producing regions. The study also aimed to optimize an integrated *in vitro* sanitation and PCR-based protocol for production of healthy material from plum plants that tested PPV-positive, for subsequent conservation and multiplication.

MATERIALS AND METHODS

Sources and locations of plant material

During the spring seasons (April to May) of 2022, 2023 and 2024, ten orchards of *Prunus domestica* 'Tropojane' were inspected for virus symptoms across seven regions of Albania. A total of 129 leaf samples were collected from Tropoja (17 samples), Kukës (12), Pukë (22), Has (18), Paskuqan (from Kukës, 30), Kamëz (from Kukës, 14), or Durrës (from Tropoja, 16 samples). Field sampling included asymptomatic and symptomatic leaves mainly exhibiting chlorotic spots, bands, and/or rings. After collection, the samples were briefly stored at 4°C for further analyses.

Serological and Molecular detection of PPV and other common Prunus *viruses*

DAS-ELISA, RT-PCR, and RT-qPCR assays

All samples were initially screened for PPV presence using a Double-Antibody Sandwich Enzyme-Linked Immunosorbent Assay (DAS-ELISA) (Clark and Adams, 1977). Monoclonal antibodies from line 5B were used to detect all known serotypes of PPV, using the commercial K-10 PPV-Universal ELISA KIT (AGRITEST) (Cambra *et al*., 1994). Sample assessments were carried out using internal positive and negative controls supplied with the kit, and absorbance was measured at $\lambda = 405$ nm using a PR 4100 Absorbance Microplate Reader (Bio-Rad). A sample was considered positive when its signal exceeded at least three times the value of the negative internal control.

Following serological screening, all samples were subjected to molecular analyses using reverse transcriptase (RT-PCR) and quantitative qPCR assays. Total nucleic acids (TNA) were extracted from 0.2 g of leaves from each sample, which was homogenized in 1 mL of grinding buffer, then isolated using silica particles, as described by Foissac *et al*. (2001). The TNA quality was checked by electrophoresis on agarose gel (1.2%) in Tris-Borate-EDTA buffer, and the extracts were stored at -20°C until used. Starting from 500 ng of TNA, cDNA was synthesized by reverse transcription, using 1 µL of random hexamer primers (0.5 mg mL^{-1}) and M-MLV reverse transcriptase, following the manufacturer's instructions (Thermo Fisher). PCR and qPCR assays were carried out on all samples using specific primers for PPV and to discriminate between M and D strains of PPV (Table 1). Positive (cDNA from plums previously infected by the PPV-M, isolate GR046, GenBank accession number PV955083) and negative (*i.e*., cDNA from a healthy plum) controls were added in the reactions.

In addition to PPV, a subset of ten samples, selected from across the seven regions (above), was also screened for Prunus necrotic ringspot virus (PNRSV), prune dwarf virus (PDV), and apple mosaic virus (ApMV; *Ilarvirus*, *Bromoviridae*) and apple chlorotic leafspot virus (ACLSV; *Trichovirus*, *Betaflexviridae*), because these viruses are often found in mixed infections with PPV in most stone fruit hosts. All the primers used in this study are listed in Table 1.

Each PCR reaction consisted of 12.5 µL of GoTaq® Green Master Mix (Promega), 2 µL of cDNA, 0.5 µL of each primer, and DNase/RNase-free water to 25µL final volume. qPCR assays were carried out using a 2× Fast SYBR™ Green Master Mix (Applied Biosystems™), a ready-to-use reaction mix optimized for dye-based qPCR on a CFX96 real-time thermocycler (BioRad).

Table 1. List of primers used in RT-PCR and RT-qPCR for detecting stone fruit viruses. The sequences (sense and antisense), amplicon sizes, and corresponding references are also reported.

Virus	Primer sequence (5´ to 3´)	PCR amplicon (bp)	Reference
PPV (PCR)	F: CAGACTACAGCCTCGCCAGA R: ACCGAGACCACTACACTCCC	243	Wetzel *et al*., 1992
PPV-D PPV-M (qPCR)	F: CGTTTATTTGGCTTGGATGGAA F: GATTAACATCACCAGCGGTGTG R: GATTCACGTCACCAGCGGTGTG	76	Olmos *et al*., 2005
ACLSV (qPCR)	F: GTTCCTGGCCGCAGAAGGCAGACCCCT R: GCTATGTTCGCGAAGATGGACTCC	86	Nickel and Fajardo,2014
ACLSV (PCR)	F: GCAGACCCCTTCATGGAAAG R: TTCGGGTCCGAAGATGTAGTC	218	Diaz-Lara *et al*., 2020
PNRSV (qPCR)	F: GGTTTGCCGAATTTGCAATC R: GCCCTGAGTGGGACCAGAG	89	Palmisano (personal communication)
PNRSV (PCR)	F: TCACTCTAGATCTCAAGCAG R: GACACTTTTGCGCGTACGCA	200	Rosner *et al*., 1997
ApMV (PCR)	F: ATCCGAGTGAACAGTCTATCCTCTAA R: GTAACTCACTCGTTATCACGTACAA	262	Menzel *et al*., 2002
	F: TAGTCGCGAGCGTTTTATTTTCAT R: CTTCGAGCTTCACAGTCCT	784	Valasevich *et al*., 2015
PDV (PCR)	F: CCGAGTGGATGCTTCACG R: CCTTTAATGAGTCCGTAGAC	220	Jarosova and Kundu,2010

Sequence analyses

Two PCR amplicons, each one amplified from a single accession, were Sanger sequenced in both directions by Macrogen Europe. The resulting sequences were then compared with those available in GenBank, using BLASTN to determine nucleotide similarity (%). Sequence alignments and phylogenetic analyses were carried out using MEGA software v. 12.1.1 to evaluate possible origins of the isolates, and to examine their overall clustering and potential strain-level differences.

Meristem excision and in vitro *regeneration of plum plantlets*

Stabilization of in vitro *cultures*. Apical shoot tips (each approx. 3–5 cm long) were collected from PPV-positive mother plants of 'Tropojane' grown in Durrës (origin Tropoja) and Paskuqan (origin Kukës). A total of five mother plants were used, and 30 apical shoots were collected *per* plant (n = 150 explants in total). The explants were sterilized with 0.01% mercuric chloride for 10 min. After several rinsing with sterile H_2O, the explants were then inserted into test tubes containing MS medium (Murashige and Skoog, 1962) supplemented with 1 mg L^{-1} of 6-benzylaminopurine (BAP), 0.1 mg L^{-1} of 1-naphthaleneacetic acid (NAA), 3% sucrose, and 0.6% agar. The pH value of the medium was set at 5.8 before autoclaving. The tubes containing explants were incubated for 4 weeks in a growth chamber at 25°C under a 16 h light/8 h dark photoperiod, with cool white fluorescent light at 46.25 µmol m^{-2} s^{-1}.

Meristem culture and PPV-testing. Meristem tips (each 0.7 to 0.9 mm) from mother plants of both origins (30 meristem tips from each geographic region) were aseptically excised using a binocular stereomicroscope, transferred to hormone-free MS medium supplemented with 3% sucrose and 0.6% agar, and incubated at 25°C under standard growth-room conditions for regeneration. Meristem-derived shoots were tested for PPV by RT-PCR at the first subculture stage at 42 to 56 d after meristem excision, when regenerated shoots reached 1.5 to 2.0 cm in length and had produced at least two to three expanded leaves.

Subculture stage and shoot regeneration. When the regenerated shoots reached 1.5 to 2 cm, they were transferred to subculture for further micropropagation. MS medium supplemented with 3% sucrose and 0.6% agar was used. Different BAP concentrations (0, 1.0, 1.5, or 2.0 mg L^{-1}) were compared to evaluating their efficiency for promoting lateral shoot growth.

Rooting and acclimatization. In vitro rhizogenesis was induced by using ½ MS medium supplemented with 1.0 mg L^{-1} of indole-3-butyric acid (IBA). Plants with well-developed roots were then acclimatized in sterilized peat in alveolate trays in an acclimatization tunnel inside a

greenhouse under controlled temperature and light conditions. After acclimatization, the plants were transferred to bags containing fertilized soil mixed with 15 to 20% agriperlite. For each treatment, 30 explants were used *per* replicate**,** and the experiment was repeated three times, resulting in a total of 90 explants per treatment.

Experimental design and data analyses. The experiment was arranged in a Completely Randomized Design (CRD). After 45 d from excision, the meristematic tips were evaluated for their regeneration potential. During the subculture stage, the effect of BAP concentration on micropropagated 'Tropojane' plum shoots was assessed using physiological and biometric parameters. The lengths of the plantlets and the numbers of new shoots *per* explant were recorded and compared. The results are analyzed with JMP 7.0 and presented as means ± standard errors.

RESULTS

Field observations and symptom expression in 'Tropojane' plum

During field inspections in the native growing areas of 'Tropojane' plum, fewer symptomatic trees were observed compared to areas where this cultivar has been introduced, such as Tiranë and Durrës. At these sites, chlorotic mosaic, interveinal chlorosis, and leaf distortion with yellowing were most frequently recorded, reflecting possible early-season manifestations of PPV (Figure 1).

Figure 1. Symptoms of PPV infections in 'Tropojane' plum trees. (a) Leaves showing mild chlorotic mosaic, light green rings and uneven green zoning (in Tiranë). (b) Leaves exhibiting pronounced mottling along with interveinal chloroses (in Durrës). (c) Leaf distortions associated with yellowing (in Durrës).

Serological and molecular detection of viruses in 'Tropojane' plum

DAS-ELISA conducted on the 'Tropojane' samples yielded 46 PPV-positive reactions out of 129 samples tested, representing an overall PPV infection rate of 35.6%. Sample evaluation was based on absorbance values measured at 405 nm after 2 h of substrate incubation, with duplicate positive controls ranging from 0.315 to 2.315, while negative controls ranged from 0.076 to 0.118. The positivity threshold was defined as three times the mean absorbance value of the negative controls (≥0.23). Accordingly, samples with absorbance values equal to or exceeding this threshold were classified as ELISA-positive, whereas those below this limit were classified as ELISA-negative.

RT-PCR and RT-qPCR screening detected 59 PPV-positive samples (45.6%), exceeding the number of positives detected by ELISA (Figure 2; Table 2), with fully consistent results between the two assays.

The regional distribution of PPV infections was heterogeneous, with the greatest prevalence observed in Durrës (87.5%), Paskuqan (86.6%), and Kamëz (85.7%). In contrast, infection rates in Kukës and Has were lower (16.6%), and only 9% of samples from Pukë tested positive. In Tropoja, the region of origin for the 'Tropojane', PPV infection was not detected in any of the sampled trees. Notable discrepancies were observed between symptom expression and infection status. Several symptomatic trees were found to be RT-PCR-negative for PPV in Tropoja, Pukë, Kukës, and Has, whereas asymptomatic RT-PCR-positive trees were detected in Paskuqan, Kamëz, and Durrës.

In parallel, screening for other stone fruit viruses, including ACLSV, PNRSV, ApMV, and PDV, showed that none of the analyzed samples were infected with these viruses. Therefore, PPV was the only virus detected in the analyzed 'Tropojane' plum samples, with no indication of mixed infections.

Sequence and phylogenetic analyses

Sequence analyses indicated a high level of similarity between the two Albanian PPV isolates partially sequenced in this study (Al_Tropojane_1 and Al_Tropojane_2). The two obtained sequences were, respectively, 213 and 212 nucleotides (nts) in length (excluding the primers sequence). Those two sequences shared 98.4% similarity. When they were compared with reference sequences available in GenBank, through BLASTN analyses, a maximum nucleotide similarity 99.5% was obtained with isolates belonging to the PPV-Rec strain

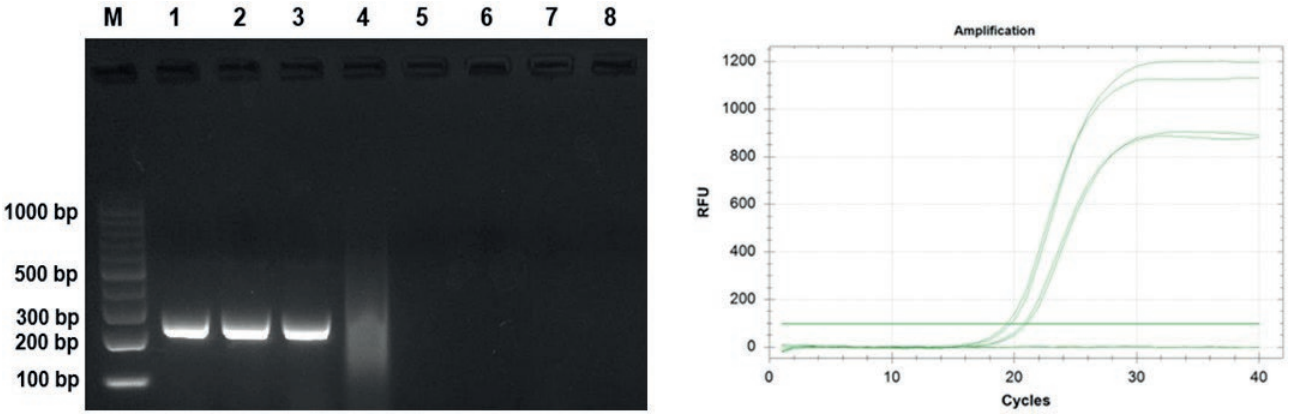

Figure 2. Representative results obtained from an RT-PCR/qPCR assay. Left image: Agarose gel electrophoresis of PCR amplicons from PPV-infected plum samples. Lane M: 100 bp DNA ladder; Lane 1: positive control (243 bp); Lanes 2 and 3: PPV-positive samples; Lanes 4 to 7: PPV-negative samples; Lane 8: sterile water used as negative control reaction. Right image: Amplification curves generated by RT-qPCR assays targeting PPV, using two different primer pairs.

Table 2. Summary of plum pox virus (PPV) detection in 'Tropojane' plum samples by ELISA, RT-PCR and RT-qPCR (2022–2024).

Region / Orchard location	Number of samples Total/Symptomatic	No. ELISA Positive	No. RT-PCR Positive	No. RT-qPCR Positive	Infection proportion (%)
Tropoja	17/3	0	0	-	0
Pukë	22/7	1	2	2	9
Kukës	12/5	1	2	2	16.6
Has	18/5	2	3	3	16.6
Kamëz - Tiranë (origin: Kukës)	14/9	10	12	12	85.7
Paskuqan - Tiranë (origin: Kukës)	30/23	20	26	26	86.6
Durrës (origin: Tropoja)	16/11	12	14	14	87.5
Total	129/63	46 (35.6%)	59 (45.6%)	59 (45.6%)	

(*i.e.*, GenBank accession numbers: EU117116, JX013532, AY690609). No recombination signals or strain-specific mutations were detected. These results support the classification of the PPV isolates from 'Tropojane' as stable, non-recombinant members of the PPV-Rec lineage.

The phylogenetic analysis to determine the strain affiliation and infer the possible origin of the Albanian isolates (Figure 3) delineated the isolates by their respective PPV strain affiliations. The two Albanian isolates clustered consistently within the PPV-Rec group, with Al_Tropojane_2 forming a well-supported subcluster (bootstrap value >80%) with isolates from Serbia (Serbia-T; GenBank accession number AY690609) and Russia (Al-Ch; GenBank accession number MN734791). In contrast, although positioned slightly basal within the Rec clade, Al_Tropojane_1 showed closest phylogenetic affinity to isolates from Poland (J4c; GenBank accession number EU117116), Croatia (Valjevka; GenBank accession number JX013532), and Ukraine (sREC; GenBank accession number KF472134), suggesting a regional evolutionary signature, and supporting absence of recent virus introductions or recombination events in this germplasm. The tip closest to the nodes belonging to PPV-M and -Rec progeny leads to the Ancestor strain (PPV-An), which gave the origin through recombination to both the above strains (Palmisano *et al.*, 2025).

Meristem culture and in vitro *plantlet regeneration*

Establishment of in vitro *cultures*

Only materials from plum mother plants grown in Durrës (origin Tropoja) and Paskuqan (origin Kukës) were used at this stage, as these tested positive for PPV. In addition to the relevant proportion of explant stabilization achieved (Figure 4a), some differences in asepsis and regeneration rates were observed between the

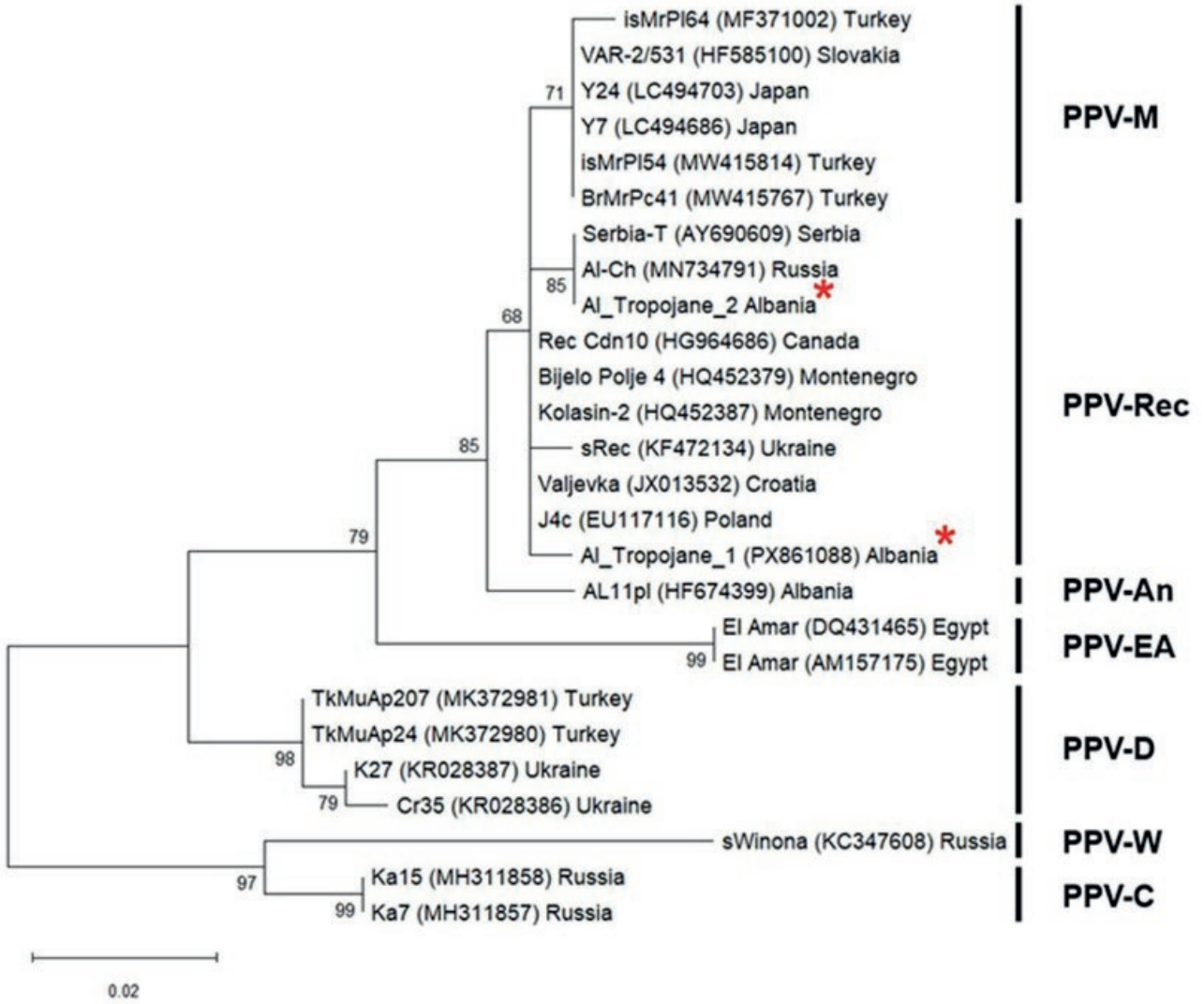

Figure 3. A maximum likelihood phylogenetic tree, constructed using nucleotide sequences of genomic 3′ end (Wetzel *et al*., 1992) PCR amplicons, of PPV isolates from Albania (indicated with red asterisks), together with reference sequences retrieved from GenBank, including their respective accession numbers and geographic origins. Bootstrap values are shown at the branch nodes.

two shoot populations. Contamination was mainly of fungal origin, characterized by fast-growing mycelium emerging from explants within the first week of culture, whereas bacterial contamination was observed less frequently, and typically appeared as turbid exudates around the explant bases. In many cases, even when explants did not show visible contamination, their survival and subsequent regeneration rates were affected by excessive polyphenol production and the release of oxidized compounds into the culture medium, which negatively affected tissue viability. Among the studied plant populations, the explants from Paskuqan (origin Kukës) exhibited the greatest degree of stabilization for both monitored parameters (Figure 5, a and b). Nevertheless, aseptic cultures were obtained from both plant populations, enabling successful regeneration of shoots and progression to the subsequent experimental stages.

Meristem survival rates after three and six weeks of culture

For both plant populations, the meristem tips were excised (Figure 4, b and c). Due to their small size (0.7 to 0.9 mm), the regeneration process was slow, and the first shoots were obtained after 6 weeks. Regeneration rates were evaluated at 3 and 6 weeks. Explants were considered regenerated when they maintained a healthy green colouration, and showed visible increases in size,

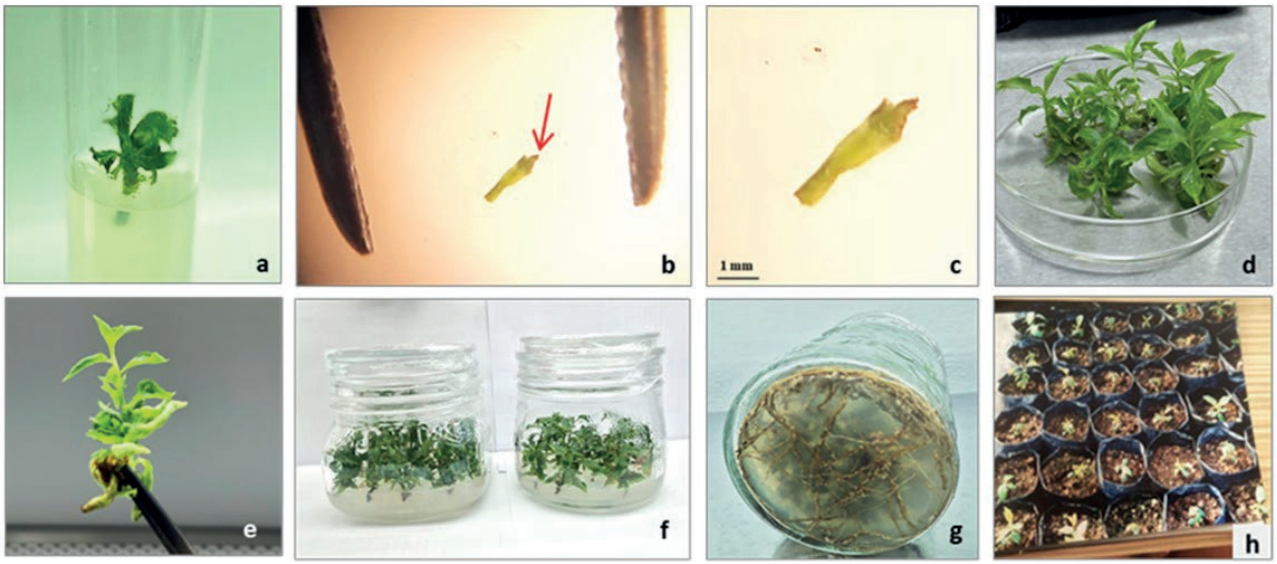

Figure 4. *In vitro* culture of *Prunus domestica* L. a) apical shoots used as primary explants. b) and c) meristematic tip isolation, d), e), and f) multiplication during the subculture stage. g) rooted plantlets. h) acclimated plants.

even if minor. Differences between the two plant populations were observed, following trends similar to those observed in the previous stage. The Paskuqan population (origin Kukës) exhibited greater regeneration rates at both evaluation points, reaching 48.6% after 3 weeks and 53.6% after 6 weeks. In contrast, the Durrës population reached 43.8% after 3 weeks and 49.1% after 6 weeks (Figure 5, c and d).

Regenerated shoots were further propagated through multiple subcultures. The *in vitro* regenerated shoots tested negative for PPV by RT-PCR at the first subculture stage, corresponding to 87% sanitation efficiency for both plant populations. These results indicated that meristem culture was effective for producing PPV-free 'Tropojane' shoots at the early regeneration stage.

Mass production of plants via *subcultures and* ex vitro *transferring*

For both plant populations, leaf numbers increased progressively with BAP concentrations up to 1.5 mg L^{-1} (Figure 6 a), indicating that cytokinins stimulated leaf development in the plum shoots during *in vitro* culture (Figure 4, d, e, and f). Across all concentrations, the Durrës/Tropoja plant material developed greater mean leaf numbers than material from Paskuqan/Kukës. Also, the shoot numbers increased progressively with increasing BAP concentrations (Figure 6 b). At 0 mg L^{-1}, both populations have low shoot production (1.3 to 1.5 shoots). Beginning at 1 mg L^{-1}, shoot proliferation increased. The greatest shoot numbers occurred at 2 mg L^{-1} BAP (Figure 4, d, e, and f). At all BAP concentration, the Durrës/Tropoja population had slightly greater shoot numbers than the Paskuqan/Kukës population. Once a sufficient number of shoots was obtained after several subcultures, they were transferred to the rooting medium. After 4 weeks, *in vitro* roots developed (Figure 4 g), and the plantlets were transferred to *ex vitro* acclimatization (Figure 4 h).

DISCUSSION AND CONCLUSIONS

Serological and molecular analyses detected PPV in 'Tropojane' plum samples with an average prevalences of 35.6% and 45.6%. These results are consistent with previous studies reporting the superior performance of PCR-based techniques over ELISA for PPV detection (Myrta *et al*. 2003; Schneider *et al*., 2004). All infected samples in the present study originated from Tiranë and Durrës, whereas all trees in the native northern region of Tropoja tested negative. One factor that may have progressively reduced the PPV inoculum in Tropoja is the systematic eradication of infected plum trees immediately after symptom appearance (Armand Haxhia, personal communication), a practice widely implemented in the region. The high altitude environment of this region, characterized by cold, prolonged winter conditions, markedly suppresses the aphid vector overwintering success rate, population growth, and early-season activity, thereby limiting virus transmission (BBRO, 2021; MSU Extension, 2020; Labonne *et al*., 1999). Addition-

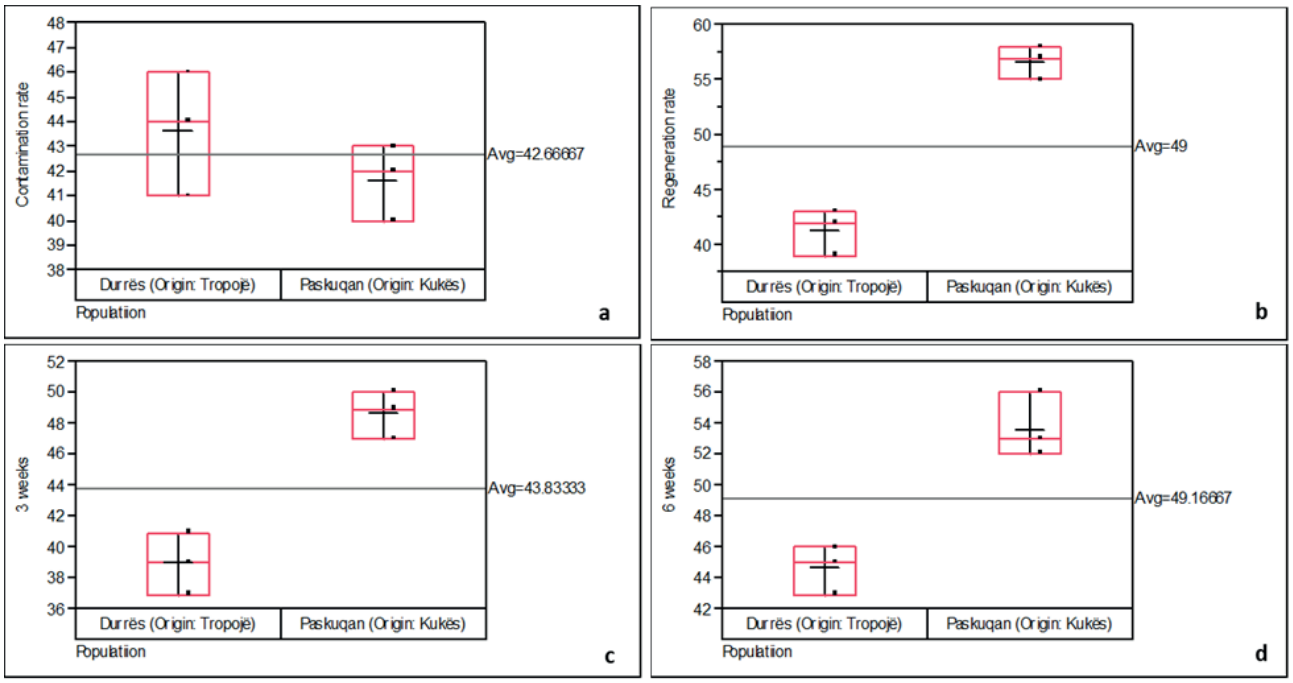

Figure 5. Parameters of *Prunus domestica* explants from two plant populations. a) contamination (%), b) regeneration (%), and survival rates of excised meristems after c) 3 or d) 6 weeks.

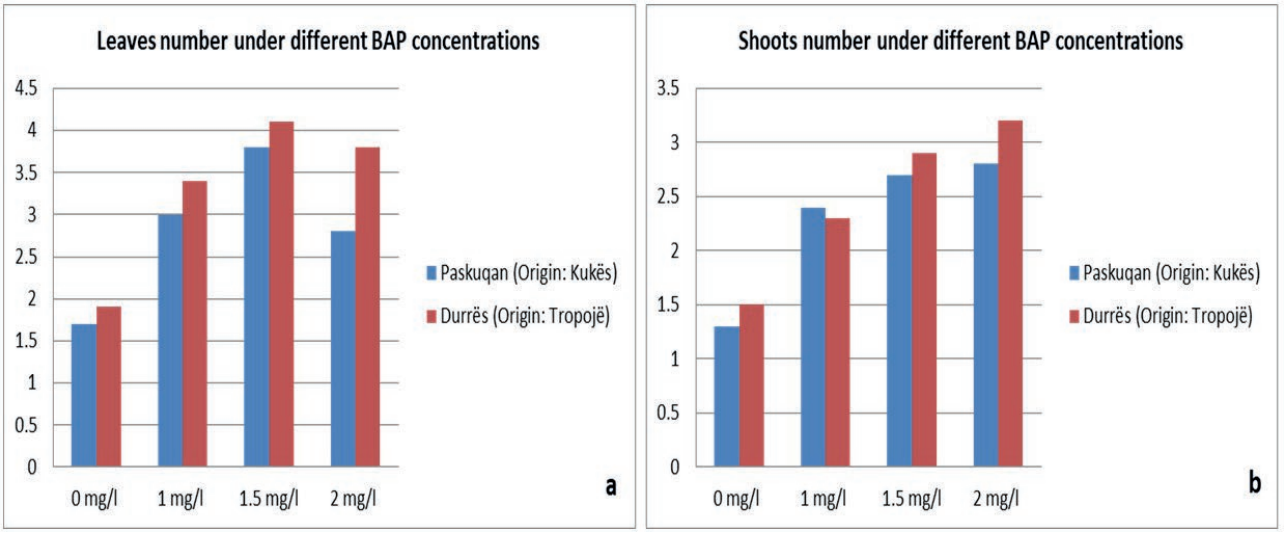

Figure 6. a) Mean leaf, and b) shoot numbers for two *Prunus domestica* types exposed to different BAP concentrations.

ally, plum production in these areas generally follows a traditional, low-input system, where trees are rarely treated with insecticides. Under such conditions, naturally occurring aphid biological control agents, including predators and parasitoids, may help regulate aphid vector populations, contributing to an ecological equilibrium that further restricts PPV dissemination.

As a consequence of a demographic shift from northern Albania toward the Tiranë and Durrës regions for economic reasons, autochthonous plum cultivars, such as 'Tropojane', were also introduced into these new areas, mainly in home gardens or small private orchards, probably favouring the spread of virus in these regions. Beyond uncontrolled movement of uncertified planting material

from the northern regions, another factor that promotes PPV spreads is the adaptability of aphid vectors to the mild climatic conditions of Tiranë and Durrës.

Symptom expression varied widely between orchards, and within individual trees, reflecting the combined influence of environmental conditions, plant phenology, virus concentration and strain, duration of infection, and fertilization regime on symptom manifestation (García *et al*., 2025). Inconsistencies between symptom expression and diagnostic results were also noted in the present study, which may indicate presence of divergent PPV strains that were not fully detected by the assays used, due to their limitations and the high genomic variability of PPV (García *et al*., 2014). However, visual detection is not always reliable, since PPV symptoms may resemble those caused by other disorders, and latent infections can occur, further complicating diagnosis. These points highlight the need for laboratory-based diagnostics using sensitive and comprehensive approaches to improve detection accuracy and support robust and reliable certification of planting material for plum orchards.

Results obtained using *in vitro* techniques demonstrated that meristem culture is effective for producing PPV-free plants. Although a large majority of regenerated plantlets tested negative for PPV at the first subculture stage, virus concentration may remain below the detection threshold during early regeneration. Therefore, confirmation of the long-term PPV-free status ideally requires re-testing after prolonged *in vitro* maintenance and/or after acclimatization (*e.g.*, ≥6 months), preferably using RT-qPCR detection, which provides greater sensitivity than RT-PCR (Kanapiya *et al*., 2024). This additional step will be included in future certification-oriented sanitation workflows. Explant size also affects regenerative potential and efficiency of virus eradication: when explants are too small, regenerative potential is lost (Vivek and Modgil, 2018; Zarghami *et al*., 2023). The efficiency of BAP as a cytokinin for the rapid biomass production of *P. domestica* aligned with reports from previous studies (Yuan *et al*., 2009; Wolella, 2017; Baziuk and Kobyletska, 2025), reinforcing its suitability for mass multiplication of the 'Tropojane' plantlets, successful establishment of *in vitro* cultures, consistent shoot proliferation, and production of PPV-free regenerated shoots. This confirms the efficiency of meristem culture techniques for this cultivar, which could serve as a routine protocol for other plum varieties.

While comparison of cytokinin concentrations is not novel, its inclusion in the present research served a practical purpose within a sanitation-to-multiplication pipeline for an autochthonous Albanian plum cultivar. Establishing stable *in vitro* cultures from field-grown 'Tropojane' material was challenging due to variable asepsis, strong phenolic oxidation, and population-dependent regeneration performance. Therefore, the present dataset demonstrates that: (i) PPV-infected local germplasm can be successfully sanitized through meristem culture; and (ii) the resulting virus-free tested lines can be rapidly multiplied using a simple and reproducible protocol suitable for implementation in national certification and conservation programs. The present study provides an operational framework for producing candidate "basic" category material of 'Tropojane' plum, which is currently lacking in Albania.

The present study underscores the need for systematic conservation and certification strategies for native plum germplasm, especially for cultivars threatened by genetic erosion. Heritage landraces such as 'Tropojane' should be preserved, either in *in situ* orchards or within organized germplasm repositories, to maintain their unique genetic makeup and agronomic traits (Priyanka, 2021; Dumont *et al*., 2025). At the same time, propagation of plum material must rely strictly on certified, virus-free nursery stock to avoid the spread of pathogens such as PPV. Implementing a national certification and traceability scheme for planting material would help safeguard local biodiversity, support future breeding programs, and ensure sustainable use of native cultivars, without risking genetic loss or disease introductions.

ACKNOWLEDGEMENTS

This study was carried out within the framework of the projects *"Use of* In Vitro *Biotechnological Methods and Molecular Biology in the Effort to Obtain 'Basic' Category Planting Material of Autochthonous Plum Cultivars"* (2022–2023), supported by NASRI (https://nasri.gov.al/), and *"Selection of Virus-Controlled Plum Plant Material for the Establishment of a Pilot Plant through Sanitation and Micropropagation (VITROCERT)"* (2022–2024), supported by the Academy of Sciences of Albania (ASA: https://akad.gov.al/). The authors also acknowledge financial support from the CryoFruit project, coordinated and financed by ASA.

AUTHOR CONTRIBUTIONS

Magdalena Cara: Sample collection, serological and molecular analyses, manuscript writing. Serafina Serena Amoia: Molecular analyses, manuscript writing. Valbona Sota: *In vitro* cultures establishment, sanitation procedures, manuscript writing. Jordan Merkuri: Sample col-

lection, serological and molecular analyses, manuscript writing. Orges Cara: Molecular and bioinformatic analyses, manuscript writing. Klevis Hoxhallari: Serological and molecular analyses, manuscript writing. Elektra Papakosta: *In vitro* procedures. Efigjeni Kongjika: *In vitro* establishment, sanitation procedures, manuscript writing. Angelantonio Minafra: Molecular analyses, manuscript writing.

LITERATURE CITED

Atanasoff D., 1932. Plum pox. A new viral disease. *Annals of the University of Sofia, Faculty of Agriculture and Silviculture* 11: 49–69.

Baziuk S., Kobyletska M., 2025. Micropropagation of plum rootstock *(Prunus domestica* L.) of 'Wavit' variety. *Studia Biologica*. Advance online publication. http://dx.doi.org/10.30970/sbi.1901.805

BBRO, 2021. How cold weather affects aphid populations and virus spread. British Beet Research Organisation, *Advisory Bulletin No. 1*. https://www.bbro.co.uk/resources/advisory-bulletin/

Bhat A.I., Rao G.P., 2020. Virus elimination by meristem-tip culture. In: *Characterization of Plant Viruses*. Springer Protocols Handbooks. Humana, New York, NY, USA. https://doi.org/10.1007/978-1-0716-0334-5_47

Çakalli A., Çiçi I., Kulla E., Myrta A., 2007. Status of Prunus germplasm in Albania. In: *Report of the 6th and 7th Meeting of ECPGR Working Group on Prunus*, 29–31.

Cambra M., Asensio M., Gorris M.T., Perez E., Camarasa E., García J.A., … Sanz A., 1994. Detection of plum pox potyvirus using monoclonal antibodies to structural and non-structural proteins. *EPPO Bulletin* 24: 569–577.

Cambra M., Vidal E., 2016. Sharka, a vector-borne disease caused by the plum pox virus: Vector species, transmission mechanism, epidemiology and mitigation strategies to reduce its natural spread. In: *III International Symposium on Plum Pox Virus* 1163, 57–68.

Cambra M., Madariaga M., Varveri C., Çağlayan K., Morca A.F., … Glasa, M., 2024. Estimated costs of plum pox virus and management of Sharka, the disease it causes. *Phytopathologia Mediterranea* 63: 343–365.

Clark M.F., Adams A.N., 1977. Characteristics of the microplate method of enzyme-linked immunosorbent assay for the detection of plant viruses. *Journal of General Virology* 34(3):475-483. https://doi.org/10.1099/0022-1317-34-3-475

Clemente-Moreno M. J., Hernández J. A., Diaz-Vivancos P., 2015. Sharka: how do plants respond to *Plum pox virus* infection? *Journal of Experimental Botany* 66: 25–35.

Dessoky E. S., Ismail A., El-Sharnouby M. 2018. Production of virus-free peach (*Prunus persica* L. Batsch) plants cv. Balady grown in Taif by meristem culture and thermotherapy. *Bioscience Research* 15(1): 124–132.

Diaz-Lara A., Stevens K., Klaassen V., Golino D., Al Rwahnih M., 2020. Comprehensive real-time RT-PCR assays for the detection of fifteen viruses infecting *Prunus* spp. *Plants* 9: 273. https://doi.org/10.3390/plants9020273

Dumont B., Rondia A., Delpierre L., Dupont P., Donis T., Ferrier V., … Lateur M., 2025. Safeguarding, evaluating and valorizing fruit tree genetic resources in Belgium: insights from nearly half a century of unsprayed orchard management. *Genetic Resources* (S2), 185–202. https://www.doi.org/10.46265/genresj.JWFV3378

EPPO, 2025. *Potyvirus plumpox*. EPPO datasheets on pests recommended for regulation. https://gd.eppo.int (accessed 2025-11-29)

Foissac X., Svanella-Dumas L., Gentit P., Dulucq M.J., Candresse T., 2001. Polyvalent detection of fruit tree Tricho, Capillo and Foveavirus by nested RT-PCR using degenerated and inosine containing primers (DOP RT-PCR). *Acta Horticulturae* 550: 37–43.

García J. A., Glasa M., Cambra M., Candresse T., 2014. Plum pox virus and Sharka: a model potyvirus and a major disease. *Molecular Plant Pathology* 15(3): 226–241. https://doi.org/10.1111/mpp.12083

García J. A., Rodamilans B., Martínez-Turiño S., Valli A. A., Simón-Mateo C., Cambra M., 2025. Plum pox virus: An overview of the potyvirus behind Sharka, a harmful stone fruit disease. *Annals of Applied Biology* 186(1): 49–75. https://doi.org/10.1111/aab.12958

Gong H., Igiraneza C., Dusengemungu L., 2019. Major In Vitro Techniques for Potato Virus Elimination and Post Eradication Detection Methods. A Review. *American Journal of Potato Research* 96: 379–389. https://doi.org/10.1007/s12230-019-09720-z

ISTAT, 2024. Plum production statistics. Institute of Statistics. https://databaza.instat.gov.al:8083/pxweb/sq/DST/START__BU__AFT/BU20/ table/tableViewLayout1/

Jarošová J., Kundu J.K., 2010. Detection of prune dwarf virus by one-step RT-PCR and its quantitation by real-time PCR. *Journal of Virological Methods* 164(1–2): 139–144. https://doi.org/10.1016/j.jviromet.2009.11.032

Kabylbekova B., Nurseitova T., Yussupova Z., Turdiyev T., Kovalchuk I., … Madenova A., 2025. Application of in vitro techniques for elimination of Plum Pox Virus (PPV) and Apple Chlorotic Leaf Spot Virus (ACLSV) in stone fruits. *Horticulturae* 11(6): 633. https://doi.org/10.3390/horticulturae11060633

Kanapiya A., Amanbayeva U., Tulegenova Z., Abash A., Zhangazin S., Dyussembayev K., Mukiyanova G., 2024. Recent advances and challenges in plant viral diagnostics. *Frontiers in Plant Science* 15: 1451790. https://doi.org/10.3389/fpls.2024.1451790

Kang C.M., Kim M.J., Hong J.S., Jeong R.D., 2025. Managing plant viruses in tissue-cultured apple and grapevine: strategies for detection and eradication. *Plant Pathology Journal* 41(5): 545–565. https://doi.org/10.5423/PPJ.RW.07.2025.0092

Kokaj T., 2025. Morphological characterization of characters of some plum cultivars in Albania country. *Journal of Biotechnology and Bioprocessing 6*(2): 2766–2314.

Labonne G., Yvon M., Quiot J. B., Avinent L., Llácer G., 1999. Aphids as vectors of Plum pox virus. *Acta Horticulturae* 472: 403–412.

Llácer G., Cambra M., 2006. Hosts and symptoms of Plum pox virus: fruiting *Prunus* species. *EPPO Bulletin* 36(2): 219–221.

Manganaris G.A., Economou A.S., Boubourakas I., Katis N., 2003. Production of virus-free plant propagation material from infected nectarine trees. *Acta Horticolturae* 616: 501–505. https://doi.org/10.17660/ActaHortic.2003.616.79

Menzel W., Jelkmann W., Maiss E., 2002. Detection of four apple viruses by multiplex RT-PCR assays with coamplification of plant mRNA as internal control. *Journal of Virological Methods* 99(1–2): 81–92. https://doi.org/10.1016/S0166-0934(01)00381-0

Mochizuki T., Ohki S.T., 2015. Detection of plant virus in meristem by immunohistochemistry and *in situ* hybridization. In: *Plant Virology Protocols* (Uyeda, I., Masuta, C., ed). Methods in Molecular Biology, vol 1236. *Humana Press*, New York, NY, USA. https://doi.org/10.1007/978-1-4939-1743-3_20

Mori K., Hosokawa D., 1977. Localization of viruses in apical meristem and production of virus-free plants by means of meristem and tissue culture. *Acta Horticolturae* 78: 389–396. https://doi.org/10.17660/ActaHortic.1977.78.49

MSU Extension, 2020**.** How insects survive cold: the potential effect of a mild winter. Michigan State University Extension. https://www.canr.msu.edu/news/how_insects_survive_cold_the_potential_effect_of_a_mild_winter

Murashige T., Skoog F., 1962. A revised medium for rapid growth and bio assays with tobacco tissue cultures. *Physiologia Plantarum* 15(3): 473–497. https://doi.org/10.1111/j.1399-3054.1962.tb08052.x

Musa A., Merkuri J., Milano R., Djelouah K., 2010. Investigation on the phytosanitary status of the main stone fruit nurseries and mother plots in Albania. *Julius-Kühn-Archive* 427: 304.

Myrta A., Di Terlizzi B., Digiaro M., 1995. A preliminary account of the sanitary status of stone fruit trees in Albania. *Acta Horticolturae* 386: 165–168. https://doi.org/10.17660/ActaHortic.1995.386.20

Myrta A., Di Terlizzi B., Boscia D., Çaglayan K., Gavriel I., ….Savino V., 1998. Detection and serotyping of Mediterranean plum pox virus isolate by means of strain specific monoclonal antibodies. *Acta Virologica* 42(4): 251–253.

Myrta A., Di Terlizzi B., Savino V., Martelli G.P., 2003. Virus diseases affecting the Mediterranean stone fruit industry: a decade of surveys. In: Myrta A., Di Terlizzi B., Savino V. (ed.). *Virus and virus-like Diseases of Stone Fruits, with Particular Reference to the Mediterranean Region*. Bari, Italy, CIHEAM, 2003. p. 15-23 (Options Méditerranéennes: Série B. Etudes et Recherches; n. 45)

Naddaf M. E., Rabiei G., Ganji Moghadam E., Mohammadkhani A., 2021. *In vitro* production of PPV-free sweet cherry (*Prunus avium* cv. Siahe-Mashhad) by meristem culture and micro-grafting. *Journal of Agricultural Sciences and Engineering* 3(1): 51–59. https://doi.org/10.22034/jpbb.2021.282382.1005

Nickel O., Fajardo T.V.M., 2014. Detection of viruses in apples and pears by real time RT-PCR using 5'-hydrolysis probes. *Journal of Plant Pathology* 96(1): 207–213.

Olmos A., Bertolini E., Gil M., Cambra M., 2005. Real-time assay for quantitative detection of non-persistently transmitted Plum pox virus RNA targets in single aphids. *Journal of Virological Methods* 128(1–2): 151–155. https://doi.org/10.1016/j.jviromet.2005.05.011

Palmisano F., Minafra A., Myrta A., Boscia D., 2015. First report of Plum pox virus strain PPV-T in Albania. *Journal of Plant Pathology* 97(2).

Palmisano F., Kawakubo S., Chiumenti M., Leonetti P., Pantaleo V., Candresse T., Minafra A., 2025. Bayesian phylogenetic and recombination analyses of plum pox virus provide a refined vision of its evolutionary history. *Virology Journal* 22: 319. https://doi.org/10.1186/s12985-025-02892-7

Pedrelli A., Panattoni A. Cotrozzi L., 2024. The Sharka disease on stone fruits in Italy: a review, with a focus

on Tuscany. *European Journal of Plant Pathology* 169: 287–300. https://doi.org/10.1007/s10658-024-02827-y

Pérez-Caselles C., Burgos L., Yelo E., Faize L., Alburquerque N., 2025. Production of HSVd- and PPV-free apricot cultivars by *in vitro* thermotherapy followed by meristem culture. *Plant Methods* 21, 23 https://doi.org/10.1186/s13007-025-01344-1

Priyanka V., 2021. Germplasm conservation: instrumental in agricultural sustainability. *Sustainability* 13(12): 6743. https://doi.org/10.3390/su13126743MDPI

Rimbaud L., Dallot S., Gottwald T., Decroocq V., Jacquot E., Soubeyrand S., Thébaud G., 2015. Sharka epidemiology and worldwide management strategies: learning lessons to optimize disease control in perennial plants. *Annual Review of Phytopathology* 53: 357–378. https://doi.org/10.1146/annurev-phyto-080614-120140

Rosner A., Maslenin L., Spiegel S., 1997. The use of short and long PCR products for improved detection of prunus necrotic ringspot virus in woody plants. *Journal of Virological Methods* 67(2): 135–141. https://doi.org/10.1016/s0166-0934(97)00088-8

Rubio M., Martínez-Gómez P., Marais A., Sánchez-Navarro J.A., Pallás V., Candresse T., 2017. Recent advances and prospects in *Prunus* virology. *Annals of Applied Biology* 171(2): 125–138

Schneider W. L., Sherman D. J., Stone A., Damsteegt V., Frederick R., 2004. Specific detection and quantification of Plum pox virus by real-time fluorescent reverse transcription-PCR, *Journal of Virological Methods* 120(1): 97–105. ISSN 0166-0934, https://doi.org/10.1016/j.jviromet.2004.04.010

Sihelská N., Glasa M., Šubr Z.W., 2017. Host preference of the major strains of Plum pox virus—Opinions based on regional and world-wide sequence data. *Journal of Integrative Agriculture* 16(3): 510–515.

Singh A., 2025. The science behind virus elimination using meristem culture. *Plant Cell Technology*. https://plantcelltechnology.com/blogs/blog/the-science-behind-virus-elimination-using-meristem-culture?srsltid=AfmBOopiMPoGo5BEroboLgH-Q6DskASU-U3YLqV3LrWF2gDy3FzzDn7XF

Stamo B., Myrta A., Boscia D., 2003. Serotyping of Albanian Plum pox virus isolates. *Options Méditerranéennes, Série B. Etudes et Recherches* 45.

Szabó L.K., Desiderio F., Kirilla Z., Hegedűs K., Várallyay E., Preininger E., 2024. A mini-review on in vitro methods for virus elimination from *Prunus* sp. fruit trees. *Plant Cell, Tissue and Organ Culture* 156, 42. https://doi.org/10.1007/s11240-023-02670-9

Valasevich N, Cieślińska M, Kolbanova E., 2015. Molecular characterization of Apple mosaic virus isolates from apple and rose. *European Journal of Plant Pathology* 141: 839–945.

Vivek M., Modgil M., 2018. Elimination of viruses through thermotherapy and meristem culture in apple cultivar 'Oregon Spur-II'. *Virus Disease* 29, 75–82. https://doi.org/10.1007/s13337-018-0437-5

Wetzel T., Candresse T., Macquaire G., Ravelonandro M., Dunez J., 1992. A highly sensitive immunocapture polymerase chain reaction method for plum pox potyvirus detection. *Journal of Virological Methods* 39: 27–37.

Wolella E.K., 2017. Surface sterilization and in vitro propagation of *Prunus domestica* L. cv. Stanley using axillary buds as explants. *Journal of Biotechnology Research* 8: 18–26. https://www.btsjournals.com/assets/2017v8p18-26.pdf

Yuan H.Y., Wu Y.X., Liao K., Gen W.J., Li J., ... Wang T., 2009. *In vitro* propagation of wild European plum (*Prunus ×domestica* L.), a rare and endangered species. *Acta Horticolturae* 839: 99–104. https://doi.org/10.17660/ActaHortic.2009.839.10

Zarghami R., Ahmadi B., 2023. Production of plum pox virus-free and *Prunus* necrotic ringspot virus-free regenerants using thermotherapy and meristem-tip culture in *Prunus persica* L. *Erwerbs-Obstbau* 65: 719–727. https://doi.org/10.1007/s10341-022-00731-5

Phytopathologia Mediterranea
The international journal of the
Mediterranean Phytopathological Union

Firenze University Press
www.fupress.com/pm

Research Papers

Occurrence of *Cylindrocarpon*-like anamorphs causing black root rot of strawberry plants in Türkiye

Havva DINLER[1], Ayhan YILDIZ[2], Seher BENLIOGLU[2], umit OZYILMAZ[2], Kemal BENLIOGLU[2,*]

[1] *Department of Plant Protection, Faculty of Agriculture, Usak University, 64200 Usak, Türkiye*
[2] *Department of Plant Protection, Faculty of Agriculture, Adnan Menderes University, 09100 Aydın, Türkiye*
*Corresponding author. E-mail: kbenlioglu@adu.edu.tr

Summary. This study aimed to identify the species of *Cylindrocarpon*-like anamorphs associated with black root rot of strawberry seedlings and field-grown plants in Aydin province, Türkiye. Samples of strawberry seedlings before planting and diseased plants after planting were collected from 41 strawberry fields during two production seasons (2009-2010 and 2010-2011) in Sultanhisar of Aydın. Incidence of pathogenic *Cylindrocarpon* spp. in seedlings was 0.11-0.54%, and fungal pathogens were isolated from 15.8% of diseased plants in 2009/2010 and were -4.6% in 2010/2011. Seven *Cylindrocarpon*-like pathogenic isolates recovered from seedling roots and 17 from diseased plants were further identified as *Dactylonectria novozelandica* (DN; 12 isolates), *Dactylonectria torresensis* (DT; nine), *Dactylonectria macrodidyma* (DM; one), and *Ilyonectria europaea* (IE; two isolates), using multilocus sequence analysis (MLSA) with sequencing of *tef1*, *tub2*, and *his3* partial genes. Cultural and morphological characteristics were determined for representative isolates of four species. Pathogenicity tests indicated that the most aggressive species could cause necrosis on detached strawberry stolons, and severity of plant decline in pots experiments was greatest from DT, less from DN and IE, and least from DM. This is the first report of *D. novozelandica, D. torresensis*, *D. macrodidyma* in Türkiye, and *I. europaea* in the world, as causes of black root rot in strawberry.

Keywords. *Dactylonectria novozelandica, D. torresensis, D. macrodidyma, Ilyonectria europaea.*

OPEN ACCESS

Citation: Dinler, H., Yildiz, A., Benlioglu, S., Ozyilmaz, U., & Benlioglu, K. (2026). Occurrence of *Cylindrocarpon*-like anamorphs causing black root rot of strawberry plants in Türkiye. *Phytopathologia Mediterranea* 65(1): 107-119. doi: 10.36253/phyto-16843

Accepted: February 24, 2026

Published: May 14, 2026

© 2026 Author(s). This is an open access, peer-reviewed article published by Firenze University Press (https://www.fupress.com) and distributed, except where otherwise noted, under the terms of the CC BY 4.0 License for content and CC0 1.0 Universal for metadata.

Data Availability Statement: All relevant data are within the paper and its Supporting Information files.

Competing Interests: The Author(s) declare(s) no conflict of interest.

Editor: Samia Gargouri, National Institute of Agricultural Research of Tunisia (INRAT), University of Carthage, Tunisia.

ORCID:
HD: 0000-0002-7011-5183
AY: 0000-0001-9443-2362
SB: 0000-0002-8437-0273
UO: 0000-0003-2314-9118
KB: 0000-0001-5338-4659

INTRODUCTION

Strawberry (*Fragaria* × *ananassa* Duchesne) is an important high-value fruit crop, grown in Türkiye for domestic consumption and export. Türkiye ranks 4th after China and the United States of America (USA), with 677 tons of strawberry production, and 5th with 222 ha of strawberry crops (FAO 2025). Aydin province is the second-leading strawberry producer in Türkiye,

producing 106 tons from 2,655 ha of under-cover (Anonymous, 2025).

The first studies investigating the effects of soil solarization and fumigants on the control of soilborne diseases of strawberries in this region indicated that *Rhizoctonia solani* and *Phytophthora cactorum* were the major plant pathogens affecting strawberries (Benlioglu *et al*., 2004; 2005). However, in recent years an apparent increase was observed in the occurrence and prevalence of disease caused by heat-tolerant fungal pathogens such as *Macrophomina phaseolina* (Marquez *et al*., 2021) and *Fusarium* spp., and in the strawberry-growing areas of Aydın, possibly due to the widespread application of soil solarization and global warming (Benlioglu *et al*., 2014). As a newly identified heat-tolerant pathogen, *Lasiodiplodia theobromae* has been reported to cause dieback on strawberry plants (Yildiz *et al*., 2014).

More recent disease surveys discovering major fungal pathogens associated with seedlings showed that *M. phaseolina* and *Fusarium* spp. were commonly isolated from crowns of dead or dying plants in strawberry-growing areas of Aydin province. Additionally, *F. oxysporum* f. sp. *fragariae* (Dinler *et al*., 2016) and *R. fragariae* (Dinler *et al*., 2018) have been recently considered as severe fungal threats to strawberry fruit yields and to transplant production in Türkiye.

Black root rot is an internationally important disease that limits strawberry yields, and is a disease complex caused by different biotic and abiotic factors interacting to darken and stunt host roots. Black root rot occurrence is caused by fungus and fungus-like pathogens including *R. fragariae,* and *Cylindrocarpon, Pythium*, and *Fusarium* spp. (Maas, 1998). A survey carried out in an intensively cultivated area of northern Italy identified *Rhizoctonia* spp. as the primary root pathogen together with several typical weak pathogens of well-known black root rot complex pathogens, including *Cylindrocarpon destructans, F. oxysporum, F. solani, Pestalotia longiseta* and others (Manici *et al*., 2005). A report from Western Australia indicated that strawberry production was severely compromised by crown and root diseases caused mainly by *F. oxysporum* and, secondarily, by *Rhizoctonia* spp., and *C. destructans* (Fang *et al*., 2011a).

In 2012, outbreaks of a destructive root disease caused by *Cylindrocarpon* sp. were observed in strawberries ('Chandler') in North Carolina, USA (Adhikari *et al*., 2013). In a 2007 to 2014 survey of black root rot of strawberries in Northern Germany, fungi with and without *Cylindrocarpon*-like anamorphs were isolated as potential pathogens. *Dactylonectria torresensis* (DT) was the most common species causing the disease, and was isolated from 18% of strawberry roots obtained from nursery plants and 37% of roots from production fields. This fungus, as well as *Ilyonectria crassa*, *Ilyonectria* sp, and *C. obtusisporium*, were found to cause typical root rot symptoms in inoculation experiments in the absence of any other predisposing factor (Weber and Entrop, 2017). Later, the first reports from Kyrgyzstan described black root rot of strawberries caused by *D. novozelandica* (Erper *et al*., 2020), and diseased greenhouse-grown strawberries in Iran were caused by *D. macrodidyma* (Habibi and Ghaderi, 2020). In China, *D. torresensis*, *D. novozelandica,* and *D. pauciseptata* caused black root rot in strawberry seedlings in different districts of Beijing (Chen *et al*., 2021), and *D. alcacerensis* caused root rot in strawberries at the same sites (Qian *et al*., 2022). Based on research between 2007 and 2014 at the fruit-growing centre Jork (Esteburg, Germany), fungi with *Cylindrocarpon*-like anamorphs, i.e., *D. torresensis* and *Ilyonectria* spp., were associated with black root rot of strawberries (Löhrer *et al*., 2022), and *D. novozelandica* was identified as the causal agent of crown and root necrosis of strawberries in Salto, Uruguay (Viglieca *et al*., 2022).

The present study was conducted to identify and assess species of *Cylindrocarpon*-like anamorphs associated with black root rot of strawberry seedlings and field-grown plants in the Aydin province of Türkiye.

MATERIALS AND METHODS

Sample collection and fungus isolation

Pre- and post-planting diseased strawberry seedlings were collected from strawberry fields of 19 growers in the 2009-2010 production season and 22 growers in the 2010-2011 production season. Seedling samples were collected in each season between 20 July and 20 August before planting, with three seedlings collected per 1,000 m^2. In each of the 41 fields, plant samples showing different amounts of decline from previously determined main plots (each consisting of ten plants per 1,000 m^2 in each sampled field) were collected during each growing period.

Sampled plants were carefully washed under running tap water to remove soil. Roots with signs of infected tissues and a crown cross-sections with discolourations were selected for further analyses. Five small pieces of the necrotic crown or root tissues per plant were then excised and subjected to surface sterilization using for one 30 s rinses in 1% sodium hypochlorite solution, followed by a 2 min rinse in sterile distilled water. The surface disinfected tissues were then plated onto 2% Potato Dextrose Agar (PDA) amended with 100 ppm streptomycin sulfate, and were then incubated at 24°C. Fungal

isolates were subcultured onto fresh PDA medium, and single-conidium isolates were obtained and were stored in filter paper at -20°C. All fungal isolates were initially identified at genus and/or species level based on visual inspections of colonies and microscopic examination of conidiophore, conidium, and hypha characteristics (Barnett and Hunter, 1998).

Molecular identification of isolates

Genomic DNA extractions from pure cultures were carried out following the method of Cenis (1992). Mycelium mats from 72 h potato dextrose broth cultures were each crushed for 1 min in 300 µL of extraction buffer, using a conical microtube pestle (Axygen®) attached to a flexible silicone tube connected to an homogenizer (IKA, Ultra Turrax®) set at 3000 rpm for 1 min. After incubation at 65°C for 10 min, 150 µL of 3 M sodium acetate (pH 5.2) was added to each tube, and the tubes were placed at -20°C for approx. 10 min. The tubes were then centrifuged (13,000 rpm for 10 min at room temperature) in a microcentrifuge, and the supernatant from each tube was transferred to another tube. DNA pellets were obtained following isopropanol precipitation and ethanol wash and were each resuspended in 50 µL of TE buffer (10 mM Tris-Cl, one mM EDTA, pH 8.0). The concentration and purity of the total genomic DNA were determined using a Picodrop® spectrophotometer, and the DNA solutions were stored at -20°C.

A conventional PCR assay was performed for each isolate sample to amplify part of the β-tubulin (*tub*), histone H3 (*his*), and translation elongation factor 1-α (*tef*) genes using a thermal cycler (BIO-RAD C1000 Touch™). Each amplification was carried out in a final volume of 40 µL, including Thermo Scientific™ DreamTaq Green PCR Master Mix, gene-specific primer pairs, and nuclease-free water. The primers were T1 (O'Donnell and Cigelnik, 1997) and Bt2b (Glass and Donaldson, 1995) for the *tub2* gene, CYLH3F/CYLH3R (Crous *et al*., 2004) for the *his3* gene, and EF1-728F/EF1-986R (Carbone and Kohn, 1999) for the *tef1*-alpha gene. The annealing temperatures for primer pairs was 58°C for T1/Bt2b and CH3F/CYPH3R and 54°C for EF1-728F/EF1-986R. The resulting amplicons were visualized under UV light on 1.5% TBE agarose gels at 45 V for 30 min, that were stained with GelRed (Biotium), and were photographed. PCR fragments were commercially sequenced by Macrogen Inc., Seoul, Korea. All sequences were firstly assembled and screened by length and quality of reads using Sequence Scanner v. 2.0 (Applied Biosystems), and were edited to resolve ambiguities. The resulting sequences were searched in the GenBank database using the Basic Local Alignment Search Tool (BLAST) to confirm isolate identities and establish their phylogenetic relationships. All sequences were submitted to GenBank (http://www.ncbi.nlm.nih.gov), and their obtained accession numbers are listed in Table 1.

Phylogenetic analyses

Homologous sequences with high sequence identities from type and non-type strains or species (Table 1) were obtained from the GenBank database to compile datasets for phylogenetic analyses. Multiple sequence alignments were performed in MEGA X (Kumar *et al*., 2018), and were manually adjusted where necessary. A multi-locus phylogenetic analysis consisting of concatenated partial sequences of *tef1*, *tub2*, and *his3* datasets was carried out using MEGA X software by the Muscle algorithm and neighbor-joining method, with 1000 bootstrap replications.

Cultural and morphological characteristics of isolated fungi

Pure cultures from representative fungal isolates of each molecularly identified species were selected to determine their colony colours, growth rates, presence of chlamydospores, and conidium types. Each representative isolate was subcultured onto PDA in triplicate and incubated at 24°C. After 7 d incubation, the radial colony growth of each isolate was measured from the underside of each culture plate and along two perpendicular colony axes. Assessments of colony colour and morphology were made on day 7. Microscope observations of conidiophores, microconidia, and one- to five-septate macroconidia of each of the triplicate subcultures were carried out using a Leica model DM/LS equipped with a DFC320 camera. Morphological, cultural, and conidium characteristics of pathogenic *Cylindrocarpon*-like species were evaluated, as described by Cabral *et al*. (2012a; 2012b), Halleen *et al*. (2004), and Lawrence *et al*. (2019).

Pathogenicity assessments

Detached stolon assays

All fungal isolates obtained in pure cultures were tested for pathogenicity on detached strawberry stolons using the method described by Yildiz and Benlioglu (2014). Strawberry stolons growing without contact to soli were collected from healthy strawberry plants 'Festival' cultivated on black plastic mulch in commercial strawberry fields in Sultanhisar, Aydın Province, during

Table 1. Fungal isolates used in this study, and their respective hosts, country locations, and GenBank accession numbers.

Species	Isolate[a]	Host	Country	*tub*	*his3*	*tef1*
Dactylonectria novozelandica	BCME1 [c]	Strawberry	Türkiye	PP216866	PP216890	PP195614
D. novozelandica	BCIG5 [d]	Strawberry	Türkiye	PP216867	PP216891	PP195615
D. novozelandica	BCNC3 [c]	Strawberry	Türkiye	PP216868	PP216892	PP195616
D. novozelandica	BCNC4 [d]	Strawberry	Türkiye	PP216869	PP216893	PP195617
D. novozelandica	FC19K [d]	Strawberry	Türkiye	PP216870	PP216894	PP195618
D. novozelandica	BFMD2 [d]	Strawberry	Türkiye	PP216871	PP216895	PP195619
D. novozelandica	BSHE5[c]	Strawberry	Türkiye	PP216872	PP216896	PP195620
D. novozelandica	BCIG4 [d]	Strawberry	Türkiye	PP216873	PP216897	PP195621
D. novozelandica	BFNO2 [d]	Strawberry	Türkiye	PP216874	PP216898	PP195622
D. novozelandica	BCOY1 [d]	Strawberry	Türkiye	PP216875	PP216899	PP195623
D. novozelandica	BCOY2 [d]	Strawberry	Türkiye	PP216876	PP216900	PP195624
D. novozelandica	FC21K [d]	Strawberry	Türkiye	PP216877	PP216901	PP195625
D. novozelandica	**CBS 113552**	*Vitis vinifera*	New Zealand	AY677237	JF735633	JF735822
D. novozelandica	Cy115	*Vitis vinifera*	USA	JF735460	JF735634	JF735823
D. novozelandica	Cy116	*Vitis vinifera*	USA	JF735461	JF735635	JF735824
D. novozelandica	JZB3310032	*Vitis vinifera*	China	OQ1296653	OQ123935	OQ122033
Dactylonectria torresensis	FS3K [d]	Strawberry	Türkiye	PP216878	PP216902	PP195626
D. torresensis	BC52K [d]	Strawberry	Türkiye	PP216879	PP216903	PP195627
D. torresensis	FC55K [d]	Strawberry	Türkiye	PP216880	PP216904	PP195628
D. torresensis	BCIG3 [c]	Strawberry	Türkiye	PP216881	PP216905	PP195629
D. torresensis	BSHE2 [d]	Strawberry	Türkiye	PP216882	PP216906	PP195630
D. torresensis	FC27K [d]	Strawberry	Türkiye	PP216883	PP216907	PP195631
D. torresensis	BCME2 [c]	Strawberry	Türkiye	PP216884	PP216908	PP195632
D. torresensis	BC33K [d]	Strawberry	Türkiye	PP216885	PP216909	PP195633
D. torresensis	BC37K [d]	Strawberry	Türkiye	PP216886	PP216910	PP195634
D. torresensis	**CBS 129086**	*Vitis vinifera*	Portugal	JF735492	JF735681	JF735870
D. torresensis	CBS 119.41	Strawberry	Netherlands	JF735478	JF735657	JF735846
D. torresensis	Cyl102	Apple (M9)	Italy	KP823885	KP823894	KP823874
Ilyonectria europaea	FC5K [d]	Strawberry	Türkiye	PP216887	PP216911	PP195635
I. europaea	FF16K [d]	Strawberry	Türkiye	PP216888	PP216912	PP195636
I. europaea	**CBS129078**	*Vitis vinifera*	Portugal	JF735421	JF735567	JF735756
I. europaea	Cy155	*Vitis vinifera*	Portugal	JF735420	JF735566	JF735755
D. macrodidyma	BCIG2 [c]	Strawberry	Türkiye	PP216889	PP216913	PP195637
D. macrodidyma	**CBS 112615**	*Vitis vinifera*	South Africa	AY677233	JF735647	JF735836
D. alcacerensis	Cy133	*Vitis vinifera*	Spain	JF735459	JF735628	JF735817
D. vitis	**CBS 129082**	*Vitis vinifera*	Portugal	JF735431	JF735580	JF735769
I. radicicola	**CBS 264.65**	*Vitis vinifera*	Netherlands	AY677256	JF735506	JF735695
I. robusta	**CBS 308.35**	Ginseng	Canada	JF735377	JF735518	JF735707
Campylocarpon fasciculare	**CBS 112613**	*Vitis vinifera*	South Africa	AY677221	JF735502	JF735691
Campylocarpon pseudofasciculare	**CBS112679**	*Vitis vinifera*	South Africa	AY772214	JF735503	JF735692

[a] Isolates in bold font are ex-type specimens, red symbolizes the isolates in this study, where first letter B indicates an isolate from a plant, F from a seedling, [d] from roots, or [c] from a plant crown.

the active plant growing period (November to December and March to June). Aseptically air-dried stolon pieces approx. 8 to 8.5 cm long and 3 to 4 mm thick were disinfected in 70% ethanol for 5 min and then rinsed in sterile distilled water. Wounded stolons on damp filter paper in Petri dishes (two stolons per dish) were then inoculated with a mycelium disk (4 mm diam,) taken from the edge of actively grown 7-d-old fungal cultures. The dishes were then incubated at 24±2°C under 16 h/8 h light/dark cycle. Control stolons were inoculated with agar disks. Isolate induced light or dark brown necrotic lesions on inoculated detached stolons after 7 d incubation were

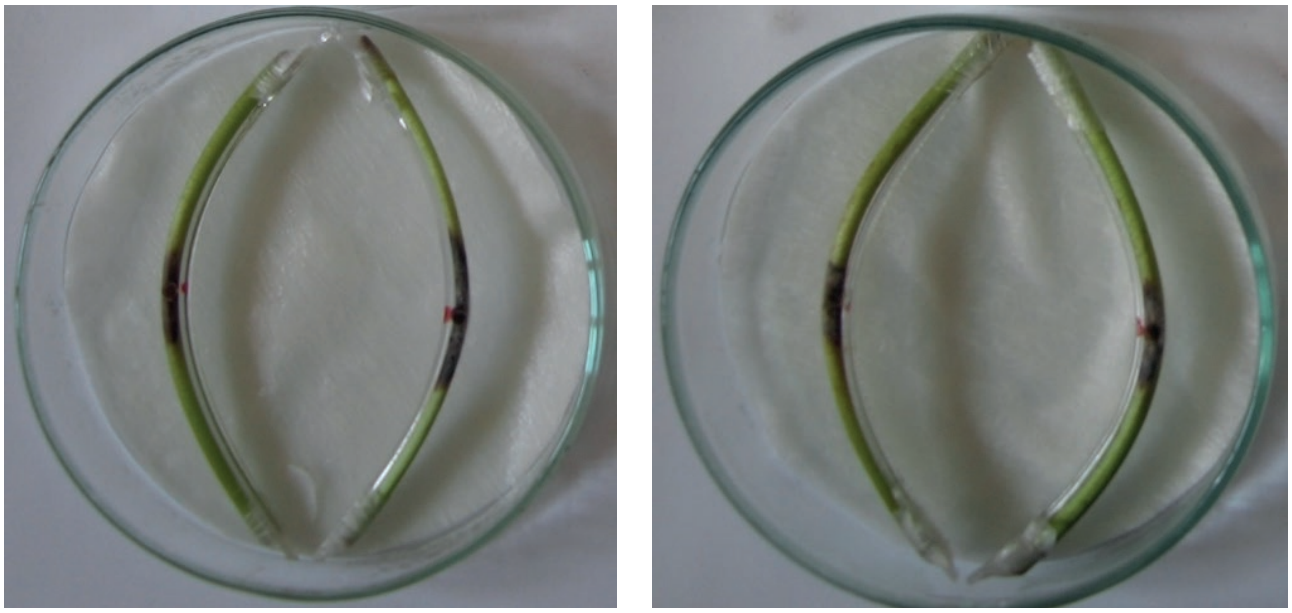

Figure 1. Necrotic lesions on the strawberry stolons 'Festival' inoculated with *Dactylonectria torresensis* isolate FC55K (left) or *Ilyonectria europea* isolate FC5K (right) after 7 d incubation at 24 ±2°C under 16h/8h light/dark conditions.

considered as indicating possible pathogenicity (Figure 1). The lesion lengths on each stolon were measured by using a caliper. The assays were conducted in triplicate for each isolate, and data analysis was performed using JMP®17.2.0 (JMP Statistical Discovery, LLC).

Potted plant assays

All *Cylindrocarpon*-like isolates were subjected to pathogenicity tests on potted seedlings after they had been molecularly identified at the species level. For these assays, healthy plantlets 'Festival' with visible peg roots at the ends of stolons without soil contact, and cultivated in black plastic mulch in commercial strawberry fields, were gathered and brought to the laboratory. The plantlets were then each planted into a 10 cm diam. plastic pot containing sterilized 2/3 sand and 1/3 peat mixture, and were then grown in a climate room at 24±2 °C and 16h/8h light/dark conditions for 6 weeks. Ten days after transplantation, the plants were each fertilized with 10 mL of NPK (18-18-18) solution containing 2 g nutrient mixture per liter for each pot, and this fertilization was repeated at 10 d intervals thereafter.

One month after setting the plants, three plants per fungal isolate were each inoculated by injecting approx. 0.3 mL of the conidium suspension (1.5×10^7 conidia mL^{-1}, based on hemacytometer counts) into the base of crown the tissue, using a 5 mL sterile syringe fitted with a 22-gauge needle (Adhikari *et al*., 2013). Plants injected with sterile distilled water were used as negative inoculation controls. Pots containing the plants were then enclosed in plastic bags for 24 h, and were then maintained in the climate room without bags. After 14 days, appearance of disease symptoms was assessed based on the disease index of Fang *et al*. (2011a), where: 0 = plant well developed, no disease symptoms; 1 = plant slightly stunted; 2 = plant stunted and yellowing; 3 = plant severely stunted and/or wilting; 4 = majority of leaves of the plant wilted or dead; 5 = plant dead. Re-isolations were made from diseased plants, and identities of resulting fungi were confirmed by comparing macroscopic and microscopic features with the original inoculated isolates to determine fulfilment of Koch's postulates.

RESULTS

Sample collection and fungus isolation

A total of 837 seedlings in the 2009-2020 growing season, and 1411 seedlings in 2010-2011, were examined for the presence of fungi. After isolation and pathogenicity tests on detached stolons, the isolation frequencies of *Cylindrocarpon* spp.-induced disease in seedlings was 0.12 in 2009–2020 and 0.64% in 2010–2011. Frequencies of isolations were 15.8% in 2009–2010 and 4.6% in 2010–2011. Seven *Cylindrocarpon*-like isolates were

recovered from seedling roots, and 17 were from diseased plants (Table 1).

Molecular identification of fungi

Conventional PCR amplifications of selected *tub*, *his3*, and *tef1* gene regions gave products of, respectively, approx. 630, 500, and 300 bp. The commercially obtained sequences of three housekeeping genes from 24 isolates were submitted to GenBank under accession numbers (Table 1). Sequence analysis of the *tub* gene separately by BLASTn (NCBI database) search indicated that 12 isolates were closest to *D. novozelandica* (100% identity) except one BCOY2 99.81% at 100% query coverage. The remaining nine isolates belonged to *D. torresensis*, two to *I. europaea*, and one to *D. macrodidyma*, with identities and query coverage of 100%. The BLASTn results from showed that nucleotide sequence comparison for *his3* genes showed that 12 isolates had 100% identity and query coverage as *D. novozelandica*. Similar results were obtained for the remaining isolates, nine belonging to *D. torresensis*, two to *I. europaea*, and one to *D. macrodidyma*, with identities and query coverage of 100% for both criteria. The sequence identities of *tef* genes for 24 isolates belonging to four species was also 100%, and the query coverage ratio was identical for all isolates in the BLASTn analyses.

The combined alignment of partial *tub*, *tef1*, and *his3* sequences was used for phylogenetic analyses for 40 taxa, including reference sequences and outgroups obtained from GenBank. *Campylocarpon fasciculare* and *Campylocarpon pseudofasciculare* were used as an outgroup. The analysis of the three genes enabled identification of four species of 24 isolates in the study. The model for phylogenetic analysis was selected by fitting the Maximum Likelihood of 24 different nucleotide substitution models, and choosing models with the lowest Bayesian Information Criterion (BIC) scores to best describe the substitution pattern.

The phylogenetic tree (Figure 2) was constructed with the Tamura-Nei model, the Neighbor-Joining method, and 1,000 bootstrap steps by the rate variation among sites modelled with a gamma distribution (shape parameter = 1). There were 1,362 positions in the final dataset, and evolutionary analyses were conducted using MEGA X software (Kumar *et al*., 2018). The first clade, with bootstrap values of 99%, consisted DN isolates from the Aydın province, Türkiye, which had almost identical sequences to those of the DN ex-type strain CBS113552 and three others of the same species from *Vitis vinifera* (Figure 2). The second clade, with bootstrap values of 100%, grouped *D. macrodidyma* isolate from Türkiye with *D. macrodidyma* ex-type specimen CBS 112615 from *Vitis vinifera* from South Africa. The third clade, with bootstrap values of 99%, consisted DT isolates from the Aydın province, Türkiye, which had almost identical sequences to those of the *D. torresensis* ex-type strain CBS129086 from *Vitis vinifera* from Portugal, and with isolate CBS119.41 from strawberry from Netherlands and Cyl102 from apple rootstock (M9) from Italy. The fourth clade, with bootstrap values of 99%, formed a monophyletic group with IE ex-type strain CBS129078 and Cy155 from Portugal (Figure 2).

Cultural and morphological characteristics of isolates

Colonies of isolates BC37K and BC52K, identified as *D. torresensis*, grew an average of 31-33 mm diam. After 7 d at 24°C on PDA, with even colony margin expansion. The aerial mycelium was cottony to felty with average to solid density, and colony colour was white to pale buff, with pale buff to amber margin (Figure 3 A). Reverse sides of colonies in were buff to amber in colour (Figure 3 B). Conidiophores were solitary, arising laterally or terminally from aerial mycelium. Macroconidia predominated and were 1-3 septate, hyaline, cylindrical, and straight or slightly curved. Microconidia were hyaline, ellipsoid to ovoid, and rarely one septate. Chlamydospores were thick-walled, globose or semi-globose, sometimes solitary or in chains, were observed in PDA cultures.

Colonies of *D. novozelandica* isolates (FC19K and FC21K) reached 28-32 mm diam. on PDA after 7 d at 24°C, with cottony to felty textures of, and buff to saffron to chestnut colour, and even margins (Figure 3C). The reverse sides of colonies were buff to saffron to chestnut (Figure 3D). Conidiophores were simple or complex, aggregated in small sporodochia, and were irregularly branched. Macroconidia pre-dominated, forming on simple and complex conidiophores, and were generally 1–3 septate, hyaline, and straight and cylindrical. Microconidia were hyaline and ellipsoid to avoid, and chlamydospores were not observed in PDA cultures.

The isolate BCIG2, identified molecularly as *D. macrodidyma*, had profuse felty aerial hyphae with yellowish colony centres, and the reverse sides were pale yellow to amber. After 7 d incubation at 24°C on PDA, colony of this isolate was 30 mm. Conidiophores were simple or complex, and ascending from aerial hyphae. Macroconidia predominated, and were 1–3 septate, straight cylindrical, or sometimes slightly curved. Microconidia were 0-1 septate and hyaline, and no chlamydospore was seen in the PDA cultures. The isolate FC5K, identified molecularly as *I. europeae*, was the most

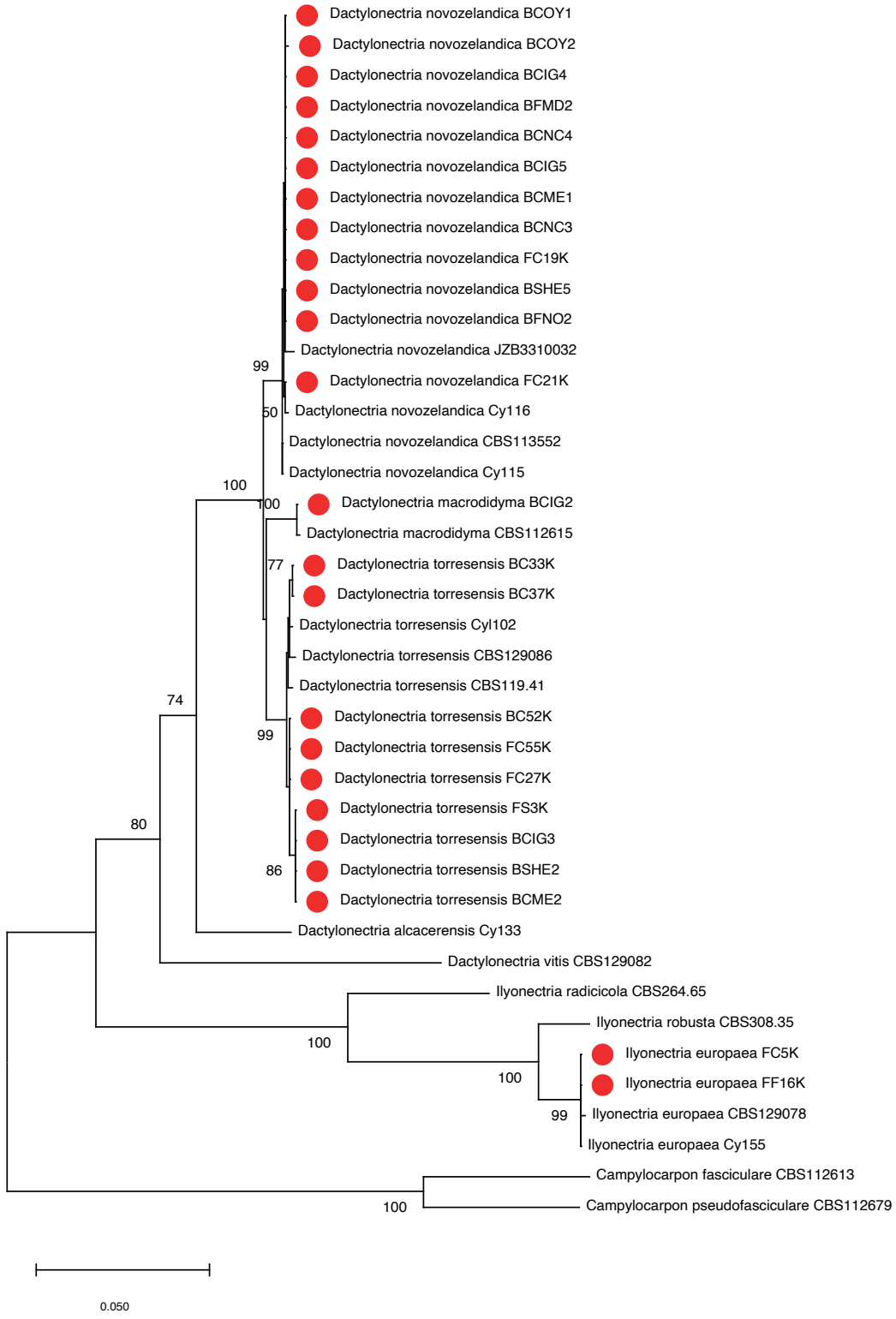

Figure 2. A neighbor-joining tree derived from a Muscle sequence alignment of combined *tub, tef1*, and *his3* sequences for 40 taxa. The percentage (>50%) of replicate value clustered in the associated taxon in the bootstrap test (1,000 replication) is shown next to each tree branch. Evolutionary distances were computed using the Tamura-Nei method and are numbers of base substitutions per site. *Campylocarpon fasciculare* and *Campylocarpon pseudofasciculare* were used as out-groups. Phylogenetic sequence data analyses were carried out using MEGA X (Kumar *et al.*, 2018). Red dots are isolates obtained in the present study, and bold font indicates ex-type isolates.

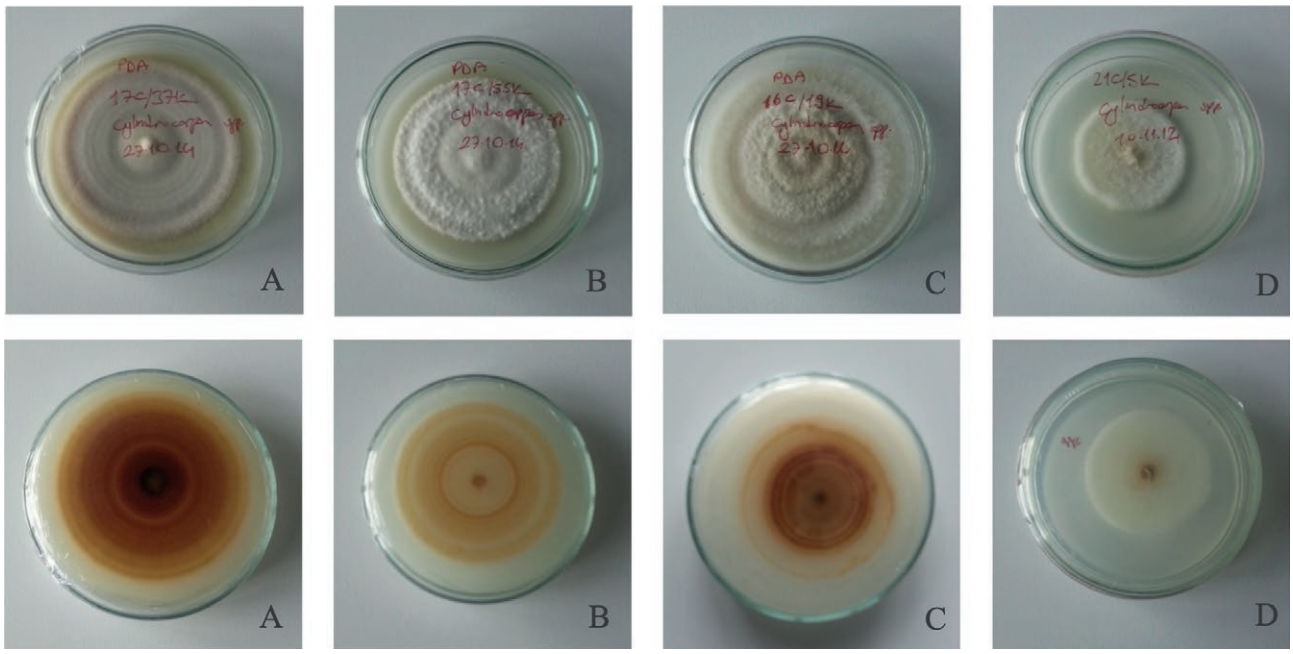

Figure 3. Upper (top row) and reverse side views of the colonies of four isolates grown on PDA at 24°C for 7 d. on the 7th day. A and B, colonies of *Dactylonectria torresensis* isolates BC37K (17C/37K) and FC55K (17C/55K). C, colony of the *Dactylonectria novozelendica* isolate FC19K (16C/19K). D, colony of *Ilyonectria europaea* isolate FC5K (21C/5K.

rapidly growing isolate among those assessed, reaching 46 mm colony diameter after 7 d at 24°C on PDA. The aerial mycelium was felty with average density, and the colonies were white to saffron with chestnut centres and even margins. Colony undersides were also white to saffron with chestnut centres. Conidiophores were solitary, arising laterally or terminally from aerial mycelium. Macroconidia predominated and were 1–3 septate, straight, and microconidia were 0–1 septate, and ellipsoid to ovoid. Few thick-walled, globose or semi-globose chlamydospores were also observed, which were solitary or in chains on PDA.

Pathogenicity tests

The light or dark-brown lesion lengths resulting from inoculations with 24 *Cylindrocarpon*-like isolates on detached 'Festival' stolons averaged between 4.4 and 13.9 mm 7 d after inoculations (Figure 1). The lesions were longer ($P < 0.0009$) than those of the controls treated with 4 mm agar disks. Figure 4 presents the pathogenicity results for all inoculated isolates, based on further lesion length analyses considering isolate molecular identifications at the species level. Nine *D. torresensis* isolates induced the longest lesions among all the stolon-inoculated species. The mean lesion length caused by inoculations with the other three species were 10.4 mm

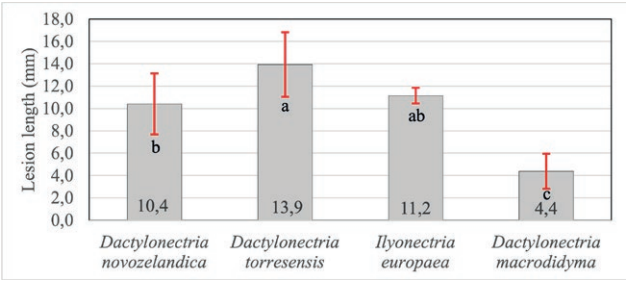

Figure 4. Mean lesion lengths on detached strawberry stolons after 7 d at 24 ±2°C following inoculations with *Dactylonectria* or *Ilyonectria* species isolated from strawberry seedlings and diseased plants. Means for each fungus are for six stolons, and bars indicate standard errors. Data were subjected to analysis of variance (ANOVA), and different letters indicate differences $P < 0.05$), according to the LSD tests.

for *D. novozelandica* (12 isolates), 11.2 mm for *I. europeae* (two isolates), and 4.49 mm for *D. macrodidyma* (one isolate). Control stolons inoculated with agar disks remained asymptomatic.

After 14 d, all the inoculated strawberry plants showed disease symptoms, including leaf necrosis, wilting, and different amounts of stunting, while inoculation control plants remained healthy (Figure 5 A and B). The average disease scores were different ($P < 0,0001$) among *Dactylonectria* and *Ilyonectria* species, varying from 1.8

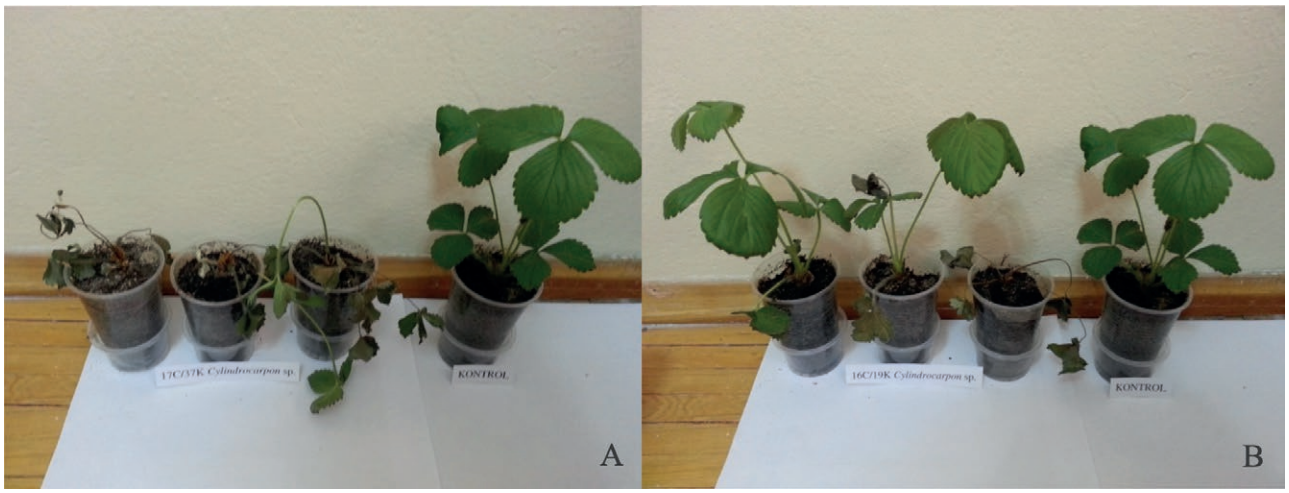

Figure 5. A Three strawberry plants 'Festival'; left) 2 weeks after inoculation with *Dactylonectria torresensis* isolate BC37K (17C/37K), and a non-inoculated control plant (right). B Three plants (left) after inoculation with *D. novozelendica* isolate FC19K (16C/19K), and a non-inoculated control plant (right).

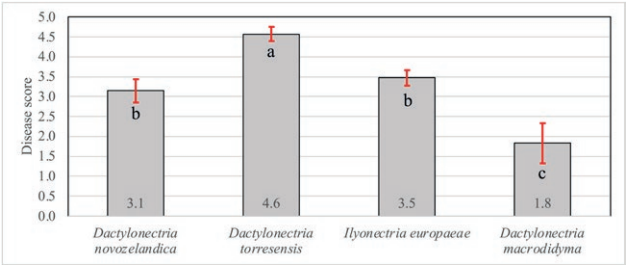

Figure 6. Mean disease scores for potted strawberry plants 2 weeks after inoculations with *Dactylonectria* or *Ilyonectria* spp. and incubation at 24 ±2°C and 16h light/8h dark cycles. Disease score means (0 to 5 scale) are each for three plants per isolate, and error bars indicate standard errors. Data were subjected to analysis of variance (ANOVA), and different letters indicate differences ($P < 0.05$), according to LSD tests.

to 4.6 (Figure 6). Similarly, the *D. torresensis* isolates induced the greatest diseased scores among the other three species assessed, with average severity scores of 3.5 from *I. europeae*, 3.2 from *D. novozelandica*, and 1.8 from *D. macrodidyma* (Figure 5). The re-isolated fungi from the inoculated plants and detached stolons had the same conidiophore and conidium morphologies and colony appearances as those of the inoculated isolates.

DISCUSSION

This is the first study to determine the presence of *Cylindrocarpon*-like anamorphs causing black root rot associated with seedling and field-grown strawberries in Aydın province of Türkiye. These results have shown that incidence of *Cylindrocarpon* spp. ranged between 0.11 to 0.54% in seedlings planted in 41 strawberry fields over two growing seasons. However, incidence of *Cylindrocarpon*-like anamorphs was greater during both vegetation periods in the same fields, and ranged between 4.6 and 15.8%. The incidence of *Cylindrocarpon* spp., either in seedlings or in field-grown plants ranked fourth after *Fusarium* spp., *Rhizoctonia* spp., and *Macrophomina phaseolina*. In most cases, *M. phaseolina* spp. (Benlioglu *et al*., 2014), *F. oxysporum* f. sp. *fragariae* (Dinler *et al*., 2016), and *R. fragariae* (Dinler *et al*.,2018) have been shown to be the most important soil-borne agents that cause decline of strawberries in Aydın province. Some reports of soil-borne fungal pathogens on seedlings or diseased strawberry plants support the present results, that showed *Cylindrocarpon* spp. occurring as typical putative weak or non-lethal pathogens, belonging to the well-known black rot root disease complex (Maas, 1998; Rigotti *et al*., 2003; Manici *et al*., 2005; Fang *et al*., 2011a).

Results from a survey study in Western Australia in 2008 to determine severity of strawberry plant decline/mortality caused by crown and root diseases in commercial strawberry fields during the peak production (August to October) were similar to those from the present study. Fang *et al*. (2011a) reported that *F. oxysporum* was the most frequently isolated pathogen (41.2%) from strawberry crowns, while *Rhizoctonia* spp. (11%) and *Cylindrocarpon destructans* (12%) were the most commonly isolated pathogens from strawberry roots.

Based on sequencing and phylogenetic analyses, four different species (DN, DT, DM, and IE), belonging to

Cylindrocarpon-like anamorphs, were identified as being associated with seven strawberry seedlings and 17 field-grown strawberry plants from different varieties (Table 1 and Figure 2). Taking into consideration that ITS was the least informative to identify the species of *Cylindrocarpon*-like anamorphs, the present study also used multilogues sequence analysis (MLSA) for *tef1*, *tub2*, and *his3* partial genes (Cabral *et al*., 2012a, 2012b). Using multilogues analysis with the same three genes and ITS sequences, Chen *et al*. (2021) obtained 46 *Dactylonectria* isolates from greenhouse strawberry seedlings showing symptoms of black root rot, in different districts of Beijing, China, and identified five representative isolates as three *D. novozelandica*, one *D. torresensis*, and one *D. pauciseptata*. In Germany, *D. torresensis* was found to be the most common species causing the disease, and was isolated from 18% of strawberry roots obtained from nursery plants and 37% of roots from production fields (Weber and Entrop, 2017).

The pathogenicity tests of the present study showed decline/death symptoms, including yellowing of the leaves, different extents of wilting, stunting, and death with internal necrosis of the crown, and blackening of entire roots. The declining and death symptoms were similar to those on plants collected from the field during the vegetation periods of both seasons, in the appearance of longitudinal sections of the crowns and blackened rots. Adhikari *et al*. (2013) obtained the similar results by injecting conidial suspensions of *Cylindrocarpon* sp. into crowns of strawberry plants 'Chandler' in their first report of crown and root rot of strawberry in North Carolina, USA. In a study comparing the virulence of fungal pathogens associated with crown and root diseases of strawberries in Western Australia, Fang *et al*. (2011b) found that *C. destructans* caused variable levels of crown and root necroses after inoculation with this fungus directly into strawberry plants. However, root and crown necrosis were much less when plants were inoculated by mixing millet seed colonized by *C. destructans* mycelia with potting mix plant growth medium. The first report of root and crown rot caused by DN on strawberries in Uruguay by Vigliecca *et al*. (2022) confirmed pathogenicity by dipping plants in conidium suspension, which resulted in root necroses and crown lesions after 137 d.

In the present study obtained three DN isolates, two of DT, and one of DM from necrotic crowns and 18 isolates (nine DN, seven DT, two IE) from blackened rot of seedling and dying strawberry plants (Table 1). Considering field symptoms and previously reports on strawberry regardless of pathogenicity tests on potted plants, symptoms associated with crown disease and root disease are probably independent of the related pathogens (Weber and Entrop, 2017; Löhrer *et al*., 2022). Pathogens associated with crown and root diseases of strawberries have often been isolated either as the sole species present or in combinations with other pathogens in crowns and roots (Fang *et al*., 2011a). However, fungal pathogens in black rot root complex, also called "root nibblers," may cause losses in marketable yields ranging from minimal up to about 80%, compared to plants grown in fumigated plots (Wood, 2001). Further investigations are required of species of *Cylindrocarpon*-like anamorphs, to determine whether they cause root rot, crown rot, or both. Combinations of these fungi with other strawberry root and crown rot pathogens, and their interactions with different strawberry cultivars under predisposing soil and climate conditions should also be investigated.

Pathogenicity tests in the present study showed that *D. torresensis*, the second frequently isolated species, caused extensive necrosis on detached strawberry stolons and severe disease on potted strawberry plants 'Festival' (Figures 4 and 6). In Northern Germany, Weber and Entrop (2017) reported that DT, causing visible symptoms in many batches of nursery plants, was frequently isolated, and could be an important source of field contamination in ongoing black root rot epidemics in strawberry and raspberry production. These results were verified by PCR-based assay and inoculations of strawberry plants (Löhrer *et al*., 2022). *Dactylonectria torresensis* associated with black root rot of strawberries has been reported in Kyrgyzstan (Erper *et al*., 2020) and China (Chen *et al*., 2021; Qian *et al*., 2022). In the present study, *D. novozelandica* was the most frequently isolated species, producing high disease scores (Figures 4 and 6). This fungus has also been reported in China (Chen *et al*., 2021) and recently from Uruguay (Vigliecca *et al*., 2022), as a pathogen causing black root rot in strawberry. In the present study, *D. macrodidyma* isolated from crowns of diseased field-grown strawberry plants was the least virulent pathogen among the four species assessed. Black root rot caused by this species was also reported in the greenhouse-grown strawberry the Kerman province of Iran (Habibi and Ghaderi, 2020). In the present study, plants the inoculated with *D. macrodidyma* showed symptoms identical to those reported in strawberry cultivation greenhouses in Iran.

The present study identified two isolates of *I. europeae* as causes of the black root rot in strawberry. These two isolates were as virulent as *D. novozelandica* in the pathogenicity tests (Figures 4 and 6). *Ilyonectria europeae* was defined by the recent taxonomic revision of *Cylindrocarpon* spp. associated with black foot of vines, and from *Actinidia chinensis* (in France), *Aesculus hippocastanum* (in Belgium), *Phragmites australis* (in Germany),

and *Vitis vinifera* (in Portugal) (Cabral *et al*., 2012a; b). *Dactylonectria macrodidyma* and *I. europeae* have been reported as the main species associated with the black foot complex of grapevines in New Zealand (Probst *et al*., 2019). However, no previous report of strawberry black root rot caused by *Ilyonectria europeae* has been found in the literature.

In conclusion, the present study isolated 24 pathogenic fungi from strawberry seedlings and diseased plants in the field. All available evidence indicates that *Cylindrocarpon*-like anamorphs, particularly *D. torresensis*, *D. novozelandica*, *D. macrodidyma*, and *I. europeae*, are principal causes of strawberry root rot. These pathogens caused typical root rot symptoms in inoculation experiments without any other predisposing factors, and Koch's postulates were fulfilled for all four species. This is the first report of *I. europeae* as a black root rot pathogen of strawberry, and of *D. novozelandica*, *D. torresensis*, *D. macrodidyma* as strawberry pathogens in Türkiye. Soil solarization has been widely used by strawberry growers in Aydin province of Türkiye, because of applicability of used polyethylene sheets covering tunnels (Yildiz *et al*., 2010). Soil solarization is known to reduce strawberry root necrosis and root infection by the primary fungal pathogens, including *Cylindrocarpon* spp. (Pinkerton *et al*., 2002; Benlioglu *et al*., 2004). Certified strawberry transplants are only approx. 24% of the certified seedlings required for total strawberry planting areas in Türkiye. The remaining 76% is transplants from runners made by strawberry growers (Benlioglu *et al*., 2018). Further investigations are required on each of these pathogens, and on appropriate disease control strategies including soil disinfection methods, possible revision of certification schemes, assessment on cultivar susceptibility, and other potential disease management techniques.

ACKNOWLEDGEMENTS

This research was supported by the Scientific Technical Research Council of Türkiye (TUBITAK), "under project No: 110R009. The authors also thank the late Nihat Ozyigit for providing the field and assisting workers during this research project.

LITERATURE CITED

Adhikari T.B., Hodges C.S., Louws F.J., 2013. First report of *Cylindrocarpon* sp. associated with root rot disease of strawberry in North Carolina. *Plant Disease* 97(9): 1251. https://doi.org/10.1094/PDIS-01-13-0116-PDN

Anonymous [Internet],2023. Türkiye İstatistikKurumu Başkanlığı (TUIK), BitkiselÜretimİstatistikleri. http://tuikapp.tuik.gov.tr/bitkiselapp/bitkisel.zul. Accessed October 15, 2025.

Barnett H.I., Hunter B.B., 1998. *Illustrated Genera of Imperfect Fungi*. 4th edn. APS press, St. Paul, MN, USA, 218 pp.

Benlioglu S., Yıldız A., Döken T., 2004. Studies to determine the causal agents of soil-borne fungal diseases of strawberries in Aydın and control them by soil disinfestation. *Journal of Phytopathology* 152: 509–513. https://doi.org/10.1111/j.1439-0434.2004.00888.x

Benlioglu S., Boz Ö., Yildiz A., Kaşkavalci G., and Benlioglu K., 2005. Alternative soil solarization treatments for the control of soil-borne diseases and weeds of strawberry in the Western Anatolia of Turkey. *Journal of Phytopathology* 153: 423–430. https://doi.org/10.1111/j.1439-0434.2005.00995.x

Benlioglu S., Yildiz A., Boz Ö., and Benlioglu K., 2014. Soil disinfestation options in Aydın province, Turkey, strawberry cultivation. *Phytoparasitica* 42: 397–403. https://doi.org/10.1007/s12600-013-0376-z

Benlioglu S., Dinler H., Yildiz A., Ozyilmaz Ü., Benlioglu K., 2018. Problems in strawberry seedlings in Türkiye, *ADÜ Ziraat Dergisi* 15(1): 221–226 (in Turkish). https://dx.doi.org/10.25308/aduziraat.359955

Cabral A., Rego C., Nascimento T., Oliveira H., Groenewald J.Z., Crous P.W., 2012a. Multi-gene analysis and morphology reveal novel *Ilyonectria* species associated with black foot disease of grapevines. *Fungal Biology* 116(1): 62–80. https://doi.org/10.1016/j.funbio.2011.09.010

Cabral A., Groenewald J.Z., Rego C., Oliveira H., Crous P.W., 2012b. *Cylindrocarpon* root rot: multi-gene analysis reveals novel species within the *Ilyonectria radicicola* species complex. *Mycological Progress* 11: 655–688. https://doi.org/10.1007/s11557-011-0777-7

Carbone I., Kohn L.M., 1999. A method for designing primer sets for speciation studies in filamentous ascomycetes. *Mycologia* 9: 553–556. https://doi.org/10.1080/00275514.1999.12061051

Cenis J.L., 1992. Rapid extraction df fungal DNA for PCR amplification. *Nucleic Acids Research* 20: 2380. https://doi.org/10.1093/nar/20.9.2380

Chen Q., Yin S.L., Zhang X.G., Ma X., Zhong S., Zhang G.Z., 2021. *Dactylonectria* species associated with black root rot of strawberry in China. *Australasian Plant Pathology* 50: 501–511. https://doi.org/10.1007/s13313-021-00804-1

Crous P.W., Groenewald J.Z., Risède J-M., Simoneau P., Hywel-Jones N.L., 2004. *Calonectria* species and

their *Cylindrocladium* anamorphs: species with sphaeropedunculate vesicles. *Studies in Mycology* 50: 415–42 9. https://doi.org/10.3114/sim.55.1.213

Dinler H., Benlioglu S., Benlioglu K., 2016. Occurrence of Fusarium wilt caused by *Fusarium oxysporum* on strawberry transplants in Aydın Province in Turkey. *Australasian Plant Disease Notes* 11:10. https://doi.org/10.1007/s13314-016-0196-3

Dinler H., Benlioglu S., Benlioglu K., 2018. *Rhizoctonia fragariae* causes black root rot on strawberry seedlings in Turkey. *Australasian Plant Disease Notes* 13:23. https://doi.org/10.1007/s13314-018-0307-4

Erper I., Ozer G., Alkan M., Zholdoshbekova S., Turkkan M., 2020. First report of *Dactylonectria torresensis* causing black root rot of strawberries in Kyrgyzstan. *Journal of Plant Pathology* 103: 379–380. https://doi.org/10.1007/s42161-020-00706-z

Fang X., Phillips D., Li H., Sivasithamparam K., Barbetti M., 2011a. Severity of crown and root diseases of strawberry and associated fungal and oomycete pathogens in Western Australia, *Australasian Plant Pathology* 40: 109–119. https://doi.org/10.1007/s13313-010-0019-5

Fang X., Phillips D., Li H., Sivasithamparam K., Barbetti M., 2011b. Comparisons of virulence of pathogens associated with crown and root diseases of strawberry in Western Australia with special reference to the effect of temperature. *Scientia Horticulturae* 131: 39–48. https://doi.org/10.1016/j.scienta.2011.09.025

FAO, 2023.FAOSTATDatabase "Food and Agriculture Organization of the United Nations". In: FAOSTAT database.https://www.fao.org/faostat/en/#data/QCL. Accessed October 15, 2025

Glass N.L., Donaldson G.C., 1995. Development of primer sets designed for use with the PCR to amplify conserved genes from filamentous ascomycetes. *Applied and Environmental Microbiology* 61: 1323–1330. https://doi.org/10.1128/aem.61.4.1323-1330.1995

Habibi A., Ghaderi F., 2020. First record of *Dactylonectria macrodidyma* causing black root rot on strawberry. *MycologiaIranica* 7(2):241-246. https://doi.org/10.22043/mi.2020.124511

Halleen F., Schroers H-J., Groenewald J.Z., Crous P.W., 2004. Novel species of *Cylindrocarpon* (*Neonectria*) and *Campylocarpon* gen. nov. associated with black foot disease of grapevines (*Vitis* spp.). *Studies in Mycology* 50: 431–455.

Kumar S., Stecher G., Li M., Knyaz C., Tamura K., 2018. MEGA X: Molecular evolutionary genetics analysis across computing platforms. *Molecular Biology and Evolution* 35:1547-1549. https://doi.org/10.1093/molbev/msy096

Lawrence D.P., Nouri M.T., Trouillas F.P., 2019.Taxonomy and multi-locus phylogeny of *Cylindrocarpon*-like species associated with diseased roots of grapevine and other fruit and nut crops in California. *Fungal Systematics and Evolution* 4: 59–75. https://doi.org/10.3114/fuse.2019.04.06

Löhrer M., Vogel L., Petrescu Dita Singer S., Erwes S., Heuprl M., Schaffrath U., 2022. PCR diagnostics for rapid detection of fungi associated with black root rot of strawberries. *Journal of Plant Diseases and Protection* 129:1053–1062. https://doi.org/10.1007/s41348-022-00594-8

Maas J.L., 1998. *Compendium of Strawberry Diseases*. 2nd ed. APS Press, St. Paul, MN, USA, 98 pp.

Manici L.M., Caputo F., Baruzzi G., 2005. Additional experiences to elucidate the microbial component of soil suppressiveness towards strawberry black root rot complex. *Annals of Applied Biology* 146: 421–431. https://doi.org/10.1111/j.1744-7348.2005.040051.x

Marquez N, Giachero M.L., Declerck S, Ducasse D.A., 2021. *Macrophomina phaseolina*: General Characteristics of Pathogenicity and Methods of Control. *Frontiers in Plant Science* 22;12:634397. https://doi.org/10.3389/fpls.2021.634397

O'Donnell K., Cigelnik E., 1997. Two divergent intragenomic rDNA ITS2 types within a monophyletic lineage of the fungus *Fusarium* are nonorthologous. *Molecular Phylogenetics and Evolution* 7: 103–116. https://doi.org/10.1006/mpev.1996.0376

Pinkerton J.N., Ivors K.L., Reeser P.W., Bristow P.R., Windom G.E., 2002. The use of soil solarization for the management of soil-borne plant pathogens in strawberry and red raspberry production. *Plant Disease* 86: 645–651. https://doi.org/10.1094/PDIS.2002.86.6.645

Probst C., Crabbe D., Ridgway H., Jaspers M.V., JonesE.E., 2019. Fate of mycelial and conidial propagules of *Ilyonectria* and *Dactylonectria* species in soil. *New Zealand Plant Protection* 72: 27–35. https://doi.org/10.30843/nzpp.2019.72.244

Qian S., Wei Z., Jiye Y., Xinghong L., 2022. Identification of pathogen causing strawberry Dactylonectria root rot. *Acta Phytopathologica Sinica* 52: 276–280. https://doi.org/10.13926/j.cnki.apps.000753

Rigotti S., Viret O., Gindrat D., 2003. Fungi from symptomless strawberry plants in Switzerland. *Phytopathologia Mediterranea* 42: 85–88. http://www.jstor.org/stable/26456650

Vigliecca M., González P., Machín A., Vicente E., Silvera E., 2022. First report of root and crown rot caused by *Dactylonectria novozelandica* on strawberry in Uruguay. *Agrociencia Uruguay* 26(2): e962. https://doi.org/10.31285/AGRO.26.962

Weber R., Entrop A., 2017. *Dactylonectria torresensis* as the main component of the black root rot complex of strawberries and raspberries in Northern Germany. *Erwerbs-Obstbau* 59: 157–169. https://doi.org/10.1007/s10341-017-0343-9

Wood M.,2001. January 4. Strawberry growers test methyl bromide alternatives. *Agriculture and Natural Resource* 49(1): 4–8.

YildizA., Benlioglu H.S., Boz O., Benlioglu K., 2010.Use of different plastics for soil solarization in strawberry growth and time-temperature relationships for the control of *Macrophomina phaseolina* and weeds. *Phytoparasitica* 38(5): 463–473. https://doi.org/10.1007/s12600-010-01237

Yildiz A., Benlioglu K., Benlioglu S., 2014. First Report of Strawberry Dieback Caused by *Lasiodiplodia theobromae. Plant Disease* 98(11): 1579. https://doi.org/10.1094/pdis-11-13-1192-pdn

Yildiz A., Benlioglu S., 2014. A laboratory bioassay for evaluating pathogenicity of *Macrophomina phaseolina* and *Rhizoctonia solani* isolates to strawberry stolons. *Phytoparasitica* 42: 367–369. https://doi.org/10.1007/s12600-013-0370-5

Phytopathologia Mediterranea
The international journal of the
Mediterranean Phytopathological Union

Firenze University Press
www.fupress.com/pm

Research Papers

Resistance and virulence patterns in the pea seed-borne mosaic virus (PSbMV) / lentil (*Lens culinaris*) pathosystem

Joop A.G. VAN LEUR[1]*, Jule H. GEORGE[1], Safaa G. KUMARI[2]

[1] *New South Wales Department of Primary Industries and Regional Development, Tamworth Agricultural Institute, Tamworth, Australia*
[2] *International Center for Agricultural Research in the Dry Areas, Terbol, Lebanon*
*Corresponding author. Email: joop.vanleur@dpi.nsw.gov.au

OPEN ACCESS

Citation: van Leur, J.A.G., George, J.H., & Kumari, S.G. (2026). Resistance and virulence patterns in the pea seed-borne mosaic virus (PSbMV) / lentil (*Lens culinaris*) pathosystem. *Phytopathologia Mediterranea* 65(1): 121-132. doi: 10.36253/phyto-17081

Accepted: April 23, 2026

Published: May 14, 2026

© 2026 Author(s). This is an open access, peer-reviewed article published by Firenze University Press (https://www.fupress.com) and distributed, except where otherwise noted, under the terms of the CC BY 4.0 License for content and CC0 1.0 Universal for metadata.

Data Availability Statement: All relevant data are within the paper and its Supporting Information files.

Competing Interests: The Author(s) declare(s) no conflict of interest.

Editor: Anna Maria D'Onghia, CIHEAM/Mediterranean Agronomic Institute of Bari, Italy.

ORCID:
JVL: 0000-0003-4640-7423
JG: 0009-0000-1455-4707
SK: 0000-0002-4492-6257

Summary. Pea seed-borne mosaic virus (PSbMV) can reach high levels of seed infection in Australian field peas, resulting in severe crop losses. Endemic, pea-derived PSbMV strains can cause lentil seed infection under experimental conditions, but PSbMV transmission has not been detected in grain harvested from lentil crops in Australia. In contrast, specialised PSbMV strains that are seed-borne in lentils occur in countries with long histories of lentil cultivation. A total of 29 PSbMV isolates were obtained from seeds of 11 exotic lentil accessions held at the Australian Grains Genebank, and the isolates were identified as the P2 pathotype using the standard set of pea differentials. However, testing with an additional set of lentil genotypes revealed two distinct pathotypes, tentatively designated P2a and P2b. Screening of lentil accessions previously reported to possess resistance to PSbMV or to bean yellow mosaic virus (BYMV), as well as Australian (25) and North American (3) cultivars, identified resistance to the P2b pathotype in several entries. In contrast, resistance to the more virulent P2a pathotype was only detected in three germplasm accessions that were previously reported to be BYMV resistant. Incursions of lentil seed-borne PSbMV strains pose major risks to the Australian lentil industry. Collaboration with research programmes in countries where lentil seed-borne PSbMV is present will facilitate resistance screening against a possible wider range of pathotypes, and support research on virulence genes and virus genes controlling seed transmission. As large-scale testing with exotic virus strains is difficult to implement in Australia, development of molecular markers for resistance to the most virulent PSbMV strains is desirable.

Keywords. Lentil seed-borne PSbMV strains, BYMV, virus resistance, pathogenicity test, pathotypes.

INTRODUCTION

Lentil (*Lens culinaris* Medik.) is one of the world's oldest domesticated crops (Zohary, 1972) and ranks third in global cool-season food legume production, after chickpea and field pea (FAOSTAT, 2026). Lentil cultivation benefits farming systems through its ability to fix nitrogen, and more generally by providing grain that is rich in protein, carbohydrates, fibre, vitamins

and minerals (Montejano-Ramírez and Valencia-Cantero, 2024).

Cultivation of lentils in Australia is recent. Less than 40 years ago, lentil was considered an experimental crop (Knights, 1987), and in 1993 the area of lentil production was estimated to be only 980 ha (FAOSTAT, 2026). By 2023, Australia was one of the world's largest producers of lentils, with 1.41 million tons of grain harvested from 0.80 million ha (FAOSTAT, 2026). This increase was made possible as Australian broad-acre grain growers recognised the benefits of introducing a grain legume into their rotations for soil health and fertility and was underpinned by research programmes that developed adapted varieties and improved agronomic practices (Materne and Reddy, 2007). Within their short history, the Australian lentil breeding programmes have focussed on improved harvestability, tolerance to boron toxicity and salinity, and resistance to Ascochyta blight and Botrytis grey mould (Materne and Reddy, 2007; Thackwray *et al*., 2024). However, comparatively little attention has been given to breeding for virus resistance.

More than 30 virus species have been reported to infect lentils. Among these, the viruses considered most economically important internationally include alfalfa mosaic virus (AMV, *Alfamovirus*), bean leafroll virus (BLRV, *Luteovirus phaseoli*), bean yellow mosaic virus (BYMV, *Potyvirus phaseoluteum*), beet western yellows virus (BWYV, *Polerovirus*), cucumber mosaic virus (CMV, *Cucumovirus*), pea enation mosaic virus 1 (PEMV-1, *Enamovirus*), pea seed-borne mosaic virus (PSbMV, *Potyvirus pisumsemenportati*) and soybean dwarf virus (SbDV, *Luteovirus glycinis*) (Kumari *et al*., 2009). Lentils are particularly vulnerable to virus infections, as they are preferred hosts for efficient virus vectors including the pea aphid (*Acyrthosiphon pisum*) (Wale *et al*., 2000).

Seed-transmitted viruses are important, because sowing infected seed results in infection foci throughout crops early in growing seasons, whereas other viruses must rely on viruliferous aphids migrating from off-season hosts. Lentil sowing rates are also substantially higher than those of larger-seeded pulses, further increasing lentil crop vulnerability to seed-borne viruses. PSbMV, CMV, AMV, BYMV and broad bean stain virus (BBSV, *Comovirus viciae*) are reported to be transmitted through lentil seed (Kumari *et al*., 2009). Of these only BBSV is not present in Australia (Jones and Congdon, 2024).

Limited virus survey data from Australian commercial lentil crops have been published. Freeman (2014) reported surveys conducted between 2000 and 2005 in Australia's main winter pulse growing regions of South Australia and Victoria and found that lentil crops were more prone to virus infections than crops of faba bean, field pea or chickpea. CMV was the most prevalent virus detected in lentils, which was attributed to high levels of seed infections. Similarly, limited information is available on lentil viruses in Canada and the United States of America (USA), despite recognition of their potential importance to pulse industries in these countries (Rashed *et al*., 2018). In contrast, much information has been published over the past three decades on the presence of lentil viruses in countries with long histories of lentil cultivation. Virus incidences determined by tissue blot immunoassays on randomly collected plants from farmer fields have been reported from nine surveys across eight countries. In five of these surveys, PSbMV was the most frequently identified virus (Table 1).

PSbMV is internationally considered a major virus in pea (*Pisum sativum*), largely because of its ability to be transmitted at high rates in pea seed (Khetarpal and Maury, 1987). In Australia, high incidences of PSbMV in commercial field pea crops were found to be strongly associated with PSbMV transmission levels in the seed used for sowing (Latham and Jones, 2001a; Freeman *et al*., 2013; Congdon *et al*., 2016). Minor levels of seed transmission were found in commercial seed lots of faba bean and chickpea (Latham and Jones, 2001b), but there are no reports of PSbMV seed transmission in Australian commercial lentil seed lots, and PSbMV infection of lentil crops has only been found near pea crops (Agriculture Victoria, 2022). Internationally, the only reported investigation of seed transmission of PSbMV in non-experimental lentil seed lots is from Ethiopia, where 84 of 270 farmer-saved seed lots were PSbMV infected, with the greatest seed-to-plant transmission rate being 16.8% (Abraham and Makkouk, 2002). Hampton (1982) detected seed-borne PSbMV in USDA Genebank accessions originating from a range of West Asian, North African, European and South American countries, indicating that PSbMV seed transmission in lentils could be widespread.

PSbMV strains isolated from lentil seed were found to be similar to pea-derived strains in host range, symptomatology, seed transmission capacity and serological reaction, but were unable to infect BYMV resistant pea varieties (Hampton, 1982; Goodell and Hampton, 1984; Alconero *et al*., 1986) and therefore considered to be a distinct pathotype. Originally coded PSbMV-L or PSbMV-L1, the lentil pathotype was renamed P2 to align with the existing nomenclature of pea-derived PSbMV strains (Kasimor *et al*., 1997).

Resistance and virulence genes within the PSbMV / *Pisum sativum* pathosystem have been studied exten-

Table 1. Published surveys in which incidences of lentil viruses were determined by tissue blot immunoassays (TBIA) on randomly collected plants from farmer fields.

Country	Year(s)	Reference	Fields surveyed	Plants tested	Virus incidence (%)[a]						Most frequently identified virus
					Seed-borne viruses					Other viruses[b]	
					PSbMV	CMV	AMV	BYMV	BBSV		
Syria	1991-1993	Kumari *et al.* (1993)	161	3,320	0.19	nt	nt	nt	0.91	nt	BBSV
Türkiye	1996	Bayaa *et al.* (1998)	39	7,800	0.03	nt	nt	0.01	0.24	nt	BBSV
Pakistan	1997	Makkouk *et al.* (2001)	29	2,085	16.26	1.06	0.00	0.00	0.00	0.72	PSbMV
Ethiopia	1998	Tadesse *et al.* (1999)	32	4,670	9.87	0.04	0.00	0.02	0.02	3.00	PSbMV
Iraq	2000	El-Muadhidi *et al.* (2001)	10	1,700	0.00	0.00	0.00	1.82	0.00	0.35	BYMV
Iran	2001, 2002	Makkouk *et al.* (2003)	34	6,080	0.61	0.00	0.16	0.05	0.66	7.81	luteo
Ethiopia	2004	Bekele *et al.* (2005)	11	810	15.43	0.00	0.00	0.12	0.00	6.05	PSbMV
Azerbaijan	2007, 2008	Mustafayev *et al.* (2011)	9	1,291	15.41	0.00	0.00	0.00	0.00	14.18	PSbMV
Nepal	2024	Khadka *et al.* (2024)	94	4,711	12.12	0.53	nt	nt	nt	nt	PSbMV

[a] nt: not tested.
[b] Other viruses: PEMV-1, luteo- and poleroviruses (as determined by the 5G4 monoclonal antibody), faba bean necrotic yellows virus (FBNYV, *Nanovirus necroflaviviciae*), chickpea chlorotic dwarf virus (CpCDV, *Mastrevirus cicerparvi*).

sively. Single, recessively inherited resistance genes have been identified in field pea that correspond to the four known pathotypes (P1–P4). These genes include: *sbm1*, which confers resistance to all four PSbMV pathotypes; *sbm1*^{1}, a different allele of the *sbm1* gene, which provides resistance to the P1 and P2 pathotypes; and *sbm2*, which confers resistance to the P2 and P3 pathotypes (Johansen *et al.*, 2001; Gao *et al.*, 2004). Among these, *sbm2* is strongly linked to the *mo* gene for BYMV resistance (Provvidenti and Alconero, 1988), or possibly the same gene with an allele of different specificity (Bruun-Rasmussen *et al.*, 2007).

In contrast, PSbMV resistance genes in lentils have received far less attention. Haddad *et al.* (1978) screened 568 lentil accessions from the USDA Genebank, using mechanical inoculations with a non-pathotyped PSbMV strain that originated from pea. Resistance was assessed based on absence of symptoms, with symptomless plants re-inoculated and their progenies tested. Of four accessions identified as immune, one (PI 368648) was crossed with two susceptible varieties, 'Tekoa' and 'Precoz', demonstrating that resistance was controlled by a single recessive gene. Crosses of PI 368648 with another of the resistant selections, PI 212610, indicated that both selections shared the same resistance gene, for which the code *sbv* was proposed. Hampton (1982) compared an isolate derived from the Greek lentil accession PI 297772 (PSbMV-L) with a pea-derived PSbMV isolate, by inoculating lentil accessions known to be either immune or susceptible to PSbMV, and found a differential reaction to both strains in some accessions. No follow-up has been reported to identify more resistant germplasm or to develop PSbMV resistant lentil varieties. Furthermore, no studies have examined potential linkages between potyvirus resistance genes in lentil, comparable to those described in pea (Provvidenti and Hampton, 1991; Bruun-Rasmussen *et al.*, 2007).

Testing seed of lentil accessions from the Australian Grains Genebank (AGG) that originated from the USDA Genebank has identified PSbMV in several lines, but no cross infection to neighbouring accessions during seed increases was detected (van Leur *et al.*, 2013a). To date, no lentil seed-borne PSbMV infections have been found in Australian commercial seed increases or production fields. However, an incursion of lentil seed-borne PSbMV strains into lentil crops could have major impacts on the Australian lentil industry, particularly as production expands from winter rainfall environments into sub-tropical regions that are likely to be virus-prone. Breeding for resistance is a cost-effective and environmentally sustainable strategy for virus management. To support this approach, Australian lentil breeding programmes require knowledge of PSbMV resistance in locally adapted varieties, and should have access to sources of PSbMV resistance.

The aim of the present study was to evaluate resistance of lentil varieties and germplasm accessions to lentil seed-derived PSbMV isolates, in order to identify potential sources of resistance that can be exploited by lentil breeding programmes to pre-emptively develop germplasm combining local adaptation with effective PSbMV resistance.

MATERIALS AND METHODS

Virus diagnostics

Tissue blot immunoassays (TBIA) were used for all diagnoses, as these assays provide a reliable, rapid, and cost-effective methodology for testing large numbers of individual plants for virus infections (Freeman *et al*., 2013; van Leur *et al*., 2025). After blotting growing tips of plants on nitrocellulose membranes (Schleiger & Schuell Protran, 0.45 µm pore size), the membranes were processed using polyclonal antibodies specific to PSbMV (DSMZ, AS-0129) or BYMV (DSMZ, AS-0717), following the procedures described by Kumari *et al.* (2022).

Germplasm tested and virus isolates used

Five lentil germplasm accessions with reported resistance or tolerance to PSbMV (Haddad *et al*., 1978; Hampton, 1982; Kumari and Makkouk, 1995), and seven accessions with reported BYMV resistance (McKirdy *et al*., 2000; Al Khalaf *et al*., 2009; Kanawaty *et al*., 2017), were obtained from the Australian Grains Genebank (AGG, Horsham, Victoria; Table 2). Single plant selections were made from several Genebank accessions to minimise possible heterogeneity. The AGG also supplied seed of additional lines that were identified during the study as potential donors of resistance. Twenty-five Australian lentil varieties were obtained from the National Lentil Breeding Program (Horsham, Victoria) or commercial seed merchants.

Four pea seed-derived PSbMV strains were used for initial screening of lentil germplasm. These were: Ps11-11/16 (P1 pathotype, isolated from a 'Kaspa' seed lot harvested at the Plant Breeding Institute in Narrabri, New South Wales (NSW)); Ps11-13/19 (P2 pathotype, isolated from a 'Dundale' seed lot harvested at the Wagga Wagga Agricultural Institute, NSW); Ps11-16/16 (P3 pathotype, isolated from an 'Excell' seed lot harvested in a farmer's field in southern NSW); and Ps11-10/2 (P4 pathotype, isolated from an 'Excell' seed lot harvested at the Wagga Wagga Agricultural Institute, NSW). Isolation and pathotyping procedures for these strains were described in a previous study (van Leur *et al*., 2025).

All PSbMV isolates obtained from lentil were first pathotyped on a *Pisum sativum* differential set (van Leur *et al*., 2025), consisting of genetically homogeneous single plant progenies from PI 193835 (*sbm1* resistance gene, resistant to all PSbMV pathotypes), PI 269774 (*sbm1*^{1} gene, resistant to P1 and P2 pathotypes) and 'Dark Skin Perfection' or 'Greenfeast' (*sbm2* gene, resistant to P2 and P3 pathotypes). Single plant progenies of lentil genotypes were used for further pathotype differentiation of lentil strains. A PSbMV- and BYMV-susceptible lentil variety ('PBA Jumbo2' or 'PBA Kelpie XT') was included as a susceptible control in each test. Tests were repeated if controls were not or poorly infected.

A total of 29 lentil seed-borne PSbMV strains were pathotyped. Fifteen strains were isolated in 2012 from seed of AGG accessions (van Leur *et al*., 2013a). These accessions were duplicates from the USDA Genebank, and had been previously reported as PSbMV infected (Hampton 1982; Goodell and Hampton, 1984). The remaining 14 strains were isolated during 2018, 2024 or 2025, and originated from AGG accessions, evaluated as part of ongoing studies to identify resistance to a range of lentil viruses. All strains were increased on PSbMV-susceptible *Vicia faba* lines, including the varieties 'PBA Amberley' or 'Fiesta' and germplasm selections Ac1206 (originating from China) or Ac1229 (from Ecuador). PSbMV infection in inoculated faba bean plants was confirmed by TBIA before leaf tissue was used as inoculum. Virus strains were preserved by drying infected faba bean tissue over silica gel and storing at 5–8°C in paper envelopes placed inside airtight plastic boxes on silica gel.

Testing for BYMV resistance in accessions reported as resistant was carried out using mechanical inoculations with BYMV isolates originating from northern NSW; isolated from faba beans growing in commercial crops (isolates By20-05 and By22-15) or from red clover (*Trifolium pratense*) growing in pastures (isolates By23-01 and By23-02). The BYMV isolates from red clover were found to be more virulent than those from faba bean, and formed a separate phylogenetic group in molecular analyses (Maina *et al*., 2025). However, all four isolates failed to infect the pea variety 'Greenfeast', which contains the single recessive *mo* gene conferring resistance to BYMV (van Leur *et al*., 2013b).

Screening tests

For each genotype / pathotype combination one 0.33 L plastic pot was sown with six seeds. The pots contained a commercial potting mixture, adjusted with lime to pH 6.8–7.0, and were after sowing placed into an aphid-proof, temperature controlled (18–24°C) greenhouse. Late emerging and poorly growing seedlings were removed 10 to 14 d after sowing, and the remaining plants were then each mechanically inoculated by rubbing a virus suspension into the first and second leaf. Virus inoculum was prepared by homogenising 3 to 5 g of fresh PSbMV infected young faba bean leaves with 3 g of silicon carbide in 15 to 25 mL of cold 0.01 M sodium phosphate buffer (pH 7.0). Plants were TBIA-tested for

Table 2. Lentil accessions and varieties with reputed resistance to PSbMV or BYMV, tested in the present study.

Name	AGG[a]	ILL[b]	PI[c]	Origin[d]	Type[d]	Virus Resistance (Reference)
ILL0217	70094	217	212610	Afghanistan	Landrace	PSbMV resistant (Haddad *et al.*, 1978) PSbMV-L resistant, PSbMV susceptible (Hampton, 1982)
ILL0277	71162	277	297745	Greece	Landrace	PSbMV resistant (Haddad *et al.*, 1978)
ILL1931	71601	1931	368648	North Macedonia	Improved cv	PSbMV resistant (Haddad et al., 1978) PSbMV-L resistant, PSbMV resistant (Hampton, 1982)
ILL1935[e]	71604	1935	368651	North Macedonia	Improved cv	PSbMV-L resistant, PSbMV susceptible (Hampton, 1982)
Red Chief	72936		477921	USA	Improved cv	PSbMV tolerant (Kumari and Makkouk, 1995)
ILL0083	74515	83		Afghanistan	Landrace	BYMV resistant (Al Khalaf *et al.*, 2009)
ILL0336	75305	336	298122	France	Unknown	BYMV resistant (Al Khalaf *et al.*, 2009)
ILL0518	71489	518	320951	India	Landrace	BYMV highly resistant (Kanawaty *et al.*, 2017)
ILL1949	71624	1949	379372	Serbia	Landrace	BYMV highly resistant (Kanawaty *et al.*, 2017)
ILL4736	75304	4736		Canada	Breeding line	BYMV resistant (Al Khalaf *et al.*, 2009)
ILL5005		5005		Spain	Landrace	BYMV moderately resistant (Kanawaty *et al.*, 2017)
ILL7163	74059	7163		Pakistan	Breeding line	BYMV highly resistant (McKirdy *et al.*, 2000) BYMV resistant (Al Khalaf *et al.*, 2009)

[a] Accession number with the Australian Grains Genebank, Horsham, Victoria, Australia (AGG).
[b] International Legume Lentil (ILL) accession number with the International Center for Agricultural Research in the Dry Areas (ICARDA).
[c] Plant Introduction (PI) accession number with the United States Department of Agriculture's Agricultural Research Service (USDA-ARS).
[d] Origin and Type, according to GENESYS (Accessed January 15, 2026, from https://www.genesys-pgr.org/).
[e] PI 368651 is heterogeneous for PSbMV-L resistance (Hampton, 1982).

virus presence 3 weeks after the inoculations. Infection percentages were calculated based on the numbers of inoculated seedlings.

BYMV inoculation procedures were the same as those described above.

Seed transmission trial

Seed transmission in mechanically inoculated lentil varieties was assessed in 2018 (five varieties) and 2019 (two of the five varieties tested in 2018), using virus strains isolated from lentil seed (three in 2018 and two in 2019) or pea seed (four in 2018 and three in 2019). Eight seeds per variety were sown into 4 L capacity pots, using the potting mixture and greenhouse conditions described above. One pot for every strain / variety combination was used in 2018. Because of poor seed yields in 2018, the number of varieties was reduced in 2019, when two pots per strain / variety combination were sown.

All emerged seedlings were inoculated at the 2-3 leaf development stage. Virus presence was assessed 2–3 weeks later, and four infected plants per pot were retained and grown to maturity. Seed harvested from these plants was grown in trays in the greenhouse, and emerged seedlings were individually TBIA-tested for presence of PSbMV. Seed-to-plant transmission percentages were calculated based on the number of emerged seedlings.

RESULTS AND DISCUSSION

Strain differentiation among lentil seed-derived PSbMV isolates

All lentil seed-derived PSbMV strains were unable to infect the *sbm1*, *sbm1*^{1} and *sbm2* pea differential lines, and were therefore classified as pathotype P2. However, initial testing of lentil seed-derived strains on ILL0277, a germplasm accession previously reported as resistant to a pea-derived PSbMV strain (Haddad *et al.*, 1978), revealed variations, even when a single-seed progeny of this accession was used. ILL0277 was resistant to all pea seed-derived PSbMV strains, but lentil seed-derived strains segregated into two distinct groups. These were tentatively classified as separate pathotypes: P2a, comprising strains able to infect ILL0277, and P2b, comprising strains unable to infect ILL0277.

Strain isolations from lentil seed in 2012 identified the more virulent P2a pathotype in two accessions originating from Chile, AGG71307 (PI 299222) and AGG71315 (PI 299233). Isolates from the Iranian accession AGG72306 (PI 432218) were mixed, with three strains pathotyped as P2a and one as P2b, whereas all four strains isolated from the Greek accession AGG71189 (PI 297772) were pathotyped as P2b (Table 3). Hampton (1982) previously isolated a PSbMV strain from PI 297772 seed (PSbMV-L), and showed a unique virulence pattern for this strain across a range of lentil germplasm.

Between 2018 to 2025, more than 500 lentil accessions were received from the AGG to be evaluated for resistance to a range of viruses of importance to the Australian lentil industry. Of these, 58 accessions were selected for seed testing based on PSbMV susceptibility and geographic origin, of which seven showed seed infections. Seven P2a pathotype strains were isolated from accessions collected in Ethiopia and Greece, and seven P2b strains were isolated from two accessions originating from Nepal (Table 3).

The germplasm accessions used for isolations have undergone multiple regeneration cycles since collection, and may have been exposed to infections originating from diverse sources. Consequently, the pathogenicity of the isolates does not necessarily reflect the PSbMV population present in the respective countries of origin.

PSbMV strain-specific resistance in lentil germplasm and breeding lines

None of the five accessions previously reported as PSbMV resistant showed resistance to the P2a strain; however, ILL1931, ILL1935 and 'Red Chief' reacted similarly to ILL0277, with resistance to the P2b strain (Table 4).

Testing of seven lentil lines with reputed BYMV resistance yielded three lines (ILL0083, ILL0518 and ILL1949) with resistance to both lentil seed-derived PSbMV pathotypes (P2a and P2b) and two lines (ILL0336 and ILL4736) that were resistant to P2b, but susceptible to P2a, exhibiting a resistance pattern similar to ILL0277.

Lentil genotype resistant to P2a and P2b, as well as those resistant only to P2b, also showed complete immunity to the four pea seed-derived pathotypes, P1, P2, P3 and P4 (Table 4).

Twenty-five Australian lentil varieties were tested with pea seed-derived PSbMV strains. The varieties 'Aldinga', 'Boomer', 'Commando', 'Nipper', 'Northfield', 'Nugget', 'PBA Blitz', 'PBA Flash', 'PBA Giant', 'PBA Greenfield', 'PBA Jumbo', 'PBA Jumbo2', 'PBA Kelpie XT', 'GIA Leader', 'GIA Metro', and 'GIA Sire' reacted as susceptible. In contrast, 'PBA Ace', 'PBA Bolt', 'PBA Hallmark XT', 'PBA Herald' and 'ALB Terrier' all showed complete resistance. 'PBA Highland XT', 'PBA Hurricane XT', 'GIA Lightning' and 'GIA Thunder' gave heterogenous reactions, with up to 25% susceptible plants. Heterogenous resistance reactions were expected, because all tested varieties were developed prior to commencement of the National Lentil Breeding Program deliberate selection for resistance to endemic (pea seed-derived) PSbMV strains in 2022. The varieties resistant to the pea seed-derived virus strains were also tested with the lentil seed-derived P2a and P2b strains. All were resistant to the P2b strain, but all were susceptible to P2a.

Improving resistance to Ascochyta blight (caused by *Ascochyta lentis*) has been a high priority for the

Table 3. Pathotyped PSbMV strains isolated from lentil seed accessions kept at the Australian Grains Genebank.

Lentil accession			Origin	Isolation Year	PSbMV strain codes	
AGG[a]	ILL[b]	PI[c]			Pathotype P2a	Pathotype P2b
71307		299222	Chile	2012	PsL12-11/1; PsL12-11/2; PsL12-11/3; PsL12-11/4	
71315	404	299233	Chile	2012	PsL12-6/1; PsL12-6/3; PsL12-6/5	
71189	304	297772	Greece	2012		PsL12-5/1; PsL12-5/3; PsL12-5/5; PsL12-5/7
72306		432218	Iran	2012	PsL12-8/2; PsL12-8/3; PsL12-8/4	PsL12-8/1
70465	4895		Ethiopia	2018	PsL18-13/1	
70527	5912		Ethiopia	2018	PsL18-14/1[d]	
73624			Greece	2024	PsL24-1/1; PsL24-1/2; PsL24-1/3	
74312	7857		Nepal	2024		PsL24-2/1; PsL24-2/2; PsL24-2/3; PsL24-2/4; PsL24-2/5; PsL24-2/6
74314	7859		Nepal	2024		PsL24-3/1
73612			Greece	2025	PsL25-1/1	
73614			Greece	2025	PsL25-2/1	

[a] Accession number with the Australian Grains Genebank, Horsham, Victoria (AGG).
[b] International Legume Lentil (ILL) accession number with the International Center for Agricultural Research in the Dry Areas (ICARDA).
[c] Plant Introduction (PI) accession number with the United States Department of Agriculture's Agricultural Research Service (USDA-ARS).
[d] PsL18-14/1 showed inconsistent reactions in eight pathogenicity tests, with six tests showing P2a reactions, and two tests showing P2b reactions.

Table 4. PSbMV and BYMV resistance[a] of selected[b] lentil accessions and varieties.

Accession name	Origin	Reported resistance	PSbMV pathotype						BYMV strain	
			P2a	P2b	P1	P2	P3	P4	Moderate[c] virulence	High[c] virulence
ILL0217[d]	Afghanistan	PSbMV	S	S	S	nt	nt	S	S	S
ILL0277[d]	Greece	PSbMV	S	R	R	R	R	R	MR	MR
ILL1931	North Macedonia	PSbMV	S	R	R	R	R	R	S	S
ILL1935	North Macedonia	PSbMV	S	R	R	nt	nt	R	R	MR
Red Chief	USA	PSbMV	S	R	R	nt	nt	R	S	S
ILL0083[d]	Afghanistan	BYMV	R	R	R	R	R	R	MR	S
ILL0336[d]	France	BYMV	S	R	R	R	R	R	S	S
ILL0518[d]	India	BYMV	R	R	R	nt	nt	R	R	MR
ILL1949[d]	Serbia	BYMV	R	R	R	nt	nt	R	R	MR
ILL4736[d]	Canada	BYMV	S	R	R	R	R	R	MR	S
ILL5005[d]	Spain	BYMV	S	S	S	nt	nt	S	MR	S
ILL7163[e]	Pakistan	BYMV	S	S	S	nt	nt	S	S	S

[a] R: complete resistance, MR: low infection (≤20% plants tested positive), S: susceptible, nt: not tested.
[b] Origin and background provided in Table 2.
[c] BYMV moderate virulence; By20-05 and By22-15 isolated from faba bean, BYMV high virulence; By23-01and By23-02 isolated from red clover (Maina *et al*., 2025).
[d] Genetically homogeneous single plant progenies used for pathogenicity tests.
[e] Two sources of ILL7163 were tested; (1) Australian Grains Genebank, (2) imported from the International Center of Agricultural Research. Both showed a similar reaction.

Australian lentil breeding programme, and the Canadian variety 'Indianhead' was used as a main donor for this resistance (Thackwray *et al*., 2024). 'Indianhead' (PI 320952, AGG 70793) is a black-seeded lentil intended for use as a green manure crop (Slinkard, 1988) and was selected at the University of Saskatchewan, Canada, from a germplasm accession originating from former Czechoslovakia (https://www.genesys-pgr.org/). In the present study, 'Indianhead' reacted similarly to ILL0277; resistant to the pea seed-derived pathotypes P1 to P4 and the lentil seed-derived pathotype P2b, but susceptible to pathotype P2a, and could be an unintentional donor of the strain-specific PSbMV resistance found in the limited number of Australian cultivars. 'Indianhead' has also been used as a donor of Ascochyta blight resistance in the lentil breeding programmes in Canada and the USA (Thackwray *et al*., 2024). The Canadian breeding line ILL4736 (University of Saskatchewan breeding code G-118), reportedly resistant to BYMV, showed a PSbMV reaction similar to ILL0277 (Table 4), although pedigree information for ILL4736 is not publicly available. The reportedly PSbMV tolerant variety 'Red Chief' also reacted like ILL0277 (Table 4). 'Red Chief' was selected at Washington State University from a cross between PI 181886 and PI 329171 (Wilson and Muehlbauer, 1983). In the present study, PI 181886 (AGG 71068, originating from Syria) was PSbMV-susceptible and PI 329171 (AGG 71505, originating from Iran), was heterogeneous for PSbMV resistance.

No recent information on PSbMV resistance in North American lentil cultivars is available, but the results from 'Indianhead', 'Red Chief' and ILL4736 indicate that resistance to the pea strains and the P2b lentil strain is present within the Canadian and USA breeding programmes.

BYMV resistance in lentil germplasm

Several accessions showed moderate resistant reactions, expressed as less than 20% of plants infected by BYMV, even after repeated tests on homogenous genotypes derived from single seed progenies. No host accession displayed complete resistance to all four of the BYMV isolates. However, two accessions previously reported as highly resistant to Syrian BYMV isolates, ILL0518 and ILL1949 (Kanawaty *et al*., 2017), were only infected by highly virulent isolates derived from red clover. The previously reported high virulence on faba bean of these isolates (Maina *et al*., 2025) was confirmed on lentils in the present study. The susceptibility of accessions previously reported to be highly BYMV resistant such as ILL7163 (McKirdy *et al*., 2000), indicates significant regional differences in pathogen virulence.

Table 5. Seed to plant transmission rates (%) of five PSbMV susceptible lentil varieties after mechanical inoculations with pea seed- and lentil seed-derived PSbMV strains in greenhouse trials.

PSbMV strain	Isolated from	Pathotype	Seed to plant transmission rates (%)						
			PBA Flash		PBA Jumbo2		PBA Blitz	Boomer	Nipper
			2018	2019	2018	2019	2018	2018	2018
PsL12-11/1	Lentil	P2a	17.5	nt[a]	0.0	nt	2.9	2.5	5.2
PsL12-6/5	Lentil	P2a	15.8	28.1	16.7	20.2	14.3	10.5	19.8
PsL12-5/3	Lentil	P2b	0.0	nt	0.0	nt	7.0	0.0	2.1
PsL12-8/1	Lentil	P2b	nt	21.3	nt	22.0	nt	nt	nt
Ps11-11/16	Pea	P1	7.9	4.3	0.0	2.2	6.5	0.0	2.2
Ps11-13/19	Pea	P2	0.0	nt	0.0	nt	nt	0.0	0.0
Ps11-16/16	Pea	P3	0.0	0.0	0.0	0.0	nh[b]	0.0	2.0
Ps11-10/2	Pea	P4	13.5	1.0	0.0	0.0	10.4	0.0	6.7

[a] nt: not tested.
[b] nh: not harvested.

While the single recessive gene (*mo*) within the *Pisum sativum* gene pool provides complete immunity to all BYMV isolates regardless of origin or virulence, no comparable gene was identified in lentil (*Lens vulgaris*) in this study.

PSbMV seed transmission in lentils under greenhouse conditions

Mechanical inoculations of PSbMV onto lentil varieties, grown in pots under greenhouse conditions, resulted in severe growth reductions, irrespective of virus isolate origin (from lentil or pea seed) or pathotype. Seed yields from the greenhouse-grown plants were very low compared with field-grown plants, and seed transmission tests were therefore conducted on only 40 to 100 harvested seeds per strain/variety combination. Seed transmission results were highly variable, but the only strain that failed to be seed transmitted in any of the tested lentil varieties was the pea seed-derived strain Ps11-13/19 (P2 pathotype). The lentil seed-derived strain PsL12-6/5 (P2a pathotype) showed the greatest level of seed transmission in both years (Table 5). Because of the limited number of seeds tested, these are only indicative results. However, they confirm earlier results showing that pea-derived PSbMV strains can be seed transmitted in lentils under experimental conditions (Hampton and Muehlbauer, 1977; Coutts *et al*., 2008).

CONCLUSIONS

The results of this study demonstrate that the PSbMV/*Lens culinaris* pathosystem is distinct from the well-characterised PSbMV/*Pisum sativum* pathosystem. When PSbMV strains isolated from lentil seed held at the Australian Grains Genebank were tested on a standard pea differential set, all were classified as pathotype P2. However, testing these strains on lentil germplasm accessions with reported PSbMV resistance revealed two distinct pathotypes, tentatively designated P2a and P2b. Lentil genotypes resistant to the P2a pathotype were also resistant to the P2b, whereas the reverse was not observed. Lentil genotypes resistant to either P2a or P2b were also resistant to all pea seed-derived PSbMV pathotypes (pathotypes P1, P2, P3 and P4).

Several recently developed Australian lentil varieties were resistant to the P2b pathotype and to pea-derived pathotypes. Australian lentil breeding programmes share research sites with pea breeding programmes, and high PSbMV infection levels are common in Australian pea crops, particularly at research stations (van Leur *et al*., 2025). Symptoms of PSbMV in field peas can be difficult to identify under field conditions (Khetarpal and Maury, 1987). However, in lentils, PSbMV can have severe effects, irrespective of whether the infecting strain originated from pea or lentil seed. It is therefore possible that Australian lentil breeders have inadvertently selected for resistance to the PSbMV pea strains present in their trial fields.

The strong linkage between BYMV resistance and resistance to PSbMV pathotype P2 in field pea (Provvidenti and Alconero, 1988) prompted the present investigation of a possible similar relationship within the PSbMV / *Lens vulgaris* pathosystem. Testing lentil lines reported as BYMV resistant did not identify a gene conferring complete immunity to all the tested BYMV isolates, comparable to the *mo* gene in field pea. However,

the most BYMV resistant lentil accessions (ILL0518 and ILL1949) were immune to all PSbMV pathotypes. Further investigations of resistance in lentils to different potyviruses would therefore be valuable.

More than 40 years ago, Goodell and Hampton (1984) warned of the risk that lentil seed-borne PSbMV strains could escape from genebanks into commercial lentil fields. Nearly three decades later, van Leur *et al.* (2013a) raised the same concern for the emerging Australian lentil industry. Since then, lentil production in the 'new' lentil producing countries – Canada, the USA, and Australia – has expanded substantially, reaching a combined area of more than 2.5 million ha in 2023, representing about half of the global lentil area (FAOSTAT, 2026). Despite this growth, and the widespread presence of PSbMV in pea crops, PSbMV seed transmission has not yet been reported in commercial lentil crops in these countries. The absence of specialised lentil seed-borne strains is the most likely explanation for this discrepancy.

In the present study, all lentil seed-derived PSbMV strains were classified as the P2 pathotype, but the P2 pathotype is not unique to lentils. Alconero and Hoch (1989) pathotyped 189 PSbMV strains isolated from seeds of a wide range of pea germplasm introductions held at the USDA Genebank, and identified 14 isolates reacting as the P2 pathotype using two pea lines capable of differentiating the four PSbMV pathotypes. In addition, a pea seed-derived P2 pathotype strain has previously been identified in Australia (van Leur *et al.*, 2025). Pathotyping of PSbMV isolates using standardised, homogenous pea and lentil genotypes is essential for pea and lentil breeding programmes to identify effective and durable resistance genes. However, single gene virulences in pathogen populations are unlikely to explain complex traits including seed transmission, which are probably controlled by multiple virus genes (Wang and Maule, 1994; Simmons and Munkvold, 2014). To fully understand the uniqueness of lentil seed-borne PSbMV strains, collaboration with research programmes in countries where these strains are endemic is needed, and should include pathotyping as well as studies of seed transmission and host resistance of local germplasm. Ademe *et al.* (2025) examined eight PSbMV strains isolated from lentils grown in farmer fields or research stations in different regions of Ethiopia. Although the strains were isolated from plants, it is likely that they were lentil seed-borne. Phylogenetic analysis showed that six isolates clustered with the published lentil seed-borne PSbMV-L1 strain (GenBank accession code: AJ252242), and were distinct from pea seed-borne strains. However, no pathotyping was undertaken by Ademe *et al.* (2025).

Strict quarantine regulations have undoubtedly played important roles in preventing introduction of lentil seed-borne strains into Australian lentil fields (Maina and Jones, 2023). However, rapidly expanding lentil cultivation, together with increasing international travel and trade, make incursions of lentil seed-borne strains very likely. Pre-emptive breeding is required, using parental material with resistance to the most virulent lentil seed-borne virus strains, but requires better understanding of the inheritance of PSbMV resistance in lentils. The only published study on PSbMV inheritance used a non-pathotyped PSbMV strain originating from field pea and identified a single recessive gene (*sbv*) in both PI 368648 and PI 212610 (Haddad *et al.*, 1978). In the present study, PI 368648 (ILL1931) was resistant to the P2b pathotype, but susceptible to the P2a pathotype, and PI 212610 (ILL0217) was found to be susceptible to PSbMV. Hampton (1982) found that PI 212610 was resistant to the lentil seed-borne strain PSbMV-L, but was susceptible to the pea seed-borne strain. This is contrary to the present study, where lentil lines resistant to a lentil seed-borne strain (either P2a or P2b) were also resistant to all pea seed-borne strains. This discrepancy likely reflects heterogeneity within the germplasm accessions, common in genebank material, and the single-plant progeny tested was not representative of the original accession.

Although the present study has demonstrated substantial differences in PSbMV virulence and resistance patterns between the field pea and lentil pathosystems, lentil germplasm accessions were identified with complete immunity to infections, similar to those observed in field pea. Detailed studies on PSbMV in field pea have revealed different alleles of resistance genes each reacting with specific pathotypes. Similar studies for PSbMV in lentils could facilitate the development of pathotype-specific resistance markers, like those developed for field pea (Swisher Grimm and Porter, 2020). Australian breeding programmes would be greatly assisted by molecular markers capable of identifying resistance to specific PSbMV pathotypes, as large-scale resistance screening using exotic virus strains is both risky and difficult to implement.

ACKNOWLEDGEMENTS

This study was financially supported by the Grains Research and Development Corporation, Australia, and the Australian Centre for International Agricultural Research.

LITERATURE CITED

Abraham A., Makkouk K.M., 2002. The incidence and distribution of seed-transmitted viruses in pea and lentil seed lots in Ethiopia. *Seed Science and Technology* 30: 567–574.

Ademe A., Kumari S.G., Moukahel A., Alemu T., Abraham A., ... Ahmed S., 2025. Phylogenetic analysis, mixed infection and seed transmission of Pea seedborne mosaic virus in Ethiopia, *Physiological and Molecular Plant Pathology* 136: 102531. https://doi.org/10.1016/j.pmpp.2024.102531

Agriculture Victoria, 2022. Temperate pulse viruses: pea seed-borne mosaic virus. Accessed March 1, 2026, from https://agriculture.vic.gov.au/

Alconero R., Provvidenti R., Gonsalves D., 1986. Three pea seedborne mosaic virus pathotypes from pea and lentil germ plasm. *Plant Disease* 70: 783–786. https://doi.org/10.1094/PD-70-783

Alconero R., Hoch J.G., 1989. Incidence of pea seedborne mosaic virus pathotypes in the US national Pisum germplasm collection. *Annals of Applied Biology* 114: 311–315. https://doi.org/10.1111/j.1744-7348.1989.tb02107.x

Al Khalaf M., Kumari S.G., Haj Kassem A., Makkouk K.M., Al Chaabi A., 2009. Differentiation between susceptible and resistant faba bean, lentil and pea genotypes to Bean yellow mosaic virus on the basis of virus movement and multiplication. *Arab Journal of Plant Protection* 27: 165–173.

Bayaa B., Kumari S.G., Akkaya A.W., Erskine W., Makkouk K.M., ... Özberk, I., 1998. Survey of major bìotìc stresses of lentil in South-East Anatolia, Turkey. *Phytopathologia Mediterranea* 37: 88–95.

Bekele B., Kumari S.G., Ali K., Yusuf A., Makkouk K.M., ... Hailu D., 2005. Survey of viruses affecting legume crops in the Amhara and Oromia Regions of Ethiopia. *Phytopathologia Mediterranea* 44: 235–246. https://doi.org/10.14601/Phytopathol_Mediterr-1803

Bruun-Rasmussen M., Moller I.S., Tulinius G., Hansen J.K.R., Lund O.S., Johansen I.E., 2007. The same allele of translation initiation factor 4E mediates resistance against two Potyvirus spp. in Pisum sativum. *Molecular Plant-Microbe Interactions* 20: 1075–1182. https://doi.org/10.1094/MPMI-20-9-1075

Congdon B.S., Coutts B.A., Renton M., Banovic M., Jones R.A.C., 2016. Pea seed-borne mosaic virus in field pea: widespread infection, genetic diversity, and resistance gene effectiveness. *Plant Disease* 100: 2475–2482. https://doi.org/10.1094/PDIS-05-16-0670-RE

Coutts B.A., Prince R.T., Jones R.A.C., 2008. Further studies on Pea seed-borne mosaic virus in cool-season crop legumes: responses to infection and seed quality defects. *Australian Journal of Agricultural Research* 59: 1130–1145. https://doi.org/10.1071/AR08113

El Muadhidi M., Makkouk K.M., Kumari S.G., Jerjess M., Murad S.S., ... Tarik F., 2001. Survey for legume and cereal viruses in Iraq. *Phytopathologia Mediterranea* 40: 224–233.

FAOSTAT, 2026. United Nations Food and Agriculture Organization, Statistics Division, Rome, Italy. Accessed April 1, 2026, from https://www.fao.org/faostat/en/#data/QCL

Freeman A., Spackman M., Aftab M., McQueen V., King S., ... Rodoni B., 2013. Comparison of Tissue blot immunoassay and high throughput PCR for virus-testing samples from a southeastern Australian pulse virus survey. *Australasian Plant Pathology* 42: 675–683. https://doi.org/10.1007/s13313-013-0252-9

Freeman A., 2014. DAV00048 - Victorian pulse pathology and virology support program – Final Report. Grains Research and Development Corporation, Canberra, Australia. Accessed December 11, 2025, from https://grdc.com.au/research/reports/report?id=319

Gao Z., Johansen I.E., Eyers S., Thomas C.L., Ellis T.H.N., Maule A.J., 2004. The potyvirus recessive resistance gene, sbm1, identifies a novel role for translation initiation factor eIF4E in cell-to-cell trafficking. *The Plant Journal* 40: 376–385. https://doi.org/10.1111/j.1365-313X.2004.02215.x

Goodell J.J., Hampton R.O., 1984 Ecological characteristics of the lentil strain of pea seedborne mosaic virus. *Plant Disease* 68: 148–150. https://doi.org/10.1094/PD-68-148

Haddad N.J., Muehlbauer F.J., Hampton R.O., 1978. Inheritance of resistance to Pea seed-borne mosaic virus in lentils. *Crop Science* 18: 613–615. https://doi.org/10.2135/cropsci1978.0011183X001800040022x

Hampton R.O., 1982. Incidence of the lentil strain of Pea seedborne mosaic virus as a contaminant of Lens culinaris germ plasm. *Phytopathology* 72: 695–698. https://doi.org/10.1094/Phyto-72-695

Hampton R.O., Muehlbauer F.J., 1977. Seed transmission of the Pea seedborne mosaic virus in lentil. *Plant Disease Reporter* 61: 235–238.

Johansen I.E., Lund O.S., Hjulsager C.K., Laursen J., 2001. Recessive resistance in *Pisum sativum* and potyvirus pathotype resolved in a gene-for-cistron correspondence between host and virus. *Journal of Virology* 75: 6609–6614. https://doi.org/10.1128/JVI.75.14.6609–6614.2001

Jones R.A.C., Congdon B.S., 2024. Australian cool-season pulse seed-borne virus research: 1. Alfalfa and

cucumber mosaic viruses and less important viruses. *Viruses* 16: 144. https://doi.org/10.3390/v16010144

Kanawaty A., Kumari S.G., van Leur J., Hammadi H., 2017. Screening of lentil genotypes for resistance to *Bean yellow mosaic virus* and effect of mixed infection on the susceptibility of some resistant lentil genotypes. *Arab Journal of Plant Protection* 35: 171–177. https://doi.org/10.22268/AJPP-035.3.171177

Kasimor K., Bagget, J.R., Hampton, R.O., 1997. Pea cultivar susceptibility and inheritance of resistance to the lentil strain (pathotype P2) of pea seedborne mosaic virus. *Journal of the American Society for Horticultural Science* 122: 325–328. https://doi.org/10.21273/JASHS.122.3.325

Khetarpal R.K., Maury Y., 1987. Pea seed-borne mosaic virus: a review. *Agronomie* 7: 215–224. https://doi.org/10.1051/agro:19870401

Khadka R.B., Kumari S., van Leur J.A.G., 2024. Prevalence and incidence of lentil viruses in Nepal. *Abstract book of the 15th Australasian Plant Virology Workshop, 29–31 October 2024, Gold Coast, Australia*. Accessed January 15, 2026, from https://hdl.handle.net/10568/159867

Knights E. J. 1987. Lentil: A potential winter grain legume crop for temperate Australia. *Journal of the Australian Institute of Agricultural Science* 53: 271–280.

Kumari S.G., Makkouk K.M., Ismail L.D., 1993. Survey of seed-borne viruses in lentil in Syria and their effects on lentil yield. *Arab Journal of Plant Protection* 11: 28–32.

Kumari S.G., Makkouk K.M., 1995. Variability among twenty lentil genotypes in seed transmission rates and yield loss induced by pea seed-borne mosaic potyvirus infection. *Phytopathologia Mediterranea* 34: 129–132.

Kumari S.G., Larsen R., Makkouk K.M., Bashir M., 2009. Virus diseases and their control. In: *The lentil: botany, production and uses.* (W. Erskine, F. J. Muehlbauer, A. Sarker and B. Sharma, ed.), Cambridge, MA, USA, CABI Press, 306–325. https://doi.org/10.1079/9781845934873.0306

Kumari S.G., Moukahel A., El Miziani I., 2022. Diagnostic tools validated by ICARDA's Germplasm Health Unit (GHU) for detection of legume seed-borne pests. International Center for Agricultural Research in the Dry Areas (ICARDA), Beirut, Lebanon. Accessed January 15, 2026, from https://hdl.handle.net/10568/126879

Latham L.J., Jones R.A.C., 2001a. Alfalfa mosaic and pea seed-borne mosaic viruses in cool season crop, annual pasture, and forage legumes: susceptibility, sensitivity and seed transmission. *Australian Journal of Agricultural Research* 52: 771–790. https://doi.org/10.1071/AR00165

Latham L.J., Jones R.A.C., 2001b. Incidence of virus infection in experimental plots, commercial crops, and seed stocks of cool season crop legumes. *Australian Journal of Agricultural Research* 52: 397–413. https://doi.org/10.1071/AR00079

Maina S., Jones R.A.C., 2023. Enhancing biosecurity against virus disease threats to Australian grain crops: current situation and future prospects. *Frontiers in Horticulture* 2: 1263604. https://doi.org/10.3389/fhort.2023.1263604

Maina S., van Leur J., Ghorbanic A., Jones R.A.C., 2025. Analysis of 40 new isolates of bean yellow mosaic virus reveal important new insights into its phylogeny, evolutionary dynamics and biology. *Proceedings of the 16th International Symposium of Plant Virus Epidemiology, São Paulo, Brazil*. Accessed January 15, 2026, from https://ispve2025.com/files/ispveprocbook.pdf

Makkouk K.M., Bashir M., Jones R.A.C., Kumari S.G., 2001. Survey for viruses in lentil and chickpea crops in Pakistan. *Journal of Plant Diseases and Protection* 108: 258–268. https://www.jstor.org/stable/45154856

Makkouk K.M., Kumari S.G., Shahraeen N., Fazlali Y., Farzadfar S., … Reza Mansouri A., 2003. Identification and seasonal variation of viral diseases of chickpea and lentil in Iran. *Journal of Plant Diseases and Protection* 110: 157–169.

Materne M., Reddy A.A., 2007. Commercial cultivation and profitability. In: *Lentil: An Ancient Crop for Modern Times.* (S.S. Yadav, D.L. McNeil and P.C. Stevenson, ed.), Dordrecht, The Netherlands, Springer, 173–186.

McKirdy S.J., Jones R.A.C., Latham L.J., Coutts B.A., 2000. Bean yellow mosaic potyvirus infection of alternative annual pasture, forage, and cool season crop legumes: susceptibility, sensitivity, and seed transmission. *Australian Journal of Agricultural Research* 51: 325–345. https://doi.org/10.1071/AR99110

Montejano-Ramírez V., Valencia-Cantero E., 2024. The importance of lentils: An Overview. *Agriculture* 14, 103. https://doi.org/10.3390/agriculture14010103

Mustafayev E., Kumari S.G., Attar N., Zeynal A., 2011. Viruses infecting chickpea and lentil crops in Azerbaijan. *Australasian Plant Pathology* 40: 612–620. https://doi.org/10.1007/s13313-011-0094-2

Provvidenti R., Alconero R. 1988. Inheritance of resistance to a lentil strain of pea seed-borne mosaic virus in *Pisum sativum*. *Journal of Heredity* 79:45-47. https://doi.org/10.1093/oxfordjournals.jhered.a110444

Provvidenti R., Hampton R.O., 1991. Chromosomal distribution of genes for resistance to seven potyviruses in *Pisum sativum*. *Pisum Genetics* 23: 26–28.

Rashed A., Feng X., Prager S.M., Porter L. D., Knodel J.J., ... Eigenbrode S.D., 2018. Vector-borne viruses of pulse crops, with a particular emphasis on North American cropping system. *Annals of the Entomological Society of America* 111: 205–227. https://doi.org/10.1093/aesa/say014

Simmons H.E., Munkvold G.P., 2014. Seed transmission in the Potyviridae. In: *Global perspectives on the health of seeds and plant propagation material*. Dordrecht, The Netherlands, Springer, 3–15.

Slinkard A.E., 1988. Indianhead lentil as an annual legume green manure crop for Western Canada. *Canadian Journal of Plant Science* 68: 838.

Swisher Grimm K.D., Porter L.D., 2020. Development and validation of KASP markers for the identification of pea seedborne mosaic virus Pathotype P1 resistance in *Pisum sativum*. *Plant Disease* 104: 1824–1830. https://doi.org/10.1094/PDIS-09-19-1920-RE

Tadesse N., Ali K., Gorfu D., Yusuf A., Abraham A., ... Kumari S.G., 1999. Survey for chickpea and lentil viruses in Ethiopia. *Phytopathologia Mediterranea* 38: 149–158.

Thackwray E.L., Materne M.A., Shunmugam A.S., Henares B.M., Lee R.C., Kamphuis L.G., 2024. The history and pedigree of Australian lentil cultivars. *Legume Science* 6: p.e70006. https://doi.org/10.1002/leg3.70006

van Leur J.A.G., Freeman A., Aftab M., Spackman M., Redden B., Materne M., 2013a. Identification of seedborne *Pea seed-borne mosaic virus* in lentil (*Lens culinaris*) germplasm and strategies to avoid its introduction in commercial Australian lentil fields. *Australasian Plant Disease Notes* 8: 75–77. https://doi.org/10.1007/s13314-013-0099-5

van Leur J.A.G., Kumari S.G., Aftab M., Leonforte A., Moore S., 2013b. Virus resistance of Australian pea (*Pisum sativum*) varieties. *New Zealand Journal of Crop and Horticultural Science* 41: 86–101. https://doi.org/10.1080/01140671.2013.781039

van Leur J., Aftab M., Freeman A., 2025. Pea seed-borne mosaic virus pathotypes isolated from Australian pea (*Pisum sativum*) seed. *Phytopathologia Mediterranea* 64: 71–76. https://doi.org/10.36253/phyto-15934

Wang D., Maule A.J., 1994. A model for seed transmission of a plant virus: Genetic and structural analysis of pea embryo invasion by Pea seed-borne mosaic virus. *The Plant Cell* 6: 777–787. https://doi.org/10.1105/tpc.6.6.777

Wale M., Jembere, B., Seyoum E., 2000. Biology of the pea aphid, *Acyrthosiphon pisum* (Harris) (Homoptera: Aphididae) on cool-season legumes. *International Journal of Tropical Insect Science* 20: 171–180. https://doi.org/10.1017/S1742758400019603

Wilson V.E., Muehlbauer F.J., 1983. Registration notice: 'Redchief' lentil. *Crop Science* 23: 802–803. https://doi.org/10.2135/cropsci1983.0011183X002300040062x

Zohary D, 1972. The wild progenitor and the place of origin of the cultivated lentil: *Lens culinaris*. *Economic Botany* 26, 326–332. https://doi.org/10.1007/BF028607

Phytopathologia Mediterranea
The international journal of the
Mediterranean Phytopathological Union

Firenze University Press
www.fupress.com/pm

Research Papers

Detection and persistence of *Bacillus*- and *Trichoderma*-based biocontrol products on lemon plants

Giuseppa Rosaria LEONARDI[1], Amanda VACCALLUZZO[1], Giorgio GUSELLA[1,*], Greta LA QUATRA[1], Alessandra PINO[1,2], Dalia AIELLO[1], Cinzia CAGGIA[1,2], Cinzia L. RANDAZZO[1,2], Giancarlo POLIZZI[1]

[1] *Department of Agriculture, Food and Environment, University of Catania, 95123 Catania, Italy*
[2] *ProBioEtna SRL, Spin off from the University of Catania, 95123 Catania, Italy*
*Corresponding author. Email: giorgio.gusella@unict.it

Summary. Knowledge of the ecology of biological control agents (BCAs), previously reported to be effective against the citrus vascular pathogen *Plenodomus tracheiphilus*, is required to improve scheduling of BCA field applications. Culture-dependent methods (dilution plate and direct plating) and culture-independent qPCR assays were used to determine survival of *Bacillus amyloliquefaciens* QST 713 and *Trichoderma asperellum* ICC 012 + *T. gamsii* ICC 080 on citrus stem and leaf tissues following foliar applications, and root endospheres and rhizospheres following root drenches with these *Trichoderma* BCAs. Viable population levels of *B. amyloliquefaciens* did not change over time on treated stems, whereas these decreased in leaf samples after 14 d. The qPCR assay detected *B. amyloliquefaciens* in all collected samples, with no temporal changes in population levels. Although the qPCR assay detected *T. asperellum* and *T. gamsii* in leaf and stem tissues, these fungi were isolated only from stem tissues, with increased isolations at 21 d post treatment compared with 7 d. Neither qPCR nor culturing detected *Trichoderma* species in citrus vascular root tissues. However, qPCR and culturing detected these fungi in host rhizospheres at 7, 14 and 21 d post inoculation, confirming their rhizosphere competence. This study has provided insights into colonization and survival within citrus plants of *B. amyloliquefaciens* and *T. asperellum* + *T. gamsii* contained in commercial biocontrol products. These indicate that integrating qPCR and culture-dependent approaches is important for detecting and quantifying these BCAs. The endophytic lifestyle of *B. amyloliquefaciens* and *T. asperellum* + *T. gamsii* makes them likely to provide long-term biological control. These results also indicate that the selected *Bacillus* and *Trichoderma* agents could spread and colonize citrus tissues over extended periods, and especially after host pruning or damage, which could promote plant colonization and protection from pathogens.

Keywords. BCA, citrus, endophytic colonization, monitoring, qPCR.

OPEN ACCESS

Citation: Leonardi, G. R., Vaccalluzzo, A., Gusella, G., La Quatra, G., Pino, A., Aiello, D., Caggia, C., Randazzo, C. L., & Polizzi, G. (2026). Detection and persistence of *Bacillus*- and *Trichoderma*-based biocontrol products on lemon plants. *Phytopathologia Mediterranea* 65(1): 133-152. doi: 10.36253/phyto-16863

Accepted: April 11, 2026

Published: May 14, 2026

©2026 Author(s). This is an open access, peer-reviewed article published by Firenze University Press (https://www.fupress.com) and distributed, except where otherwise noted, under the terms of the CC BY 4.0 License for content and CC0 1.0 Universal for metadata.

Data Availability Statement: All relevant data are within the paper and its Supporting Information files.

Competing Interests: The Author(s) declare(s) no conflict of interest.

Editor: Ali Siah, UMR 1158 BioEcoAgro, Yncréa HdF, Lille, France.

ORCID:
GRL: 0000-0002-4676-5100
AV: 0000-0002-4902-1799
GG: 0000-0002-0519-1200
AP: 0000-0001-8246-106X
DA: 0000-0002-6018-6850
CC: 0000-0002-2688-9536
CLR: 0000-0002-1243-5357
GP: 0000-0001-8630-2760

INTRODUCTION

Citrus types are among the most economically important fruit crops, appreciated by consumers for the high amounts they contain of health-pro-

moting nutrients and bioactive compounds, such as flavonoids, phenolic acids, vitamins, carotenoids, pectins, and fatty acids (Liu *et al.,* 2022). Citrus cultivation is distributed in tropical, subtropical and Mediterranean climatic regions, expanded from East Asia to all continents on a total of 12.7 million ha (FAOSTAT, 2024; Istat, 2024). Italy is the second-largest producer of oranges and the third-largest producer of lemons, reaching production of nearly 3.1 million tons (FAOSTAT, 2024; Istat, 2024).

Several abiotic and biotic factors affect citrus production (Timmer *et al.,* 2000). Several Ascomycete fungi, which infect wood through natural openings or pruning wounds and colonize host vascular tissues, are involved in twig, branch, and trunk diseases of citrus. Wind, hail and frost damage, sunscald, overhead irrigation, and mechanical injuries can facilitate citrus infections by fungi (Fawcett 1936; Aiello *et al.,* 2023; Leonardi *et al.,* 2023a). *Plenodomus tracheiphilus* (syn. *Phoma tracheiphila*), the causal agent of Mal secco disease, is considered to be the major destructive fungal disease, causing twig and branch wilt and dieback, with serious economic impacts on citrus industry of the Mediterranean and Black Sea regions (Catara and Cutuli, 1972; Solel and Salerno, 2000). *Colletotrichum* spp. are generally recognized as important pathogens in all cultivated *Rutaceae*, causing stem-end rots, and twig and branch dieback (Timmer *et al.,* 2000; Mayorquin *et al.,* 2019; Leonardi *et al.,* 2023a). Species in *Botryosphaeriaceae* and *Diaporthaceae* have also been reported to cause cankers, gummosis, blight and dieback in different citrus-producing countries (Polizzi *et al.,* 2009; Huang *et al.,* 2013; Guarnaccia and Crous, 2017; Gusella *et al.,* 2025), as well as other fungal genera including *Fusarium*, *Neocosmospora*, *Peroneutypa*, and *Phaeoacremonium* (Timmer 2000; Mayorquin *et al.,* 2016; Sandoval-Denis *et al.,* 2018; Espargham *et al.,* 2020; Gusella *et al.,* 2025).

Management of fungal pathogens affecting the vascular systems and woody tissues of plants is difficult, because no effective treatments can protect hosts once pathogens have colonized internal host tissues. Management relies on application of fungicides or on agronomic practices (e.g., sanitation), when varietal resistance cannot be achieved (EFSA PHL, 2014; 2023; Vitale *et al.,* 2021). Frequent use of chemical fungicides in agriculture has raised concerns about phytotoxicity, development of resistant pathogen strains, soil accumulation, and negative effects on environments and human health (European Chemicals Agency, 2018; Piel *et al.,* 2019; Triantafyllidis *et al.,* 2020; Dao *et al.,* 2021; Burandt *et al.,* 2024). Based on scientific assessments of chemical toxicity, the European Union (EU) has approved laws that result in banning or restriction of their use by imposing decreased maximum residue limits (MRLs) (Clark *et al.,* 2002; EFSA 2020; European Commission, 2020). Some chemicals, such as copper compounds authorized for the control of *Alternaria* spp., *Colletotrichum* spp., and *P. tracheiphilus*, have been classified by the EU as candidates for substitution (European Commission, 2018), with the aim of finding alternative substances that are environmentally friendly and cost-effective.

Biological control of plant diseases using endophytic microorganisms able to colonize the same ecological niches as pathogens, and that have antagonist activity, have been widely investigated. Among biological control agents (BCAs), bacteria and fungi that are used to manage plant diseases are reported as rapid colonizers of phyllospheres, endospheres or rhizosphere (Kalai-Grami *et al.,* 2014a, 2014b; Dimaria *et al.,* 2023; Giordano *et al.,* 2023; Nascimento *et al.,* 2023; Tan *et al.,* 2025).

Bacillus and *Trichoderma* spp. have been widely studied for abilities to control citrus plant pathogens, through different biocontrol mechanisms (Weideman and Wehner, 1993; Agostini *et al.,* 2003; Kalai-Grami *et al.,* 2014a, 2014b; Kupper *et al.,* 2011, 2019; Chen *et al.,* 2020; Ferreira *et al.,* 2020; Kalimutu *et al.,* 2020; Ezrari *et al.,* 2021; Silvia, 2021; Aiello *et al.,* 2022; Calcagnile *et al.,* 2022; Khuong *et al.,* 2023; Leonardi *et al.,* 2023b; Phal *et al.,* 2023; Lombardo *et al.,* 2024; Zhou *et al.,* 2024). Activity of these microorganisms is linked to production of biodegradable biological molecules that can inhibit pathogen growth, induce systemic resistance, and/or compete with pathogens for nutrient resources (Lugtenberg and Kamilova, 2009; Ezrari *et al.,* 2021).

Trichoderma and *Bacillus* are part of the microbiota of healthy plant tissues, without causing disease but assisting host plants to defend against biotic and abiotic stresses (Chen *et al.,* 2020; Fontana *et al.,* 2021). For these reasons, several *Trichoderma* and *Bacillus* species have been identified as potential biocontrol agents, and some have been developed as biocontrol agents in commercial formulations. Among these, Serenade®Aso, containing *Bacillus amyloliquefaciens* strain QST 713 (formerly *B. subtilis*), and Remedier®, containing *T. asperellum* isolate ICC 012 and *T. gamsii* isolate ICC 080, are currently registered in Italy (Ministero della Salute, 2025). Recent studies have demonstrated the efficacy of these agents for controlling symptoms of leaf vein chlorosis caused by *P. tracheiphilus* on Volkamer lemon plants in controlled growth conditions (Aiello *et al.,* 2022; Leonardi *et al.,* 2023b; Leonardi *et al.,* 2026).

Because of increased interest in the use of BCAs in integrated management of citrus diseases, knowledge on their colonization and survival within plant systems is important for achievement of disease control, and for

scheduling BCA applications (Torsvik and Øvreås, 2002; Timofeeva *et al.,* 2023). Some *Trichoderma* and *Bacillus* species inhabit soil and plants, with ability to colonize rhizospheres and endospheres of several crop plants (Bae *et al.,* 2009; Labiadh *et al.,* 2021; Tseng *et al.,* 2020; Wang *et al.,* 2021). However, few investigations have assessed endophytic colonization ability of *Bacillus amyloliquefaciens* in citrus plants, and these have only used culture-dependent methods (Kalai-Grami *et al.,* 2014a; Aiello *et al.,* 2022). Although time-consuming for field monitoring, culture-dependent methods have been the most widely used for quantifying BCA population levels. Alternative culture-independent methods, including quantitative polymerase chain reactions (qPCRs), have been proposed for more sophisticated detection and quantification of *Bacillus* spp. and *Trichoderma* spp. selected as plant pathogen BCAs (Rubio *et al.,* 2005; Savazzini *et al.,* 2008; Johansson *et al.,* 2014; Mendis *et al.,* 2018; Stummer *et al.,* 2020; Xie *et al.,* 2020; Li *et al.,* 2021; Su *et al.,* 2024). qPCR assays have been validated on grapevine bunches, wood and soil for quantification of *Bacillus* and *Trichoderma* (Rotolo *et al.,* 2016; Gerin *et al.,* 2018).

The aim of the present study was to accurately detect and quantify, over time, the levels of *B. amyloliquefaciens* QST 713 and *T. asperellum* ICC 012 + *T. gamsii* ICC 080 within the vascular tissues of lemon seedlings, after application of these two formulations under controlled growth conditions, using culture-dependent and molecular methods.

MATERIALS AND METHODS

Plant material and growth conditions

Ten-month-old seedlings of Volkamer lemon (*Citrus volkameriana*) were previously grown in a nursery greenhouse in Catania province (Eastern Sicily, Italy), and were maintained in plastic trays (850 mm^2 and 900 mm deep). The plants were obtained by sowing healthy seeds on a commercial substrate (90% blond peat + 10% perlite) to which had been added an organic fertilizer (35–40% KNO_3, 0.3–1% $CuSO_4 \cdot 5H_2O$, 0.1–0.2% BH_3O_3, 0.1–0.2% $ZnSO_4$) at 1 kg m^{-3}), and a micronutrient fertilizer (15% Fe, 2.5% Mn, 0.20% B, 1% Cu, 1% Zn, 0.04% Mo) at 300 g m^{-3}. Two weeks before experiments were carried out, the seedling trays were transferred to a growth chamber at the Department of Agriculture, Food and Environment, University of Catania, which was maintained at 25°C, 80% relative humidity (RH), and with a daily cycle of 16 h light and 8 h darkness.

BCA selection and preparation

To assess the endophytic colonization ability of the BCAs on citrus plants, the commercial BCA formulations Serenade® Aso, containing *B. amyloliquefaciens* (formerly *B. subtilis*) isolate QST 713 at 1.05×10^{12} CFU L^{-1} (Bayer CropScience) and Remedier®, containing *T. asperellum* isolate ICC 012 + *T. gamsii* isolate ICC 080 at 3×10^7 CFU g^{-1} (Gowan Crop Protection), were selected from BCAs that had previously been shown to minimize symptoms caused by *P. tracheiphilus* (Aiello *et al.,* 2022; Leonardi *et al.,* 2023b; Leonardi *et al.,* 2026). Before commencing applications to the plants, the viability of the BCAs was confirmed by plating the respective product suspensions on Potato Dextrose Agar (PDA) (Lickson).

Foliage and root applications

Colonization ability of *B. amyloliquefaciens* into *C. volkameriana* plants was assessed on leaves and stems (from foliar applications), whereas *Trichoderma* spp. colonization was assessed on leaves and stems (foliar applications), into root endospheres and into soil rhizospheres (root applications). Each of these was considered as a distinct experimental treatment, since effectiveness had been previously confirmed through root drench applications (Leonardi *et al.,* 2026). Prior to the foliar BCA applications, wounds were made by pruning plant stem tips to 5 cm length to favour microbial colonization of the vascular systems.

Both commercial products were prepared according to the label rates (167 g hL^{-1} for the *Trichoderma*-based product, and 533 mL hL^{-1} for the *Bacillus*-based product). Inoculations were carried out by spraying 300 mL of each formulation (100 mL per replicate) onto all plant canopy with a manual sprayer. For the foliar treatments, inoculation controls consisted of seedlings pruned and then sprayed with sterile deionized water (SDW). Root applications each consisted of a 30 mL drench of the commercial products at the rates described above. Experimental control treatments were with 30 mL of SDW. The foliar-treated plants were then allowed to dry for around 4 h, and all plants were then transferred into a growth chamber maintained at 25 ± 1°C, 80% relative humidity (RH), with a photoperiod of 16 h light and 8 h darkness. A total of 45 seedlings were used for each treatment (foliar or root), with three replicates per treatment, each including 15 seedlings.

Leaf and stem collections

To evaluate development of *Bacillus* or *Trichoderma* within the inoculated tissues after treatments, three post-treatment collection were made at 7, 14, and 21 d after treatments. At each collection, 15 seedlings (five per replicate) were randomly selected for analyses. From each plant, a 5 cm stem section from the artificial wound was collected, together with three leaves from the same stem portion, so each seedling was divided into stem and leaf tissue. The samples were washed under tap water and surface sterilized using the protocols of Mushtaq *et al.* (2019) for endophyte isolation from citrus leaf vascular tissues, and Araújo *et al.* (2002) for isolation from stems, with some modifications. Leaf samples were sterilized in 1% sodium hypochlorite solutions for 5 min, followed by three washes in SDW. Stem samples were sterilized in 70% ethanol for 5 min, sodium hypochlorite solution (2.5% available Cl^-) for 5 min, and 70% ethanol for 30 s, followed by two washes in SDW. To confirm that leaf and stem samples were disinfested of contaminants, aliquots of the sterile distilled water used in each final rinse were plated on PDA, and the plates were examined for microbial growth after incubation at 25 ± 1°C for 3 to 5 d. After thorough drying, the leaves and stems (after aseptic bark removal), were cut longitudinally. Half of the leaf and stem tissues was then processed for culture-dependent analysis, and the other half for qPCR analysis.

Rhizosphere and root collections

Collection of rhizosphere samples was carried out as described by Xu *et al.* (2022), with modifications. Fine roots (approx. 1 mm diam.) were collected from each plant to a depth of 5-6 cm, and were gently shaken to remove soil not tightly attached to the roots. Adherent soil surrounding the roots was then carefully scraped off with a hairbrush, and collected to obtain 2 g per replicate (each of five plants). One g of rhizosphere soil was immediately stored at -80°C for DNA extraction. The fine roots were used to determine populations of *Trichoderma* in the endospheres.

Culture-dependent detection of Bacillus *from leaf and stem tissues*

A total of 1 g of each leaf or stem tissue sample was homogenized by mortar and pestle in 5 mL of sterile-filtered phosphate-buffered saline (PBS 1X; Thermo Scientific), and serial dilutions (10^{-1} to 10^{-4}) from each sample were plated onto PDA plates. A total of nine plates per replicate were used, with three replicates per time after inoculation. The plates were incubated at 25 ± 1°C for 48 h, and developed bacterial colonies were then subcultured onto Nutrient Agar (NA) and identified based on colony morphology. Bacterial population densities were estimated by counting the colonies, and were expressed as colony-forming units (CFU) per g of sample fresh weight determined from numbers of CFU mL^{-1} of sample plated, and the dilution factors.

Colonies morphologically identified as *Bacillus* were molecularly characterized. Their DNA was extracted and sent to Macrogen Inc. (Seoul, Republic of Korea) for PCR and sequencing. The 16S rDNA was amplified using the primers 27F/1492R (Somerville *et al.,* 2020), and the *gyrA* gene regions were amplified using primers 42f/1066r (Chun and Bae 2000). The DNA sequences generated were assembled with Lasergene SeqMan Pro (DNASTAR), deposited in GenBank (https://www.ncbi.nlm.nih.gov/), and compared with the NCBI GenBank nucleotide database using the standard nucleotide Basic Local Alignment Search Tool (BLAST) (https://blast.ncbi.nlm.nih.gov/Blast.cgi).

Culture-dependent detection of Trichoderma *from leaf and stem tissues*

For fungal isolations, leaf and stem samples were surface sterilized and processed using the methods described above for *Bacillus*-treated plants. Although PDA was used under the same conditions to allow simultaneous recovery of fungi and bacteria, to ensure accurate detection and quantification of *Trichoderma* and to allow for rapid growth of these fungi, isolations from plant samples treated with *Trichoderma* were also carried out on Rose Bengal-chloramphenicol agar (RBA; Biolife), a selective medium for these fungi (Qiao *et al.,* 2018; Zanfaño *et al.,* 2024).

In addition to the plate dilution technique, direct plating was also used for *Trichoderma*, because rapid growth and filamentous habit of these fungi can affect colony separation. Stem and leaf sections were cut into 4 to 6 mm pieces, and placed onto RBA amended with 100 mg L^{-1} of streptomycin sulfate (Sigma-Aldrich) to prevent bacterial growth. Plates were then incubated at 25 ± 1°C in the dark for 4 to 6 d or until fungal growth was observed. Population densities were estimated by calculating the isolation frequency (IF) as the percentage of tissue fragments that yielded colonies morphologically resembling *T. asperellum* or *T. gamsii*, out of the total number of fragments plated per replicate (including tissue collected from five plants). Other *Trichoderma*-like

colonies were not counted, but representative colonies were chosen and molecularly characterized to confirm their identities. A total of nine plates per replicate, each containing eight leaf or stem fragments, were used for isolations at each collection time. *Trichoderma asperellum* and *T. gamsii* colonies obtained were firstly identified based on culture characteristics (colony appearance, upper and lower surface colours, borders, texture, conidia), and were molecularly characterized.

The collected colonies distinguished based on morphotype were grown on PDA for 5 d, and genomic DNA was then extracted. Mycelium was scraped off and processed using the Wizard Genomic DNA Purification Kit® according to the manufacturer's protocol (Promega Corporation). DNA samples obtained were stored at 4°C until processed. The DNA-directed RNA polymerase II second largest subunit gene (*rpb2*) was amplified with primers RPB2-5F2 (Sung *et al.,* 2007) and fRPB2-7cr (Liu *et al.,* 1999), and the PCR amplification products were estimated visually by electrophoresis on 1% agarose gels and sent to Macrogen Inc. (Seoul, Republic of Korea) for purification and sequencing. The DNA sequences generated were assembled, deposited in GenBank, and compared with reference sequences in the NCBI GenBank nucleotide database, as outlined (above) for *Bacillus*.

Culture-dependent detection of Trichoderma *from roots and rhizospheres*

Root samples were washed with tap water and sterilized using the methods of Trivedi *et al.* (2011), with some modifications. Root segments were immersed in sodium hypochlorite solution (2.5% available Cl^-) for 5 min, and then washed five times in SDW. For a sterility checks, aliquots of each last rinse water were plated onto PDA and RBA plates. Isolation of fungi from roots were carried out using agar dilution and direct plating of wood fragments. Samples (1 g each) were homogenized using a mortar and pestle in 5 mL of sterile PBS, and the homogenized samples were then used to prepare serial dilutions (10^{-1} to 10^{-4}) which were plated on RBA amended with 100 mg L^{-1} of streptomycin sulfate. Roots were also cut into fragments and plated onto RBA medium amended with 100 mg L^{-1} of streptomycin sulfate to prevent bacterial growth. Plates were then incubated at 25 ± 1°C in the dark for 6 d until fungal growth was observed.

Isolations from rhizospheres were carried out using the plate-dilution method of Xu *et al.* (2022). Collected rhizosphere soil (1 g) was suspended in 9 mL of PBS buffer, and then shaken at 250 rpm for 40 min. The resulting suspension was serially diluted at tenfold intervals to 10^{-4} dilution. Aliquots of each dilution were then spread onto three replicate RBA plates.

Trichoderma population densities were estimated by counting fungal colonies on plates, and were expressed as CFU g^{-1} fresh weight of soil or root, and (only for roots), calculating the IF as described above. A total of nine plates per replicate were used for direct plating, each containing eight root fragments, with three replicates per interval. *Trichoderma* colonies obtained from treated and untreated rhizosphere soil were first identified based on culture characteristics, and pure cultures were also molecularly characterized based on the *rpb2* gene, as described above.

Extractions of total bacterial and fungal genomic DNA from plant tissue and rhizosphere samples

Leaf, stem and root tissues, collected at 7, 14 and 21 d, were crushed and ground to powder in liquid nitrogen, and totals of 300 or 600 mg of plant tissue was collected from each replicate and stored at -80°C until DNA extraction. Total bacterial and fungal genomic DNA (gDNA) were extracted using the DNeasy Plant Pro kit (Qiagen), according to the manufacturer's instructions and with slight modifications. To improve the extraction yields, the samples were each twice homogenized with a Precellys Evolution homogenizer (Bertin Technologies) at 4,500 rpm, with each homogenizing separated by a pause on ice. After tissue destruction, the samples were subjected to extraction and purification steps according to the kit procedures.

The same protocol and extraction kit were adopted (with modifications) for DNA isolations from soil samples. Prior to the bead beating step, DNA yield was improved by heating each soil samples (100 mg) to 65°C for 10 min in the presence of lysis solution. After incubation, the steps described above were followed.

For all the samples, the gDNA concentrations were determined with a Qubit 4.0 fluorometer (Invitrogen), and purity was checked with a NanoDrop spectrophotometer (Thermo Scientific). The gDNA templates obtained were stored at -20°C, and were subjected to qPCR detection.

qPCR monitoring of Bacillus amyloliquefaciens

For the molecular detection of *B. amyloliquefaciens* QST 713, species-specific primers were used to detect colonization of the inoculated BCA, at different sampling times. The protocol of Rotolo *et al.* (2016) was used for the qPCR analyses. The reaction mixtures each consisted of 10 µL of QuantiNovaTM SYBR Green PCR

Kit (Qiagen), 10 µM of each primer BS_yndJ-F (AATGACCGTGCTCCATCTGTAA) and BS_yndJ-R (TTCCGATCTTACGGATTGCT), 5 µL of Dnase/Rnase-free water and 3 µL of templated gDNA. The amplification cycles included an initial pre-denaturation step (Hold) at 95°C for 3 min, followed by 40 cycles, each of denaturation at 95°C for 10 s, annealing at 58°C for 45 s, and extension 72°C for 60 s. The melting temperatures were set between 55°C and 95°C. The slope of the regression curve obtained by plotting the logarithm of DNA concentrations against corresponding mean cycle thresholds (Ct values) was used to determine primer efficiency, according to the equation: E=0.5 (10(-1(-1*slope*)) × 100.

To assess reaction efficiency, gDNA from the *B. amyloliquefaciens* QST 713 isolate (Serenade® Aso) was extracted using the PureLink™ Genomic DNA Mini Kit (Thermo Fisher Scientific), and was used as a reference sample to generate standard curves. Standard curves were established by serially diluting the QST 713 gDNA to obtain concentrations ranging between 12 and 5 log CFU mL^{-1}. Quantitative PCR assays were carried out using a Rotor-Gene Q thermocycler (Qiagen), and each sample was analyzed in triplicate.

qPCR monitoring of Trichoderma asperellum *and* Trichoderma gamsii

For detections of *T. asperellum* and *T. gamsii*, a Duplex-qPCR was set up, following the protocol of Gerin *et al.* (2018), to monitor the colonization by fungal formulation at different sampling times. The reaction mixtures were each prepared using 10 µL of QuantiNovaTM SYBR Green PCR Kit (Qiagen), 0.25 µM of each of the primers, and 0.15 µM of each of the probes as:
for *T. asperellum*;
Ta_rpb_fw (GGAGGTCGTTGAGTACGAA),
Ta_rpb2_rev_3 (TTGCAATAGGATTTACGACGAGT),
Ta_rpb2_probe (FAM-CGCTGAGGTATCCCCATGCGACA-BHQ1),
and for *T. gamsii*;
Tg_rpb2_fw (GCCACCTGGTTGACCAAGGA),
Tg_rpb2_rev (CGCACCAGCCCTGATCA), and
Tg_rpb2_probe (HEX-CCTCCAGAAGACCCAAGCATGAAGCTC-BHQ1).

Dnase/Rnase-free water (5.4 µL) and 2 µL of templated DNA was included in each reaction. The amplification cycles each included an initial pre-denaturation step (Hold) at 95°C for 2 min, followed by 40 cycles each of denaturation at 95°C for 5 s, annealing at 62°C for 30 s, and extension 65°C for 30 s. The melting temperature was set in the range of 65°C to 95°C. The slopes of the regression curves were calculated as described above.

To ensure reaction efficiency, total gDNA of the *T. asperellum* and *T. gamsii* mixture isolates was isolated using the QIAamp DNA Mini kit, with some adjustments in the initial steps (below). Mycelium of the two species, grown on agar plates, was collected and dissolved in phosphate buffered saline (PBS, pH 8.0), to allow washing of conidia and removal of extracellular parts. Each solution was centrifuged at 7,500 rpm for 10 min. Subsequently, the resulting pellet was resuspended in 180 µL of 2 mM EDTA solution and incubated in Thermomix for 30 min at 37°C. Following this, 20 µL of proteinase K and 200 µL of lysis buffer (provided with the kit) were added, and the samples were then incubated at 56°C for 30 min and then at 95°C for 15 min. The solutions were then transferred to bead-beater vials for mechanical lysis (9,000 rpm for 2 min with pause on ice). The solutions were transferred to purification columns provided by the kit for the final purification steps, according to the kit manufacturer instructions. qPCR standard curves were each obtained by serially diluting the DNA mixture to concentrations from 1.13×10^{10} to 1.13×10^{3} conidia mL^{-1}. The qPCR reactions were carried out with a Rotor Gene Q instrument (Qiagen). Each sample was assayed in triplicate.

Data analyses

All CFU data from dilution plate isolations and from qPCR assays were log-transformed, and the percentage IFs from direct plating isolations were arcsine (sin^{-1} square root x) transformed, to meet the assumptions of homogeneity of variance, which were determined using Levene's test. A primary analysis of variance (ANOVA) was then carried out for each experimental treatment, by calculating F and the associated P values to evaluate whether effects of single factors (i.e. treatment, time, and sample type) and their interactions, were statistically significant. *Post hoc* comparisons were conducted on significant interactions using Tukey's HSD test ($\alpha = 0.05$). When no significant interaction was detected, the main effect of a single factor was evaluated separately using one-way ANOVA.

RESULTS

Culture-dependent detection of Bacillus amyloliquefaciens *in leaf and stem tissues*

At each collection time, bacterial colonies developed from treated samples as determined using the culture-dependent method (Figures 1 and 2). Developed colonies

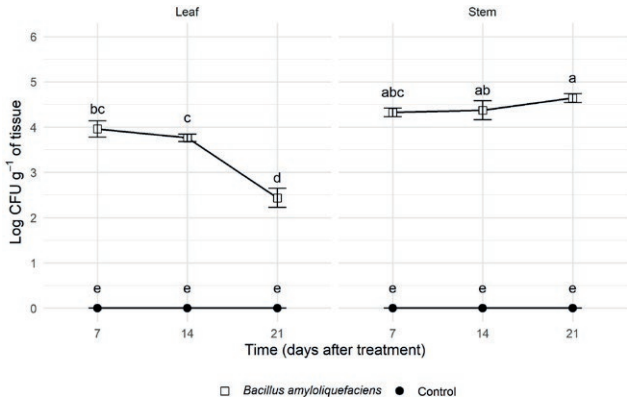

Figure 1. Mean numbers (± standard errors) of *Bacillus amyloliquefaciens* (expressed as Log CFU g^{-1} of tissue) detected in citrus leaf or stem tissues at 7, 14 or 21 d after treatment using a culture-dependent method. Results were from *Bacillus*-treated (open symbols) and control plants (close symbols) using the agar dilution technique. Different letters accompanying symbols indicate differences ($\alpha = 0.05$) among combined factors (treatment × sample × time), according to Tukey's HSD tests.

in the cultures had smooth and sticky surfaces, and were protruding with slightly irregular edges (Figure 2) (Qiao *et al.,* 2024). A culture of a representative strain (BA1) was molecularly characterized, and 16S rDNA (Acc. No. PX559962) and *gyrA* (Acc. No. PX571115) gene sequences of this culture were deposited in GenBank. Comparison of the sequences obtained with those present in the NCBI nucleotide database showed 99.75% similarity for 16S rDNA with different *Bacillus* species isolates (including *B. amyloliquefaciens* isolate D3, Acc. No. KR871014.1), and 99.80% similarity for the *gyrA* gene with different *B. amyloliquefaciens* isolates (including, INH2-4b Acc. No. CP061852). No colonies resembling *Bacillus* were obtained from the controls through using the culture-based method.

Bacillus amyloliquefaciens concentrations from leaf samples were 3.96 log CFU g^{-1} after 7 d, 3.76 log CFU g^{-1} after 14 d, and 2.43 log CFU g^{-1} after 21 d in culture. From stem samples, *B. amyloliquefaciens* concentrations were 4.32 log CFU g^{-1} after 7 d, 4.32 log CFU g^{-1} after 14 d, and 4.64 log CFU g^{-1} after 21 d in culture. Homogeneity of variances was confirmed by Levene's test ($F = 0.9311$, $P = 0.53$). The multifactor ANOVA showed that the single factors, (treatment, sample type, collection time), and the combinations of these factors, influenced the respective *Bacillus* populations ($P < 0.001$). Tukey's *post hoc* test of the combined factors (treatment × sample type × collection time), showed that *Bacillus*-treated samples differed in microbial populations within leaf and stem tissues from those of untreated plants, at each of the three collection times ($P < 0.001$). The populations of *B. amyloliquefaciens* recorded in the leaf sam-

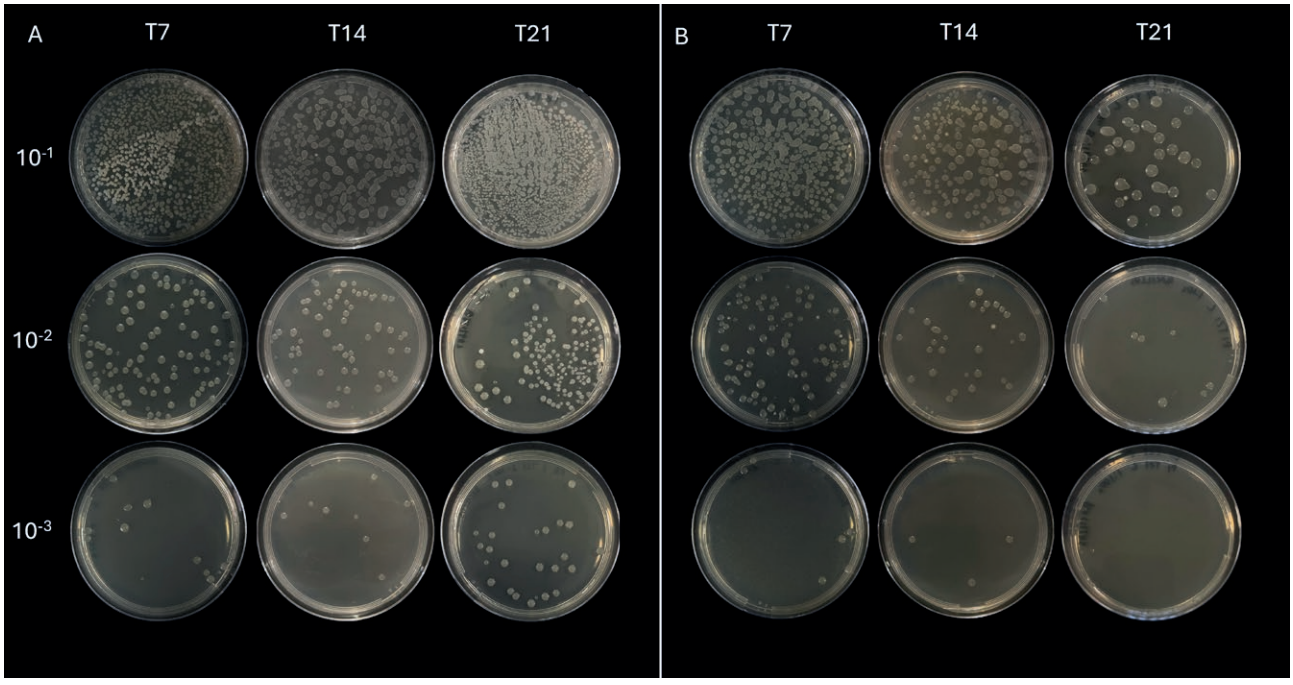

Figure 2. Representative *Bacillus amyloliquefaciens* isolation plates from citrus stem (A) or leaf (B) tissues, at different collection times (T7, T14, or T21 d after treatments), showing colony growth on potato dextrose agar across serial dilutions (from 10-1 to 10-3).

ples using the culture-dependent method did not differ ($P > 0.05$) between 7 and 14 d after culturing, but were reduced after 21 d (Figure 1). Populations of *B. amyloliquefaciens* in the stem tissue samples did not change with time, although a slight increasing population trend was observed from 14 to 21 d. Populations of the bacterium in stem tissues at 14 and 21 d differed significantly from those detected in the leaf tissues at each of the three assessment times.

Culture-indipendent detection of Bacillus amyloliquefaciens *in leaf and stem tissues*

Bacillus amyloliquefaciens detection was assessed by qPCR assays of leaf and stem samples. The detection threshold was calculated from standard curves, and ranged from a maximum of 12 log CFU mL^{-1} (cycle threshold (Ct) = 10.6) to a minimum of 5 log CFU mL^{-1} (Ct = 31.7). No DNA copies were detected from the negative controls (Ct = 39.2). The obtained slope value was -3.17308, and the coefficient of determination (R^2) was 99.1%. For the leaf samples, the inoculated bacteria were detected at concentrations of 6.92 log CFU g^{-1} after 7 d, 6.55 log CFU g^{-1} after 14 d, and 6.46 log CFU g^{-1} after 21 d. For the stem samples, the bacteria were detected at concentrations of 8.27 log CFU g^{-1} after 7 d, 7.85 log CFU g^{-1} after 14 d, and 7.72 log CFU g^{-1} after 21 d. The Ct data confirmed the cell densities detected, with Ct values (for the three sampling times) of 25.44, 26.44 and 26.26 for the leaf samples, and 21.62, 23.90 and 23.75 for stem samples (Supplementary Table I).

The qPCR analyses revealed presence of *B. amyloliquefaciens* DNA in the control plants, with concentrations in the leaf tissues of 1.79 log CFU g^{-1} (Ct= 33.43) at 7 d, 1.73 log CFU g^{-1} (Ct = 33.11) at 14 d, and 1.66 log CFU g^{-1} (Ct = 34.05) at 21 d. Control plant populations in the stem tissues were 5.48 log CFU g^{-1} at 7 d (Ct = 31.69), 5.02 log CFU g^{-1} at 14 d (Ct = 32.04), and 5.47 log CFU g^{-1} at 21 d (Ct = 31.88). Homogeneity of variances of DNA concentrations was confirmed by Levene's test (F = 1.03, $P = 0.45$). The multifactor analysis of variance (ANOVA) showed that the single factors (treatment, plant tissue, collection time), and the combined factor treatment × sample influences detection of *Bacillus* ($P < 0.001$). Tukey's *post hoc* test of the combined factors (treatment × sample) showed that *Bacillus*-treated samples differed in microbial concentrations within the leaf and stem tissue samples from those of untreated plants (Figure 3). Although the levels of *B. amyloliquefaciens* detected in stem tissues were greater than in leaf tissues, there were no statistically significant population changes ($P > 0.05$) during 21 d post inoculation in either the leaf or stem tissue samples.

Culture-dependent detection of Trichoderma asperellum *and* Trichoderma gamsii *in leaf and stem tissues*

Trichoderma was isolated from stem tissue samples using direct plating (Figures 4 and 5), but no *Trichoderma*-like colonies were obtained from leaves using plate dilution or direct plating. Two distinct *Trichoderma*-like colonies were consistently obtained from the stems of treated plants, so representative isolates were collected for each of the two *Trichoderma* morphotypes (named TA and TG), which were distinguishable by colony morphology. Comparisons of the *rpb2* sequences of one representative isolate per morphotype, TA1 (Acc. No. PX597589) and TG1 (Acc. No. PX597590), with those present in the NCBI nucleotide database, showed 99.61% similarity of TA1 with *T. asperellum* isolate ICC 012 (Acc. No. MU868004.1), and 98.97% similarity of TG1 with *T. gamsii* isolate T065 (Acc. No. OK813898.1). The overall IFs of the two *Trichoderma* morphotypes from wood fragments of treated plants were 8.5% after 7 d, 10.6% at 14 d, and 55.6% at 21 d after treatment. Although both morphotypes were recovered, TG was consistently less frequently recovered than TA. No colonies were recorded from the untreated control treatments. The assumption of homogeneity of variances for IFs was confirmed by Levene's test (F = 2.91, $P = 0.06$). The two-way analysis of variance (ANOVA) showed that

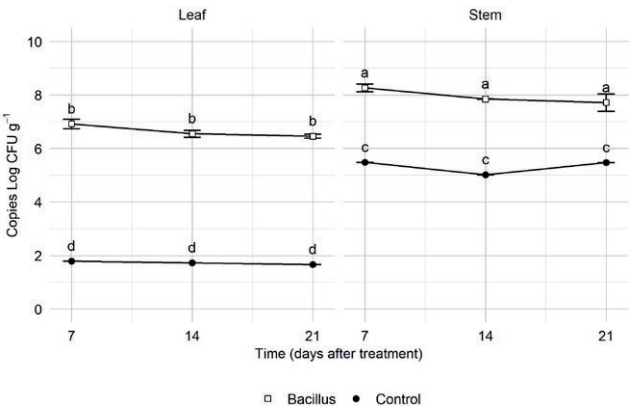

Figure 3. Mean numbers (± standard errors) of *Bacillus amyloliquefaciens* (expressed as copies Log CFU g^{-1} of tissue) detected in citrus leaf or stem tissues detected at 7, 14 or 21 d after treatment using a culture-indipendent method. Results were from *Bacillus*-treated (open symbols) and control plants (close symbols) using the qPCR assay. Different letters accompanying symbols indicate differences ($\alpha = 0.05$) among combined factors (treatment × sample), according to Tukey's HSD tests.

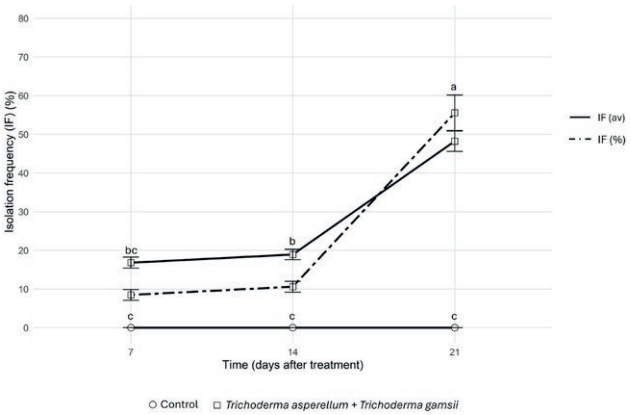

Figure 4. Mean numbers (± standard errors) of *Trichoderma asperellum* + *Trichoderma gamsii* (expressed as isolation frequency, IF) detected in citrus stem tissues, detected at 7, 14 or 21 d after treatment using a culture-dependent method. Results were from *Trichoderma*-treated (square symbols) and control plants (circle symbols). Different letters accompanying symbols indicate differences (α = 0.05) among combined factors (treatment × time), according to Tukey's HSD tests performed on arcsine square-root transformed data (av).

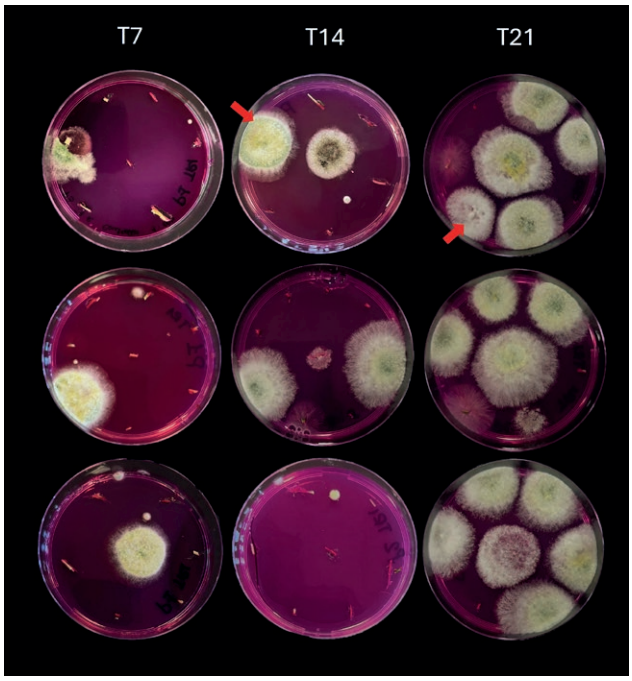

Figure 5. Representative isolation plates of the two *Trichoderma* morphotypes (red arrows) from plants treated with *Trichoderma asperellum* ICC 012 + *Trichoderma gamsii* ICC 080 at different collection times (T7, T14, or T21 d after treatments) on Rose Bengal-chloramphenicol Agar (RBA) medium.

the single factors, treatment (F = 223.60, $P < 0.001$) and collection time (F = 85.23, $P < 0.001$), and the combined factors (treatment × collection time) (F = 85.23, $P < 0.001$), all influenced detection of *Trichoderma* (angular-transformed value). Tukey's *post hoc* test of the combined factors showed that *Trichoderma* from treated plants differed significantly in IFs from those from untreated plants at each of the three collection times. Incidence of the two *Trichoderma* species was greater after 21 d than that recorded at 7 or 14 d ($P < 0.001$) (Figures 4 and 5).

Culture-independent detection of Trichoderma asperellum *and* Trichoderma gamsii *in leaf and stem tissues*

The culture-independent approach was used to determine trends of *Trichoderma* spp. in leaf and stem samples. Detection thresholds were calculated from standard curves, and ranged from a maximum of 10 log CFU g^{-1} (Ct = 16.29) to a minimum of 3 log CFU g^{-1}, (Ct = 34.68). The slope was -2.87841 and the coefficient of determination (R^2) was 99.2%. The negative experimental control gave Ct values of 39 to 40, with no DNA copies detected. *Trichoderma* spp. were detected in leave tissues at concentrations of 5.33 copies log CFU g^{-1} after 7 d culture, 5.69 copies log CFU g^{-1} after 14 d, and 4.87 copies log CFU g^{-1} after 21 d, and in stem tissues at 5.72 copies log CFU g^{-1} after 7 d, 5.70 copies log CFU g^{-1} after 14 d, and 5.66 copies log CFU g^{-1} after 21 d. The Ct values for leaf samples were 32.01 after 7 d, 32.09 after 14 d, and 34.14 after 21 d, and for stem samples were 31.97 after 7 d, 31.16 after 14 d, and 31.83 after 21 d (Supplementary Table II). No amplification was detected from the control samples. Homogeneity of variances of data was confirmed by Levene's test (F = 1.70, $P = 0.13$). The ANOVA showed that only treatment influenced the survivability of *Trichoderma* in leaf and stem tissues (F = 1442.1, $P < 0.001$). Tukey's *post hoc* test ($\alpha = 0.05$) showed differences in detection of *Trichoderma* spp. at each collection time in treated and control leaf and stem tissue samples ($P < 0.001$). However, the qPCR assays did not detect statistically significant differences in *T. asperellum* and *T. gamsii* populations between the leaf and stem samples (Figure 6), with no statistically significant decreases up to 21 d after treatment.

Culture-dependent detection of Trichoderma asperellum *and* Trichoderma gamsii *from roots and soil-rhizospheres*

Culture-based methods (dilution and direct plating techniques) did not detect *T. asperellum* and *T. gamsii* from vascular root tissues. For rhizospheres, *Trichoderma* colonies were isolated from treated plants using the

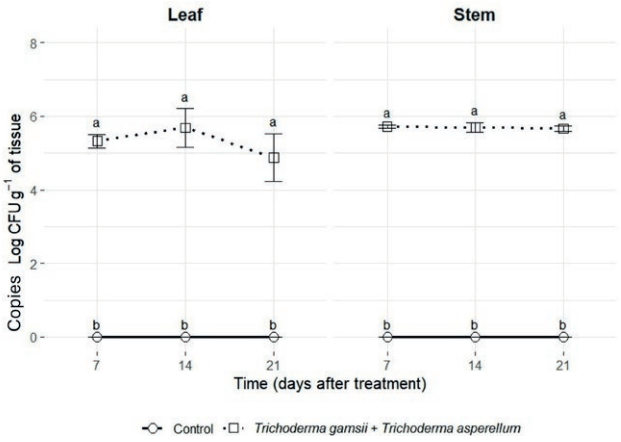

Figure 6. Mean numbers (± standard errors) of *Trichoderma asperellum* + *Trichoderma gamsii* (expressed as copies Log CFU g^{-1} of tissue) detected in citrus stem and leaf tissues, detected at 7, 14 or 21 d after treatment using a qPCR assay. Results were from *Trichoderma*-treated (square symbols) and control plants (circle symbols). Different letters accompanying symbols indicate differences (α = 0.05) according to Tukey's HSD tests.

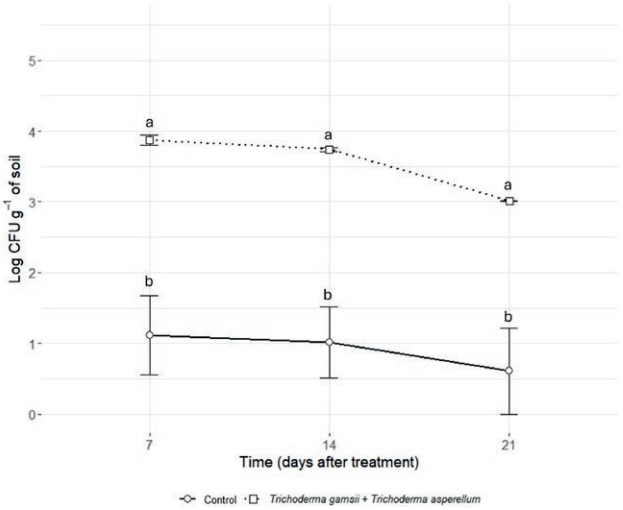

Figure 7. Mean numbers (± standard errors) of *Trichoderma asperellum* + *Trichoderma gamsii* (expressed as Log CFU g^{-1} of tissue) detected in the soil rhizosphere, detected at 7, 14 or 21 d after treatment using the agar dilution technique. Results were from *Trichoderma*-treated (square symbols) and control plants (circle symbols). Different letters accompanying symbols indicate differences (α = 0.05) according to Tukey's HSD tests.

dilution plating (Figures 7A and 8A). However, some *Trichoderma*-like colonies were isolated from the rhizospheres of untreated plants (Figures 7 B and 8 B). Some of these colonies were morphologically different from those collected from treated plants (Figure 8 B). Based on the *rpb2* gene region, the representative *Trichoderma* isolates S-TA (Acc. No. PX597587) and S-TG (Acc. No. PX597588) collected from rhizospheres of treated plants gave 100% of identity with *T. asperellum* ICC 012 (Acc. No. MU868004.1) and 100% identity with several *T. gamsii* isolates, including *T. gamsii* strain PPRI 14668 (Acc. No. MF043068.1). In contrast, the four representative isolates obtained from experimental controls were identified, based on their *rpb2* gene regions, as *T. virens* for S1 (Acc. No. PX571116) and for S3 (Acc. No. PX571117), with 99.72% similarity and 99.91% of identity with *T. virens* strain TRA1-50 (Acc. No. MW325767.1), for S4 *T. harzianum* (Acc. No. PX597586) having 98.93% similarity with *T. harzianum* strain Vimi-17.0073 (Acc. No. MZ675885.1), and for S2 *Trichoderma asperellum* (S2 Acc. No. PX597585), which showed 99.91% of identity with *T. asperellum* strain CGMCC 6422 (Acc. No. KF425755.1), but only 97.34% similarity with *T. asperellum* ICC 012 (Acc. No. MU868004.1). *Trichoderma asperellum* and *T. gamsii* were isolated from treated samples at concentrations of 4.73 log CFU g^{-1} after 7 d, 4.63 log CFU g^{-1} after 14 d, and 4.37 log CFU g^{-1} after 21 d (Figure 7 A). Since control plates yielded colonies of different *Trichoderma* species, only colonies resembling *T. asperellum* were included in the plate count data. These showed overall concentrations of *T. asperellum* colonies in the control plates as 1.12 log CFU g^{-1} after 7 d, 1.02 log CFU g^{-1} after 14 d, and 0.61 log CFU g^{-1} after 21 d. Homogeneity of variances was confirmed by Levene's test (F = 0.62, *P* = 0.68), and ANOVA showed that only the treatment significantly influenced the survivability of *Trichoderma* spp. in soil rhizospheres (F = 65.68, *P* < 0.001). A one-way ANOVA showed differences (F = 67.32, *P* < 0.001) in the amounts of *T. gamsii* + *T. asperellum* in the soil rhizospheres of the treated and untreated plants. Although not statistically significant, small decreases, over time, in populations of these fungi were detected in the control and treated samples (Figure 7).

Culture-independent detection of Trichoderma asperellum *and* Trichoderma gamsii *in roots and rhizosphere soil*

The same qPCR reaction protocol used for leaf and stem samples was applied for the detection of *Trichoderma* spp. in the endospheres of roots and rhizosphere samples. The qPCR assay did not detect *T. asperellum* or *T. gamsii* from root vascular tissues. For rhizospheres, the qPCR assay detected these fungi at concentrations of 5.79 log CFU g^{-1} (Ct = 31.92) after 7 d, 5.93 log CFU g^{-1} (Ct = 31.47) after 14 d, and 6.01 log CFU g^{-1} (Ct = 31.21) after 21 d (Figure 9). Homogeneity of variances was confirmed by Levene's test (F = 1.76, *P* = 0.19), and the two-

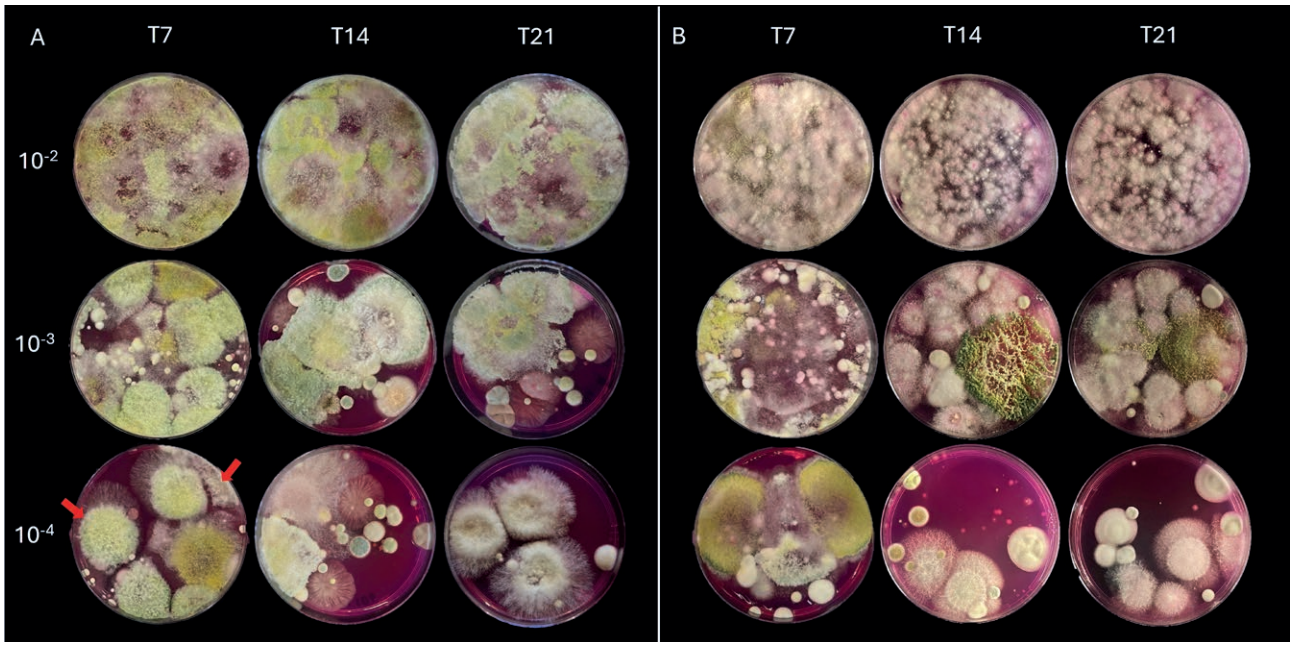

Figure 8. Representative isolation plates of *Trichoderma* spp. from rhizosphere treated with *Trichoderma asperellum* ICC 012 + *Trichoderma gamsii* ICC 080 (A) (red arrows) and controls (B) at different collection times (T7, T14, or T21 d after treatments), showing colony growth across serial dilution (from 10^{-2} to 10^{-4}) on Rose Bengal-chloramphenicol Agar (RBA) medium.

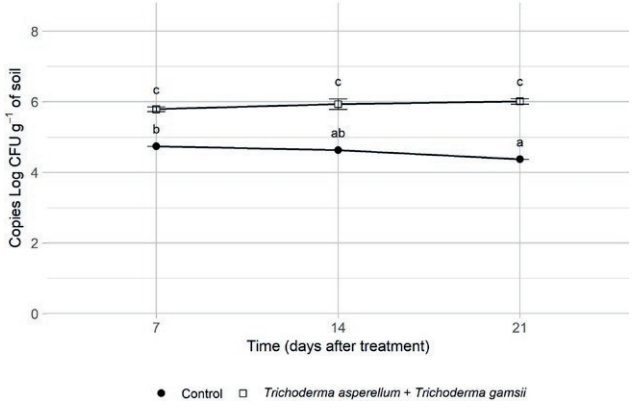

Figure 9. Mean numbers (± standard errors) of *Trichoderma asperellum* + *Trichoderma gamsii* (expressed as copies Log CFU g^{-1} of tissue) detected in the soil rhizosphere, detected at 7, 14 or 21 d after treatment using the qPCR assay. Results were from *Trichoderma*-treated (square symbols) and control plants (circle symbols). Different letters accompanying symbols indicate differences (α = 0.05) according to Tukey's HSD tests.

way ANOVA showed that the treatment affected population dynamics of *T. asperellum* and *T. gamsii* in the soil rhizospheres (F =15.37, $P < 0.001$) (Figure 9). The Tukey post hoc analysis ($\alpha = 0.05$) showed differences in population levels detected through the qPCR assays among the treated and control samples ($P < 0.01$). However, no statistically significant differences were detected due to collection time.

DISCUSSION

Bacillus amyloliquefaciens isolate QST 713 and *T. asperellum* ICC 012 + *T. gamsii* ICC 080 are beneficial microorganisms that can have important roles in management of citrus Mal secco disease (Aiello *et al.,* 2022; Leonardi *et al.,* 2023b; Leonardi *et al.,* 2026). Accurate quantification of BCAs over time, within plant vascular tissues and in soil rhizospheres, is important for improving effectiveness these agents, and for improved rating and scheduling their applications (Mathre *et al.,* 1999; McGuire, 2000; Whipps, 2001; Ojiambo and Scherm, 2006). The levels of colonization and persistence of BCAs in niches of pathogens are key factors underlying their biocontrol activity (Mohandoss and Suryanarayanan, 2009; Rodriguez *et al.,* 2009; Lahlali *et al.,* 2022), and to be effective BCAs must also densely colonize the host sites where pathogens are likely to infect (Card *et al.,* 2016). The present study assessed, using culture-dependent and culture -independent methods, quantitative differences in the endophytic colonization by *Bacillus* and *Trichoderma* in different citrus tissues. A qPCR methodology was developed and validated for the quan-

titative and specific detection of the biocontrol agents *B. amyloliquefaciens* and *T. asperellum* + *T. gamsii* on grapevine berries, wood and associated soil (Rotolo *et al.,* 2016 Gerin *et al.,* 2018). The present used qPCR to investigate the population dynamics of the same BCAs within vascular tissues of *C. volkameriana*. This citrus species, previously used to assess the efficacy of BCAs against *P. tracheiphilus* (Aiello *et al.,* 2022; Leonardi *et al.,* 2023b; Leonardi *et al.,* 2026), is a widely used rootstock in citrus-producing countries, including Italy (Bowman and Joubert, 2020).

Results from the present study confirmed that *B. amyloliquefaciens* persisted in grapevine stem vascular tissues. Good agreement was usually found between culture-dependent detection methods and qPCR results for stationary trends over time, except for leaf samples. From these, detections of *Bacillus* decreased after 14 d post-treatment. Endophytic colonization ability of *Bacillus* in vascular tissues of plants has been previously reported (Gagne *et al.,* 1987), and attributed to the large gene cluster responsible for the secretion of antibiotics and siderophores that promote *Bacillus* competitive ability in the root environments, and colonization of host plants (Chen *et al.,* 2020; Compant *et al.,* 2010). Kalai-Grami *et al.* (2014a) recovered endophytic *B. amyloliquefacies* TEB1 from treated *Citrus aurantium* seedlings after 30 d, reporting greater levels of endophytic colonization in stem and root samples than leaves. In a preliminary study, Aiello *et al.* (2022) isolated *B. amyloliquefaciens* QST 713 at 10^3 to 10^4 CFU g^{-1} (3 to 4 log CFU g^{-1}) from internal woody tissues of Volkamer lemon, 50 d after two treatments. Although Aiello *et al.* (2022) used a similar isolation protocol from stem tissue for detecting *B. amyloliquefaciens*, differences in number of treatments and the stem wounds could have influenced bacterial colonization and persistence. In the present study *B. amyloliquefaciens* was detected in leaf and stem samples from untreated citrus plants only using qPCR, while no cells were isolated on nutrient media, confirming the high sensitivity of qPCR and allowing detection of low bacterial populations in non-treated experimental control leaves.

The greater persistence of *B. amyloliquefaciens* recorded with qPCR assays than determined from culture-dependent methods in all the samples analyzed (stem, leaf, and soil), could have been because qPCR detects total DNA, including that from non-viable or viable but non-culturable (VBNC) cells, while culture-dependent methods only detect actively growing populations (Postollec *et al.,* 2011; Gorsuch *et al.,* 2019). Isolation methods could show false negative detections of VBNC bacteria which remain metabolically active but below detection levels (Morawska and Kuipers, 2022; Pinto *et al.,* 2015). Different stress factors for bacteria, such as microbial competition, nutrient-limited conditions, high salt or low pH environments, may lead to bacterial dormancy, which make these organisms undetectable by isolation on nutrient media (Foster, 1999; Xu *et al.,* 2008a, 2008b; Wang *et al.,* 2011; Guo *et al.,* 2019). Therefore, consistent with the literature (Chen *et al.,* 2020; Kalai-Grami *et al.,* 2014a), *Bacillus* may be a natural endophyte in citrus plants, although in the present study it was below the culturing detection limit. Similarly, Aiello *et al.* (2022) reported that no cells were isolated from untreated plants using a culture-dependent method.

Although different strains of *Trichoderma* spp. have been reported to be endophytes (Jaklitsch *et al.,* 2006; Gazis *et al.,* 2011; Muñoz-Guerrero *et al.,* 2021), and some have shown promising activity against pathogens of citrus (de Lima *et al.,* 2017; Ferreira *et al.,* 2020; Choudhary *et al.,* 2021; Muñoz-Guerrero *et al.,* 2021; Garzón *et al.,* 2022; Leonardi *et al.,* 2023b, 2026; Phal *et al.,* 2023), colonization and survival of these fungi in citrus plants and in soil has been little investigated (Ohr *et al.,* 1972; Camprubí *et al.,* 1995; Nemec *et al.,* 1996). In the present study, *T. asperellum* was recovered from wounded stem tissues at 21 d post-treatment only with direct plating, whereas no growth was observed from leaf or root tissues using two culture-dependent techniques. However, from the molecular data, *Trichoderma* was detected from citrus leaves and stems, so for *Trichoderma*-treated leaf samples, there was no agreement between isolation and qPCR results. For root samples, however, the qPCR accurately reflected the results from culturing methods, showing that *Trichoderma* did not colonize the citrus internal vascular tissues. Comparison of results from qPCR and culturing also highlighted a discrepancy in the population dynamics observed over time. While qPCR results showed that DNA levels of *Trichoderma* in stem tissues remained stable across all collection times, culture isolations showed increases in colony IFs 21 d post-inoculation. Greater PCR detection of *Trichoderma* in leaves qPCR than from culturing could be attributed to several factors, including different sensitivities of the two methods, presence of non-viable cells, the types of plant tissue, and presence of stem wounds that permit internal colonization by fungi (Carro-Huerga *et al.,* 2022; Bretträger *et al.,* 2022).

The qPCR assay can detect nucleic acid from damaged, stressed, or non-viable cells, whereas the traditional isolations rely on recovery of actively viable propagules above minimum detection thresholds. Xu *et al.,* (2025) reported that DNA quantification of *T. asperellum*

strain T34 from live strawberry leaf, flower or root cells using the PMA-qPCR was, in some cases, less than the total DNA quantified using the qPCR. This indicated that normal qPCR possibly leads to over-estimation of viable population sizes of specific microorganisms. However, Xu *et al.,* (2025) found that dynamics of total DNA and PMA-qPCR DNA did not differ over time, suggesting that conventional qPCR techniques can be used to estimate changes in viable population sizes.

Plant tissues can contain different levels of phenolics, flavonoids, or terpenes, with defense functions that can reduce *Trichoderma* viability, allowing DNA to remain detectable without corresponding *in vitro* isolations. Scott *et al.* (2023) found that endophytic *Trichoderma* isolates had greater diversity of biosynthetic gene clusters (BGC) and degradative gene clusters (DGC) than non-endophytic isolates, allowing colonization of plant rhizospheres or phyllospheres. Plant metabolites in these habitats may be toxic or restrictive for colonization of non-endophytic *Trichoderma*. Several studies have highlighted ability of *Trichoderma* to colonize roots and rhizospheres, but presence of these fungi within phyllospheres is little understood (Guzmán-Guzmán *et al.,* 2025). Genes with potential roles in endophytic colonization by the *Trichoderma* isolates used in the present study have not been identified, but this study has indicated that they can be detected within citrus stem vascular tissues, but not in these tissues of leaves or roots. These results indicate that *T. asperellum* and *T. gamsii* may only be able to superficially colonize these plant tissues, as has been reported elsewhere for other crop plants (Sarrocco *et al.,* 2021). For rhizospheres, the detection level of *T. asperellum* + *T. gamsii* assessed using qPCR gave similar patterns to those from the culture-dependent method. The rhizosphere samples showed persistence of the fungi after 21 d, through plate counts and qPCR assays, confirming rhizosphere competence of *Trichoderma* (Woo *et al.,* 2023).

Although the present study did not track individual BCA isolates within citrus tissues, it provides the first insights into the endophytic ability of *B. amyloliquefaciens*, and of *T. asperellum* + *T. gamsii* in these plants after foliar and root applications. The study was based on species-level identifications, indicating that the qPCR primers and probe assessed can be used for monitoring these BCAs in citrus orchards, without appreciable interference from closely related microorganisms. Although the culture-dependent approach is laborious, time-consuming and requires well-trained personnel, combination of qPCR and culturing methods is important for detection and quantification of BCAs within plant tissues. This will facilitate improved scheduling of BCA field applications. The present study results also indicate that high colonization rates by *Trichoderma* spp. and *Bacillus* sp. could be achieved after long periods, and that application of these BCAs after pruning or damage could protect citrus plants from pathogen infections, as has been reported for other host crops (John *et al.,* 2005; Halleen *et al.,* 2010; Mutawila *et al.,* 2011; Kotze *et al.,* 2011). Results from the present study showed that the recovered isolates (identified at species level) from treated plants matched with the applied BCAs, supporting the inference of their persistence within plant tissues.

Endophytic colonization allows microorganisms to remain protected from environmental influences and fluctuations that could threaten their survival and reduce biocontrol efficacy (Card *et al.,* 2016). This enables *Bacillus* and *Trichoderma* to provide more stable biocontrol effects, and are also ideal for biological control. Nevertheless, as the present study used particular experimental conditions, deeper insights are required into endophyte functioning under varied experimental conditions and with different plant genotypes. The endophytic behaviour of these BCAs in healthy plants may change when host plants are grown under unfavourable or stress conditions (Hardoim *et al.,* 2015). Further research should assess BCA applicability in the field, since it is well-known that UV light, lack of nutrients, and other environmental factors can reduce colonization of above-ground plant surfaces, and that only adapted microorganisms can survive and enter host plants via stomata, wounds, and hydathodes (Hallmann 2001; Compant *et al.,* 2010; Carro-Huerga *et al.,* 2022).

FUNDING

This research was funded by: Agritech National Research Center (European Union Next-Generation EU, PIANO NAZIONALE DI RIPRESA E RESILIENZA, PNRR – MISSIONE 4 COMPONENTE 2, INVESTIMENTO 1.4—D.D. 1032 17/06/2022, CN00000022, CUP: E63C22000960006) Spoke 2 (Task 2.2.4: 'Biopesticide and biostimulants'), AGRIVITA project "Difesa degli Agrumeti Italiani dal Malsecco – AGRIVITA", CUP: C83C23000650006, and the University of Catania through a PhD grant to Giuseppa Rosaria Leonardi.

LITERATURE CITED

Agostini J.P., Bushong P.M., Timmer L.W., 2003. Greenhouse evaluation of products that induce host resistance for control of scab, melanose, and *Alternaria*

brown spot of citrus. *Plant Disease* 87(1): 69–74. https://doi.org/10.1094/PDIS.2003.87.1.69

Aiello D., Leonardi G.R., Di Pietro C., Vitale A., Polizzi G., 2022. A new strategy to improve management of citrus Mal secco disease using bioformulates based on *Bacillus amyloliquefaciens* strains. *Plants* 11(3): 446. https://doi.org/10.3390/plants11030446

Aiello D., Bregant C., Carlucci A., Guarnaccia V., Gusella G., … Polizzi G., 2023. Current status of *Botryosphaeriaceae* species in Italy: impacts on agricultural crops and forest ecosystems. *Phytopathologia Mediterranea* 62(3): 381–412. https://doi.org/10.36253/phyto-14711

Araújo W.L., Marcon J., Maccheroni W. Jr, van Elsas J.D., van Vuurde J.W., Azevedo J.L., 2002. Diversity of endophytic bacterial populations and their interaction with *Xylella fastidiosa* in citrus plants. *Applied and Environmental Microbiology* 68(10): 4906–4914. https://doi.org/10.1128/AEM.68.10.4906-4914.2002

Bae H., Sicher R.C., Kim M.S., Kim S.H., Strem M.D., … Bailey, B.A., 2009. The beneficial endophyte *Trichoderma hamatum* isolate DIS 219b promotes growth and delays the onset of the drought response in *Theobroma cacao*. *Journal of Experimental Botany* 60: 3279–3295. https://doi.org/10.1093/jxb/erp165

Bowman K. D., and Joubert J., 2020. Citrus rootstocks, In: The genus citrus (M. Talon, M. Caruso, F. Gmitter jr, ed.), Woodhead Publishing, Sawston, Cambridge CB22 3HJ, United Kingdom.105-127.

Bretträger M., Becker T., Gastl M., 2022. Screening of mycotoxigenic fungi in barley and barley malt (*Hordeum vulgare* L.) using real-time PCR—a comparison between molecular diagnostic and culture technique. *Foods* 11(8): 1149. https://doi.org/10.3390/foods11081149

Burandt Q.C., Deising H.B., von Tiedemann A., 2024. Further limitations of synthetic fungicide use and expansion of organic agriculture in Europe will increase the environmental and health risks of chemical crop protection caused by copper-containing fungicides. *Environmental Toxicology and Chemistry* 43(1): 19–30. https://doi.org/10.1002/etc.5766

Calcagnile M., Tredici M.S., Pennetta A., Resta S.C., Talà A., … Alifano P., 2022. *Bacillus velezensis* MT9 and *Pseudomonas chlororaphis* MT5 as biocontrol agents against citrus sooty mold and associated insect pests. *Biological Control* 176: 105091. https://doi.org/10.1016/j.biocontrol.2022.105091

Camprubí A., Calvet C., Estaún V., 1995. Growth enhancement of *Citrus reshni* after inoculation with *Glomus intraradices* and *Trichoderma aureoviride* and associated effects on microbial populations and enzyme activity in potting mixes. *Plant and Soil* 173: 233–238. https://doi.org/10.1007/BF00011460

Card S., Johnson L., Teasdale S., Caradus J., 2016. Deciphering endophyte behaviour: the link between endophyte biology and efficacious biological control agents. *FEMS Microbiology Ecology* 92(8): 114. https://doi.org/10.1093/femsec/fiw114

Carro-Huerga G., Compant S., Gorfer M., Cardoza R.E., Schmoll M., … Casquero, P.A., 2022. Colonization of *Vitis vinifera* L. by the endophyte *Trichoderma* sp. strain T154: biocontrol activity against *Phaeoacremonium minimum*. *Frontiers in Plant Science* 11: 1170. https://doi.org/10.3389/fpls.2020.01170

Catara A., Cutuli G., 1972. Osservazioni sulla suscettibilità di alcune Rutacee alle infezioni epigee di *Phoma tracheiphila*. *Annali dell'Istituto Sperimentale per l'Agrumicoltura di Acireale* 5: 29–43.

Chen K., Tian Z., He H., Long C., Jiang F., 2020. *Bacillus* species as potential biocontrol agents against citrus diseases. *Biological Control* 151: 104419. https://doi.org/10.1016/j.biocontrol.2020.104419

Choudhary A.K., Singh N., Singh D., 2021. Evaluation of the bioformulation of potent native strains of *Trichoderma* spp. against the foot rot/gummosis of Kinnow mandarin. *Egyptian Journal of Biological Pest Control* 31(1): 90. https://doi.org/10.1186/s41938-021-00437-y

Chun J., Bae K.S., 2000. Phylogenetic analysis of *Bacillus subtilis* and related taxa based on partial *gyrA* gene sequences. *Antonie van Leeuwenhoek* 78: 123–127. https://doi.org/10.1023/A:1026555830014

Clark T., Harris C.A., Tomerlin J.R., 2002. The regulation of pesticides in Europe—Directive 91/414. *Journal of Environmental Monitoring* 4(2): 28N–31N.

Compant S., Clément C., Sessitsch A., 2010. Plant growth-promoting bacteria in the rhizo- and endosphere of plants: their role, colonization, mechanisms involved and prospects for utilization. *Soil Biology and Biochemistry* 42(5): 669–678. https://doi.org/10.1016/j.soilbio.2009.11.024

Dao T.T., Tran T.T., Nguyen A.M., Nguyen L.N., Pham P.T., … Nguyen M.N., 2021. Fungicide application can intensify clay aggregation and exacerbate copper accumulation in citrus soils. *Environmental Pollution* 288: 117703. https://doi.org/10.1016/j.envpol.2021.117703

de Lima F.B., Felix C., Osorio N., Alves A., Vitorino R., … Esteves A.C., 2017. *Trichoderma harzianum* T1A constitutively secretes proteins involved in the biological control of *Guignardia citricarpa*. *Biological Control* 106: 99–109. https://doi.org/10.1016/j.biocontrol.2017.01.003

Dimaria G., Mosca A., Anzalone A., Paradiso G., Nicotra D., … Catara V., 2023. Sour orange microbiome is affected by infections of *Plenodomus tracheiphilus* causal agent of citrus Mal secco disease. *Agronomy* 13(3): 654. https://doi.org/10.3390/agronomy13030654

EFSA (European Food Safety Authority) PLH Panel, 2014. Scientific opinion on the pest categorisation of *Plenodomus tracheiphilus* (Petri) Gruyter, Aveskamp & Verkley (syn. *Phoma tracheiphila* (Petri) L.A. Kantschaveli & Gikashvili). *EFSA Journal* 12(7): 3775. https://doi.org/10.2903/j.efsa.2014.3775

EFSA (European Food Safety Authority) PLH Panel, Bragard C., Baptista P., Chatzivassiliou E., Di Serio F., Gonthier P., … Reignault P.L., 2023. Scientific opinion on the pest categorisation of *Neoscytalidium dimidiatum*. *EFSA Journal* 21(5): e08001. https://doi.org/10.2903/j.efsa.2023.8001

EFSA (European Food Safety Authority), Abdourahime H., Anastassiadou M., Arena M., Auteri D., Barmaz S., … Villamar-Bouza, L., 2020. Peer review of the pesticide risk assessment of the active substance mancozeb. *EFSA Journal* 18(12): e05755. https://doi.org/10.2903/j.efsa.2020.5755

Espargham N., Mohammadi H., Gramaje D.A., 2020. Survey of trunk disease pathogens within citrus trees in Iran. *Plants* 9: 754. https://doi.org/10.3390/plants9060754

EFSA (European Food Safety Authority, Arena M., Auteri D., Barmaz S., Bellisai G., Brancato A., … Villamar-Bouza L., 2018. Peer review of the pesticide risk assessment of the activesubsttribasic copperance copper compounds copper(I), copper(II) variants namely copper hydroxide, copper oxychloride, tribasic copper sulfate, copper(I) oxide, Bordeaux mixture. *EFSA Journal* 16(1): 5152. https://doi.org/10.2903/j.efsa.2018.5152

European Commission, 2018. Regulation (EU) 2018/1981 of 13 December 2018 renewing the approval of copper compounds. Available online at: https://eur-lex.europa.eu/legal-content/EN/TXT/PDF/?uri=CELEX:32018R1981&from=EN (accessed August 2025).

European Commission, 2020. Implementing Regulation (EU) 2020/2087 of 14 December 2020 concerning the non-renewal of the approval of the active substance mancozeb. Available online at: https://eur-lex.europa.eu/legal-content/EN/TXT/PDF/?uri=CELEX:32020R2087&from=EN (accessed August 2025).

Ezrari S., Mhidra O., Radouane N., Tahiri A., Polizzi G., Lazraq A., Lahlali R., 2021. Potential role of rhizobacteria isolated from citrus rhizosphere for biological control of citrus dry root rot. *Plants* 10(5): 872. https://doi.org/10.3390/plants10050872

FAOSTAT, 2024. Available online at: https://www.fao.org/faostat/en/#data (accessed June 26, 2025).

Fawcett, H.S., 1936. *Citrus Diseases and Their Control (2nd edition)*. McGraw-Hill Book Company, Inc., New York and London: xv + 656 pp.

Ferreira F.V., Herrmann-Andrade A.M., Calabrese C.D., Bello F., Vázquez D., Musumeci M.A., 2020. Effectiveness of *Trichoderma* strains isolated from the rhizosphere of citrus tree to control *Alternaria alternata*, *Colletotrichum gloeosporioides* and *Penicillium digitatum* A21 resistant to pyrimethanil in post-harvest oranges (*Citrus sinensis* L. Osbeck). *Journal of Applied Microbiology* 129(3): 712–727. https://doi.org/10.1111/jam.14657

Fontana D.C., de Paula S., Torres A.G., de Souza V.H.M., Pascholati S.F., … Dourado Neto, D., 2021. Endophytic fungi: biological control and induced resistance to phytopathogens and abiotic stresses. *Pathogens* 10: 570. https://doi.org/10.3390/pathogens10050570

Foster J.W., 1999. When protons attack: microbial strategies of acid adaptation. *Current Opinion in Microbiology* 2: 170–174. https://doi.org/10.1016/S1369-5274(99)80030-7

Garzón M.A., Mártiz J., Valdés-Gómez H.A., 2022. Characterization of *Fusarium* species that affect orange trees (*Citrus* × *sinensis* L.) and *in vitro* biocontrol essays with *Trichoderma* spp. In: *XIV International Citrus Congress. Acta Horticulturae* 1399: 417–422. https://doi.org/10.17660/ActaHortic.2024.1399.52

Gazis R., Rehner S., Chaverri P., 2011. Species delimitation in fungal endophyte diversity studies and its implications in ecological and biogeographic inferences. *Molecular Ecology* 20(14): 3001–3013. https://doi.org/10.1111/j.1365-294X.2011.05110.x

Gerin D., Pollastro S., Raguseo C., De Miccolis Angelini R.M., Faretra F., 2018. A ready-to-use single- and duplex-TaqMan-qPCR assay to detect and quantify the biocontrol agents *Trichoderma asperellum* and *Trichoderma gamsii*. *Frontiers in Microbiology* 9: 2073. https://doi.org/10.3389/fmicb.2018.02073

Giordano D.F., Pastor N.A., Rouws L.F.M., Moura de Freitas K., Erazo J.G., … Torres A.M., 2023. *Trichoderma harzianum* ITEM 3636 colonizes peanut roots as an endophyte and protects the plants against late leaf spot. *Symbiosis* 89: 337–352. https://doi.org/10.1007/s13199-023-00913-z

Gorsuch J., LeSaint D., VanderKelen J., Buckman D., Kitts C.L., 2019. A comparison of methods for enumerating bacteria in direct fed microbials for animal feed. *Journal of Microbiological Methods* 160: 124–129. https://doi.org/10.1016/j.mimet.2019.04.003

Guarnaccia V., Crous P.W., 2017. Emerging citrus diseases in Europe caused by species of *Diaporthe*. *IMA Fungus* 8(2): 317–334. https://doi.org/10.5598/imafungus.2017.08.02.07

Guo L., Ye C., Cui L., Wan K., Chen S., ... Yu X., 2019. Population and single-cell metabolic activity of UV-induced VBNC bacteria determined by CTC-FCM and D2O-labeled Raman spectroscopy. *Environment International* 130: 104883. https://doi.org/10.1016/j.envint.2019.05.077

Gusella G., Leonardi G.R., La Quatra G., Aiello D., Voglmayr H., Polizzi G., 2025. Re-evaluating the etiology of citrus "Dothiorella gummosis" in Italy. *Plant Disease* First Look. https://doi.org/10.1094/PDIS-02-25-0441-RE

Guzmán-Guzmán P., Etesami H., Santoyo G., 2025. *Trichoderma*: a multifunctional agent in plant health and microbiome interactions. *BMC Microbiology* 25: 434. https://doi.org/10.1186/s12866-025-04158-2

Halleen F., Fourie P.H., Lombard P.J., 2010. Protection of grapevine pruning wounds against *Eutypa lata* by biological and chemical methods. *South African Journal of Enology and Viticulture* 31(2): 125–132.

Hallmann J., 2001. Plant interactions with endophytic bacteria. In: *Biotic interactions in plant-pathogen associations* (M. J. Jeger, N.J. Spence ed.), CAB International, Wallingford, United Kingdom, 87–119. https://doi.org/10.1079/9780851995120.0000

Hardoim P.R., van Overbeek L.S., Berg G., Pirttilä A.M., Compant S., ... Sessitsch, A., 2015. The hidden world within plants: ecological and evolutionary considerations for defining functioning of microbial endophytes. *Microbiology and Molecular Biology Reviews* 79(3): 293–320. https://doi.org/10.1128/MMBR.00050-14

Huang F., Hou X., Dewdney M.M., Fu Y., Chen G., ... Li, H., 2013. *Diaporthe* species occurring on citrus in China. *Fungal Diversity* 61: 237–250. https://doi.org/10.1007/s13225-013-0245-6

ISTAT, 2024. Available online at: http://dati.istat.it/ (accessed June 27, 2025).

Jaklitsch W.M., Samuels G.J., Dodd S.L., Lu B.S., Druzhinina I.S., 2006. *Hypocrea rufa/Trichoderma viride*: a reassessment, and description of five closely related species with and without warted conidia. *Studies in Mycology* 56(1): 135–177. https://doi.org/10.3114/sim.2006.56.04

Johansson A.H., Bejai S., Niazi A., Manzoor S., Bongcam-Rudloff E., Meijer J., 2014. Studies of plant colonisation by closely related *Bacillus amyloliquefaciens* biocontrol agents using strain-specific quantitative PCR assays. *Antonie van Leeuwenhoek* 106: 1247–1257. https://doi.org/10.1007/s10482-014-0295-0

John S., Wicks T. J., Hunt J. S., Lorimer M. F., Oakey H., Scott E. S., 2005. Protection of grapevine pruning wounds from infection by *Eutypa lata* using *Trichoderma harzianum* and *Fusarium lateritium*. *Australasian Plant Pathology* 34(4): 569–575. https://doi.org/10.1071/AP05075

Kalai-Grami L., Ben Slimane I., Mnari-Hattab M., Rezgui S., Aouani M.A., ... Limam, F., 2014a. Protective effect of *Bacillus amyloliquefaciens* against infections of *Citrus aurantium* seedlings by *Phoma tracheiphila*. *World Journal of Microbiology and Biotechnology* 30(2): 529–538. https://doi.org/10.1007/s11274-013-1471-5

Kalai-Grami L., Saidi S., Bachkouel S., Slimene I.B., Mnari-Hattab M., ... Limam, F., 2014b. Isolation and characterization of putative endophytic bacteria antagonistic to *Phoma tracheiphila* and *Verticillium albo-atrum*. *Applied Biochemistry and Biotechnology* 174(1): 365–375. https://doi.org/10.1007/s12010-014-1062-4

Kalimutu P.K., Mahardika I.B.K., Sagung P.R.A.A.A., 2020. Antagonism test of *Trichoderma atroviride* and *Gliocladium* sp. Bali local isolates as a disease control of blendok disease (*Botryodiplodia theobromae*) in grapefruit (*Citrus grandis* L. Osbeck). *SEAS (Sustainable Environment Agricultural Science)* 4(2): 102–110. https://doi.org/10.22225/seas.4.2.2311.102-110

Khuong N.Q., Nhien D.B., Thu L.T.M., Trong N.D., Hiep P.C., ... Xuan, D.T., 2023. Using *Trichoderma asperellum* to antagonize *Lasiodiplodia theobromae* causing stem-end rot disease on pomelo (*Citrus maxima*). *Journal of Fungi* 9(10): 981. https://doi.org/10.3390/jof9100981

Kotze C., Van Niekerk J., Mostert L., Halleen F., Fourie P., 2011. Evaluation of biocontrol agents for grapevine pruning wound protection against trunk pathogen infection. *Phytopathologia Mediterranea* 50: S247–S263.

Kupper K.C., Corrêa É.B., Moretto C., Bettiol W., Goes A.D., 2011. Control of *Guignardia citricarpa* by *Bacillus subtilis* and *Trichoderma* spp. *Revista Brasileira de Fruticultura* 33: 1111–1118. https://doi.org/10.1590/S0100-29452011000400009

Kupper K.C., Moretto R.K., Fujimoto A., 2019. Production of antifungal compounds by *Bacillus* spp. isolates and its capacity for controlling citrus black spot under field conditions. *World Journal of Microbiology and Biotechnology 36*(1), 7. https://doi.org/10.1007/s11274-019-2772-0

Labiadh M., Dhaouadi S., Chollet M., Chataigne G., Tricot C., ... Kallel S., 2021. Antifungal lipopeptides from *Bacillus* strains isolated from rhizosphere

of citrus trees. *Rhizosphere* 19: 100399. https://doi.org/10.1016/j.rhisph.2021.100399

Lahlali R., Ezrari S., Radouane N., Kenfaoui J., Esmaeel Q., … Barka E.A., 2022. Biological control of plant pathogens: a global perspective. *Microorganisms* 10(3): 596. https://doi.org/10.3390/microorganisms10030596

Leonardi G.R., Aiello D., Camilleri G., Piattino V., Polizzi G., Guarnaccia V., 2023a. A new disease of kumquat (*Fortunella margarita*) caused by *Colletotrichum karsti*: twig and branch dieback. *Phytopathologia Mediterranea* 62(3): 333–348. https://doi.org/10.36253/phyto-14544

Leonardi G.R., Polizzi G., Vitale A., Aiello D., 2023b. Efficacy of biological control agents and resistance inducer for control of Mal secco disease. *Plants* 12(9): 1735. https://doi.org/10.3390/plants12091735

Leonardi G.R., Vitale A., Mavica S., Catara V., Polizzi G., Aiello D., 2026. Efficacy of *Trichoderma*-based formulates against Mal secco disease of citrus. *Organic Agriculture* 16: 16. https://doi.org/10.1007/s13165-025-00542-4

Li S., He P., Fan H., Liu L., Yin K., … Zheng, S.J., 2021. A real-time fluorescent reverse transcription quantitative PCR assay for rapid detection of genetic markers' expression associated with Fusarium wilt of banana biocontrol activities in *Bacillus*. *Journal of Fungi* 7(5): 353. https://doi.org/10.3390/jof7050353

Liu Y.J., Whelen S., Hall B.D., 1999. Phylogenetic relationships among ascomycetes: evidence from an RNA polymerase II subunit. *Molecular Biology and Evolution* 16(12): 1799–1808. https://doi.org/10.1093/oxfordjournals.molbev.a026092

Liu S., Lou Y., Li Y., Zhang J., Li P., … Gu Q., 2022. Review of phytochemical and nutritional characteristics and food applications of *Citrus* L. fruits. *Frontiers in Nutrition* 9: 968604. https://doi.org/10.3389/fnut.2022.968604

Lombardo M.F., Panebianco S., Azzaro A., Timpanaro G., Polizzi G., Cirvilleri G., 2024. Copper-alternative products to control anthracnose and *Alternaria* brown spot on fruit of Tarocco sweet oranges and lemon in Italy. *Crop Protection* 176: 106520. https://doi.org/10.1016/j.cropro.2023.106520

Lugtenberg B., Kamilova F., 2009. Plant-growth-promoting rhizobacteria. *Annual Review of Microbiology* 63(1): 541–556. https://doi.org/10.1146/annurev.micro.62.081307.162918

Mathre D.E., Cook R.J., Callan N.W., 1999. From discovery to use: traversing the world of commercializing biocontrol agents for plant disease control. *Plant Disease* 83(11): 972–983. https://doi.org/10.1094/PDIS.1999.83.11.972

Mayorquin J.S., Nouri M.T., Peacock B.B., Trouillas F.P., Douhan G.W., … Eskalen, A., 2019. Identification, pathogenicity, and spore trapping of *Colletotrichum karstii* associated with twig and shoot dieback in California. *Plant Disease* 103(7): 1464–1473. https://doi.org/10.1094/pdis-08-18-1425-re

Mayorquin J.S., Wang D.H., Twizeyimana M., Eskalen A., 2016. Identification, distribution, and pathogenicity of *Diatrypaceae* and *Botryosphaeriaceae* associated with citrus branch canker in the southern California desert. *Plant Disease* 100(12): 2402–2413. https://doi.org/10.1094/pdis-03-16-0362-re

McGuire R.G., 2000. Population dynamics of postharvest decay antagonists growing epiphytically and within wounds on grapefruit. *Phytopathology* 90(11): 1217–1223. https://doi.org/10.1094/PHYTO.2000.90.11.1217

Mendis H.C., Thomas V.P., Schwientek P., Salamzade R., Chien J.T., … De La Fuente, L., 2018. Strain-specific quantification of root colonization by plant growth-promoting rhizobacteria *Bacillus firmus* I-1582 and *Bacillus amyloliquefaciens* QST713 in non-sterile soil and field conditions. *PLoS One* 13(2): e0193119. https://doi.org/10.1371/journal.pone.0193119

Ministero della Salute, 2025. Banca Dati dei Prodotti Fitosanitari. Available online at: www.fitosanitari.salute.gov.it (accessed January 20, 2025).

Mohandoss J., Suryanarayanan T.S., 2009. Effect of fungicide treatment on foliar fungal endophyte diversity in mango. *Sydowia* 61(1): 11–24.

Morawska L.P., Kuipers O.P., 2022. Antibiotic tolerance in environmentally stressed *Bacillus subtilis*: physical barriers and induction of a viable but nonculturable state. *Microlife* 3: uqac010. https://doi.org/10.1093/femsml/uqac010

Muñoz-Guerrero J., Guerra-Sierra B.E., Alvarez J.C., 2021. Fungal endophytes of Tahiti lime (*Citrus* × *latifolia*) and their potential for control of *Colletotrichum acutatum* J.H. Simmonds causing anthracnose. *Frontiers in Bioengineering and Biotechnology* 9: 650351. https://doi.org/10.3389/fbioe.2021.650351

Mushtaq S., Shafiq M., Ashraf T., Haider M.S., Ashfaq M., Ali M., 2019. Characterization of plant growth-promoting activities of bacterial endophytes and their antibacterial potential isolated from citrus. *Journal of Animal & Plant Sciences* 29(4): 978–991.

Mutawila C., Fourie P.H., Halleen F., Mostert L., 2011. Grapevine cultivar variation to pruning wound protection by *Trichoderma* species against trunk pathogens. *Phytopathologia Mediterranea* 50: S264–S276. https://www.jstor.org/stable/26458726

Nascimento Brito V., Lana Alves J., Sírio Araújo K., de Souza Leite T., Borges de Queiroz C., … de Queiroz,

M.V., 2023. Endophytic *Trichoderma* species from rubber trees native to the Brazilian Amazon, including four new species. *Frontiers in Microbiology* 14: 1095199. https://doi.org/10.3389/fmicb.2023.1095199

Nemec S., Datnoff L.E., Strandberg J., 1996. Efficacy of biocontrol agents in planting mixes to colonize plant roots and control root diseases of vegetables and citrus. *Crop Protection* 15(8): 735–742. https://doi.org/10.1016/S0261-2194(96)00048-8

Ohr H.D., Munnecke D.E., Bricker J.L., 1972. *Trichoderma* spp. as modified by methyl bromide. *Phytopathology* 63: 965–973.

Ojiambo P.S., Scherm H., 2006. Biological and application-oriented factors influencing plant disease suppression by biological control: a meta-analytical review. *Phytopathology* 96(11): 1168–1174. https://doi.org/10.1094/PHYTO-96-1168

Phal P., Soytong K., Poeaim S., 2023. Natural product nanofibers derived from *Trichoderma hamatum* K01 to control citrus anthracnose caused by *Colletotrichum gloeosporioides*. *Open Agriculture* 8(1): 20220193. https://doi.org/10.1515/opag-2022-0193

Piel C., Pouchieu C., Carles C., Beziat B., Boulanger M., … Renier, M., 2019. Agricultural exposures to carbamate herbicides and fungicides and central nervous system tumour incidence in the cohort AGRICAN. *Environment International* 130: 104876. https://doi.org/10.1016/j.envint.2019.05.070

Pinto D., Santos M.A., Chambel L., 2015. Thirty years of viable but nonculturable state research: unsolved molecular mechanisms. *Critical Reviews in Microbiology* 41(1): 61–76. https://doi.org/10.3109/1040841X.2013.794127

Polizzi G., Aiello D., Vitale A., Giuffrida F., Groenewald J.Z., Crous P.W., 2009. First report of shoot blight, canker, and gummosis caused by *Neoscytalidium dimidiatum* on citrus in Italy. *Plant Disease* 93(11): 1215–1215. https://doi.org/10.1094/PDIS-93-11-1215A

Postollec F., Falentin H., Pavan S., Combrisson J. and Sohier D., 2011. Recent advances in quantitative PCR (qPCR) applications in food microbiology. *Food Microbiology*, 28(5): 848–861. https://doi.org/10.1016/j.fm.2011.02.008

Qiao M., Du X., Zhang Z., Xu J., Yu, Z., 2018. Three new species of soil-inhabiting *Trichoderma* from southwest China. *MycoKeys* 44: 63. https://doi.org/10.3897/mycokeys.44.30295

Qiao W., Kang X., Ma X., Ran L., Zhen Z., 2024. New strain of *Bacillus amyloliquefaciens* G1 as a potential downy mildew biocontrol agent for grape. *Agronomy*, 14(7): 1532. https://doi.org/10.3390/agronomy14071532

Rodriguez R.J., White Jr. J.F., Arnold A.E., Redman R.A., 2009. Fungal endophytes: diversity and functional roles. *New Phytologist* 182(2): 314–330. https://doi.org/10.1111/j.1469-8137.2009.02773.x

Rotolo C., De Miccolis Angelini R.M., Pollastro S., Faretra F., 2016. A TaqMan-based qPCR assay for quantitative detection of the biocontrol agents *Bacillus subtilis* strain QST713 and *Bacillus amyloliquefaciens* subsp. *plantarum* strain D747. *BioControl* 61(1): 91–101. https://doi.org/10.1007/s10526-015-9701-4

Rubio M.B., Hermosa M.R., Keck E., Monte E., 2005. Specific PCR assays for the detection and quantification of DNA from the biocontrol strain *Trichoderma harzianum* 2413 in soil. *Microbial Ecology* 49(1): 25–33. https://doi.org/10.1007/s00248-003-0171-3

Sandoval-Denis M., Guarnaccia V., Polizzi G., Crous P.W., 2018. Symptomatic citrus trees reveal a new pathogenic lineage in *Fusarium* and two new *Neocosmospora* species. *Persoonia* 40(1): 1–25. https://doi.org/10.3767/persoonia.2018.40.01

Sarrocco S., Esteban P., Vicente I., Bernardi R., Plainchamp T., … Dufresne, M., 2021. Straw competition and wheat root endophytism of *Trichoderma gamsii* T6085 as useful traits in the biological control of Fusarium head blight. *Phytopathology* 111(7): 1129–1136. https://doi.org/10.1094/PHYTO-09-20-0441-R

Savazzini F., Longa C.M.O., Pertot I., Gessler C., 2008. Real-time PCR for detection and quantification of the biocontrol agent *Trichoderma atroviride* strain SC1 in soil. *Journal of Microbiological Methods* 73(2): 185–194. https://doi.org/10.1016/j.mimet.2008.02.004

Scott K., Konkel Z., Gluck-Thaler E., Valero David G.E., Simmt C.F., … Slot, J., 2023. Endophyte genomes support greater metabolic gene cluster diversity compared with non-endophytes in *Trichoderma*. *PLoS One* 18(12): e0289280. https://doi.org/10.1371/journal.pone.0289280

Silvia M., 2021. Application of *Trichoderma* as an alternative to the use of sulfuric acid pesticides in the control of Diplodia disease on pomelo citrus. In: *IOP Conference Series: Earth and Environmental Science*. 11 November, 2020, Kuala Lumpur, Malaysia, 819(1): 012007. https://doi.org/10.1088/1755-1315/819/1/012007

Solel Z., Salerno M., 2000. Mal secco. In: *Compendium of Citrus Diseases (*L.W. Timmer, S.M. Garnsey, J.H. Graham, ed.), 2nd ed. American Phytopathological Society, Saint Paul, MN, 33–35.

Somerville T.F., Corless C.E., Sueke H., Neal T., Kaye S.B., 2020. 16S ribosomal RNA PCR versus conventional diagnostic culture in the investigation of suspected bacterial keratitis. *Translational Vision Science*

and Technology 9(13): 2–2. https://doi.org/10.1167/tvst.9.13.2

Stummer B.E., Zhang Q., Zhang X., Warren R.A., Harvey P.R., 2020. Quantification of *Trichoderma afroharzianum*, *Trichoderma harzianum* and *Trichoderma gamsii* inoculants in soil, the wheat rhizosphere and *in planta* suppression of the crown rot pathogen *Fusarium pseudograminearum*. *Journal of Applied Microbiology* 129(4): 971–990. https://doi.org/10.1111/jam.14670

Su Z., Liu G., Li C., Liu X., Guo Q., … Qu, Y., 2024. Establishment and application of quantitative detection of *Bacillus velezensis* HMB26553, a biocontrol agent against cotton damping-off caused by Rhizoctonia. *Biotechnology Journal* 19(2): 2300412. https://doi.org/10.1002/biot.202300412

Sung G.H., Sung J.M., Hywel-Jones N.L., Spatafora J.W., 2007. A multi-gene phylogeny of Clavicipitaceae (Ascomycota Fungi): identification of localized incongruence using a combinational bootstrap approach. *Molecular Phylogenetics and Evolution* 44(3): 1204–1223. https://doi.org/10.1016/j.ympev.2007.03.011

Tan Q., Zhang Y., Zhou T., Xiong Y., Huang Q., … Manawasinghe I., 2025. Endophytic *Trichoderma* (Sordariomycetes, Hypocreaceae) species associated with citrus in Guangdong province, China. *New Zealand Journal of Botany* 63(2–3): 251–277. https://doi.org/10.1080/0028825X.2024.2445352

Timmer L.W., Roberts P.D., Darhower H.M., Bushong P.M., Stover E.W., … Ibáñez, A.M., 2000. Epidemiology and control of citrus greasy spot in different citrus-growing areas in Florida. *Plant Disease* 84(12): 1294–1298. https://doi.org/10.1094/PDIS.2000.84.12.1294

Timmer L.W., Garnsey S.M., Grahameditors J.H., 2000. *Compendium of Citrus Diseases*. 2nd edition. American Phytopathological Society, APS Press, St. Paul, MN, USA, 92 pp.

Timofeeva A.M., Galyamova M.R., Sedykh S.E., 2023. Plant growth-promoting bacteria of soil: designing of consortia beneficial for crop production. *Microorganisms* 11(12): 2864. https://doi.org/10.3390/microorganisms11122864

Torsvik V., Øvreås L., 2002. Microbial diversity and function in soil: from genes to ecosystems. *Current Opinion in Microbiology* 5(3): 240–245. https://doi.org/10.1016/S1369-5274(02)00324-7

Triantafyllidis V., Zotos A., Kosma C., Kokkotos E., 2020. Environmental implications from long-term citrus cultivation and wide use of Cu fungicides in Mediterranean soils. *Water, Air, & Soil Pollution 231*(5): 218. https://doi.org/10.1007/s11270-020-04577-z

Tseng Y-H., Rouina H., Groten K., Rajani P., Furch A.C.U., … Oelmüller R., 2020. An endophytic *Trichoderma* strain promotes growth of its hosts and defends against pathogen attack. *Frontiers in Plant Science* 11: 573670. https://doi.org/10.3389/fpls.2020.573670

Vitale A., Aiello D., Azzaro A., Guarnaccia V., Polizzi G., 2021. An eleven-year survey on field disease susceptibility of citrus accessions to *Colletotrichum* and *Alternaria* species. *Agriculture* 11(6): 536. https://doi.org/10.3390/agriculture11060536

Vu T.X., Tran V. T., 2020. Isolation and characterization of *Trichoderma* strains antagonistic against pathogenic fungi on orange crops. *VNU Journal of Science: Natural Sciences and Technology* 36(3): 1–10. https://doi.org/10.25073/2588-1140/vnunst.5086

Wang H., Zhang R., Duan Y., Jiang W., Chen X., Shen X., Yin C., Mao Z., 2021. The endophytic strain *Trichoderma asperellum* 6S-2: an efficient biocontrol agent against apple replant disease in china and a potential plant-growth-promoting fungus. *Journal of Fungi* 7: 1050. https://doi.org/10.3390/jof7121050

Wang L., Zhao X., Chu J., Li Y., Li Y., … Zhong Q., 2011. Application of an improved loop-mediated isothermal amplification detection of *Vibrio parahaemolyticus* from various seafood samples. *African Journal of Microbiology Research* 5(31): 5765–5771. https://doi.org/10.5897/AJMR11.1237

Weideman H., Wehner F.C., 1993. Greenhouse evaluation of *Trichoderma harzianum* and *Fusarium oxysporum* for biological control of citrus root rot in soils naturally and artificially infested with *Phytophthora nicotianae*. *Phytophylactica* 25(2): 101–106.

Whipps J.M., 2001. Microbial interactions and biocontrol in the rhizosphere. *Journal of Experimental Botany* 52(suppl_1): 487–511. https://doi.org/10.1093/jexbot/52.suppl_1.487

Woo S.L., Hermosa R., Lorito M., Monte E., 2023. *Trichoderma*: a multipurpose, plant-beneficial microorganism for eco-sustainable agriculture. *Nature Reviews Microbiology* 21(5): 312–326. https://doi.org/10.1038/s41579-022-00819-5

Xie S., Yu H., Wang Q., Cheng Y., Ding T., 2020. Two rapid and sensitive methods based on TaqMan qPCR and droplet digital PCR assay for quantitative detection of *Bacillus subtilis* in rhizosphere. *Journal of Applied Microbiology* 128(2): 518–527. https://doi.org/10.1111/jam.14481

Xu X., Fagg G., Passey T., 2025. Population dynamics of three commercial biocontrol organisms on strawberry plants grown in coir substrate under protection. *Plant Pathology* 74(5): 1302–1314. https://doi.org/10.1111/ppa.14093

Xu H., Yan L., Zhang M., Chang X., Zhu D., ... Chen W., 2022. Changes in the density and composition of rhizosphere pathogenic *Fusarium* and beneficial *Trichoderma* contributing to reduced root rot of intercropped soybean. *Pathogens* 11(4): 478. https://doi.org/10.3390/pathogens11040478

Xu Z., Li L., Alam M. J., Zhang L., Yamasaki S., Shi L., 2008a. First confirmation of integron-bearing methicillin-resistant *Staphylococcus aureus*. *Current Microbiology* 57(3): 264–268. https://doi.org/10.1007/s00284-008-9187-8

Xu Z., Shi L., Alam M.J., Li L., Yamasaki S., 2008b. Integron-bearing methicillin-resistant coagulase-negative staphylococci in South China, 2001–2004. *FEMS Microbiology Letters* 278(2): 223–230. https://doi.org/10.1111/j.1574-6968.2007.00994.x

Zanfaño L., Carro-Huerga G., Rodríguez-González Á., Mayo-Prieto S., Cardoza R.E., ... Casquero P.A., 2024. Trichoderma carraovejensis: a new species from vineyard ecosystem with biocontrol abilities against grapevine trunk disease pathogens and ecological adaptation. *Frontiers in Plant Science*, *15*: 1388841. https://doi.org/10.3389/fpls.2024.1388841

Zhou Z., Lu S., Liu T., Liu J., Deng J., ... Yi T., 2024. Biocontrol of citrus melanose *Diaporthe citri* by *Bacillus subtilis* M23. *Biological Control* 197: 105608. https://doi.org/10.1016/j.biocontrol.2024.105608

Phytopathologia Mediterranea
The international journal of the
Mediterranean Phytopathological Union

Firenze University Press
www.fupress.com/pm

Research Papers

Synergism of abiotic stresses and Hop Stunt Viroid infections causing citrus decline in Jahrom Orchards, Iran

Seyed Ali Akbar BAGHERIAN[1,*], Behzad HAJIEGHRARI[2], Mojahed KAMALIZADEH[2]

[1] *Department of Horticultural science, College of Agriculture, Jahrom University, Jahrom, Iran*
[2] *Department of Agricultural Biotechnology, College of Agriculture, Jahrom University, Jahrom, Iran*
*Corresponding author. Emails: bagherian@jahromu.ac.ir; sabagherian@gmail.com

Summary. Citrus is an economically important crop in subtropical regions including Jahrom, Iran. Productivity of these fruit crops can severely decline due to biotic and abiotic stresses. Interactions were investigated between Hop Stunt Viroid (HSVd) infections and abiotic stress factors (drought and soil salinity) for effects on orchard decline. HSVd infection, a key biotic factor causing citrus cachexia, along with abiotic stresses of drought, high temperatures, and poor orchard management, compromise tree health by disrupting water balance and causing stunting and bark damage. Combined effects of HSVd infection and environmental stresses on citrus decline were assessed. Experimental treatments of healthy (experimental control), HSVd infected, abiotic decline-affected, and HSVd + abiotic decline was assessed in three citrus orchards. Compared with controls, trees from the other three treatments had reduced yields, plant heights, crown sizes, and fruit diameters. Plant heights varied among orchards, while fruit diameters did not. Healthy (control) plants grew and yielded best, while yields from plants infected with HSVd and subjected to climate change yielded least. Trees under climate-induced decline had increased fruit diameters, likely due to reduced fruit set under drought stress and redirected assimilates to reduced numbers of developing fruits. Similar responses have been reported in citrus under water stress conditions. Molecular diagnostics (RT-PCR and dot-blot hybridization) confirmed HSVd presence exclusively in symptomatic trees (samples of 10 trees per orchard), while assays for citrus Tristeza Virus (CTV) were negative. These results are consistent with HSVd being the primary biotic agent associated with the observed citrus decline, although causal confirmation requires controlled inoculation studies. Stresses negatively impacted citrus productivity in 85 orchards in Jahrom. Given the observed associations between HSVd presence, abiotic decline indicators, and reduced productivity, integrated citrus crop management is recommended. This should include reductions of drought (through optimized irrigation scheduling), and soil salinity (mitigation of sodium adsorption ratio), and appropriate phytosanitary measures. Phytosanitation should include use of certified viroid-free planting material, and targeted molecular surveillance for viroid infections. Implementation of these strategies should be guided by follow-up studies that verify absence/presence of other graft-transmissible pathogens, quantify rootstock effects, and test mitigation strategies in controlled and replicated field trials.

Keywords. Abiotic stresses, HSVd infections, citrus decline, Lisbon lemon.

OPEN ACCESS

Citation: Bagherian, S. A. A., Hajieghrari, B., & Kamalizadeh, M. (2026). Synergism of abiotic stresses and Hop Stunt Viroid infections causing citrus decline in Jahrom Orchards, Iran. *Phytopathologia Mediterranea* 65(1): 153-164. doi: 10.36253/phyto-16995

Accepted: April 19, 2026

Published: May 14, 2026

© 2026 Author(s). This is an open access, peer-reviewed article published by Firenze University Press (https://www.fupress.com) and distributed, except where otherwise noted, under the terms of the CC BY 4.0 License for content and CC0 1.0 Universal for metadata.

Data Availability Statement: All relevant data are within the paper and its Supporting Information files.

Competing Interests: The Author(s) declare(s) no conflict of interest.

Editor: Nihal Buzkan, Kahramanmaraş Sütçü Imam University, Turkey.

ORCID:
SAAB: 0000-0003-4330-2335
BH: 0000-0002-7470-046X
MK: 0000-0002-8694-3928

INTRODUCTION

Citrus includes a diverse group of fruit plant species and cultivars, that produce oranges, limes, grapefruit, and sour oranges (Wu *et al*., 2018). These fruits are internationally valued for their distinctive flavours, vibrant colours, and nutritional content (Lv *et al*., 2015). These fruits are native to subtropical and tropical regions, typically found between latitudes 40°N and 40°S (Raju *et al*., 2024). Citrus is one of the most economically important fruit crops cultivated in these regions, including the Jahrom area in Fars Province, Iran.

The Jahrom region (28°30′N, 53°33′E), in the semiarid Fars Province of Iran, exemplifies the environmental challenges facing citrus production in the era of climate change. This region has average annual rainfall of less than 170 mm, occurring almost entirely outside the winter-spring growing season, necessitating heavy reliance on groundwater irrigation for fruit production. These aquifers are increasingly stressed and often salinized, with reported sodium adsorption ratios (SAR) exceeding 13 in some agricultural wells (Bagherian *et al*., 2021). Summertime temperatures regularly surpass 40°C, accompanied by low relative humidity (often <25%) and high evapotranspiration rates (>8 mm d^{-1}). These common conditions of water scarcity, endemic soil salinity, and high temperatures challenge citrus cultivation; and create persistent abiotic stress that pre-disposes trees to secondary pathogens. Consequently, Jahrom region offers a representative case study for investigating how orchard decline may be affected a synergy between abiotic factors (drought, salinity, high temperature) and the biotic agent *Citrus hop stunt viroid* (HSVd).

HSVd interferes with host plant regulatory and metabolic networks (Marquez-Molins *et al*., 2021; Di Serio *et al*., 2024). Although not typically lethal, HSVd causes chronic damage to citrus plants, that includes stunted growth, reduced fruit size and quality, stem pitting, bark gummoses, and overall decline. While HSVd infections may remain asymptomatic or produce mild symptoms under normal conditions, their effects are intensified under environmental stress (Hadidi *et al*., 2024).

Citrus orchards internationally, including those in Jahrom, Iran, have experienced significant declines in productivity and vitality, which have been due to a complex interplay of biotic and abiotic factors. A key biotic constraint are infections by HSVd, the causal agent of citrus cachexia (Vamenani *et al*., 2019). Concurrently, several abiotic stressors, including extreme temperature fluctuations, prolonged drought, flooding, and elevated soil and water salinity, have been exacerbated by climate change, posing severe threats for citrus cultivation (Dahro *et al*., 2023). Notably, the HLB-associated bacterium 'Candidatus Liberibacter asiaticus' has been detected in citrus trees in Fars Province, Iran, including the Jahrom region (Rahimpour *et al*., 2025; Faghihi *et al*., 2025), adding another potential biotic stressor to the complex decline syndrome affecting local orchards.

In Jahrom, additional challenges including use of substandard planting materials, degraded soil quality, inconsistent rainfall patterns, and suboptimal orchard management practices, further contribute to citrus decline. Among abiotic stressors, drought remains the most pressing issue, driven by high temperatures, inadequate rainfall, poor irrigation management, and soil water deficits. Physical constraints, including soil compaction, poor drainage, and excessive salinity, also limit root access to water and nutrients, intensifying the effects of drought stress.

High temperatures, particularly when accompanied by elevated evaporation losses, severely affect citrus physiology by disrupting the balance between water absorption and transpiration (Moore *et al*., 2021; Chen *et al*., 2025). In the Jahrom region, this imbalance is a key contributor to physiological decline observed in citrus trees. The optimal temperature range for citrus plant growth is between 22 and 34°C; temperatures exceeding this range cause fruit drop, reduced fruit size, and impaired overall tree productivity. Although some citrus varieties can tolerate temperatures above 40°C without showing immediate visible symptoms, the long-term physiological stress incurred leads to reduced growth and low fruit yields.

Infections by viroids, which are circular, single-stranded RNA molecules ranging from 246 to 401 nucleotides, are another important factor in citrus decline. They are classified into two families, the *Pospiviroidae* and *Avsunviroidae* (Di Serio *et al*., 2014). Citrus trees are natural hosts to several viroid species, all belonging to *Pospiviroidae*. Among these, pathogenic variants of HSVd are responsible for citrus cachexia, a disease that prevails in most citrus-producing regions, including Jahrom (Belabess *et al*., 2021). HSVd is mechanically transmissible *via* sap and contaminated tools. Infected trees typically exhibit symptoms of stunting, leaf chloroses, bark gummoses, stem pitting, and general decline, although leaf and fruit symptoms may be absent in HSVd-infected plants (Marquez-Molins *et al*., 2021).

The present study aimed to evaluate the combined effects of abiotic stresses and HSVd infection on citrus trees in the Jahrom region. Disease severity was assessed in the context of local climatic conditions, and the interactive roles were assessed of environmental and pathogen factors in citrus orchard decline. This knowl-

edge could support development of integrated management strategies to enhance citrus resilience and sustainability under changing environmental conditions. The study controlled for potential confounding factors, by focusing on one citrus rootstock across the sampled orchards, and also made assessments for other major pathogens.

MATERIALS AND METHODS

This study was carried out during 2022 and 2023, across multiple commercial citrus orchards in the Jahrom region, Fars Province, Iran. Hereafter, 'growth condition' refers to pre-existing orchard health categories (healthy, HSVd-affected, abiotic decline, or HSVD/abiotic decline combined) used for comparative analyses, but that were not experimentally imposed treatments. Specifically, the treatments corresponded to orchard health/status categories, which were: (A) Healthy control orchards (no visual decline symptoms, no molecular evidence of HSVd); (B) HSVd-affected orchards (trees exhibiting stem-pitting/shaqqaq symptoms, and HSVd detection confirmed by molecular assays); (C) abiotic decline orchards (trees meeting predefined abiotic decline criteria described below); or (D) orchards showing both HSVd-associated symptoms and abiotic decline indicators. Each "treatment" thus represented a natural orchard category used for observational comparisons.

The following abiotic stress factors were quantified in this study:

- Soil salinity: Measured as sodium adsorption ratio (SAR), using ICP-OES, with SAR > 13 classified as severe salinity stress.
- Drought stress: Assessed by actual irrigation volume applied (L per tree per day) compared to recommended rates (80–100 L per tree per day in summer; 40–50 L per tree per day in winter).
- Heat stress: Recorded as number of days per growing season with maximum temperatures exceeding 40°C.
- Soil structural degradation: Evaluated using assessments of soil organic matter content and texture (hydrometer method), with low organic matter (< 1%) considered a contributing factor.
- Canopy light limitation: Measured as percentage light interception using a ceptometer (AccuPAR LP-80), with < 60% interception indicating poor canopy development.
- Evaporative water loss: Assessed indirectly by presence/absence of organic mulch (target: 10–15 cm depth under canopy).

Trees were classified as experiencing "abiotic decline" (treatment category 3) if they exhibited SAR > 13, light interception < 60%, and at least two visual decline symptoms (leaf chlorosis score ≥ 3, canopy thinning > 30%, or terminal branch dieback).

All sampled trees had the same scion cultivar, rootstock, age, and phenological stage, to minimize variability unrelated to the factors under study. Specifically, the study focused on 'Lisbon' lemon (*Citrus limon* L. 'Lisbon') grafted onto sour orange (*Citrus aurantium* L.) rootstock. All selected trees were 12 to 15 years old, at full commercial maturity, and had been consistently fruit-bearing for at least 6 years prior to the study. Trees exhibiting obvious signs of juvenility or senescence were excluded from samplings. This uniformity ensured that observed differences in decline severity could be attributed primarily to treatment effects (HSVd infection, abiotic stress, or their combination) rather than to genetic or developmental variation.

Healthy orchards (control group) were selected based on optimal tree growth, high fruit quality, and the absence of significant pests and diseases. HSVd infections were diagnosed by symptomatology and confirmed molecularly. Leaf and symptomatic bark samples were tested by RT-PCR with the HSVd-specific primers described by Bagherian and Izadpanah (2010). Representative RT-PCR amplicons (n = 6) were gel-purified and Sanger-sequenced; BLASTn comparison of these sequences against NCBI nt confirmed HSVd identities with ≥ 99% nucleotide similarity to reference HSVd sequences (Bagherian and Izadpanah, 2010). Amplification controls included a positive control (RNA from HSVd-infected sweet lime), and a negative control (RNA from viroid-free seedlings). Dot-blot hybridization using DIG-labelled HSVd probes corroborated RT-PCR results. Young, fully expanded leaves and symptomatic bark tissues were collected from ten randomly selected trees per orchard, including symptomatic and asymptomatic trees. The samples were promptly placed in sterile polyethylene bags, stored on ice, and transported to the laboratory within 6 h, before being assessed using RT-PCR. Total nucleic acids were extracted using the optimized high titer viroid extraction method described by Semancik *et al.* (1975). For RNA extraction and viroid enrichment, citrus tissues were homogenized in extraction buffer containing 0.1 M Tris–HCl, 0.1 M NaCl, 0.01 M EDTA, and 1% SDS, pH 8.0. After centrifugation, nucleic acids were fractionated by adding 2 M LiCl, selectively precipitating high-molecular-weight RNA and DNA. The viroid-enriched supernatant was then precipitated using ethanol. The resulting RNA pellets were resuspended in TKM buffer (10 mM Tris–HCl, 10 mM KCl,

0.1 mM $MgCl_2$, pH 7.4), and were then stored at −80°C until used. Reverse transcription-polymerase chain reaction (RT-PCR) detection of HSVd, was carried out using HSVd-specific primers targeting the full-length viroid genome (Bernad and Durán-Vila 2006):

Forward primer: 5′-GGGGCAACTCTTCTCAGAATCC-3′
Reverse primer: 5′-GGGGCTCCTTTCTCAGGTAAGTC-3′

Complementary DNA (cDNA) syntheses were carried out using RevertAid M-MuLV reverse transcriptase (Thermo Scientific), followed by PCR amplification with Taq DNA polymerase (Invitrogen). Thermal cycling conditions were as follows: initial denaturation at 94°C for 3 min; 35 cycles, each of denaturation at 94°C for 30 sec, annealing at 55°C for 30 sec, and extension at 72°C for 45 sec; then a final extension at 72°C for 7 min. PCR products (~300 bp) were separated on 1% agarose gels, were stained with SYBR Safe DNA gel stain, and were visualized under UV illumination.

To rule out co-infections with other prevalent pathogens, all sampled trees were also tested for citrus tristeza virus (CTV) using CTV-specific primers (Ayllón *et al.*, 2001). Each CTV-specific RT-PCR run included a positive control (RNA from CTV-infected citrus tissue) and a negative control (RNA from viroid- and virus-free citrus seedlings). All sampled trees tested negative for CTV. To confirm RT-PCR results, dot-blot hybridization assays were carried out, following the method of Li *et al.* (1995). Full-length HSVd cDNA probes were labelled with digoxigenin (DIG) using the PCR DIG Probe Synthesis Kit (Roche). Nucleic acid extracts were applied to positively charged nylon membranes, and were hybridized with DIG-labelled probes at 50°C. Detection was carried out using anti-DIG alkaline phosphatase-conjugated antibodies, followed by chromogenic development with NBT/BCIP substrate.

Abiotic citrus decline was diagnosed based on a combination of field symptoms and environmental stress indicators, following the protocol of Bagherian *et al.* (2021). Citrus trees were classified as experiencing only abiotic decline if they met all the following criteria:

- Soil sodium adsorption ratio (SAR) > 13 (determined by ICP-OES)
- Canopy light interception < 60% (measured by ceptometer at midday)
- At least two of the following visual decline symptoms: persistent leaf chlorosis (score ≥ 3); canopy thinning > 30%; annual terminal branch dieback.

Soil analyses

Composite soil samples (0–30 cm depth) were collected and analyzed for texture using the hydrometer method (Mwendwa, 2022), and sodium adsorption ratios (SAR) were calculated from Na^+, Ca^{2+}, and Mg^{2+} concentrations (Pansu and Gautheyrou, 2006) determined by inductively coupled plasma optical emission spectrometry (ICP-OES).

Canopy shading

Light interception was measured using a ceptometer (AccuPAR LP-80, Decagon Devices), at midday on clear days. Ten readings were taken under each assessed canopy, and ten outside (open sky), in each tree quadrant, and percentage light interception was calculated.

Tree vigour assessments

Tree trunk circumferences, shoot growth rates, and incidence of branch dieback were assessed as indicators of tree vigour. Trees were classified as experiencing abiotic decline only if they met all of the following criteria:

(a) Soil SAR > 2 (determined by ICP-OES),
(b) Canopy light interception < 60% (based on ceptometer readings), and
(c) At least two visual symptoms of decline, including: Persistent leaf chlorosis (chlorosis score ≥ 3), Canopy thinning > 30% or Annual terminal branch dieback.

The experimental groups represented distinct phytosanitary and edaphic conditions found in the region. To minimize variability unrelated to the factors under study, all sampled trees were of the same cultivar and age, grafted on a common rootstock, and managed under similar horticultural practices prior to the onset of decline symptoms. For consistency, all sampled trees belonged to one citrus cultivar, were of similar age, and exhibited uniform pre-treatment health conditions. To reduce variability, the trees were at 6 m spacings and were managed under identical cultural practices, apart from the treatment-specific interventions.

Three orchards were selected based on similar cultivar, age, and general management practices. Although irrigation systems and soil types varied slightly, these were accounted for as random effects in the statistical model to minimize confounding variability between orchards. At the fruit ripening stage, data were collected using systematic random sampling. Each selected tree was divided into four quadrants (north, south, east, or

west), and samples were taken from three canopy levels (upper, middle, or lower) to account for intra-canopy variations.

The experimental design was a Repeated Measures Completely Randomized Design (RM-CRD). Treatments were randomly assigned to experimental units. The following morphological and yield-related traits were measured for each tree:

- Fruit yield (kg per tree): All harvested fruits were weighed using a high-precision digital scale.
- Tree height (m): Measured from the tree base to the canopy apex using a telescopic measuring pole.
- Canopy diameter (m): Calculated by averaging two measuring tape measurements at right angle to each other.
- Fruit diameter (cm): Measured from a random sample of 100 fruits per tree, collected from various canopy positions. A digital caliper with ±0.1 mm accuracy was used, and all measurements were carried out in triplicate.

Data obtained were assessed for normality prior to analyses. Statistical analyses were carried out using Minitab software. A one-way analysis of variance (ANOVA) was conducted to examine effects of treatments on tree growth and fruit production. Where statistically significant effects were detected, Tukey's *post hoc* test was used to identify pairwise differences among treatment means. Results were expressed as means ± standard errors (SE), with statistical significance set at $P < 0.05$.

Although citrus greening (HLB) caused by 'Candidatus Liberibacter asiaticus' has been reported in Fars Province (Faghihi *et al*., 2025), the sampled trees in the present study did not exhibit characteristic HLB symptoms, such as asymmetrical chloroses, blotchy mottle, or lopsided fruit with aborted seeds. Therefore, HLB was not considered an important biotic factor in the present study, although its potential presence in the region underscores the complexity of citrus decline etiology.

RESULTS

RT-PCR assays successfully amplified approx. 300 bp fragments specific to HSVd in all leaf and bark samples collected from trees showing stem pitting symptoms (Groups B and D). In contrast, samples from asymptomatic trees (Groups A and C) did not show any amplifications. Positive (infected sweet lime) and negative (virus-free seedlings) controls confirmed specificity of the assay. Dot-blot hybridization further confirmed these results. All RT-PCR-positive samples exhibited strong hybridization signals with DIG-labeled HSVd probes, while RT-PCR-negative samples did not give detectable signals. These molecular results indicated direct association between HSVd infections and the stem pitting symptoms observed in the field. Nevertheless, given the limited sample size (ten trees per orchard) and the observational design, these data demonstrate HSVd association rather than causation.

The ANOVA results showed significant differences in fruit yields across the treatments ($P = 0.001$). This indicates that the treatments affected yield, and at least one treatment produced a significantly different result compared to the others. This indicates that the applied treatment type influenced yield in comparison to the control (Table 1). Combined HSVd + abiotic-decline trees experienced the greatest yield losses (≈85% relative to controls). To evaluate whether this reduction represented synergy rather than independent effects, the observed combined loss (85%) was compared with the expected combined loss under an independent (multiplicative) model: expected combined loss = $1 - (1 - 0.38) \times (1 - 0.60) = 75.2\%$. Because the observed loss (85%) exceeded the expected independent effect (75.2%) and the interaction term in the mixed-effects model was statistically significant ($\chi^2 = 12.7$, $P < 0.001$), these results are consistent with a synergistic interaction between HSVd infection and abiotic decline.

The *post hoc* Tukey's test analysis grouped the treatments into four distinct four groups. Group A: the control (greatest yield), Group B: Hop Stunt Viroid-infected trees, Group C: climate change threatened decline, and Group D: combined effect of HSVd and decline (least yield). Healthy plants yielded more than plants in the other three treatments. The combined HSVd and decline treatment yielded the least (Figure 1). The ANOVA for plant height data showed statistically significant differences between the treatments ($P = 0.001$), and between the orchards ($P = 0.035$), indicating that treatments and orchards affected plant height (Table 2).

Plant height was the most affected of the growth parameters assessed. and the orchards also affected

Table 1. Analysis of Variance (ANOVA) for fruit yield data obtained in this study.

Source	DF	Adj SS	Adj MS	F-Value	*P*-Value
Treatment	3	3924427	1308142	634.15	< 0.001
Orchard	2	5008	2504	1.21	0.297
Error	2258	4657836	2063		
Lack-of-Fit	6	18300	3050	1.48	0.181
Pure Error	2252	4639536	2060		
Total	2263	8587484			

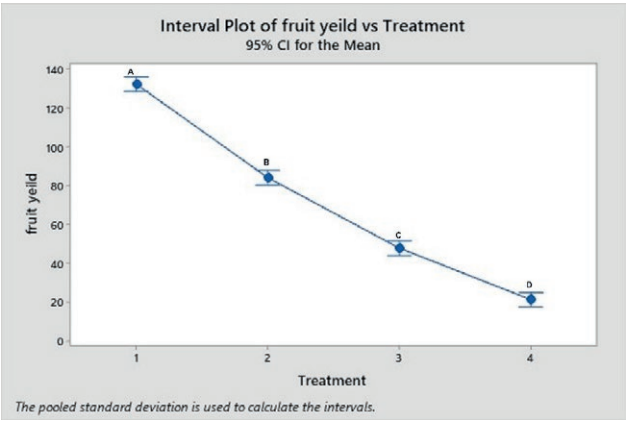

Figure 1. Mean Citrus plant yields (kg) from "healthy" plants (Treatment 1) or plants with Hop Stunt Viroid (HSVd) infections (Treatment 2), climate change-induced decline (Treatment 3), or combined HSVd plus climate-induced stress (Treatment 4). Means accompanied by different letters are ($P < 0.05$; Tukey's HSD tests).

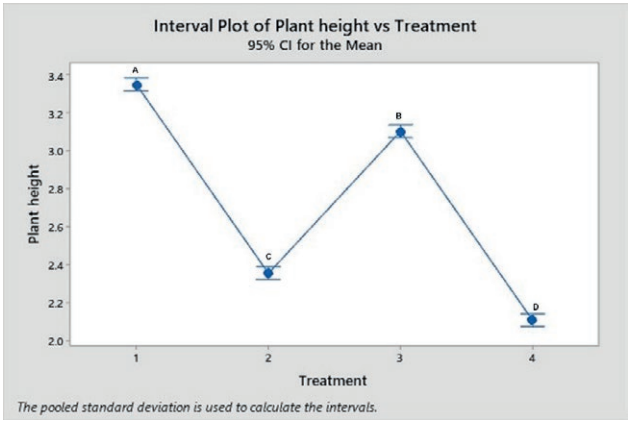

Figure 2. Effects of Hop Stunt Viroid Infection, climate change-induced decline, and their interaction on citrus tree height (m). (1) healthy control, (2) HSVd-infected trees, (3) trees exhibiting decline due to climate-related stressors, and (4) trees exposed to both HSVd infection and climate-induced decline. Means with different letters are significantly different at $P < 0.05$ (Tukey's HSD).

Table 2. Analysis of Variance (ANOVA) for plant height data obtained in this study.

Source	DF	Adj SS	Adj MS	F-Value	*P*-Value
Treatment	3	598.215	199.405	1199.67	0.001
Orchard	2	1.120	0.560	3.37	0.035
Error	2258	375.317	0.166		
Lack-of-Fit	6	0.493	0.082	0.49	0.814
Pure Error	2252	374.824	0.166		
Total	2263	974.571			

Table 3. The Analysis of Variance (ANOVA) for plant crown diameter data obtained in this study.

Source	DF	Adj SS	Adj MS	F-Value	*P*-Value
Treatment	3	207.31	69.1049	88.67	0.001
Orchard	2	0.47	0.2358	0.30	0.739
Error	2258	1759.77	0.7793		
Lack-of-Fit	6	4.60	0.7663	0.98	0.435
Pure Error	2252	1755.17	0.7794		
Total	2263	1967.54			

this parameter. However, the primary source of plant height differences was due to the treatments. *Post-hoc* Tukey's test results showed the following growth condition grouping: Group A: the control (tallest plants), Group B: climate changes threatened decline, Group C: HSVd infected trees, and Group D: HSVd infected and decline (shortest plants). The healthy plants were the tallest plants, which were taller than the climate changes threatened decline, the Hop Stunt Viroid-infected trees, and for the trees in the HSVd plus decline treatment. Although HSVd-infected trees were shorter than the climate plus decline trees, the overall growth suppression (including canopy densities and yields) was more severe in the climate plus decline trees, indicating the broader physiological limitation of these two factors. The combined effect of HSVd plus decline resulted in the shortest plants, indicating that the treatment interaction caused greatest growth reduction (Figure 2). The ANOVA for tree crown diameter indicated significant differences between the treatments ($P = 0.001$). Growth condition was also associated with crown diameter (Table 3).

Post hoc, the Tukey tests showed that the control plants had the largest crown diameters. The mean crown diameters in HSVd-infected trees, climate change threatened trees, and the combined effects of HSVd and decline were all less than for the controls. This indicated that the combined effect HSVd plus decline had the greatest impact on crown diameter, which could impede overall plant growth and development (Figure 3). For fruit diameter, there were significant differences between the treatments ($P = 0.001$), differences between the three orchards were not significant ($P = 0.125$) (Table 4).

Post hoc analyses grouped the treatments as follows: Group A: climate changes threatened decline (greatest fruit diameter), Group B: the control, Group C: HSVd infected trees, and Group D: combined HSVd and decline (least fruit diameter). Although fruit diameter was greater in climate stressed trees,

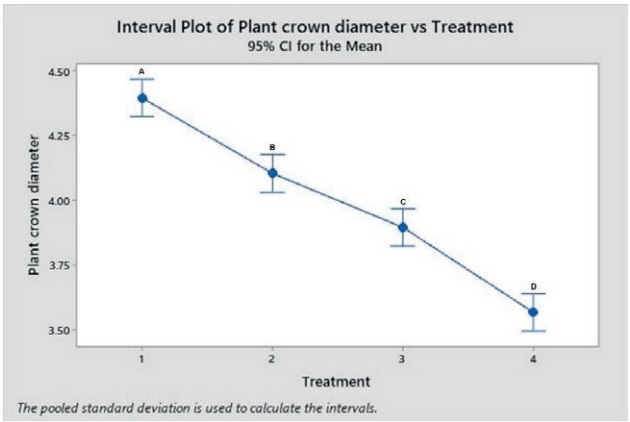

Figure 3. Effects of Hop Stunt Viroid Infection, climate change-induced decline, and their combination on crown diameter of citrus trees (m). (1) healthy control, (2) HSVd-infected trees, (3) trees exhibiting decline due to climate-related stressors, and (4) trees exposed to both HSVd infection and climate-induced decline. Means with different letters are significantly different at $P < 0.05$ (Tukey's HSD).

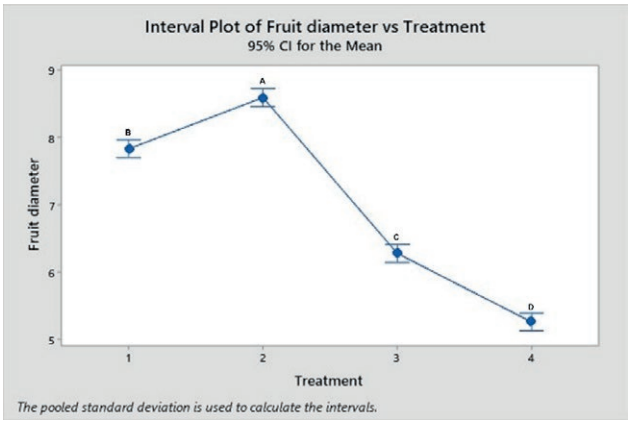

Figure 4. Effects of Hop Stunt Viroid Infection, climate change-induced decline, and Their Interaction on Fruit Diameter in Citrus Trees (cm). (1) healthy control, (2) HSVd-infected trees, (3) trees exhibiting decline due to climate-related stressors, and (4) trees exposed to both HSVd infection and climate-induced decline. Means with different letters are significantly different at $P < 0.05$ (Tukey's HSD).

Table 4. Analysis of Variance (ANOVA) of fruit diameter data obtained in this study.

Source	DF	Adj SS	Adj MS	F-Value	*P*-Value
Treatment	3	3831.25	1277.08	482.97	0.001
Orchard	2	10.99	5.49	2.08	0.125
Error	2258	5970.62	2.64		
Lack-of-Fit	6	18.99	3.17	1.20	0.304
Pure Error	2252	5951.63	2.64		
Total	2263	9813.23			

this should be interpreted with caution due to the concurrent yield reductions, which would undermine the practical value of increased fruit size. However, the combined effect of HSVd plus decline produced the smallest fruits (Figure 4). A strong negative correlation was observed between leaf chlorosis index and fruit yields (r = -0.79, $P < 0.001$), confirming that leaf chlorosis is an indicator of reduced citrus productivity. There was also a negative correlation between SAR and fruit yields (r = -0.72, $P < 0.01$).

Overall, healthy plants gave the greatest fruit yields, were the tallest, and had the greatest crown diameters compared with the other three treatments applied in this study. Climate change threatened decline was the best for enhancing fruit diameter, suggesting it might be more suitable for improving fruit size. The combined effect of HSVd plus decline consistently resulted in the greatest negative effects on plant growth and fruit productivity.

DISCUSSION

This study has provided field-based evidence for synergistic interaction between HSVd infections and abiotic stress as causes of decline of Lisbon lemon trees grafted on sour orange rootstock in Jahrom. The study has also demonstrated a direct link between the observed biotic stress to HSVd, by confirming HSVd infections molecularly and excluding CTV co-infections. Citrus decline is an increasing concern for international citrus production, and is particularly severe in Jahrom, a region recognized for its vibrant and productive citrus industry. Once a hallmark of agricultural success in southern Iran, Jahrom now faces a serious threats to citrus sustainability. While numerous factors contribute to this decline, the two interrelated stressors of climate change and HSVd infections have emerged as the most detrimental and complex challenges facing citrus growers in this region (Kovalskaya and Hammond, 2014; Belabess *et al.*, 2021). Furthermore, while HLB has been detected elsewhere in Fars Province (Faghihi *et al.*, 2025), the absence of characteristic HLB symptoms in the trees sampled in the present study indicate that decline in Jahrom is primarily caused by HSVd and abiotic stresses rather than by Liberibacter infections.

The present study has provided field-based evidence of individual and combined effects of HSVd infection, manifesting as stem pitting ("shaqqaq"; Bagerian and Izadpanah, 2010), and abiotic stress-induced reductions on growth, productivity, and survival of Lisbon lemon (*Citrus limon* L. 'Lisbon') trees in a

semi-arid environment. These results provide valuable insights into the pathophysiological mechanisms affecting citrus tree degeneration under complex, multifactorial stress conditions.

The correlation between stem pitting symptoms and molecular detection of HSVd (and absence of CTV) strengthens evidence that HSVd was the biotic component in tree decline, which is consistent with the report of Bagherian *et al.* (2021). HSVd-infected trees were also smaller than the healthy trees (~30% compared to healthy trees) and had moderate canopy contractions, results that are similar to those of Bagherian and Izadpanah (2010). Viroid-induced disruption of phloem function, characterized by callose deposition and collapse of vascular tissues, has been previously reported, and may play a central role in symptom development, particularly growth stunting and impaired assimilate transport (Di Serio *et al*., 2023). Phloem disruption It likely causes the stunted growth phenotype by impairing assimilate transport and meristem activity. Shaqqaq-only trees had yield losses of approx. 38%, consistent with previous results for HSVd-infected citrus (Navarro *et al*., 2012), highlighting potential economic, though sublethal, effects of these infections. The mild to moderate chloroses indicate impaired nutrient transport or water relations rather than complete systemic failure. The genetic diversity of HSVd populations in Mediterranean regions (Alaxin *et al*., 2023) could explain the variability in symptom expression.

Over the past decade, climate patterns in Jahrom have shifted, with increasing average temperatures, prolonged drought periods, erratic rainfall, and increased evapotranspiration. These abiotic stressors impose adverse physiological effects on citrus trees, disrupting water and nutrient uptake, impairing photosynthesis, and causing hormonal imbalances (Kumari *et al*., 2022; de Souza Junior *et al*., 2025). Direct consequences include reduced size, yield and quality of fruit, stunted vegetative growth, and general plant vigour decline.

Abiotic decline independently exerted adverse effects on tree performance, including yield reductions exceeding 60%, reductions in crown diameters (~11%), and moderate foliar chlorosis. These results are consistent with multi-year studies conducted in comparable semi-arid citrus-growing regions, where factors such as soil compaction, elevated sodium adsorption ratio (SAR), and excessive shading have been identified as key contributors to citrus decline (Navarro *et al*., 2012; Di Serio *et al*., 2023). Salt stress disrupts plant osmotic balance, induces ion toxicity, and promotes oxidative damage, while poor soil aeration impairs root respiration and nutrient uptake (Tian *et al*., 2022; Ahmed *et al*., 2023). Trees with abiotic decline showed minimal height reductions, indicating that root-zone stressors primarily limited canopy development and fruit production, rather than plant height. In the decline-only orchards, the moderate plant death (~15%) reflected the progressive nature of abiotic decline, where tree vigour gradually weakens over several growing seasons before tree death. In addition, a significant negative correlation was detected between leaf chlorosis and yield, emphasizing the importance of monitoring chlorosis as a reliable indicator of citrus decline. Negative correlation was also detected between SAR and fruit yields, indicating that salinity stress adversely affected tree productivity.

Drought stress, in particular, exacerbated by suboptimal irrigation practices and water scarcity, further weakens tree health and compromises defense systems (Seleiman *et al*., 2021). Reduced fruit set under drought stress may lead to the accumulation of photosynthates in the remaining fruits, resulting in increased fruit diameters (Liu *et al*., 2023). Under these conditions, citrus trees become more vulnerable to opportunistic pathogens such as HSVd. This abiotic-biotic interaction creates a compounding effect, where climate stress amplifies the host susceptibility and the impacts of viroid infections. This effect was particularly evident in Jahrom, where stressed trees exhibited severe viroid-induced symptoms and failed to recover or maintain productivity.

The symptoms caused by HSVd, including leaf chlorosis, reduced vigour, and fruit deformation, can be mistaken for, or masked by, drought-related damage. This overlap complicates early diagnoses, delays disease management interventions, and facilitates the spread of HSVd, often through contaminated tools and inadequate sanitation protocols.

The results of the present study reinforce the impacts of the HSVd–climate stress interaction. Growth condition type was found to influence all the measured plant performance indicators, including fruit yield, tree height, canopy diameter, and fruit size. Healthy control trees consistently outperformed all the other growth condition groups, highlighting the importance of maintaining plant health for optimal growth and productivity.

The observed 85% yield loss under combined stress conditions exceeded the theoretical additive effect of HSVd infection and abiotic decline (38% + 60% = 98%; $P < 0.001$), indicating a synergistic rather than additive effect. The increasing incidence of HSVd in Mediterranean citrus orchards further emphasizes the importance of stress interactions and their impacts on orchard sustainability. In the present study, trees with infected by HSVd and affected by abiotic stress had yield reductions (> 85%), severe chlorosis (mean index = 4.2), mor-

tality rates (> 40% within 2 years), and reductions in tree height and crown diameter. These results provide strong evidence for the synergistic interaction between biotic and abiotic stressors. Several mechanisms may underlie this interaction. Compromised vascular function may result from HSVd-induced stem pitting which disrupts phloem integrity, compounding the effects of water stress associated with salinity and impaired root function. Enhanced oxidative stress can result from simultaneous presence of biotic and abiotic stressors to synergistically increase reactive oxygen species (ROS) accumulation, overwhelming antioxidant systems and triggering programmed cell death. Suppression of host defense mechanisms occurs when viroid infections modulate host gene expression, downregulating pathways involved in abiotic stress resistance and increasing the host plant vulnerability to environmental challenges. Synergistic interactions between viral pathogens and drought or salinity stress have been documented in other perennial crops (Prasad *et al*., 2022). However, quantitative characterization of these interactions involving viroids in citrus under commercial field conditions remains scarce, highlighting the novelty and importance of the present study results. Abiotic stresses probably exacerbate viroid replication by disrupting the host RNA silencing mechanisms.

The combined HSVd + climate-induced decline resulted in the most pronounced reduction in all the key measured plant performance traits. These results emphasize the urgent need to revise and improve orchard management strategies, especially in regions facing viroid infections and climate-related pressures. This interaction has socio-economic implications. Citrus production is a key source of income and employment in Jahrom, and the observed decline threatens economic stability of local farming communities. Sustaining citrus cultivation requires an integrated management approach that addresses viroid control and climate adaptation.

The present study had several limitations. Firstly, while CTV was confirmed as absent, potential interactions with other non-assessed or soil-borne pathogens cannot be ruled out. Secondly, the rootstock used (sour orange) is known to be sensitive to abiotic stresses; so the observed synergy might also be rootstock-influenced, and studies on different rootstocks are needed. Thirdly, the term "treatment" in our experimental design refers to pre-existing field conditions rather than actively applied treatments, which is a constraint of observational field studies. Fouthly, the mechanistic basis of the observed synergy requires molecular physiological investigations to confirm hypotheses involving vascular dysfunction or oxidative stress.

The present study results have implications for the development of effective orchard management strategies. These include:

- Enhanced viroid surveillance. Systematic molecular monitoring (e.g., RT-PCR, dot-blot hybridization) for HSVd should be prioritized, particularly in regions where shaqqaq symptoms are prevalent. Early detection of HSVd is important for minimizing viroid-related losses in productivity and citrus tree lifespans.
- Systematic molecular monitoring for HSVd is essential. When detected, infected trees should be immediately removed, as this is the only effective management strategy, as no known cure exists. For infection rates less than 5%, only positive trees should be removed; for rates of 5 to 20%, positive trees plus a two tree buffer should be removed; for infection rates greater than 20%, whole-orchard removal should be undertaken, followed by a fallow period before replanting with certified viroid-free stock.
- Improved soil and water management, to maintain citrus plant vigour and productivity. Drip irrigation systems should be used, to apply 80 to 100 L per tree per day in summer, or 40 to 50 L per tree per day in winter. Irrigate every 2 to 3 d during heat waves (>40°C). Soil salinity management should be used where SAR values exceed 13, and should include application of gypsum (2 to 5 tons ha^{-1} annually). For the 5 to 20% soil leaching fraction, 10 to 20 tons ha^{-1} of manure should be added each year. Organic mulch (10 to 15 cm depth) should be maintained under crop canopies to reduce evaporation and salt accumulation. Every 6 months, soil tests should be carried out to monitor SAR, EC, and pH.
- Integrated stress management. An holistic approach is essential, that simultaneously addresses biotic and abiotic stressors. Specific integrated practices include: (i) combine HSVd testing with soil SAR/EC monitoring in each citrus orchard; (ii) coordinated tree removal (rogueing) with irrigation upgrades and gypsum applications; (iii) planting of viroid-free scions on salt- and viroid-tolerant rootstocks (e.g., 'Rangpur' lime) instead of sour orange; and (iv) training for growers emphasizing that solving abiotic stress alone does not eliminate HSVd decline.
- Sanitation and use of clean planting material. This should rely on RT-PCR certified viroid-free nursery stock. Five percent of each shipment should be tested, and all plants should be rejected if viroid infections are detected. Disinfect pruning tools with 10% bleach or 2% NaOH for 30 seconds between trees. Rinse after bleach treatment, but not required for

NaOH. Immediately remove HSVd-positive trees. For 5 to 20% infections, remove a 2-tree buffer around each infected tree. After whole-orchard removals, leave fallow for 6–12 months before replanting. Carry out annual workshops on citrus crop sanitation, emphasizing that non-certified budwood is the most common route for HSVd introductions. To prevent the spread of HSVd, prioritize removing severely affected trees and using only certified viroid-free propagation material in orchards.

In conclusion, the interplay between climate change and pathogens such as HSVd is a major cause of citrus decline in the Jahrom region. Field observations and molecular assays have shown that orchard health category (growth condition type), particularly concurrence of HSVd-associated symptoms and diagnostic evidence plus abiotic decline indicators, is associated with reduced tree performance (height, crown diameter, yield). However, because this study was observational, and because potential confounders (rootstock variation, undetected co-infections) were not ruled out across all the surveyed citrus orchards, these results are evidence of association and synergistic interactions between HSVd and abiotic factors, rather than definitive causal proof. Controlled inoculation experiments and complete pathogen assessments are required to conclusively attribute causality. Without timely interventions, these dual threats pose a serious risk to the long-term viability of citrus orchards. To mitigate their impacts, a comprehensive management strategy is essential. This should include improved irrigation systems, the use of drought-tolerant and disease-resistant rootstocks, optimized nutrient and pruning practices, and robust viroid surveillance and control measures. Long-term solutions may also involve the development of HSVd-resistant citrus cultivars and adoption of climate-integrated agricultural technologies. Survival of productive citrus farming in Jahrom requires proactive, science-based, and locally tailored interventions that address environmental and pathological dimensions.

ACKNOWLEDGEMENTS

This research was supported by Jahrom University. No external financial support was received; all expenses related to the research were fully covered by the authors. ChatGPT-5 (OpenAI) was used for improving English language in the paper manuscript, preliminary draft editing, and for data formatting. The scientific content, study design and data analyses presented in this paper were conceived, validated, and approved by the authors.

DATA AVAILABILITY

The data supporting the findings of this study are not available elsewhere and will be made available in accordance with the data availability policy for *Phytopathologia Mediterranea*.

LITERATURE CITED

Ahmed R., Uddin M., Quddus M.A., Islam M.A., Hossain M.M., 2023. Impact of foliar application of zinc and zinc oxide nanoparticles on growth, yield, nutrient uptake and quality of tomato. *Horticulturae* 9(2): 162. https://doi.org/10.3390/horticulturae9020162

Alaxin P., Predajňa L., Achs A., Šubr Z., Mrkvová M., Glasa M., 2023. Analysis of hop stunt viroid diversity in grapevine (*Vitis vinifera* L.) in Slovakia: Coexistence of two particular genetic groups. *Pathogens* 12(2): 205. https://doi.org/10.3390/pathogens12020205

Ayllón M.A., López C., Navas-Castillo J., Garnsey S.M., Guerri J., Flores R., Moreno P., 2001. Polymorphism of the 5′ terminal region of Citrus tristeza virus (CTV) RNA: incidence of three sequence types in isolates of different origin and pathogenicity. *Archives of Virology* 146: 27–40. https://doi.org/10.1007/s007050170188

Bagherian S.A.A., Izadpanah K., 2010. Two novel variants of Hop stunt viroid associated with yellow corky vein disease of sweet orange and split bark disorder of sweet lime. 21st *International Conference on Virus and other Graft Transmissible Diseases of Fruit Crops in Julius-Kühn-Archiv* 427: 105–113.

Bagherian S.A.A., Ghani A., Sanie Khatam A.R., 2021. The most important abiotic factors affecting the occurrence of citrus decline in *Citrus limon* cv. 'Lisbon'. *Journal of Horticultural Science* 35(1): 39–53. https://doi.org/10.22067/jhorts4.v35i1.85365

Belabess Z., Radouane N., Sagouti T., Bencheikh M., Labhal A., 2021. A current overview of two viroids prevailing in citrus orchards: Citrus exocortis viroid and Hop stunt viroid. *Citrus - Research, Development and Biotechnology*. https://doi.org/10.5772/intechopen.95914

Bernad L., Duran-Vila N., 2006. A novel RT-PCR approach for detection and characterization of citrus viroids. *Molecular and Cellular Probes* 20(2): 105–113. https://doi.org/10.1016/j.mcp.2005.11.001

Chen, F., Cui, N., Jiang, S., Zhang, Y., Wang, Y. 2025. Effects of deficit drip irrigation at different growth stages on citrus leaf physiology, fruit growth, yield,

and water productivity in South China. *Agricultural Water Management*. 307:109206. https://doi.org/10.1016/j.agwat.2024.109206

Dahro B., Li C., Liu J.H, 2023. Overlapping responses to multiple abiotic stresses in citrus: from mechanism understanding to genetic improvement. *Horticultural Advances* 1: 4. https://doi.org/10.1007/s44281-023-00007-2

de Souza Junior J.P., Kadyampakeni D.M., Shahid M.A., Chen Q., Nascimento C.A.C., 2025. Mitigating abiotic stress in citrus: the role of silicon for enhanced productivity and quality. *Plant Stress* 16: 100837. https://doi.org/10.1016/j.stress.2025.100837

Di Serio F., Flores R., Verhoeven J.T.J., Li S.F., Owens R.A., 2014. Current status of viroid taxonomy. *Archives of Virology*159: 3467–3478. https://doi.org/10.1007/s00705-014-2200-6

Di Serio F., Owens R.A., Li S. F., Matoušek J., Pallás V., Randles J.W., 2024. ICTV Report Consortium. ICTV virus taxonomy profile: Pospiviroidae. *Journal of General Virology* 102(2): 001543. https://doi.org/10.1099/jgv.0.001543

Di Serio F., Owens R.A., Navarro B., Li S.F., Verhoeven J.T.J., 2023. Role of RNA silencing in plant-viroid interactions and in viroid pathogenesis. *Virus Research* 323: 198964. https://doi.org/10.1016/j.virusres.2022.198964

Faghihi M., Maleki M., Alizadeh Aliabadi A., 2025. Microbiota dynamic communities in sweet orange infected by "huanglongbing" in Iran. *Phytopathologia Mediterranea* 64(1), 129-143. https://doi.org/10.36253/phyto-15662

Hadidi A., Czosnek H.H., Kalantidis K., Flores R., Barba M., 2024. Viroids and satellites and their vector interactions. *Viruses* 6(10): 1598. https://doi.org/10.3390/v16101598

Kovalskaya N., Hammond R.W., 2014. Molecular biology of viroid–host interactions and disease control strategies. *Plant Science* 228: 48–60. https://doi.org/10.1016/j.plantsci.2014.05.006

Kumari V.V., Banerjee P., Verma V.C., Sukumaran S., Yadav A.K., 2022. Plant nutrition: An effective way to alleviate abiotic stress in agricultural crops. *International Journal of Molecular Sciences* 23(15): 8519. https://doi.org/10.3390/ijms23158519

Li S.F., Onodera S., Sano T., Hataya T., Shikata E., 1995. Gene diagnosis of viroids: comparisons of return-PAGE and hybridization using DIG-labeled DNA and RNA probes for practical diagnosis of hop stunt, citrus exocortis and apple scar skin viroids in their natural host plants. *Japanese Journal of Phytopathology* 61: 381–390. https://doi.org/10.3186/jjphytopath.61.381

Liu X., Gao T., Liu C., Ma X., Chen J., 2023. Fruit crops combating drought: Physiological responses and regulatory pathways. *Plant Physiology* 192(3): 1768–1784. https://doi.org/10.1093/plphys/kiad202

Lv X., Zhao S., Ning Z., Chen Y., Zhang J., 2015. Citrus fruits as a treasure trove of active natural metabolites that potentially provide benefits for human health. *Chemistry Central Journal* 9: 68. https://doi.org/10.1186/s13065-015-0145-9

Marquez-Molins J., Gomez G., Pallas V., 2021. Hop stunt viroid: A polyphagous pathogenic RNA that has shed light on viroid-host interactions. *Molecular Plant Pathology* 22(2): 153–162. https://doi.org/10.1111/mpp.13022

Moore C.E., Meacham-Hensold K., Lemonnier P., Guan K., Bernacchi C.J., 2021. The effect of increasing temperature on crop photosynthesis: from enzymes to ecosystems. *Journal of Experimental Botany* 72(8): 2822–2844. https://doi.org/10.1093/jxb/erab090

Mwendwa S. M., 2022. Revisiting soil texture analysis: Practices towards a more accurate Bouyoucos method. *Heliyon* 8(5): e09395. https://doi.org/10.2139/ssrn.4002346

Navarro B., Gisel A., Rodio M. E., Delgado S., Flores R., Di Serio F., 2012. Viroids: how to infect a host and cause disease without encoding proteins. *Biochimie* 94(7): 1474-1480. https://doi.org/10.1016/j.biochi.2012.02.020

Pansu M., Gautheyrou J., 2006. *Handbook of Soil Analysis: Mineralogical, Organic and Inorganic Methods*. Springer, Berlin.

Prasad A., Sett S., Prasad M., 2022. Plant-virus-abiotic stress interactions: A complex interplay. *Environmental and Experimental Botany* 199: 104869. https://doi.org/10.1016/j.envexpbot.2022.104869

Rahimpour H., Talebi A.A., Raz, A., Azarbad H., Mehrabadi M., 2025. Geographic variation and diversity of bacterial endosymbionts in Asian citrus psyllid, Diaphorina citri, from Iran. *Pest Management Science* 81(12): 7919-7927. https://doi.org/10.1002/ps.70100

Raju C., Pazhanivelan S., Perianadar I.V., Vimalraj P., Praveen G., 2024. Climate change as an existential threat to tropical fruit crop production—A review. *Agriculture* 14: 2018. https://doi.org/10.3390/agriculture14112018

Seleiman M.F., Al-Suhaibani N., Ali N., Alotaibi M., Ibrahim M., 2021. Drought stress impacts on plants and different approaches to alleviate its adverse effects. *Plants (Basel)* 10(2): 259. https://doi.org/10.3390/plants10020259

Semancik J.S., Morris T.J., Weathers L.G., Reddy J.D., Dodds J.A., 1975. Physical properties of a minimal

infectious RNA (viroid) associated with the exocortis disease. *Virology* 63(1): 160–167. https://doi.org/10.1016/0042-6822(75)90381-5

Tian T., Wang J., Wang H., Zhang J., Li Y,. 2022. Nitrogen application alleviates salt stress by enhancing osmotic balance, ROS scavenging, and photosynthesis of rapeseed seedlings (*Brassica napus*). *Plant Signaling and Behavior* 17(1), 2081419. https://doi.org/10.1080/15592324.2022.2081419

Vamenani R., Rahimian H., Alavi S.M., Najafi A., Javan-Nikkhah M., 2019. Genetic diversity of Hop stunt viroid from symptomatic and asymptomatic citrus trees in Iran. *Journal of Phytopathology* 67: 484–489. https://doi.org/10.1111/jph.12821

Wu G., Terol J., Ibanez V., Lopez-Garcia A., Perez-Roman E., 2018. Genomics of the origin and evolution of Citrus. *Nature* 554: 311–316. https://doi.org/10.1038/nature25447

Phytopathologia Mediterranea
The international journal of the
Mediterranean Phytopathological Union

Firenze University Press
www.fupress.com/pm

Research Papers

Spatial distribution and molecular characterization of persistently aphid-transmitted viruses causing yellowing and stunting in faba bean and chickpea crops in Tunisia

Samia MGHANDEF[1,2,*], Safaa G. KUMARI[3], Abdulrahman MOUKAHEL[3], Imen HAMDI[1], Arvind VARSANI[4], Asma NAJAR[1]

[1] *Institut National de la Recherche Agronomique de Tunisie (INRAT), Tunis, Tunisie*
[2] *Faculté des Sciences de Bizerte (FSB), Université de Carthage Jarzouna, 7021 Bizerte, Tunisie*
[3] *Seed Health/Virology Laboratory, International Center for Agricultural Research in the Dry Areas (ICARDA), Terbol Station, Zahle, Lebanon*
[4] *The Biodesign Center for Fundamental and Applied Microbiomics, Center for Evolution and Medicine, School of Life Sciences, Arizona State University, Tempe, Arizona, United States of America*
* Correspondence author. Email: mghandefsamia91@yahoo.com

Summary. Field surveys were conducted in the northeastern and northwestern regions of Tunisia between 2013/2014 and 2018/2019 growing seasons to identify viruses that infect faba bean and chickpea crops. Field observations showed that 18.8% of the faba bean and 21.0% of the chickpea fields surveyed had virus-like symptoms. These rates exceeded 20% during the growing seasons from 2013/2014 to 2018/2019, and were most common in the 2014/2015 growing season (28.6% of surveyed faba bean fields and 37.5% of chickpea fields showed virus-like symptoms in more than 20%). Totals of 1,538 faba bean and 1,511 chickpea plant samples showing yellowing and stunting symptoms were collected from 144 faba bean and 124 chickpea fields, . All collected samples were tested by tissue blot immunoassay (TBIA) using six monoclonal antibodies. These results showed that chickpea chlorotic stunt virus (CpCSV; *Polerovirus CPCSV*) was the most prevalent in faba bean and chickpea, with incidences of 20.2% and 37.6%, respectively, followed by beet western yellows virus (BWYV; *Polerovirus BWYV*) (13.5 and 9.7%), bean leafroll virus (BLRV; *Luteovirus phaseoli*) (3.7 and 3.3%), and faba bean necrotic yellows virus (FBNYV; *Nanovirus necroflaviviciae*) detected only in faba bean (6.6% of faba bean samples tested). In addition, TBIA results indicated that single virus infections were more prevalent than mixed infections in both crops. Mixed infections were predominantly co-infections involving viruses in *Polerovirus* (*Solemoviridae*), particularly CpCSV and BWYV (93% in faba bean and 69% in chickpea). Twenty-six samples that reacted positively with different monoclonal antibodies were assessed with reverse transcription-polymerase chain reaction (RT-PCR) using generic and specific primers followed by sequencing of the partial coat protein (*CP*) gene. The sequence analyses confirmed presence of CpCSV, BWYV, BLRV, brassica yellows virus (BrYV; *Polerovirus TUYV*), and turnip yellows virus (TuYV; *Polerovirus TUYV*). Comparative sequence analyses of the Tunisian iso-

OPEN ACCESS

Citation: Mghandef, S., Kumari, S. G., Moukahel, A., Hamdi, I., Varsani, A., & Najar, A. (2026). Spatial distribution and molecular characterization of persistently aphid-transmitted viruses causing yellowing and stunting in faba bean and chickpea crops in Tunisia. *Phytopathologia Mediterranea* 65(1): 165-184. doi: 10.36253/phyto-16680

Accepted: April 14, 2026

Published: May 14, 2026

© 2026 Author(s). This is an open access, peer-reviewed article published by Firenze University Press (https://www.fupress.com) and distributed, except where otherwise noted, under the terms of the CC BY 4.0 License for content and CC0 1.0 Universal for metadata.

Data Availability Statement: All relevant data are within the paper and its Supporting Information files.

Competing Interests: The Author(s) declare(s) no conflict of interest.

Editor: Sabine Banniza, University of Saskatchewan, Canada.

ORCID:
SM: 0009-0008-8972-9135
SGK: 0000-0002-4492-6257
AM: 0000-0003-4297-771X
IH: 0000-0001-6973-860X
AV: 0000-0003-4111-2415
AN: 0000-0002-9576-6476

lates indicated that 13 CpCSV sequences had nucleotide sequence similarities of 95 to 99% with the reference isolate (EU541266) belonging to serotype I, and six BLRV isolates had similarities of 96 to 99% with BLRV reference isolate (PP333098). One sample (TuCp265-19) had a mixed infection with CpCSV and BLRV. Six isolates initially detected using BWYV-specific primers were sequenced and analyzed. BLASTn results showed that only three isolates were closely related (98 to 100%) to BWYV (OM419176), while the remaining four isolates were identified as *Polerovirus TUYV* and showed greatest similarity to BrYV (LC428361) and TuYV (OP699039), indicating co-occurrence of two distinct *Polerovirus* species within the analyzed samples. There is no information on the genetic variability of legume viruses in Tunisia, so this study shows that these viruses should be considered when developing disease management strategies to improve faba bean and chickpea production in Tunisia.

Keywords. CpCSV, BWYV, BLRV, *Polerovirus*, mixed infections, sequencing, phylogenetic analyses.

INTRODUCTION

Chickpea (*Cicer arietinum* L.) and faba bean (*Vicia faba* L.) are the two major pulse crops grown in West Asia and North Africa (WANA) (Makkouk, 2020). In Tunisia, faba bean and chickpea are among the most widely cultivated legumes, grown in northern Tunisia. In 2024, faba bean covered 55,212 ha, with an average yield of 1.34 ton ha^{-1}, while chickpea covered 6,743 ha with an average yield of 1.43 ton^{-1} (FAOSTAT, 2026). These two crops are key components of the Tunisian cereal-based production system, and their productivity is affected by parasitic weeds, diseases and insect pests. Viruses and their vectors are among the most important obstacles to production of these two key crops, and the disease management practices available to farmers are limited.

Several viruses associated with yellowing and stunting symptoms in cool-season food legumes are among the most internationally important diseases (Makkouk *et al*., 2003; Makkouk, 2020). These viruses are predominantly transmitted by aphid vectors, either persistently circulative, as reported for the viruses investigated in the present study, or less commonly those that are non-persistently transmitted (Makkouk *et al*., 2003; Kumar *et al*., 2008; Kumari *et al*., 2009; Makkouk *et al*., 2014). Some of these viruses have been reported in Tunisia, include: faba bean necrotic yellows virus (FBNYV; *Nanovirus necroflaviviciae*, *Nanoviridae*), bean leafroll virus (BLRV; *Luteovirus phaseoli*, *Luteovirus, Tombusviridae*), soybean dwarf virus (SbDV; *Luteovirus glycinis*, *Luteovirus*, *Tombusviridae*), beet western yellows virus (BWYV; *Polerovirus BWYV*, *Polerovirus*, *Solemoviridae*), and chickpea chlorotic stunt virus (CpCSV; *Polerovirus CPCSV*, *Polerovirus*, *Solemoviridae*) (Najar *et al*., 2000a; 2003; 2011; Kumari *et al*., 2015). The main aphids transmitting legume viruses are *Aphis craccivora* and *Acyrthosiphon pisum* (Asaad *et al*., 2009; Abraham and Vetten, 2022).

Serological differentiation of closely related virus species within *Solemoviridae*, particularly *Polerovirus* species, may be limited by cross-reactivity when antibodies are raised against conserved epitopes, highlighting the importance of sequence-based approaches for accurate virus identification (Moukahel *et al*., 2021; Ademe *et al*., 2025). Uses of molecular techniques for chickpea showing yellowing/stunting symptoms that showed cross-reactivity between the specific monoclonal antibodies have led to identification of four new viruses in *Polerovirus* that infect chickpea in Sudan (Moukahel *et al*., 2021).

Accurate identification of viruses affecting legume crops is crucial for breeding for resistance to these diseases they cause and for developing crop disease management methods. Viruses infecting food legume crops can be identified using serology, but molecular approaches have not been widely used to identify additional viruses that may cause economic losses in Tunisia. To address this knowledge gap, field surveys were conducted in major chickpea and faba bean production areas to determine whether new viruses are associated with yellowing/stunting symptoms. Results of these surveys are reported in this paper.

MATERIALS AND METHODS

Field surveys, visual disease assessments, and sample collection

Field surveys were carried out each growing season from 2013/2014 to 2018/2019, in the main faba bean and chickpea growing areas of Tunisia during the flowering and pod setting stages of crop growth. The surveys were carried out in the northeastern regions (Bizerte, and Cap Bon) and northwestern regions (Kef, Jendouba, and Béja) of Tunisia (Figure 1). Totals of 1,538 faba bean and 1,511 chickpea samples, showing symptoms including yellowing, stunting, leaf rolling, and/or reddening, were collected from 144 faba bean and 124 chickpea fields (Table 1). In each field, plants were inspected using a standardized survey format, that recorded crop condition, growth stage, disease symptoms, disease incidence,

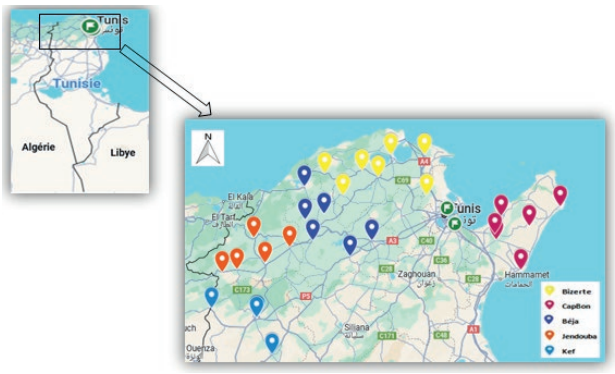

Figure 1. A map showing the location of fields surveyed in the northeastern (Bizerte, Cap Bon) and the northwestern (Kef, Jendouba, Béja) regions of Tunisia between 2013-2019.

and aphid populations. Virus incidence was estimated in each field as the percentage of plants exhibiting virus-like symptoms per square meter at different randomly selected locations within the field. Incidence values were then classified into five categories: <1%, 1 to 5%, 6 to 20%, 21 to 50%, and >50%. All samples were placed in labelled plastic bags and transported to the ICARDA Virology Laboratory in Tunis for virus testing. For these, fresh stems from each plant sample were blotted onto nitrocellulose membrane (NCM, 0.45 µm, Bio-Rad, Cat No. 1620115) in ten replicates. Leaves from each sample were freeze-dried for subsequent molecular analysis.

Serological assays

All samples blotted onto NCM were tested by tissue-blot immunoassay (TBIA) using the method of Makkouk and Kumari (1996). A monoclonal antibody (MAb) specific for FBNYV (3-2E9; Franz *et al*., 1996), and a broad-spectrum legume MAb (5G4; Katul, 1992) that detects legume virus species in *Solemoviridae* and *Tombusviridae*, were used for the assessments. Samples that reacted positively with 5G4 MAb were subsequently tested with specific MAbs for BWYV (A5977; Agdia), BLRV (4B10; Katul, 1992), SbDV (PVAS-650, ATCC, United States of America) and a mixture of three MAbs (5-2B8, 5-3D5 and 5-5B8) produced against a Syrian isolate of CpCSV (Abraham *et al*., 2006; 2009).

Virus molecular characterizations, genetic diversity and phylogenetic analyses

Based on serological reactions with different MAbs, 26 samples (four from faba bean and 22 from chickpea) (Table 2), representing all the surveyed regions, were selected for further molecular characterizations (seven of these samples only reacted with 5G4 Mab, ten samples reacted positively with 5G4 and CpCSV MAbs, six samples reacted positively with 5G4 and BWYV MAbs, and three samples reacted positively with 5G4 and BLRV MAbs (Table 2). Total RNA was extracted from plant samples, and cDNA syntheses were carried out as described by Moukahel *et al*. (2021).

Virus detections were carried out using reverse transcription-polymerase chain reactions (RT-PCR) that included a pair of generic primers (AS3/Pol3870F) to amplify 370 bp of the partial coat protein (*CP*) gene of several Luteo- and polero-viruses. Samples amplified using a pair of generic primers were reprocessed by multiplex RT-PCR (MP-PCR) (Moukahel *et al*., 2021), using the generic reverse primer AS3 with species-specific primers for CpCSV, BWYV, SbDV, BLRV, phasey bean mild yellows virus (PBMYV; *Polerovirus PBMYV*; *Polerovirus*; *Solemoviridae*), and cucurbit aphid-borne yellows virus (CAbYV; *Polerovirus CABYV, Polerovirus*, *Solemoviridae*). Each MP-PCR amplification mixture was divided in two multiplex master mixes due to the proximity in product sizes for some primers: master mix-I include AS3 with primers BLRV3589F, BWYV3969F, SbDV3731F, and PBMYV3396F (amplify, respectively, 551, 276, 418 and 838 bp of the partial *CP*); and master mix-II consisted of AS3 with primers CpCSV3705F and CABYV3635F (amplify, respectively, 566 and 474 bp). Primers, PCR amplification conditions and electrophoresis analyses were carried out using the protocol described by Moukahel *et al*. (2021).

High-quality PCR products were directly sequenced in both directions using the Sanger method by Macrogen, South Korea. The sequences were compared with available database sequences (Table 3), using the basic local alignment search tool BLAST program (Altschul *et al*., 1997; 2005). Sequences were analyzed to estimate nucleotide polymorphism parameters with DnaSP software version 6.0 (Rozas *et al*., 2017). Virus genetic diversity was quantified using haplotype diversity (Hd), numbers of haplotype (h) (Tajima, 1989), numbers of segregating sites (S), and nucleotide diversity (Pi) (Jukes and Cantor, 1969). Pairwise sequence identities were calculated using the Sequence Demarcation Tool (SDT) v1.2 (Muhire *et al*., 2014). Phylogenetic relationships were inferred using the Maximum Likelihood method based on Jukes-Cantor model with 1,000 bootstrap replicates. Evolutionary analyses were conducted in MEGA X (Kumar *et al*., 2018).

Table 1. Results of serological tests (tissue blot immunoassay, TBIA) for faba bean and chickpea symptomatic samples collected from different regions of Tunisia during 2013-2019.

Crop / Season	Region	Number of fields surveyed	Number of samples tested	Number of samples reacted positively with MAbs[a]						% of virus infection based on the TBIA results of the 1st test
				1st test	2nd test for samples, which reacted with 5G4					
				FBNYV	5G4	CpCSV	BWYV	BLRV	Unidentified	
Faba bean										
2013/2014	Bizerte	10	141	0	34	17	11	4	0	24.1
	Cap Bon	6	75	0	24	14	8	0	6	32.0
	Kef	5	79	0	15	15	0	0	0	19.0
	Béja	2	32	0	6	6	0	0	0	18.8
	Jendouba	5	81	0	21	15	5	0	2	25.9
2014/2015	Bizerte	17	268	0	68	32	19	0	18	25.4
	Cap Bon	16	172	0	64	5	30	0	30	37.2
	Kef	2	19	0	6	0	2	0	4	31.6
	Béja	14	140	0	48	12	18	0	12	34.3
2016/2017	Bizerte	4	36	23	18	5	0	11	2	100.0
	Cap Bon	3	25	8	11	2	0	5	4	76.0
	Kef	6	49	29	10	0	4	7	0	79.6
	Béja	7	50	10	17	1	0	6	10	54.0
	Jendouba	2	12	1	0	0	0	0	0	8.3
2017/2018	Bizerte	7	86	10	63	33	47	3	0	84.9
	Cap Bon	8	114	0	105	98	43	1	2	92.1
	Kef	3	17	0	13	12	1	0	4	76.5
	Béja	4	38	5	28	27	16	0	0	86.8
	Jendouba	2	12	0	12	12	1	0	0	100.0
2018/2019	Bizerte	8	32	11	14	3	0	9	1	78.1
	Cap Bon	5	22	3	0	0	0	0	0	13.6
	Kef	2	12	2	3	1	0	1	0	41.7
	Béja	3	18	0	6	0	0	4	2	33.3
	Jendouba	3	8	0	8	0	2	6	0	100.0
Subtotal faba bean		144	1538	102	594	310	207	57	97	45.3
Chickpea										
2014/2015	Bizerte	29	504	0	342	262	26	0	54	67.9
	Cap Bon	4	73	0	6	3	4	0	1	8.2
	Béja	7	148	0	61	59	15	0	0	41.2
	Jendouba	8	158	0	71	55	16	0	4	44.9
2015/2016	Bizerte	4	32	0	22	13	6	0	3	68.8
	Cap Bon	9	78	0	34	30	9	0	0	43.6
	Kef	3	21	0	16	4	11	0	1	76.2
	Béja	3	28	0	7	2	1	0	4	25.0
	Jendouba	6	78	0	69	42	28	0	0	88.5
2016/2017	Bizerte	6	56	0	22	10	6	19	0	39.2
	Cap Bon	7	63	0	42	36	12	13	0	66.7
	Kef	3	18	0	13	12	0	0	1	72.2
	Béja	5	41	0	21	9	4	0	8	51.2
	Jendouba	4	30	0	6	2	0	0	4	20.0
2018/2019	Bizerte	3	12	0	4	1	1	0	2	33.3
	Cap Bon	12	91	0	38	6	4	16	12	41.8
	Kef	4	21	0	19	15	0	0	4	90.5
	Béja	6	47	0	14	6	3	1	4	29.8
	Jendouba	1	12	0	1	1	0	0	10	8.3
Subtotal chickpea		124	1511	0	808	568	146	49	112	53.5
Total		268	3049	102	1402	878	353	106	209	49.3

[a] FBNYV: faba bean necrotic yellows virus (3-2E9 MAb); 5G4: broad-spectrum legume luteovirid monoclonal antibody; CpCSV: chickpea chlorotic stunt virus (mixture of 5-2B8, 5-3D5 and 5-5B8 MAbs); BWYV: beet western yellows virus (A5977 MAb from Agdia); BLRV: bean leafroll virus (4B10 MAb).
All samples were negative for Soybean dwarf virus (PVAS-650 MAb from ATCC, USA).

RESULTS

Assessments of virus-like symptoms in the field

During field visits, colonies of the potential virus-transmitting aphids *Aphis fabae, Aphis craccivora, Acyrthosiphon pisum* and *Myzus persicae* were observed congregating on the stems, leaves and shoots of young faba bean plants. Faba bean plants exhibiting symptoms commonly associated with virus diseases were collected, including yellowing, chlorosis, stunting and leaf rolling. Virus-like symptom incidence was estimated based on these observable field symptoms. Symptom incidence varied among seasons, crop types, and surveyed regions. Approximately 18.8% of faba bean and 21.8% of chickpea fields had more 20% of plants with virus-like symptoms during the 2013/2014 to 2018/2019 growing seasons, with the 2014/2015 growing season having the most severe diseases (28.6% of faba bean and 37.5% chickpea fields had more than 20% of plants with virus-like symptoms) (Figure 2). Not all symptomatic plants were confirmed to be virus-infected; as similar symptoms may also result from other factors, such as abiotic stresses.

Virus identifications based on serological tests

Serological results (TBIA) from 1,538 faba bean and 1,511 chickpea symptomatic samples showed that overall incidence of the detected viruses in chickpea samples was 53.5%, whereas in faba bean this was 45.3% (Table 1). Greatest incidence was recorded for luteoviruses, where 808 chickpea (53.5%) and 594 faba bean samples (38.6%) reacted positively with the broad-spectrum legume virus MAb (5G4). In contrast, FBNYV was detected in 102 (6.6%) of the faba bean samples (Table 1). Based on serological tests with the MAbs used in this study, 54.7% of the faba bean samples and 46.5% of the chickpea samples were virus-free (Table 1).

When samples that had reacted positively to the 5G4 MAb were retested with the specific MAbs, CpCSV, BWYV, and BLRV were detected, respectively, in 310, 207 and 57 faba bean samples, and in 568, 146 and 46 chickpea samples. SbDV was not detected in any of the assessed samples. In addition, 209 samples (97 from faba bean and 112 from chickpea) reacted only with 5G4 MAb, but not with the specific MAbs used in the study (Table 1).

Mixed virus infections

Mixed virus infections were less frequent than single infections in both crop types. In faba bean, 123 out of 594 (20.7%) 5G4-positive samples showed mixed infections, whereas in chickpea, 71 out of 808 (8.8%) 5G4-positive samples had mixed infections (Table 4). These infections were mostly CpCSV + BWYV co-infections, which accounted 114 of 123 mixed infections (92.7%) in faba bean and 50 of the 71 mixed infections (69%) in chickpea. Other combinations were less frequent, including CpCSV + BLRV (detected in one faba bean and 13 chickpea samples), while triple infections were rare, occurring in two faba bean and three chickpea samples (CpCSV + BWYV + BLRV) and in one faba bean sample (CpCSV + BWYV + FBNYV) (Table 4).

Regionally, CpCSV and BWYV co-infections were most prevalent in Bizerte, representing 59% of mixed infections in faba bean and 52% in chickpea, followed by Cap Bon where they accounted for 37% of mixed infections in faba bean and 26% of those in chickpea (Figure 3). Overall, CpCSV was the most frequently detected virus in mixed infections affecting the chickpea and faba bean crops.

Molecular characterizations of viruses

The generic primer pair AS3/Pol3870F amplified a fragment of approx. 370 bp, corresponding to a partial *CP* gene of luteo- and polero-viruses. MP-PCR using specific primers detected CpCSV, BWYV and BLRV in, respectively, four, six and two samples, with the expected amplicon size of each virus (566 bp for CpCSV, 276 bp for BWYV, and 551 bp for BLRV). In addition, two mixed infections were detected: isolate TuCp265-19 (CpCSV + BLRV) and isolate TuCp275-19 (CpCSV + BWYV) (Table 2). Eleven samples were amplified by the generic primer pair AS3/Pol3870F, but not by the specific primers used. Therefore, these together, in addition to those amplified with specific primers, were subjected to Sanger sequencing (Table 2). No sample was amplified with the primers for SbDV, PBMYV, or CAbYV.

Analysis of 26 partial *CP* genes (one amplicon from 24 samples, and two amplicons from one sample TuCp265-19) confirmed presence of CpCSV (in 13 samples), BLRV (in six samples), BWYV (in three samples), brassica yellows virus (BrYV; *Polerovirus TUYV; Polerovirus; Solemoviridae*) (two samples) and turnip yellows virus (TuYV; *Polerovirus TUYV*) (two samples) (Table 2). BLASTn analyses showed that Tunisian CpCSV isolates shared 95%-99% nucleotide similarity with the Moroccan faba bean CpCSV-serotype I isolate (EU541266) (Table 2, Figure 4).

Among the 13 CpCSV isolates, five isolates (GenBank accession numbers MT739413, MT739414, MT739415, MT739416, and MT739418) were 100% iden-

Table 2. Geographic origins, comparison and identity with reference GenBank accessions of chickpea and faba bean isolates collected from Tunisia in 2016, 2018, and 2019.

Isolate code[a]	Crop	Region	Genbank accession number	TBIA reaction with MAbs	RT-PCR reaction with primers[b]	Virus sequences Blastn reference GenBank accessions	Blastn similarity %
TuCp08-19	Chickpea	Cap Bon	PQ526601	5G4, CpCSV	Generic only	CpCSV; EU541266	98
TuCp15-19	Chickpea	Cap Bon	PQ526602	5G4, CpCSV	Generic only	CpCSV; EU541266	98
TuCp37-19	Chickpea	Cap Bon	PQ526603	5G4, CpCSV	Generic only	CpCSV; EU541266	98
TuCp98-19	Chickpea	Bizerte	PQ526604	5G4, CpCSV	Generic, CpCSV	CpCSV; EU541266	98
TuCp100-19	Chickpea	Bizerte	PQ526605	5G4, CpCSV	Generic only	CpCSV; EU541266	98
TuCp108-19	Chickpea	Bizerte	PQ526606	5G4, BLRV	Generic only	CpCSV; EU541266	98
TuCp160-19	Chickpea	Jendouba	PQ526607	5G4, CpCSV	Generic, CpCSV	CpCSV; EU541266	95
TuCp195-19	Chickpea	Beja	PQ526608	5G4	Generic, CpCSV	CpCSV; EU541266	99
TuCp207-19	Chickpea	Beja	PQ526609	5G4, CpCSV	Generic only	CpCSV; EU541266	98
TuCp261-19	Chickpea	Beja	PQ526610	5G4	Generic only	CpCSV; EU541266	98
TuCp265-19	Chickpea	Beja	PQ526611	5G4, CpCSV	Generic, CpCSV, BLRV	CpCSV; EU541266	98
TuCp290-19	Chickpea	Cap Bon	PQ526612	5G4, BLRV	Generic only	CpCSV; EU541266	99
TuFa109-18	Faba bean	Cap Bon	MT739415	5G4, CpCSV	Generic, CpCSV	CpCSV; EU541266	98
TuFa62-16	Faba bean	Bizerte	PQ526614	5G4, BWYV	Generic, BWYV	BWYV; OM419176	100
TuFa72-16	Faba bean	Bizerte	PQ526615	5G4, BWYV	Generic, BWYV	BWYV; OM419176	98
TuCp58-19	Chickpea	Cap Bon	PQ526617	5G4, BWYV	Generic, BWYV	BWYV; OM419176	99
TuCp104-19	Chickpea	Bizerte	PQ526618	5G4	Generic, BWYV	BrYV; LC428361	98
TuCp275-19	Chickpea	Cap Bon	PQ526620	5G4	Generic, CpCSV, BWYV	BrYV; LC428361	91
TuCp16-19	Chickpea	Cap Bon	PQ526616	5G4, BWYV	Generic, BWYV	TuYv; OP699039	96
TuCp229-19	Chickpea	Beja	PQ526619	5G4, BWYV	Generic, BWYV	TuYV; OP699039	94
TuFa101-18	Faba bean	Cap Bon	PQ526622	5G4	Generic, BLRV	BLRV; PP333098	98
TuCp36-19	Chickpea	Cap Bon	PQ526623	5G4, BLRV	Generic, BLRV	BLRV; PP333098	99
TuCp38-19	Chickpea	Cap Bon	PQ526624	5G4	Generic only	BLRV; PP333098	96
TuCp172-19	Chickpea	Jendouba	PQ526625	5G4	Generic only	BLRV; PP333098	96
TuCp258-19	Chickpea	Beja	PQ526626	5G4, BWYV	Generic only	BLRV; PP333098	98
TuCp265-19	Chickpea	Beja	PQ526627	5G4, CpCSV	Generic, CpCSV, BLRV	BLRV; PP333098	98

[a] The last two numbers refer to year of collection.
[b] Generic primers (AS3/Pol3870F); CpCSV: chickpea chlorotic stunt virus (CpCSV3705F primers); BWYV: beet western yellows virus (BWYV3969F primers); BLRV: bean leafroll virus (BLRV3589F primers).

tical to each other, and therefore only isolate MT739415 was used as the representative sequence for the whole set. Sequence analyses of seven isolates amplified with BWYV-specific primers revealed that three isolates shared 98 to 100% similarity with BWYV from coriander in Cyprus (OM419176) (Table 2, Figure 5 A), whereas four isolates showed 91 to 99% similarity with TuYV. Among these, two isolates were closely related (94 to 99%) to a TuYV isolate from the Czech Republic (OP699039), while two clustered with a Japanese rapeseed isolate (91 to 98%) previously described as BrYV (LC428361), currently classified within the *Polerovirus TUYV* species (Table 2, Figure 5 B). The *CP* of the five Tunisian BLRV isolates shared 96 to 99% nucleotide identity with a BLRV isolate originated from alfalfa in Spain (PP333098) (Table 2, Figure 6). All 26 *CP* sequences generated in this study were deposited in GenBank under the accession number listed in Table 2.

Genetic diversity

The *CP* sequences of 26 Tunisian virus isolates from this study (Table 2) together with 47 references sequences retrieved from GenBank (Table 3) were analysed using DnaSP version 6.0 (Rozas *et al*., 2017). For CpCSV, analysis of the complete dataset (24 sequences) revealed 16 polymorphic sites (S), ten haplotypes (hd), and high haplotype diversity (Hd = 0.841), with nucleotide diversity Pi (JC = 0.0266). However, Tunisian CpCSV showed no variable sites, indicating very low local genetic variability. For TuYV, analysis of the four Tunisian isolates revealed three haplotypes (h = 3), with high haplotype diver-

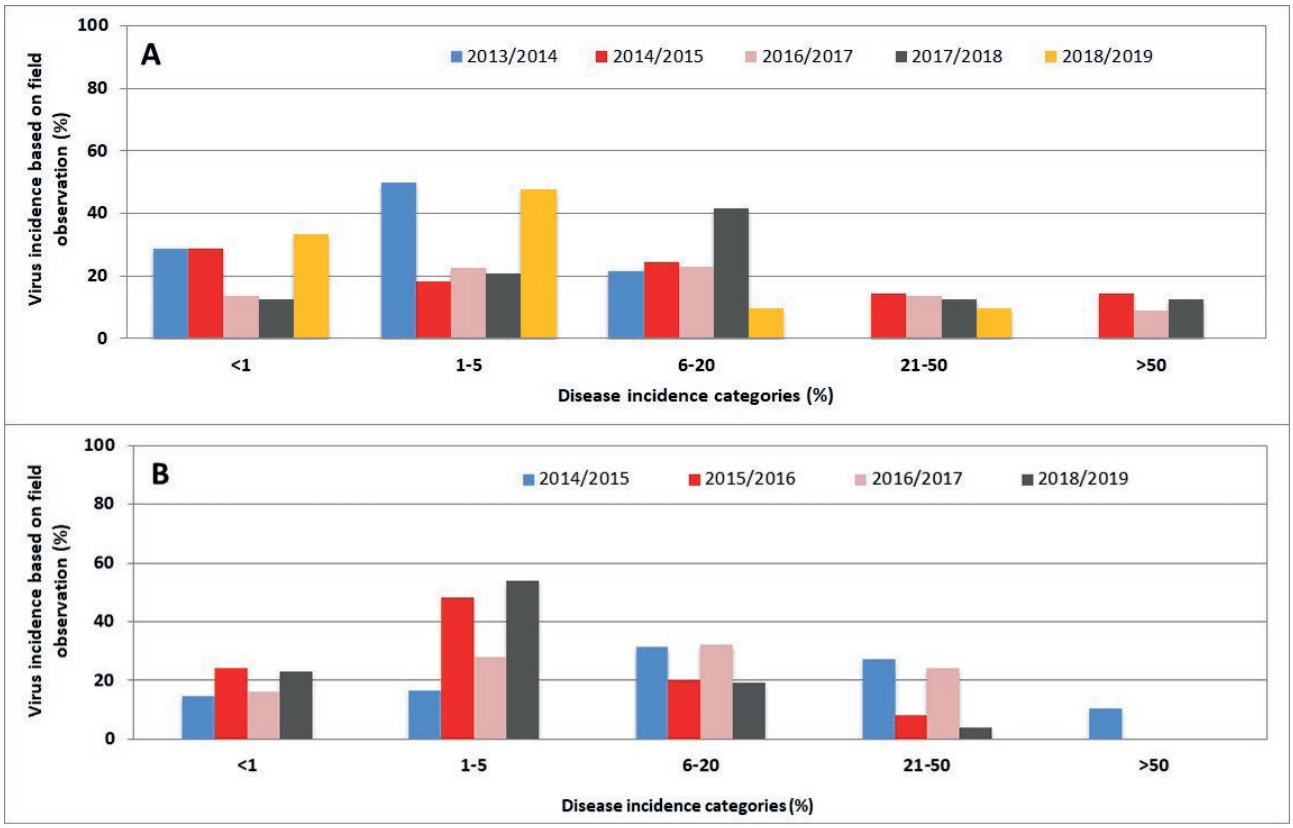

Figure 2. Fields of faba bean (A) and chickpea (B) showing virus-like symptoms during surveys conducted in Tunisia between 2013–2019.

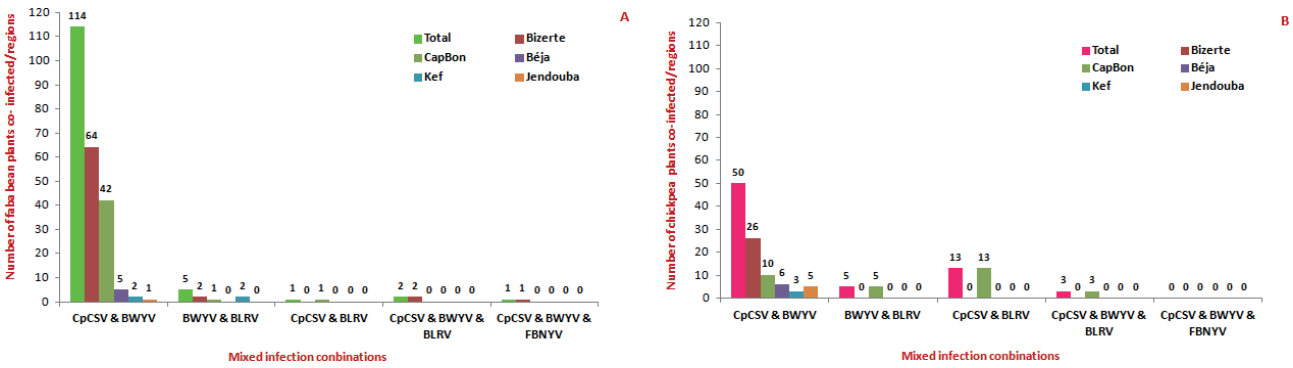

Figure 3. Distribution of mixed infection combinations involving chickpea chlorotic stunt virus (CpCSV), beet western yellows virus (BWYV), bean leafroll virus (BLRV), and baba bean necrotic yellows virus (FBNYV) across five regions of Tunisia, based on serological Tissue-Blot Immunoassay (TBIA) of surveys conducted in faba bean (A) and chickpea (B) crops (2013-2019). Bars indicate to the number of plants co-infected by each virus combination per region, relative to the total mixed-infected plants.

sity (Hd = 0.833), 26 polymorphic sites, and nucleotide diversity Pi (JC) = 0.058. When the complete dataset of 14 sequences was analyzed, nine haplotypes were detected (Hd= 0.879) with the same 26 polymorphic sites and Pi (JC) = 0.058. For BWYV, analysis of nine sequences revealed 35 polymorphic sites, resulting in six haplotypes (h = 6) and high haplotype diversity (Hd = 0.889). Nucleotide diversity was high (Pi (JC) = 0.0586), with an average 11.99 nucleotide differences, indicating substantial genetic differentiation among the BWYV isolates.

Analysis restricted to the three Tunisian BWYV variants identified five polymorphic sites, forming three dis-

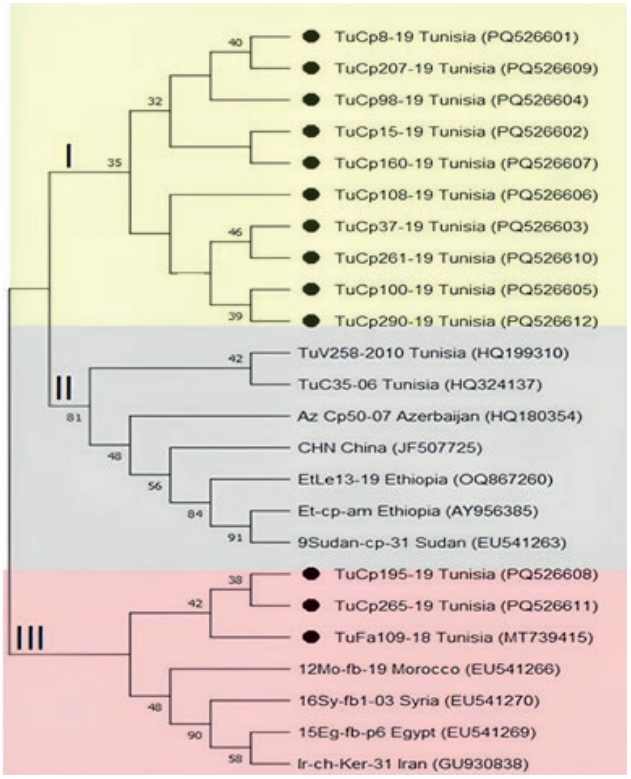

Figure 4. Maximum likelihood phylogenetic analysis of the partial CP gene of 24 chickpea chlorotic stunt virus (CpCSV, species *Polerovirus CPCSV*) isolates from chickpea and faba bean. Isolates from this study are indicated by black circles.

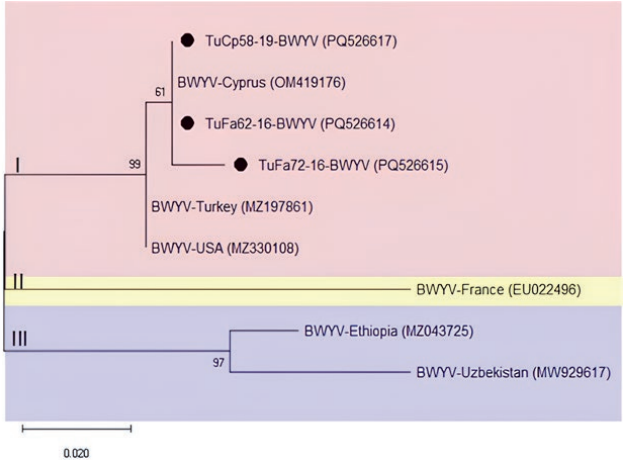

Figure 5. Maximum likelihood phylogenetic analysis of the partial CP gene of 9 beet western yellows virus (BWYV, species *Polerovirus BWYV*) isolates from chickpea and faba bean. Isolates from this study are indicated by black circles.

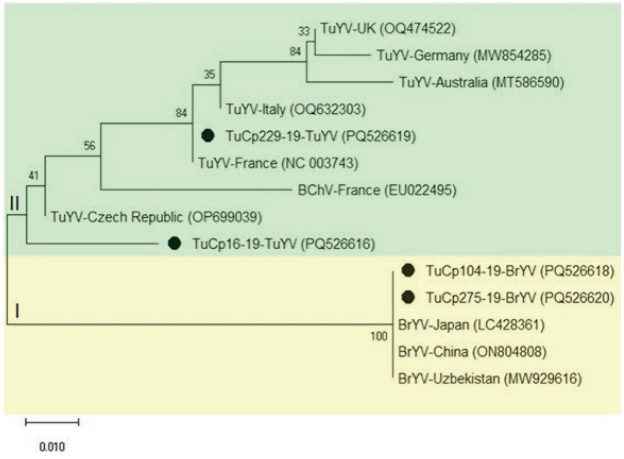

Figure 6. Maximum likelihood phylogenetic analysis of the partial CP gene of 14 TuYV/BrYV (species *Polerovirus TUYV*) isolates from chickpea and faba bean. Isolates from this study are indicated by black circles.

Figure 7. Maximum likelihood phylogenetic analysis of the partial CP gene of 26 bean leafroll virus (BLRV, species *Luteovirus phaseoli*) isolates from chickpea and faba bean. Isolates from this study are indicated by black circles.

tinct haplotypes (Hd = 1.0), suggesting clear genetic differentiation among these isolates. For BLRV, analysis of the complete dataset (26 isolates) revealed 18 haplotypes with high haplotype diversity (Hd = 0.957) and nucleotide diversity of approx. Pi (JC) = 0.1, based on 39 variable sites detected among the CP sequences.

Phylogenetic analyses for specific viruses

CpCSV - The Maximum Likelihood (ML) phylogenetically grouped CpCSV isolates (Figure 4), into three well-defined groups (I, II, and III). Group I comprised most of the new Tunisian isolates, which clustered closely together, indicating high genetic relatedness and suggesting local diversification of CpCSV within Tunisia. All isolates within this subgroup originated only from chickpea, and were collected during the survey conducted in 2019, which indicates existence of a temporally and host-associated lineage. Group II included earlier reported Tunisian isolates together with isolates from Azerbaijan, China, Ethiopia, or Sudan, reflecting a geographically mixed lineage and possible historical introductions. The older Tunisian variants were recovered from two different host plants (chickpea and faba bean), indicating broad host adaptation. In contrast, Group III clustered several Tunisian isolates with isolates from Morocco, Syria, Egypt, and Iran, forming a distinct regional lineage independent of sampling year or host, and indicating ongoing circulation of CpCSV across North Africa and the Middle East. Overall, the phylogenetic structure this virus highlights substantial genetic diversity within CpCSV, and indicates that Tunisian isolates are distributed across multiple evolutionary lineages.

BWYV - The ML phylogenetic analysis resolved BWYV isolates into three clades (I, II, and III) (Figure 5). Clade I encompassed all Tunisian isolates, together with isolates from Cyprus, Turkey, and the United States of America, showing high nucleotide sequence similarity with the Cypriot coriander isolate from Cyprus (OM419176). Clade II was monophyletic and contained only the French sugar beet isolate (EU022496), highlighting the distinct evolutionary lineage of Clade II. Clade III grouped with chickpea isolates from Ethiopia (MZ043725) and Uzbekistan (MW929617). Overall, Clades II and III exhibited host-associated structuring (sugar beet for Clade II and chickpea for Clade III), whereas Calades I showed low host specify, including Citrus (MZ330108), *Capsicum annuum* (MZ197861), chickpea (PQ526617), faba bean (PQ526615, PQ526614), or coriander (OM419176) (Figure 5).

BrYV/TuYV (Polerovirus TUYV) - Phylogenetic analysis of *Polerovirus TUYV* resolved the dataset into two main groups (labeled I and II), largely structured by geographic origins (Figure 6). Group I comprised isolates closely related to European isolates, whereas group II clustered with isolates associated with Asian lineages. Despite the recent taxonomic revision unifying TuYV and BrYV into a single species (*Polerovirus TUYV*), isolates previously designated as TuYV remained separated into their respective lineages. This pattern indicates that the taxonomic unification did not take consideration of underlying genetic structure, and that geographic origin remains a key factor shaping the genetic diversity of *Polerovirus TUYV* (Figure 6).

BLRV - The ML phylogenetic analysis of BLRV isolates showed limited but detectable genetic variation. The Tunisian isolates (TuCp38-19, TuCp172-19, TuFa101-18, TuCp258-19, TuCp36-19, and TuCp265-19) were interspersed among sequences from different geographic origins, rather than forming well-supported, distinct clusters (Figure 7). Most Tunisian isolates showed close relationships with European isolates (from Spain, France, Germany, and Greece) as well as isolates from Saudi Arabia, Australia, or the United States of America, indicating high genetic similarity across these regions. One isolate (TuCp265-19) showed a more divergent position, clustering closer to isolates from Libya, Ethiopia, and China. Overall, these results indicate low genetic diversity among Tunisian BLRV isolates and weak geographic structuring, consistent with the broad international distribution of BLRV (Figure 7).

Pairwise identity

A pairwise identity matrix of partial CP sequences was calculated using the Sequences Demarcation Tool (SDT) (Muhire *et al*., 2014) to evaluate genetic relationships among the analyzed isolates.

CpCSV - Similarity values ranged from 91 to 100% among CpCSV isolates (Figure 8). The 13 Tunisian isolates showed high intra-grouped similarities (95 to 100%), indicating a genetically homogeneous local population. The closest sequences corresponded to previously reported Tunisian isolates from faba bean, chickpea, or pea, sharing 93 to 97% nucleotide similarity. In contrast, comparisons with international CpCSV isolates showed slightly lower similarity values (90 to 98%), indicating moderate genetic divergence at the international level. These results support the phylogenetic relationships inferred from the ML analysis, confirming the presence of two main CpCSV lineages, despite their occurrence in different host plants (Figure 8).

BWYV - Pairwise nucleotide similarity analysis revealed values ranging from 98 to 99% among BWYV isolates. The three Tunisian BWYV isolates (PQ526614, PQ526615, and PQ526617) showed high similarity among themselves (98 to 99%), indicating a closely related local lineage. The closest sequences corresponded to the coriander isolate from Cyprus, with high nucleotide similarity. In contrast, lower similarity values were observed with sugar beet-derived BWYV isolates from

Table 3. Lists of GenBank sequences used for phylogenetic analysis

No.	Isolate	Geographical origin	Virus[b]	Host	GenBank accession No.
Isolates used in phylogenetic analysis of CpCSV					
1	12Mo-fb-19	Morocco	CpCSV	Faba bean	EU541266
2	16Sy-fb1-03	Syria	CpCSV	Faba bean	EU541270
3	15Eg-fb-p6	Egypt	CpCSV	Faba bean	EU541269
4	Ir-ch-Ker-31	Iran	CpCSV	Chickpea	GU930838
5	CHN	China	CpCSV	Pea	JF507725
6	Et-cp-am	Ethiopia	CpCSV	Chickpea	AY956385
7	EtLe13-19	Ethiopia	CpCSV	Lentil	OQ867260
8	9Sudan-cp-31	Sudan	CpCSV	Chickpea	EU541263
9	TuV258-2010	Tunisia	CpCSV	Faba bean	HQ199310
10	TuC35-06	Tunisia	CpCSV	Chickpea	HQ324137
11	Az Cp50-07	Azerbaijan	CpCSV	Chickpea	HQ180354
Isolates used in phylogenetic analysis of BWYV					
1	21506527b	Cyprus	BWYV	Coriander	OM419176
2	866	Turkey	BWYV	Bell pepper	MZ197861
3	IV400	USA	BWYV	*Citrus medica*	MZ330108
4	W1403a_2009	United Kingdom	TuYV	*Brassica napus*	OQ474522
5	MK107	Australia	TuYV	*Brassica napus*	MT586590
6	DSMZ PV-1209	Germany	TuYV	*Physalis pubescens*	MW854285
7	No8agrosCZ	Czech Republic	TuYV	*Papaver rhoeas*	OP699039
8	NAP	Japan	BrYV	Rapeseed	LC428361
9	BrYV-lnc	China	BrYV	Rapeseed	ON804808
10	FL1	France	TuYV	lettuce	NC_003743
11	ITA1	Italy	TuYV	*Phytolacca americana*	OQ632303
12	UzCp100-13	Uzbekistan	BrYV	Chickpea	MW929616
13	EthCp16-18	Ethiopia	BWYV	Chickpea	MZ043725
14	UzCp76-13	Uzbekistan	BWYV	Chickpea	MW929617
15	N20	France	BWYV	Sugar beet	EU022496
16	G43	France	BChV	Sugar beet	EU022495
Isolates used in phylogenetic analysis of BLRV					
1	SIN4	Spain	BLRV	Alfalfa	PP333098
2	ALF1067	USA	BLRV	Alfalfa	ON669091
3	Manfredi	Argentina	BLRV	Alfalfa	KR261610
4	SA-11	Australia	BLRV	Alfalfa	MF075256
5	Salzlandkreis-2_17	Germany	BLRV	Field pea	MN412735
6	12835-Norfolk-BFS-consensus	UK	BLRV	Field pea	PP744500
7	SA-49	Australia	BLRV	Alfalfa	MF075258
8	Restinclieres/2015	France	BLRV	Alfalfa	MW676129
9	DSMZ PV-0331	Germany	BLRV	Field pea	MW961159
10	MS16	Tunisia	BLRV	Chickpea	HQ840723
11	Gr-7	Greece	BLRV	Lentil	KT382811
12	UzCp84-13	Uzbekistan	BLRV	Chickpea	MW929604
13	MS28	Libya	BLRV	Faba bean	HQ840724
14	MS31	Ethiopia	BLRV	Lentil	HQ840725
15	BLRV-43	Spain	BLRV	Faba bean	AY616761
16	Chickpea-Sierra-NCIS-21-Bozeman-MT	USA	BLRV	Chickpea	MK070175
17	AKM-1	Uzbekistan	BLRV	Chickpea	OQ123402
18	Vf-khuzestan	Iran	BLRV	Faba bean	MF780974
19	ZM1_NX3	China	BLRV	Alfalfa	OL521667
20	BLRV-Hotah	KSA	BLRV	Alfalfa	KJ847770

[a] CpCSV: chickpea chlorotic stunt virus, BWYV: beet western yellows virus, TuYV: turnip yellows virus, BrYV: brassica yellows virus, BLRV: bean leafroll virus, BChV: beet chlorosis virus.

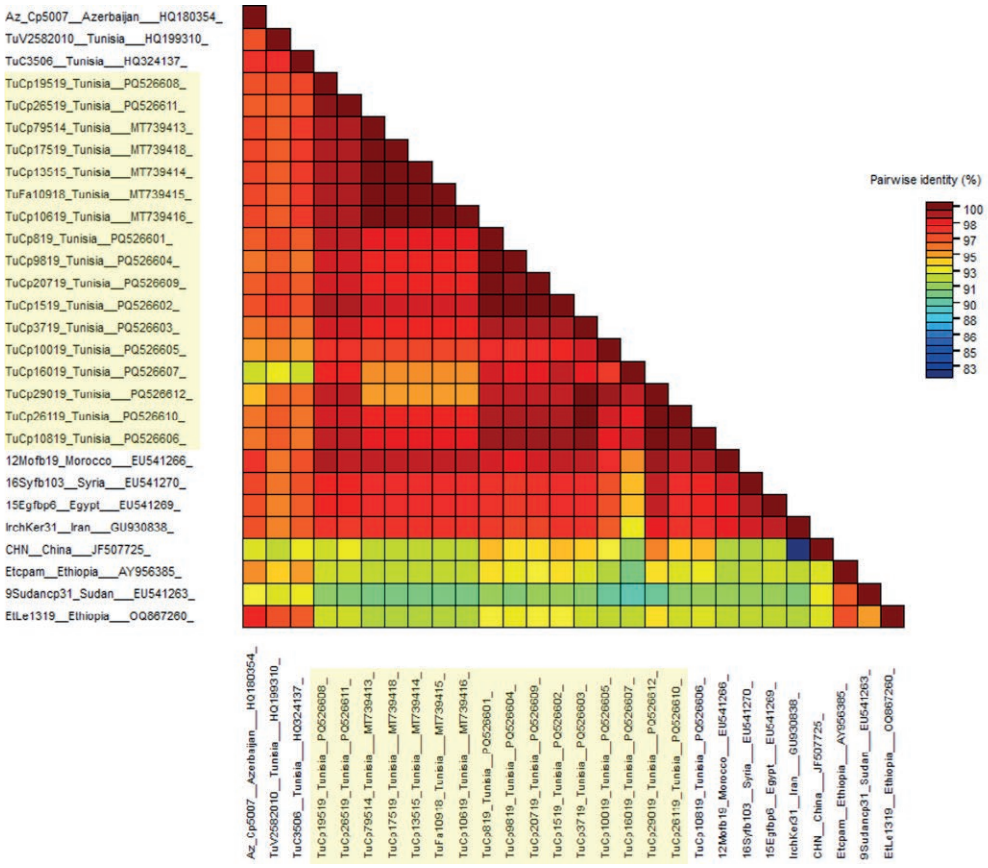

Figure 8. Pairwise nucleotide identity matrix of 24 chickpea chlorotic stunt virus (CpCSV, species *Polerovirus CPCSV*) sequences generated using SDTv1.3. Isolates characterized in this study are highlighted.

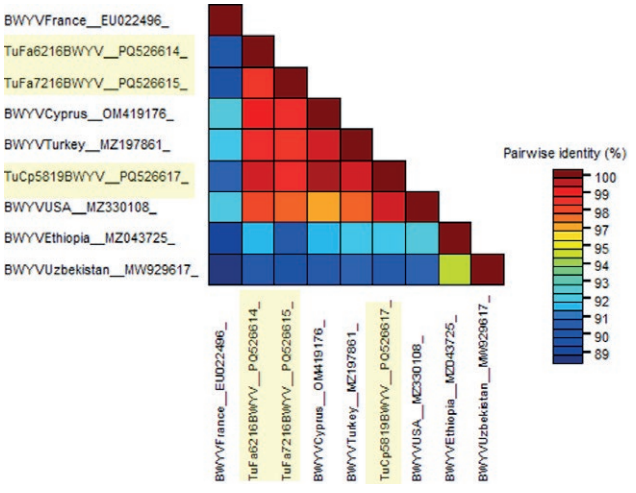

Figure 9. Pairwise nucleotide identity matrix of 9 beet western yellows virus (BWYV, species *Polerovirus BWYV*) sequences generated using SDTv1.3. Isolates characterized in this study are highlighted

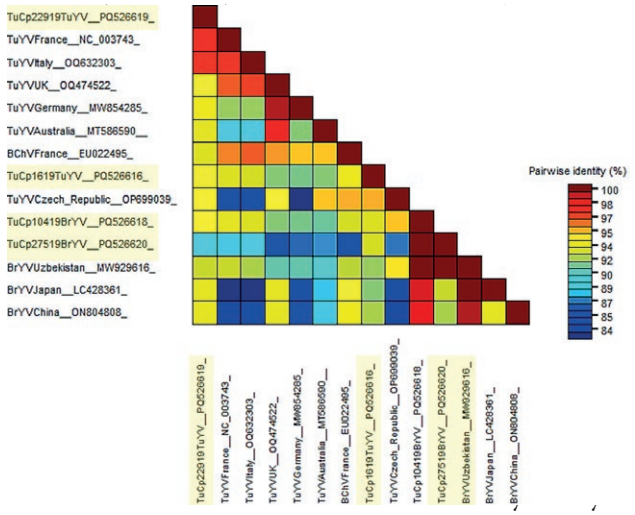

Figure 10. Pairwise nucleotide identity matrix of 14 TuYV/BrYV (species *Polerovirus TUYV*) sequences generated using SDTv1.3. Isolates characterized in this study are highlighted

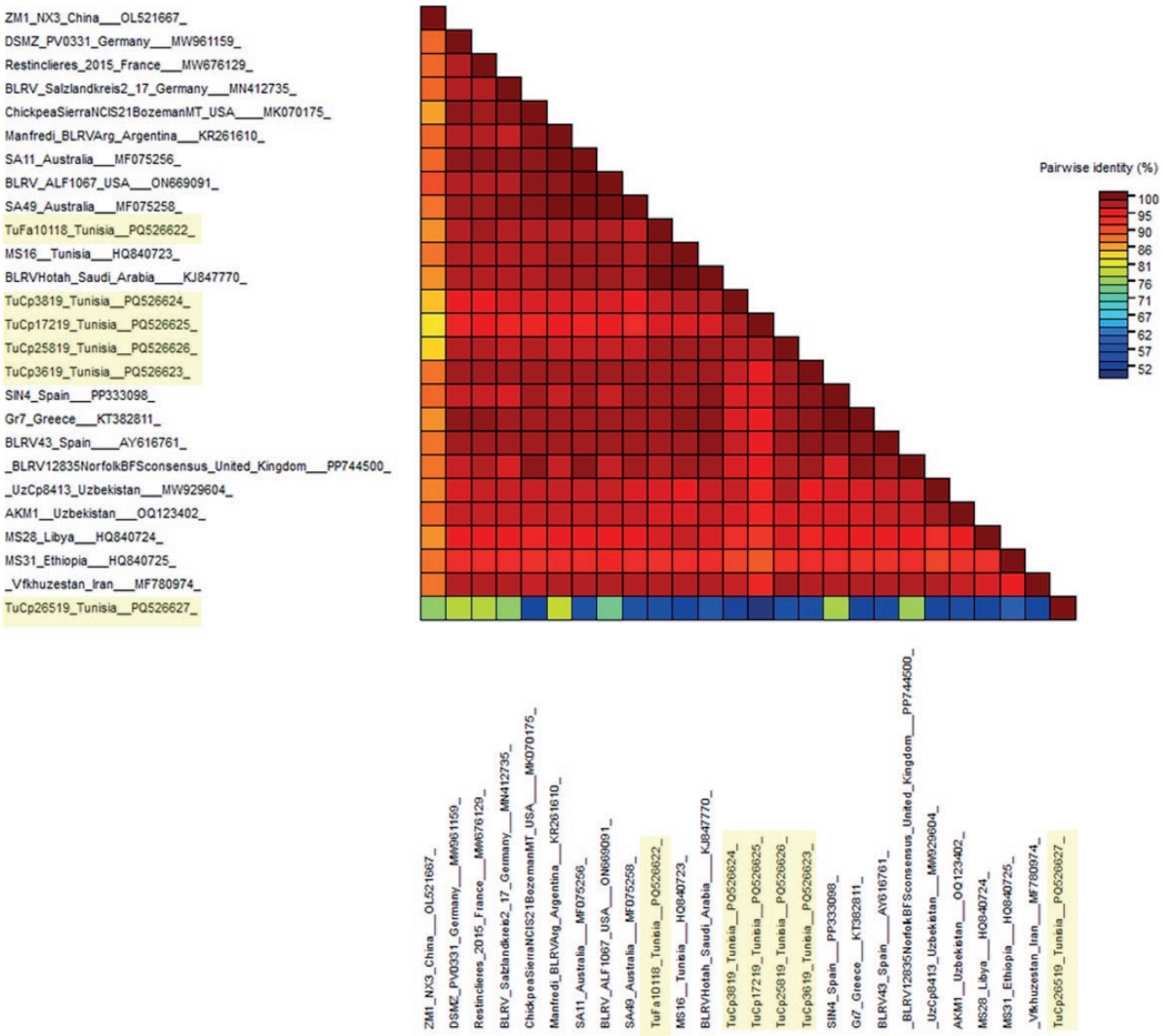

Figure 11. Pairwise nucleotide identity matrix of 26 bean leafroll virus (BLRV, species *Luteovirus phaseoli*) sequences generated using SDTv1.3. Isolates characterized in this study are highlighted

revealed values ranging from 50 to 98% among BLRV isolates. Most isolates showed high similarity (92 to 98%), consistent with the limited genetic diversity observed in the phylogenetic analysis. However, isolate TuCp265-19 displayed a markedly lower similarity (50 to 57%) compared with other isolates, indicating substantial sequence divergence within the analyzed region. The closest reference sequence to the main BLRV cluster was the Spanish isolate SIN4 (PP333098; from *Medicago sativa*), sharing 95 to 99% similarities with most isolates, but only 77% similarity with TuCp265-19 (Figure 11). These results suggest that TuCp265-19 is a highly divergent variant, although additional genomic regions would be required to clarify its precise taxonomic position.

DISCUSSION

This study has shown that CpCSV and BWYV (*Polerovirus*) were the most frequently detected viruses in faba bean and chickpea samples exhibiting yellowing and stunting symptoms. The survey was geographically extensive and was carried out during multiple growing seasons for these legumes. The field surveys also showed

Table 4. Tissue blot immunoassay (TBIA) reaction with Luteo- and polerovirus monoclonal antibodies (MAbs) of faba bean and chickpea samples collected from Tunisia between 2013-2019. All the plants tested were selected on the basis of reaction with broad-spectrum legume luteovirus MAb 5G4

Year	Crop	No. of samples reacted with 5G4 MAb	No. of plants with single infection	No. of samples reacted positively to MAbs[a]					Total of mixed infection
				CpCSV + BWYV	BWYV + BLRV	CpCSV + BLRV	CpCSV + BWYV + BLRV	CpCSV + BWYV + FBNYV	
2013/2014	Faba bean	100	77	21	1	0	1	0	23
2014/2015	Faba bean	186	174	12	0	0	0	0	12
	Chickpea	480	455	25	0	0	0	0	25
2015/2016	Chickpea	148	142	6	0	0	0	0	6
2016/2017	Faba bean	56	51	3	1	1	0	0	5
	Chickpea	104	72	13	5	11	3	0	32
2017/2018	Faba bean	221	140	78	1	0	1	1	81
2018/2019	Faba bean	31	29	0	2	0	0	0	2
	Chickpea	76	68	6	0	2	0	0	8
Total	Faba bean	594	471	114	5	1	2	1	123
	Chickpea	808	737	50	5	13	3	0	71

[a] CpCSV: chickpea chlorotic stunt virus (mixture of 5-2B8, 5-3D5 and 5-5B8 MAbs); BWYV: beet western yellows virus (A5977 MAb from Agdia); BLRV: bean leafroll virus (4B10 MAb); FBNYV: faba bean necrotic yellows virus (3-2E9 MAb).

the frequent presence of aphid colonies, particularly *Aphis craccivora* and *Acyrthosiphon pisum,* on faba bean plants. These aphid species are recognized as efficient vectors of CpCSV (Abraham *et al*., 2006; Asaad *et al*., 2009), and their abundance in the surveyed fields likely contributed to the high incidence of CpCSV detected in this study.

CpCSV has previously been reported on faba bean and chickpea in Tunisia, based on molecular characterization (Najar *et al*., 2011), whereas BWYV has been reported on faba bean using serological analyses (Najar *el al*., 2000b). Since first reported in Ethiopia (Abraham *et al*., 2006), CpCSV has been identified in several food legume crops, including chickpea, faba bean, lentil and pea, across many countries of the WANA region (Abraham *et al*., 2006; Kumari *et al*., 2008; Abraham *et al*., 2009; Asaad *et al*., 2009, Kumari *et al*., 2018). The virus has also been reported infecting several leguminous weeds and four non-legume wild plant species (Asaad *et al*., 2009). Although epidemics of CpCSV have been documented in Syria, Tunisia, and Ethiopia (Abraham *et al*., 2006; Kumari *et al*., 2007; Asaad *et al*., 2009; Kumari *et al*., 2009; Najar *et al*., 2011), quantitative data on yield losses due to this virus remain limited (Abraham and Vetten, 2022). This highlights the need for further studies to better assess the impacts of CpCSV on legume crop productivity.

FBNYV was detected only in faba bean during the 2016/17, 2017/18, and 2018/19 growing seasons, and at low incidence. This virus was previously reported in Tunisia by Najar *et al*. (2000a), and is considered one of the most damaging viruses of faba bean in the WANA region, where it has reached epidemic levels and caused substantial yield losses in several countries (Makkouk *et al*., 2003; Kumari and Makkouk, 2007). Such severe outbreaks of FBNYV were repeated in Egypt during the 1992/1993 and 1997/1998 growing seasons, resulting in a complete of the faba bean crop productivity (Makkouk*et al*.,1998).

Environmental conditions in the Cap Bon region of northeastern Tunisia are particularly favourable for establishment and spread of aphid-borne viruses. This coastal area is characterized by a sub-humid Mediterranean climate with mild temperatures and frequent winds (Hlaoui *et al*., 2019), factors known to strongly influence aphid survival, reproduction, and dispersal (Irwin and Thresh, 1988; Ng and Perry, 2004; Puthanveed *et al*., 2023; Roonjha *et al*., 2025). The polyphagous aphid *Myzus persicae*, which feeds on more than 400 plant species (Blackman and Eastop, 2000), is an economically important pest in Tunisia, and is an efficient vector of numerous plant viruses (Boukhris-Bouhachem *et al*., 2007; Guesmi *et al*., 2010; Boukhris-Bouhachem *et al*., 2011; Mdellel and Kamel, 2014; Charaabi *et al*., 2016).

The complex life cycle of *M. persicae*, involving host alternation between primary woody and herbaceous plants and prolonged parthenogenetic reproduction, enables aphid populations to persist year-round and move readily among crops (Simon *et al*., 2002; Mdellel and Ben Halima, 2012). In the Cap Bon region, the close proxim-

ity of peach orchards, potato fields, brassica crops, cucurbit and pepper crops, and legume fields further facilitates movement of winged aphids (Stevens *et al*., 2005; Hlaoui *et al*., 2019, 2022; Roonjha *et al*., 2025), and favours the spread of persistently transmitted viruses such as BWYV. In contrast, BLRV has a more restricted host range mainly limited to legumes, so vectoring of BLRV may be less favoured under these ecological conditions.

Weeds and invasive plants may also contribute to virus epidemiology by acting as reservoir hosts ("Green Bridge") for viruses and their aphid vectors (Wisler and Norris, 2005; Kazinczi *et al*., 2007). Because many aphid-transmitted viruses infect cultivated and wild plants, they can persist in alternative hosts between cropping seasons, increasing infection pressure on nearby crops (Aguiar *et al*., 2018; Hussein Aliyu *et al*., 2021; Yazdkhasti *et al*., 2021). Poleroviruses such as BWYV and CpCSV have been reported as infecting numerous cultivated plants and weeds (Abraham *et al*., 2006; Kumari *et al*., 2008; Venkataravanappa *et al*., 2023), highlighting the roles of reservoir hosts in virus persistence and spread.

Serological analysis using TBIA showed that 54.7% of faba bean and 46.5% of chickpea symptomatic samples tested negative for the antibodies used, suggesting the presence of additional viruses not detected in the present study. These results highlight the need for expanded diagnostic approaches using additional antisera and molecular assays for detecting an increased spectrum of virus pathogens.

The results of this study have shown clear predominance of single virus infections in chickpea and faba bean crops in Tunisia, as determined by TBIA. Chickpea crops had the greatest proportion of singly infected plants (77%), whereas faba bean crops had a relatively greater proportion of mixed virus infections (21%). This difference may be related to host plant traits influencing aphid feeding behaviour and virus transmission. Faba bean plants have large canopies and soft tissues, that attract aphid vectors and promote repeated feeding events, increasing the likelihood of acquiring and transmitting multiple viruses. In contrast, chickpea plants generally have small and rigid leaves, that may reduce aphid settling and feeding duration, favouring single virus infections. Similar patterns have been reported in other legume cropping systems where plant morphology and nutritional traits influence aphid colonization and dynamics of virus transmission (Ghorbani *et al*., 2010; Chiquito Almanza *et al*., 2017; Mulenga *et al*., 2022; Ademe *et al*., 2025). These results underscore the importance of considering vector-mediated processes alongside host susceptibility when developing strategies to manage virus spread in legume cropping systems (Lei *et al*., 2025).

Mixed infections were predominantly associated with *Polerovirus* (*Solemoviridae*) viruses, particularly CpCSV and BWYV, accounting for 95% of mixed infections in faba bean and 69% in chickpea. Virus-virus interactions in mixed infections may influence virus accumulation, host range, symptom severity, and vector transmission efficiency (Moreno and López-Moya, 2020; Sánchez-Tovar *et al*., 2025). The frequent association of CpCSV and BWYV has been previously reported in legume crops (Abraham *et al*., 2009; Moukahel *et al*., 2021; Maina and Jones, 2023), although the nature of the interaction between these two viruses remains unclear.

While serological assays (TBIA) frequently suggested co-infections by CpCSV and BWYV, molecular analyses detected only single *Polerovirus* species per sample. This discrepancy probably reflects the limitations of serological diagnostics for closely related viruses, as CpCSV and BWYV share conserved coat protein epitopes that may lead to antibody cross-reactivity (Martin and D'Arcy, 1990; Oshima *et al*., 1990; Fortass *et al*., 1997; Kidanemariam and Abraham, 2023). Consequently, molecular analyses occasionally reveal mixed infections not detected by TBIA, highlighting the complementary nature of serological and molecular diagnostic approaches. While TBIA remains a rapid and cost-effective tool for large-scale virus surveillance (Makkouk and Kumari, 1996), molecular techniques such as MP-PCR provide increased sensitivity and specificity for detecting closely related viruses and mixed infections (Abraham *et al.,* 2008; Deb and Anderson, 2008; Abraham and Vetten, 2022). The present study results also showed that CpCSV was the most prevalent virus involved in mixed infections in chickpea and faba bean crops. This predominance may be explained by the broader host range of CpCSV than of BWYV host range, and efficient persistent transmission by *A. craccivora*, which was frequently observed during field surveys (Abraham *et al*., 2006; Asaad *et al*., 2009; Abraham and Vetten, 2022). In the Bizerte region where winters are mild, CpCSV and BWYV co-infections were particularly common, representing 59% of mixed infections in faba bean crops and 52% in chickpea. A similar pattern was observed in Cap Bon, where these co-infections accounted for 37% of mixed infections in faba bean and 26% of mixed infections in chickpea. These results highlight the ecological adaptability and transmission efficiency of CpCSV in cool-season legume cropping systems.

The present study observations are consistent with previous studies demonstrating that climate change, agricultural history, and the invasion or persistence of alter-

native host plants strongly influence vector dynamics and virus emergence at regional scales (Robert and Lemire, 1999; Jones and Barbetti, 2012; Jones, 2016; Trebicki, 2020). They also emphasize the importance of weed and reservoir host management as key components of integrated strategies aimed at reducing virus inoculum and limiting epidemic development (Wisler and Norris, 2005).

The use of the partial *CP* gene in the present study was a strategic choice to combine practical feasibility with phylogenetic relevance. Virus *CP* remains a reliable and accessible molecular marker for initial identification and diagnosis, because of its structural role and its conservation among related viruses. Despite its conserved nature, the partial *CP* gene has also been shown to contain sufficient variability to discriminate between isolates, and to reveal phylogeographic structuring in several *Polerovirus* species, including CpCSV.

Previous studies have demonstrated clear phylogeographic structuring in CpCSV populations. Abraham *et al*. (2009) identified two major strains associated with geographic origins, Strain I (from Ethiopia and Sudan) and Strain II (from Morocco, Syria, and Egypt), separated by approx. 8 to 10% nucleotide divergence in the CP. Similarly, Najar *et al*. (2011) reported that Tunisian isolates of CpCSV clustered into these two groups. Consistent with these findings, the present study phylogenetic analysis showed that ten newly characterized Tunisian isolates clustered with Ethiopian and Sudanese isolates (Strain I), whereas three isolates grouped with isolates from Morocco, Egypt, Syria, and Iran (Strain II). These results confirm the coexistence of at least two CpCSV lineages in Tunisia, and indicate that geographic origin rather than host species drives CpCSV genetic differentiation. Presence of distinct strains may also have epidemiological and host resistance breeding implications, as different isolates may vary in symptom severity and resistance-breaking potential (Abraham *et al*., 2009).

BWYV is widely distributed and infects chickpea and numerous other plant species, with reported yield losses due to BWYV infections ranging from 8 to 90% (Abraham, 2025). Despite this broad host range, previous studies have reported limited sequence variability among BWYV isolates (Yoshiba and Tamada, 2019). In agreement with these observations, SDT pairwise similarity analysis revealed high nucleotide conservation among the Tunisian BWYV isolates (98 to 99%), indicating circulation of a genetically homogeneous lineage. However, these isolates were clearly differentiated from sugar beet derived BWYV variants (89 to 90%), and from chickpea isolates from Ethiopia and Uzbekistan (89 to 92%), suggesting existence of host- or geography-associated lineages.

Sequencing of amplicons obtained with BWYV-specific primers also showed presence of TuYV/BrYV in addition to BWYV. This is consistent with recent studies showing that many poleroviruses previously identified as BWYV by serology correspond to TuYV or related species (Abraham, 2025). The discrepancy between PCR detection and sequencing probably results from primer annealing in conserved genomic regions shared among poleroviruses, which may result in cross-detection of closely related species (Hauser *et al*., 2000; 2002; D'Arcy and Domier, 2005). These results highlight the limitations of PCR targeting conserved regions, and emphasize the need for additional genomic markers for accurate species identification.

TuYV, formerly known as BWYV, belongs to *Polerovirus* within *Solemoviridae*. BrYV shares approx. 80% nucleotide similarity with TuYV and has been subdivided into several strains associated with different brassica hosts. Phylogenetic analyses indicate that TuYV and BrYV share a common evolutionary origin, and recombination has been recognized as an important driver of their diversification (Filardo *et al*., 2021; Peng *et al*., 2023). In some cases, whole-genome analyses have indicated that BrYV may represent a divergent lineage within the TuYV species complex, rather than being a distinct species (Filardo *et al*., 2021). These findings highlight the taxonomic complexity within the TuYV/BrYV group, and the importance of highly specific molecular diagnostic tools. More recently, high-throughput sequencing studies detected BWYV-related sequences in Citrus, including an isolate associated with citrus yellow vein-associated virus and "fatal yellows" disease (Keremane *et al*., 2024). Consistent with these observations, Pierre *et al.* (2026) developed and validated a real-time RT-PCR assay for specific detection of BWYV and related poleroviruses, which demonstrated improved sensitivity and specificity compared with generic ELISA and RT-PCR assays.

Phylogenetic and SDT analysis further showed that Tunisian TuYV isolates form a genetically homogeneous cluster closely related to international TuYV populations, with clustering largely associated with geographic origin. In contrast, BLRV isolates showed both high conservation and notable divergence. Most Tunisian isolates clustered with sequences from Europe, the United States, Australia, and Spain, sharing 95 to 99% nucleotide similarity, suggesting a cosmopolitan lineage. However, one isolate (TuCp265-19) exhibited marked divergence (50 to 57% similarity) compared with other Tunisian isolates, indicating the possible presence of a highly divergent variant or distinct lineage. Similar patterns of divergence within BLRV populations have been reported previously; for example, Hajiyusef *et al*. (2017) showed that an

Iranian BLRV isolate formed two subgroups with other international isolates, while maintaining high similarity within each subgroup.

The present study has highlighted the diversity of viruses infecting chickpea and faba bean in Tunisia, with poleroviruses (CpCSV and BWYV) as the predominant pathogens. Phylogenetic analyses revealed two CpCSV strains, and high conservation among BWYV and TuYV isolates. The detection of TuYV/BrYV among BWYV-positive samples underscores the importance of molecular diagnostics for virus pathogens. These results provide essential baseline data for improving virus surveillance and management in Tunisian legume crops.

FUNDING

This research was partly supported by the Germplasm Health Units Component of the CGIAR Genebanks and CGIAR Sustainable Farming Science Program, supported by the CGIAR Trust Fund Donors.

LITERATURE CITED

Abraham A.D., 2025. Virus diseases of economic importance on food legumes in Africa and their control. *Viruses* 17(12): 1555. https://doi.org/10.3390/v17121555

Abraham A.D., Menzel W., Lesemann D.E., Varrelmann M., Vetten H.J., 2006. Chickpea chlorotic stunt virus: a new polerovirus infecting cool-season food legumes in Ethiopia. *Phytopathology* 96: 437–446. https://doi.org/10.1094/PHYTO-96-0437

Abraham A.D., Menzel W., Varrelmann M., Vetten H.J., 2009. Molecular, serological and biological variation among chickpea chlorotic stunt virus isolates from five countries of North Africa and West Asia. *Archives of virology* 154: 791–799. https://doi.org/10.1007/s00705-009-0374-0

Abraham A.D., Varrelmann M., Vetten H.J., 2008. Molecular evidence for the occurrence of two new luteoviruses in cool-season food legumes in northeast Africa. *African Journal of Biotechnology* 7(4): 414–420.

Abraham A., Vetten H.J., 2022. Chickpea chlorotic stunt virus: a threat to cool-season food legumes. *Archives of virology* 167: 21–30. https://doi.org/10.1007/s00705-021-05288-4

Ademe A., Kumari S.G., Moukahel A., Alemu T., Abraham A., ... Kemal S.A., 2025. Phylogenetic analysis, mixed infection and seed transmission of Pea seed-borne mosaic virus in Ethiopia. *Physiological and Molecular Plant Pathology* 136: 102531. https://doi.org/10.1016/j.pmpp.2024.102531

Aguiar R.W.S., Alves G.B., Queiroz A.P., Nascimento I.R., Lima, M.F., 2018. Evaluation of weeds as virus reservoirs in watermelon crops. *Planta Daninha* 36. https://doi.org/10.1590/S0100-83582018360100032

Altschul S.F., Madden T.L., Schaffer A.A., Zhang Z.H., Zhang Z., ... Lippman D.J., 1997. Gapped BLAST and PSIBLAST: A new generation of protein database search programs. *Nucleic Acids Research* 25(17): 3389–3402. https://doi.org/10.1093/nar/25.17.3389

Altschul S.F., Wootton J.C., Gertz E.M., Agarwala R., Morgulis A., ... Yu Y-K., 2005. Protein database searches using compositionally adjusted substitution matrices. *FEBS Journal* 272(20): 5101–5109. https://doi.org/10.1111/j.1742-4658.2005.04945.x

Asaad N.Y., Kumari S.G., Haj-Kassem A.A., Shalaby A.A., Al-Shaabi S., Malhotra R.S., 2009. Detection and characterisation of chickpea chlorotic stunt virus in Syria. *Journal of Phytopathology* 157(11-12): 756–761. https://doi.org/10.1111/j.1439-0434.2009.01574.x

Blackman R.L., Eastop V.F., 2000. *Aphids on the World's Crops: an Identification and Information Guide*. 2nd ed. John Wiley & Sons, Ltd.: Chichester, UK.

Boukhris-Bouhachem S., Souissi R., Turpeau E., Rouzé-Jouan J., Fahem M., ... Hulle M., 2007. Aphid (Hemiptera: Aphidoidea) diversity in Tunisia in relation to seed potato production. *Annales de la Société Entomologique de France* 43(3): 311–318. https://doi.org/10.1080/00379271.2007.10697526

Boukhris-Bouhachem S., Rouzé-Jouan J., Souissi R., Glais L., Hullé M., 2011. Transmission efficiency of the strain PVYNTN by commonly captured aphids in Tunisian potato fields. *Plant Pathology Journal* 10(1): 22–28. https://doi.org/10.3923/ppj.2011.22.28

Charaabi K., Boukhris-Bouhachem S., Makni M., Fenton B., Denholm I., 2016. Genetic variation in target-site resistance to pyrethroids and pirimicarb in Tunisian populations of the peach potato aphid, *Myzus persicae* (Sulzer) (Hemiptera: Aphididae). *Pest Management Science* 72(12): 2313–2320. https://doi.org/10.1002/ps.4276

Chiquito-Almanza E., Acosta-Gallegos J.A., García-Álvarez N.C., Garrido-Ramírez E.R., Montero-Tavera V., Anaya López J.L., 2017. Simultaneous detection of both RNA and DNA viruses infecting dry bean and occurrence of mixed infections by BGYMV, BCMV and BCMNV in the Central-West region of Mexico. *Viruses* 9(4): 63. https://doi.org/10.3390/v9040063

D'Arcy C.J., Domier L.L., 2005. Luteoviridae. In: *Virus Taxonomy. Eight Report of the International Committee on Taxonomy of Viruses* (C.M. Faugnet, M.A.

Mayo, J. Maniloff, U. Desselberger, L.A. Ball, ed.), Elsevier Academic Press, London, UK, 343–352.

Deb M., Anderson J.M., 2008. Development of a multiplexed PCR detection method for *Barley* and *Cereal yellow dwarf viruses*, *Wheat spindle streak virus*, *Wheat streak mosaic virus* and *Soil-borne wheat mosaic virus*. *Journal of Virological Methods* 148(1-2): 17–24. https://doi.org/10.1016/j.jviromet.2007.10.015

FAOSTAT. 2026. United Nations Food and Agriculture Organization, Statistics Division, Rome, Italy. Available at: https://www.fao.org/faostat/en/#data/QCL. Accessed April 2, 2026.

Filardo F., Nancarrow N., Kehoe M., McTaggart A.R., Congdon, B., … Sharman, M., 2021. Genetic diversity and recombination between turnip yellows virus strains in Australia. *Archives of Virology* 166(3): 813–829. https://doi.org/10.1007/s00705-020-04931-w

Fortass M., van der Wilk F., van den Heuvel J.F.J.M., Goldbach R.W., 1997. Molecular evidence for the occurrence of beet western yellows virus on chickpea in Morocco. *European Journal of Plant Pathology* 103: 481–484. https://doi.org/10.1023/A:1008687629522

Franz A., Makkouk K.M., Katul L., Vetten H.J., 1996. Monoclonal antibodies for the detection and differentiation of faba bean necrotic yellows virus isolates. *Annals of Applied Biology* 128(2): 255–2268. https://doi.org/10.1111/j.1744-7348.1996.tb07321.x

Ghorbani S.G.M., Shahraeena N., Elahinia S.A., 2010. Distribution and impact of virus associated diseases of common bean (*Phaseolus vulgaris* L.) in northern Iran. *Archives of Phytopathology and Plant Protection* 43(12): 1183–1189. https://doi.org/10.1080/03235400802366834

Guesmi J., Ben Halima K.M., Almohandes-Dridi B., 2010. Identification and population evolution of aphids infesting artichoke in Tunisia. *Tunisian Journal of Plant Protection* 5: 83–89.

Hajiyusef T., Shahraeen N., Maleki M., 2017. Serological and molecular detection of *Bean leaf roll* and *Chickpea chlorotic stunt* luteoviruses in chickpea from Iran. *Journal of Plant Protection Research* 57(2): 136–143. https://doi.org/10.1515/jppr-2017-0018

Hauser S., Stevens M., Mougel C., Smith H.G., Fritsch C., … Lemaire O., 2000. Biological, serological, and molecular variability suggest three distinct Polerovirus species infecting beet or rape. *Phytopathology* 90(5): 460–466. https://doi.org/10.1094/PHYTO.2000.90.5.460

Hauser S., Stevens M., Beuve M., Lemaire O., 2002. Biological properties and molecular characterization of beet chlorosis virus (BChV). *Archives of Virology* 147: 745–762. https://doi.org/10.1007/s007050200023

Hlaoui A., Boukhris-Bouhachem S., Sepúlveda D.A., Correa M.C., Briones L.M., … Figueroa C.C., 2019. Spatial and temporal genetic diversity of the peach potato aphid *Myzus persicae* (Sulzer) in Tunisia. *Insects* 10(10): 330. https://doi.org/10.3390/insects10100330

Hlaoui A., Chiesa O., Figueroa C.C., Souissi R., Mazzoni E., Boukhris-Bouhachem S., 2022. Target site mutations underlying insecticide resistance in Tunisian populations of *Myzus persicae* (Sulzer) on peach orchards and potato crops. *Pest Management Science* 78(4): 1594–1604. https://doi.org/10.1002/ps.6778

Hussein Aliyu T.H., Takim F.O., Olatinwo L.K., Arogundade O., Funmilayo Omotesho K.F., Oladoja D.A., 2021. Severity of viral diseases and types of weeds as alternative viral hosts in Dioscorea fields in southern guinea savannah agroecology of Nigeria. *Journal of Food and Agriculture,* 14(2): 1–16. https://doi.org/10.4038/jfa.v14i2.5242

Irwin M.E., Thresh J.M., 1988. Long-range aerial dispersal of cereal aphids as virus vectors in North America. *Philosophical Transactions of the Royal Society of London. B, Biological Sciences*, 321(1207): 421–446. http://www.jstor.org/stable/2396815

Jones R.A.C., 2016. Future scenarios for plant virus pathogens as climate change progresses. *Advances in Virus Research* 95: 87–147. https://doi.org/10.1016/bs.aivir.2016.02.004

Jones R. A., Barbetti M.J., 2012. Influence of climate change on plant disease infections and epidemics caused by viruses and bacteria. *CABI Reviews* 1–13. https://doi.org/10.1079/PAVSNNR20127022

Jukes T.H., Cantor C.R., 1969. Evolution of protein molecules. In: *Mammalian Protein Metabolism* (H.N. Munro, ed.), Academic Press, New York, 21–132.

Katul L., 1992. *Serological and Molecular Characterization of Bean leaf roll virus (BLRV) and Faba bean necrotic yellows virus (FBNYV).* PhD Thesis, University of Göttingen, Germany, 115 pp.

Kazinczi G., Horvath J., Takacs A., 2007. Toposviruses on ornamental plants. *Plant Viruses* 2: 142– 162.

Keremane M., Singh K., Ramadugu C., Krueger R.R., Skaggs T.H., 2024. Next generation sequencing, and development of a pipeline as a tool for the detection and discovery of citrus pathogens to facilitate safer germplasm exchange. *Plants* 13(3): 411. https://doi.org/10.3390/plants13030411

Kidanemariam D., Abraham A., 2023. Luteoviruses. In: *Plant RNA Viruses* (R.K. Gaur, B.P. Patil, R. Selvarajan, ed.), London: Academic Press, 57–77.

Kumar P.L., Kumari S.G., Waliyar F., 2008. Virus diseases of chickpea. In*: Characterization, Diagnosis and Management of Plant Viruses: Vegetable and Pulse Crops,* Vol 3 (G.P. Rao, P.L. Kumar, R.J.H. Penna, ed.), Texas, USA: Studium Press LLC, 213–234.

Kumar S., Stecher G., Li M., Knyaz C., Tamura K., 2018. MEGA X: Molecular Evolutionary Genetics Analysis across computing platforms. *Molecular Biology and Evolution* 35(6): 1547–1549. https://doi.org/10.1093/molbev/msy096

Kumari S.G., Makkouk K.M., 2007. Virus diseases of faba bean (*Vicia faba* L.) in Asia and Africa. *Plant Viruses* 1(1): 93–105. https://www.globalsciencebooks.info/Online/GSBOnline/images/0706/PV_1(1)/PV_1(1)93-105o.pdf

Kumari S.G., Makkouk K.M., Asaad N., Attar N., Hlaing Loh M., 2007. Chickpea chlorotic stunt virus affecting cool-season food legumes in West Asia and North Africa. *In: Abstract book of 10th International Plant Virus Epidemiology Symposium, on the theme "Controlling Epidemics of Emerging and Established Plant Virus Diseases—The Way Forward",* 15–19 October 2007, Hyderabad, India, 157 (abstract).

Kumari S.G., Makkouk K.M., Loh M.H., Negassi K., Tsegay S., ... Tesfatsion, Y., 2008. Viral diseases affecting chickpea crops in Eritrea. *Phytopathologia Mediterranea* 47(1): 42–49. https://www.jstor.org/stable/26463297

Kumari S.G., Larsen R., Makkouk K.M., Bashir M., 2009. Virus diseases of lentil and their control. In: *The Lentil: Botany, Production and Uses* (W. Erskine, F.J. Muehlbauer, A. Sarker, B. Sharma, ed.). CABI, UK, 306–325.

Kumari S.G., Najar A., Timoumi S., Male M.F., Kraberger S., Varsani A., 2015. First report of Chickpea chlorotic dwarf virus naturally infecting chickpea in Tunisia. *New Disease Reports* 32(1): 16. https://doi.org/10.5197/j.2044-0588.2015.032.016

Kumari S.G., Moukahel A.R., Hamed A.A., Sharman M., 2018. First report of Cucurbit aphid-borne yellows virus affecting chickpea (*Cicer arietinum* L.) in Sudan. *Plant Disease* 102(10): 2048. https://doi.org/10.1094/PDIS-02-18-0347-PDN

Lei, J., Yuan J., Chen M., Mao Q., 2025. Insect-specific viruses and their emerging role in plant disease mitigation. *Viruses* 17(9): 1269. https://doi.org/10.3390/v17091269

Maina S., Jones R.A.C., 2023. Enhancing biosecurity against virus disease threats to Australian grain crops: current situation and future prospects. *Frontiers in Horticulture* 2: 1263604. https://doi.org/10.3389/fhort.2023.1263604

Makkouk K.M., 2020. Plant pathogens which threaten food security: viruses of chickpea and other cool season legumes in West Asia and North Africa. *Food Security* 12: 495–502. https://doi.org/10.1007/s12571-020-01017-y

Makkouk K.M., Kumari S.G., 1996. Detection of ten viruses by the tissue-blot immunoassay (TBIA). *Arab Journal of Plant Protection* 14(1): 3–9 (in Arabic).

Makkouk, K.M., Vetten, H.J., Katul, L., Franz, A., Madkour, M.A., 1998. Epidemiology and control of faba bean necrotic yellows virus. (Chapter 40). In: *Plant Virus Disease Control* (A. Hadidi, R.K. Khetarpal, H. Koganezawa, ed.). APS Press, The American Phytopathological Society, St. Paul, Minnesota, USA, 534–540

Makkouk K.M., Kumari S.G., Hughes J.d'A., Muniyappa V., Kulkarni N.K., 2003. Other legumes: Faba bean, chickpea, lentil, pigeonpea, mungbean, blackgram, lima bean, horegram, bambara groundnut and winged bean. In: *Virus and Virus-like Diseases of Major Crops in Developing Countries* (G. Loebenstein, G. Thottappilly, ed.). Kluwer Academic Publishers, Dordrecht, The Netherlands, 447–476.

Makkouk K.M., Kumari S.G., van Leur J.A., Jones R.A., 2014. Control of plant virus diseases in cool-season grain legume crops. *Advances in Virus Research* 90: 207–253. https://doi.org/10.1016/B978-0-12-801246-8.00004-4

Martin R.R., D'Arcy C.J., 1990. Relationships among luteoviruses based on nucleic acid hybridization and serological studies. *Intervirology* 31(1): 23–30. https://doi.org/10.1159/000150130

Mdellel L., Ben Halima M.K., 2012. Aphids on almond and peach: preliminary results about biology in different areas of Tunisia. *REDIA* 95: 3–8.

Mdellel L., Kamel M.B.H. 2014. Effects of different varieties of pepper (*Capsicum annum* L.) on the biological parameters of the green peach aphid *Myzus persicae* Sulzer *(Hemiptera, Aphididae)* in Tunisia. *European Journal of Environmental Sciences* 4(2): 102–105. https://doi.org/10.14712/23361964.2014.4

Moreno A.B., López-Moya J.J., 2020. When viruses play team sports: mixed infections in plants. *Phytopathology* 110(1): 29–48. https://doi.org/10.1094/PHYTO-07-19-0250-FI

Moukahel A., Kumari S., Hamed A., Sharman M., Kemal S., 2021. Distribution and identification of luteovirids affecting chickpea in Sudan. *Phytopathologia Mediterranea* 60(2): 199–214. https://doi.org/10.36253/phyto-12135

Muhire B.M., Varsani A., Martin D.P., 2014. SDT: a virus classification tool based on pairwise sequence align-

ment and identity calculation. *PLOS ONE* 9: e108277. https://doi.org/10.1371/journal.pone.0108277

Mulenga R.M., Miano D.W., Al Rwahnih M., Kaimoyo E., Akello J., ... Alabi O.J., 2022. Survey for Virus Diversity in Common Bean (*Phaseolus vulgaris*) Fields and the Detection of a Novel Strain of *Cowpea polerovirus 1* in Zambia. *Plant Disease* 106(9): 2380–2391. https://doi.org/10.1094/PDIS-11-21-2533-RE

Najar A., Kumari S.G., Makkouk K.M., Daaloul A., 2003. A survey of viruses affecting faba bean (*Vicia faba*) in Tunisia includes first record of *Soybean dwarf virus*. *Plant Disease* 87(9): 1151. https://doi.org/10.1094/PDIS.2003.87.9.1151B

Najar A., Kumari S.G., Attar N., Lababidi S., 2011. Present status of some virus diseases affecting legume crops in Tunisia and partial characterization of Chickpea chlorotic stunt virus. *Phytopathologia Mediterranea* 50(2): 310–315. https://www.jstor.org/stable/26458704

Najar A., Makkouk K.M., Boudhir H., Kumari S.G., Zarouk R., ... Ben Othman F., 2000a. Viral diseases of cultivated legume and cereal crops in Tunisia. *Phytopathologia Mediterranea* 39: 423–432. https://www.jstor.org/stable/26456574

Najar A., Makkouk K.M., Kumari S.G., 2000b. First record of *Faba bean necrotic yellows virus* and *Beet western yellows virus* infecting faba bean in Tunisia. *Plant Disease* 84(9): 1046. https://doi.org/10.1094/PDIS.2000.84.9.1046A

Ng J.C.K., Perry, K.L., 2004. Transmission of plant viruses by aphid vectors. *Molecular Plant Pathology* 5(5): 505–511. https://doi.org/10.1111/j.1364-3703.2004.00240.x

Oshima K., Inoue A.K., Ishikawa Y., Shikata E., Takashi H., 1990. Production and application of monoclonal antibodies specific to ordinary strain and necrotic strain of potato virus Y. *Japanese Journal of Phytopathology* 56(4): 508–514. https://doi.org/10.3186/jjphytopath.56.508 (in Japanese).

Peng Q., Li W., Zhou X., Sun C., Hou Y., ... Lei L., 2023. Genetic diversity analysis of Brassica yellows virus causing aberrant color symptoms in oilseed rape. *Plants* 12(5): 1008. https://doi.org/10.3390/plants12051008

Pierre H., Ellen E., Elisabeth D., Pauline R., Yordan M., ... Stéphan S., 2026. Comparative analysis of beet western yellows virus detection methods: Development and validation of a novel real-time RT-PCR assay also targeting beet leaf yellowing virus. *Journal of Virological Methods* 342: 115352. https://doi.org/10.1016/j.jviromet.2026.115352

Puthanveed V., Singh K., Poimenopoulou E., Pettersson J., Siddique A.B., ... Kvarnheden A., 2023. Milder autumns may increase risk for infection of crops with Turnip yellows virus. *Phytopathology* 113(9): 1788–1798. https://doi.org/10.1094/PHYTO-11-22-0446-V

Robert Y., Lemaire O., 1999. Epidemiology and control strategies. In: The Luteoviridae. H.J. Smith and H. Barker (ed.). CABI Publishing, UK. Pp 211–219.

Rozas, J., Ferrer-Mata A., Sánchez-DelBarrio J.C., Guirao-Rico S., Librado P., Ramos-Onsins S.E., Sánchez-Gracia A., 2017. DnaSP 6: DNA Sequence Polymorphism Analysis of Large Data Sets. *Molecular Biology and Evolution* 34(12): 3299–3302. https://doi.org/10.1093/molbev/msx248

Roonjha M.A., Roonjho R., Ali M., Anas M., Khalid H., Jan A., 2025. Aphid-transmitted plant viruses: Epidemiology and integrated vector management. *International Journal of Agricultural Innovations and Cutting-Edge Research* 3(3): 109–126. https://jai.bworesearches.com/index.php/jwr/article/view/157

Sánchez-Tovar M.R., Rivera-Bustamante R.F., Saavedra-Trejo D.L., Guevara-González R.G., Torres-Pacheco I., 2025. Mixed plant viral infections: complementation, interference and their effects, a review. *Agronomy* 15(3): 620. https://doi.org/10.3390/agronomy15030620

Simon J.C., Rispe C., Sunnucks P., 2002. Ecology and evolution of sex in aphids. *Trends in Ecology & Evolution* 17(1): 34–39. https://doi.org/10.1016/S0169-5347(01)02331-X

Stevens M., Freeman B., Liu H.Y., Herrbach E., Lemaire O., 2005. Beet poleroviruses: close friends or distant relatives?. *Molecular Plant Pathology* 6(1): 1–9. https://doi.org/10.1111/j.1364-3703.2004.00258.x

Tajima F., 1989. Statistical methods to test for nucleotide mutation hypothesis by DNA polymorphism. *Genetics* 123(3): 585–595. https://doi.org/10.1093/genetics/123.3.585

Trebicki P., 2020. Climate change and plant virus epidemiology. *Virus Research* 286: 198059. https://doi.org/10.1016/j.virusres.2020.198059

Venkataravanappa V., Ashwathappa K.V., Hiremath S., Manjunatha L., Shankarappa K.S., ... Lakshminarayana Reddy C.N., 2023. Begomovirus and DNA-satellites association with mosaic and leaf curl disease of *Solanum nigrum* and *Physalis minima*: the new hosts for chilli leaf curl virus. *VirusDisease* 34(4): 504–513. https://doi.org/10.1007/s13337-023-00850-x

Wisler G.C., Norris R.F., 2005. Interactions between weeds and cultivated plants as related to management of plant pathogens. *Weed Science* 53(6): 914–917. https://doi.org/10.1614/WS-04-051R.1

Yoshida N., Tamada T., 2019. Host range and molecular analysis of *Beet leaf yellowing virus*, *Beet west-*

ern yellows virus-JP and *Brassica yellows virus* in Japan. *Plant Pathology* 68(6): 1045–1058. https://doi.org/10.1111/ppa.13023

Yazdkhasti E., Hopkins R.J., Kvarnheden A., 2021. Reservoirs of plant virus disease: Occurrence of Wheat dwarf virus and Barley/Cereal yellow dwarf viruses in Sweden. *Plant Pathology* 70(11): 1552–1561. https://doi.org/10.1111/ppa.13414

Phytopathologia Mediterranea
The international journal of the
Mediterranean Phytopathological Union

Firenze University Press
www.fupress.com/pm

New or Unusual Disease Reports

First report of *Fusarium clavum* and Fusarium venenatum causing leaf spots on *Magnolia grandiflora*

Michele NARDUZZI[1], Carlo BREGANT[2], Anna Maria VETTRAINO[1,*]

[1] *Department for Innovation in Biological, Agro-Food and Forest Systems (DIBAF), University of Tuscia, Viterbo 01100, Italy*
[2] *Department of Land, Environment, Agriculture and Forestry (TESAF), University of Padova, Padova 35020, Italy*
* Corresponding author. Email: vettrain@unitus.it

Summary. *Magnolia grandiflora* is an important ornamental tree in urban areas. In 2025, leaf spot symptoms were observed on *M. grandiflora* leaves in Viterbo, Italy. The causal agents were isolated and identified through morphological characterization and multilocus phylogenetic analysis of EF1-α, RPB1 and RPB2 gene sequences, and were identified as *Fusarium venenatum* and *F. clavum*. Pathogenicity tests on healthy *M. grandiflora* leaves produced characteristic brown leaf spots within 3 d post-inoculation. Re-isolations of the inoculated fungi confirmed Koch's postulates. This study demonstrated that *F. venenatum* and *F. clavum* caused the leaf spot symptoms on Magnolia, and is the first report of this disease in Italy. These results provide the basis for developing targeted disease management strategies for emerging diseases caused by these fungi in urban areas.

Keywords. Emerging disease, *Nectriaceae*, urban trees.

OPEN ACCESS

Citation: Narduzzi, M., Bregant, C., & Vettraino, A. M. (2026). First report of *Fusarium clavum* and *Fusarium venenatum* causing leaf spots on *Magnolia grandiflora*. *Phytopathologia Mediterranea* 65(1): 185-189. doi: 10.36253/phyto-17048

Accepted: April 29, 2026

Published: May 14, 2026

© 2026 Author(s). This is an open access, peer-reviewed article published by Firenze University Press (https://www.fupress.com) and distributed, except where otherwise noted, under the terms of the CC BY 4.0 License for content and CC0 1.0 Universal for metadata.

Data Availability Statement: All relevant data are within the paper and its Supporting Information files.

Competing Interests: The Author(s) declare(s) no conflict of interest.

Editor: Juan A. Navas-Cortes, Spanish National Research Council (CSIC), Cordoba, Spain.

ORCID:
MN: 0009-0004-2205-8649
CB: 0000-0003-1353-7993
AMV: 0000-0003-0797-3297

INTRODUCTION

Magnolia (*Magnolia grandiflor*a L.) is a popular ornamental species that is widely planted in both public and private green areas for its evergreen foliage, large and fragrant flowers, and high aesthetic value. Beyond its ornamental significance, *M. grandiflora* contributes to the ecological balance of urban ecosystems, providing shade, improving air quality and supporting urban biodiversity (Sjöman *et al.,* 2018; Novak *et al*., 2023). Among the approx. 200 species within *Magnolia*, *M. grandiflora* is particularly valued for its notable tolerance to drought conditions (Vastag *et al*., 2020). Nonetheless, like other urban trees species, magnolias planted in cities are frequently subjected to multiple stress factors, including soil compaction, air pollution and restricted rooting space (Balraju *et al*., 2023; Vettraino *et al*., 2025a, b). Such conditions can weaken tree vitality and increase their susceptibility to biotic agents.

Global warming and changes in temperature and humidity can influence the development, survival and spread of pests and pathogens, as well as the spread and survival of natural enemies, competitors and vectors. Consequently, abiotic stress, together with the impacts of climate change and high risks of introducing infected plant material from nurseries into urban environments, creates a complex and potentially dangerous scenario (Garrett *et al*., 2021; Antonelli *et al*., 2023; Raum *et al*., 2023;Antonelli *et al*., 2024; Lahlali *et al*., 2024;). In recent years, foliar diseases have become increasingly prevalent in urban trees, posing dual threats by compromising their aesthetic values and physiological functions, including photosynthesis, nutrient transport and overall plant health (Knox *et al*., 2012; Esmaeilzadeh *et al*., 2020; Hu *et al*., 2023; Huang *et al*., 2025;).

Leaf diseases of magnolia plants commonly manifest as brown spots that impair the visual quality of the foliage, and substantially reduce photosynthetic performance, with negative consequences for tree growth, vigour and resilience.

During routine monitoring of urban trees in April 2025, brown leaf spots were observed on two mature magnolia trees located in Viterbo (Central Italy). This study aimed to determine the etiology of this disease, to provide knowledge as the basis for effective disease management.

MATERIALS AND METHODS

Field observation and fungi identification

In April 2025, leaves of *M. grandiflora* exhibiting leaf spot symptoms were collected in Viterbo, Italy (42.4186°N; 12.1042°E). About 10% of the leaves exhibited brown- spots distributed on the leaf surface (Figure 1).

A total of ten leaves showing brown spots symptoms were collected, transported to the laboratory in sterile plastic bags, and processed within 24 h of collection. Tissue samples were sterilized according to Vettraino *et al.* (2021), with procedural adjustments. Specifically, the leaves were immersed in 75% ethanol for 1 min, and were then rinsed three times with sterile distilled water to remove residual disinfectant. Tissue sections exhibiting spots were aseptically cut into fragments. A total of 100 fragments were placed on PDS medium (39 g L^{-1} Potato dextrose agar [PDA; Oxoid] supplemented with 0.06 g L^{-1} streptomycin sulfate), and the culture plates were incubated at 25 ± 2°C. Each of the resulting distinct colonies was subcultured by transferring a hyphal tip onto a fresh PDA plate for purification.

The isolates obtained (35) were grouped based on colony morphology and pigment production observed after 7 d incubation. Conidium morphology was examined using a Zeiss Axio Imager A2m microscope.

Figure 1. *Magnolia grandiflora* leaves showing leaf spot symptoms.

Two isolates (R3 and R7) were selected as representative strains of the total isolates obtained, and their morphological characterizations were confirmed by molecular analyses. Genomic DNA was extracted from fresh mycelium using the NucleoSpin® Plant II kit (Macherey-Nagel), according to the manufacturer's instructions. Molecular identification of cultures was achieved based on the amplification and sequencing of the gene regions translation elongation factor 1 alpha (EF–1α), RNA polymerase largest subunit (RPB1), and RNA polymerase second largest subunit (RPB2) (O'Donnell *et al*., 2008; Jiang *et al*., 2020). Phylogenetic trees were constructed using the neighbour-joining (NJ) algorithm combined with the Kimura 2-parameter model implemented in MEGA 11 (Tamura *et al*., 2021). Bootstrap analysis was conducted with 1,000 replicates. Sequences of related *Fusarium* species were retrieved from GenBank for comparisons. The dataset consisted of sequences from isolates characterized in this study and ten taxa from the *Fusarium* species complex.

Pathogenicity tests

Pathogenicity tests were carried out on detached healthy *M. grandiflora* leaves to confirm the etiological roles of isolates R3 and R7. For each isolate, 5 mm mycelium plugs collected from 7-d-old PDA cultures were placed on leaf surfaces that had been previously

wounded using a sterile scalpel (wound length 4mm). Inoculation control leaves received sterile PDA plugs. All leaves were then placed in plastic trays with moist paper towels to maintain approx. 90% relative humidity, and were incubated at 25 ± 1°C. Petioles of the leaves were wrapped in wet cotton to prevent desiccation. Each treatment consisted of five replicates per isolate. Development of symptoms was monitored daily, for 3 d after inoculation. Fungal re-isolations were made from symptomatic tissues assess fulfilment of Koch's postulates. The pathogenicity tests were repeated twice to confirm reproducibility.

RESULTS

Isolation and characterization of fungal isolates

Isolates R3 and R7 both produced fast-growing, pale to bright- coloured colonies with dense aerial mycelium. Isolate R3 developed orange to pink aerial mycelium. Macroconidia were hyaline and two to five septate, of lengths 35 to 50 µm, while microconidia were absent. Chlamydospores were abundant, and were globose to oval, and were intercalary and lateral, and measured 7 to 11 µm. Isolate R7 formed white aerial mycelium and produced hyaline, non-septate, single-celled, ovoid microconidia measuring 6 to 8 µm. This isolate also produced abundant globose to oval chlamydospores, measuring 6 to 11 µm. Macroconidia of R7 were falcate, hyaline, one to six-septate, and were 30 to 45 µm in length.

The two isolates were coded as *Fusarium*, and species identity was verified through analysis of the EF1-α, RPB1 and RPB2 sequences using BLAST searches against the NCBI database. Isolate R3 corresponded to *F. venenatum*, and isolate R7 corresponded to *F. clavum*. The phylogenetic analysis based on the concatenated sequences of TEF-1α, RPB1 and RPB2, using the NJ method, was consistent with the result of the BLASTn comparison (Figure 2).

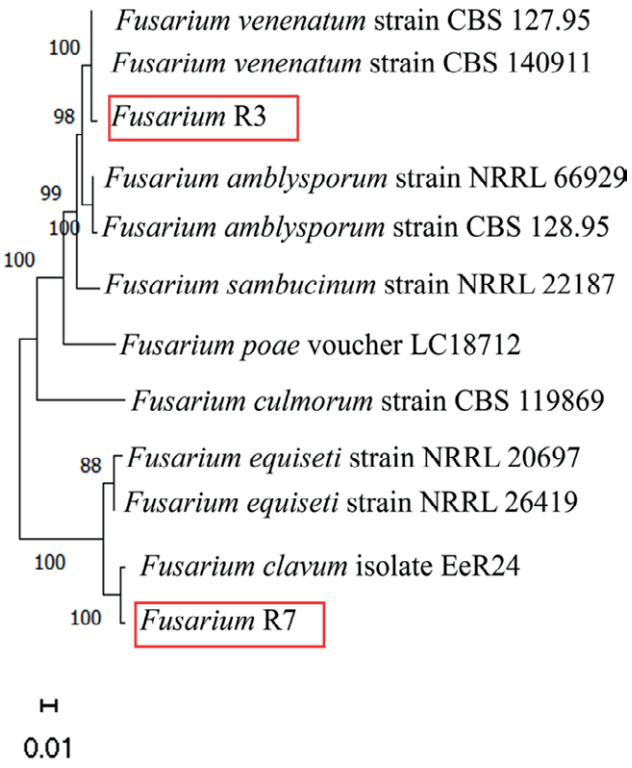

Figure 2. Neighbour-Joining (NJ) phylogenetic tree based on concatenated sequences of TEF-1α, RPB1 and RPB2 genes, including sequences of already known *Fusarium* species and of isolates R3 and R7 obtained in the present study. Bootstrap values greater than 50% (expressed as percentages of 1,000 replications) are shown at the nodes. The isolates characterized in this study are each highlighted with a red-bordered rectangle.

Pathogenicity tests

Three days following inoculations, brown leaf spots appeared on all leaves inoculated with isolates R3 and R7, in both experimental repetitions. No symptoms were observed on control leaves (Figure 3). The symptoms were similar to those previously observed on *M. grandiflora* trees under field conditions. Fungi identical to *F. venenatum* R3 were re-isolated from diseased tissues inoculated with this isolate, and similarly for *F. clavum* R7, confirming Koch's postulates for both fungi.

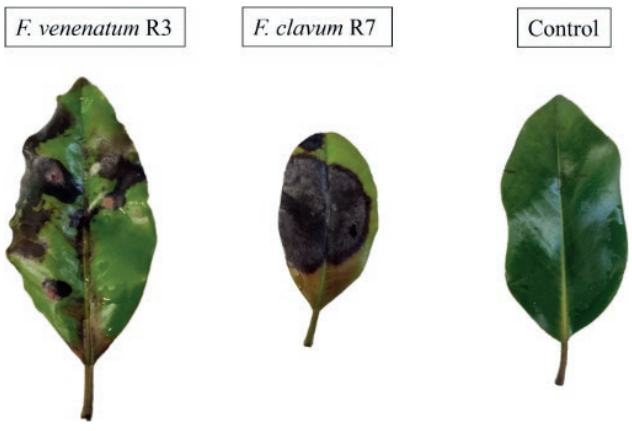

Figure 3. Symptoms on *Magnolia grandiflora* leaves after inoculations with *Fusarium* isolates R3 or R7, compared to an uninoculated control leaf.

DISCUSSION

Magnolia grandiflora is a widely valued ornamental tree in urban and peri-urban landscapes, providing key ecosystem services such as air purification, shade, aesthetic value, and habitats for biodiversity. However, introductions of new pests and pathogens pose significant risks to magnolia health and the benefits provided by these trees. The fungi isolated from leaf spots on *M. grandiflora* during the survey in Viterbo, Italy were identified as *F. venenatum* (isolate R3) and *F. clavum* (isolate R7), based on morphological and molecular analyses.

Fusarium Link (*Hypocreales*, *Nectriaceae*) includes several aggressive plant pathogens that cause root rot, cankers and vascular wilt on a variety of urban trees (Skarmoutsou & Skarmoutsos, 1999; Guo *et al*., 2021). *Fusarium venenatum* has been previously reported in association with dry rot in potato tubers (Stefancyzk *et al*., 2016; De Jesús Díaz Aguilar *et al*., 2023), and root and collar rot, damping-off, and foliar necroses in herbaceous crops (Ayoubi & Soleimani, 2016), citrus trees and strawberry plants. Similarly, *F. clavum* has been associated with leaf spot and blight symptoms, appearing as necrotic lesions that sometimes expand and lead to premature senescence (Sandoval-Denis *et al*., 2018; Matic *et al.,* 2020; Gilardi *et al*., 2021).

The present study has identified, for the first time, natural infections of *M. grandiflora* by *F. venenatum* and *F. clavum*. This is the first documented report of *F. venenatum* and *F. clavum* associated with diseases of *M. grandiflora*. Occurrence of these fungi in symptomatic leaves collected from urban green spaces extends the known host range of both species, and indicates their adaptability to actively colonize foliar tissues, rather than acting merely as secondary saprophytes, highlighting the adaptability of *Fusarium* species to urban tree environments.

These results emphasize the vulnerability of urban trees to emerging fungal pathogens, and the importance of regular disease surveillance in green city areas. To mitigate the impacts of these pathogens, management strategies should emphasize preventive cultural practices that limit pathogen spread and establishment, including minimal and well-timed pruning of dead or diseased branches, rapid removal of symptomatic tissues, and strict application of pruning hygiene methods.

LITERATURE CITED

Antonelli C., Biscontri M., Tabet D., Vettraino A.M., 2023. The never-ending presence of *Phytophthora* species in Italian nurseries. *Pathogens* 12: 15. https://doi.org/10.3390/pathogens12010015

Antonelli C., Soulioti N., Linaldeddu B.T., Tsopelas P., Biscontri M., … Vettraino A.M., 2024. *Phytophthora nicotianae* and *Ph. mediterranea*: A biosecurity threat to *Platanus orientalis* and *P.* x *acerifolia* in urban green areas in Greece. *Urban Forestry & Urban Greening* 95: 128281. https://doi.org/10.1016/j.ufug.2024.128281

Ayoubi N. Soleimani M.J., 2016. Morphological and molecular identification of pathogenic *Fusarium* spp. on strawberry in Iran. *Sydowia An International Journal of Mycology* 163–171. https://doi.org/10.12905/0380.sydowia68-2016-0163

Balraju W., Upadhyay K.K., Tripathi S.K., 2023. Assessing toxic element accumulation trend in *Magnolia champaca* tree rings at Tuirial dumping site in Mizoram, Northeast India using dendrochemical analysis. *Water, Air, & Soil Pollution* 234: 726. https://doi.org/10.1007/s11270-023-06648-3

De Jesús Díaz Aguilar R., Chávez E.C., Velázquez Guerrero J.J., Roque Enriquez A., Rodríguez Pagaza Y., Ochoa Fuentes Y.M., 2023. First report of *Fusarium clavum* causing garlic bulb rot in Mexico. *Plant Disease* 107: 3317. https://doi.org/10.1094/PDIS-12-22-2853-PDN

Esmaeilzadeh A., Zafari D., Bagherabadi S., 2020. First report of *Phyllosticta capitalensis* causing leaf spots on ornamental *Magnolia grandiflora* and *Syringa reticulata* in Iran. *New Disease Reports* 41: 7–7. https://doi.org/10.5197/j.2044-0588.2020.041.007

Garrett K.A., Nita M., De Wolf E.D., Esker P.D., Gomez-Montano L., Sparks A.H., 2021. Plant pathogens as indicators of climate change. In: *Climate Change*, Elsevier, 499–513.

Gilardi G., Matic S., Guarnaccia V., Garibaldi A., Gullino M.L., 2021. First report of *Fusarium clavum* causing leaf spot and fruit rot on tomato in Italy. *Plant Disease* 105: 2250. https://doi.org/10.1094/PDIS-05-20-1096-PDN

Guo Z., Yu Z., Li Q., Tang L., Guo T., … Luo S., 2021. *Fusarium* species associated with leaf spots of mango in China. *Microbial Pathogenesis* 150: 104736. https://doi.org/10.1016/j.micpath.2021.104736

Hu L.-J., Li Y., Zhai M., Xuan J.-P., Mo Z.-H., Hua Y.-L., 2023. First report of leaf spot on *Magnolia grandiflora* caused by *Lasiodiplodia theobromae* in Jiangsu. *Plant Disease* 107: 950. https://doi.org/10.1094/PDIS-05-22-1038-PDN

Huang S., Cao J., Zhang L., Feng J., 2025. *Diaporthe cercidis* causing leaf blight on *Magnolia grandiflora* in China. *Crop Protection* 198: 107389. https://doi.org/10.1016/j.cropro.2025.107389

Jiang H., Wu N., Jin S., Ahmed T., Wang H., ... Zhang J.-Z., 2020. Identification of rice seed-derived *Fusarium* spp. and development of LAMP assay against *Fusarium fujikuroi*. *Pathogens* 10: 1. https://doi.org/10.3390/pathogens10010001

Knox G.W., Klingeman W.E., Paret M., Fulcher A., 2012. Management of pests, plant diseases and abiotic disorders of *Magnolia* species in the Southeastern United States: A review. *Journal of Environmental Horticulture* 30: 223–234. https://doi.org/10.24266/0738-2898.30.4.223

Lahlali R., Taoussi M., Laasli S.-E., Gachara G., Ezzouggari R., ... Barka E.A., 2024. Effects of climate change on plant pathogens and host-pathogen interactions. *Crop and Environment* 3: 159–170. https://doi.org/10.1016/j.crope.2024.05.003

Matic, S., Tabone, G., Guarnaccia, V., Gullino, M.L., & Garibaldi, A. (2020). Emerging leafy vegetable crop diseases caused by the *Fusarium incarnatum-equiseti* species complex. *Phytopathologia Mediterranea* 59, 303–317. https://doi.org/10.14601/Phyto-10883

Nowak D.J., 2023. Improved air quality and other services from urban trees and forests. In: *Engineering and Ecosystems* (B.R. Bakshi, ed.), Cham, Springer International Publishing, 215–245.

O'Donnell K., Sutton D.A., Fothergill A., McCarthy D., Rinaldi M.G., ... Geiser D.M., 2008. Molecular phylogenetic diversity, multilocus haplotype nomenclature, and in vitro antifungal resistance within the *Fusarium solani* species complex. *Journal of Clinical Microbiology* 46: 2477–2490. https://doi.org/10.1128/JCM.02371-07

Raum S., Collins C.M., Urquhart J., Potter C., Pauleit S., Egerer M., 2023. Tree insect pests and pathogens: a global systematic review of their impacts in urban areas. *Urban Ecosystems* 26: 587–604. https://doi.org/10.1007/s11252-022-01317-5

Sandoval-Denis M., Guarnaccia V., Polizzi G., Crous P.W., 2018. Symptomatic *Citrus* trees reveal a new pathogenic lineage in *Fusarium* and two new *Neocosmospora* species. *Persoonia - Molecular Phylogeny and Evolution of Fungi* 40: 1–25. https://doi.org/10.3767/persoonia.2018.40.01

Sjöman H., Hirons A.D., Bassuk N.L., 2018. Magnolias as urban trees – a preliminary evaluation of drought tolerance in seven magnolia species. *Arboricultural Journal* 40: 47–56. https://doi.org/10.1080/03071375.2017.1415554

Skarmoutsou H., Skarmoutsos G., 1999. First report of *Fusarium* wilt disease of mimosa in Greece. *Plant Disease* 83: 590–590. https://doi.org/10.1094/PDIS.1999.83.6.590D

Stefańczyk E., Sobkowiak S., Brylińska M., Śliwka J., 2016. Diversity of *Fusarium* spp. associated with dry rot of potato tubers in Poland. *European Journal of Plant Pathology* 145: 871–884. https://doi.org/10.1007/s10658-016-0875-0

Tamura K., Stecher G., Kumar S., 2021. MEGA11: Molecular Evolutionary Genetics Analysis Version 11. *Molecular Biology and Evolution* (F.U. Battistuzzi, ed.) 38: 3022–3027. https://doi.org/10.1093/molbev/msab120

Vastag E., Orlović S., Konôpková A., Kurjak D., Cocozza C., ... Stojnić S., 2020. *Magnolia grandiflora* L. shows better responses to drought than *Magnolia* × *soulangeana* in urban environment. *iForest - Biogeosciences and Forestry* 13: 575–583. https://doi.org/10.3832/ifor3596-013

Vettraino A.M., Luchi N., Rizzo D., Pepori A.L., Pecori F., Santini A., 2021. Rapid diagnostics for *Gnomoniopsis smithogilvyi* (syn. *Gnomoniopsis castaneae*) in chestnut nuts: new challenges by using LAMP and real-time PCR methods. *AMB Express* 11: 105. https://doi.org/10.1186/s13568-021-01266-w

Vettraino A.M., Matošević D., 2025. Sustainable management strategies for enhancing urban tree health and resilience. *Urban Forestry & Urban Greening* 128859. https://doi.org/10.1016/j.ufug.2025.128859

Vettraino A.M., Soulioti N., Matosevic D., Tuğba Doğmuş Lehtijarvi H., Woodward S., ... Luchi N., 2025. Management of fungal diseases of *Platanus* under changing climate conditions: Case studies in urban areas. *Urban Forestry & Urban Greening* 107: 128750. https://doi.org/10.1016/j.ufug.2025.128750

Mediterranean Phytopathological Union

Founded by Antonio Ciccarone

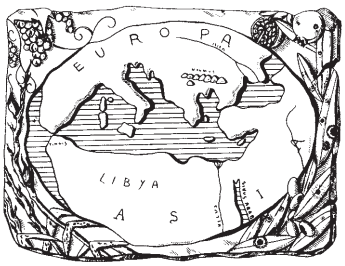

The Mediterranean Phytopathological Union (MPU) is a non-profit society open to organizations and individuals involved in plant pathology with a specific interest in the aspects related to the Mediterranean area considered as an ecological region.
The MPU was created with the aim of stimulating contacts among plant pathologists and facilitating the spread of information, news and scientific material on plant diseases occurring in the area. MPU also intends to facilitate and promote studies and research on diseases of Mediterranean crops and their control.
The MPU is affiliated to the International Society for Plant Pathology.

MPU Governing Board

President
Salah M. Abdel-Momen, Agricultural Research Center, Giza, Egypt,
E-mail: salah1993@yahoo.com

Immediate Past President
Dimitrios Tsitsigiannis, Agricultural University of Athens, Greece
E-mail: dimtsi@aua.gr

Board members
Nihal Buzkan, Faculty of Agriculture, Avşar Campus, 46100 Kahramanmaraş, Türkiye
Diana Fernandez, INRAE, Institute Agro, Montpellier, France
Juan A. Navas-Cortés, Institute for Sustainable Agriculture, Spanish National Research Council, Córdoba, Spain

Honorary President - Treasurer
Giuseppe Surico, DAGRI, University of Florence, Firenze, Italy
E-mail: giuseppe.surico@unifi.it

Secretary
Anna Maria D' Onghia, CIHEAM-Mediterranean Agronomic Institute of Bari, Valenzano, Bari, Italy – E-mail: donghia@iamb.it

Treasurer
Laura Mugnai, DAGRI, University of Florence, Firenze, Italy
E-mail: laura.mugnai@unifi.it

Coordinator of the Advisory Committee
Maria Do Céu Silva, University of Lisbon, Portugal,
E-mail: mariaceusilva@isa.ulisboa.pt

MPU National Society Members

Croatian Plant Protection Society
Egyptian Phytopathological Society (EPS)
French Society of Plant Pathology (SFP)
Hellenic Phytopathological Society (HPS)
Israeli Phytopathological Society (IPS)
Italian Association for Plant Protection (AIPP)
Italian Phytopathological Society (SIPAV)
Italian Nematological Society (SIN)
Palestinian Plant Production and Protection Society (PPPPS)
Plant Protection Society in Bosnia and Herzegovina
Plant Protection Society of Serbia
Plant Protection Society of Slovenia
Portuguese Phytopathological Society (PPS)
Spanish Phytopathological Society
Turkish Phytopathological Society (SEF)

MPU Affiliated Members

Arab Society of Plant Pathology
Euphresco
CIHEAM-Bari
International Mycotoxicology Society
International Society for Plant Pathology

2026 Information for authors of the Open Access journal *Phytopathologia Mediterranea*

Only MPU members are eligible to publish according to MPU membership categories (see https://oajournals.fupress.net/index.php/pm/about):

– All authors belonging to an MPU National Society Member (see list above) or to an MPU Affiliated Member (international organizations or networks), that signed a Memorandum of Understanding with MPU, are entitled to publish with a contribution to publication cost (https://oajournals.fupress.net/index.php/pm/about)

– All Individual Members (not in the above categories), including members of profit or non-profit entities, and physical person.

To become an Individual Member see www.mpunion.org or contact secretariat@mpunion.org

To receive the paper version of the journal please contact phymed@unifi.it

For information visit the MPU web site:
www.mpunion.org
or contact us at: Phone +39 39 055 2755861/862 – E-mail: phymed@unifi.it

Phytopathologia Mediterranea
Volume 65, April, 2026

Contents

Phytopathologia Mediterranea is an Open Access Journal published by Firenze University Press (available at www.fupress.com/pm/) and distributed under the terms of the Creative Commons Attribution 4.0 International License (CC-BY-4.0) which permits unrestricted use, distribution, and reproduction in any medium, provided you give appropriate credit to the original author(s) and the source, provide a link to the Creative Commons license, and indicate if changes were made.
The Creative Commons Public Domain Dedication (CC0 1.0) waiver applies to the data made available in this issue, unless otherwise stated.
Copyright © 2026 Authors. The authors retain all rights to the original work without any restrictions.
Phytopathologia Mediterranea is covered by AGRIS, BIOSIS, CAB, Chemical Abstracts, CSA, ELFIS, JSTOR, ISI, Web of Science, PHYTOMED, SCOPUS and more

Direttore responsabile: Giuseppe Surico • Autorizzazione del Tribunale di Firenze n. 4923 del 5-1-2000 • *Printed by* Logo S.r.l. - Padova, May 2026